Isolation and molecular characterization of single circulating rare cells : developing innovative methods for predictive oncology and non-invasive prenatal diagnosis

Lucile Broncy

NNT : 2017SACLS391

Thèse de doctorat
de
l'Université Paris-Saclay
préparée à
l'Université Paris Sud

Ecole Doctorale n° 577
Structure et dynamique des systèmes vivants (SDSV)
Spécialité de doctorat : sciences de la vie et de la santé

Par

Lucile Broncy

Isolement et caractérisation moléculaire de cellules rares circulantes individuelles : développement de nouvelles approches méthodologiques en oncologie prédictive et diagnostic prénatal.

Thèse présentée et soutenue à Paris, le 7 novembre 2017

Composition du Jury :

M. Saule, Simon	Professeur, Université Paris-Sud	Président
Mme Taly, Valérie	Directeur de recherche, Université Paris-Descartes	Rapporteur
Mme Brevet, Marie	Professeur, Centre de biologie et pathologie EST Lyon	Rapporteur
M. Cussenot, Olivier	Professeur, Centre de recherche sur les pathologies prostatiques	Examinateur
Mme Paterlini-Bréchot, Patrizia	Professeur, Université Paris-Descartes	Directeur de thèse
Mme Ezine, Sophie	Directeur de recherche, Université Paris-Descartes	Co-directeur de thèse

Summary

Special thanks

First, I would like to thank the CIFRE doctoral grant programme from ANRT (Association Nationale de la Recherche et de la Technologie) that provided essential funding to support my work. I am also equally grateful to both co-directors of the SDSV (Science et Dynamique des Systèmes Vivants) Doctoral School, Professors Pierre Capy and Jean-Luc Pernodet, as well as to the Paris-Saclay University, who believed in my research project when others didn't.

I would also like to express my most sincere gratitude to the brilliant woman who agreed to direct my work and provided much appreciated guidance regarding multiple aspects of both academic and private research sectors: Professor Patrizia Paterlini-Bréchot. Her humble dedication and continuously renewed tenacious efforts towards improving medical care practices for patients all over the world never ceases to impress.

I am also very grateful to Dr. Sophie Ezine for her additional guidance and support as co-director as well as for her persistent optimism throughout the course of my doctoral research.

Additionally, I am very grateful to all my collaborators from INSERM (Institut National de la Santé et de la Recherche Médicale) and the Necker Institute as well as to all my colleagues at the firm Rarecells Diagnostics who took part in any aspect of the work presented here and invested their time, energy and resources in order to provide their valued contributions to this doctoral research, including (but not restricted to) Basma Ben Nijma, Ingrid Pfeifer, Sophie Laget, Davide Bréchot, Katia Hormigos, Karine Prévost, Gabriela Petkova-Campbell and Jane Muret.

I am also thankful for both private and academic research collaboration opportunities provided by Stephen Jackson and Dalia Dhingra (Thermofisher Scientific – United States of America), Filip Van Nieuwerburgh and Lieselot Deleye (Ghent University – Belgium), Chris Wetzel (Molecular Machines & Industries – Germany), Paul Hofman and Marius Ilie (Centre Hospitalo-Universitaire de Nice – France) as well as Laurent Farinelli (Fasteris – Switzerland).

Special thanks are addressed to my father as well as to my roommate and best friend for putting up with my late working hours and fluctuant moods while never ceasing to believe in me.

And finally, extra special thanks are further addressed to my original research mentor, Dr Thierry Capiod, for his many teachings, professional integrity, open-mindedness and esteemed friendship that proved essential in guiding my first steps towards medical research in oncology.

List of Figures and Tables

List of acronyms in oncology research

ATP: Adenosine TriPhosphate
BMDC: Bone Marrow-Derived Cells
BMP: Bone Morphogenetic Proteins
CAF/TAF: Cancer-/Tumor-Associated Fibroblasts
ccRCC: clear cell Renal Cell Carcinoma
CDH1: epithelial CaDHerin protein coding gene
CEpC: Circulating Epithelial Cells
COPD: Chronic Obstructive Pulmonary Disease
CSC: Cancer Stem Cells
CTC: Circulating Tumor Cells
CTM: Circulating Tumor Microemboli
Cx: Connexins
DNA: DesoxyriboNucleic Acids
DTC: Disseminated Tumor Cells
ECM: ExtraCellular Matrix
EGF: Epidermal Growth Factor
EGFR: EGF Receptor
EMT: Epithelial to Mesenchymal Transition
EndMT: Endothelial to Mesenchymal Transition
EpCAM: Epithelial Cell Adhesion Molecule
ERK: Extracellular signal-Regulated Kinases
F-Actin: Actin Filaments
FAK: Focal Adhesion Kinases
FDA: Food & Drugs Administration
GAS: Growth Arrest-Specific proteins
HER2: Human EGF Receptor 2
HIF: Hypoxia Inducible Factor
HNSCC: Head & Neck Squamous Cell Carcinoma
ICAM: InterCellular Adhesion Molecule
IFN-γ: InterFeroN gamma
IL: InterLeukin
iPS: induced Pluripotent Stem cells
ISET: Isolation by SizE of Tumor/Trophoblastic cells
ITH: Intra-Tumor Heterogeneity
JAM: Junction Adhesion Molecule
KRAS: Kirsten RAt Sarcoma viral oncogene homolog
LEC: Lymphatic Endothelial Cells
lncRNA: long non-coding RNA
MAPK: Mitogen-Activated Protein Kinases
MDSC: Myeloid-Derived Suppressor Cells
MET: Mesenchymal to Epithelial Transition
miR: microRNA
MMP: Matrix MetalloProteinases
mRNA: messenger RNA
NF-κB: Nuclear Factor kappa B
NSCLC: Non-Small-Cell Lung Cancer
OSCC: Oral Squamous Cell Carcinoma
PAMR: Perijunctional Acto-Myosin Ring
PDGF: Platelet-Derived Growth Factor
PECAM: Platelet/Endothelial Cell Adhesion Molecule
PI3K: PhosphoInositide 3 Kinase
PTEN: Phosphatase & TENsin homolog
RNA: RiboNucleic Acids
SDF-1: Stromal cell-Derived Factor one
TAM: Tumor-Associated Macrophage
TANK: Tumor-Associated Natural Killer cells
TCIPA: Tumor Cell-Induced Platelet Aggregation
TF: Tissue Factor
TGFβ: Transforming Growth Factor beta
Treg: regulatory T lymphocytes
VCAM: Vascular Cell Adhesion Molecule
VE-cadherin: Vascular Endothelial cadherin
VEGF: Vascular Endothelial Growth Factor
VEGFR: VEGF Receptor
VHL: Von Hippel-Lidau
VM: Vasculogenic Mimicry
VTE: Venous Thrombo-Embolism
Wnt: Wingless integration site glycoproteins
ZO: *Zona Occludens* proteins

List of acronyms in prenatal research

CF: Cystic Fibrosis

cfDNA: cell-free DNA

cffDNA: cell-free fetal DNA

CFTC: Circulating Fetal Trophoblastic Cells

CGH: Comparative Genomic Hybridization

CVS: Chorionic Villus Sampling

ddPCR: droplet digital PCR

EVT: ExtraVillous Trophoblasts

iEVT: interstitial EVT

ISET®: Isolation by SizE of Tumor/Trophoblastic cells

IUGR: IntraUterine Growth Retardation

IVF: *In Vitro* Fecundation

LCM: Laser Capture Microdissection

NGS: Next-Generation Sequencing

NIPD: Non-Invasive Prenatal Diagnosis

NIPT: Non-Invasive Prenatal Testing

PCR: Polymerase Chain Reaction

PEP: Primer Extension Preamplification

SMA: Spinal Muscular Atrophy

STR: Short Tandem Repeat

SynT: SyncytioTrophoblasts

TCC sampling: TransCervical Cell sampling

TOP: Termination Of Pregnancy

vEVT: vascular EVT

WG: Weeks of Gestation

Introduction

1. Tumor invasion, dormancy and metastasis

1.1. Introduction: an overview on tumor invasion/metastasis

Tumor invasion and subsequent metastatic spread are responsible for 90% of human cancer-related deaths worldwide (Siegel *et al.*, 2015). Tumor invasion/metastasis was originally thought to be a linear process where the primary tumor develops by acquiring a series of genetic and epigenetic characteristics until a fully malignant profile of cancer cells emerges (Fidler, 2003). For instance, the activation of oncogenic drivers such as BRAF, KRAS, EGFR and PI3K, among other genetic alterations, are known to confer malignant proliferative capacities to their cellular carriers. In the linear progression model, fully malignant tumor cells possess invasive properties that allow them to detach from the primary tumor and migrate through the basement membrane and underlying interstitial matrix. The tumor vasculature develops by neoangiogenesis and invasive cancer cells can exploit existing vasculature to disseminate into the lymphatic system and the bloodstream by intravasation, they are then called circulating tumor cells (CTC). Survival in the circulation is however difficult even for invasive CTC and most of them die during the journey (Fidler, 1975). But for those that do survive, extravasation at distant organ sites or regional lymph nodes results in effective dissemination and those cells are therefore called disseminated tumor cells (DTC).

The assumption that DTC colonize specific target organs depending on the primary tumor origin comes from the observation of recurrent patterns of metastasis depending on the type of cancer diagnosed as primary tumor. For example, breast cancer is known to give rise to lung, liver, brain, lymph nodes and bone metastasis preferentially (Viadana *et al.*, 1973). This theory was first proposed by Stephen Paget in 1889 (Paget, 1889) with the "seed and soil" metaphor in which tumor cells are the seed that only grows on a specific soil, namely specific organ sites that enable successful development of metastasis.

One of the key aspects of the linear model is that dissemination of fully malignant cells occurs mostly

in advanced cancers because clonal expansion is linked to tumor size (Cairns, 1975). The model also implies that metastatic cells can always be traced back to the primary tumor and should therefore exhibit a core of genetic features identical to those of primary cancer cells, with potential few additional features gained during metastasis development. And finally, linear metastatic progression associates with the concept of metastatic cascades which suggests that metastases are also capable of seeding invasive cancer cells to distant organs, thereby initiating secondary metastasis in a distinct location.

However, studies from the 1950s quantifying human cancer growth rates concluded that early initiation of metastasis, meaning initiation long before clinical evidence of a primary tumor arises, is required for the timely emergence of metastatic lesions compared with that of the primary tumor, given their respective growth rates (Collins *et al.*, 1956). Additional evidences contradicting the linear model include the diagnosis of metastasis in early-stage cancer patients at first clinical presentation (representing 5% of breast cancer patients diagnosed with primary tumors smaller than 5 cm), malignant neoplasms of unknown primary tumor origin (accounting for 5-10% of diagnoses in Europe and the US), multiple coexisting metastases which appear to derive from genetically unrelated tumor clones, and the finding that DTC extracted from the bone marrow of breast, prostate and oesophageal cancer patients exhibit significantly fewer genetic aberrations than primary tumor cells (Klein, 2009). The above-mentioned observations prompted for a different theoretical approach to model cancer development towards invasion and metastasis.

Accumulating substantial evidence now points to a parallel progression of primary tumors and metastases. For example, murine breast cancer models suggest that dissemination of cancer cells occurs early in tumor development (Hüsemann *et al.*, 2008) and that even untransformed mammary epithelial cells (lacking activation of known oncogenic drivers) can survive injection into the blood stream, disseminate in the lung and assume a low-proliferative or dormant state until oncogene activation leads them to initiate malignant growth (Podsypanina *et al.*, 2008). Additionally, the presence of epithelial cells circulating in the peripheral blood of patients with benign inflammatory

bowel diseases and their comparative absence in healthy control subjects (Pantel *et al.*, 2012) clearly demonstrates that proliferative malignancy is not required for epithelial cells to invade the blood stream, particularly when sustained inflammation governs their microenvironment.

The parallel progression model of tumor invasion/metastasis postulates that dissemination of cells throughout the body starts very early in the natural history of cancer and may even predate the full acquisition of proliferative malignancy (Klein, 2009). Such a model can account with much more fidelity for the disparate array of clinical observations reported so far. It is indeed much more accurate in predicting the level of genetic heterogeneity observed between malignant cells from distinct biological locations in the same individual. It could even provide a sensible explanation for malignant neoplasms of unknown primary origin; because if pre-malignant cells disseminate and stay dormant at distant organ sites, then hypothetical situations become possible where malignant transformation of DTC occurs before or even without acquisition of malignancy by sister cells in the primary organ of origin.

The idea that malignant transformation is merely accessorial to the blood-borne dissemination of epithelial cells begs the question of what other mechanisms are required for such invasion to arise. Important clues come from studies on animal models of cancer. In particular, mouse models of pancreatic cancer revealed that pre-neoplastic tumor cells can undergo epithelial-mesenchymal transition (EMT) in order to disseminate prior to the acquisition of a detectable malignancy (Rhim *et al.*, 2012). Interestingly, these authors also reported that induction of inflammation through pancreatitis resulted in increased numbers of circulating pancreatic cells. Indeed, the presence of mesenchymal CTC in the blood of cancer patients has been linked to disease progression and resistance to chemotherapy (Mego *et al.*, 2012; Yu *et al.*, 2013). Transitioning to a mesenchymal phenotype confers motility to epithelial cells by loss of polarity and cell-cell adhesions which correlates to the occurrence of EMT in normal embryo development (Nieto, 2011). Increasing evidence links EMT to invasive cancer cells. However, this transition also associates with reduced proliferation capacities and quiescence of tumor cells (Mejlvang *et al.*, 2007), thereby protecting

them from apoptosis mechanisms that induce cell death (Vega *et al.*, 2004). *In vitro* experiments conducted on cancer cell lines suggest that mesenchymal tumor cells have increased invasive capabilities but are also unable to metastasize without reverting to an epithelial phenotype (Tsuji *et al.*, 2008; Celià-Terrassa *et al.*, 2012). Indeed, the counterpart mechanism that reverts EMT (mesenchymal-epithelial transition, MET) also plays an important role in normal embryonic development and cancer metastasis since proliferating metastatic cells are mainly epithelial (Chaffer *et al.*, 2006). Furthermore, the fact that even dormant DTC have exclusively been described as epithelial cells suggests that survival of DTC in distant organs relies on the recovery of an epithelial phenotype. Therefore, it is more likely that a high degree of phenotypic plasticity, rather than just EMT, favors tumor invasion and subsequent metastatic spread (Brabletz, 2012).

Another example of phenotypic plasticity of tumor cells is their ability to differentiate into endothelial-like cells and reorganize to form tubular structures which are filled with extracellular matrix components and divert red blood cells from the existing vasculature to irrigate hypoxic regions of the tumor. This phenomenon, referred to as vasculogenic mimicry (VM), was first evidenced in melanoma by Maniotis and colleagues (Maniotis *et al.*, 1999). VM was later associated with poor prognosis of patients with different types of neoplasms including non-small-cell lung cancer, sarcoma, melanoma, colorectal cancer and hepatocellular carcinoma (Cao *et al.*, 2013). Interestingly, a recent study on murine models and human breast cancer reported that anti-angiogenic treatment with sunitinib promotes an adaptive switch of triple negative breast tumors towards VM whereas less aggressive breast tumors (non-triple negative) did not exhibit such a phenomenon and did not relapse immediately after treatment arrest (Sun *et al.*, 2017). Those results highlight the complex intertwining of intrinsic and extrinsic factors, including genetic factors and therapeutic pressures, cooperating to orchestrate cancer development. Likewise, epithelial-mesenchymal plasticity is highly influenced by molecular and cellular components of the microenvironment, as suggested by previously cited studies linking invasion and EMT to inflammation (Pantel *et al.*, 2012; Rhim *et al.*, 2012). Furthermore, induction, maintenance and exit

of DTC dormancy also depend on effectors present in the microenvironment such as hypoxia-related signaling (Lu *et al.*, 2010).

Conversely, the emerging concept of cancer stem cells postulates that a small fraction of tumor initiating cells possess intrinsic stem-like properties that allow them to reshape their microenvironment along with their own proliferative capabilities (Brabletz *et al.*, 2005). Like other types of cancer cells, circulating cancer stem cells can be found in the blood of cancer patients (Tinhofer *et al.*, 2014; Mirzaei *et al.*, 2015). CTC (including circulating cancer stem cells) represent an informative and easily-accessible source of cancer material that is rapidly gaining interest from scientists as targets enabling a "liquid biopsy" of cancer. However, the heterogeneity and extreme rarity in blood of CTC have hampered their comprehensive analysis and its application in clinical settings (Alix-Panabières and Pantel, 2016).

Another interesting concept suggested by animal models is that of tumor self-seeding. Although difficult to prove in human cancer patients, tumor self-seeding was evidenced in a mouse model of breast cancer where fluorescently labeled tumor cells injected intravenously migrated back to the primary tumor and recruited stromal cells along the way to promote tumor growth and angiogenesis (Kim *et al.*, 2009).

All the above-mentioned mechanisms of cancer development (for a general overview, please see **Figure 1**) rely on complex molecular cross-talk between cells of various origins and functions. Assuming the parallel progression of primary tumors and metastases, the following chapters will further detail the cellular and molecular mechanisms involved in the main steps of tumor invasion/metastasis which were introduced here.

Figure 1: *Parallel progression of tumor and metastasis (see legend on the following page)*

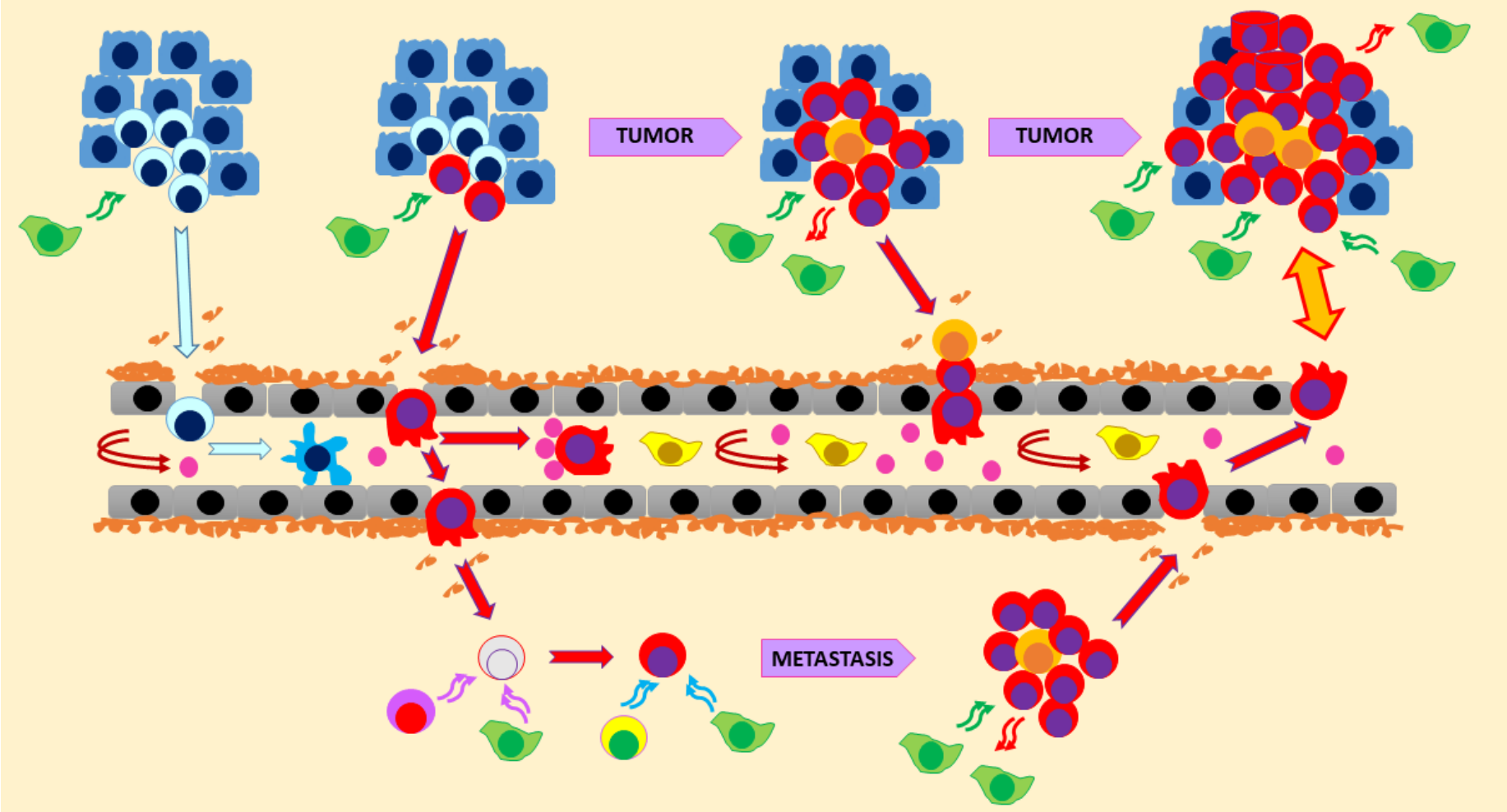

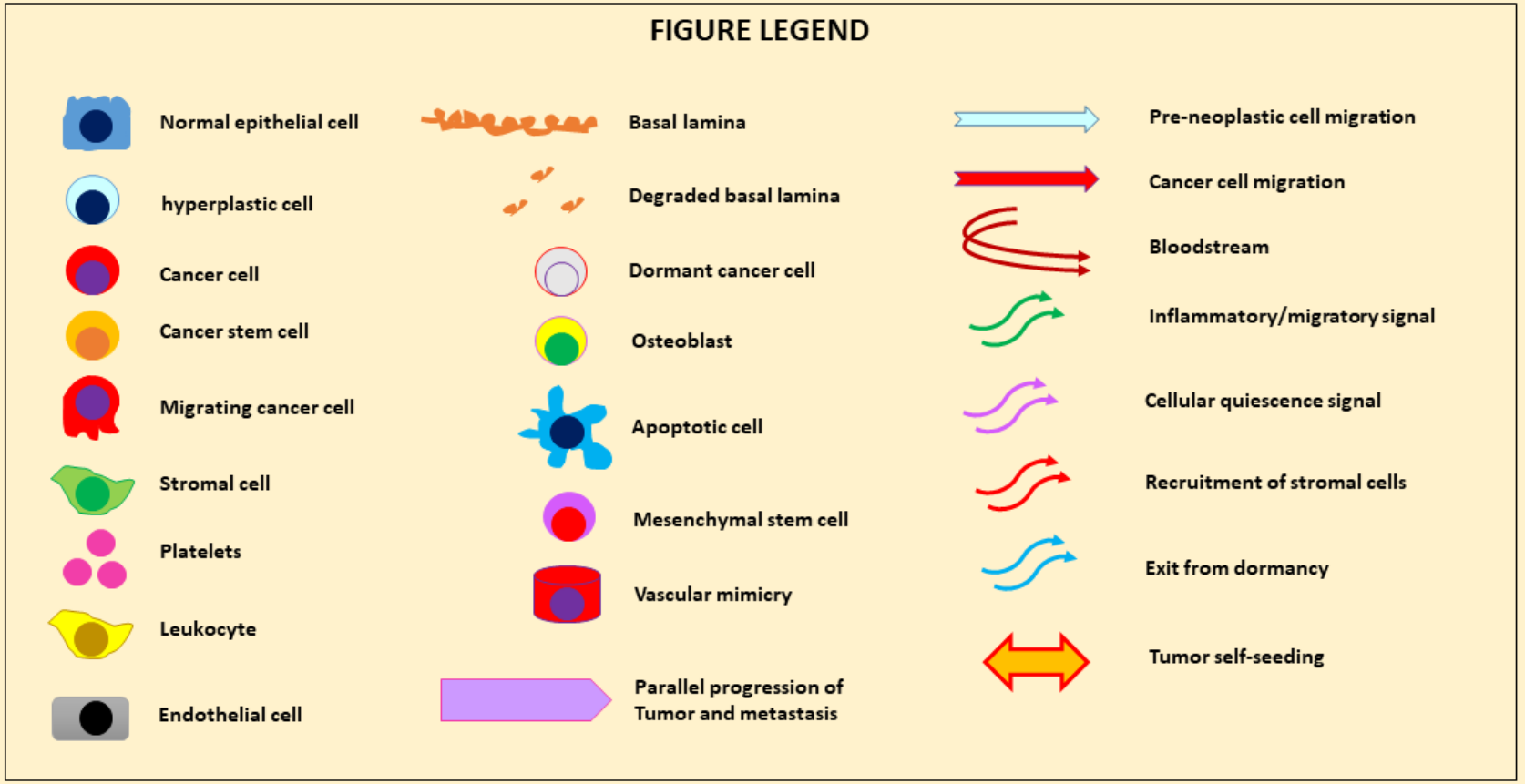
FIGURE LEGEND
Normal epithelial cell
hyperplastic cell
Cancer cell
Cancer stem cell
Migrating cancer cell
Stromal cell
Platelets
Leukocyte
Endothelial cell
Basal lamina
Degraded basal lamina
Dormant cancer cell
Osteoblast
Apoptotic cell
Mesenchymal stem cell
Vascular mimicry
Parallel progression of Tumor and metastasis
Pre-neoplastic cell migration
Cancer cell migration
Bloodstream
Inflammatory/migratory signal
Cellular quiescence signal
Recruitment of stromal cells
Exit from dormancy
Tumor self-seeding

1.2. Cell motility, attachment and cytoskeleton dynamics

Most solid cancers derive from epithelia. Epithelial cells are typically polarized and firmly attached to one another through the formation of adherens junctions, tight junctions and desmosomes. They are capable of creating continuous barriers to separate distinct biological microenvironments and to function in absorption. In contrast, mesenchymal and stromal cells are loosely organized in the extracellular matrix and possess faster intrinsic motile functions (Thiery *et al.*, 2009). Cell motility and adhesion are crucially mediated by cytoskeleton dynamics. This section will therefore highlight the main molecular mechanisms implicated in cell motility and attachment.

Cytoskeleton dynamics in animal cells are mainly operated through fast rearranging proteins such as microtubules, actin and intermediate filaments. Microtubules are cylindrical polymers of alternating alpha- and beta-tubulin monomers guiding the long-range transport of vesicles through the cytoplasm and the segregation of chromosomes during cell division. Microtubules are polarized and associate with motor proteins that migrate along the tubular structure towards the minus end (dynein) or the plus end (kinesin). Likewise, actin filaments also function as polarized polymer structures of beta- and gamma-actin monomers providing internal mechanical support (cell stiffness and cell shape), enabling cell adhesion and associating with a myosin motor protein to drive cell motility and finalize cell division by separating plasma membranes. Actin filaments also participate in the short-range transport of vesicles and provide force to internalize endocytic vesicles from the plasma membrane (Pollard and Cooper, 2009). Intermediate filaments enable further plasticity of intracellular tensions (cell stiffness) and their molecular composition can significantly vary from one cell-type to another. For example, intermediate filaments in epithelial cells are mainly composed of members of the keratin family of proteins (also called cytokeratins) whereas mesenchymal cells rely on vimentin proteins. Conversely, human endothelial cells mainly express vimentin but some members of the keratin family such as K7 and K18 are also found in subsets of normal endothelia (Miettinen and Fetsch, 2000).

1.2.1. Cell attachment

Many membrane and cytoplasmic components of cell-cell attachment are guided through the cytoplasm and delivered at junctions by microtubule-binding motor proteins (Sluysmans *et al.*, 2017). In epithelial cells for instance, efficient assembly of adherens junctions relies on the interaction of dynein and β-catenin (Ligon and Holzbaur, 2007). β-catenin associates with the intra-cytoplasmic domain of the transmembrane adhesion protein E-cadherin (in epithelial cells) to activate a conformational change in its extracellular domain, thereby enabling attachment to neighboring cells by formation of homodimers of activated cadherins. Similarly, kinesin interacts with desmosomal cadherins to guide them along microtubules towards desmosomes where they bind intermediate filaments (Nekrasova *et al.*, 2011).

On the apical-basal axis of polarized epithelial cells, adherens junctions are located just below tight junctions that form at the apical extremity. Both adherens and tight junctions are zonular, which means they form a continuous ring around the apex of the cell (Sluysmans *et al.*, 2017). Actin filaments (or F-actin) associate with nonmuscle myosin-II to form the perijunctional acto-myosin ring (PAMR) that sustains adherens junctions of epithelial cells on the cytoplasmic side of the plasma membrane. Parallel F-actin bundles connect to the transmembrane junctional proteins of adherens junctions (nectins and cadherins) via afadin and catenin-vinculin complexes. The PAMR has a contractile function that infers junction disruption leading to internalization of junctional proteins (Kartenbeck *et al.*, 1991). Both adherens and tight junctions are affected by contraction of the PAMR because endocytosis of the cadherin complex indirectly disrupts neighboring tight junctions. Assembly, remodeling and contractility of the PAMR are regulated by RhoA, Rac1 and Cdc42 which are all members of the Rho family of small GTPases (Sluysmans *et al.*, 2017).

Importantly, the integrity of tight junctions is crucial to the barrier function of epithelia. Tight junctions occur between apposing plasma membranes to eliminate the intercellular space. They are composed of homodimers of transmembrane proteins such as claudins, occludins and junction adhesion molecules (JAM). Those transmembrane proteins bind to a submembrane scaffold of

zonula occludens proteins (ZO-1 and ZO-2 heterodimers) that tether to the cytoplasmic network of actin filaments (Furuse, 2010). Another zona occludens protein (ZO-3) more likely regulates the acto-myosin cytoskeleton by influencing the activity of small Rho GTPases. Interestingly, experimental modulation of the expression of each zona occludens protein affects the acto-myosin cytoskeleton in a cell-type dependent manner, suggesting a more complex interconnection of signaling pathways.

Cell junctions also enable epithelial and endothelial cells to respond to intracellular or extracellular tensions by mechanotransduction. In normal epithelia, increased tension on F-actin (intracellular) or on the extracellular domain of E-cadherin leads to a conformational change of the beta-catenin bound alpha-catenin that increases its affinity to vinculin (Kim *et al.*, 2015). Specific tension on E-cadherin also infers activation of the PI3-kinase (PI3K) which results in myosin-II contraction at focal adhesion sites (cell-matrix attachment). In endothelial cells, specific junction molecules include VE-cadherin, receptors for the vascular endothelial growth factor (VEGFR2/3) and platelet-endothelial cell adhesion molecules (PECAM-1, also known as CD31). Shear stress and other types of extracellular tensions induce phosphorylation of VEGFR2/3 by the Src kinase (controlling endothelial growth and repopulation after injury) and activation of the Pi3K pathway which recruits actin filaments to strengthen VE-cadherin homologous binding. Additionally, PECAM-1 recruits vimentin upon phosphorylation by the Fyn tyrosine kinase upstream of MAPK and ERK1/2 pathways (Sluysmans *et al.*, 2017).

Another important type of protein complex mediating cell contact and communication is referred to as gap junctions. The connective transmembrane channel formed by gap junctional proteins allow connected cells to exchange various small metabolites, ions, second messengers, electrical impulses and water by passive diffusion from one cytoplasm to another (Söhl and Willecke, 2004). Hemi-channels (also called connexons) form in the plasma membrane by assembly of six protein subunits called connexins (Cx) that slide along each other to assume open or closed conformations of the connexon. In juxtaposed cells, connexin extracellular domains bind each other to form gap junction

channels composed of two colocalized connexons. In human cells, 21 connexin isoforms have been identified and some of them are expressed in a cell-type specific manner. For example, cardiomyocytes were found to express Cx40, Cx43 and Cx45 whereas Cx37 and Cx40 form gap junctions between endothelial cells (Söhl and Willecke, 2004). Junctions forming between epithelial cells are summarized in **Figure 2**.

Figure 2: *Cell attachment in normal epithelia*

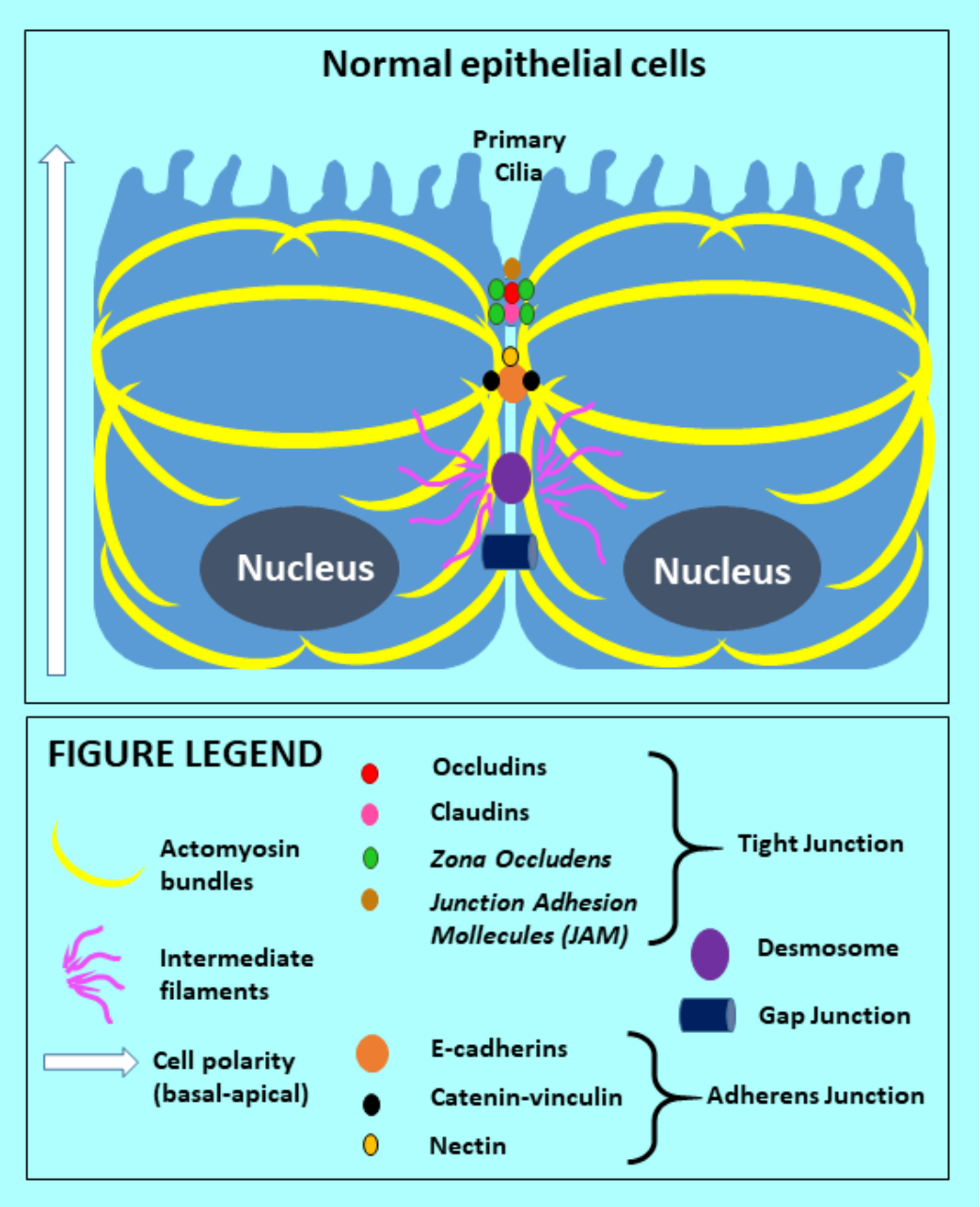

1.2.2. Cell motility

Cytoskeletal proteins play an important role in cell attachment at focal adhesion sites and cellular protrusion-retraction mechanisms which altogether govern cell motility. Cellular migration is crucial to normal embryonic development, tissue regeneration and wound healing (Krawczyk, 1971). Importantly, cellular motility can occur at single-cell level and as collective migration both in normal development and in cancer invasion.

The crawling-like motion of individual cells on a substrate involves 4 major steps: protrusion at the leading edge, adhesion to the substrate, retraction at the rear edge and de-adhesion (Pollard and Borisy, 2003). Dynamic polymerization of actin filaments can induce changes in cell shape to form protrusions at the leading edge (also called lamellipodia and filopodia). It is worth noting that spontaneous polymerisation of unbranched actin filaments can occur *in vitro* depending on (and at a speed proportional to) the concentration of actin monomers in the medium. Because formation of lamellipodia requires both fast and branched polymerization of actin filaments, migrating single-cells produce a number of specific proteins to enable protrusion at the leading edge. The branching of F-actin relies on the binding of activated Arp2/3 complex and WASp (Wiskott-Aldrich syndrome protein) /Scar protein. The small Rho GTPases Cdc42 and Rac1 activate WASp/Scar proteins and Arp2/3 complex respectively, but activated WASp/Scar proteins can also activate Arp2/3 complex independently of Rac1 upon binding with actin filaments (Pollard and Borisy, 2003). Interestingly, human leukocytes concentrate remarkably high levels of Arp2/3 complex in their cytoplasm. Moreover, fast elongation of F-actin requires the maintenance of a high concentration of unpolymerized actin monomers at the leading edge of the migrating cell. Capping proteins bind the extremity of F-actin to terminate elongation where necessary. In parallel, monomer-binding proteins such as profilin and thymosin-β4 inhibit spontaneous and uncontrolled polymerization of F-actin. In human platelets and leukocytes, profilin controls the pool of polymerization-ready actin by blocking assembly on the single relevant side of the monomer while thymosin-β4 ensures the maintenance of a backup pool by blocking actin assembly at both ends of the monomer. Importantly, compared

to thymosin-β4, the higher affinity of profilin to bind actin monomers allows platelets and leukocytes to repurpose a fraction of the backup pool whenever faster motility is required (Pollard and Borisy, 2003). Mysosin II contractility provides the force necessary to push the plasma membrane, resulting in lamellipodium formation at the leading edge. Faster actin turnover at the leading edge is ensured by ADF/cofilin proteins which depolymerize aged filaments. Nascent focal adhesions (also called focal complexes) form at the leading edge and mature through β1-integrin-dependant mechanisms in mesenchymal migrating cells while amoeboid migration (leukocytes, platelets) does not rely on β1-integrins. Nascent adhesions incorporate paxilin and can either be disassembled to recycle their molecular components or develop into mature focal adhesions, incorporating other molecules such as alpha-actinin, and slide inward towards the cell body (Webb *et al.*, 2003).

The lamellum, which designates the central area of the cell directly following the leading edge, is characterized by unbranched filaments, a slower retrograde flow of actin and mature focal adhesions (Alexandrova *et al.*, 2008). In mesenchymal migrating cells, actin stress fibers form an essential intracytoplasmic scaffold of thicker actin bundles incorporating myosin II and alpha-actinin. The tension mediated by theses stress fibers is essential to focal adhesion maturation. Three types of actin stress fibers have been identified: dorsal stress fibers, transverse arcs and ventral stress fibers, as depicted in **Figure 3**. At the leading edge, dorsal stress fibers connect on one side to nascent focal adhesions and attach on the opposite side to perpendicularly oriented transverse arcs which mediate tension to the leading edge adhesions. Conversely, ventral stress fibers are only found in the trailing area and connect with focal adhesions at both ends (Vallenius, 2013). Myosin II contractility allows both mechanosensing at focal adhesion sites and retraction of the trailing edge during migration. The specific molecular mechanisms involved in stress fibers assembly remain partially uncharacterized but sufficient evidence links mDia1 (a formin family member) to the assembly of dorsal stress fibers while mDia2 and Arp2/3 complex cooperate to assemble transverse arcs via end-to-end annealing of short actin bundles. Furthermore, distinct isoforms of myosin II (myosin IIA and mysosin IIB) are thought to mediate distinct functions of stress fibers. For example,

myosin IIB was implicated in the regulation of directional cell migration trough ventral stress fibers contractility whereas myosin IIA localizes primarily at the leading edge. However, myosin IIB is also found on a portion of transverse arcs and implicated in leading edge adhesions (Vallenius, 2013). Further studies are required in order to better understand the molecular mechanisms linking cytoskeletal proteins to the specific components of cellular motility.

Figure 3: *Single-cell motility of mesenchymal cells*

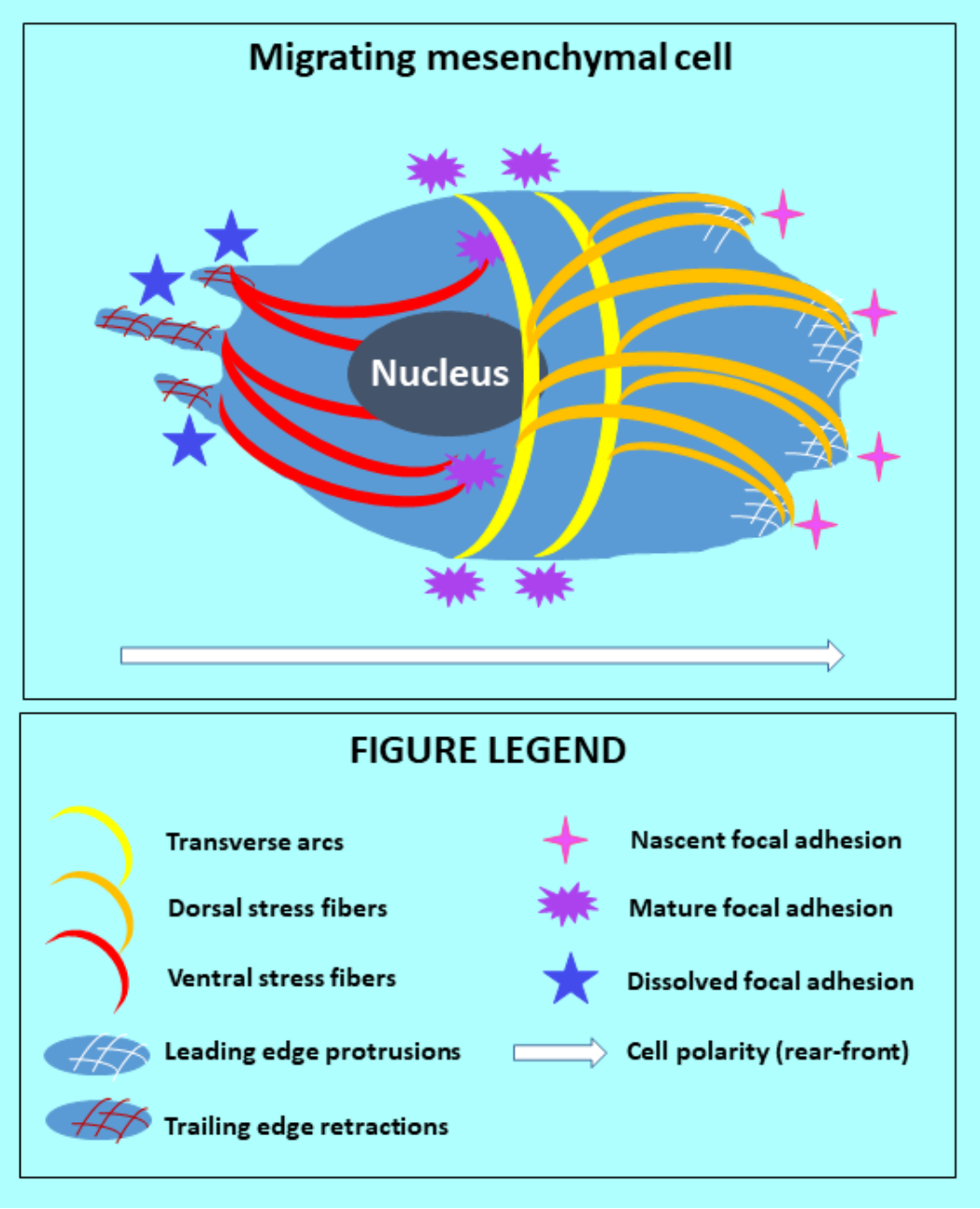

In contrast, collective cell migration can occur with or without protrusion at the leading edge, the

latter representing less well characterized mechanisms which have been implicated in normal embryo development (Uechi and Kuranaga, 2017). Collectively migrating cells can organize and communicate to enable formation of protrusions at the leading edge of the cluster and cohesive links between follower cells and leader cells. Cadherin-mediated adherens junctions tether the follower cells to their leaders and inhibit the formation of protrusions in the plasma membrane of the followers. Leader cells also interact with each other and coordinate the retrograde flow of F-actin-bound adherens junctions, creating a constant treadmilling along the lateral sides of adjacent leading cells which is supported by a polarized recycling of cadherins. In models of wound healing for instance, the coordinated retrograde flow of N-cadherin engaged in adherens junctions of collectively migrating astrocytes depends on the internalization of N-cadherin at the rear and its recycling to the front, guided by a polarized gradient of p120-catenin phosphorylation (Peglion *et al.*, 2014). In another wound healing model, cohesive attachment of migrating epithelial cells allows for formation of finger-like extensions of the cell sheet where very few leader cells generate thick actin cables that exert traction forces on several rows of followers via F-actin tethered to adherens junctions (Reffay *et al.*, 2014). Interestingly, accumulation of activated RhoA molecules colocalizes with the multicellular distribution of traction forces in collectively migrating epithelia and mirrors the intracytoplasmic distribution of activated RhoA in migrating single-cells, further demonstrating the regulation of actomyosin contractility by the small GTPase (Reffay *et al.*, 2014). Adherens junctions mediate traction forces and their loss results in fast rearrangement of motility while tight junctions, gap junctions and desmosomes also participate in the strength of cell-cell contacts but do not modulate velocity upon disassembly (Bazellières *et al.*, 2015).

Importantly, the leaders of collective migration are not intrinsically defined by cell types. Instead, environmental cues and direct proximity with neighboring cells regulates the functional assignment of each cell in the collective as leader or follower, and those roles can be switched during migration. For example, in a mouse model of angiogenesis, Arima and colleagues demonstrated the dynamic exchange of positions and functions between respective endothelial cells at the tip and the trunk of

the neovasculature during both elongation and branching of vessels *in vivo* (Arima *et al.*, 2011). Furthermore, leader cells provide more than just traction forces to the collective. By sensing soluble factors present in the microenvironment, leaders effectively infer directional guidance of the migrating group. They can also fully control such guidance by secreting their own soluble factors and by producing enzymes capable of remodeling extracellular matrix components such as members of the matrix metalloproteinase (MMP) family (Wang *et al.*, 2010).

1.3. Strong effectors of the microenvironment

The microenvironment of a given cell is composed of extracellular matrix (ECM) proteins arranging in fibers such as various types of collagen and fibronectin, directly or indirectly neighboring cells and the soluble factors they secrete into the ECM such as cytokines and growth factors. For example, stromal cells such as fibroblasts are capable of producing and remodeling ECM components and they have been directly implicated in the formation of a tumor microenvironment (Erdogan and Webb, 2017).

1.3.1. Stromal cells

Stromal cells are crucial mediators of ECM stiffness which can promote both tumor invasion and initiation, as evidenced in a transgenic mouse model expressing collagen dense mammary stroma (Provenzano *et al.*, 2008). ECM fibers such as collagen and fibronectin, arrange in a meshwork among other connective proteins to provide physical guidance to motile stromal cells as well as invasive cancer cells that detach from the tumor. For example, higher collagen 1 (Col1) fiber volumes and increased numbers of fibroblast-like cells have been correlated to invasive and metastatic properties of the ECM in prostate cancer (Penet *et al.*, 2017). Fibroblasts being subjected to tumor signaling in the stromal proximity of a tumor have been described as cancer- or tumor-associated fibroblasts (CAF/TAF). But this terminology broadly designates all activated fibroblast-like cells in the tumor microenvironment which can derive from mesenchymal stem cells, epithelial and endothelial cells through phenotypic plasticity and transdifferentiated normal tissue cells such as pericytes,

adipocytes and smooth muscle cells in breast cancer (Qiao *et al.*, 2016). By producing enzymes of the matrix metalloproteinases (MMP) familly, CAF/TAF can actively remodel ECM fibers (Nabeshima *et al.*, 2002). The contribution of CAF/TAF to the formation of a sustained pro-invasive tumor microenvironment has been reported through various mechanisms in a number of neoplastic malignancies including prostate (Penet *et al.*, 2017), lung (Yu *et al.*, 2016), breast (Wang *et al.*, 2002), liver (Kubo *et al.*, 2016), endometrial (Teng *et al.*, 2016), pancreatic (Lee *et al.*, 2011) and colorectal (Bai *et al.*, 2015) cancer. It is also worth noting that CAF/TAF can physically bind tumor cells by forming heterotypic E-cadherin/N-cadherin adherens junctions and exert mechanical forces to drag them, thereby inducing collective migration of epithelial tumor cells by acting as leaders (Labernadie *et al.*, 2017).

Importantly though, cancer is not the only context in which quiescent stromal cells can be activated. In normal wound healing for instance, inflammatory signals trigger the activation of stromal cells to promote proliferation and migration of epithelial cells which are both required for an efficient healing process to occur (Bussard *et al.*, 2016). Similarly, hepatic stellate cells responding to liver injury activate and start secreting ECM proteins, which can lead to accumulation of Col1 and hepatic fibrosis in cases of chronic injury induced by frequent ethanol consumption, viral hepatitis and iron deposition, for example (Brenner *et al.*, 2000). Other examples include smoking-induced cardiorenal fibrosis (Drummond *et al.*, 2016) and chronic obstructive pulmonary disease (COPD) which has been linked to a higher risk of developing lung cancer (Barreiro *et al.*, 2016). Moreover, normal fibroblasts subjected to sublethal doses of irradiation have been shown to activate and induce malignant transformation of normal mammary epithelial cells when co-transplanted in mice (Kuperwasser *et al.*, 2004). This suggests that activated stromal cells play an important role even at the earliest steps of carcinogenesis.

Additionally, immune cells can also be recruited to the tumor stroma such as T regulatory lymphocytes (Treg), tumor-associated natural killer cells (TANK) and myeloid-derived suppressor cells (MDSC) which can differentiate into dendritic cells or tumor-associated macrophages (TAM).

Interestingly, TAM have recently been further characterized as capable of remodeling the ECM through synthesis, assembly and cross-linking of various types of collagen proteins (Afik *et al.*, 2016). However, the strongest ECM effectors that both tumor cells and tumor-associated stromal cells can produce in order to form a pro-invasive tumor microenvironment are growth factors and cytokines.

1.3.2. Growth factors and cytokines

Upon binding to their respective receptors on the plasma membrane, growth factors and cytokines present in the microenvironment trigger multiple intracellular signaling pathways involved in controlling cell migration, proliferation, differentiation and survival. Those are complex mechanisms that can trigger angiogenic or inflammatory signals as well as specific responses to oxidative stress and hypoxia within the tumor. This part will however focus primarily on the molecular mechanisms by which growth factors and cytokines facilitate the earliest steps of tumor invasion before tumor cells can access the circulation by intravasation into nearby lymphatic or blood vessels.

Induction of migration by growth factor and cytokine signaling can occur through separate or parallel modulations of cell-cell and cell-matrix adhesions. For instance, epidermal growth factor (EGF) upon binding with its receptor (EGFR) can induce both activation of the EMT transcription factor Snail resulting in the downregulation of E-cadherin at cell-cell junctions (Lu *et al.*, 2003) and downregulation of focal adhesion kinase (FAK) which weakens cell-matrix attachment in various epithelial tumor cells (Lu *et al.*, 2001). Downregulation of cell attachment both to neighboring cells and to the surrounding ECM favors single-cell amoeboid migration of tumor cells which detach from the tumor and migrate through the ECM by weak interactions without forming mature focal adhesions (Friedl and Wolf, 2010). However the deregulations of growth factor and cytokine signaling which are frequently observed in cancer seem to function somewhat differently depending on the cell type. In head and neck squamous cell carcinoma (HNSCC) cells for instance, EGF signaling affects cell-cell junctions by upregulating MMP9 production which enables enzymatic cleavage of E-cadherin (Zuo *et al.*, 2011) rather than by downregulating E-cadherin itself. Conversely, stromal cell-derived factor 1 (SDF-1, also called by its cytokine name: CXCL12) can increase cell-matrix adhesion

by upregulating β6 integrins through activation of the ERK pathway in colorectal cancer (Wang *et al.*, 2014a). Enhanced adhesion to the ECM favors mesenchymal-like migration of tumor cells either as single cells or clusters depending on the strength of cell-cell adhesions in the molecular context of a particular tumor microenvironment. Single-cell mesenchymal migration of epithelial cells occurs mainly by induction of EMT, which can be mediated by growth factor and cytokine signaling from the microenvironment. Hypoxia-inducible factor 1 (HIF-1), for example, has been shown to activate EMT transcription factors Snail, Zeb and Twist (Zhou *et al.*, 2012). In untransformed human hepatocytes, activation of Snail1 expression is necessary and sufficient to induce EMT and confer resistance to TGFβ-mediated apoptosis (Franco *et al.*, 2010). Interestingly, TGFβ through binding with its receptor TGFβR1 on hepatocellular carcinoma cells upregulates Snail1 expression by activating the nuclear factor-kappa B (NF-κB) pathway (Franco *et al.*, 2010). In colorectal cancer however, stimulations with transforming growth factor beta 1 (TGFβ1) or the chemokine CXCL12 (SDF-1) reinforce E-cadherin-based junctions and result in collective cell migration (Hwang *et al.*, 2012). Interestingly, collective migration may be a strategy for poorly invasive cancer cells to migrate on unfavorable substrates. Indeed, to reach nearby vessels and disseminate throughout the body, tumor cells first need to cross the laminin-rich basal membrane before accessing the collagen- and fibronectin-rich ECM of interstitial tissues. Accordingly, Ramos et al. reported that poorly invasive oral squamous cell carcinoma (OSCC) cell lines expressing high levels of E-cadherin display increased RhoA activity and migrate collectively on fibronectin-rich substrates while highly invasive OSCC cell lines expressing low levels of E-cadherin rather display increased Rac1 activity and adopt a single-cell strategy of migration on fibronectin (Ramos *et al.*, 2016). In contrast, Lobastova and colleagues reported that thyroid carcinoma cells migrate more efficiently as collectives on plastic surfaces in a Rac1-dependent manner (Lobastova *et al.*, 2017). These studies highlight the complex regulation of tumor cell behavior depending on intrinsic and extrinsic factors. Moreover, growth factors and cytokines also impact invasive properties and behavior of cancer cells in a context-dependent manner. Indeed, live intravital imaging techniques have enabled researchers to locate invasive

behavior of tumor cells at the border, called invasive front, of the tumor. For example, Giampieri et al. demonstrated that TGFβ signaling is transiently and locally activated in breast cancer cells at the invasive front of the tumor where it promotes single cell motility (Giampieri *et al.*, 2009). Importantly, TGFβ signaling can also promote growth arrest and (in early stages) apoptosis of tumor cells and is therefore repressed in highly proliferative locations inside the tumor (Derynck *et al.*, 2001). As a truly context-dependent effector capable of both antitumor and pro-tumorigenic effects, TGFβ exemplifies the complex and heterogeneous distribution of intracellular and intercellular regulation of signaling pathways across a single tumor mass.

1.4. Intratumor heterogeneity

Intratumor heterogeneity (ITH) was first evidenced in animals in the 1950s when studies on chromosomal changes occurring in primary tumors during disease progression fueled the later concept of clonal evolution of tumor cell populations that arose in the 1970s (Nowell, 1976; Dexter *et al.*, 1978). The clonal theory actually relates to the Darwinian concept of evolution as it postulates that only the "fittest" clone will expand to dominate the tumor population in a given tumor environment defined by selective internal and external pressures (Gatenby and Vincent, 2003). This is well exemplified by the acquisition of specific genetic alterations and/or expansion of clonal populations that provide an adaptive advantage for resisting therapeutic pressures in the context of neoadjuvant therapies (Balko *et al.*, 2014). Furthermore, a recent study built on analysis of 1165 tumor exomes across 12 different cancer types reported that 86% of all samples contained at least two distinct clonal populations, with an increased mortality risk associated to samples containing more than two coexisting tumor clones (Andor *et al.*, 2016). Genetic ITH could therefore serve as a prognostic factor in various types of cancer. Importantly though, ITH is often underestimated at genetic level by current methodologies and has further been evidenced at other levels with regards to non-genetic factors such as epigenetic differentiation and environmental contributions.

From a genetic viewpoint, multiple sampling at distinct tumor locations together with important

technological developments regarding high throughput sequencing have greatly expanded our understanding of ITH. For example, Gerlinger et al. studied 10 cases of clear cell renal cell carcinoma (ccRCC) and applied multiregion exome sequencing to identify the level of ITH during disease progression and treatment (Gerlinger *et al.*, 2014). More precisely, they determined that 73-75% of all driver genetic alterations were found at the sub-clonal level, meaning that they were not represented in every biopsy sampled from the same tumor. Decreased ITH was attributed to specific treatment regimens targeting predominant tumor clones. This is important because, in the advent of personalized anticancer therapies, treatment decision is unfortunately still often made based on analysis of a single tumor sample, leading to underestimation of ITH and recurrence of the disease after treatment. Despite continuous progress in bioinformatics, important limitations in current technical strategies restrict our capability to accurately assess genetic ITH from bulk tumor sample sequencing, even when applying multiple sampling from distinct regions of the same tumor. This is in part due to significant error rates attributed to high throughput sequencing technologies that do not allow for an accurate description of small tumor populations which harbor genetic alterations present at allele frequencies below 1% in the whole sample. A potent example of this limitation was provided by a single-cell sequencing study in melanoma which enabled the identification of a minor tumor subpopulation exhibiting a resistant phenotype prior to therapy (Tirosh *et al.*, 2016). Single-cell sequencing therefore provides an essential distinction between acquired resistance to therapy and selection of resistant tumor subclones by therapeutic pressure; a distinction that current bulk tumor sequencing technologies are unable to infer reliably. Moreover, the assumption that a given genetic alteration occurs at the same allelic frequency in all cancer cells and represents a single given tumor clone is highly biased, as shown by comparative single-cell sequencing and alternate statistical methodologies (Roth *et al.*, 2016; Mroz and Rocco, 2017). In acute myeloid leukemia, for instance, the commonly associated driver mutations in FTL3 and NPM1 genes were recently reported to occur both in homozygous and heterozygous states at single-cell level and be distributed among at least nine distinct clonal populations (Paguirigan *et al.*, 2015). These observations also suggest

that distinct tumor clones found in separate locations inside the same tumor can adopt seemingly convergent evolutionary strategies. Indeed, genetic convergence of unrelated clones, through activation of known oncogenic pathways such as EGFR, KRAS and PI3K, has been well established by studies of inter-tumor heterogeneity between unrelated patients. Similarly, distinct tumor subclones coexisting in the same patient have been shown to independently acquire convergent genetic alterations in both pancreatic (Campbell *et al.*, 2010) and renal cancers (Voss *et al.*, 2014). Additionally, the Darwinian concept of inter-clonal competition for survival has further been complemented by reports highlighting the occurrence of functional cooperation between distinct clonal populations of the same tumor. For example, in a mouse model of glioblastoma, Inda and colleagues found that some tumors harbored a minority of EGFR mutants that sustained the growth of the dominant wild-type EGFR clones by secreting cytokines such as leukemia inhibitory factor (LIF) and interleukin 6 (IL-6), thereby activating EGFR in wild-type neighboring cells (Inda *et al.*, 2010). Similarly, in a mouse model of breast cancer, Marusyk *et al.* determined that minor subclones expressing IL-11 promoted tumor growth in a non-cell-autonomous fashion and that depletion of IL-11 expressing clones significantly reduced tumor growth and clonal expansion (Marusyk *et al.*, 2014). Although derived from animal studies, the concept of inter-clonal collaboration is in agreement with clinical observations relating to acquired treatment resistance in human colorectal cancer. More precisely, the limited fraction of KRAS mutant cancer cells observed in samples of patients exhibiting resistance to targeted anti-EGFR therapy was reported to sustain the growth of the wild-type drug-sensitive clonal populations through the secretion of TGF alpha and amphiregulin (Hobor *et al.*, 2014). These studies highlight the complex contributions of both genetic and non-genetic factors to the survival and clonal evolution of cancer cells.

Indeed, components of the microenvironment have significant effects on ITH but other non-genetic parameters are also at play, such as epigenetic factors. Epigenetic modifications mainly comprise altered DNA methylation, differential expression of non-coding RNA (including microRNA) and histone modifications. While oncogenic effects of specific types of microRNA, such as miR-21, have

only recently been discovered (Abrahamsson and Dabrosin, 2015), altered DNA methylation in cancer has been studied since the early 1980s (Gama-Sosa *et al.*, 1983; Goelz *et al.*, 1985). DNA methylation is enzymatically reversible and replicates with lower fidelity than DNA sequences through mitosis. Surprisingly though, efforts to infer evolutionary history of a tumor through comparative genetic and epigenetic analyses have yielded highly concordant phylogenies depicting similar patterns of evolution (Mazor *et al.*, 2016). Those results likely reflect a certain degree of co-dependency existing between epigenetic and genetic alterations since aberrant epigenetic states may promote genetic instability or may result from genetic alterations. Nevertheless, studying epigenetic ITH on bulk tumor samples imposes similar technical and analytical limitations to those previously mentioned in the context of genetic analysis. Furthermore, very few studies have explored the epigenomic landscape of cancer at single-cell resolution, partly due to a lack of reliable methods to do so. One interesting report from Buenrostro and colleagues recently identified sets of transcription factors with highly variable chromatin accessibility from one cell to another and further linked those factors to the regulation of cellular differentiation states (Buenrostro *et al.*, 2015).

Additional studies are still required in order to fully understand the extent of ITH and single-cell analysis offers great potential to explore any kind of cell-cell variability. However, analysis of available ITH data has already fostered important discoveries regarding tumor initiation, propagation and relapse. Notably, following the description of genetic ITH in the 1950s, the quest to identify a specific subtype of tumor-initiating cells led to the emergence of the concept of cancer stem cells (Makino, 1956).

1.5. Cancer stem cells

Despite an ongoing debate about the origin of cancer stem cells (CSC), accumulating evidence supports their role in tumor initiation and metastasis. Stem cells have unique properties to self-renew and give rise to multiple cell lineages through various differentiation programs. Numerous reports have identified such properties in subsets of cancer cells, therefore termed cancer stem cells.

The existence of stem-like tumorigenic cells has been demonstrated in the 1960's by Kleinsmith and Pierce who performed single cell grafts of embryonal carcinoma cells and obtained 43 teratocarcinomas, each containing at least 14 different somatic tissues (Kleinsmith and Pierce, 1964). However, the first report characterizing molecular markers of a specific subset of tumor cells presenting stem-like capacities dates back to 1997 and identified acute myeloid leukemia-initiating cells as those presenting with a CD34+ and CD38- marker signature (Bonnet and Dick, 1997). Since then, researchers have identified specific molecular signatures of CSC in breast (Al-Hajj *et al.*, 2003), brain (Singh *et al.*, 2004), prostate (Collins *et al.*, 2005), colon (O'Brien *et al.*, 2007), pancreatic (Li *et al.*, 2007), gastric (Takaishi *et al.*, 2009), ovarian (Curley *et al.*, 2009), liver (Terris *et al.*, 2010), skin (Boiko, 2013) and lung cancer (Zhang *et al.*, 2012). In the study by Al-Hajj *et al.*, a rare subset of breast cancer cells exhibiting a CD44+ and CD24low phenotype could initiate the growth of heterogeneous tumors from as few as 100 cells transplanted into mice, whereas transplanting tens of thousands of breast cancer cells with alternate phenotypes failed to form tumors (Al-Hajj *et al.*, 2003). It is worth noting that most of the current CSC surface markers are also present on normal embryonic or adult stem cells, which led researchers to think that CSC may predominantly originate from normal stem cells through accumulation of a series of epigenetic and genetic alterations. For example, CD133 is a glycosylated transmembrane protein that has been used as a CSC marker in brain, lung, pancreas and prostate cancer (Islam *et al.*, 2015). Although its precise function remains unknown, CD133 may regulate cell membrane topology and is also typically found on human embryonic and adult stem cells (Grosse-Gehling *et al.*, 2013). However, CD133 is also present on the surface of differentiated epithelial cells in a variety of tissues where it assumes different tertiary conformations that impact its ligand domain (Kim and Ryu, 2017), suggesting that alternative splicing variants can either maintain or restrict the stem-like phenotype. Indeed, CD133's transcription is controlled by five alternative promoters generating 16 distinct splicing variants in a tissue-specific manner (Grosse-Gehling *et al.*, 2013). Transcriptional and post-transcriptional modifications greatly impact the structure and function of CSC surface markers and CD44 is another

great example. The CD44 gene contains 20 exons of which 10 are alternatively spliced to form variant isoforms of the CD44 transmembrane glycoprotein (CD44v1-10). All isoforms of the CD44 marker, including the standard form containing only the 10 conserved exons (CD44s), possess a ligand-binding site which recognizes hyaluronan, a component of the ECM mediating cell-matrix adhesion and inducing migration of a variety of cancer cells (Thapa and Wilson, 2016). Multivalent interactions of CD44 isoforms can activate or regulate several oncogenic pathways through indirect interaction with Src kinases, small GTPases and growth factor receptors such as EGFR, HER2 and TGFβR1. Interestingly, CD44 isoforms are expressed on the surface of both normal and cancer cells at varying levels and while some isoforms have an antitumor effect, others clearly mediate pro-tumorigenic signals. For example, expression or overexpression of CD44v6 correlates with poor prognosis of pancreatic adenocarcinoma, acute myeloid leukemia, non-Hodgkin's lymphoma, urothelial carcinoma and non-small-cell lung cancer (Thapa and Wilson, 2016).

The discovery and further characterization of CSC phenotypes has led to a hierarchical model of cancer development driven by highly tumorigenic and self-renewing CSC. Examples of phenotypic plasticity such as the trans-differentiation of tumor cells into endothelial cells during vasculogenic mimicry (Ricci-Vitiani *et al.*, 2010) further support the pluripotent properties of some cancer cells. However, considering that several properties of stem-like cells in cancer have been shown to arise from alternative splicing of mRNA precursors which is regulated by epigenetic mechanisms, the cellular origin of CSC remains controversial. Suva and colleagues have shown that the induced expression of a combination of four specific transcription factors (POU3F2, Sox2, SALL2 and OLIG2) is necessary and sufficient to reprogram non-tumorigenic glioblastoma cells into tumor-propagating glioblastoma cells that recapitulate the epigenetic and phenotypic landscape of native glioblastoma CSC (Suvà *et al.*, 2014). This suggests a more complex hierarchy where dedifferentiation of cancer cells is also possible. Indeed, dedifferentiation through the induction of combinations of transcription factors has been widely used to convert specific cells to different lineages and to yield induced pluripotent stem cells (iPS). For example, Takahashi and Yamanaka reported that introduction of

four specific transcription factors (Oct3/4, Sox2, c-Myc and Klf4) was necessary and sufficient to reprogram normal fibroblasts into iPS (Takahashi and Yamanaka, 2006). Interestingly, Oct3/4 and c-Myc are both encoded by hypoxia-responsive genes that have been shown to activate following deregulation of the hypoxia-response pathway in renal cancer cells, leading to cellular dedifferentiation (Patel and Simon, 2008). Furthermore, the rare but documented occurrence of tumor cell fusion with bone marrow-derived cells (BMDC) including macrophages and erythrocytes was suggested as a biological mechanism generating CSC *in vivo* (Pawelek and Chakraborty, 2008). Indeed, Jacobsen et al. described spontaneous fusions of human tumor cells with mouse fibroblasts after injection of malignant mammary human cells in mice with 30% of cells derived from the tumor presenting hybrid hyperploid nuclei containing both human and mouse chromosomes and 8% carrying mouse/human translocations (Jacobsen *et al.*, 2006). Horizontal transfer of DNA including oncogenes through release and uptake of apoptotic bodies has also been reported (Holmgren *et al.*, 1999). For example, the deletion or silencing of p53 (an apoptosis inducer) in normal murine cells was reported to enable phagocytosis of apoptotic bodies from oncogene transformed rat fibroblasts and subsequent mouse/rat chromosomal rearrangements resulting in aneuploidy and transfer of the activated HRAS and c-Myc oncogenes to the murine host cells (Bergsmedh *et al.*, 2001).

Regardless of their cellular origin, CSC often share abnormal activation of specific signaling pathways such as Wnt/β-catenin, Hedgehog and Notch signaling which are developmental pathways. Abnormal activation of Notch signaling has been evidenced in CSC from breast and pancreatic cancer while Wnt signaling deregulation is involved in colorectal, breast, skin and lung cancer (Koury *et al.*, 2017). Those pathways are crucially mediating CSC self-renewal by regulating the expression of oncogenes such as c-Myc and SOX2. Notably, activating those pathways can be achieved through several strategies, including genetic mutations activating oncogenic signaling (PI3K, KRAS) and/or inactivating tumor suppressor genes (PTEN, TP53), transcriptional regulation mediated by epigenetic factors and extracellular activation of transmembrane receptor signaling induced by binding of specific ligands present in the microenvironment such as hypoxia-inducible factors and stromal cell

secretions (Peitzsch *et al.*, 2017). While genetic mutations can insure a relatively stable activation of signaling pathways (until conflicting genetic alterations occur or strong epigenetic factors override specific transcriptional instructions), external activation through receptor signaling depends on the maintenance of extrinsic factors in the microenvironment. This probably explains why CSC localize in specific types of microenvironments such as hypoxic regions, invasive fronts and perivascular niches and why they actively recruit stromal cells, immune cells and mesenchymal stem cells to insure remodeling or maintenance of environmental cues. A brief overview of stem cell niches is presented in **Figure 4**.

Besides self-renewal and differentiation into various lineages, CSC also exhibit resistance to conventional anticancer therapies which has led scientists to believe that this specific subset of cancer cells is responsible for tumor recurrence.

Figure 4: *Cancer stem cell niches in human solid tumors*

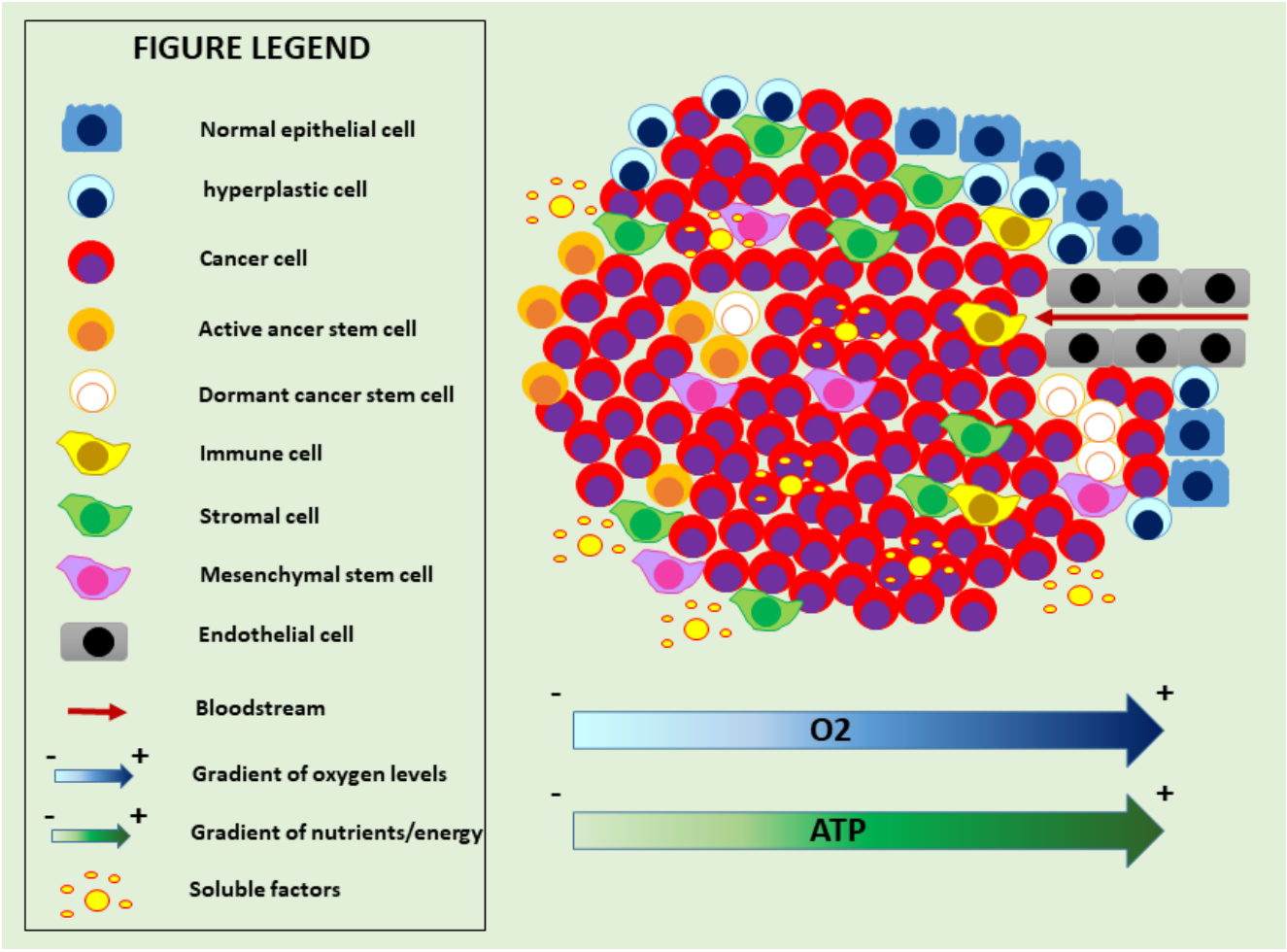

1.6. Tumor cell dissemination and dormancy

Tumor relapse poses significant clinical issues because residual disease is often undetectable by standard clinical tools and patients can remain asymptomatic for years following primary neoplasm excision (Karrison *et al.*, 1999). A growing body of evidence points to the establishment of dormant phenotypes within disseminated tumor cells (DTC) after extravasation into specific types of environments, called dormant niches.

Importantly, cancer dormancy refers to a state in which the detectable tumor burden stagnates without visible progression of the disease and has been divided into the three following categories (Aguirre-Ghiso, 2007). Cellular dormancy refers to single or small groups of DTC entering cellular quiescence due to intrinsic and/or extrinsic molecular mechanisms. Angiogenic dormancy characterizes constancy of tumor masses which is believed to be governed by a balance between proliferating tumor cells and cells that die due to extreme hypoxic conditions inferred by poor vascularization. And immune-mediated dormancy characterizes proliferating tumor masses which are kept constant by persistent cytotoxic activity of the immune system. The latter two categories recapitulate tumor population-based dormancy which may be more accurately referred to as homeostatic mechanisms than dormancy mechanisms (Klein, 2011) since they imply an active regulation of variables that seemingly results in the constancy of parameters.

Tumor dormancy was first described in 1934 by Willis and further defined by Hadfield in 1954 (Hadfield, 1954) as a temporary mitotic arrest. Dormancy was thought to arise from lack of mitogenic signaling. However, it now appears that cellular dormancy of DTC involves a differential regulation of genes which resembles that of quiescent normal stem cells (Adam *et al.*, 2009; Cheung and Rando, 2013). This implies that signals regulating dormancy also function by repressing oncogene signaling in order to induce quiescence of DTC. Although much is still to be learned regarding the molecular components of dormancy regulation, evidences point to a strong impact of the microenvironment. For example, in gastric cancer, DTC are often found in the bone marrow of patients in a non-proliferative state while bone metastasis is much rarer for gastric cancer patients

(Sosa *et al.*, 2014). Similarly, breast cancer DTC are often found in the bone marrow of patients without clinical evidence of bone metastasis (Braun *et al.*, 2005).

Indeed, as a hematopoietic stem cell niche, the bone marrow functions as a dormancy-permissive microenvironment where bone stromal cells secrete effectors such as growth arrest-specific protein 6 (GAS6) involved in leukemia and prostate cancer DTC dormancy *in vitro*, bone morphogenetic proteins 4 and 7 (BMP4 contributing to DTC dormancy of mouse breast cancer cells in the lungs and BMP7 inducing dormancy of DTC from prostate cancer cell lines injected into the bone) and transforming growth factor-β2 (TGFβ2) which infers activation of p38 and p27 proteins resulting in quiescence of bone marrow DTC from head and neck squamous cell carcinoma (HNSCC) (Sosa *et al.*, 2014).

Furthermore, the frequent development of delayed bone metastasis in human cancers such as breast (Pierga *et al.*, 2003), prostate (Manca *et al.*, 2017) and lung (Liu *et al.*, 2017) points to a reversible quiescence of dormant DTC. Indeed, recent experimental evidences support the theory of a so called switch that regulates escape from dormancy. For example, in the bone environment, recruitment of osteoclasts progenitors by VCAM1 expressing breast cancer DTC which bind the β1 integrins expressed by osteoclasts was shown to mediate escape from dormancy and induce osteolytic bone metastasis formation (Lu *et al.*, 2010). In triple negative breast cancer, overexpression of CXCL12 and IGF1 by CAF/TAF in the primary tumor selects tumor clones towards expression of CXCR4, the receptor for the CXCL12 ligand which is abundantly produced by bone stromal cells, and has been shown to predict bone metastasis (Zhang *et al.*, 2013b).

Although the underlying mechanisms of dormancy escape are still poorly understood, studies have reported that microenvironmental changes may participate in DTC escape from dormancy in a cell type-specific and organ-specific manner (Cheng *et al.*, 2009a). For example, dormant breast DTC in the lung were reported to exit dormancy by secreting the BMP4 inhibitor protein CoCo, which specifically accumulates in the pericellular matrix to neutralize BMP4 secreted by the stroma, thereby illustrating a process that is specific to BMP-rich target organs (Gao *et al.*, 2012). Other examples of

this include modulation of dormancy by changes in extracellular matrix stiffness related to increased TGFβ1 signaling which was reported for hepatocellular carcinoma cells *in vitro* (Schrader *et al.*, 2011) and disseminated breast cancer cells in fibrotic lungs characterized by a dense type I collagen ECM (Barkan *et al.*, 2010).

Like in the bone marrow (Lawson *et al.*, 2015), evidences of simultaneous presence of both dormant and proliferative DTC in the lungs (Ghajar *et al.*, 2013) and brain (Kienast *et al.*, 2010) suggest an intra-organ diversity of microenvironmental signals. The observations of Ghajar et al. who recreated a stable microvascular endothelium with human cells *in vitro* point to the perivascular niche as a specific intra-organ localization of dormant DTC where quiescence is induced by endothelial-derived thrombospondin-1 (TSP-1) associated to the basement membrane of mature microvasculature (Ghajar *et al.*, 2013). In contrast, these same authors reported that DTC in contact with neovascular endothelial tip cells secreting TGFβ1 and periostin (POSTN) exhibited enhanced proliferation. Since the dissemination of tumor cells invariably leads them to the perivascular niche, these findings raise the question of whether only DTC extravasating in activated endothelial tips of the neovasculature, or in partially degraded "leaky" vasculature, may immediately start to proliferate (Linde *et al.*, 2016). Additionally, evidences of thrombospondin (TSP) upregulation in dormant tumor masses with poor angiogenic features further suggest that intrinsic regulators of the vascular switch induced by poor oxygenation may also regulate DTC dormancy in liposarcoma (Almog *et al.*, 2006), glioblastoma and osteosarcoma (Almog *et al.*, 2009) models *in vivo*. In line with the observations of Ghajar *et al.*, real-time in situ imaging of breast cancer and melanoma DTC in the mouse brain confirmed their strict perivascular localization and direct contact with endothelial cells (Kienast *et al.*, 2010). Together, these observations suggest that endothelial cells might mediate cellular dormancy before the occurrence of angiogenic population-based dormancy (or homeostasis).

Conversely, to this day there is no definitive proof that immune-mediated dormancy operates strictly either at population level or at cellular level by induction of quiescence. There is however substantial evidence that the immune system can keep proliferative malignancies in check. This is well

exemplified by the fact that seemingly cancer-free organs, once transplanted into artificially immunosuppressed recipients, can elicit rapid tumor growth (Chapman *et al.*, 2013). However, observations linking chronic inflammation to cancer and studies depicting crosstalk between cancer cells and immune cells in the microenvironment clearly indicate that tumor cells develop mechanisms to evade immune cytotoxicity and further reprogram immune cells to participate to the formation of pre-metastatic niches in distant organs (Mantovani *et al.*, 2008).

1.7. The pre-metastatic niche

Invasive tumor cells that disseminate into suitable microenvironments, termed pre-metastatic niches, may subsequently initiate metastatic spread in distant organs. Studies have shown that the induction of pre-metastatic niches can be an early event in cancer progression, meaning that signals from the primary tumor can prepare specific organs for the arrival of DTC even before they acquire invasive behavior and leave the primary tumor. For example, animal models of breast cancer have indicated that the recruitment of specific types of myeloid derived suppressor cells (MDSC) to the lungs, eliciting transformation of the lung microenvironment into a pre-metastatic niche, predates both the arrival of DTC in the lungs and the presence of CTC in the peripheral blood (Hiratsuka *et al.*, 2006; Yan *et al.*, 2010). More precisely, Yan and colleagues reported that myeloid cells expressing the granulocyte marker Gr-1 infiltrate the lung of breast cancer-bearing mice before the dissemination of breast tumor cells and arrange in clusters that delineate pre-metastatic lesions (Yan *et al.*, 2010). Gr-1+ MDSC subsequently inhibit interferon gamma (IFN-ɣ) production in resident macrophages and up-regulate the secretion of interleukins (IL-4, IL-5, IL-9 and IL-10), thereby conferring immune-suppressive effects to the microenvironment. Gr-1+ MDSC clustering in pre-metastatic lungs also resulted in elevated levels of basic fibroblast growth factor (FGF2) and insulin-like growth factor 1 (IGF1) which are characteristic of a proliferative microenvironment. Additionally, the presence of Gr-1+ MDSC clusters strongly correlated with elevated levels of pro-inflammatory cytokines (IL-1β, SDF-1), matrix-remodeling enzymes (MMP9, MMP2) and vascular endothelial

growth factor receptor 1 (VEGFR1) leading to the disorganization and leakage of the lung vasculature, thereby facilitating the dissemination of breast tumor cells (Yan *et al.*, 2010). Another study employing the same animal model further established the role of tumor-secreted TGFβ in recruiting myeloid cells to the lungs to produce a pre-metastatic environment (Ye *et al.*, 2015). Like breast cancers, renal cancers also frequently metastasize to the lungs and the formation of the pre-metastatic niche, through upregulation of VEGFR1, MMP2 and MMP9, was reported to be specifically induced by renal CSC-derived microvesicles (Grange *et al.*, 2011). Indeed, extracellular vesicles of all sizes (including apoptotic bodies, microvesicles and exosomes) contain functional proteins, DNA fragments and epigenetic regulators such as microRNA (miR) and long non-coding RNA (lncRNA) which participate to the intercellular communication at both short and long ranges throughout the body. A recent study on oral squamous cell carcinoma (OSCC) identified miR-21-enriched exosomes that derived from hypoxic OSCC cells as inducers of a prometastatic phenotype in normoxic OSCC cells (Li *et al.*, 2016). Another study on breast cancer reported that tumor-derived extracellular vesicles containing miR-122 and delivered to the lungs and brain through the circulation induced metabolic changes in stromal cells of the pre-metastatic niches towards lower glucose uptake, thereby reducing the competition for nutrients with highly glucose-dependent breast tumor cells before they effectively disseminate to those target organs (Fong *et al.*, 2015).

It is important to note that the molecular mechanisms governing the onset of a pre-metastatic niche depend on functional features of both the primary tumor preparing for dissemination and distant organ sites being prepared for colonization. However, once the soil has been effectively fertilized, any viable tumor seed may take the advantage to grow. This was suggested by Kaplan et al. who studied the recruitment of VEGFR1 expressing bone marrow-derived cells to specific organ sites upon stimulation with tumor-conditioned media from distinct tumor cell types (Kaplan *et al.*, 2005). More precisely, using conditioned media from a melanoma cell line to treat wild type nude mice, they observed an increase in fibronectin expression followed by the recruitment of VEGFR1+ hematopoietic progenitors to the specific organ sites that typically host melanoma metastasis,

including lung, liver, spleen, testis and kidney. In contrast, treatment of wild type nude mice with conditioned media from Lewis lung carcinoma cells resulted in fibronectin accumulation and recruitment of VEGFR1+ cells restricted to the lung and liver, consistent with the usual metastatic pattern of this type of cancer. Interestingly though, injection of Lewis lung carcinoma cells into wild type nude mice previously treated with conditioned media from melanoma cells redirected lung cancer metastasis to the organ sites frequently colonized by melanoma including kidney, spleen and oviducts. The authors further noted that tumor-conditioned media from melanoma cells contained significantly higher levels of placental growth factor (PlGF) which signals specifically through VEGFR1 (Kaplan *et al.*, 2005). Despite the absence of microRNA analysis, this study highlights the importance of tumor-derived factors in directing and preparing organ-specific metastasis. Subsequent evidence demonstrated that melanoma-derived exosomes containing high levels of the MYC oncoprotein receptor are responsible for the reprogramming of bone marrow progenitors towards modeling of the pre-metastatic niche (Peinado *et al.*, 2012). Further research elucidated the role of exosomes in organ-specific tropism of metastasis by demonstrating that specific integrins present at the surface of tumor-derived exosomes direct them towards specific organs. For instance, exosomes presenting integrins α6β4 and α6β1 were associated with lung metastasis whereas integrin αvβ5 directed exosomes toward formation of a pre-metastatic niche in the liver (Hoshino *et al.*, 2015).

Indeed the lungs, liver and bone marrow contain a more fenestrated vasculature which suggests that metastasis formation in those organs may predominantly result from the active remodeling of the microenvironment towards metastasis-permissive conditions rather than from an adaptation of tumor cells seeded in those organs. However, metastasis formation ultimately depends on the arrival of circulating tumor cells at distant organ sites.

2. Circulating tumor cells (CTC)

2.1. Defining circulating tumor cells (CTC)

Circulating tumor cells (CTC) are cells that have detached from a given tumor mass, migrated

through interstitial tissues and intravasated into the blood or lymphatic circulation. In the blood those cells are very rare compared to the abundant haematogeneous population; 1 or few tumor cells can be found among 10 million leukocytes and 5 billion erythrocytes in each milliliter of blood (Paterlini-Bréchot, 2014). CTC are a very heterogeneous population of cells, recapitulating the whole array of distinct tumor clones and phenotypes that enabled passive or active intravasation at any given location harboring malignant neoplastic colonization, including cancer cells shed from the primary tumor and from the single or multiple coexisting metastatic site(s), viable and apoptotic cancer cells, epithelial, mesenchymal, hybrid and cancer stem cells. Despite their extensive heterogeneity in tumorigenic potential, cellular deformability and cell size, CTC are generally larger than most circulating normal blood cells, ranging from 10 µm in small cell lung cancer up to 70 µm in breast, pancreatic and non-small-cell lung cancer and might occasionally reach 100 µm in prostate cancer while lymphocytes and monocytes comprise cells of 6 to 20 µm in size (Thiele *et al.*, 2017). With increased tumorigenic potential, CTC also exhibit increased cytoskeletal deformability, as evidenced by comparing normal epithelial mammary cells (MCF-10A), malignant but poorly metastatic breast cancer cells (MCF-7) and highly invasive and metastatic breast cancer cells (MDA-MB-231) (Guck *et al.*, 2005), which may reflect their increased capacity to squeeze between endothelial cells during intravasation. And with increased cytoskeletal deformability come greater variations in measurable cell size (Park *et al.*, 2014), which are also influenced by CTC isolation techniques.

Following their discovery by Ashworth in 1869 (Ashworth, 1869), CTC were correlated to shorter survival times more than a century later (Salsbury, 1975) and have been ferociously investigated by researchers for several decades now. However, the significant technical challenge that CTC isolation and analysis represent, due to their extensive heterogeneity and relative rarity in blood samples, has hampered the transfer of CTC analyses from research labs to routine clinical tests. Indeed, the CellSearch® platform (Veridex, USA) is the first and only FDA-approved prognostic test based on CTC isolation for metastatic breast (Cristofanilli *et al.*, 2004), colorectal (Cohen *et al.*, 2008) and

prostate cancers (Danila *et al.*, 2007) and has greatly contributed to the study of CTC. Yet the CellSearch® approach, as well as other techniques based on the use of epithelial markers such as EpCAM and cytokeratins for CTC selection and/or identification, are truly lacking in specificity since a significant portion of CTC do not retain expression of all the common epithelial markers and especially considering that non-malignant epithelial cells can also circulate in the bloodstream in response to chronic inflammation (Pantel *et al.*, 2012).

Moreover, specific parameters such as the relevant cutoff in CTC numbers enabling the statistical deduction of clinical outcomes are closely linked to the specific technical approach used for CTC detection/analysis and cannot be universally transferred to studies employing distinct methodologies. This implies that correlating CTC with clinicopathological features requires extensive and separate validation for each CTC detection/analysis method, which probably contributes to the extremely high ratio of research publications on CTC, more than 10 000, versus clinically validated applications of CTC analysis, especially considering that more than 40 distinct techniques have been developed for CTC detection (Joosse *et al.*, 2015). Those will be further discussed hereafter and include methods based on the selection of specific cell surface antigens, size-based enrichment and other techniques using biomechanical and biophysical cellular properties to isolate CTC from the background of normal blood cells. Notably, size-based enrichment of CTC has already been proven useful for the early diagnosis (Ilie *et al.*, 2014), prognosis (Hofman *et al.*, 2011), treatment decision (Faugeroux *et al.*, 2014), follow-up and monitoring of recurrence (Abdallah *et al.*, 2016; Poruk *et al.*, 2016) of cancer.

Given the life-threatening impact of metastasis development on cancer patients, CTC represent an easily accessible source of cancer material that is still strikingly underrepresented in current clinical practices and deserves further consideration. The following chapters will provide essential details regarding the biology, analytical strategies and clinical utility/validity of CTC.

2.2. Phenotypic plasticity

Phenotypic plasticity is now considered to be a hallmark of cancer cell invasion and metastasis. At the invasive front of the tumor, interactions between cancer cells and the tumor stroma induce a partial or complete switch of epithelial cells towards a mesenchymal phenotype which allows them to acquire invasive and migratory capacities. The process of EMT can be defined by the loss of epithelial markers such as keratins, E-cadherin, claudin and occludin accompanied by an increased expression of mesenchymal markers such as vimentin, N-cadherin, fibronectin and matrix-remodeling enzymes. Since downregulation of E-cadherin expression is tightly linked to EMT programs, much effort has been deployed to characterize transcription repressors of E-cadherin. Transcription factors such as Snail, Zeb, Zeppo1, E47 and KLF8 directly bind the CDH1 gene promoter to suppress E-cadherin transcription whereas Twist, FoxC2, E2.2 and Goosecoid transcription factors act indirectly upstream of E-cadherin transcription, often by interacting with direct E-cadherin transcription repressors (Nieto, 2011). EMT inducers also cross-react with important signaling pathways regulating stem cell pluripotency and cell fate. For example TGF-β, which is a potent EMT inducer as previously mentioned, also induces alpha catenin phosphorylation and the subsequent β-catenin nuclear translocation that activates the Wnt/β-catenin pathway, thereby providing self-renewal capacities to CSC from pancreatic carcinoma (Principe *et al.*, 2014). An underlying layer of epigenetic regulation further modulates the complex intertwining of signaling pathways that regulate phenotypic plasticity and non-coding RNA species such as long non-coding RNA (lncRNA) and microRNA (miRNA) have emerged as potent regulators of cell state and phenotype. As an example of regulation of cellular differentiation states by non-coding RNA species, Kim *et al.* reported that the loss of p53 function induced by non-sense mutations of the tumor suppressor gene TP53 in colorectal cancer can constitutively activate the Wnt/β-catenin pathway through loss of miR-34 expression (Kim *et al.*, 2011). Notably, while protein-coding transcripts (mRNA) represent approximately 2% of the total cellular content of RNA species, non-coding RNA constitute the remaining 98% of the total cellular production of RNA species (Zhang *et al.*, 2017b).

It is also important to note that regulation of cell signaling by non-coding RNA species now appears to be more complex than classical signaling pathways defined by protein interactions. This is a potent statement considering the plethora of cross-reactivity, feedback and feedforward loops of signaling as well as post-transcriptional and post-translational modifications that regulate protein interactions. However, non-coding RNA species act upstream of protein signaling pathways by simultaneously regulating multiple mRNA targets and are therefore involved in shaping and reshaping cellular behaviors by controlling the vast landscape of protein expression.

MiRNA are small single-stranded RNA molecules containing approximately 18-24 nucleotides which mature from hairpin structured precursors (pre-miRNA) via cleavage operated by the Dicer family of enzymes (Zhao *et al.*, 2017b).

Unlike messenger RNA (mRNA), microRNA do not require further translation into proteins to fulfill their biological functions since binding their target mRNA is sufficient to block the translation of proteins encoded by those targets. Additionally, miRNA can also actively regulate each other. In breast cancer for example, miR-103 and miR-107 induce EMT by targeting Dicer1 and downregulating the expression of members of the miR-200 family (miR-200a, miR-200b, miR-200c, miR-141 and miR-429) which are crucially involved in silencing Zeb1 and Zeb2 transcription factors by binding their mRNA precursors to ensure the maintenance of an epithelial phenotype (Martello *et al.*, 2010). Notably, members of the miR-200 family are also involved in promoting a differentiated state by negatively regulating the translation of stem cell factors and other inducers of stemness such as BMI1 (Shimono *et al.*, 2009). Feedback loops are also at play in epigenetic mechanisms regulating phenotypic plasticity since Zeb transcription factors also inhibit the transcription of miR-200 family members (Burk *et al.*, 2008). Likewise, miR-34 family members (miR-34a, miR-34b and miR-34c) block the translation of Snail1 while Snail1 itself inhibits the transcription of miR-34 family members (Brabletz, 2012). Examples of EMT regulation by miRNA species are depicted in **Figure 5**.

Figure 5: *Regulation of phenotypic plasticity by microRNA species*

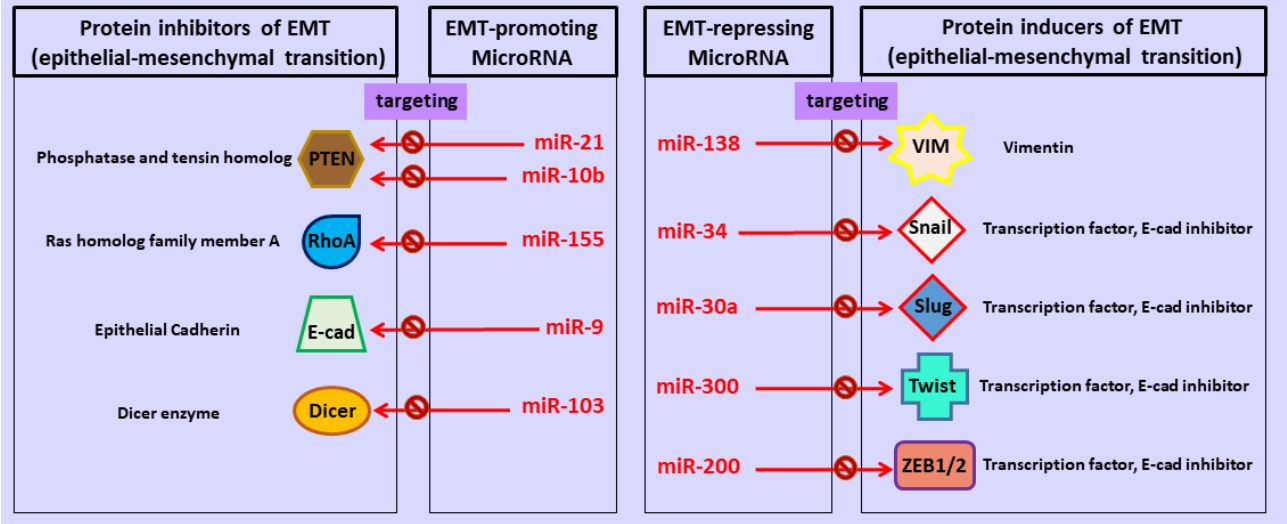

In contrast, long non-coding RNA (lncRNA) are functional RNA molecules defined by a length greater than 200 nucleotides and those are also actively involved in regulating the transcription of specific genes, either by directly binding a target DNA sequence and recruiting protein effectors such as transcription factors, or by directly targeting diverse functional proteins, including histones which can modulate chromatin conformation and accessibility (Ponting *et al.*, 2009). As such, lncRNA are expressed in a highly tissue-specific manner and are even largely heterogeneous from one cell to the next within a given tissue, as shown by Hu and colleagues who used single-cell analysis of lncRNA in glioblastoma to reveal a further extent of intra-tumor heterogeneity (Hu *et al.*, 2015). As potent regulators of cellular differentiation states, lncRNA are also actively implicated in regulating phenotypic plasticity through epigenetic modulation of transcription, including by targeting multiple miRNA molecules as competing endogenous RNA. In colorectal cancer for instance, the specific lncRNA H19 was reported to promote EMT by sequestering both miR-138 and miR-200a which are crucial repressors of Zeb2 and vimentin expression (Liang *et al.*, 2015). Multiple distinct lncRNA are involved in regulating phenotypic plasticity including, though not limited to, HOTAIR, BANCR, TUG1, GHET1 and lncRNA-ATB which can all participate in activating EMT signaling pathways and thus result in enhanced cell-survival, migratory capacities and tumorigenic potential of cancer cells (Li *et al.*, 2017a).

Importantly, EMT is a reversible process on which differentiated epithelial cells may depend to acquire the migratory and stem-like phenotype that enables invasion. And the counterpart MET is an equally relevant process whereby quiescent tumor cells differentiate to recover their proliferative capacities which are necessary for metastatic growth. Thus a pattern of phenotypic plasticity emerges where transient phenotypes are mainly acquired in response to changes in the microenvironment. A potent example of this type of plasticity lies in the behavior of epithelial cells during wound healing which is triggered by inflammatory signals in the vicinity of the wound and involves the acquisition of temporary mesenchymal traits that stably coexist with the initial epithelial markers (Nieto, 2011). Similarly, CTC frequently present with various types of intermediate (or hybrid) phenotypes comprising both epithelial and mesenchymal traits and this also makes their reliable identification more difficult. However, when it comes to tumor cells, the hybrid phenotype is not necessarily transient since collective migration, which requires the coexistence of both epithelial and mesenchymal traits, can be maintained all the way during the journey from primary tumors to metastases. Indeed, the presence of clusters of tumor cells, called circulating tumor microemboli (CTM), in the blood of metastatic breast cancer patients has been reported to result from collective migration of oligoclonal cancer cells that detached from the primary tumor as a group (Aceto *et al.*, 2014). Furthermore, a recent study by Jolly and colleagues shed some light on the molecular mechanisms involved in the stabilization of the hybrid phenotype (Jolly *et al.*, 2016). More precisely, the authors identified phenotypic stability factors (PSF) such as OVOL which inhibits both Zeb and miR-200 family members and GRHL2 which is involved in its own negative regulatory feedback loop with Zeb. Interestingly, this study showed that knockdown of OVOL and GRHL2 in hybrid lung cancer cells migrating collectively results in the completion of the transition towards the mesenchymal phenotype and a switch from collective to single-cell migration (Jolly *et al.*, 2016).

Conversely, collective migration can also be induced intrinsically without any gain of mesenchymal features and independently of any growth factor or cytokine signaling, as shown by Godinho et al. who correlated increased invasiveness of breast cancer cells with centrosome amplification (Godinho

et al., 2014). More precisely, this study reported that the amplification of microtubule-tethering centrosomes, which has been correlated with tumor aggressiveness in breast cancer, activates Rac1 through unknown mechanisms and promotes the formation of actin- and microtubule-rich membrane protrusions by subsequent activation of the Arp2/3 complex downstream of Rac1. This newly discovered and still modestly understood mechanism, although not exactly qualifying as phenotypic plasticity, illustrates how intrinsic defects such as genetic or epigenetic aberrations can provide advantageous conditions for a cancer cell to override its initial biology.

Despite our growing understanding of the cellular and molecular mechanisms involved in cancer invasion/metastasis, many questions currently remain unanswered. For example, while single-cell intravasation of nascent CTC has been described and crucially involves single-cell transendothelial migration, the mechanism by which collectively migrating cancer cells intravasate into blood vessels remains largely elusive.

2.3. Endothelial tropism and tumor cell intravasation

Spontaneous tumor cell intravasation within vessels of the primary tumor is difficult to study in humans *in vivo* because it would require sophisticated live intravital imaging of the primary tumor at early stages of tumor development. Therefore, studies describing molecular and cellular components of tumor cell intravasation have so far only been conducted in animal models and *in vitro* models using co-cultures of human cancer cells with endothelial and/or stromal cells. However, most of those studies were based on clinical evidences of human cancer biology, thanks to reports characterizing the intra-tumor and peripheral stromal organization of cells along with the various molecular components of the ECM in resected human primary tumors from metastatic patients.

One interesting observation regarding human breast cancer biopsies is that the specific alignment of collagen fibers can serve as a prognostic and predictive marker for breast cancer patients (Bredfeldt *et al.*, 2014). Indeed, tumor-associated collagen signatures comprise well aligned collagen fibers oriented perpendicularly to the tumor border and this pattern has been described in human

resected tumors as well as in organoid models *in vitro* and animal models *in vivo* (Provenzano *et al.*, 2006). Interestingly, a recent study described the behavior of tumor cells migrating along collagen fibers into the surrounding stroma and determined that collagen fibers aligned perpendicularly to the invasive front of the tumor provide advantageous guidance for migrating cancer cells (Han *et al.*, 2016). This study and many others illustrate the crucial part that active remodeling of the tumor microenvironment plays at the earliest steps of invasion, similar to the role that the induction of pre-metastatic niches plays in metastasis development.

Induction of angiogenesis is another important step towards cancer invasion in primary tumor development and the so called angiogenic switch is considered to be a major stepping stone in the transition from primary non-invasive neoplasms to invasive carcinomas. Hypoxia signaling within the tumor triggers VEGF secretion by tumor cells and elevated levels of active VEGF induce disorganized vessel sprouting and reduced pericite coverage leading to a sustained immature vascular network (Greenberg *et al.*, 2008). However, the simple secretion of active VEGF molecules by cancer cells is not sufficient to induce angiogenesis since active VEGF molecules remain essentially bound to ECM fibers in the microenvironment. At the earliest stages, the bioavailability of tumor-secreted VEGF relies on the active recruitment of stromal cells and tumor-infiltrating leukocytes such as neutrophils and monocytic precursors of macrophages which produce matrix remodeling enzymes capable of releasing active VEGF through ECM fiber cleavage (Deryugina and Quigley, 2015). In turn, tumor-associated stromal cells and tumor-infiltrating leukocytes respond to tumor-secreted factors by sustaining angiogenic signaling, remodeling the ECM architecture and inducing EMT in cancer cells. In that sense, cancer invasion is truly a cooperative effort. Partial or complete EMT enables tumor cells to migrate collectively or as single cells depending on their specific cellular biology and adaptability to the molecular composition and 3D organization of ECM proteins. Indeed, phenotypic plasticity can give rise to various expression patterns depending on the cell type and the multiparametric signaling of the specific microenvironment which results in distinct cellular behaviors. For example, highly invasive fibrosarcoma and breast cancer cell lines express specific

types of membrane-bound matrix metalloproteinases (MT1-MMP, also called MMP14) that are required for invasion into highly crosslinked collagen fibers, as demonstrated by *in vitro* spheroid co-culture with reconstituted full length type I collagen matrices (Sabeh *et al.*, 2009). In contrast, the same tumor cells can invade much faster and independently of MT1-MMP activity in pepsin-extracted collagen matrices composed of weakly crosslinked fibers by switching from a mesenchymal-like to an amoeboid-like migration tactic (Sabeh *et al.*, 2009). However, in the absence of co-cultured fibroblasts, both *in vitro* models incorporating highly and weakly crosslinked collagen fibers do not account for the pre-existing tubular tracks left by migrating tumor-associated stromal cells within the ECM, which has been reported to be involved in collective migration of squamous cell carcinoma cells (Gaggioli *et al.*, 2007). Conversely, *in vivo* animal models cannot be fully representative of human cancer cell behavior since in the mammary gland, for example, human interstitial tissue is composed of denser collagen fibers than mouse ECM which is embedded in adipose tissue (Parmar and Cunha, 2004). Those simple observations call for scientific vigilance and rigor regarding specific experimental models used to describe cancer cell invasion.

The MMTV-PyMT murine model of breast cancer (expressing the polyomavirus middle T-antigen (PyMT) of the mouse mammary tumor virus (MMTV)) is one of the most extensively studied *in vivo* models of cancer invasion because the resulting spontaneous tumor histology resembles that of human primary breast cancers. In this model, a paracrine loop signaling between tumor associated macrophages (TAM) expressing EGF and breast cancer cells expressing the colony-stimulating factor 1 (CSF-1) is responsible for the induction of EMT and tumor cell migration through collagen (Goswami *et al.*, 2005). Meanwhile, TAM are organized as small clusters or single macrophages at the stromal periphery of blood vessels and produce a gradient of secreted EGF molecules that serves as the main directional guidance for migrating breast cancer cells. This was evidenced by Wyckoff et al. who used multiphoton intravital imaging to directly visualize macrophage-assisted tumor cell intravasation (Wyckoff *et al.*, 2007). In particular, this study determined that murine breast tumor cells migrate towards perivascular macrophages in streams of single cells where they form close

contacts with the vascular endothelium and intravasate specifically in direct proximity of the perivascular TAM. In this model, tumor cell intravasation was significantly associated with the density of perivascular macrophages irrespective of the blood vessel density. Later studies determined that a specific subpopulation of TAM expressing high levels of the Tie2 tyrosine kinase and VEGFA specifically migrate towards perivascular niches in MMTV-PyMT breast tumors and induce local and transient vascular permeability by releasing bursts of VEGF-A upon direct contact with migrating tumor cells (Harney *et al.*, 2015). Indeed, the binding of VEGF-A to VEGFR2 on blood-vascular endothelial cells induces ZO-1 and VE-cadherin endocytosis leading to endothelial junction disassembly and temporary vascular permeability (Nakayama and Berger, 2013).

Interestingly, the presence of perivascular macrophages has also been described in a mouse model of glioblastoma where the perivascular TAM population was reported to arise exclusively from the recruitment of bone marrow-derived cells at a very early stage of disease progression (Chen *et al.*, 2017). Indeed, different types of cancer cells may adopt converging strategies to reach and enter nearby blood vessels, such as EGFR overexpression which enables MMP-9 production and active VEGF release in glioblastoma as well as head and neck, lung and breast carcinoma cells *in vitro* (Deryugina and Quigley, 2015). Conversely, renal cell carcinoma (RCC) cells use the prostaglandin E2 receptor 4 (EP4) to enable CD24 expression which in turn mediates adhesion to P-selectin-presenting endothelial cells from blood vessels (Zhang *et al.*, 2017c). Additionally, the same cancer cells can use distinct mechanisms to invade either blood or lymphatic vessels.

Despite clinical evidence of collective cancer cell migration and the detection of CTM in the blood of metastatic cancer patients, to this day direct visualization of collective intravasation of tumor cells in blood vessels has not been reported *in vivo*. However, substantial *in vitro* evidence links collective cancer cell invasion to the lymphatic vasculature. For example, Giampieri et al. reported that blocking TGF-β signaling in rat mammary cancer cells *in vivo* prevents single cell migration but not collective migration and restricts intravasation to the lymphatic vessels, which suggests that clusters of cancer cells can only invade collectively through the lymphatic vasculature (Giampieri *et al.*, 2009).

Lymphatic endothelial cells (LEC) are arranged in a single layer deprived of both pericyte and smooth muscle cell coverages and do not form tight junctions with each other, allowing for both luminal and transmural lymph flows to occur (Alitalo *et al.*, 2005). Due to the absence of basement membrane coating around most lymphatic vessels, the transmural flow can carry a rich content of high molecular weight proteins which can diffuse further away from the vessels and into the surrounding tissue when lymph flow rates increase in response to local or systemic inflammation (Miteva *et al.*, 2010). Higher luminal and transmural flow rates also cause LEC to increase their production of cytokines and adhesion molecules such as E-selectin, ICAM-1, VCAM-1 and CCL21 which positively correlates with increased attachment and *in vitro* transmigration of highly invasive breast cancer cells (MDA-MB-231) expressing the CCR7 receptor that binds the CCL21 ligand (Pisano *et al.*, 2015). As shown by Pan and colleagues, CCR7 can be upregulated in breast cancer cells via EP2/EP4 signaling pathways (Pan *et al.*, 2009). Additionally, tumor cells and cancer-associated stromal cells can promote lymphangiogenesis by releasing VEGF-C and VEGF-D molecules, which have been significantly correlated to lymph node metastasis (Stacker *et al.*, 2002).

Furthermore, poorly invasive breast cancer cells (MCF-7) can also invade the lymphatic circulation as clusters. This was reported by Vonach and colleagues who used a 3D co-culture model of MCF-7 and LEC to evidence the induction by breast tumor cells of an endothelial to mesenchymal transition (EndMT) causing LEC to migrate individually along the vessel and away from the tumor cells, thereby providing a sufficiently large opening for MCF-7 clusters to collectively penetrate the lymphatic vessel (Vonach *et al.*, 2011). Interestingly, this study showed that the circular openings resulting from the EndMT of LEC caused by invading clusters of cancer cells do not retract after intravasation of the cluster but rather persist as permanent defects in the LEC monolayer, possibly causing lymphatic leakage and attracting even more cancer cells. Other experiments using similar co-culture models demonstrated that lymphatic intravasation crucially depends on the formation of heterocellular gap junctions between LEC and melanoma cells as well as breast and lung cancer cells *in vitro* (Karpinich and Caron, 2015), a process that is not required for tumor cells to invade blood vessels.

There is currently an ongoing debate regarding the ability of lymphatic CTC to colonize distant organs such as lungs, liver and bone marrow despite the presence of both blood and lymph vessels in those organs. On the other hand, the fact that collective cancer cell invasion has been reported to occur solely through the lymphatic vasculature is somewhat puzzling given that CTM have been observed clinically in the blood. One possible hypothesis on the subject, considering that CTM are predominantly found in the blood of metastatic cancer patients, is that although cancer cell clusters may be unable to penetrate intact blood vessels collectively, the disorganized and immature blood vasculature that develops in growing primary tumors along with the leaky blood vasculature promoted in the metastatic niche could potentially support collective cancer cell intravasation. Such a mechanism would better correspond to a passive rather than an active mode of intravasation. Moreover, the possible transmission of tumor cells from the lymph to the bloodstream at specific locations where both circulatory systems meet, such as the junction of the left subclavian and the internal jugular veins (Alitalo *et al.*, 2005), needs to be considered and investigated.

In addition, it is worth mentioning that intravasation is not a strict requirement for metastasis to occur. Notably, angiotropism refers to a mechanism by which cancer cells migrate along abluminal vascular surfaces, that is along the external border of the vasculature, and has been reported as an independent prognostic marker of metastasis in both cutaneous and uveal melanomas (Barnhill *et al.*, 2017). Nonetheless, the blood compartment is currently still considered as the main route for cancer cells towards metastasis at distant organ sites and represents the most easily accessible source of CTC. Interestingly, highly vascular tumors with sinusoidal vessels, such as renal cell carcinoma (RCC) and hepatocellular carcinoma (HCC) tumors tend to release whole tumor fragments organized as heterocellular clusters containing pericytes, endothelial, stromal and cancer cells in venous outflow, as evidenced by several groups (Sugino *et al.*, 2004; Küsters *et al.*, 2007; Kats-Ugurlu *et al.*, 2009), thus illustrating an EMT-independent mode of tumor invasion through hematogenous spread. Several distinct strategies of cancer cell migration/invasion are depicted in **Figure 6**.

Figure 6: *Differential strategies of cancer cell migration/invasion*

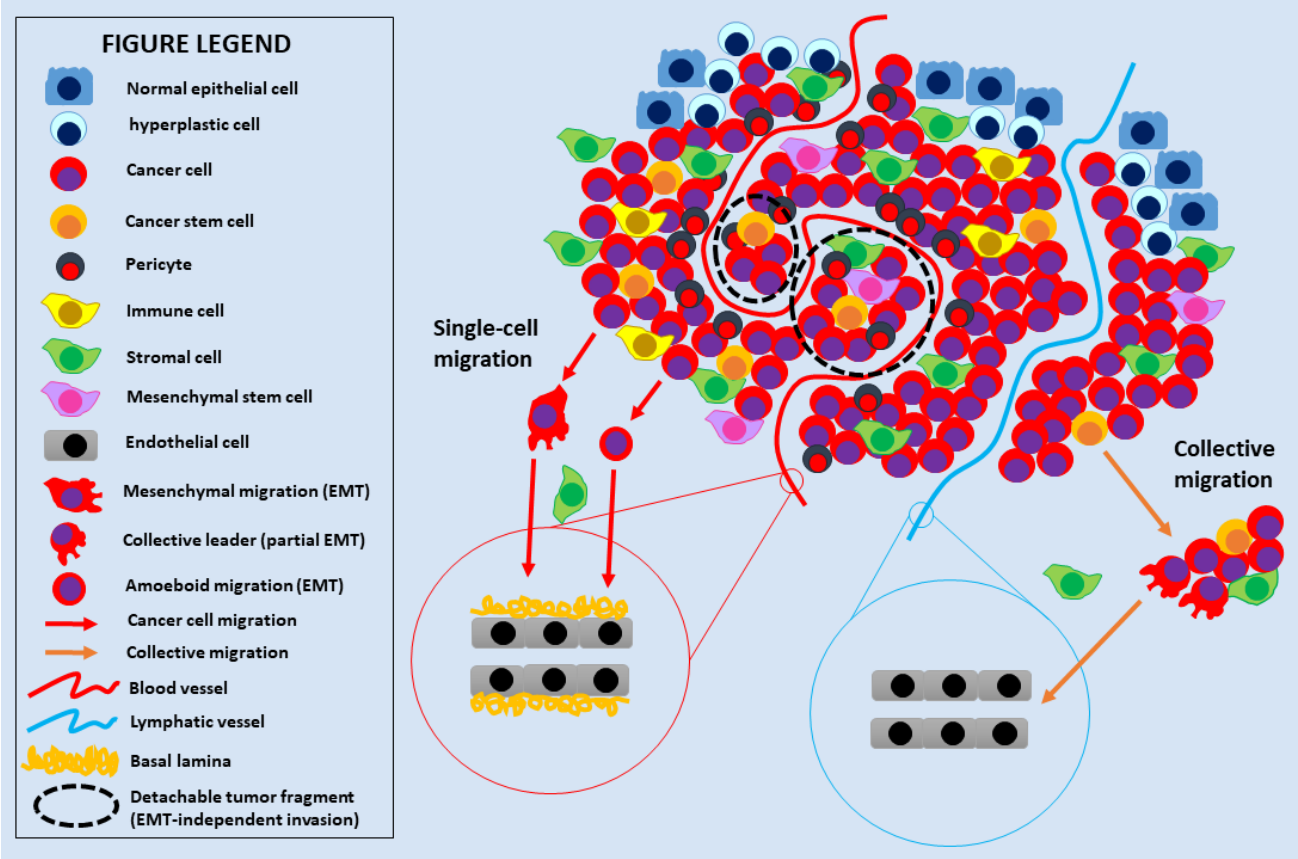

2.4. The blood compartment

Once intravasated into blood vessels, tumor cells discover an entirely new microenvironment. The bloodstream can be a hostile environment for CTC. First, tumor cells have to resist anoikis, an apoptotic mechanism that induces epithelial cell death upon loss of contact with the ECM and neighboring cells. Shear forces in the blood flow and cytolytic attacks from immune cells, particularly natural killer (NK) cells, represent additional obstacles to the survival of tumor cells. CTC having undergone partial or complete EMT during their initial migration from the tumor acquire crucial traits that support their survival in the circulation. However, since EMT is transiently induced by stromal cells of the tumor microenvironment, single CTC may depend on the maintenance of this transient phenotype during their journey, which is often mediated by interactions with fellow travelers in the bloodstream. Those include bone marrow-derived cells at various levels of differentiation, endothelial cells, fibroblasts, mast cells, leukocytes and platelets (Joyce and Pollard, 2009).

Platelets (also called thrombocytes) are anuclear and discoid blood cells that are released by megakaryocytes as cytoplasmic bodies to fulfill a major anti-hemorrhagic function by inducing blood coagulation in case of vascular injury. As such, platelets are highly reactive to injured or altered endothelial lining and exposed underlining basement membrane components inside the vasculature. Upon detection of disrupted vascular integrity, platelets activate and avidly bind endothelial cells, smooth muscle cells, fibroblasts and ECM components such as collagen, fibronectin and laminin (Ruggeri, 2009). Activated platelets in turn recruit other neighboring platelets to promote aggregation and coagulation by conversion of fibrinogen into crosslinked fibrin as well as lymphocytes and bone marrow progenitors to prevent infection. They do so by releasing effectors from dense and alpha-granules such as platelet-derived growth factor (PDGF), VEGF, TGF-β, proinflammatory cytokines and matrix metalloproteinases, all of which can profoundly influence the fate of CTC in blood (Gay and Felding-Habermann, 2011). For example, TGF-β secreted by activated platelets has been shown to induce downregulation of NKG2D (member D of the activating immunoreceptor natural killer group 2) on NK cells, thereby enabling CTC to evade antitumor immunity (Kopp *et al.*, 2009). Platelet membrane receptors and surface markers are highly advantageous targets for CTC since activated platelets can transfer the major histocompatibility complex (MHC class I) to bound CTC which also protects them from antitumor immunity (Placke *et al.*, 2012). Moreover, rapid turnover and mass production are characteristics of platelets which make them likely to be the first cells to interact with CTC in the bloodstream, since the human body produces and clears 10^{11} platelets daily to maintain a normal blood count (Grozovsky *et al.*, 2015). In this context it is not surprising that thrombocytosis (elevated platelet count) correlates with poor prognosis in a number of proliferative malignancies such as lung, colon, breast, brain, gastric, renal, pancreatic, endometrial, cervical and ovarian cancers (Gay and Felding-Habermann, 2011). And it has for long been known that platelet depletion (or defective production) significantly reduces metastasis (Gasic *et al.*, 1968).

In addition to immune evasion, tumor cell-induced platelet aggregation (TCIPA) can provide CTC

with the necessary signals to maintain the EMT phenotype. Indeed, TGF-β signaling from activated platelets induces upregulation of several EMT transcripts in breast and colon cancer cell lines, such as vimentin, MMP9 and the Snail transcription factor, which help decrease apoptotic signals that normally arise from loss of contact in epithelial cells (Labelle *et al.*, 2011). Platelet-induced protection from apoptosis through mitochondrial uncoupling has also been reported in leukemia (Velez *et al.*, 2014). Furthermore, PDGF signaling contributes to the nuclear translocation of β-catenin in hepatocellular carcinoma cells *in vitro* which activates the Wnt signaling pathway, thereby protecting malignant hepatocytes from anoikis (Fischer *et al.*, 2007). PDGF signaling is also involved in EMT through gain of vimentin as well as loss of E-cadherin and ZO-1 expression in prostate cancer cells *in vitro* (Kong *et al.*, 2008). In turn, activated platelets can recruit other leukocytes to form a heterogeneous cluster that further shields CTC from cytotoxic immune cells and shear forces of the bloodstream (Gay and Felding-Habermann, 2011). All these examples illustrate the considerable advantage that platelet-binding represents for CTC in the bloodstream, but only a fraction of all the CTC released in the circulation are able to use that advantage. Interestingly, Alves and colleagues demonstrated that CD44 expressed at the surface of colon cancer cells serves as the major ligand to bind fibrin and P-selectin on the cytoplasmic membrane of platelets under shear flow (Alves *et al.*, 2008). The use of CD44 knockdown colon cancer cells did not allow for further characterization of the specific CD44 splicing variant implicated in platelet and fibrin binding. However, this study suggests that the blood compartment can act as a major selection factor in determining the metastatic advantage of stem-like tumorigenic cells.

Other than platelets, CTC have been described to associate with various cell types in the blood compartment such as circulating neutrophils (Zhang *et al.*, 2016) and activated circulating endothelial cells (Yadav *et al.*, 2015) that provide enhanced resistance to anoikis and protection against immune attacks. Importantly, collective migration of CTC clusters (CTM) also provides a significant advantage for CTC to survive their haematogeneous journey (Hou *et al.*, 2012). Indeed, the maintenance of epithelial traits together with the acquisition of mesenchymal properties that

characterize most collectively migrating cancer cells provide enhanced adaptability to the various types of microenvironments that can be encountered throughout the human body. In the bloodstream, CTM have been identified as clusters of 2 to 50 cancer cells (Joosse *et al.*, 2015) and associated with poor clinical outcome in a number of malignancies, including pancreatic (Chang *et al.*, 2016), skin (Long *et al.*, 2016), colorectal (Zhang *et al.*, 2017a), lung (Hou *et al.*, 2012) and breast (Uga *et al.*, 2012) cancers. Tumor cells have been shown to produce and release tissue factor (TF), a natural ligand able to initiate the coagulation cascade, which is associated with an elevated risk of venous thromboembolism (VTE), including pulmonary embolism (PE) and deep venous thrombosis (DVT), in cancer patients (Lou *et al.*, 2015). However, CTM are especially thought to contribute to VTE because their relative larger size compared to single CTC could make them prone to entrapment in small capillaries (Aceto *et al.*, 2014). But this hypothesis was recently challenged by an *in vitro* study reporting that CTM, selected from patients as rounded clusters of up to 20 cancer cells, are able to reorganize into a single chain-like geometry and squeeze into small blood-filled capillaries of 5 to 10 µm in diameter, from which they emerge viable and quickly rearrange to recover the rounded shape of the initial cluster (Au *et al.*, 2016). This interesting mechanism, further recapitulated *in vivo* by injection of CTM in zebrafish (Au *et al.*, 2016), suggests that physical entrapment of CTM may not be the predominant factor leading to VTE. Instead, biochemical interactions between cancer cells and leukocytes as well as endothelial cells may favor CTC and CTM arrest in the vasculature, possibly leading to intravascular proliferation of CTM and passive extravasation through rupture of small capillaries, or active CTC extravasation, depending on the conditions encountered in distinct locations throughout the blood vasculature.

2.4. Extravasation mechanisms

To this day, there is still much to be learned about the specific molecular interactions which govern the extravasation of circulating tumor cells through the vascular endothelium. Several experimental settings have shown the preferred extravasation of tumor cells at specific distant sites in a cell-type

specific manner which depends on key molecular players of intercellular communication and cell-cell attachment.

It has been proposed that CTC extravasation mechanisms somewhat resemble those governing leukocyte extravasation (Strell and Entschladen, 2008) which is vital for immune surveillance and inflammation. The extravasation process of leukocytes is composed of three major steps: 1) rolling which describes loose interactions with vascular endothelial cells at the fringe of the blood stream, resulting in a rolling motion of the circulating cell along the intravascular border, 2) adhesion where the attachment to endothelial cells strengthens via interaction with cell surface molecules that differ from the ones implicated in the rolling phase, and 3) diapedesis which results in the effective crossing of the endothelium layer.

Leukocytes achieve rolling and adhesion to the endothelium mainly by expressing N-cadherin and several types of β2-integrins which bind the cellular adhesion molecules (CAM) and junction adhesion molecules (JAM) present at the surface of endothelial cells. In contrast, CTC do not express β2-integrins and are thought to mediate rolling mainly through expression of selectins, CD24, N-cadherin and intercellular adhesion molecule 1 (ICAM1) which binds β2-integrins present on surrounding leukocytes and platelets, thus using normal blood cells as bridge for attachment (Strell *et al.*, 2007). CTC can then successfully adhere to the endothelium by expressing variants of CD44, MUC1, β1- and β7-integrins. Indeed, the upregulation of several integrins was recently shown to characterize pan-cancer transcriptomic datasets (Yadavalli *et al.*, 2017). The variant CD44v6 and MUC1 are known to bind galectin-3 at the surface of endothelial cells (Yu *et al.*, 2007). Galectins are a family of β-galactoside-binding proteins containing one or several carbohydrate-recognition domains (CRD) which are known to play a role in modulating pro- and anti-inflammatory functions as well as migration through extracellular matrix, cell-cell adhesion and angiogenesis (Hughes, 2001; Thijssen *et al.*, 2007). Galectin-3 slightly differs from other galectins in its molecular architecture because, in addition to the CRD motif, it contains an N-terminal domain that determines cellular localization in a phosphorylation-dependent manner (Barondes *et al.*, 1994). Interestingly, galectin-

3 has also been shown to play a role in apoptotic functions depending on its cellular localization (Stillman *et al.*, 2006), suggesting that CTC binding on the intravascular endothelium can induce apoptosis of endothelial cells.

Once strongly attached to the endothelium, leukocytes mediate diapedesis through two distinct mechanisms: paracellular and transcellular migrations. Leukocytes can be extravasated without permanently disrupting the endothelium by binding the platelet/endothelial cell adhesion molecule (CD31, also called PECAM-1) and junction adhesion molecules (JAM-A, JAM-B and JAM-C, also called JAM1, JAM2 and JAM3) which mediate homogeneous cell-cell adhesion between endothelial cells of the vasculature (Strell and Entschladen, 2008). Leukocytes thereby squeeze between viable endothelial cells to cross the endothelium with minimal disruption and achieve paracellular migration. However, a much faster route exists where leukocytes simply infer apoptosis of endothelial cells by cell-specific molecular interactions which are less well known. For example, in early stages of inflammation, transendothelial migration of neutrophils was reported to implicate the $P2Y_2$ purinergic receptor on endothelial cells *in vitro* whereas ICAM-1 and IL-8 upregulation play an important role in neutrophil extravasation at later stages of inflammation (Kukulski *et al.*, 2010). This permanently disruptive extravasation mechanism, termed transcellular migration, does not seem to be the preferred route for cancer cells (Reymond *et al.*, 2013), although transcellular migration of colorectal cancer cells has been observed *in vitro* (Tremblay *et al.*, 2008), such a mechanism still awaits demonstration *in vivo*.

Moreover, tumor cell interaction with platelets acts beyond protection during circulation by facilitating CTC extravasation. Although little is known about the specific molecular interactions governing platelet-mediated CTC extravasation, experimental models have suggested that platelet-derived adenine nucleotides (such as ATP molecules secreted by platelet dense granules) bind and activate the $P2Y_2$ receptor on endothelial cells, thereby enabling early stage CTC extravasation (Schumacher *et al.*, 2013) while upregulation of TGF-β secretion by tumor-activated platelets promote cancer cell extravasation at later stages of cancer progression (Labelle *et al.*, 2011). Cancer

cells can also associate with a variety of leukocytes to enable extravasation, such as neutrophils, natural killer or monocytes/macrophages, and platelet-coating of CTC also enhances leukocyte attraction (Reymond *et al.*, 2013), as depicted in **Figure 7**.

Passive extravasation due to intravascular proliferation of cancer cells has been proposed as an additional mechanism of cancer cell homing to distant organ sites. In particular, CTM arrest in the vasculature, by causing regional elevations of thrombin (Phillips *et al.*, 2015) and initiating intravascular proliferation (Wong *et al.*, 2002), is considered to potentiate passive extravasation.

Therefore, both CTC and CTM represent highly informative cancer material and their non-invasive collection through sequential blood samplings offers the opportunity to perform kinetic studies on cancer development, treatment and recurrence at virtually any biological level (genetic, transcriptomic and protein level). Such studies are impractical at best and impossible in many cases via repeated invasive samplings like biopsies of both the primary tumor and multiple metastatic sites.

Figure 7: *Interactions facilitating CTC extravasation*

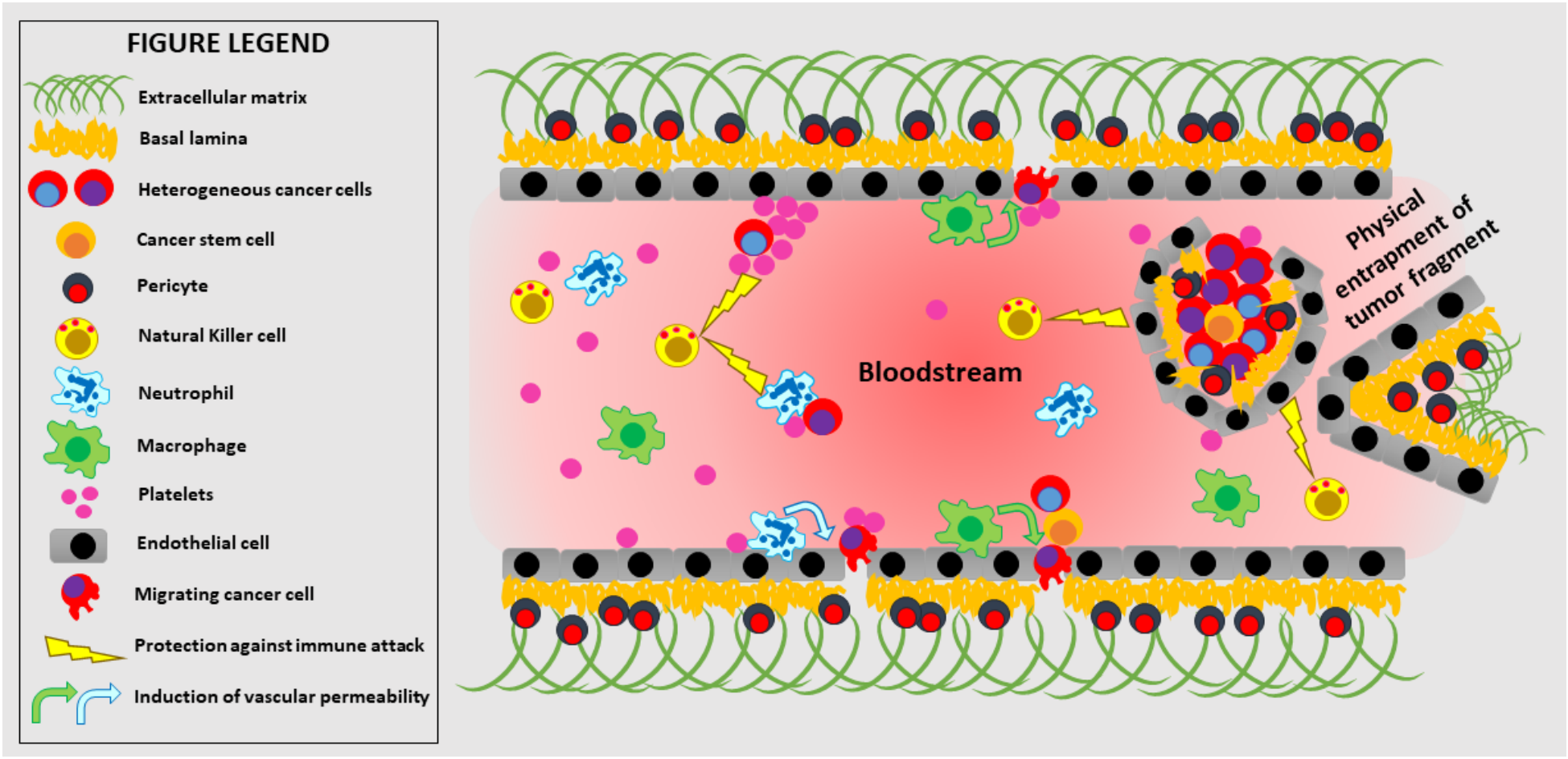

2.5. Technical challenges in CTC/CTM isolation and characterization

Indeed, CTC/CTM constitute extremely attractive targets for many researchers and scientists looking to unveil the complex cellular and molecular biology underlying blood-borne metastasis. On the other hand, the possibility to correlate CTC/CTM numbers and/or biochemical properties with patients' clinicopathological features (further detailed in the next chapter), including potential response or resistance to therapy, has also attracted many clinicians and oncopharmacological companies to the field of CTC study. However the technical aspect of this field is far from trivial and, just like the CTC population itself, highly heterogeneous. As mentioned earlier, more than forty distinct methods have been developed for the purpose of CTC isolation/detection and those generally fall into one of the two following categories: surface marker-dependent and marker–independent approaches. In order to better understand the substantial challenge that CTC isolation/detection represents, let's first have a closer look at the very heterogeneous population of circulating rare cells (CRC).

2.5.1 Circulating Rare Cells (CRC)

Circulating Rare Cells (CRC) are rare and heterogeneous cells derived from organs which circulate in blood. They include circulating tumors cells (CTC) as well as non-tumorous, non-haematological cells, mainly of epithelial or endothelial origin. Distinguishing CTC from other circulating non-haematological cells is a task far from trivial. For example, tumor-derived circulating endothelial cells exhibiting hyperplastic morphologies and distinct genetic alterations than those of tumor cells were found in the blood of colorectal cancer patients (Cima *et al.*, 2016). While circulating endothelial cells can inform on the overall damage to the human vasculature during cancer development and therapy, it is also crutial to distinguish them from cancer cells. Endothelial cells may express both vimentin and certain cytokeratins (Miettinen and Fetsch, 2000), markers that are also associated with CTC undergoing EMT, thus phenotypic markers cannot on their own distinguish CTC from other CRC. Cancer cells with a stem phenotype can also circulate in blood (Easwaran *et al.*, 2014) and those represent an even rarer subpopulation of CTC. Additionally, non-tumorous epithelial cells can also invade the bloodstream in cases of sustained inflammation (Pantel *et al.*, 2012) and circulating

fetal cells (CFC) can also be found in the blood of pregnant women (Saker *et al.*, 2006). To this day, the only method proven to bear diagnostic significance for CTC detection consists in the cytomorphological assessment of CRC (Hofman *et al.*, 2011c), possibly combined with immunelabelling, which can be applied only to fixed cells following cytological staining. Still, many other methods for CTC detection have been reported and combined to various enrichment approaches, as further detailed below.

2.5.2 CTC isolation/detection methods based on surface marker selection

When based on antigen expression, positive antibody-mediated selection of CTC usually involves targeting the epithelial cell adhesion molecule (EpCAM), as cancer cells were initially thought to remain exclusively epithelial in nature. Among those, the semi-automated CellSearch® platform is the most commonly used since it is still the only CTC detection technique that received clearance by the U.S. food and drug administration (FDA). Typically, the CellSearch® system performs an immunomagnetic selection of EpCAM-presenting cells in 7.5 mL of peripheral blood and further requires fluorescent immunolabeling of the selected and fixed cells to guide CTC identification. In this system, CTC are defined as nucleated with positive DAPI staining, epithelial with positive cytokeratin staining and non-haematogeneous in nature with negative staining of the CD45 leukocyte antigen (Cristofanilli *et al.*, 2005). Such a definition is truly lacking in specificity since a significant portion of CTC do not retain expression of the common EpCAM marker. For example, the absence of detectable EpCAM expression has been shown to characterize the specific subset of breast cancer CTC capable of initiating brain metastasis (Zhang *et al.*, 2013a). Additionally, as mentioned previously, non-malignant epithelial cells can also circulate in the bloodstream.

Many other EpCAM-based selection methods exist, including the AdnaTest (Tewes *et al.*, 2009), the MagSweeper (Talasaz *et al.*, 2009), various types of microfluidic devices and platforms such as IsoFlux and the CTC-Chip (Joosse *et al.*, 2015) as well as the CellCollector™, an EpCAM-coated medical guidewire that is inserted into a patient's cubital vein for 30 minutes and thereby enables the *in vivo* capture of EpCAM-positive cells from an estimated 1.5 liters of flowing blood (Saucedo-

Zeni *et al.*, 2012). As inventive as those techniques may be, any EpCAM-based selection method would suffer the same limitations as CellSearch® does. Therefore, all results obtained from blood samples by any epithelial marker-dependent selection/detection method will from here on out be referred to as characterizing circulating epithelial cells (CEpC) rather than CTC.

Ultimately, full CTC characteristics are likely to be patient-specific, which implies that any positive selection of CTC based on a single preselected biomarker would introduce biases. Emerging technologies such as those using specific aptamers tailored to the surface-biology of cancer cells are very promising because they offer the possibility of a positive selection based on multiple and unselected biomarkers. Aptamers are small single-stranded oligonucleotides (DNA or RNA molecules of 20 to 80 nucleotides) produced by associating random sequences with flanking universal probes and can be selected for their affinity to bind cellular surface markers (Ouyang *et al.*, 2016). In a study by Zamay and colleagues, for instance, specific aptamer cocktails were selected on the basis of their strong positive affinity to bind bulk cancer cells extracted from a biopsy specimen of lung cancer, as well as strict negative affinity for non-cancerous cells from the same patient (Zamay *et al.*, 2015). Those aptamer pools were then sequenced and synthesized to enable the tailored isolation of pure yet heterogeneous CTC populations in a patient-specific manner. While aptamers hold great promise for CTC capture, substantial limitations such as the stability of aptamers in whole blood have hampered translation to clinical aplications (Song *et al.*, 2017). Additionally, studies have employed 3D nano-surfaces made in synthetic materials, like for example silicon nanopillars (Wang *et al.*, 2009), carbon nanotubes (Abdolahad *et al.*, 2012) or polymer nanofibers (Zhao *et al.*, 2013), as biomimetic nanostructures to enhance antibody- or aptamer-depedent binding of CTC for a more sensitive isolation.

In contrast, negative selection (depletion) methods typically consist in targeting the CD45 antigen present at the surface of leukocytes. For example, the EasySep® kit from Stemcell Technologies uses biantibody-coated magnetic beads to enable leukocyte depletion, which offers the possibility to recover live cells (Yin *et al.*, 2015). Using this strategy, the viable cells enriched can be cultured *in*

vitro and used for further downstream analysis (Denève *et al.*, 2013). CD45-mediated depletion of leukocytes enables the selection of all cancer cell phenotypes but has also been reported to result in lower purities (Harouaka *et al.*, 2014), because first, red blood cells are still in the way and, second, even after erythrocyte lysis the entire population of rare cells is selected, including non-malignant epithelial, mesenchymal and endothelial cells. This is why leukocyte depletion methods are often used in combination with other types of CTC enrichment techniques.

2.5.3 CTC isolation/detection methods based on biomechanical and biophysical properties

Understanding biomechanical and biophysical properties of cancer cells in general, such as their polarized electric charge, intrinsic density, variable deformability as well as global size/volume, enabled scientists to target CTC based on various aspects of their biology.

One of the first methods employed for CTC isolation was developed on the basis of the differential densities observed for red blood cells, leukocytes and cancer cells by S. H. Seal in the late 1950s (Seal, 1959). The resulting method of density-based gradient separation in blended silicon oils further evolved to include centrifugation and a synthetic polysaccharide was added to the mixture of silicon oils to create the Ficoll-Paque® solution, which then became a gold standard approach to separate peripheral blood mononuclear cells (PBMC) from the denser erythrocytic and granulocytic populations of cells in whole blood (Boyle and Chow, 1969). After density gradient centrifugation, targeted molecular analysis can be applied to detect specific mutations by PCR (polymerase chain reaction) or the expression of specific transcripts by RT-PCR (reverse transcription PCR). The latter was applied by Weitz and colleagues to detect the expression of cytokeratin 20 transcripts by putative CTC in the whole PBMC fraction (Weitz *et al.*, 1998). However, this approach also lacks in specificity since it cannot allow counting of CTC nore discriminate CTC from other circulating epithelial cells in the PBMC fraction.

Back in the 1950s, S. H. Seal also proposed the first size-based enrichment method for CTC isolation, using an experimental filtration device (Seal, 1956, 1964). This pioneering technique incorporated filtration membranes defined by relatively small pores, on average between 3 and 5 microns in

diameter, because it was meant to recover and concentrate the entire cellular fraction involved in "cell spillage" during surgical interventions. Almost half a century and multiple technical adjustments later, the ISET® (Isolation by SizE of tumor/trophoblastic cells) filtration method was introduced by Vona and colleagues (Vona *et al.*, 2000). The ISET® method, by using a filtration synthetic membrane with an average pore size of 8 microns, following erythrocyte lysis achieved by a pretreatment step, enables the recovery of all the circulating rare cells including subpopulations of CTC from virtually any type of invasive solid cancer. Unbiased selection of even the smallest types of CTC was reported in studies using ISET® to enumerate and characterize EMT-induced phenotypic plasticity in CTC from small-cell lung cancer (SCLC) patients (Lecharpentier *et al.*, 2011; Krebs *et al.*, 2012). The counterpart to avoiding size-based selection biases is the resulting low purity of CTC obtained after enrichment, since all the circulating cells with average diameters larger than 8 microns are retained, including the larger portion of polynuclear and monocytic cell populations. Therefore, filtration technologies developed for CTC isolation, such as ISET® and ScreenCell®, rely on morphophenotypic criteria examined after classical histopathological staining and immunohistochemical labeling to enable the diagnosis and further characterization of both single CTC and malignant clusters (CTM). Different filtration parameters can influence the performance of any given filtration technique. For example, ScreenCell® applies uncontrolled and unmonitored negative pressure to aspirate 3 ml of blood through a filter using a seringe and a vacutainer tube (Pinzani *et al.*, 2013). By contrast, ISET® applies a controlled modulable negative pressure to aspirate 10 ml of blood through a filter membrane, a process which keeps cell morphology intact (Vona *et al.*, 2000).

3D filtration technologies based on biomechanical and biophysical properties of cancer cells, such as specific types of microfluidic devices, can achieve far greater purity levels in isolating large CRC than 2D filtration by incorporating multiple sequential steps of discrimination based on distinct criteria of cell size, cytoskeletal deformability and/or electrical polarity (Harouaka *et al.*, 2013) but the approach markedly decreases sensitivity . The possibility to isolate viable CTC by microfluidic enrichment is

attractive, especially for scientists studying the tumorigenic potential of distinct CTC subpopulations, which requires xenografting viable tumor cells into immunodeficient mice (Baccelli *et al.*, 2013). However, the need to combine additional enrichment strategies with microfluidic devices that cannot handle whole blood, as well as the very low throughput levels imposed by those capable of processing whole blood (1h processing time on average for each milliliter of blood analyzed) represent significant limitations to those technologies.

Additionally, dielectrophoresis (DEP) can be used to select CRC based on their relative electromagnetic properties by applying a strong electromagnetic field to which cells react either by moving towards or by moving away from the signal source. A good example of such technology is the DEPArray™ from Silicon Biosystems which unfortunately primarily relies on phenotypic immunomolecular characterization of CRC to identify CTC (defined as nucleated cytokeratin-positive and CD45-negative cells), thus possibly producing both false negative and false positive results, and demonstrating variable recovery rates from 11.6% to 86% when tested using tumor cells from cell lines spiked in blood (Fabbri *et al.*, 2013).

It is also worth noting that CTC detection strategies do not always include a preliminary enrichment step. One example of such strategy consists in combining red blood cell lysis with cell-spinning or -smearing on glass slides to enable subsequent assessment of cytomorphological features and immunomolecular characteristics of CTC subtypes among the entire population of nucleated blood cells by microscopic imaging techniques such as automated digital microscopy or fiber-optic array scanning technology (Krivacic *et al.*, 2004). Accordingly, Nieva and colleagues used this approach on a cohort of 28 SCLC patients and reported CTC detection rates as low as 3 CTC per 10 mL of blood at study enrollment, with detection rates increased to an average 134 CTC per 10 mL of blood in later follow-up samples (Nieva *et al.*, 2012). This strategy however bears the main limitations of requiring sample fixation prior to analysis and of potentially producing false negative and false positive results since CTC are identified on the basis of cytokeratin expression.

In summary, an ideal CTC isolation/detection technique should allow a relatively practical sensitive

recovery of viable cancer cells while discarding a large portion of the background of normal blood cells without introducing selection biases. With that in mind, drawing accurate conclusions from results obtained after CTC enrichment requires careful evaluation of the multiple performance parameters that define each CTC isolation/detection technology, such as the repeatability and reliability of results, capture efficiency, cell viability, enrichment capacity, processing speed and blood volumes analyzed (Harouaka *et al.*, 2013). And ultimately, cost-effectiveness can also significantly impact the potential clinical implementation of any type of biotechnology. Examples of current CTC isolation/detection techniques are depicted in **Figure 8**.

Figure 8: *Examples of CTC isolation/detection methods*

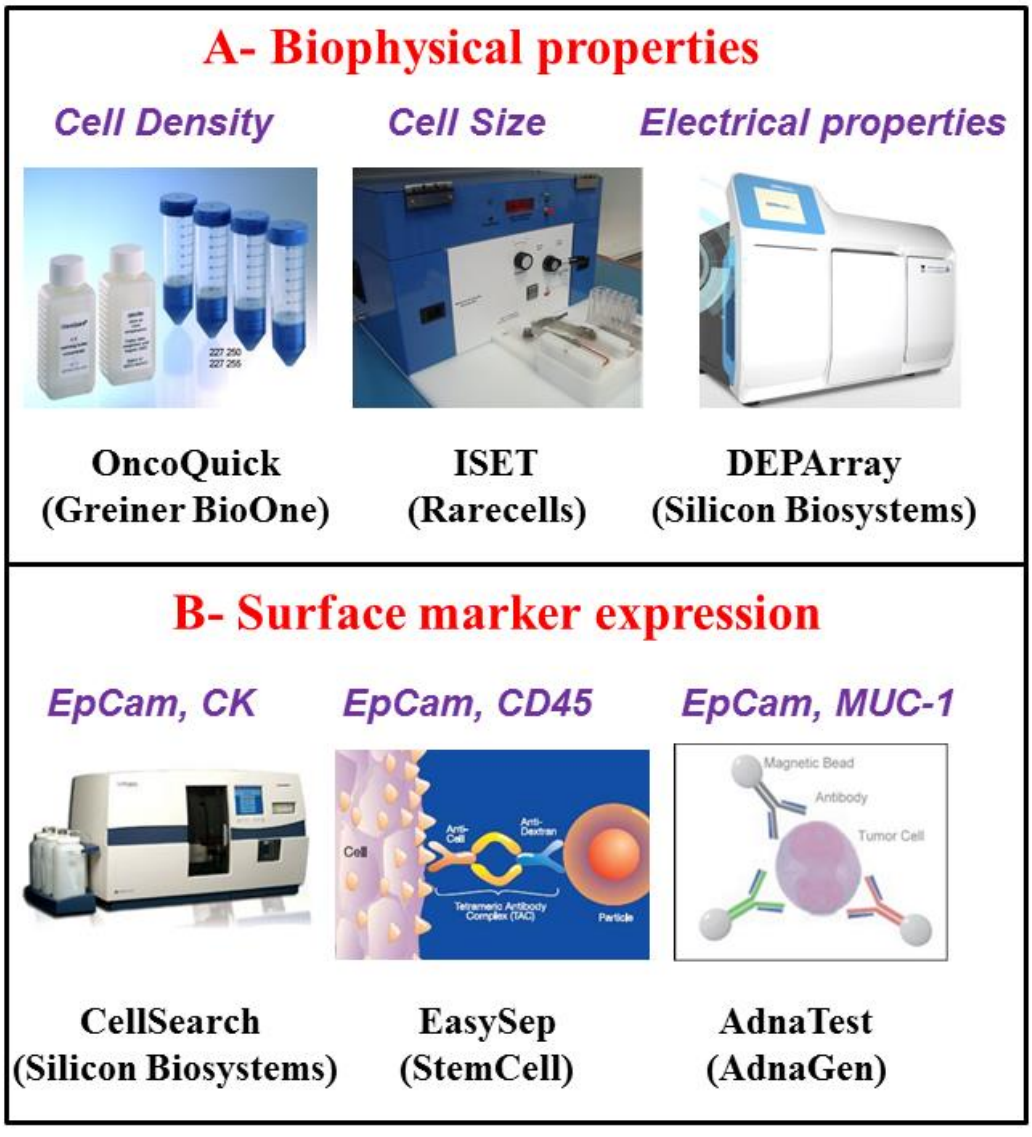

2.6. Clinical interest of studying CTC

Considering the costly, time-consuming, highly invasive and poorly repeatable aspects of surgical tumor samplings such as biopsies, reliable blood-based cancer biomarkers enabling a so-called "liquid biopsy" of cancer would have tremendous impacts on patients' care if successfully implemented in clinical settings. Notably, recent developments in circulating tumor DNA (ctDNA) analysis have introduced another non-invasive way of interrogating single nucleotide variations (SNV) in blood for patients with both locally advanced and metastatic cancer stages (Bidard *et al.*, 2013). In fact, the very first liquid biopsy test to receive approval by the US FDA (June 2016) consists in detecting mutations on exons 19 and 21 of the EGFR gene by ctDNA analysis and was proposed by Roche under the name "Cobas® EGFR Mutation Test V2" for personalized treatment of non-small-cell lung cancer (NSCLC) patients (Han *et al.*, 2017). However, the detection of complex DNA alterations such as chromosomal translocations remains difficult to perform on ctDNA (Cabel *et al.*, 2017). Moreover, owing in part to the relative abundance of cell-free DNA (cfDNA) released in the bloodstream by non-cancerous cells compared to ctDNA levels, even the most sensitive methods based on the identification of genetic mutations for ctDNA detection cannot currently provide a reliable diagnosis of early-stage cancers (Alix-Panabières and Pantel, 2016; Abbosh *et al.*, 2017). In contrast, CTC can serve as a non-invasively collected tumor surrogate for a much wider array of biological analyses, including genetic, epigenetic, transcriptomic and protein characterization. Furthermore, by definition, CTC can inform on the invasive nature of the tumor while ctDNA rather reflects the extent of tumor necrosis (Abbosh *et al.*, 2017) Those CTC-based analyses could potentially improve patients' care at multiple levels with regards to the current standard practices in clinical oncology.

2.6.1 CTC detection for early diagnosis of cancer

As of August 2017, to my knowledge only one study reported the possibility of employing CTC detection for early cancer diagnosis. Using ISET® filtration and cytomorphological analysis to screen the blood of individuals at high risk of lung cancer, Ilie et al. could detect CTC years before

conventional computed tomography (CT) scanning could detect a corresponding small tumor mass (Ilie *et al.*, 2014). In a cohort of 168 patients with chronic obstructive pulmonary disease (COPD) and without clinical diagnosis of cancer, along with a control group of 77 healthy individuals, this study reported the detection of CTC in the blood of 5 (3% of) COPD patients and in none of the healthy individuals. An annual monitoring by low-dose computed tomography (CT)-scan identified lung nodules in each of those five patients after 1 to 4 years following CTC detection, leading to surgical resection and diagnosis of early-stage lung cancer (Ilie *et al.*, 2014). Although larger studies are warranted to confirm this striking result, and one is in fact currently undergoing, the possibility of using CTC detection for early cancer diagnosis in high-risk patients would be of high clinical interest.

2.6.2. Prognostic and predictive values of CTC and CEpC

Despite its previously stated shortcomings, the CellSearch® platform has fostered numerous large-scale clinical studies on metastatic cancer patients which provided extensive data on the prognostic and predictive values of circulating epithelial cells (CEpC).

In metastatic breast cancer, Bidard et al. reported a pooled meta-analysis of CEpC count from 1944 individual cancer patients and determined that patients presenting with elevated CEpC counts (5 or more CEpC detected in 7.5 mL of whole blood by CellSearch®) at baseline had significantly decreased progression-free survival (PFS) and overall survival (OS) compared to patients with lower CEpC counts (Bidard *et al.*, 2014). In this meta-analysis study, further incorporating CEpC counts evaluated after 3-5 and 6-8 weeks of therapy along with baseline counts into standard clinicopathological predictive models enhanced the accuracy of survival predictions whereas levels of standard serum tumor-markers (carcinoembryonic antigen (CEA) and cancer antigen 15-3 (CA15-3)) did not. Conversely, in another large-scale multicenter study conducted on 2026 non-metastatic primary breast cancer patients before adjuvant chemotherapy, Rack and colleagues reported that any number of detectable CEpC could predict poor prognosis for patients, with shorter PFS and OS compared to patients without detectable CEpC (Rack *et al.*, 2014). In this study, CEpC were found

in 21.5% of 2026 breast cancer patients with only 3.1% of patients harbouring at least 5 CEpC in 30 mL of blood while 57.9% of the cohort presented with locally advanced stages (T2-T4) of breast cancer. Additionally, 4.9% of the 84 healthy individuals tested as negative controls also harboured CEpC in their blood, demonstrating the lack of specificity of the method to identify CTC (Rack *et al.*, 2014).

In other large-scale clinical trials and publication-based meta-analyses, CEpC presence or numbers detected by CellSearch® in the blood of patients were confirmed as independent predictors of poor prognosis in terms of objective response rate (ORR) to therapy or PFS and OS in metastatic colorectal cancer (Huang *et al.*, 2015), locally advanced colorectal cancer (Krebs *et al.*, 2015) and metastatic castration-resistant prostate cancer (Scher *et al.*, 2015). Smaller-scaled studies also suggested a prognostic significance of CEpC in advanced and relapsed NSCLC patients (Krebs *et al.*, 2011; Punnoose *et al.*, 2012). In NSCLC as well as breast and prostate cancers at metastatic stages, studies using CellSearch® for prognostic assessment have applied the FDA-approved cutoff placing patients with at least 5 CEpC detected in 7.5 mL of blood in the "high risk" group while studies on colorectal cancer and other cancers at locally advanced stages have used less uniform cutoffs to stratify patients, ranging from 1 to 3 CEpC per 7.5 mL of blood. Importantly though, very low detection rates were reported for non-metastatic cancer patients at locally-advanced stages using CellSearch®, with the notable exception of small-cell lung cancer (SCLC) patients where CellSearch® detected CEpC in 85% of 97 patients with a median number of 24 CEpC per 7.5 mL of blood (Hou *et al.*, 2012). Moreover, the limited sensitivity and specificity of the CellSearch® method are well exemplified by its lack of applicability to early-stage cancers (Alix-Panabières and Pantel, 2016).

Meanwhile, in early-stage (I-IIIA) NSCLC patients, epithelial CTC were detected after surgical resection by simultaneous assessment of cytomorphological features and immunostaining of cytokeratins following enrichment by immunomagnetic selection of CK-positive cells in peripheral blood samples (Bayarri-Lara *et al.*, 2016). It must be noted that detecting CEpC after surgical intervention on the basis of cytokeratin expression (or other epithelial markers such as EpCAM) does

not reflect the spontaneous entry of tumor cells into the circulation since surgical procedures are known to induce forced shedding of cells into the bloodstream (Yao *et al.*, 2014). Although CEpC were reported to be independent predictors of postoperative disease relapse, with patients exhibiting significantly shorter PFS when compared to patients without detectable epithelial CRC after surgery (Bayarri-Lara *et al.*, 2016), such conclusions derive from methodologies that do not enable a proper distinction of CTC from other CRC.

In contrast, using size-based enrichment (ISET® filtration) followed by cytopathological diagnosis of CTC (defined as circulating non-hematological cells (CNHC) with malignant morphological features), Hofman and colleagues detected preoperative CTC in 36% of 208 patients with resectable NSCLC at very early stages (I-II) (Hofman *et al.*, 2011). Furthermore, by placing a cutoff at 50 CNHC in 10 mL of blood, the authors reported a significant correlation of elevated CNHC levels with poor prognosis, demonstrating shorter PFS and OS for patients with more than 50 preoperative CNHC.

Notwithstanding the clinical value of those studies, evaluating CTC strictly on the basis of their number does not enable a full assessment of their vast informative potential. Given that various phenotypic traits and distinct levels of tumorigenicity can be found among the numerous coexisting CTC subpopulations, establishing cutoff values of epithelial CRC for clinical assessment does not account for the highly malignant mesenchymal CTC and thus fails to assess the entire population of heterogeneous CTC. Furthermore, considering that the dynamic evolution of CTC subpopulations can reflect or predict response to treatments, molecular subtyping of CTC populations should demonstrate great potential for clinical application.

2.6.2. Molecular subtyping of CTC populations

Most CTC isolation/detection techniques allow for a subsequent immunolabeling step to characterize CTC on the basis of their epithelial and mesenchymal traits. Those are often interesting to evidence since various levels of EMT may determine resistance of those CTC to current systemic therapies, as shown for Adriamycin-based chemotherapy resistance in breast cancer (Li *et al.*, 2009), by Snail-mediated radioresistance and chemoresistance of ovarian cancer cells (Kurrey *et al.*, 2009) and by

resistance to immunotherapies of Snail-expressing melanoma cells (Kudo-Saito *et al.*, 2009). For example, Bulfoni and colleagues used a cocktail of antibodies against both epithelial and mesenchymal markers to characterize circulating cells after CD45-mediated immunomagnetic depletion of leukocytes from the blood of metastatic breast cancer patients (Bulfoni *et al.*, 2016). By demonstrating a significant correlation of hybrid EMT phenotypes in CD45-negative circulating cells with shorter PFS and OS of metastatic breast cancer patients treated by chemotherapy, this study highlighted the importance of characterizing distinct phenotypes in circulating cell populations for clinical assessment, therapeutic decision-making and follow-up of cancer patients. However, clinical assessment and follow-up of cancer patients would benefit from a more specific characterization of CRC populations in order to distinguish cancer cells from other CRC such as endothelial cells and from tumor-associated immune and stromal cells which can also circulate in blood. Characterizing the EMT status of CTC can be achieved at protein level by concomitant immunohistochemical or fluorescent staining of Vimentin and various members of the Keratin family. As already mentioned, reliable CTC identification by cytomorphological assessment is required with phenotypic characterization because concommittant expression of Vimentin and certain members of the Keratin family can also characterize populations of circulating endothelial cells (Miettinen and Fetsch, 2000; Cima *et al.*, 2016). In a cohort of 50 pancreatic ductal adenocarcinoma (PDAC) patients, for example, Poruk and colleagues used ISET® filtration and cytomorphological assessment to identify CTC before characterizing distinct phenotypic subpopulations by immunostaining. This study demonstrated that detection of hybrid CTC expressing both vimentin and cytokeratin could serve as an independent predictor of disease recurrence (Poruk *et al.*, 2016).

Other protein markers of chemoresistance can be evidenced in CTC and correlated to therapeutic responses in various cancer types. In metastatic colorectal cancer for instance, increased expression of thymidylate synthase in CTC enriched by filtration together with elevated CTC counts (more than 2 CTC per mL of blood) was reported to significantly correlate with a worse prognosis for patients treated by 5-FU-based chemotherapy (Abdallah *et al.*, 2015).

Furthermore, in the advent of personalized anti-cancer treatments and immunotherapies, numerous molecular targets, including changes in nucleic acids and proteins, are known to induce resistance to current treatment strategies. Detecting and assessing the timely evolution of those biomarkers expressed by specific CTC subpopulations at distinct time points (before, during and after therapy) could enable to predict patients' responses and manage evolving treatment decisions based on sequential liquid biopsies. Although large-scale studies are still required to validate the clinical utility (capacity to improve patient outcome) of CTC molecular characterization, numerous prospective studies have already provided encouraging results.

In metastatic castration-resistant prostate cancer (mCRPC), expression and nuclear localization in CTC of a specific splicing variant of the androgen receptor (ARv7), which corresponds to a constitutively active and truncated form of the receptor with no ligand-binding site, has been shown to correlate with initial or acquired resistance of patients to anti-androgen targeted therapies (Antonarakis *et al.*, 2014; Scher *et al.*, 2016).

In the context of breast cancer, treatment regimens targeting the human epidermal growth factor receptor 2 (HER2) such as the humanized monoclonal antibody trastuzumab are currently administered only to patients exhibiting HER2 expression in a significant portion of biopsied primary tumor cells. However, in a phase II clinical trial, Georgoulias and colleagues reported that early-stage breast cancer patients with HER2-expressing CTC detected in the blood and without significant HER2 expression levels in primary tumor specimens could also benefit from trastuzumab treatment, with significantly prolonged DFS compared to untreated control patients initially exhibiting similar cancer characteristics (Georgoulias *et al.*, 2012).

Conversely, in metastatic melanoma patients, the presence of CTM expressing high levels of TRF2, SOX10 and CD10, as determined by immunolabeling of filtration-enriched circulating cancer cell populations, was found to correlate with a poor prognosis and reduced OS independently of applied treatment strategies (Long *et al.*, 2016).

And finally, the possibility of characterizing CTC and CTM from cancer patients after short-term *in*

vitro expansion offers great potential to interrogate the predictive value of CTC/CTM regarding patient response or resistance to various types of therapeutic approaches, as reported by Khoo and colleagues in the context of primary and metastatic breast cancers (Khoo *et al.*, 2015).

Since invasive cancer cells are the vessels potentiating metastatic spread of the disease, improving the lives and medical care of cancer patients could be achieved in the near future if robust technical approaches enabling sensitive, specific and comprehensive analyses of CTC and CTM can be successfully applied in clinical settings. Performing such analyses at multiple time points could complement and improve current medical practices, from early diagnosis to real-time personalized therapeutic strategies and monitoring of potential recurrence of the disease.

In fact, cancer is not the only medical field that could benefit from non-invasive sampling methods enabling to study the biology of circulating rare cells (CRC).

3. Prenatal diagnosis and circulating trophoblastic cells

3.1. Circulating fetal trophoblastic cells (CFTC) and human placentation

Considerable evidence has shown that fetal cells can enter the maternal blood circulation as an early-occurring and persisting event during pregnancy. In the blood of pregnant mothers, circulating fetal trophoblastic cells (CFTC) are part of the rare cells population since approximately 1-2 CFTC can be found in one milliliter of maternal blood, depending on the time of collection during pregnancy.

In humans, the earliest steps of embryo development typically involve attachment of the blastocyst to the maternal endometrium (7 days after coitus), proliferation and maturation of trophoblastic progenitor cells such as mono-nucleated cytotrophoblasts or giant polyploid syncytiotrophoblasts (SynT) resulting from cellular fusion events, and invasive migration of those trophoblastic cells to form the tree-shaped multicellular extensions of the developing placenta, termed chorionic villi (Doridot *et al.*, 2013). Trophoblast invasion is a crucial event during embryonic implantation and placentation because it is required for the remodeling of maternal arteries to construct an effective uteroplacental vasculature capable of sustaining the vital transfer of molecules between maternal and fetal tissues, including import of nutrients and export of toxic metabolites to and from the fetus respectively (Kervancioglu Demirci *et al.*, 2016).

The human placenta is a complex chimeric organ composed of both maternal and fetal cellular structures and the first trimester of the pregnancy is mainly dedicated to placentation (Maltepe *et al.*, 2010). Placentation starts with adhesion of the premature villous tree to the intrauterine epithelium through proliferation and differentiation of villous cytotrophoblasts located underneath SynT and initially firmly attached to the basement membrane that surrounds the mesenchymal core of the anchoring villous structure (Hunkapiller and Fisher, 2008). By acquiring invasive capabilities through differentiation, cytotrophoblasts are able to migrate away from the villous tree to form extravillous trophoblasts (EVT). A particular set of EVT called endovascular EVT (vEVT) specifically migrates towards maternal arteries to form plugs, locally clogging the maternal circulation. This allows for an efficient remodeling of maternal arteries which involves the transdifferentiation of vEVT

into endothelial-like progenitors (vascular mimicry) that displace the maternal endothelium and induce apoptosis of part of the surrounding smooth muscle cells in order to direct the spiral arteries towards the developing placenta (Hunkapiller and Fisher, 2008). As early as 15 days post-coitus, cytotrophoblasts start migrating to become EVT, some of them arranging in clusters to initiate the remodeling of maternal arterioles. While those vEVT invade the maternal circulation, interstitial EVT (iEVT) migrate through the maternal tissue of the decidua (Kervancioglu Demirci *et al.*, 2016). And until the 11th or 12th week of gestation (WG) marking the end of the first trimester, when the clogs of vEVT naturally dissolve after vascular remodeling to let the maternal blood flow fully irrigate the placental intervillous space, trophoblast invasion is considered as the main source of fetal cells' shedding into the maternal circulation. An overview of the major steps of placentation can be found in **Figure 9**.

Although the molecular components regulating trophoblast invasion remain to this day incompletely understood, substantial progress has been made in the past decades. Studies on human trophoblast cell lines migrating *in vitro* have reported that distinct sets of specific chemokines may be involved in regulating trophoblast invasion. For example, Hannan and colleagues observed that invasion of vEVT is induced by endometrial cell secretion of CX3CL1 (also called fractalkine) that binds and activates the CX3CR1 receptor on vEVT while iEVT expressing the CCR3 receptor exhibit enhanced invasive behavior in presence of another ligand, the CCL4 chemokine (Hannan *et al.*, 2006). Other studies have focused on describing the complex epigenetic mechanisms regulating lineage differentiation of trophoblast progenitors either *in vitro* or *in vivo*. Numerous publications have reported the use of *in vivo* mouse models to highlight molecular mechanisms involved in placentation and early embryonic development (Rossant and Cross, 2001). Although fully extrapolating those findings to apply to human biology would remain essentially speculative, results obtained on animal models have highlighted the complex transcriptional regulation of trophoblast differentiation at various levels during animal placentation, as for induction of trophoblast migration and invasion (Maltepe *et al.*, 2010). Importantly, further *in vitro* investigations enabled to formally identify some

of the molecular components regulating invasion of human trophoblasts, including specific transcription factors such as Id-2, one of the four family members of Inhibitors of DNA-binding proteins (from Id-1 to Id-4) (Janatpour *et al.*, 2000), as well as members of the basic helix-loop-helix (bHLH) family of tissue-specific transcription factors which are crucial regulators of trophoblast differentiation during placentation (Meinhardt *et al.*, 2005). Furthermore, specific sets of miRNA are also implicated at post-transcriptional level in regulating trophoblast differentiation into EVT and further inducing invasion of vEVT, or conversely insuring maintenance of stemness features and proliferative capacities of the villous cytotrophoblasts. Examples of miRNA regulation of cell fate in human trophoblasts include miR-34a, which inhibits invasion by binding and blocking the translation of Notch1 and Jagged1 mRNA, as well as miR-141 which is involved in the maintenance of proliferative capacities, hence its progressive downregulation in trophoblasts during the second and third trimesters of gestation (Morales-Prieto *et al.*, 2012). Additionally, lower levels of miR-34a were evidenced in pathological placentas corresponding to preeclamptic pregnancies, suggesting that aberrant epigenetic imbalances can drive abnormal placentation, causing elevated risks of premature delivery as well as maternal and fetal morbidity and mortality during gestation (Doridot *et al.*, 2014). In general, it is interesting to note that aberrantly expressed miRNA species that were first evidenced as characteristics of epigenetic deregulation in the context of cancer are also involved in regulating placentation during pregnancy.

Further along during pregnancy, cross-placental trafficking of fetal cells into the maternal circulation occurs through various other release mechanisms that contribute to the shedding of a wide variety of fetal cell types, as shown in **Figure 9**. Circulating fetal cells have been described to include lymphocytes, erythroblasts (also called nucleated red blood cells), neutrophils, natural killer cells, endothelial progenitors and possibly mesenchymal stem cells, in addition to the early EVT and apoptotic or necrotic fragments of SynT (Hahn *et al.*, 2005).

Figure 9: *The major steps of human placentation*

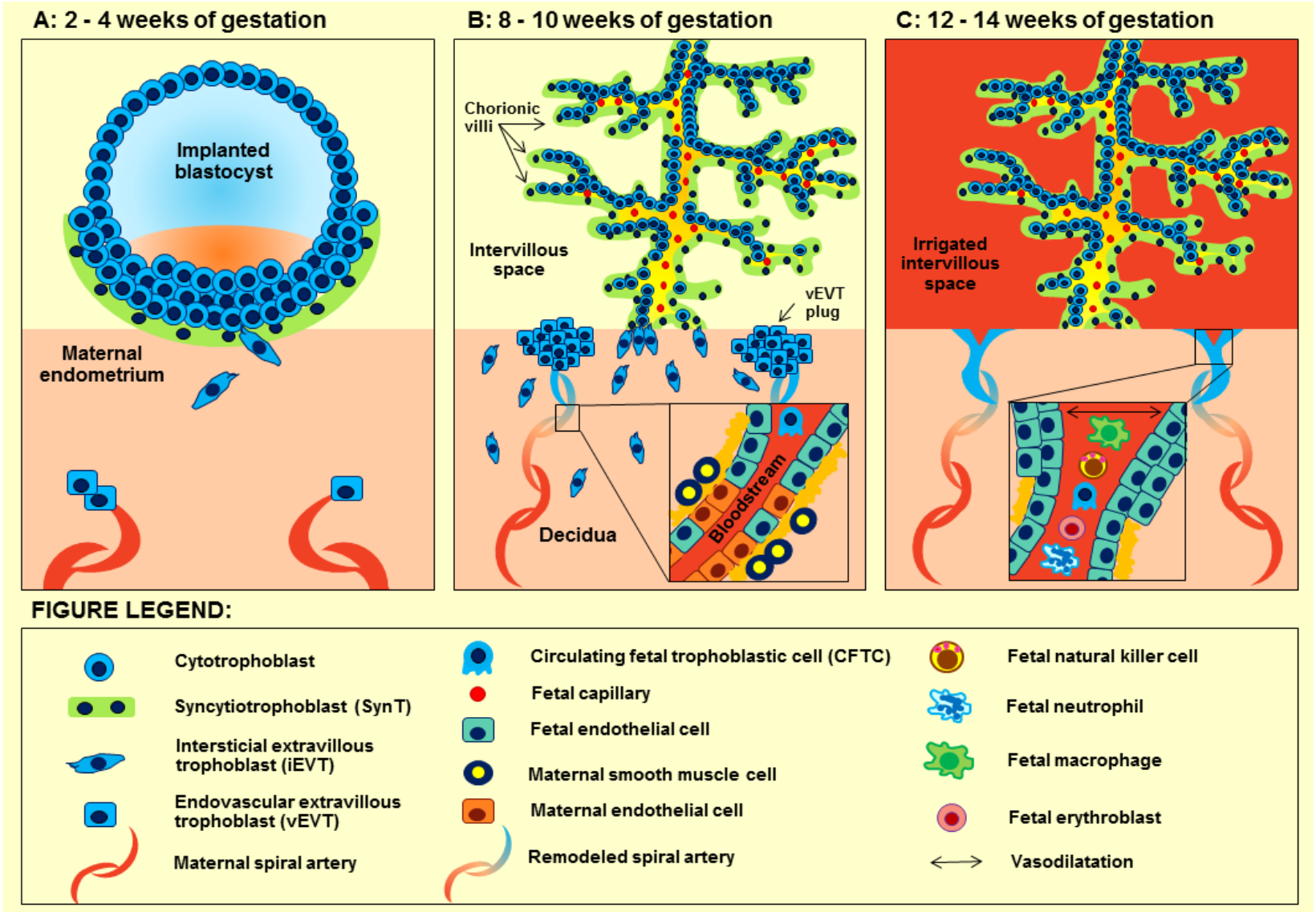

Notably, using ISET® filtration to study the kinetics of CFTC in weekly-drawn blood samples from pregnant mothers between the 4th and 12th week of gestation (WG), Mouawia and colleagues reported that CFTC could be reliably detected in all samples tested from as early as the 5th WG (Mouawia *et al.*, 2012). This latter study also reported striking results on the diagnosis of cystic fibrosis and spinal muscular atrophy via genetic analysis of filtration-enriched CFTC. By reaching 100% diagnostic sensitivity and specificity compared to invasive chorionic villus sampling (CVS) procedures in a cohort of 63 pregnant women, the study validated the possibility of using filtration-enriched CFTC for the early and non-invasive prenatal diagnosis (NIPD) of recessive single-gene disorders (Mouawia *et al.*, 2012).

3.2. Prenatal diagnosis

Historically, prenatal diagnosis of genetic disorders has primarily relied on the use of invasive procedures to recover fetal genetic material such as amniocentesis or chorionic villus sampling (CVS). Yet those invasive techniques bear well-known risks for fetal health, miscarriage being the most severe outcome occurring in up to 1% of pregnant mothers tested invasively at mid-pregnancy and with even higher incidences when invasive procedures are performed at early gestational ages, namely before 10 WG for CVS and before 15 WG for amniocentesis (Tabor and Alfirevic, 2010). Consequently, for amniocentesis, because test results are generally not available before the 16th WG, termination of pregnancy (TOP) in cases of unfavorable diagnoses requires relatively heavy and stressful medical procedures. In this context, implementing non-invasive methods into routine clinical practices in order to replace or at least reduce the need for invasive procedures has been a long-standing goal in the field and it is only now beginning to reach success for a limited array of genetic disorders.

Clinically applied strategies for routine non-invasive prenatal testing (NIPT) currently rely exclusively on the detection and analysis of cell-free fetal DNA (cffDNA) that can be found in maternal blood samples. Following its first description by Lo et al. in 1997 (Lo *et al.*, 1997), cffDNA has become

increasingly studied and valued for clinical application, especially owing to a recent burst of technological advances, among which high throughput next-generation sequencing (NGS) and droplet digital PCR (ddPCR) have proven most useful in reducing false or inconclusive results (Lench *et al.*, 2013). In a recently published meta-analysis, cffDNA-based NIPT was reported to bear diagnostic significance only when assessing fetal sex and rhesus D status, with estimated sensitivity levels of 98.9% and 99.3% as well as specificities of 99.6% and 98.4% respectively (Mackie *et al.*, 2017). Although evaluating those parameters for the detection of trisomy 21 and trisomy 18 through the same approach yielded very similar if not higher performances, this latter study highlighted the need to confirm positive NIPT results for those aneuploidies by invasive methods because of potential false-positive results arising from confined placental mosaicism. Moreover, detection of trisomy 13 and monosomy X by the same approach displayed lower sensitivity levels, reaching just above 90% and 92% respectively. The authors therefore concluded that despite its undeniable value as a screening test, the search for aneuploidy disorders by cffDNA-based NIPT cannot currently bear diagnostic significance (Mackie *et al.*, 2017). Nevertheless, even as a preliminary screening test, NIPT applied to the detection of trisomy 21 has already demonstrated its significant clinical utility by restricting the need for invasive prenatal procedures to pregnancies for which three distinct alleles of a genetic marker located on the 21st chromosome can be found in cffDNA by NIPT (Lench *et al.*, 2013). However, to insure the absence of false negative results of aneuploidy detection by NIPT, cffDNA levels in maternal blood must exceed 4% of the total cell-free DNA (cfDNA) load in the sample which contains a large majority of maternal DNA. Accordingly, NIPT is currently restricted to tests performed from 10 WG onward, when cffDNA levels generally span 4-10% of the total cfDNA content of plasma samples (Jain *et al.*, 2016). It is also important to note that, despite the tremendous technological progress already achieved, current methods for cffDNA analysis do not allow for an accurate detection of maternally-inherited single-gene disorders, nor that of complex chromosomal rearrangements such as large chromosomal deletions or duplications, inversions, balanced or unbalanced translocations and also struggle with the presence of low or confined

mosaicism causing false-positive aneuploidy screening results (Hayata *et al.*, 2017).

In contrast, intact fetal cells collected non-invasively represent a source of pure and complete fetal genomes that could inform on an extended variety of genetic disorders and as early as 5 WG (Mouawia *et al.*, 2012). In agreement, the recent publication from Breman and colleagues serves as a proof of concept that large chromosomal deletions and confined placental mosaicism can be accurately detected by high-throughput analyses (NGS and array CGH) performed on CFTC after density gradient centrifugation of maternal blood samples (Breman *et al.*, 2016). Furthermore, increased numbers of fetal cells in maternal blood samples have been associated to specific genetic anomalies, such as trisomy 21 which relates to a release of 3-5 times more fetal cells in the maternal circulation than normal pregnancies (Krabchi *et al.*, 2006). Detecting trisomy 21 in fetal erythroblasts and fetal trophoblasts collected non-invasively can be achieved through comparative genomic hybridization (CGH) (Yang *et al.*, 2006), fluorescence in situ hybridization (FISH) using chromosome-specific probes (Yang *et al.*, 2003) and more recently targeted multiplex NGS analysis (Jain *et al.*, 2016).

And finally, since preeclampsia is associated with an increase in both cffDNA and CFTC release in the blood, with a specific median amount of trophoblasts per milliliter of blood from the uterine vein reported as 37 times higher in preeclamptic pregnancies compared to control cases (Hahn *et al.*, 2005), implementing CFTC analysis in clinical settings could complement cffDNA-based NIPT and help to reach diagnostic significance for a wider range of fetal conditions. Indeed, CFTC have a great potential to help furthering clinical applications of NIPD and it is important to note that trophoblastic cells can also be recovered from the cervix during the first trimester of pregnancy, thus potentially offering additional material for prenatal diagnosis (Imudia *et al.*, 2009).

The work presented hereafter was conducted as part of a collaborative effort bridging public research and private commercial interests for the purpose of developing reliable methods of molecular analysis suited for single-cell characterization of ISET®-enriched circulating rare cells (CRC) and destined to applications in predictive oncology as well as non-invasive prenatal diagnosis (NIPD).

Methods & Results

1. Single cells analysis of CRC isolated by ISET® for non-invasive prenatal diagnosis (NIPD)

In the context of non-invasive prenatal diagnosis, single-cell molecular analysis constitutes an important prerequisite for the reliable identification of fetal trophoblastic cells because there is currently no unique cytological marker known to be specific to all human trophoblasts. Previous work from our scientific team demonstrated that amplification of short tandem repeat (STR) markers from single CFTC enriched by ISET® enables both the molecular validation of their fetal nature and an accurate diagnosis of recessive genetic disorders such as cystic fibrosis (CF) and spinal muscular atrophy (SMA) (Mouawia *et al.*, 2012). CF is an autosomal recessive inherited disorder caused by mutations in the gene coding for the cystic fibrosis transmembrane regulator (CFTR) and bearing frequent lethal implications for affected individuals (Saker *et al.*, 2006). Following CF, SMA is the second most common recessive disease which arises in the vast majority of cases from homozygous deletions of the spinal motor neuron (SMN) gene: SMN1 while 4% of cases are caused by concomitant heterozygous deletion and inactivating mutation of each SMN1 allele respectively (Béroud *et al.*, 2003).

The main challenge regarding CFTC analysis relates to their extremely low abundance in the bloodstream, a particular feature that is common to all CRC. In order to ensure a maximum recovery of trophoblastic cells via non-invasive procedures, we sought to introduce non-invasive collection of fetal trophoblasts from the cervix of pregnant women. Cells recovered from the cervix were transferred to ISET® filters and subjected to molecular analysis, as described in the methods section of the following publication (Pfeifer *et al.*, 2016).

(http://dx.doi.org/10.1016/j.placenta.2015.11.002)

Cervical Trophoblasts for non-invasive single-cell genotyping and prenatal diagnosis.

I. Pfeifer[1]*, A. Benachi[2]*, A. Saker[1], J. P. Bonnefont[3], H. Mouawia[1], R Frydman[4], M. L. Brival[5], B. Lacour[6], R. Dachez[7], P. Paterlini-Bréchot[1,6]#, L. Broncy[1]

1 INSERM Unit 1151 - team 13, Paris Descartes University, Paris, France

2 Department of Gyncology, Antoine Béclère Hospital, Clamart, France

3 Laboratory of Medical Genetics, Necker-Enfants Malades Hospital, Paris, France

4 Department of Reproduction, Foch Hospital, Suresnes, France.

5 Department of Maternity, Les Lilas, France

6 Laboratoiry of Biochemistry A, Necker-Enfants Malades Hospital, Paris, France

7 Alfred Fournier Institute, Paris, France

*Authors I. Pfeifer[1] and A. Benachi[2] contributed equally to this work.

Corresponding author: P. Paterlini-Bréchot

E-mail: patriziapaterlini@gmail.com

Address: Unité Inserm Unit 1151 – équipe 13, Université Paris Descartes, Bâtiment Leriche, Porte 14, 14 rue Maria Helena Vieira Da Silva, 75014 Paris, France.

Tel: +33(0)172606461; Fax: +33(0)172606460

Short title: Cervical Trophoblasts for Non Invasive Prenatal Diagnosis

Key words: ISET®, trophoblasts, non-invasive prenatal diagnosis, cystic fibrosis, spinal muscular atrophy

ABSTRACT

Objective

We aimed at developing a method to recover trophoblastic cells from the cervix through a completely non-invasive approach and obtaining a genetic proof of their fetal nature implying that they can be used for non-invasive prenatal diagnosis (NIPD).

Methods

We studied obstetrical samples from 21 pregnant women between 8 and 12 weeks of gestation scheduled for chorionic villus sampling or undergoing elective termination of pregnancy. A cytobrush was used to extract cells from the external parts of the cervix and transferred to 10 ml of preservative solution. Cells were layered on filters with 8 micron pores using the ISET system (Isolation by SizE of Tumor/Trophoblastic cells) and stained. Putative fetal cells were collected by single cell laser-assisted microdissection and identified as fetal or maternal cells by Short Tandem Repeat genotyping. NIPD was blindly performed on 6 mothers at risk of having a fetus with Cystic Fibrosis or Spinal Muscular Atrophy.

Results

Trophoblastic cells were recovered from all tested cervical samples with a frequency of 2 to 12 trophoblasts per 2 ml. NIPD was blindly obtained and verified in 6 mothers at risk of having a fetus with Cystic Fibrosis or Spinal Muscular Atrophy.

Discussion

Although larger confirmation studies are required, this is the first report providing a solid proof of principle that trophoblasts can be consistently and safely recovered from cervical samples. Since they are a source of pure fetal DNA, i.e. fetal DNA not mixed with maternal DNA, they constitute an ideal target to develop NIPD of recessive diseases, which is a technical challenge for methods based on cell free DNA.

INTRODUCTION

In order to avoid the risk of miscarriage linked to amniocentesis and chorionic villus sampling (CVS) [1], fetal DNA can be, in principle, retrieved non-invasively from three sources: circulating fetal cells in maternal blood [2], transcervical trophoblastic cells [3] and cell-free fetal DNA in maternal blood [4]. The analysis of cell-free fetal DNA has allowed developing reliable non-invasive tests for prenatal detection of aneuploidies [4]. However, the use of cell-free fetal DNA, which is mixed with maternal cell-free DNA in variable proportions, for non-invasive prenatal diagnosis (NIPD) of single-gene disorders and recessive diseases is particularly challenging [5]. In this setting, targeting genetic tests to the pure fetal DNA contained in fetal cells remains an attractive aim.

The presence of fetal cells in the endocervix was first demonstrated by Shettles in 1971 [6]. However, until now the rarity of these cells and the difficulty to collect them through a completely non-invasive approach has prevented their implementation for NIPD. Different methods, all collecting fetal cells from the inner part of the cervix and/or the lower pole of the uterine cavity, called transcervical cell (TCC) sampling, were developed, including: intrauterine lavage, endocervical lavage, endocervical mucus aspiration as well as endocervical sampling by a cytobrush [7-17,18]. Studies have established

that uterine and endocervical lavage are the most effective methods to yield fetal cells as early as 5 weeks of gestation [3,7-11]. All these methods however present one major risk: fetal loss [3,19,20]. On the one hand, samples were collected immediately prior to termination of pregnancy in the majority of studies, hence their safety has not been sufficiently examined. On the other hand, establishing the sampling method's safety on a large casistic is difficult for evident reasons. These observations prompted us to test another approach. We reasoned that the Papanicolaou (PAP) test is currently performed on pregnant women during the first trimester of pregnancy [21], and that its safety has been extensively demonstrated throughout the world. Our aim was to test if this sampling approach could consistently detect trophoblastic cells. Interestingly, no study using the PAP-test sampling method to collect cervical trophoblasts had been previously reported.

We also combined this method with our genetic approach to reliably identify trophoblastic cells in blood [22] and avoided the use of antibodies which could lower the sensitivity of trophoblasts detection.

In this study, we aimed at developing a completely non-invasive method to recover trophoblastic cells from the cervix and obtaining a genetic proof of their fetal nature implying that they can be used for non-invasive prenatal diagnosis (NIPD).

MATERIALS AND METHODS

We have tested 21 pregnant women at risk for having a baby affected by CF or SMA (between 8 and 12 weeks of gestation, including 6 (Necker-Enfants Malades Hospital Paris, France) tested immediately before CVS) and 15 women tested before elective termination of pregnancy (Antoine Béclère, Clamart Hospital, France; Maternity "des Lilas", Les Lilas, France).

Cells were obtained with the use of a cytobrush, but unlike the reported TCC sampling methods [3], the brush was not inserted into the endocervical canal but rather rotated at the external os, as done during a routine PAP test. Cytobrushes were transferred to 10 ml of a specific preservative solution (Cytrofix, Rarecells® Diagnostics, Paris, France). We also obtained 1 ml of blood (collected on EDTA) from each woman and from the father for genomic DNA extraction and testing.

ISET was carried out as previously described [2, 22-25] with only minor modifications. In order to layer the cells and eliminate the liquid 1 ml of each Cytofix sample was diluted 50 fold in bi-distilled, sterile water and subsequently filtered through the Rarecells® Device using a Rarecells® consumable containing an 8 microns pores filter (Rarecells® Diagnostics, Paris, France; www.rarecells.com). The filter was then stained with a 0.1 % nuclear fast red stain/5 % aluminium sulphate solution (Sigma-Aldrich, St. Louis, MO, USA), incubated for 2 minutes and then thoroughly rinsed with water. Filters were dried on air.

We examined the morphology of cytotrophoblasts by microdissecting putative cytotrophoblasts and analyzing them by short tandem repeat (STR) genotyping. Single cells displaying a cytotrophoblast-like or syncytiotrophoblast-like morphology were retrieved from the filters by laser-capture microdissection using the Nikon TE 2000-U (Nikon Paris, France and MMI Zurich, Switzerland) laser-equipped microscope. Each single cell was lifted from the filter and transferred onto the lid of a microfuge tube suited for PCR.

Each microdissected cell was lysed in 15 µL of lysis buffer (100 mmol/L Tris-HCl, pH 8; 400 µg/mL proteinase K) for 2 h at

60°C, followed by proteinase K inactivation at 94°C for 15 min. For primer extension preamplification (PEP) [26], to the lysed cell we added 5 µL of a 400 µM solution of random primers (Kit genPEP 75 OD, Genetix, Boston, USA), 6 µL of PCR buffer (25 mM MgCl2/gelatin (1 mg/mL), 100 mM Tris-HCl, pH 8.3, 500 mM KCl), 3 µL of a mixture of four dNTPs (each at 2 mM) and 1 µL (5 U) of Taq polymerase (Applied Biosystem, Foster City, CA, USA) in a final volume of 60 µL. Single-cell genotyping was performed to identify cells having a fetal genome by using STR primers found to be informative through the analysis of paternal and maternal genomic DNA. For genotyping we used 10 different sets of STR genotyping primers from 10 selected STR regions shown in Table 1. Amplification was performed in 60 µL containing 6 µL of the PEP product, 10 mM Tris-HCl, 50 mM KCl, 2.5 mM MgCl2, 200 µM of each deoxynucleotide, 0.5 µM of each STR 'outer' primer and 2 U of Taq Gold (Applied Biosystems, Foster City, CA, USA). 2 µl of a 1:10 diluted PCR outer product were re-amplified in a nested PCR in 20 µL final volume using 'inner' fluoresceinated STR primers and the same PCR protocol. One µL of the 1:20 diluted inner PCR product (amplicon) was then mixed with 13.5 µL of deionised Hi-Di formamide and 0.5 µL of Genescan 400 HD (ROX) marker (Applied Biosystems) and loaded into an ABI Prism 3100 automated sequencer (Applied Biosystems). Profiles were analyzed using the Genescan and Genotyper software programs (Applied Biosystems).

The NIPD of CF and SMA was performed blindly and carried out as described in other studies [2,24,25].

Invasive diagnoses were carried out at Hôpital Necker-Enfants Malades, Laboratoire de Génétique Médicale, Paris, France.

RESULTS

We screened a total of 21 cervical samples from pregnant women at risk for having a baby affected by CF or SMA between 8 and 12 weeks of gestation, including 6 tested before CVS, and 15 undergoing elective TOP. In all cases cervical samples were obtained by cytobrush exclusively at the level of the external os, as in the completely safe PAP test. As shown in Figure 1B, an exocervical squamous epithelial cell (marked with an arrow) is easily morphologically recognized in microscopic images. We were looking for cells displaying a cytotrophoblast-like morphology: round cells with large, irregular hyperchromatic nuclei (Figure 1A).

However, some rare maternal endocervial cells and fetal cytotrophoblasts may have a similar morphology and are therefore much harder to differentiate morphologically (see Figures 1A and 1B) without genetic tests. Fetal genotypes were all verified by fluorescent PCR analysis of informative STR markers (Figure 1C, Table I). Syncytiotrophoblasts were very rarely found (Table I). They have dense nuclei and are multinucleated (Figure 2).

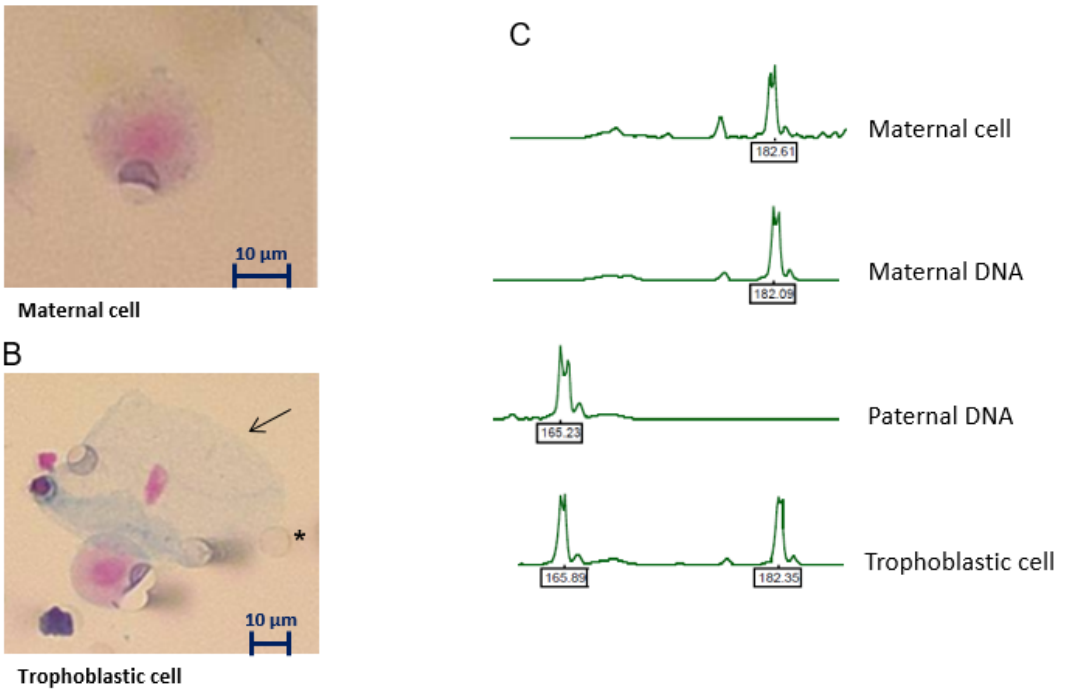

Figure 1.
Detection of a maternal cell (A) and a fetal cell (B) in a sample collected non-invasively from the cervix. Nuclei were colored with nuclear red stain. Marked with an arrow (B) is an exocervical squamous epithelial cell which is easily distinguished from smaller fetal and maternal cells (magnification x 40). An asterisk (B) indicates one of the 8-µm-diameter cylindrical pores on the ISET® filter.

Genetic profiles (C), obtained by single-cell genotyping with the informative STR marker D21S1435. Profiles show that the cell in A is maternal, and that the cell in B is fetal (trophoblastic) as compared to the maternal and paternal DNA

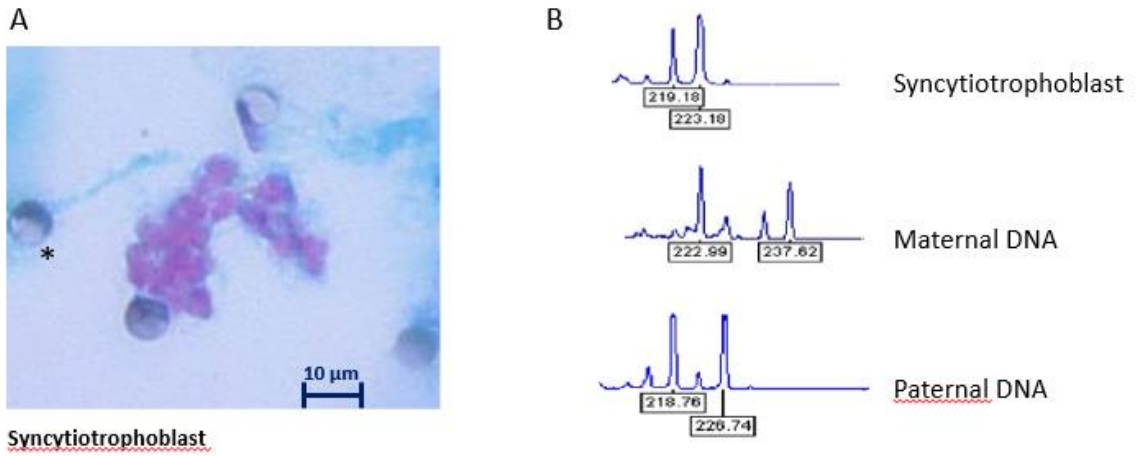

Figure 2.
Detection of a syncytiotrophoblast (A) in a sample collected non-invasively from the cervix. Nuclei were colored with nuclear red stain (magnification x 40). Its genetic profile obtained through STR-genotyping with the D21S11 STR marker is fetal (trophoblastic) as compared to the maternal and the paternal DNA (B).

Table I. Isolation of fetal cells from 21 cervical samples obtained non-invasively and exemplary non-invasive prenatal diagnoses (NIPD) of cystic fibrosis (CF) and spinal muscular atrophy (SMA).

Couple	Term of pregnancy (WG)	Informative STR marker	Cytotrophoblasts/ Syncytiotrophoblasts* - NIPD**	N° of microdissected cells
1(CF)	12	D7S486/D7S523	4 - carrier	10
2(CF)	12	D7S523	6 - carrier	12
3(CF)	12	D16S539/D7S523	10 - carrier	19
4 (SMA)	12	D5S816/D21S1437	6 – not affected	13
5 (SMA)	12	D21S1435	10 – not affected	21
6 (SMA)	12	D16S539/D7S523	6 – not affected	13
7#	12	D5S816/D21S1437	5	11
8#	12	D16S539	3/2	9
9#	11	D16S539/D5S816	4/2	10
10#	12	D21S1435	10	21
11#	12	D21S1435	6	14
12#	12	D16S3018	7	13
13#	12	D21S1435/D7S523	6	14
14#	12	D16S539/D5S816	2	6
15#	12	D21S11	8/2	16
16#	12	D16S539/D21S1435	12	21
17#	9	D16S3018/D5S615	6	12
18#	9	D5S615/D16S539	4	9
19#	8	D16S539/D5S816	4	10
20#	11	D16S539/D21S11	3	7
21#	8	D5S615/D5S816	3/1	8

*in 2 ml of sample ; WG: Week of Gestation; #TOP: Termination of pregnancy; **NIPD was consistent with invasive diagnosis

We identified fetal cells (either cytotrophoblasts or cytotrophoblasts and syncytiotrophoblasts) in all 21 samples, with a frequency of 2 to 12 fetal cells per 2 ml of sample (Table I). We found approximately 1 cytotrophoblast every two microdissected cells (Table I).

In order to show that our previously published protocols for NIPD of CF and SMA can be successfully applied to fetal cells isolated from the cervix, NIPD was blindly performed in six cases of pregnant women at risk for having a baby affected by CF or SMA (Table I). NIPD of CF was based on the presence or absence of the DelF508 mutated allele(s) as both parents in the 3 couples (Couples 1, 2 and 3, Table 1) were carrier of the DelF508 mutated allele [2,25]. We determined that all 3 fetuses were carriers of the DelF508 mutation. NIPD of SMA was carried out in fetal cells from couples 4, 5, 6 (Table I) using our previously published method [2,24]. We determined that none of the 3 fetuses was affected by SMA. Our analyses were performed blindly and results were consistent with those obtained by invasive prenatal diagnosis performed after CVS.

DISCUSSION

Our results show that trophoblasts, (also called trophectodermal cells) were recovered non-invasively from all tested 21 pregnant women and allowed blind NIPD in 6 mothers at risk of having a fetus with Cystic Fibrosis (CF) or Spinal Muscular Atrophy (SMA). The goal of our study was to determine if trophoblastic cells could be consistently isolated from the cervix using a completely safe sampling method. This goal implied using the PAP-test sampling approach, layering the collected cells on a filter by ISET, using cell morphology to target cells eligible for individual genotyping and identifying every trophoblastic cell by STR genotyping. No study had been performed in the past using a completely non-invasive collection method [3], proven to be safe by previous extensive and routine use. This is the case for the PAP-test sampling method collecting cells from the exocervix, which has been routinely performed on pregnant women for several decades [21].

Trophoblastic cells are thought to be shed from regressing chorionic villi in the uterine cavity, which disappears between 11 and 12 weeks of gestation following the fusion of the *decidua basalis* and *parietalis*, and from it towards the cervix [6,27]. Hence the possibility of collecting trophoblastic cells from cervix is expected to be transient and restricted to early terms of pregnancy.

We treated the samples with ISET, a technology developed in our laboratory, which layers the cells onto a membrane and poises them for single cell microdissection followed by STR genotyping. Using this approach, we were able to demonstrate the collection of trophoblastic cells in all tested cases through the analysis of only 2 ml of each 10 ml sample. We believe that the success of our approach is linked to several factors: we decided arbitrarily 1) to collect the cells using the PAP-test sampling approach, to ensure safety; 2) to filtrate the cells, to avoid their overlapping (and loss of detection of rare cells); 3) not to use antibodies to identify trophoblastic cells, to avoid loss of sensitivity; 4) to verify the fetal nature of putative trophoblasts through single cell STR genotyping.

We did not use antibodies to identify trophoblastic cells as we were concerned by the fact that these cells are very rare and that the use of antibodies would probably lead to the loss of some of them. In fact, it is thought that identification of fetal cells through immunological labeling is exposed to the risk of false positive and false negative results [28,29]. In the past several studies have used antibody staining and/or cell morphology without validation by molecular testing [11,30-32]. Two groups used immunolabelling with NDOG-1 antibody in combination with genetic analyses [18,33]. Whereas one of them [33] reported that only half of their samples contained fetal cells, the other showed detection of fetal cells in all 22 screened samples with a frequency of 5-10 fetal cells per sample [18] and found syncytiotrophoblasts in 116 of 207 (56%) TCC samples [18]. However, samples were obtained through endocervical mucus aspiration, a semi-invasive procedure carried out under general anesthesia immediately prior to termination of pregnancy. In other studies, employing antibodies anti-HLA-G [32, 34], samples were obtained with the least, but still invasive TCC sampling method, using a cytobrush inserted about 2 cm into the endocervical canal to retrieve cervical mucus. Although no direct adverse effects were observed, it can be imagined that pregnant women would be reluctant towards such TCC sampling. Imundia et al. [32] identified putative cytotrophoblasts in 35 out of 37 TCC samples but did not confirm their fetal nature by genetic analysis.

Bolnick et al. [34] used Y chromosome Fluorescence *In Situ* Hybridization (FISH) to validate the fetal origin of 99% of the cells they had retrieved. But since their FISH approach could only confirm fetal origin of throphoblastic cells retrieved from male fetuses, the author did not extend the study to the 9 female specimens identified amongst the 20 pregnancies tested. Choosing a different and entirely non-invasive approach, we used cell morphology to select cells for further genotyping analyses. In fact, we learnt about the morphology of cytotrophoblasts by microdissecting putative cytotrophoblasts and analyzing them by STR genotyping. We observed undeniably that fetal cells are generally smaller and have a smaller cytoplasm when compared to the majority of cervical maternal cells. By using this approach, we found 2 to 12 fetal cells per 2 ml of a 10 ml sample, potentially 10 to 60 trophoblastic cells per cervical sample.

Our pilot study shows that trophoblastic cells are located at the external zone of the cervix and can be consistently recovered by the PAP test sampling approach. This is a very encouraging news for collecting these precious rare cells without any risk for the fetus.

In summary, we have performed an original study which provides a proof of principle for consistent and safe collection of trophoblastic cells from cervical samples at an early stage of pregnancy and for their use in NIPD of recessive diseases. Although these results require a larger scale study to obtain further confirmation, this is the first report on a completely safe and successful approach to isolate trophoblastic cells from cervix aiming at non-invasive prenatal diagnosis testing. In particular, antibodies reported to be specific to trophoblastic cells should be tested in parallel with our approach not relying on antibodies to assess their efficiency and sensitivity for trophoblastic cells identification. This is clearly a key issue related to the cost of a potential future test and its possible “routinisation” [5]. However, exploring the diagnostic potential of fetal cells collected non-invasively seems a clinically interesting path, which could benefit from recent advances showing the use of Next Generation Sequencing for single blastomers’ molecular analyses [35].

ACKNOWLEDGEMENTS

This study was supported by grants from: PHRC program, Assistance Publique-Hôpitaux de Paris; Fondation Bettencourt-Schueller; INSERM (Institut National de Santé et Recherche Médicale), Université Paris Descartes, Association Anjou Mucoviscidose.

REFERENCES

[1] Mujezinovic F, Alfirevic Z. Procedure-related complications of amniocentesis and Chorionic villous sampling: a systematic review. Obstet Gynecol 2007; 110:687-694.

[2] Mouawia H, Saker A, Jais JP, Benachi A, Bussieres L, Lacour B, Bonnefont JP, Frydman R, Simpson JL, Paterlini-Brechot P. Circulating trophoblastic cells provide genetic diagnosis in 63 fetuses at risk for cystic fibrosis or spinal muscular atrophy. Reprod Biomed Online 2012; 25:508-520.

[3] Imudia AN, Kumar S, Diamond MP, DeCherney AH, Armant DR. Transcervical retrieval of fetal cells in the practice of modern medicine: a review of the current literature and future direction. Fertility and Sterility (Modern Trends) 2010; 93:1725-1730.

[4] Lo JO, Cori DF, Norton ME, Caughey AB. Noninasive prenatal testing. Obstet Gynecol Surv. 2014; 69:89-99.

[5] Lench N, Barrett A, Fielding S, McKay F, Hill M, Jenkins L, White H, Chitty LS. The clinical implementation of non-invasive prenatal diagnosis for single-gene disorders: challenges and progress made. Prenatal Diagnosis 2013; 33:555-562.

[6] Shettles LB. Use of the Y chromosome in prenatal sex determination. Nature 1971; 230:52-53.

[7] Ergin T, Baltaci V, Zeyneloglu HB, Duran EH, Ergenell MH, Batioglu S. Non-invasive early prenatal diagnosis using fluorescent in situ hybridization on transcervical cells: comparison of two different methods for retrieval. Eur J Obstet Gynecol Reprod Biol 2001;95:37-41.

[8] Cioni R, Bussani C, Bucciantini S, Scarselli G. Fetal cells in a transcervical cell sample collected at 5 weeks of gestation. J Mat-Fet Neonat Med 2005; 18:271-273.

[9] Cioni R, Bussani C, Scarselli B, Bucciantini S, Marchionni M, Scarselli G. Comparison of two techniques for transcervical cell sampling performed in the same study population. Prenat Diagn 2005; 25:198-202.

[10] Bussani C, Scarselli B, Cioni R, Bucciantini S, Scarselli G. Use of the quantitative fluorescent-PCR assay in the study of fetal DNA from micromanipulated transcervical samples. Mol Diagn 2004; 8:259-263.

[11] Kingdom J, Sherlock J, Rodeck C, Adinolfi M. Detection of trophoblast cells in transcervical samples collected by lavage or cytobrush. Obstet Gynecol 1995; 86: 283-288.

[12] Massari A, Novelli G, Colosimo A, Sangiuolo F, Palka G, Calabrese G, Camurri L, Ghirardini G, Milani G, Giorlandino C, Gazzanelli G, Malatesta M, Romanini C, Dallapiccola B. Non-invasive early prenatal molecular diagnosis using retrieved transcervical trophoblast cells. Hum Genet 1996; 97:150-155.

[13] Overton TG, Lighten AD, Fisk NM, Bennett PR. Fetus-Placenta-Newborn: Prenatal diagnosis by minimally invasive first-trimester transcervical sampling is unreliable. Am J Obstet Gynecol 1996; 175:382-387.

[14] Fejgin MD, Diukman R, Cotton Y, Weinstein G, Amiel A. Fetal cells in the uterine cervix: a source for early non-invasive prenatal diagnosis. Prenat Diagn 2001; 21:619-621.

[15] Cioni R, Bussani C, Scarselli B, Bucciantini S, Barciulli F, Scarselli G. Fetal cells in cervical mucus in the first trimester of pregnancy. Prenat Diagn 2003; 23:168-171.

[16] Sherlock J, Halder A, Tutschek B, Delhanty J, Rodeck C, Adinolfi M. Prenatal detection offetal aneuploidies using transcervical cell samples. J Med Genet 1997; 34:302-305.

[17] Falcinelli C, Battafarano S, Neri C, Mazza V, Ranzi A, Forabosco A. Analysis of fetal sex in TCC sample DNA: a contribution to the validation of this approach. Prenatal Diagnosis 1998; 18:1109-1116.

[18] Mantzaris D, Cram D, Healy C, Howlett D, Kovacs G. Preliminary report: correct diagnosis of sex in fetal cells isolated from cervical mucus during early pregnancy. Australian and New Zealand J Obstet Gynaecol 2005; 45:529-532.

[19] Chang SD, Lin SL, Chu KK, His BL. Minimally-invasive early prenatal diagnosis using fluorescence in situ hybridization on samples from uterine lavage. Prenat Diagn 1997; 17:1019-1025.

[20] Chou MM, Lin SK, Ho ES. Severe limb reduction defects after uterine lavage at 7-8 weeks' gestation. Prenat Diagn 1997; 17:77-80.

[21] Foster JC, Smith HL. Use of the Cytobrush for Papanicolaou smear screens in pregnant women. J Nurse Midwifery 1996; 41:211-217.

[22] Vona G, Beroud C, Benachi A, Quenette A, Bonnefont JP, Romana S, Munnich A, Vekemans M, Dumez Y, Lacour B, Paterlini-Bréchot P. Enrichment, immunomorpho-logical, and genetic characterization of fetal cells circulating in maternal blood. Am J Path 2002; 160:51-58.

[23] Vona G, Sabile A, Louha M, Sitruk V, Romana S, Schütze K, Capron F, Franco D, Pazzagli M, Vekemans M, Lacour B, Bréchot C, Paterlini-Bréchot P. Isolation by size of epithelial tumor cells: a new method for the immunomorphological and molecular characterization of crirculating tumor cells. Am J Pathol. 2000; 156:57-63.

[24] Beroud C, Karliova M, Bonnefont JP, Benachi A, Munnich A, Dumez Y, Lacour B, Paterlini-Bréchot P. Prenatal diagnosis of spinal muscular atrophy by gentic analysis of circulating fetel cells. Lancet 2003; 361:1013-4

[25] Saker A, Benachi A, Bonnefont JP, Munnich A, Dumez Y, Lacour B, Paterlini-Bréchot P. Genetic characterisation of circulating fetal cells allows non-invasive prenatal diagnosis of cystic fibrosis. Prenatal Diagn. 2006; 26:906-16.

[26] Zhang L, Cui X, Schmitt K, Hubert R, Navidi W, Arnheim N. Whole genome amplification from a single cell: implications for genetic analysis. Proc Natl Acad Sci U S A 1992; 89:5847-5851.

[27] Rhine SA, Cain JL, Cleary RE, Palmer CG, Thompson JF. Prenatal sex detection with endocervical smears: successful results utilizing Y-bodyfluorescence. Am J Obstet Gynecol 1975; 122:155-160.

[28] Bulmer JN, Cioni R, Bussani C, Cirigliano V, Sole F, Costa C, Garcia P, Adinolfi M. HLA-G positive trophoblastic cells in transcervical samples and their isolation and analysis by laser microdissection and QF-PCR. Prenat Diagn 2003; 23:34-39.

[29] Tjoa ML, Delli-Bovi L, Johnson KL, Bianchi DW. Antibodies to trophoblast antigens HLA-G, placenta growth factor, and neuroD2 do not improve detection of circulating trophoblast cells in maternal blood. Fetal Diagn Ther 2007; 22:85-89.

[30] Bussani C, Cioni R, Scarselli B, Barciulli F, Bucciantini S, Simi P, Fogli A, Scarselli G. Strategies for the isolation and detection of fetal cells in transcervical samples. Prenat Diagn 2002; 22:1098-1101.

[31] Fang CN, Kan YY, Hsiao CC. Detection of fetal cells from transcervical mucus plug before first-trimester termination of pregnancy by cytokeratin-7 immunohistochemistry. J Obstet Gynaecol Res 2005; 31:500-507.

[32] Imudia AN, Suzuki Y, Kilburn BA, Yelian FD, Diamond MP, Romero R, Armant DR. Retrieval of trophoblast cells from the cervical canal for prediction of abnormal pregnancy: a pilot study. Hum Reprod 2009; 24:2086-2092.

[33] Katz-Jaffe MG, Mantzaris D, Cram DS. DNA identification of fetal cells isolated from cervical mucus: potential for early non-invasive prenatal diagnosis. BJOG 2005; 112: 595-600.

[34] Bolnick JM, Kilburn BA, Bajpayee S, Reddy N, Jeelani R, Crone B, Simmerman N, Singh M, Diamond MP, Armant R. Trophoblast retrieval and isolation from the cervix (TRIC) for noninvasive prenatal screening at 5 to 20 weeks of gestation. Fertil Steril 2014; 102:135-42.

[35] Fiorentino F, Biricik A, Bono S, Spizzichino L, Cotroneo E, Cottone G, Kokocinski F, Michel CE. Development and validation of a next-generation sequencing-based protocol for 24-chromosome aneuploidy screening of embryos. Fertil Steril 2014; 101:1375-1382.

2. Single cells analysis of CRC isolated by ISET® for non-invasive predictive oncology

Despite the obvious improvements to mother and child care that NIPD promises to instore, my personal focus was initially drawn to predictive oncology because single-cell molecular analysis of CTC bears tremendous potential to further improve current medical practices through refined strategies for early detection of invasive cancers, personalized anticancer therapy and non-invasive real-time follow-up of the disease as well as to uncover new aspects of cancer biology, concomitant objectives that are in fact fundamentally connected and depend on each other for success.

Application to clear cell renal cell carcinoma (ccRCC) of the combined molecular and cytopathological analyses of single CRC isolated by ISET® was motivated by two important facts ascertained at the time this study was initiated. First, insights from other studies have shown that reliable identification and molecular analysis of CTC in the context of ccRCC presents substantial methodological and analytical challenges (Gradilone *et al.*, 2011; El-Heliebi *et al.*, 2013). And second, the reliable identification of CTC in ccRCC patients, although considered as a difficult task, appears to be a particularly relevant liquid biopsy approach also because cell-free circulating tumor DNA (ctDNA) has been shown to be barely detectable in plasma samples of ccRCC patients (Corrò *et al.*, 2017) We therefore analyzed the VHL gene sequence in individual CRC identified through cytomorphological assessment and classification following ISET® enrichment. The full spectrum of methods used and results obtained in this study can be found in the recently submitted article inserted hereafter.

Title: Single-cell genetic analysis helps to validate cytopathological identification of Circulating Cancer Cells in patients with Clear Cells Renal Cell Carcinoma.

Authors

1. Broncy Lucile (a)
2. Ben Njima Basma (b)
3. Méjean Arnaud (c)
4. Béroud Christophe (d)
5. Ben Romdhane Khaled (b)
6. Ilie Marius (e)
7. Hofman Veronique (e)
8. Muret Jane (f)
9. Hofman Paul (e)
10. Chaabouni Habiba (b)
11. Paterlini-Bréchot Patrizia (a) (g)

Affiliations:

(a): INSERM Unit 1151 team 13, Faculté de Médecine Paris Descartes, Paris, France.

(b): Genetics and Pathology Departments, University of Tunis, Tunis, Tunisia.

(c): Service d'Urologie, Hôpital Européen Georges Pompidou, Paris, France.

(d): INSERM Unit S910, Faculté de Médecine de La Timone, Université de médecine Aix-Marseille, Marseille, France.

(e): Laboratoire de pathologie clinique et expérimentale, Centre Hospitalo-Universitaire de Nice, Nice, France.

(f): Institut Curie, PSL Research University, Département d'Anesthésie Réanimation Douleur, Paris, France.

(g): Laboratoire de Biochimie A, Hôpital Necker-Enfants Malades, Paris, France.

Contact information:

Name: Patrizia Paterlini-Bréchot

Address: Faculté de Medecine Paris Descartes, Bâtiment Leriche - Porte 14

14 rue Maria Helena Vieira Da Silva - CS 61431, 75993 Paris Cedex 14

Phone number: +33 (0) 172 60 64 66

Facs number: +33 (0) 172 60 64 60

E-mail address: patriziapaterlini@gmail.com

Key-words: Liquid biopsy. Circulating Cancer Cells. ISET® technology. Clear cell Renal Cell Carcinoma. VHL mutation.

Abstract:

Context: Circulating Rare Cells (CRC) are non-haematological cells circulating in blood. They include, among other cells, Circulating Cancer Cells (CCC) and cells with uncertain malignant features (CRC-UMF) according to cytomorphological criteria. Clear cell Renal Cell Carcinomas (ccRCC) frequently bear a mutated Von Hippel-Lindau (VHL) gene.

Aim: Blind genetic analysis of CRC and tumor samples to help cytopathological decision.

Methods: 30 ccRCC patients gave blood for CRC isolation by ISET® (Isolation by SizE of Tumour/Trophoblastic cells). CRC cytopathological and single-cell VHL mutation analyses were performed blindly and compared to VHL mutation analysis of tumor tissues and normal leukocytes.

Results: 29/30 patients harboured CRC (20 harboured CCC, 29 CRC-UMF) and 25/29 patients carried VHL mutations in their tumour tissue. 205 single CRC (64 CCC, 141 CRC-UMF) provided genetic data. 57/57 CCC and 104/125 CRC-UMF from the 25 patients with VHL-mutated tumor carried the same VHL mutation detected in the tumorous tissue. Seven CCC and 16 CRC-UMF did not carry VHL mutations but were found in patients with wild-type VHL tumor tissue.

Conclusions: All the CCC and 83,2% (104/125) of the CRC-UMF were found to carry the same VHL mutation identified in the corresponding tumorous tissue, thus helping to consider these CRC-UMF with inconclusive cytological diagnosis as cancer cells.

Introduction:

Circulating Rare Cells (CRC) are rare and heterogeneous cells circulating in blood and deriving from organs. They include circulating tumors cells (CTC) as well as non-tumorous, non-haematological cells, mainly of epithelial or endothelial origin (to be distinguished from cancer cells).

CTC represent an accessible source of tumor material for monitoring tumor invasion and response to treatment, and for detecting predictive molecular biomarkers to identify patients eligible for targeted treatments.

CTC can be isolated either by marker-dependent or -independent technologies. Importantly though, because CTC populations consist of very heterogeneous phenotypes and may express epithelial markers, or mesenchymal markers or sometimes both [1–3], markers alone are barely diagnostic and cytopathology remains the reference method for circulating cancer cells diagnosis. [4] Furthermore, marker-dependent isolation approaches may lead to selection biases, false positive and false negative results. [4–6] Isolation by SizE of Tumor/Trophoblastic cells (ISET®) is a marker-independent technology that relies on the fact that blood cells are the smallest cells in the body, thus on the larger size of CRC including all types of cancer cells derived from solid cancers. CRC are retained on a filter, while erythrocytes are lysed and the majority of leucocytes are lost through the 8 µm pores. [7] This permits a very sensitive isolation of CRC from blood, without marker-related bias, keeping them intact, thus allowing their cytopathological diagnosis, and further immunomorphological and molecular analysis. The superior sensitivity of ISET® has been demonstrated by independent studies both in vitro [2,8–10] and in vivo, [11] including in comparative tests (reviewed in [12]).

In this setting, since the term circulating tumor cells (CTC) has been applied to cells extracted from blood using epithelial markers and is therefore associated to possible false positive and false negative results, the term circulating cancer cell (CCC) has been introduced to strictly designate cancer cells, of epithelial or mesenchymal origin, isolated from blood without bias and diagnosed by cytopathology. [4]

Under cytopathological analysis, CRC can be distinguished in CRC with malignant features (CRC-MF), also called Circulating Cancer Cells (CCC) and CRC with uncertain malignant features (CRC-UMF). Importantly, CRC isolated by ISET® can

undergo further characterization such as genetic analyses at single-cell level [7,12–16] which could help the cytopathological diagnosis in uncertain cases provided that the tumor displays tumor-specific genetic mutations.

Some leukemias are known to be characterized by specific mutations which are not present in non-tumor cells. Thus, the presence of a particular mutation not only confirms the diagnosis of leukemia but also identifies the leukemia's subtype. [17]

In the field of solid cancers, the knowledge about subtype-specific mutations is currently limited. However, the classification of sarcoma, previously based on the site of the tumor (bone or soft tissue), currently also relies on immunohistochemistry and detection, in selected cases, of mutations associated with specific histological subtypes. [18]

Furthermore, clear cell renal cell carcinoma (ccRCC), which accounts for approximately 75% of cases of renal cell carcinoma (RCC), [19] is characterized in up to 83% of cases by mutations of the Von Hippel-Lindau (VHL) gene. [20] Together with inactivating epigenetic alterations and loss of heterozygosity (LOH), VHL gene mutations contribute to more than 90% of patients exhibiting loss of function (LOF) of the VHL protein (pVHL). [21]

ccRCC is an aggressive form of RCC which typically presents with a highly vascularized stroma, haemorrhagic areas [22–24] and frequent intravenous tumor embolization [25] suggesting that CCC may represent interesting prognostic and predictive markers to monitor disease progression and response to therapy.

Furthermore, reliable identification of CCC in ccRCC patients, although considered as a difficult task [26], appears to be a particularly relevant liquid biopsy approach also because cell-free circulating tumor DNA (ctDNA) has been shown to be barely detectable. [27]

This study has been planned to assess the feasibility of helping a reliable diagnosis of CCC in ccRCC patients by combining CRC cytomorphological analysis with their single-cell VHL-targeted genetic analysis. Our results show that certain CRC-UMF carry the same mutation found in the tumor tissue, thus the uncertainty about their tumor nature can be solved and they can be considered as circulating cancer cells based on a combination of morphological and genetic data.

Results:

Genetic analysis of DNA from tumor tissues and corresponding leukocytes:

Tumor tissue DNA analyses from the 30 patients included in this study revealed that four patients (13.3%) had no detectable VHL mutations in their tumor samples. Interestingly, three patients (10%) harboured two simultaneous VHL mutations in their primary tumor sample, each located on a different exon of the VHL gene. The rest of the cohort presented single VHL mutations located either on exon one (33.4% of patients), exon two (13.3% of patients) or exon three (30% of patients) of the VHL gene. We identified 18 distinct VHL mutations including nine (50%) mutations located on exon one, four (22%) mutations on exon two and five (28%) mutations on exon three (**Table 1**), consistently with previous literature. [28,29] Genetic analysis of tumor DNA samples revealed that 38.9% of patients had deletions inducing frameshifts, 44.4% presented transversions and 16.7% harboured transitions (see **Table 1**). Importantly, all patients exhibited a wild type VHL gene sequence in the DNA from the corresponding single leukocytes tested as reference, demonstrating the accuracy of our molecular results and confirming the absence of germline VHL mutations in our cohort. Overall, 92 individually microdissected leukocytes gave informative data on all three VHL exons, providing at least three single cell controls per patient.

Table 1: Types of VHL mutations detected in ccRCC tumorous tissues

Exon, Codon	Detected in patient n°	Nucleotide change	Type of mutation (codon change)	Amino acid change	Zygosity	Predicted impact on pVHL functions	References in past litterature
1, 9	03	c.27G>T	Transversion (GAC>TAC)	D9Y	Heterozygous	Missense: Location on CpG island predicts impact on transcription initiation.	No published record, newly identified mutation
1, 18	01, 07	c.53C>A	Transversion (GCA>GAA)	A18E	Heterozygous	Missense: possibly pathogenic (binding to unknown target altered)	(Kishida *et al.*, 1995)
1, 61	09	c.183C>G	Transversion (CCC>CCG)	P61P	Heterozygous	Silent mutation: no functional impact	(Gallou *et al.*, 1999)
1, 65	20	c.194C>A	Transversion (TCG>TAG)	S65X	Heterozygous	Truncation: loss of all functions on one allele	(Gallou *et al.*, 1999)
1, 69	04	c.205-206delCG	Frameshift (CGC>delCG)	E69fsX62	Homozygous	Truncation: biallelic loss of all functions	(Gallou *et al.*, 1999)
1, 88	06, 19	c.263G>A	Transition (TGG>TAG)	W88X	Heterozygous	Truncation: loss of all functions on one allele	(Gallou *et al.*, 2001)
1, 92	12	c.275delA	Frameshift (GAC>delA)	D92fsX67	Homozygous	Truncation: biallelic loss of all functions	(Gallou *et al.*, 1999)
1, 100	27	c.299delC	Frameshift (ACG>delC)	T100fsX59	Homozygous	Truncation: biallelic loss of all functions	(Gallou *et al.*, 1999)
1, 109	08, 29	c.327delC	Frameshift (ATC>delC)	H109fsX50	Homozygous	Truncation: biallelic loss of all functions	(Gallou *et al.*, 1999)
2, 116	01	c.346C>G	Transversion (CTT>GTT)	L116V	Heterozygous	Missense: pathogenic (altered 3D conformation)	(Forman *et al.*, 2009)
2, 118	05, 10, 16	c.353T>C	Transition (CTC>CCC)	L118P	Heterozygous	Missense: pathogenic (HIF-1/2α accumulation)	(Forman *et al.*, 2009)
2, 140	21	c.418delC	Frameshift (CTC>delC)	L140fsX19	Homozygous	Truncation: biallelic loss of all functions	(Zhuang *et al.*, 1996)
2, 145	03	c.435G>T	Transversion (CAG>CAT)	Q145H	Heterozygous	Missense: pathogenic (HIF-2α accumulation)	(Miller *et al.*, 2005)
3, 158	23	c.472delC	Frameshift (CTG>delC)	L158X	Homozygous	Truncation: biallelic loss of all functions	(Razafinjatovo *et al.*, 2017)
3, 163	02, 14, 17	c.486delC	Frameshift (TGC>delC)	L163fsX7	Homozygous	Truncation: biallelic loss of all functions	(Razafinjatovo *et al.*, 2017)
3, 176	24	c.526A>T	Transversion (AGG>TGG)	R176W	Heterozygous	Missense: no functional impact on protein	(Gossage *et al.*, 2014a)
3, 183	04, 11, 26, 28	c.548C>A	Transversion (TCG>TAG)	S183X	Homozygous	Truncation: biallelic loss of all functions	(Zhou *et al.*, 2004)
3, 207	13	c.620C>T	Transition (GCA>GTA)	A207V	Heterozygous	Missense: pathogenic (unknown mechanism)	(Kanno *et al.*, 1997)

Cytopathological and molecular analysis of circulating rare cells (CRC):

Among the 30 patients included in this study, 29 had detectable CCC and/or CRC-UMF in their blood samples. From the 29 patients, 327 CRC were individually laser microdissected, their DNA was lysed and preamplified before targeted amplification of the three VHL exons. Among those 327 CRC, we obtained the amplification of the three VHL exons for 205 single cells, representing an amplification success rate of 62.7%.

Cytopathological reading performed before single cell laser microdissection allowed to classify the CRC as circulating cancer cells (CCC) or CRC-UMF as described in the Methods section. Based on cytopathology, 64 cells derived from 20 patients were classified as CCC and 141 cells from 29 patients as CRC-UMF. **Table 2** shows the clinicopathological characteristics of our patients. No correlation was found between the presences of CCC and/or CRC-UMF and clinicopathological data as the majority of our patients had early stage cancer and only two were metastatic patients.

Table 2: Patients characteristics

Clinical characteristics	Number of patients (%) (n = 30)
Tumor stage	
T1	17 (56.7 %)
T2	2 (6.7 %)
T3	7 (23.3 %)
Tx	4 (13.3 %)
Adenopathy	
No	21 (70.0 %)
N1	1 (3.3 %)
N2	1 (3.3 %)
Nx	7 (23.3 %)
Metastases	
M1	2 (6.7 %)
M0	28 (93.3 %)
Fuhrman nuclear grade	
I	4 (13.3 %)
II	13 (43.3 %)
III	8 (26.7 %)
IV	1 (3.3 %)
Unknown	4 (10.4 %)

Our molecular data, obtained blindly, validated the presence of a VHL mutation in 57 of the 64 CRC identified as CCC and in 125 of the 141 CRC identified as CRC-UMF by the cytopathologists. Examples of morphological and molecular profiles are shown in **Figure 1**.

Figure 1: Examples of morphological features of CRC with corresponding VHL alterations.

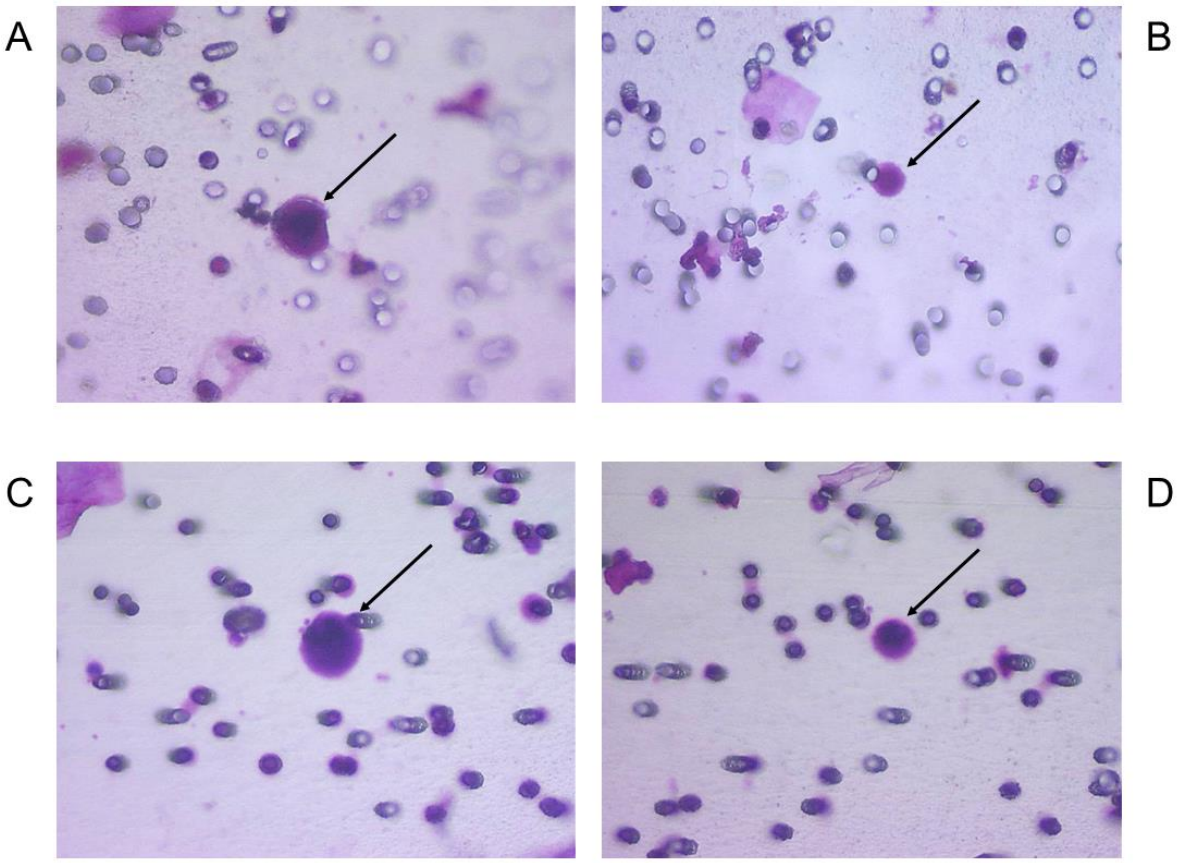

Legend: A: CCC with c.353T>C mutation; B: CRC-UMF with c.353T>C mutation; C: CCC with c.183C>G mutation; D: CRC-UMF with c.183C>G mutation; with black arrows pointing to each cell of interest.

The remaining seven CCC and sixteen CRC-UMF without VHL mutation were all found to derive from the four patients harbouring a wild type VHL sequence in their tumor tissue. Thus, while our molecular results showed a complete correlation of absence of VHL mutation in the tumor and in the CCC and CRC-UMF derived from the same patient, the 23 CRC derived from the four patients without VHL mutation in their tumor tissue could not help the diagnosis of CCC versus CRC-UMF. Remarkably, the type of VHL mutation detected in the 57 validated CCC as well as in 104 CRC-UMF correlated exactly with that detected in the corresponding tumor samples, raising the issue of the neoplastic nature of cells classified as CRC-UMF by the cytopathologists. We also found 21 CRC-UMF derived from 11 patients and exhibiting a distinct VHL mutational profile than that found in the corresponding tumor tissue, raising the issue of their tumor or possible pre-tumor nature.

At genetic level, from our 30 cases, 25 (83.3% of) tumor samples were characterized by mutations in the VHL gene. One hundred and sixty-one CRC (CCC and CRC-UMF) isolated from the blood of these 25 patients showed mutations of the VHL gene identical and 21 CRC-UMF displayed mutations of the VHL gene different from those detected in the corresponding tumor tissue. In these 182 CRC detected in 25 patients, we found 18 different VHL mutations affecting the three exons of the VHL gene: seven are missense mutations that induce an amino acid change within the VHL protein in eight (26.7% of) patients, one is a silent mutation with no effect at protein level found in a single patient, seven are deletions resulting in frameshifts and three are nonsense mutations that generate premature stop codons and result in a truncated VHL protein for 16 patients.

While nonsense mutations and frameshifts are generally considered to abrogate all functions of the VHL protein (pVHL), the significance of missense mutations requires further investigation because single amino acid changes affecting specific regions of pVHL may have an impact on distinct functions of the protein and result in distinct biological effects. **Table 1** also shows the analysis of each mutation's impact on pVHL function. All missense mutations along with two out of three nonsense mutations were found at heterozygous state, which can coexist with biallelic loss of VHL function since the remaining wild-type allele can be epigenetically silenced via promoter or intronic alterations.

Concerning the CCC, we found an identical VHL gene sequence in 100% of the CCC and corresponding tumor samples from the 20 patients, including two patients harbouring wild type VHL sequences in their CCC and corresponding tumor samples. Concerning the CRC-UMF, we found an identical VHL gene sequence in 85.1% of CRC-UMF and corresponding tumor samples from the 29 cases, including four patients harbouring wild type VHL sequences in all their CRC-UMF and corresponding tumor samples.

Interestingly, our cohort contained two patients who harboured two missense mutations in the tumor tissue as well as in each of the single CRC analysed. One of them exhibited both A18E (c.53C>A) and L116V (c.346C>G) mutations while the other had both D9Y (c.27G>T) and Q145H (c.435G>T) mutations. Since mutations A18E, L116V and Q145H have been shown to inactivate important regulatory functions of pVHL [30–32] (see Table 1) and considering that all missense mutations were found at heterozygous state in our cohort, it is possible that the tumor cells from these two patients harboured biallelic loss of VHL, with each VHL allele bearing a distinct missense mutation. This view implies that D9Y mutation significantly impairs pVHL functions, which is plausible since it affects the initial CpG island of the VHL gene. [33,34] However, further studies are needed to assess the functional impact of this previously undescribed missense mutation found in our cohort of ccRCC patients.

Among the 161 CRC (CCC and CRC-UMF) bearing concordant VHL mutational profiles with respect to paired tumor tissues, 97 cells (60.2 %) had mutations on the first exon, 36 cells (22.3 %) had mutations on the second exon, and 47 cells (29.2 %) had mutations on the third exon. Interestingly, double mutations were found in 19 of the 205 CRC analysed (9.3%), all belonging to three patients bearing the same double mutations in their tumor tissue samples. Examples of matching molecular profiles are shown in **Figure 2** and mutational status of all CRC compared to corresponding tumor samples are detailed in **Table 3**.

Importantly, our results show a 100% specificity of the cytopathological diagnosis of CCC, based on concordance of VHL genetic profiles obtained from all the CCC identified in 20 patients, including 2 patients with wild type VHL sequence in CCC and corresponding tumor samples. The reliability of our molecular approach was assessed through the analysis of at least three individual leukocytes per patient, serving as reference controls, all of which consistently demonstrated the absence of germline VHL mutations in our cohort. Additionally, we specifically designed our experiments in order to minimize the potential effects of allele drop out (ADO) on our molecular results (see Methods). Because ADO is stochastic and affects one or the other allele at a frequency of around 10%, it affects the same allele at a frequency of one in 20 analyses (5%). [26] Concerning both homozygous and heterozygous VHL mutations, the concordance of genetic profiles found in all 64 validated CCC and in 120 CRC-UMF compared to corresponding tumor samples (including for the patients harbouring a wild type VHL sequence in their CRC and corresponding tumor samples) indicates that our quality control of both WGA and PCR products were successful in minimizing the impact of ADO on our single-cell molecular results.

Table 3: VHL genetic profiles detected in CRC and corresponding tumor samples

Patient	VHL mutations found in primary tumor DNA	Number of single CRC	Number of CCC (CRC-MF)		Number of CRC-UMF		
			With same mutations as primary tumor	Without VHL mutation	With same mutations as primary tumor	With different mutations than primary tumor	Without VHL mutation
01	c.53C>A c.346C>G	8	5	0	3	0	0
02	c.486delC	10	7	0	3	0	0
03	c.27G>T c.435G>T	6	2	0	4	0	0
04	c.205-206delCG c.548C>A	5	4	0	1	0	0
05	c.353T>C	13	5	0	5	3	0
06	c.263G>A	17	2	0	13	2	0
07	c.53C>A	9	2	0	7	0	0
08	c.327delC	7	0	0	6	1	0
09	c.183C>G	18	10	0	7	1	0
10	c.353T>C	8	1	0	6	1	0
11	c.548C>A	8	2	0	5	1	0
12	c.275delA	2	0	0	2	0	0
13	c.620C>T	7	3	0	2	2	0
14	c.486delC	1	0	0	1	0	0
15	**Wild Type**	4	0	0	0	0	4
16	c.353T>C	1	0	0	1	0	0
17	c.486delC	8	1	0	7	0	0
18	**Wild Type**	3	0	0	0	0	3
19	c.263G>A	11	3	0	8	0	0
20	c.194C>A	15	3	0	8	4	0
21	c.418delC	6	0	0	4	2	0
22	**Wild Type**	9	0	5	0	0	4
23	c.472delC	2	1	0	1	0	0
24	c.526A>T	2	0	0	2	0	0
25	**Wild Type**	7	0	2	0	0	5
26	c.548C>A	4	3	0	1	0	0
27	c.299delC	6	1	0	3	2	0
28	c.548C>A	5	2	0	1	2	0
29	c.327delC	3	0	0	3	0	0

Patient	VHL mutations found in primary tumor DNA	Number of single CRC	Number of CCC (CRC-MF)		Number of CRC-UMF		
			With same mutations as primary tumor	Without VHL mutation	With same mutations as primary tumor	With different mutations than primary tumor	Without VHL mutation
TOTAL		205	57	7	104	21	16

Figure 2: Examples of matching DNA profiles

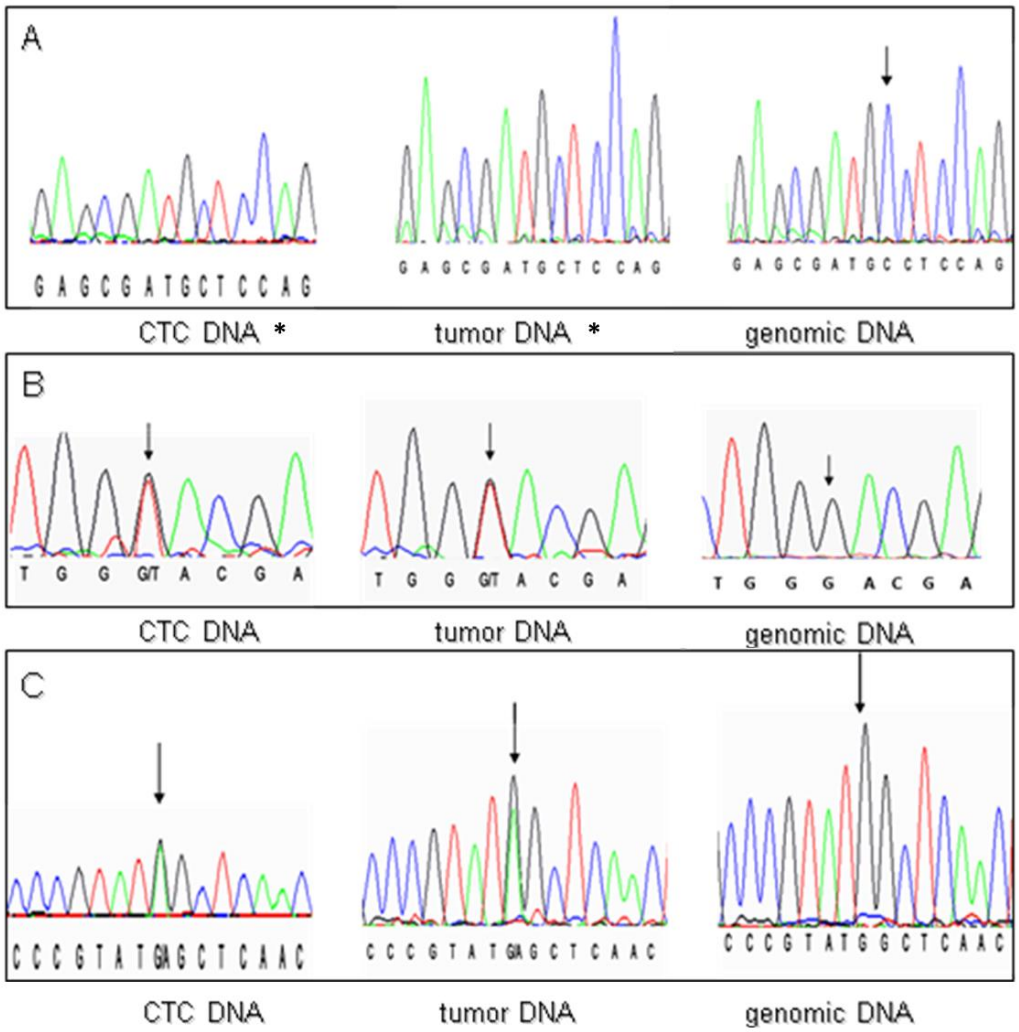

Legend: A: exon 3 codon 163; B: exon 1 codon 9; C: exon 1 codon 88.
Black arrows point to each nucleotide of interest, except when the nucleotide is deleted by the mutation (*)

In the attempt to use the genetic analysis of the VHL mutations as an indicator of the tumorous nature of CRC, we focused our analysis on the 25 patients having VHL mutations in the tumor tissue thus excluding the four patients with wild type VHL in the tumor and the single patient without CRC. At the cellular level, we also excluded the CRC-UMF found to harbour discordant VHL mutations with respect to paired tumor samples. We thus focused our study on 57 CCC and 104 CRC-UMF from our 25 patients (see **Table 4**).

Table 4: VHL-mutations detected in CRC according to their expected functional impact on pVHL

		VHL mutations expected to change pVHL function (n=23)	VHL mutations without expected impact on pVHL function (n=2)	Total number of informative patients (with VHL mutation in the tumor and CRC in blood) (n=25)
Number of patients	harboring CCC diagnosed by cytopathology	17	1	18
	harboring CRC-UMF with the same VHL mutation found in the tumor	23	2	25
	harboring CCC or CRC-UMF with the same VHL mutation found in the tumor	23	2	25
Number of single cells	classified as CCC by cytopathology	47	10	57
	classified as CRC-UMF & with the same VHL mutation found in the tumor	95	9	104
	classified as CCC or CRC-UMF with the same VHL mutation found in the tumor	142	19	161

Discussion:

The reliable identification of Circulating Cancer Cells (CCC) is a biomedical challenge with potentially highly relevant clinical implications. [4] While DNA mutations are recognized as a key element in cancer development and pathogenesis, cancer diagnosis is largely based on histopathological and/or cytopathological examination and assessment. However, the diagnostic identification of CCC in blood has to take into account the Circulating Rare Cells (CRC) morphological heterogeneity and the presence in blood of non-tumorous, non-haematological cells, mainly of epithelial or endothelial origin, to be distinguished from CCC. Cytopathological diagnosis is based on interpretation of cytological aspects by experts and would benefit from complementary immunomolecular information. [35]

In the present study, we used a cohort of 30 patients with clear cell renal cell carcinoma (ccRCC) and took advantage of the occurrence of VHL mutations in the tumorous tissue of 83.3% of them to match, at single cell level, cytopathological assessment and presence of VHL mutations. Our results show that the cytopathological diagnosis of CCC matches, in all cells, with the presence of a VHL mutation identical to that found in the tumor tissue, thus demonstrating the complete specificity of cytopathology performed by expert cytopathologists and taking into account strict morphological criteria (see Methods). Furthermore, our results show that the cytopathological diagnosis of CRC-UMF also matches, in a proportion of cells (83.2%), with the presence of a VHL mutation identical to that found in the tumor tissue, thus demonstrating that genetic studies can complete uncertain cytomorphological assessments and reveal the tumor cell nature of CRC.

RCC is a very invasive and chemoresistant disease which is often treated by surgical resection as it also responds poorly to radiotherapy. [36] Importantly, more than 30% of localized RCC recur or metastasize after treatment. [37] Even in RCC cases believed to be curable by radical nephrectomy, distant metastasis can develop 5-10 years after surgery. [38] The more frequent RCC subtype is referred to as "clear cell" carcinoma because of high lipid content in the cytoplasm of ccRCC cells which is washed away during staining procedures, resulting in observation of unstained or faintly eosinophilic

cytoplasms with well-defined membrane borders during pathological examination. [39] Clear cell RCC tumors typically present with a highly vascularized stroma and frequently show haemorrhagic areas. [22] It is noteworthy that ccRCC is also an aggressive form of RCC. [23,24] Evidences of long dormancy and high metastatic potential of ccRCC, together with frequent intravenous tumor embolization, sometimes extending to the inferior vena cava, [25] suggest that circulating and disseminated tumor cells (CTC, DTC) may represent interesting prognostic and predictive markers to monitor disease progression as well as patients' response to therapy.

However, only few studies have been published on DTC [40] and CTC analysis [25,32–37] in patients with sporadic ccRCC. This is partly because cancer cells from ccRCC patients are prone to EMT and often lack epithelial antigens, which impairs their capture from blood and analysis when epithelial marker-dependent selection/identification methods are used. [43,44] For example, using the CellSearch system (relying on the epithelial marker known as EpCAM for selection), Gradilone et al. detected CTC only in 16% of 25 metastatic ccRCC patients. [43] Consistently, using immunostaining of cytokeratins (CK8/18) after hematopoietic cell-depletion, Bluemke et al. found positive expression of CK8/18 in only 4.5% of 154 RCC patients while blood samples from another 38% of patients harboured CK-negative cells with large blue-stained nuclei. [44]

Several studies using density gradient blood centrifugation to recover mononuclear cells, followed by hematopoietic cell-depletion, have reported results on CTC identification when in fact those results profiled CRC of heterogeneous nature, possibly including circulating stem cells (CSC) and non-tumor cells of epithelial and/or endothelial origin. [44,45] The recent report by Nel et al. uncovered an extensive phenotypic heterogeneity among CRC derived from individual patients. [45] Interestingly, using both phenotyping- and gene expression-focused molecular approaches, these authors were able to correlate the presence of mesenchymal (N-cadherin-positive) and stem-like (CD133-positive) cells in blood with a decreased expression of genes coding for the first alpha subunit identified within hypoxia-inducible factors (HIF-1α) and the receptor for the vascular-endothelial growth factor (VEGFR) as well as with shorter progression-free survival (PFS) among the 14 metastatic RCC patients tested, including 12 ccRCC. [45] However, the lack of proper distinction between CTC and CRC, exemplified by the finding of "false" CTC in healthy controls, prompted Nel et al. to apply statistical cut-offs in order to distinguish healthy donors from the 64% of metastatic RCC patients exhibiting panCK-positive CRC.

An approach based on molecular data consists in detecting VHL gene alterations present in the peripheral blood of ccRCC patients. This analysis was done by Ashida et al. in a study where mutation-specific primers tailored to each individual ccRCC patient were designed for nested RT-PCR targeted to the pooled mononuclear cells extracted from blood by density gradient centrifugation. The authors reported a 75% concordance of the VHL gene alterations detected in peripheral blood with those obtained on matched tumor samples. [38] However, this approach is time-consuming as it requires the synthesis of specific molecular probes tailored to the mutation(s) found in the tumor tissue of each individual patient, and it would be difficult to implement in a routine clinical setting. Furthermore, it cannot provide the CTC count. Nonetheless, targeting the VHL gene appears as an interesting strategy for the study of CTC in ccRCC patients.

Loss of VHL function in humans has been correlated to cellular dedifferentiation, illustrated by a gain of expression of the mesenchymal marker vimentin in epithelial kidney cells. [46] This process is characteristic of an early EMT which favours acquisition of invasive properties of kidney cells and is induced by the biallelic inactivation of the VHL gene in humans, [47] but not in mice, [48] illustrating species-specific functions of the VHL protein (pVHL). Indeed, pVHL was first characterized as an effector mediating the proteolytic degradation of alpha subunits of hypoxia-inducible factors (HIF-1α and HIF-2α) through binding of Elongins B and C as stabilizing cofactors. [51–53] On its own, this hypoxia-related function of pVHL has tremendous biological impacts since HIF are potent transcription factors known to target over 800 genes.

[52] It is interesting to note that some missense VHL mutations may favour HIF-2α accumulation while others result in activation of both HIF-1α and HIF-2α since those transcription factors target different genes. [53]

However, subsequent studies identified numerous other functions of pVHL, including its putative contribution to immune surveillance by maintaining expression of the vascular cell adhesion molecule 1 (VCAM-1) in human kidney cells. [54] The multiplicity of pVHL roles (the major ones are depicted in **Figure 3** along with the main pVHL-binding cofactors) highlights the multimodal impact of the biallelic inactivation of VHL, [55] which occurs at an exceptionally high rate in sporadic ccRCC and mainly involves distinct genetic or epigenetic alterations of each copy of the VHL gene. Loss of heterozygosity (LOH) by deletion of the VHL locus on one allele of chromosome three (LOH at 3p) has been described to occur in over 90% of sporadic ccRCC tumors. [56] Thus VHL represents an interesting genetic driver of ccRCC, which importantly is absent from the genetic background of other RCC subtypes. [19,57,58]

Figure 3: Protein cofactors and major physiological functions of wild type pVHL reported in past literature for human kidney cells.

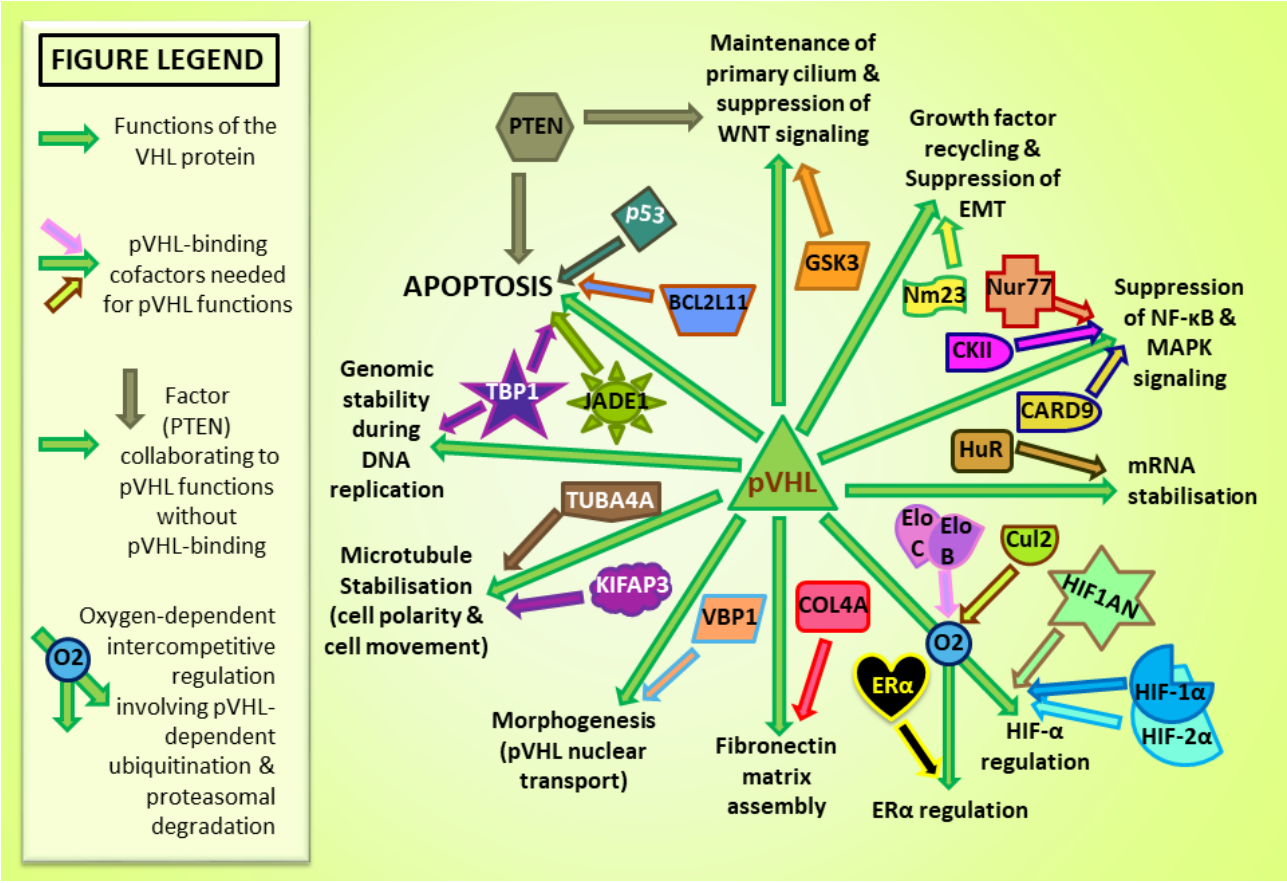

Legend: Green arrows represent links to pVHL functions and distinctly colored arrows converging with green arrows indicate pVHL-binding cofactors implicated in respective pVHL functions.

El-Heliebi et al. have isolated CRC from RCC patients by blood filtration and used a combination of morphological criteria and genetic analysis in the aim of identifying malignant cells. [26] Their conclusion is that, for patients with renal tumors, cytomorphological classification alone is not sufficient to allow for reliable detection of single CTC or clusters of CTC, also

called circulating tumor microemboli (CTM), and needs immunocytochemical and/or molecular methods. However, the authors do not provide any guide for identifying CTC or CTM as, in their study, molecular results are not consistent with immunological nor immunomorphological data. They found that all the CRC clusters identified in 30 RCC patients, including 25 ccRCC and 5 papillary RCC, were of endothelial origin, based on their CD31 positivity and only one was of tumor origin, based on carbonic anhydrase nine (CAIX) positivity, used as a marker of RCC-derived tumor phenotype. The authors also found that 5 out of 14 tested CRC with malignant phenotype were CAIX-positive while none of the clusters with malignant phenotype (and one of 16 with uncertain phenotype) was CAIX-positive. Furthermore, out of 12 CRC-clusters studied by GCH array, including 6 with tumor phenotype, only two showed CGH abnormalities, including one with tumor phenotype and one with uncertain phenotype, but in both cases the genomic abnormalities were different from those detected in the tumorous tissue. The authors thus failed to provide any guideline concerning detection of circulating tumor cells and tumor microemboli in patients wih RCC. [26]

It is to be noted that the morphological criteria used in the study from El-Heliebi et al. and applied to individual CRC were in fact less stringent than those described by Hofman et al. [59,60] Specifically, El-Heliebi et al. defined malignant individual cells as displaying at least three of five morphological criteria of malignancy whereas the "reference" definition of CCC published by Hofman and colleagues [59,60] relies on the presence of at least four of those same criteria (anisonucleosis (ratio >0.5), nuclei larger than three times the calibrated pore size of 8 µm (i.e. >24 µm), irregular nuclei, high nuclear/cytoplasmic ratio and presence of tridimensional sheets). It is noteworthy that a recent study on early lung cancer detection by Mascalchi and colleagues used the same filtration technique as El-Heliebi et al. but applied Hofman's criteria faithfully and demonstrated a 100% specificity of the cytopathological identification of CTC/CTM compared to diagnostic results of core biopsy or fine needle aspiration of suspicious pulmonary nodules. [61] Furthermore, in the study of El-Heliebi et al., CAIX immunostaining was used as a specific marker of RCC-derived tumor cells while CAIX can also be expressed in hypoxic or necrotic tissues regardless of their tumor origin. In fact, CAIX is a specific marker of HIF-1α accumulation as the CA9 gene encoding CAIX is transcriptionally activated by the HIF-1α transcription factor. [62,63] Indeed, HIF-1α accumulation characterizes a metabolic switch induced by the complete loss of functional pVHL. However, VHL alterations favouring HIF-2α accumulation would not cause this CAIX-positive phenotype among ccRCC patients. [64] The study by El-Heliebi et al. also included 5 papillary RCC and this subtype is not associated with LOH at 3p nor with CAIX expression. [23]

To note, Yang and colleagues analysed RCC and hemangioblastoma tumors associated with loss of pVHL function and discovered an inverse correlation between pVHL levels and CD31 expression, suggesting that CD31 expression may not be restricted to non-malignant endothelia and could also occur in tumor cells, a finding which has not been considered by El-Heliebi et al. [65] Thus, RCC-derived tumor cells with low expression of pVHL should be further investigated regarding possible concomitant expression of CD31.

Furthermore, Kats-Ugurlu et al. analysed tumor fragments in renal venous outflow of 42 ccRCC patients and determined that 33% of them harboured circulating clusters containing a core of cancer cells surrounded by an external coating of endothelial cells. [66] Importantly, this report confirms previous observations made by Sugino et al. regarding CD31-positive endothelia-coated tumor microemboli observed inside large blood vessels on sections of RCC tissues. [67]

Actually, the non-consistent CGH array results obtained on circulating cell clusters by El-Heliebi and colleagues are puzzling and difficult to explain. They could in part reflect the analysis of tumor-derived circulating endothelial cell clusters, since those circulating clusters have been described by Cima and colleagues to bear cytomorphological anomalies without corresponding tumor-associated genetic alterations in the context of early stage colorectal cancer. [68] Additionally, those

results could be related to the mixtures of endothelial and cancer cells, also possibly including other non tumor cells in the cluster like pericytes, smooth muscle cells, immune and stromal cells, as described by Kats-Ugurlu et al. in ccRCC blood samples, [66,69] in agreement with other publications focused on resected human ccRCC tumors [67] or murine xenograft models. [70] As suggested in the literature, [71–73] different quantitative contributions of each cell type to those heterogeneous clusters could potentially give rise to both balanced and unbalanced CGH array results such as those found by El-Heliebi and colleagues.

Taken together, these arguments challenge the conclusions of El-Heliebi and colleagues [26] and stimulate to perform further investigations.

In this setting, we carried out a comparative study, at single-cell level, of cytopathological diagnosis of CCC according to the reference criteria reported by Hofman et al. [59,60] and genetic analysis of VHL mutations. Consistently, our protocol included the genetic characterization, performed blindly, of the VHL gene in the CRC isolated by ISET® from 30 patients affected by ccRCC and, as controls, in the corresponding tumorous tissues, and several individual leukocytes.

The present study did not include healthy donors. However, 254 healthy donors have already been studied in our previously published contributions and CCC/CRC-UMF were not found in healthy donors. [14,59,60,74] .

CRC-UMF and CCC were identified by cytomorphological analysis in respectively 29 (96.7%) and 20 (66.7%) of the 30 patients included, using previously defined morphological criteria. [59,60] In this cohort, 25 (83.3%) patients harboured a mutated VHL gene in the primary tumor sample and allowed us to perform the comparison study in the CRC. Overall, 20 patients harboured CCC, including 2 with a wild type VHL gene in the tumor tissue, and 29 harboured CRC-UMF, with or without coexisting CCC, including 4 patients with a wild type VHL gene in the tumor tissue.

A 100 % correlation was observed between the diagnosis of CCC and the detection, by their single-cell analysis, of the same VHL sequence detected in the tumor tissue. Eighteen patients harbouring a VHL-mutated tumor tissue were found with the same VHL mutation in the CCC diagnosed by cytopathology, and 2 patients with a VHL-wild type tumor tissue were found with the same wild type VHL sequence in their CCC diagnosed by cytopathology.

VHL mutations were not found in CCC or in CRC-UMF derived from the four patients with the tumor lacking VHL mutation. Each of our 25 patients with VHL-mutated tumors exhibited CCC and/or CRC-UMF with VHL mutational profiles matching that of the tumor while 11 of those cases also presented a total of 21 CRC-UMF bearing distinct VHL mutations than that of the primary tumor. Among the 25 patients with a VHL-mutated tumor, no CCC nor CRC-UMF were found without VHL mutation.

Understanding the role of VHL mutations in driving ccRCC tumorigenesis is important to assess their diagnostic value, in particular when VHL mutations identical to those found in the tumorous tissue are also found in CRC classified as CRC-UMF according to cytopathological criteria.

VHL mutations are thought to represent the earliest events in ccRCC tumorigenesis. [46] However, although frequent, the VHL mutations presently known do not represent the full spectrum of genetic components that may drive the onset and subsequent development of sporadic ccRCC. [75] It is known that VHL mutations affecting pVHL functions invariably predate malignant transformation [46,76–81] and that VHL mutations can also be found in hyperplastic cells derived from human benign kidney lesions, [46] thus questioning their diagnostic significance as tumor marker. Studies focusing on patients affected by the hereditary VHL disease, which is defined by inactivation of one VHL allele at germline level and predisposes affected individuals to the occurrence of multiple types of malignancies, including ccRCC, [82] have shown that both malignant neoplasms and "benign" precursor cystic lesions of the kidney display complete loss of functional pVHL. [46,76]

In mice kidneys, the conditional biallelic inactivation of the Vhl gene in distal tubules and collecting ducts was found to elicit benign cystic lesions with severe concomitant fibrosis that were considered as precursors of ccRCC. [78,81] Interestingly, the same authors determined that benign Vhl-null lesions were mainly driven by HIF-1α activation while another study reported that a switch from HIF-1α to HIF-2α could be observed in VHL-null human kidney cells during malignant transformation of the precursor cystic lesions. [46]

However, once precursor lesions progress and patients are diagnosed with ccRCC, several reports have shown that genetic alterations of the VHL locus are the only ubiquitous drivers found to be identical in all regions of the tumor, including when comparing multiple metastatic sites to the primary tumor. [83–86] For instance, using multiregion sampling and high throughput deep sequencing to uncover intratumor heterogeneity (ITH), Gerlinger et al. determined that 75% of all driver aberrations found in each ccRCC patient were subclonal while VHL alterations, including LOH at 3p and epigenetic silencing, were the only ubiquitous events found across all 79 tumor sites sampled from 10 ccRCC patients. [85] Such observations are consistent with the role of VHL inactivation as a critical founder event in the majority of ccRCC.

In this context, our finding that 21 CRC-UMF from 11 patients exhibited discordant VHL mutational profiles when compared to corresponding tumor samples raises questions concerning the origin of those cells. Several hypotheses can be proposed to explain such results. It must be noted that up to 25% of patients with RCC are known to present with multifocal tumor at diagnosis and that genetic analyses performed on a cohort of 26 multifocal ccRCC cases revealed that 46% of those patients were in fact carrying several coexisting tumors of distinct genetic origins and separate intra-organ localization. [87] Thus, multifocal ccRCC tumors of distinct origins can be expected in approximately 11.5% of ccRCC cases and could in part explain a discordance of VHL mutational profiles found in CRC-UMF with respect to the specific tumor sample analysed.

On the other hand, those CRC exhibiting uncertain morphology and distinct genetic profiles from that of the tumor could also represent hyperplastic non-neoplastic cells derived from distinct precursor lesions of the kidney, since those can coexist with ccRCC and have been shown to directly result from VHL inactivation. [46,80] Therefore, the tumorous nature of these 21 CRC-UMF could not be proven by either cytopathology or VHL genetic analysis.

In order to analyse our results in depth, we stratified our ccRCC patients based on their VHL mutational profiles. As detailed in Table 4, complete loss of functional pVHL due to truncating homozygous VHL mutations was found in 13 patients (43.3%) of our cohort. These mutations, based on previous literature, [21,88–91] can be considered a molecular genetic hallmark of tumor phenotype. Thus, in these cases, not only the CCC but also all the CRC-UMF displaying the same VHL mutational profiles found in the tumor tissue are proven to be tumor cells. For this group of patients, cytopathological assessment of CCC bears complete (100%) specificity, while sensitivity is 61.5%, demonstrating that VHL mutational analysis could reliably complement and extend the capacity of cytopathology to identify tumor cells. This group of patients can be considered a model for circulating cancer cells diagnosis based on cytomorphological and molecular characteristics.

In another group of 10 patients (33%) we found in the tumor tissue VHL mutations inducing a partial loss of the VHL function, i.e. heterozygous inactivating VHL mutations (Table 4). It has to be considered that Kondo et al. studied a cohort of 202 ccRCC patients and found that a complete loss of pVHL function is significantly likely to occur in cases bearing functionally inactivating VHL mutations detected on one allele. [88] Furthermore, previous reports have identified inactivating splicing site mutations and promoter hypermethylation of VHL in a variable proportion of ccRCC cases. [20,76–78] In a cohort of 240 ccRCC patients, Sato and colleagues found LOH at 3p in 94% of cases and further reported that 98% of those ccRCC tumors displayed promoter hypermethylation or genetic alterations responsible for inactivating the remaining functional VHL allele. [21]

In the present study, we performed the sequencing analysis of the coding regions of the VHL gene, thus potentially missing the presence of intronic mutations with functional relevance on pVHL expression. In fact, aberrant splicing of mRNA precursors can lead to loss of whole exons and translation into truncated and/or abnormally rearranged forms of the VHL protein. [92,93] Also, we could not address epigenetic alterations such as promoter hypermethylation with silencing effect and histone modifications affecting chromatin conformation which can both influence transcription of the VHL gene.

Therefore, it is probable that all or part of these 10 patients displaying heterozygous inactivating VHL mutations in the tumor tissue did in fact harbour complete loss of functional pVHL expression caused by concomitant epigenetic (intronic or promoter) alterations of the remaining VHL allele. In this setting, the CCC and CRC-UMF found in these cases and displaying the same mutations found in the tumor tissue should be considered as cancer cells.

Consistent with this view is also the fact that, among the 10 cases bearing heterozygous inactivating VHL mutations, two patients harboured double missense VHL mutations in the tumor tissue that were found identical in the corresponding CRC (including seven CCC and seven CRC-UMF). These double missense VHL mutations could either be located separately on the two VHL alleles, thus leading to biallelic inactivation of the VHL gene, or affect the same VHL allele and coexist with a fully functional VHL allele. In any case, the probability that the exact same two VHL alterations would have occurred separately in distinct kidney cells when more than 500 distinct exonic VHL mutations have been described so far (see methods for VHL database references) is very low or absent. So, at least for those two additional patients, we can reliably state that the VHL mutations we found in their CRC are diagnostic for their tumorous nature, i.e. all the CRC carrying those two mutations are cancer cells even if seven have been classified as CRC-UMF. Adding those two patients to our analysis of the 13 cases with complete pVHL loss of function still supports a 100% specificity of the cytopathological diagnosis while bringing its clinical sensitivity up to 66.7%.

Additionally, Dagher and colleagues recently reported on 98 ccRCC patients, after characterizing both genetic and epigenetic alterations of the VHL gene in resected tumors, and determined that ccRCC harbouring heterozygous VHL alterations while partially retaining functional pVHL expression (encoded from one allele only) were significantly associated with a higher nuclear grade IV, metastases, sarcomatoid component, and vascular endothelial growth factor overexpression (>30%) when compared with ccRCC displaying complete loss of functional pVHL. [94] Thus, monoallelic inactivation of VHL can be considered to predispose to a more aggressive form of ccRCC than biallelic VHL inactivation through an accumulation of distinct genetic alterations. [94]

Additionally, although wild type VHL genetic profiles remain restricted to a minority among ccRCC cases, [21,28,29,75,88,89,91,95–105] it is important to note that the absence of detectable VHL mutation does not exclude the presence of ccRCC. [106] When it comes to patients that constitute the "wild type" VHL group, obtaining informative molecular data would require performing more complex extensive analysis of single CRC than the strictly VHL-targeted approach presented here.

Other VHL-neighbouring tumor suppressor genes such as PBRM1, BAP1 and SETD2 have all been shown to localize on the short arm of the third chromosome (3p21) and represent simultaneous targets of depletion by LOH at 3p. [105] For example, in a cohort of 227 ccRCC patients, truncating mutations of PBRM1 impacting the chromatin remodelling function of the encoded protein were found in 41% of cases. [104] Furthermore, concomitant inactivation of VHL and PBRM1 was recently reported to display synergistic effects of metabolic deregulation in ccRCC cell lines in vitro. [107] Additionally, expression of functional PBRM1 has been shown to restrain VHL loss-driven ccRCC progression, thus illustrating the existence of distinct subtypes of VHL-null ccRCC. [108] Conversely, in tumors displaying functional pVHL expression, high throughput molecular studies have shown that activation of the oncogenic pathway related to HIF-α transcription factors

can be achieved through distinct genetic alterations that display mutual exclusiveness with inactivating VHL mutations. For instance, mutations in the ELOC gene (also called TCEB1) together with LOH at its 8p locus were found to inactivate the Elongin C cofactor of pVHL in 40% of ccRCC patients with wild type pVHL expression. [21]

Despite said limitations, to our knowledge, our study is the first to combine highly experienced cytopathological analysis according to the "reference" criteria [59,60] with blind single-cell genetic analysis of cells previously assessed by cytopathological study. This approach needed to overcome specific technical challenges. In fact, the DNA of fixed single cells is particularly difficult to analyse and cell-staining adds further technical difficulties, as illustrated by the 62.7% successful amplification of the three VHL exons from all the individual CRC that were microdissected in our study.

With the continuous improvement of molecular testing applied to single-cell analyses, we can hope that in the future whole genome, transcriptome and maybe proteome analyses of fixed and stained single cells could become available, thus increasing our capacity to investigate CRC and detect their tumorous nature.

Comparative studies targeting CRC isolated from patients with ccRCCC and from patients with benign kidney diseases including patients affected by hereditary VHL disease at the pre-cancerous stage could also help to assess the diagnostic value of specifically targeted DNA mutations, including VHL mutations. Unfortunately, we did not have access to such patients.

Nonetheless, it is striking that, in our study performed blindly, all the 57 CCC defined by "reference" cytopathological criteria [59,60] were carrying the same VHL mutation found in the corresponding tumorous tissue, which was always absent from normal leukocyte controls. This finding is consistent with a complete specificity of the cytopathological approach. In addition to this, 104 single cells classified as CRC-UMF by morphological examination were also found to carry the same VHL mutation detected in the corresponding tumorous tissue. We can consider that, since we found VHL mutations identical to those found in the tumor tissue in CRC having partial tumor phenotypes (CRC-UMF) and having acquired the capability to circulate in blood, those CRC with VHL mutation are in fact tumor cells. Under this view, cytopathology appears as having 100% specificity and 72% sensitivity.

Detecting CCC may represent our best chance to take advantage from liquid biopsy in the follow up of patients with ccRCC. In fact, detecting ctDNA in ccRCC patients was recently reported as particularly inefficient for assessing the tumor burden since ccRCC tumors seem to be characterized by reduced shedding and higher clearance of ctDNA [27]

In conclusion, our study provides a proof of principle demonstrating that combined cytomorphological and single-cell molecular analysis of CRC shows great potential to expand our diagnostic capabilities to identify cancer cells circulating in blood, thus helping personalized treatment strategies and early detection of disease relapse through CRC isolation and cyto-molecular characterization.

Methods:

Patients:

Thirty patients with clear cell renal cell carcinoma (ccRCC) scheduled for either partial (n=9) or total (n=21) nephrectomy were enrolled in this study. All patients with ccRCC as part of a hereditary VHL disease (bearing germline VHL mutations) were excluded from this study. Our panel consists of twenty-two men and eight women with an average age of 68.5 years. Two of our patients presented with metastatic ccRCC. Informed consent was obtained from all patients participating in this study.

Tumor DNA extraction and molecular analysis:

Thirty thick sections of frozen tumors were recovered from all thirty patients. These sections were provided by the Department of Anatomy and Cytology of the Necker Hospital after careful selection based on standard histological criteria of malignancy. Manual macrodissection of samples was performed after histopathological examination to collect tumor tissue only. Tumor-DNA extraction was then carried out after incubation of the tissue section with Proteinase K (Tris-HCL 50 mmol / L, pH 8, proteinase K 800 g / ml) at 50 °C overnight. Proteinase K was then denatured at 94 °C for 10 minutes and DNA extraction was performed using the QIAamp® DNA kit (Qiagen, USA) as per manufacturer's instructions.

Amplification of the VHL gene was performed on extracted tumor DNA by nested PCR using Taq Gold at 0.05 U/µL with 1X PCR Gold buffer (Thermofisher, USA), MgCl2 at 2.5 mM and mixed dNTP at 0.2 mM. All three exons of the VHL gene were independently amplified by applying 2 consecutive cycles of nested PCR in respective total volumes of 40 µl containing 4 µl of extracted tumor DNA and 20 µl containing 2 µl of the first PCR product (PCR1). Primers and conditions used for the amplification of the coding regions of the VHL gene are detailed in **Table 5**. The first VHL exon being located on a CpG island makes it more difficult to study. [109] We therefore chose to cut this exon in three parts. PCR primers and conditions were optimized, as described elsewhere, [110] to ensure a minimal error rate during amplification.

Table 5: PCR primers and conditions

Location	Forward primer (5'-3')	Reverse primer (5'-3')	Annealing	Amplicon
Exon 1 Part 1	CGCGCGTTCCATCCTCTAC	GGCCTCCATCTCCTCCTCG	55°C	300 bp
Exon 1 Part 2	GAGTACGGCCCTGAAGAAGA	CCGTCGAAGTTGAGCCATAC	TouchDown 65°C to 60°C	215 bp
Exon 1 Part 3	GCCGAGGAGGAGATGGAG	GCTTCAGACCGTGCTATCGT	54°C	248 bp
Exon 2	ACCGGTGTGGCTCTTTAACA	TCCTGTACTTACCACAACAACCTT	56°C	215 bp
Exon 3	GCCACTGAGGATTTGGTTTT	CAAAAGCTGAGATGAAACAGTG	58°C	215 bp

Reactions were incubated in a GeneAmp 9700 thermal cycler (Applied Biosystems, USA) at 95°C for five minutes before 35 cycles of amplification (including 30 seconds at annealing temperature) and a final extension step of five minutes at 72°C were applied. Final PCR (PCR2) products were then purified using the DNA Clean & Concentrator™-5 kit (Zymo Research, USA) as per manufacturer's instructions. Purified PCR2 products were diluted 1:10 in sterile water prior to sequencing of both strands with Big Dye terminators version 3.1 (Applied Biosystems, USA) as per manufacturer's instructions. Sequencing data were collected raw from a 3130xl Genetic Analyser (Applied Biosystems, USA) and analysed using both Sequencing Analysis® and SeqScape® softwares (Applied Biosystems, USA).

All sequences were analyzed by visual inspection of the individual sequencing files. Sanger sequencing of DNA extracted from whole populations predictably informs on the dominant clonal population present in each sample. As reported elsewhere, the possible contamination of tumor samples with normal infiltrating cells would not constitute a dominant clonal population in ccRCC surgical samples and should not represent more than 10% of the total DNA extracted from the tumor. [111] Therefore, concerning tumor DNA, heterozygous transitions and transversions were defined as those presenting a single nucleotide change compared with the wild type sequence and for which the minor allele peak height represented >20% of the major allele peak. Homozygous mutations inducing frameshifts (insertions/deletions) were defined as those ablating or adding a number of nucleotides not divisible by three and for which the sequence showed a

single signal for each nucleotide following the frameshift and no other peaks higher than 20% of the major allele peak over the reading frame of the sequence (at least 20 nucleotides following the frameshift).

Blood filtration by ISET®:

Peripheral blood samples (10 ml) were collected on buffered EDTA (EthyleneDiamine Tetraacetic Acid) before surgery, transported to the laboratory within 3 hours after collection and processed by ISET® filtration. [7] Briefly, each 10 mL blood sample was diluted 1:10 with the Rarecells® Buffer (Rarecells Diagnostics, France) containing formaldehyde, incubated with gentle stirring for 10 minutes at room temperature, and filtered on the Rarecells® Device as per manufacturer's instructions. Enriched CRC from each blood sample were recovered fixed on ten circular areas (spots) of the filter.

Cytopathological staining and diagnostic identification of Circulating Cancer Cells (CCC):

One or more spots (up to ten), each one corresponding to 1 ml of filtered blood, were stained with haematoxylin and eosin as described elsewhere [10]. CRC were first analysed and diagnosed by four cytopathologists who confronted their results to come to an agreement, then blindly and individually microdissected for genetic analysis by an independent operator. According to Hofman et al. [59,60], CCC, also called CRC-MF (circulating rare cells with malignant features), are characterized by at least 4 of the following five criteria of malignancy [35]: anisonucleosis (ratio >0.5), nuclei larger than three times the calibrated pore size (i.e. >24 µm), irregular nuclei, presence of tridimensional sheets, and a high nuclear/cytoplasmic ratio. Past studies have also included other criteria such as nuclear hyperchromatism or the size and number of nucleoli [112] which were not considered in this study. CRC exhibiting at least one and up to three morphological features of malignancy were classified as CRC-UMF (circulating rare cells with uncertain malignant features).

Molecular analysis of CCC/CRC-UMF at single-cell level:

Laser microdissection of each individual cell selected was performed using an Eclipse microscope (Nikon, Japan) equipped with the Cell Cut System (Molecular Machines and Industries, Germany). Each microdissected single cell underwent enzymatic lysis and amplification of DNA by the PEP (Primer Extension Preamplification) protocol, as described previously. [113] Amplification of the VHL gene was then performed by nested PCR using the same protocol as the one described above for tumor DNA analysis except that 6 µL of PEP product served as template in the first round of amplification (PCR1) and that PCR2 products were not diluted prior to sequencing. To check for the absence of contamination, tubes containing only the lysis buffer (negative controls) were included at the cell lysis step and run to the end of each PCR run, further adding appropriate negative (containing PCR buffer only) and positive (containing 1 ng of genomic DNA) PCR controls.

At single-cell level, the global preamplification step necessary to obtain sufficient DNA quantities for mutational analysis is known to introduce bias such as allele drop out (ADO) or overrepresentation of one allele. [114] Therefore, we optimized PCR primers, selected only samples of sufficient quality to inform on all three VHL exons and defined heterozygous mutations as those for which the minor allele peak height represented >10% of the major allele peak, as reported elsewhere in the context of fixed single-cell analysis. [115] Similarly, homozygous mutations inducing frameshifts (insertions/deletions) were defined as those ablating or adding a number of nucleotides not divisible by 3 and for which the sequence showed a single signal for each nucleotide following the frameshift and no other signals higher than 10% of the major allele peak over the reading frame of the sequence (20 nucleotides following the frameshift).

Molecular analysis of genomic DNA from normal leukocytes:

Genomic DNA extraction and analysis was performed for each patient on several replicates of individually microdissected leukocytes using the same protocol as described for single CRC analysis.

Genotype – phenotype correlations:

All VHL mutations found in single circulating cells and corresponding tumor tissues were investigated to determine their phenotypic impact on pVHL functions by searching the following databases: the VHL Universal Mutation Database (http://www.umd.be/VHL/), the Catalogue Of Somatic Mutations In Cancer (http://cancer.sanger.ac.uk/cosmic), the database of pVHL interactions (http://vhldb.bio.unipd.it), and records of ccRCC in The Cancer Genome Atlas (https://portal.gdc.cancer.gov/).

Conflicts of Interest:

Professors Patrizia Paterlini-Bréchot and Paul Hofman are coinventors of ISET® patents belonging to University Paris Descartes, INSERM and Assistance Publique Hopitaux de Paris, exclusively licensed to Rarecells Diagnostics, France. These authors do not receive payments from Rarecells Diagnostics. The present study was conducted independently by academic research teams.

Acknowledgements:

We would like to thank Dr Gabriela Petkova-Campbell for reviewing the manuscript's English language and Dr Raoudha Doghri for cytopathological assistance. This work was supported by funds from: Fondation pour la Recehrche Médicale, Fondation Bettencourt Schueller, Fondation Lefort-Beaumont de l'Institut de France and INSERM.

References:

1. Lecharpentier A, Vielh P, Perez-Moreno P, Planchard D, Soria JC, Farace F. Detection of circulating tumour cells with a hybrid (epithelial/mesenchymal) phenotype in patients with metastatic non-small cell lung cancer. Br J Cancer. 2011; 105: 1338–41. doi: 10.1038/bjc.2011.405.

2. Krebs MG, Hou J-M, Sloane R, Lancashire L, Priest L, Nonaka D, Ward TH, Backen A, Clack G, Hughes A, Ranson M, Blackhall FH, Dive C. Analysis of circulating tumor cells in patients with non-small cell lung cancer using epithelial marker-dependent and -independent approaches. J Thorac Oncol Off Publ Int Assoc Study Lung Cancer. 2012; 7: 306–15. doi: 10.1097/JTO.0b013e31823c5c16.

3. Hofman V, Ilie M, Long E, Guibert N, Selva E, Washetine K, Mograbi B, Mouroux J, Vénissac N, Reverso-Meinietti J, Milano G, Mazières J, Marquette C-H, et al. Detection of circulating tumor cells from lung cancer patients in the era of targeted therapy: promises, drawbacks and pitfalls. Curr Mol Med. 2014; 14: 440–56.

4. Paterlini-Bréchot P. Circulating Tumor Cells: Who is the Killer? Cancer Microenviron Off J Int Cancer Microenviron Soc. 2014; 7: 161–76. doi: 10.1007/s12307-014-0164-4.

5. Pantel K, Denève E, Nocca D, Coffy A, Vendrell J-P, Maudelonde T, Riethdorf S, Alix-Panabières C. Circulating epithelial cells in patients with benign colon diseases. Clin Chem. 2012; 58: 936–40. doi: 10.1373/clinchem.2011.175570.

6. Alix-Panabières C, Pantel K. Challenges in circulating tumour cell research. Nat Rev Cancer. 2014; 14: 623–31. doi: 10.1038/nrc3820.

7. Vona G, Sabile A, Louha M, Sitruk V, Romana S, Schütze K, Capron F, Franco D, Pazzagli M, Vekemans M, Lacour B, Bréchot C, Paterlini-Bréchot P. Isolation by size of epithelial tumor cells : a new method for the immunomorphological and molecular characterization of circulatingtumor cells. Am J Pathol. 2000; 156: 57–63. doi: 10.1016/S0002-9440(10)64706-2.

8. Kallergi G, Politaki E, Alkahtani S, Stournaras C, Georgoulias V. Evaluation of Isolation Methods for Circulating Tumor Cells (CTCs). Cell Physiol Biochem Int J Exp Cell Physiol Biochem Pharmacol. 2016; 40: 411–9. doi: 10.1159/000452556.

9. Chinen LTD, Mello CAL, Abdallah EA, Ocea LM, Buim ME, Breve NM, Gasparini JL, Fanelli MF, Paterlini-Bréchot P. Isolation, detection, and immunomorphological characterization of circulating tumor cells (CTCs) from patients with different types of sarcoma using isolation by size of tumor cells: a window on sarcoma-cell invasion. OncoTargets Ther. 2014; 7: 1609–17. doi: 10.2147/OTT.S62349.

10. De Giorgi V, Pinzani P, Salvianti F, Panelos J, Paglierani M, Janowska A, Grazzini M, Wechsler J, Orlando C, Santucci M, Lotti T, Pazzagli M, Massi D. Application of a filtration- and isolation-by-size technique for the detection of circulating tumor cells in cutaneous melanoma. J Invest Dermatol. 2010; 130: 2440–7. doi: 10.1038/jid.2010.141.

11. Ilie M, Hofman V, Long-Mira E, Selva E, Vignaud J-M, Padovani B, Mouroux J, Marquette C-H, Hofman P. "Sentinel" circulating tumor cells allow early diagnosis of lung cancer in patients with chronic obstructive pulmonary disease. PloS One. 2014; 9: e111597. doi: 10.1371/journal.pone.0111597.

12. Laget S, Broncy L, Hormigos K, Dhingra DM, BenMohamed F, Capiod T, Osteras M, Farinelli L, Jackson S, Paterlini-Bréchot P. Technical Insights into Highly Sensitive Isolation and Molecular Characterization of Fixed and Live Circulating Tumor Cells for Early Detection of Tumor Invasion. PloS One. 2017; 12: e0169427. doi: 10.1371/journal.pone.0169427.

13. Morrow CJ, Trapani F, Metcalf RL, Bertolini G, Hodgkinson CL, Khandelwal G, Kelly P, Galvin M, Carter L, Simpson KL, Williamson S, Wirth C, Simms N, et al. Tumourigenic non-small-cell lung cancer mesenchymal circulating tumour cells: a clinical case study. Ann Oncol Off J Eur Soc Med Oncol. 2016; 27: 1155–60. doi: 10.1093/annonc/mdw122.

14. Vona G, Estepa L, Béroud C, Damotte D, Capron F, Nalpas B, Mineur A, Franco D, Lacour B, Pol S, Bréchot C, Paterlini-Bréchot P. Impact of cytomorphological detection of circulating tumor cells in patients with liver cancer. Hepatol Baltim Md. 2004; 39: 792–7. doi: 10.1002/hep.20091.

15. Buim ME, Fanelli MF, Souza VS, Romero J, Abdallah EA, Mello CA, Alves V, Ocea LM, Mingues NB, Barbosa PN, Tyng CJ, Chojniak R, Chinen LT. Detection of KRAS mutations in circulating tumor cells from patients with metastatic colorectal cancer. Cancer Biol Ther. 2015; 16: 1289–95. doi: 10.1080/15384047.2015.1070991.

16. Pinzani P, Salvadori B, Simi L, Bianchi S, Distante V, Cataliotti L, Pazzagli M, Orlando C. Isolation by size of epithelial tumor cells in peripheral blood of patients with breast cancer: correlation with real-time reverse transcriptase-polymerase chain reaction results and feasibility of molecular analysis by laser microdissection. Hum Pathol. 2006; 37: 711–8. doi: 10.1016/j.humpath.2006.01.026.

17. Arber DA, Orazi A, Hasserjian R, Thiele J, Borowitz MJ, Le Beau MM, Bloomfield CD, Cazzola M, Vardiman JW. The 2016 revision to the World Health Organization classification of myeloid neoplasms and acute leukemia. Blood. 2016; 127: 2391–405. doi: 10.1182/blood-2016-03-643544.

18. Pennacchioli E, Tosti G, Barberis M, De Pas TM, Verrecchia F, Menicanti C, Testori A, Mazzarol G. Sarcoma spreads primarily through the vascular system: are there biomarkers associated with vascular spread? Clin Exp Metastasis. 2012; 29: 757–73. doi: 10.1007/s10585-012-9502-4.

19. Lopez-Beltran A, Scarpelli M, Montironi R, Kirkali Z. 2004 WHO classification of the renal tumors of the adults. Eur Urol. 2006; 49: 798–805. doi: 10.1016/j.eururo.2005.11.035.

20. Nickerson ML, Jaeger E, Shi Y, Durocher JA, Mahurkar S, Zaridze D, Matveev V, Janout V, Kollarova H, Bencko V, Navratilova M, Szeszenia-Dabrowska N, Mates D, et al. Improved identification of von Hippel-Lindau gene alterations in clear cell renal tumors. Clin Cancer Res Off J Am Assoc Cancer Res. 2008; 14: 4726–34. doi: 10.1158/1078-0432.CCR-07-4921.

21. Sato Y, Yoshizato T, Shiraishi Y, Maekawa S, Okuno Y, Kamura T, Shimamura T, Sato-Otsubo A, Nagae G, Suzuki H, Nagata Y, Yoshida K, Kon A, et al. Integrated molecular analysis of clear-cell renal cell carcinoma. Nat Genet. 2013; 45: 860–7. doi: 10.1038/ng.2699.

22. Czarnecka AM, Kornakiewicz A, Kukwa W, Szczylik C. Frontiers in clinical and molecular diagnostics and staging of metastatic clear cell renal cell carcinoma. Future Oncol Lond Engl. 2014; 10: 1095–111. doi: 10.2217/fon.13.258.

23. Ficarra V. Open radical nephrectomy versus open partial nephrectomy: is it still an issue? Eur Urol. 2007; 51: 593–5. doi: 10.1016/j.eururo.2006.11.031.

24. Kuthi L, Jenei A, Hajdu A, Németh I, Varga Z, Bajory Z, Pajor L, Iványi B. Prognostic Factors for Renal Cell Carcinoma Subtypes Diagnosed According to the 2016 WHO Renal Tumor Classification: a Study Involving 928 Patients. Pathol Oncol Res POR. 2017; 23: 689–98. doi: 10.1007/s12253-016-0179-x.

25. Park W-H, Eisen T. Prognostic factors in renal cell cancer. BJU Int. 2007; 99: 1277–81. doi: 10.1111/j.1464-410X.2007.06828.x.

26. El-Heliebi A, Kroneis T, Zöhrer E, Haybaeck J, Fischereder K, Kampel-Kettner K, Zigeuner R, Pock H, Riedl R, Stauber R, Geigl JB, Huppertz B, Sedlmayr P, et al. Are morphological criteria sufficient for the identification of circulating tumor cells in renal cancer? J Transl Med. 2013; 11: 214. doi: 10.1186/1479-5876-11-214.

27. Corrò C, Hejhal T, Poyet C, Sulser T, Hermanns T, Winder T, Prager G, Wild PJ, Frew I, Moch H, Rechsteiner M. Detecting circulating tumor DNA in renal cancer: An open challenge. Exp Mol Pathol. 2017; 102: 255–61. doi: 10.1016/j.yexmp.2017.02.009.

28. Gallou C, Joly D, Méjean A, Staroz F, Martin N, Tarlet G, Orfanelli MT, Bouvier R, Droz D, Chrétien Y, Maréchal JM, Richard S, Junien C, et al. Mutations of the VHL gene in sporadic renal cell carcinoma: definition of a risk factor for VHL patients to develop an RCC. Hum Mutat. 1999; 13: 464–75. doi: 10.1002/(SICI)1098-1004(1999)13:6<464::AID-HUMU6>3.0.CO;2-A.

29. Gallou C, Longuemaux S, Deloménie C, Méjean A, Martin N, Martinet S, Palais G, Bouvier R, Droz D, Krishnamoorthy R, Junien C, Béroud C, Dupret JM. Association of GSTT1 non-null and NAT1 slow/rapid genotypes with von Hippel-Lindau tumour suppressor gene transversions in sporadic renal cell carcinoma. Pharmacogenetics. 2001; 11: 521–35.

30. Kishida T, Stackhouse TM, Chen F, Lerman MI, Zbar B. Cellular proteins that bind the von Hippel-Lindau disease gene product: mapping of binding domains and the effect of missense mutations. Cancer Res. 1995; 55: 4544–8.

31. Forman JR, Worth CL, Bickerton GRJ, Eisen TG, Blundell TL. Structural bioinformatics mutation analysis reveals genotype-phenotype correlations in von Hippel-Lindau disease and suggests molecular mechanisms of tumorigenesis. Proteins. 2009; 77: 84–96. doi: 10.1002/prot.22419.

32. Miller F, Kentsis A, Osman R, Pan Z-Q. Inactivation of VHL by tumorigenic mutations that disrupt dynamic coupling of the pVHL.hypoxia-inducible transcription factor-1alpha complex. J Biol Chem. 2005; 280: 7985–96. doi: 10.1074/jbc.M413160200.

33. McRonald FE, Morris MR, Gentle D, Winchester L, Baban D, Ragoussis J, Clarke NW, Brown MD, Kishida T, Yao M, Latif F, Maher ER. CpG methylation profiling in VHL related and VHL unrelated renal cell carcinoma. Mol Cancer. 2009; 8: 31. doi: 10.1186/1476-4598-8-31.

34. Jones PA. Functions of DNA methylation: islands, start sites, gene bodies and beyond. Nat Rev Genet. 2012; 13: 484–92. doi: 10.1038/nrg3230.

35. Hofman VJ, Ilie M, Hofman PM. Detection and characterization of circulating tumor cells in lung cancer: Why and how? Cancer Cytopathol. 2016; 124: 380–7. doi: 10.1002/cncy.21651.

36. Motzer RJ, Bander NH, Nanus DM. Renal-cell carcinoma. N Engl J Med. 1996; 335: 865–75. doi: 10.1056/NEJM199609193351207.

37. Lam JS, Shvarts O, Leppert JT, Figlin RA, Belldegrun AS. Renal cell carcinoma 2005: new frontiers in staging, prognostication and targeted molecular therapy. J Urol. 2005; 173: 1853–62. doi: 10.1097/01.ju.0000165693.68449.c3.

38. Ashida S, Okuda H, Chikazawa M, Tanimura M, Sugita O, Yamamoto Y, Nakamura S, Moriyama M, Shuin T. Detection of circulating cancer cells with von hippel-lindau gene mutation in peripheral blood of patients with renal cell carcinoma. Clin Cancer Res Off J Am Assoc Cancer Res. 2000; 6: 3817–22.

39. López JI. Renal tumors with clear cells. A review. Pathol Res Pract. 2013; 209: 137–46. doi: 10.1016/j.prp.2013.01.007.

40. Buchner A, Riesenberg R, Kotter I, Hofstetter A, Stief C, Oberneder R. Frequency and prognostic relevance of disseminated tumor cells in bone marrow of patients with metastatic renal cell carcinoma. Cancer. 2006; 106: 1514–20. doi: 10.1002/cncr.21775.

41. Li G, Passebosc-Faure K, Gentil-Perret A, Lambert C, Genin C, Tostain J. Cadherin-6 gene expression in conventional renal cell carcinoma: a useful marker to detect circulating tumor cells. Anticancer Res. 2005; 25: 377–81.

42. Ohlmann C-H, Ozgür E, Schrader AJ, Konrad L, Hofmann R, Engelmann U, Heidenreich A. Detection of circulating tumor cells in patients with renal cell carcinoma by reverse transcriptase polymerase chain reaction for G250/MNCA-9: results of a prospective trial. Urol Oncol. 2006; 24: 287–93. doi: 10.1016/j.urolonc.2005.10.004.

43. Gradilone A, Iacovelli R, Cortesi E, Raimondi C, Gianni W, Nicolazzo C, Petracca A, Palazzo A, Longo F, Frati L, Gazzaniga P. Circulating tumor cells and "suspicious objects" evaluated through CellSearch® in metastatic renal cell carcinoma. Anticancer Res. 2011; 31: 4219–21.

44. Bluemke K, Bilkenroth U, Meye A, Fuessel S, Lautenschlaeger C, Goebel S, Melchior A, Heynemann H, Fornara P, Taubert H. Detection of circulating tumor cells in peripheral blood of patients with renal cell carcinoma correlates with prognosis. Cancer Epidemiol Biomark Prev Publ Am Assoc Cancer Res Cosponsored Am Soc Prev Oncol. 2009; 18: 2190–4. doi: 10.1158/1055-9965.EPI-08-1178.

45. Nel I, Gauler TC, Bublitz K, Lazaridis L, Goergens A, Giebel B, Schuler M, Hoffmann A-C. Circulating Tumor Cell Composition in Renal Cell Carcinoma. PloS One. 2016; 11: e0153018. doi: 10.1371/journal.pone.0153018.

46. Mandriota SJ, Turner KJ, Davies DR, Murray PG, Morgan NV, Sowter HM, Wykoff CC, Maher ER, Harris AL, Ratcliffe PJ, Maxwell PH. HIF activation identifies early lesions in VHL kidneys: evidence for site-specific tumor suppressor function in the nephron. Cancer Cell. 2002; 1: 459–68.

47. Harten SK, Shukla D, Barod R, Hergovich A, Balda MS, Matter K, Esteban MA, Maxwell PH. Regulation of renal epithelial tight junctions by the von Hippel-Lindau tumor suppressor gene involves occludin and claudin 1 and is independent of E-cadherin. Mol Biol Cell. 2009; 20: 1089–101. doi: 10.1091/mbc.E08-06-0566.

48. Albers J, Rajski M, Schönenberger D, Harlander S, Schraml P, von Teichman A, Georgiev S, Wild PJ, Moch H, Krek W, Frew IJ. Combined mutation of Vhl and Trp53 causes renal cysts and tumours in mice. EMBO Mol Med. 2013; 5: 949–64. doi: 10.1002/emmm.201202231.

49. Linehan WM, Lerman MI, Zbar B. Identification of the von Hippel-Lindau (VHL) gene. Its role in renal cancer. JAMA. 1995; 273: 564–70.

50. Maxwell PH, Wiesener MS, Chang GW, Clifford SC, Vaux EC, Cockman ME, Wykoff CC, Pugh CW, Maher ER, Ratcliffe PJ. The tumour suppressor protein VHL targets hypoxia-inducible factors for oxygen-dependent proteolysis. Nature. 1999; 399: 271–5. doi: 10.1038/20459.

51. Stebbins CE, Kaelin WG, Pavletich NP. Structure of the VHL-ElonginC-ElonginB complex: implications for VHL tumor suppressor function. Science. 1999; 284: 455–61.

52. Gossage L, Eisen T, Maher ER. VHL, the story of a tumour suppressor gene. Nat Rev Cancer. 2015; 15: 55–64. doi: 10.1038/nrc3844.

53. Martínez-Sáez O, Gajate Borau P, Alonso-Gordoa T, Molina-Cerrillo J, Grande E. Targeting HIF-2 α in clear cell renal cell carcinoma: A promising therapeutic strategy. Crit Rev Oncol Hematol. 2017; 111: 117–23. doi: 10.1016/j.critrevonc.2017.01.013.

54. Labrousse-Arias D, Martínez-Alonso E, Corral-Escariz M, Bienes-Martínez R, Berridy J, Serrano-Oviedo L, Conde E, García-Bermejo M-L, Giménez-Bachs JM, Salinas-Sánchez AS, Sánchez-Prieto R, Yao M, Lasa M, et al. VHL promotes immune response against renal cell carcinoma via NF-κB-dependent regulation of VCAM-1. J Cell Biol. 2017; 216: 835–47. doi: 10.1083/jcb.201608024.

55. Gossage L, Pires DEV, Olivera-Nappa Á, Asenjo J, Bycroft M, Blundell TL, Eisen T. An integrated computational approach can classify VHL missense mutations according to risk of clear cell renal carcinoma. Hum Mol Genet. 2014; 23: 5976–88. doi: 10.1093/hmg/ddu321.

56. Kondo K, Klco J, Nakamura E, Lechpammer M, Kaelin WG. Inhibition of HIF is necessary for tumor suppression by the von Hippel-Lindau protein. Cancer Cell. 2002; 1: 237–46.

57. Moch H. An overview of renal cell cancer: pathology and genetics. Semin Cancer Biol. 2013; 23: 3–9. doi: 10.1016/j.semcancer.2012.06.006.

58. Hsieh JJ, Purdue MP, Signoretti S, Swanton C, Albiges L, Schmidinger M, Heng DY, Larkin J, Ficarra V. Renal cell carcinoma. Nat Rev Dis Primer. 2017; 3: 17009. doi: 10.1038/nrdp.2017.9.

59. Hofman V, Long E, Ilie M, Bonnetaud C, Vignaud JM, Fléjou JF, Lantuejoul S, Piaton E, Mourad N, Butori C, Selva E, Marquette CH, Poudenx M, et al. Morphological analysis of circulating tumour cells in patients undergoing surgery for non-small cell lung carcinoma using the isolation by size of epithelial tumour cell (ISET) method. Cytopathol Off J Br Soc Clin Cytol. 2012; 23: 30–8. doi: 10.1111/j.1365-2303.2010.00835.x.

60. Hofman VJ, Ilie MI, Bonnetaud C, Selva E, Long E, Molina T, Vignaud JM, Fléjou JF, Lantuejoul S, Piaton E, Butori C, Mourad N, Poudenx M, et al. Cytopathologic detection of circulating tumor cells using the isolation by size of epithelial tumor cell method: promises and pitfalls. Am J Clin Pathol. 2011; 135: 146–56. doi: 10.1309/AJCP9X8OZBEIQVVI.

61. Mascalchi M, Maddau C, Sali L, Bertelli E, Salvianti F, Zuccherelli S, Matucci M, Borgheresi A, Raspanti C, Lanzetta M, Falchini M, Mazza E, Vella A, et al. Circulating tumor cells and microemboli can differentiate malignant and benign pulmonary lesions. J Cancer. 2017; 8: 2223–30. doi: 10.7150/jca.18418.

62. Raval RR, Lau KW, Tran MGB, Sowter HM, Mandriota SJ, Li J-L, Pugh CW, Maxwell PH, Harris AL, Ratcliffe PJ. Contrasting properties of hypoxia-inducible factor 1 (HIF-1) and HIF-2 in von Hippel-Lindau-associated renal cell carcinoma. Mol Cell Biol. 2005; 25: 5675–86. doi: 10.1128/MCB.25.13.5675-5686.2005.

63. Patel SA, Simon MC. Biology of hypoxia-inducible factor-2alpha in development and disease. Cell Death Differ. 2008; 15: 628–34. doi: 10.1038/cdd.2008.17.

64. Gordan JD, Lal P, Dondeti VR, Letrero R, Parekh KN, Oquendo CE, Greenberg RA, Flaherty KT, Rathmell WK, Keith B, Simon MC, Nathanson KL. HIF-alpha effects on c-Myc distinguish two subtypes of sporadic VHL-deficient clear cell renal carcinoma. Cancer Cell. 2008; 14: 435–46. doi: 10.1016/j.ccr.2008.10.016.

65. Yang C, Huntoon K, Ksendzovsky A, Zhuang Z, Lonser RR. Proteostasis modulators prolong missense VHL protein activity and halt tumor progression. Cell Rep. 2013; 3: 52–9. doi: 10.1016/j.celrep.2012.12.007.

66. Kats-Ugurlu G, Roodink I, de Weijert M, Tiemessen D, Maass C, Verrijp K, van der Laak J, de Waal R, Mulders P, Oosterwijk E, Leenders W. Circulating tumour tissue fragments in patients with pulmonary metastasis of clear cell renal cell carcinoma. J Pathol. 2009; 219: 287–93. doi: 10.1002/path.2613.

67. Sugino T, Yamaguchi T, Ogura G, Saito A, Hashimoto T, Hoshi N, Yoshida S, Goodison S, Suzuki T. Morphological evidence for an invasion-independent metastasis pathway exists in multiple human cancers. BMC Med. 2004; 2: 9. doi: 10.1186/1741-7015-2-9.

68. Cima I, Kong SL, Sengupta D, Tan IB, Phyo WM, Lee D, Hu M, Iliescu C, Alexander I, Goh WL, Rahmani M, Suhaimi N-AM, Vo JH, et al. Tumor-derived circulating endothelial cell clusters in colorectal cancer. Sci Transl Med. 2016; 8: 345ra89. doi: 10.1126/scitranslmed.aad7369.

69. Kats-Ugurlu G, Oosterwijk E, Muselaers S, Oosterwijk-Wakka J, Hulsbergen-van de Kaa C, de Weijert M, van Krieken H, Desar I, van Herpen C, Maass C, de Waal R, Mulders P, Leenders W. Neoadjuvant sorafenib treatment of clear cell renal cell carcinoma and release of circulating tumor fragments. Neoplasia N Y N. 2014; 16: 221–8. doi: 10.1016/j.neo.2014.03.007.

70. Küsters B, Kats G, Roodink I, Verrijp K, Wesseling P, Ruiter DJ, de Waal RMW, Leenders WPJ. Micronodular transformation as a novel mechanism of VEGF-A-induced metastasis. Oncogene. 2007; 26: 5808–15. doi: 10.1038/sj.onc.1210360.

71. Fiegler H, Geigl JB, Langer S, Rigler D, Porter K, Unger K, Carter NP, Speicher MR. High resolution array-CGH analysis of single cells. Nucleic Acids Res. 2007; 35: e15. doi: 10.1093/nar/gkl1030.

72. Vieira J, Henrique R, Ribeiro FR, Barros-Silva JD, Peixoto A, Santos C, Pinheiro M, Costa VL, Soares MJ, Oliveira J, Jerónimo C, Teixeira MR. Feasibility of differential diagnosis of kidney tumors by comparative genomic hybridization of fine needle aspiration biopsies. Genes Chromosomes Cancer. 2010; 49: 935–47. doi: 10.1002/gcc.20805.

73. Adam J, Couturier J, Molinié V, Vieillefond A, Sibony M. Clear-cell papillary renal cell carcinoma: 24 cases of a distinct low-grade renal tumour and a comparative genomic hybridization array study of seven cases. Histopathology. 2011; 58: 1064–71. doi: 10.1111/j.1365-2559.2011.03857.x.

74. Hofman V, Bonnetaud C, Ilie MI, Vielh P, Vignaud JM, Fléjou JF, Lantuejoul S, Piaton E, Mourad N, Butori C, Selva E, Poudenx M, Sibon S, et al. Preoperative circulating tumor cell detection using the isolation by size of epithelial tumor cell method for patients with lung cancer is a new prognostic biomarker. Clin Cancer Res Off J Am Assoc Cancer Res. 2011; 17: 827–35. doi: 10.1158/1078-0432.CCR-10-0445.

75. Li J, Guo L, Ai Z. An integrated analysis of cancer genes in clear cell renal cell carcinoma. Future Oncol Lond Engl. 2017; 13: 715–25. doi: 10.2217/fon-2016-0473.

76. Lubensky IA, Gnarra JR, Bertheau P, Walther MM, Linehan WM, Zhuang Z. Allelic deletions of the VHL gene detected in multiple microscopic clear cell renal lesions in von Hippel-Lindau disease patients. Am J Pathol. 1996; 149: 2089–94.

77. Mack FA, Rathmell WK, Arsham AM, Gnarra J, Keith B, Simon MC. Loss of pVHL is sufficient to cause HIF dysregulation in primary cells but does not promote tumor growth. Cancer Cell. 2003; 3: 75–88.

78. Rankin EB, Tomaszewski JE, Haase VH. Renal cyst development in mice with conditional inactivation of the von Hippel-Lindau tumor suppressor. Cancer Res. 2006; 66: 2576–83. doi: 10.1158/0008-5472.CAN-05-3241.

79. Mehta GU, Shively SB, Duong H, Tran MGB, Moncrief TJ, Smith JH, Li J, Edwards NA, Lonser RR, Zhuang Z, Merrill MJ, Raffeld M, Maxwell PH, et al. Progression of epididymal maldevelopment into hamartoma-like neoplasia in VHL disease. Neoplasia N Y N. 2008; 10: 1146–53.

80. Montani M, Heinimann K, von Teichman A, Rudolph T, Perren A, Moch H. VHL-gene deletion in single renal tubular epithelial cells and renal tubular cysts: further evidence for a cyst-dependent progression pathway of clear cell renal carcinoma in von Hippel-Lindau disease. Am J Surg Pathol. 2010; 34: 806–15. doi: 10.1097/PAS.0b013e3181ddf54d.

81. Pritchett TL, Bader HL, Henderson J, Hsu T. Conditional inactivation of the mouse von Hippel-Lindau tumor suppressor gene results in wide-spread hyperplastic, inflammatory and fibrotic lesions in the kidney. Oncogene. 2015; 34: 2631–9. doi: 10.1038/onc.2014.197.

82. Richard S, Gardie B, Couvé S, Gad S. Von Hippel-Lindau: how a rare disease illuminates cancer biology. Semin Cancer Biol. 2013; 23: 26–37. doi: 10.1016/j.semcancer.2012.05.005.

83. Gerstung M, Beisel C, Rechsteiner M, Wild P, Schraml P, Moch H, Beerenwinkel N. Reliable detection of subclonal single-nucleotide variants in tumour cell populations. Nat Commun. 2012; 3: 811. doi: 10.1038/ncomms1814.

84. Gerlinger M, Rowan AJ, Horswell S, Larkin J, Endesfelder D, Gronroos E, Martinez P, Matthews N, Stewart A, Tarpey P, Varela I, Phillimore B, Begum S, et al. Intratumor heterogeneity and branched evolution revealed by multiregion sequencing. N Engl J Med. 2012; 366: 883–92. doi: 10.1056/NEJMoa1113205.

85. Gerlinger M, Horswell S, Larkin J, Rowan AJ, Salm MP, Varela I, Fisher R, McGranahan N, Matthews N, Santos CR, Martinez P, Phillimore B, Begum S, et al. Genomic architecture and evolution of clear cell renal cell carcinomas defined by multiregion sequencing. Nat Genet. 2014; 46: 225–33. doi: 10.1038/ng.2891.

86. Gulati S, Martinez P, Joshi T, Birkbak NJ, Santos CR, Rowan AJ, Pickering L, Gore M, Larkin J, Szallasi Z, Bates PA, Swanton C, Gerlinger M. Systematic evaluation of the prognostic impact and intratumour heterogeneity of clear cell renal cell carcinoma biomarkers. Eur Urol. 2014; 66: 936–48. doi: 10.1016/j.eururo.2014.06.053.

87. Cheng L, MacLennan GT, Zhang S, Wang M, Zhou M, Tan P-H, Foster S, Lopez-Beltran A, Montironi R. Evidence for polyclonal origin of multifocal clear cell renal cell carcinoma. Clin Cancer Res Off J Am Assoc Cancer Res. 2008; 14: 8087–93. doi: 10.1158/1078-0432.CCR-08-1494.

88. Kondo K, Yao M, Yoshida M, Kishida T, Shuin T, Miura T, Moriyama M, Kobayashi K, Sakai N, Kaneko S, Kawakami S, Baba M, Nakaigawa N, et al. Comprehensive mutational analysis of the VHL gene in sporadic renal cell carcinoma: relationship to clinicopathological parameters. Genes Chromosomes Cancer. 2002; 34: 58–68.

89. Banks RE, Tirukonda P, Taylor C, Hornigold N, Astuti D, Cohen D, Maher ER, Stanley AJ, Harnden P, Joyce A, Knowles M, Selby PJ. Genetic and epigenetic analysis of von Hippel-Lindau (VHL) gene alterations and relationship with clinical variables in sporadic renal cancer. Cancer Res. 2006; 66: 2000–11. doi: 10.1158/0008-5472.CAN-05-3074.

90. Dalgliesh GL, Furge K, Greenman C, Chen L, Bignell G, Butler A, Davies H, Edkins S, Hardy C, Latimer C, Teague J, Andrews J, Barthorpe S, et al. Systematic sequencing of renal carcinoma reveals inactivation of histone modifying genes. Nature. 2010; 463: 360–3. doi: 10.1038/nature08672.

91. Razafinjatovo C, Bihr S, Mischo A, Vogl U, Schmidinger M, Moch H, Schraml P. Characterization of VHL missense mutations in sporadic clear cell renal cell carcinoma: hotspots, affected binding domains, functional impact on pVHL and therapeutic relevance. BMC Cancer. 2016; 16: 638. doi: 10.1186/s12885-016-2688-0.

92. Brauch H, Weirich G, Brieger J, Glavac D, Rödl H, Eichinger M, Feurer M, Weidt E, Puranakanitstha C, Neuhaus C, Pomer S, Brenner W, Schirmacher P, et al. VHL alterations in human clear cell renal cell carcinoma: association with advanced tumor stage and a novel hot spot mutation. Cancer Res. 2000; 60: 1942–8.

93. Taylor C, Craven RA, Harnden P, Selby PJ, Banks RE. Determination of the consequences of VHL mutations on VHL transcripts in renal cell carcinoma. Int J Oncol. 2012; 41: 1229–40. doi: 10.3892/ijo.2012.1561.

94. Dagher J, Kammerer-Jacquet S-F, Brunot A, Pladys A, Patard J-J, Bensalah K, Perrin C, Verhoest G, Mosser J, Lespagnol A, Vigneau C, Dugay F, Belaud-Rotureau M-A, et al. Wild-type VHL Clear Cell Renal Cell Carcinomas Are a

Distinct Clinical and Histologic Entity: A 10-Year Follow-up. Eur Urol Focus. 2016; 1: 284–90. doi: 10.1016/j.euf.2015.06.001.

95. Shuin T, Kondo K, Torigoe S, Kishida T, Kubota Y, Hosaka M, Nagashima Y, Kitamura H, Latif F, Zbar B. Frequent somatic mutations and loss of heterozygosity of the von Hippel-Lindau tumor suppressor gene in primary human renal cell carcinomas. Cancer Res. 1994; 54: 2852–5.

96. Kanno H, Shuin T, Kondo K, Yamamoto I, Ito S, Shinonaga M, Yoshida M, Yao M. Somatic mutations of the von Hippel-Lindau tumor suppressor gene and loss of heterozygosity on chromosome 3p in human glial tumors. Cancer Res. 1997; 57: 1035–8.

97. Béroud C, Joly D, Gallou C, Staroz F, Orfanelli MT, Junien C. Software and database for the analysis of mutations in the VHL gene. Nucleic Acids Res. 1998; 26: 256–8.

98. Schraml P, Struckmann K, Hatz F, Sonnet S, Kully C, Gasser T, Sauter G, Mihatsch MJ, Moch H. VHL mutations and their correlation with tumour cell proliferation, microvessel density, and patient prognosis in clear cell renal cell carcinoma. J Pathol. 2002; 196: 186–93. doi: 10.1002/path.1034.

99. Cheng L, Zhang S, MacLennan GT, Lopez-Beltran A, Montironi R. Molecular and cytogenetic insights into the pathogenesis, classification, differential diagnosis, and prognosis of renal epithelial neoplasms. Hum Pathol. 2009; 40: 10–29. doi: 10.1016/j.humpath.2008.09.009.

100. Cowey CL, Rathmell WK. VHL gene mutations in renal cell carcinoma: role as a biomarker of disease outcome and drug efficacy. Curr Oncol Rep. 2009; 11: 94–101.

101. Frew IJ, Moch H. A clearer view of the molecular complexity of clear cell renal cell carcinoma. Annu Rev Pathol. 2015; 10: 263–89. doi: 10.1146/annurev-pathol-012414-040306.

102. Razafinjatovo CF, Stiehl D, Deininger E, Rechsteiner M, Moch H, Schraml P. VHL missense mutations in the p53 binding domain show different effects on p53 signaling and HIFα degradation in clear cell renal cell carcinoma. Oncotarget. 2017; 8: 10199–212. doi: 10.18632/oncotarget.14372.

103. Tennenbaum DM, Manley BJ, Zabor E, Becerra MF, Carlo MI, Casuscelli J, Redzematovic A, Khan N, Arcila ME, Voss MH, Feldman DR, Motzer RJ, Benfante NE, et al. Genomic alterations as predictors of survival among patients within a combined cohort with clear cell renal cell carcinoma undergoing cytoreductive nephrectomy. Urol Oncol. 2017; . doi: 10.1016/j.urolonc.2017.03.015.

104. Varela I, Tarpey P, Raine K, Huang D, Ong CK, Stephens P, Davies H, Jones D, Lin M-L, Teague J, Bignell G, Butler A, Cho J, et al. Exome sequencing identifies frequent mutation of the SWI/SNF complex gene PBRM1 in renal carcinoma. Nature. 2011; 469: 539–42. doi: 10.1038/nature09639.

105. Cancer Genome Atlas Research Network. Comprehensive molecular characterization of clear cell renal cell carcinoma. Nature. 2013; 499: 43–9. doi: 10.1038/nature12222.

106. Patard J-J, Rioux-Leclercq N, Masson D, Zerrouki S, Jouan F, Collet N, Dubourg C, Lobel B, Denis M, Fergelot P. Absence of VHL gene alteration and high VEGF expression are associated with tumour aggressiveness and poor survival of renal-cell carcinoma. Br J Cancer. 2009; 101: 1417–24. doi: 10.1038/sj.bjc.6605298.

107. Gao W, Li W, Xiao T, Liu XS, Kaelin WG. Inactivation of the PBRM1 tumor suppressor gene amplifies the HIF-response in VHL-/- clear cell renal carcinoma. Proc Natl Acad Sci U S A. 2017; 114: 1027–32. doi: 10.1073/pnas.1619726114.

108. Nargund AM, Pham CG, Dong Y, Wang PI, Osmangeyoglu HU, Xie Y, Aras O, Han S, Oyama T, Takeda S, Ray CE, Dong Z, Berge M, et al. The SWI/SNF Protein PBRM1 Restrains VHL-Loss-Driven Clear Cell Renal Cell Carcinoma. Cell Rep. 2017; 18: 2893–906. doi: 10.1016/j.celrep.2017.02.074.

109. Illingworth RS, Bird AP. CpG islands--'a rough guide'. FEBS Lett. 2009; 583: 1713–20. doi: 10.1016/j.febslet.2009.04.012.

110. Saker A, Benachi A, Bonnefont JP, Munnich A, Dumez Y, Lacour B, Paterlini-Brechot P. Genetic characterisation of circulating fetal cells allows non-invasive prenatal diagnosis of cystic fibrosis. Prenat Diagn. 2006; 26: 906–16. doi: 10.1002/pd.1524.

111. Arai E, Kanai Y. Genetic and epigenetic alterations during renal carcinogenesis. Int J Clin Exp Pathol. 2010; 4: 58–73.

112. Jang SJ, Gardner JM, Ro JY. Diagnostic approach and prognostic factors of cancers. Adv Anat Pathol. 2011; 18: 165–72. doi: 10.1097/PAP.0b013e31820cb39e.

113. Pfeifer I, Benachi A, Saker A, Bonnefont JP, Mouawia H, Broncy L, Frydman R, Brival ML, Lacour B, Dachez R, Paterlini-Bréchot P. Cervical trophoblasts for non-invasive single-cell genotyping and prenatal diagnosis. Placenta. 2016; 37: 56–60. doi: 10.1016/j.placenta.2015.11.002.

114. Riba J, Renz N, Niemöller C, Bleul S, Pfeifer D, Stosch JM, Metzeler KH, Hackanson B, Lübbert M, Duyster J, Koltay P, Zengerle R, Claus R, et al. Molecular Genetic Characterization of Individual Cancer Cells Isolated via Single-Cell Printing. PloS One. 2016; 11: e0163455. doi: 10.1371/journal.pone.0163455.

115. Court CM, Ankeny JS, Sho S, Hou S, Li Q, Hsieh C, Song M, Liao X, Rochefort MM, Wainberg ZA, Graeber TG, Tseng H-R, Tomlinson JS. Reality of Single Circulating Tumor Cell Sequencing for Molecular Diagnostics in Pancreatic Cancer. J Mol Diagn JMD. 2016; 18: 688–96. doi: 10.1016/j.jmoldx.2016.03.006.

116. Zhuang Z, Gnarra JR, Dudley CF, Zbar B, Linehan WM, Lubensky IA. Detection of von Hippel-Lindau disease gene mutations in paraffin-embedded sporadic renal cell carcinoma specimens. Mod Pathol Off J U S Can Acad Pathol Inc. 1996; 9: 838–42.

117. Zhou MI, Wang H, Foy RL, Ross JJ, Cohen HT. Tumor suppressor von Hippel-Lindau (VHL) stabilization of Jade-1 protein occurs through plant homeodomains and is VHL mutation dependent. Cancer Res. 2004; 64: 1278–86.

3. Methodological developments targeting single cells analysis of CRC isolated by ISET®

Considering the extensive heterogeneity uncovered by recent "high throughput" molecular studies on virtually all types of solid cancers, it appeared crucial to develop reliable methods to interrogate a wide-spread reading frame of genomic and, potentially, transcriptomic data from CRC isolated by ISET®. To that aim, we used human and mouse cell lines to assess the *in vitro* performance of several methodological improvements developed specifically for ISET® applications.

First, ISET® filtration itself was experimented in order to enable recovery of viable circulating cells from blood. Multiple parameters were assessed and repeated quality control tests were applied in order to establish the mean performance of this new variant ISET® protocol. Then, cytological and molecular experiments were conducted as proofs of concept validating the use of single viable cells recovered through this innovative ISET® procedure for high throughput characterization of CRC, as described in the last publication presented here (Laget *et al.*, 2017).

RESEARCH ARTICLE

Technical Insights into Highly Sensitive Isolation and Molecular Characterization of Fixed and Live Circulating Tumor Cells for Early Detection of Tumor Invasion

Sophie Laget[1], Lucile Broncy[1,2☯], Katia Hormigos[1☯], Dalia M. Dhingra[3], Fatima BenMohamed[2], Thierry Capiod[2], Magne Osteras[4], Laurent Farinelli[4], Stephen Jackson[3], Patrizia Paterlini-Bréchot[2]*

1 Rarecells Diagnostics, Paris, France, **2** Unité INSERM U1151 (Eq 13), Faculté de Médecine Paris Descartes, Paris, France, **3** Thermo Fisher Scientific, South San Francisco, California, United States of America, **4** Fasteris SA, Geneva, Switzerland

☯ These authors contributed equally to this work.
* patriziapaterlini@gmail.com

OPEN ACCESS

Citation: Laget S, Broncy L, Hormigos K, Dhingra DM, BenMohamed F, Capiod T, et al. (2017) Technical Insights into Highly Sensitive Isolation and Molecular Characterization of Fixed and Live Circulating Tumor Cells for Early Detection of Tumor Invasion. PLoS ONE 12(1): e0169427. doi:10.1371/journal.pone.0169427

Editor: Masaru Katoh, National Cancer Center, JAPAN

Received: May 3, 2016

Accepted: December 16, 2016

Published: January 6, 2017

Data Availability Statement: All relevant data are within the paper and its Supporting Information files

Funding: This work was supported by Fondation Bettencourt-Schueller, Fondation Lefort-Beaumont de l'Institut de France, INSERM, Universite´ Paris Descartes and Rarecells Diagnostics. Rarecells Diagnostics, Thermo Fisher Scientific and Fasteris SA provided support in the form of salaries for authors SL, LB, KH, DMD, SJ, MO and LF, but did

Abstract

Circulating Tumor Cells (CTC) and Circulating Tumor Microemboli (CTM) are Circulating Rare Cells (CRC) which herald tumor invasion and are expected to provide an opportunity to improve the management of cancer patients. An unsolved technical issue in the CTC field is how to obtain highly sensitive and unbiased collection of these fragile and heterogeneous cells, in both live and fixed form, for their molecular study when they are extremely rare, par- ticularly at the beginning of the invasion process. We report on a new protocol to enrich from blood live CTC using ISET® (Isolation by SizE of Tumor/Trophoblastic Cells), an open sys- tem originally developed for marker-independent isolation of fixed tumor cells. We have assessed the impact of our new enrichment method on live tumor cells antigen expression, cytoskeleton structure, cell viability and ability to expand in culture. We have also explored the ISET® *in vitro* performance to collect intact fixed and live cancer cells by using spiking analyses with extremely low number of fluorescent cultured cells. We describe results con- sistently showing the feasibility of isolating fixed and live tumor cells with a Lower Limit of Detection (LLOD) of one cancer cell per 10 mL of blood and a sensitivity at LLOD ranging from 83 to 100%. This very high sensitivity threshold can be maintained when plasma is col- lected before tumor cells isolation. Finally, we have performed a comparative next genera-
tion sequencing (NGS) analysis of tumor cells before and after isolation from blood and culture. We established the feasibility of NGS analysis of single live and fixed tumor cells enriched from blood by our system. This study provides new protocols for detection and characterization of CTC collected from blood at the very early steps of tumor invasion.

not have any additional role in the study design, data collection and analysis, decision to publish, or preparation of the manuscript. The specific roles of these authors are articulated in the 'author contributions' section.

Competing Interests: This study was partly funded by Rarecells Diagnostics, the employer of Sophie Laget, Lucile Broncy and Katia Hormigos. Dalia M. Dhingra and Stephen Jackson are employed by Thermo Fisher Scientific and Magne Osteras and Laurent Farinelli by Fasteris SA. PPB, TC and SL are co-inventors of the ISET® patents which protect the Rarecells® Device and its consumables, as well as the analyses performed on cells isolated using the Rarecells® System: Method and device for the separation of biological particles contained in a liquid by means of vertical filtration (FR 0502945; PPB), Process for multi-analyses of rare cells extracted or isolated from biological samples through filtration (US 2013/0316347 A1; PPB, SL, TC). PPB is founder of Rarecells Diagnostics which commercializes the ISET® technology, holds license for the ISET® patents, and is a spin-off of University Paris Descartes, Assistance Publique Hôpitaux de Paris and Institut National de la Santé et Recherche Médicale (INSERM), public Institutions which are owners of the ISET® patents. Life technologies commercialize Hotspot Cancer Panel v2, and Fasteris a service company specialized in next-generation sequencing. There are no further patents, products in development or marketed products to declare. This does not alter our adherence to all the PLOS ONE policies on sharing data and materials, as detailed online in the guide for authors.

Introduction

The most challenging goal in the Circulating Tumor Cells (CTC) field is their unbiased and reliable detection when they are extremely rare, namely at the beginning of the invasion pro- cess. At clinical level, this goal implies the possibility to detect invasive cancers when they are still curable, raising the hope of tremendously reducing cancer mortality [1-4]. At biological level, the initial spread of CTC may provide an outstanding source of material to understand the biology of early tumor invasion. Furthermore, high sensitivity is needed to obtain a suffi- cient number of tumor cells for theranostic analyses.

In this setting, technical challenges remain to be addressed and rigorous *in vitro* perfor- mance validations are required targeting unbiased isolation and detection of CTC when they are very rare, due to their low abundance, fragility, heterogeneity and lack of specific markers [2]. Approximately, forty different CTC isolation/detection methods have been published [5-9]. To our knowledge, however, no report specifically addresses the analytical issues of the use of these technologies for the purpose of early detection of invasive cancers. This implies the isolation without bias of selection and the identification without mistake of the very rare CTC that are spread at the beginning of the tumor invasion process. Early detection of aggressive cancers also implies studying the immune-molecular profile of the rare CTC as well as their growth potential. CTC populations consist of cancer cells with very different phenotypes, including epithelial tumor cells, mesenchymal tumor cells, epithelial to mesenchymal hybrid tumor cells, stem tumor cells and clusters of tumor cells called Circulating Tumor Microemboli (CTM) [2, 4, 10-13]. Furthermore, identification of cancer cells in blood is challenging because of their sim- ilarities to non-tumor Circulating Rare Cells (CRC) such as circulating epithelial-normal cells, epithelial-atypical cells, endothelial cells, normal stem cells and physiological-state dependent cells (such as giant monocytes, micromegakaryocytes and fetal cells in pregnant and ex-preg- nant women) [2]. Taking into account the vast heterogeneity of circulating rare cells and the lack of circulating tumor cells-specific markers, the use of epithelial and/or organ specific anti- bodies at the isolation/enrichment step or for the identification of CTC may lead to selection/ detection biases [2, 4, 13-15].

In 2000, we reported on ISET® (Isolation by SizE of Tumor/Trophoblastic Cells), the first antibody-independent whole blood filtration-based approach for CTC isolation. This method relies on the larger size of all types of CRC as compared to the majority of leukocytes [10].

ISET® is performed within 5 hours after blood collection and carefully preserves the cell mor- phology. When combined with cytopathology, the filtration method has been shown to allow distinguishing circulating malignant cells derived from practically all types of solid tumors from circulating benign cells including those derived from organs [2,4,16].

Several studies have shown the feasibility of characterizing CTC isolated by ISET® using simple or multiple immuno-fluorescence labeling [11, 17, 18], simple or multiple immuno- cytochemistry labeling [10, 12, 19, 20], FISH analyses [10, 21-23] and targeted molecular analyses [10, 17, 24-26].

ISET®'s sensitivity threshold (lower limit of detection (LLOD)) was initially determined at one tumor cell per mL of blood using a prototype [10], a result which has been subsequently confirmed by an independent team [25]. In 2006, our team has developed a device and con- sumables (ISET® System) specifically designed to make our approach reproducible in other laboratories. Independent teams have since then confirmed its *in vitro* LLOD of one tumor cell per mL of blood [12, 27-29] and shown its *in vivo* superior sensitivity [3], including in com- parative tests [12, 17, 20, 22, 23, 30-32].

We report here the careful assessment of the ISET® System's *in vitro* analytical performance. We have studied its LLOD as well as its sensitivity at the sensitivity threshold (LLOD). Until now, studies have only demonstrated the ISET® System's ability to isolate fixed CTC capturing them attached to filters. However, their sensitive enrichment as living cells is required for a deeper investigation of their molecular code and to explore their possible use for culture and drug sensitivity assays. In the present report a new variant protocol of the ISET® System to enrich live CTC from blood and its analytical assessment is demonstrated. Our results show that our system and protocols allow collecting fixed and live CTC from blood with a LLOD of one CTC per 10 mL of blood. We also show that live tumor cells isolated from blood using the new protocol maintain their initial antigen expression levels, their viability and ability to grow. Finally, we compared by next generation sequencing (NGS) molecular profiles of tumor cells before and after isolation from blood and culture. We address the feasibility of analyzing by NGS the genetic code of individual cells enriched from blood by our system.

These results and developments should foster clinical and fundamental studies targeting the very early steps of tumor cells invasion.

Material and Methods

A- Blood samples collection

Blood from healthy volunteers was obtained from the French Blood Bank (Etablissement Français du Sang) according to the local ethics rules (agreement number 2014000051/U1151). Blood samples were drawn preferentially in liquid K_3EDTA tubes (Becton Dickinson, USA) with immediate gentle agitation after blood collection. If samples were not processed immedi- ately after blood withdrawal, the tubes were left on a blood agitator until processing within 5 hours after blood collection.

B- Cell lines, cell size analysis of cells from cell lines

A549 (human lung adenocarcinoma), HeLa (human cervical epithelioid carcinoma), MCF-7 (human breast adenocarcinoma) and LNCaP (human prostate adenocarcinoma) cells were obtained from American Type Culture Collection (ATCC, USA). Mouse MMTV-PyMT cells, obtained by mammary gland-specific expression of the polyomavirus middle T antigen [33], were a kind gift from Dr. Takemi Tanaka (Oklahoma University, USA). H_2/H_3-GFP-HCT116 cells (human colon cancer) were a kind gift from Dr. Guido Kroemer (Institut Gustave Roussy, France). A549, LNCaP and MMTV-PyMT cells were cultured in RPMI media supplemented with 10% Fetal Calf Serum (FCS) and 1% penicillin-streptomycin (P/S). MCF-7 cells were grown in DMEM media supplemented with 10% FCS and 1% P/S. HCT116 were grown in MacCoy media supplemented with 10% FCS and 1% P/S. All cells were cultured at 37˚C with 5% CO_2, and passaged regularly as previously described [10, 34].

For cell size analysis on ISET® filters, trypsin-treated cultured cells were fixed with the Rarecells® Buffer (ref. 54 0203) for 10 minutes, when mixed with blood, or for 3 minutes without blood and filtered through ISET® filters with a nominal pore size of 8 or 5 μm. Cells on filters were stained with the May-Grünwald Giemsa (MGG) cytopathological staining, as described previously [35]. Analysis of cell size on ISET® filters was performed with an Eclipse micro- scope (Nikon, Japan) equipped with the Cell Cut System using the pre-calibrated software (Molecular Machines and Industries, Germany). The size of at least 100 individual MGG- stained cells was analyzed for each cell line.

C- Isolation from blood of fixed tumor cells using the ISET® system

The CE-IVD labeled Rarecells® Device and its consumables (Rarecells Diagnostics, France) were used to assess the *in vitro* performance of the ISET® standard protocol for marker-inde- pendent isolation of fixed tumor cells from blood (Fig 1A). The Rarecells® Buffer solution (ref. 54 0203) was reconstituted according to the manufacturer instructions. The reconstituted buffer solution can be stored frozen at -20˚C for up to 6 months. Before use, the pH is adjusted to 7.2. Formaldehyde is then added for cell fixing and to obtain a 0.74% final concentration. 90 mL of Rarecells buffer is then used to dilute ten mL of blood (10-fold dilution) to prepare it for filtration. Blood pretreatment has to take place for exactly 10 minutes under constant gentle stirring on a horizontal mixer (CAT Ingenieurbüro model# RM5-40).

A disposable cartridge (Rarecells® Block) containing a filter having proprietary characteris- tics and 8 microns nominal pores size is set into the device. The cartridge contains 6 compart- ments: a large compartment for filtration of 5 mL of blood and 5 smaller compartments, each one for filtration of 1 mL of blood. The compartments are independent, allowing filtering vari- able volumes of blood from 10 μL to 10 mL of blood (100 μL to 100 mL of diluted blood).

Empty compartments have to be closed during filtration with Rarecells® Block lids.

The protocol starts with filtration of 50 mL of sterile PBS to hydrate the filter, then the diluted blood is loaded (100 mL of 1:10 diluted blood) into the Rarecells® Block and filtered at a typical standard calibrated depression of -10 kPa. Blood filtration lasts no longer than a minute.

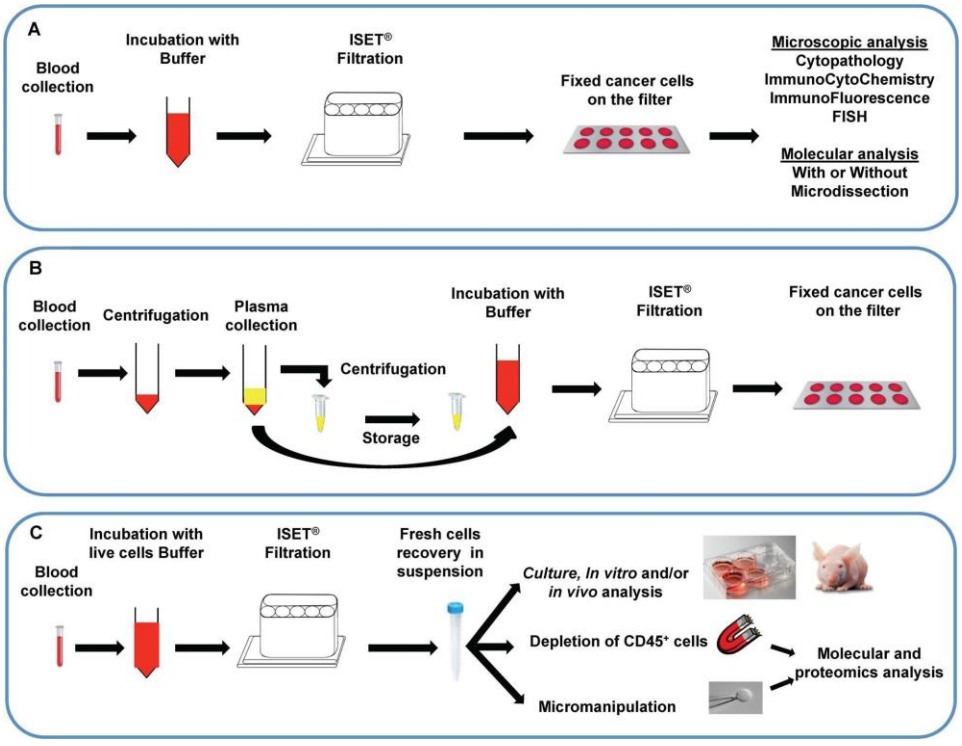

Fig 1. Overview of ISET® filtration workflows. (A) ISET® workflow for isolation and downstream analysis of fixed Circulating Rare Cells (CRC) from 10 mL of whole blood (See Methods section 3 for details). The filter can subsequently be sent by post or stored in biobank for years [21] for further CRC staining, cyto-morphological analysis and counting, immuno-labeling, *in situ* hybridization and molecular analyses (with or without laser capture microdissection). (B) ISET® workflow for dual collection of plasma and enrichment of fixed CRC from whole blood (See Methods, section 4 for details). (C) ISET® workflow for enrichment and downstream analysis of live CRC from whole blood (See Methods, section 5 for details). Optionally, single-cells can be isolated by micromanipulation for further analyses or CRC can be purified by immune-magnetic depletion of $CD45^+$ cells before further molecular or cell growth assays.

doi:10.1371/journal.pone.0169427.g001

Since the degree of blood cellularity may be variable due to physiological or pathologi- cal conditions and may increase blood resistance to filtration, the device allows increasing the depression for a few seconds if needed in order to complete filtration. This method allows maintaining a minimum shear force and sticks the cells to the filter avoiding their loss. The tubes that contained the diluted blood are then rinsed with 100 mL of sterile PBS that is also filtered in a few seconds. The cartridge is released from the device and disassembled in order to extract and gently rinse the ISET® filter with sterile distilled water. Fixed cells are left to dry and attach firmly to the filter at room temperature for 15 to 30 minutes.

The filter contains 10 circular areas (spots) and each spot contains the CRC that were, before filtration, in one mL of blood along with some residual leukocytes.

The technical characteristics of the Block allow processing 1 to 10 mL of blood by ISET®, while the number of spots still corresponds to the number of milliliters of blood filtered. The counting of the number of CTC per mL then conveniently corresponds to the number of spots counted.

Tumor cells distribution (intra-assay precision and accuracy) analyses. In order to verify the random distribution of CTC on the five spots located in the large compartment of the Rarecells® Block, cultured A549 cells were made fluorescent and precisely counted as described in section 6. An aliquot of 100 μL of the diluted suspension containing 50 cells was added to 5 mL of healthy donor' s blood and processed by filtration (Fig 1A).

The number of tumor cells found on each spot (each corresponding to the filtration of 1 mL of blood) was recorded.

For each experiment, we calculated the average number of tumor cells found if considering randomly only 1 spot, only 2 spots, only 3 spot and only 4 spots. We analyzed all possible single spots or randomly grouped spots (any 1, any 2, any 3, any 4 spots) and calculated corresponding mean values and their standard deviations. Intra-assay precision (percent coefficient of variation, %CV) and accuracy (%Error) were calculated (formula given in section 6).

Counting of residual leukocytes. In order to evaluate the number of remaining White Blood Cells (WBC), one mL of blood from four different healthy donors was filtered and stained with Hematoxylin and Eosin. Leucocytes were then carefully counted under microscope.

D- Dual collection of plasma and fixed tumor cells

We have assessed the feasibility of recovering plasma from whole blood, collected on EDTA as previously described, without losing fixed CTC (Fig 1B). Fluorescent tumor cells were added to blood by individual cell micropipetting according to the protocol described in section 6 and Fig 2A. Two aliquots of 5 mL of blood were transferred into 2 x 50 mL Falcon tubes and centrifuged at 150 g for 10 minutes and 2 x 1 mL of the upper phase (plasma) were carefully pipetted without disturbing the interphase and transferred to a micro-centrifuge tube. The collected plasma was then centrifuged at 15000 g for 10 minutes (to eliminate potential debris), the supernatant carefully transferred to a new microcentrifuge tube and stored at -20˚C for further analyses. The remaining 2 x 4 mL of blood were then carefully diluted to 50 mL volume each with the Rarecells® Buffer (ref 54 0203) and mixed by a gentle and slow inversion of the tube at least 20 times. The diluted blood was then left for 10 minutes under horizontal mild agita- tion and processed by the ISET® system to isolate fixed tumor cells as described above.

E- Isolation from blood of live tumor cells and their characterization: tumor cells' size, antigen expression, viability, culture and study of cytoskeleton markers

The Rarecells® Device and Block were used with a new protocol developed to obtain the marker-independent enrichment of live tumor cells from blood without sticking them to the

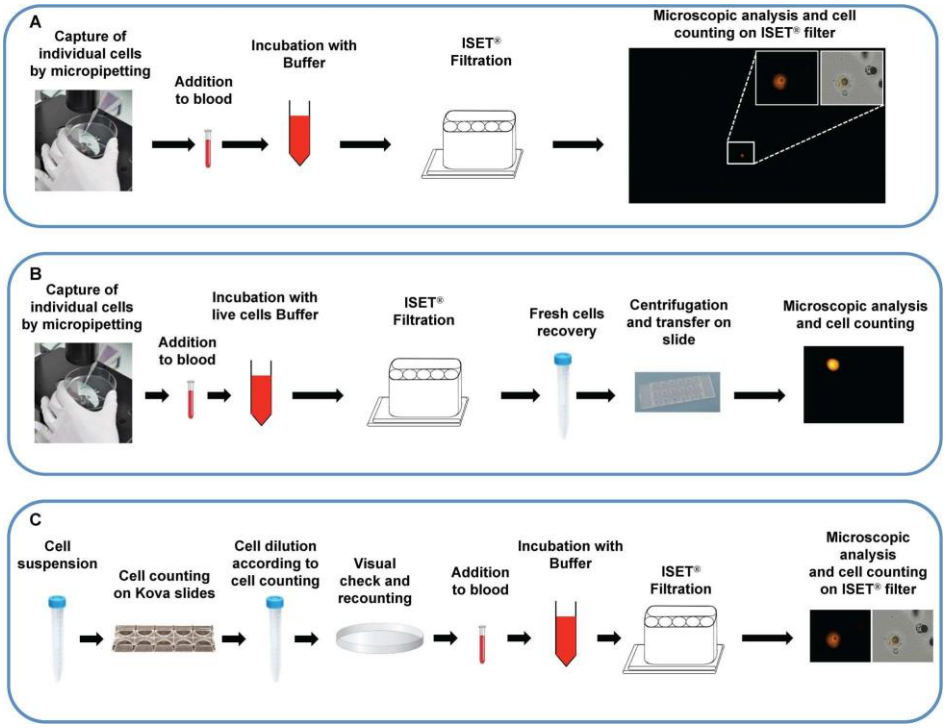

Fig 2. ISET® sensitivity *in vitro* assays using individually micropipetted tumor cells. (A) *In vitro* sensitivity assay using the ISET® workflow described in Fig 1A (See Methods sections 3 and 6 for details). Image: example of recovered fixed cell stained with Cell Tracker™ Orange (larger panel: TRITC filter only, lower magnification, or smaller panels (higher magnification, TRITC filter only or merge of TRITC filter and brightfield)). (B) *In vitro* sensitivity assay using the ISET® workflow described in Fig 1C (See Methods, sections 5 and 6 for details). Image: example of recovered live cell stained with Cell Tracker™ Orange (TRITC filter). (C) *In vitro* sensitivity assay using the ISET® workflow described in Fig 1A (See Methods sections 3 and 6 for details) with precise counting of cells by dilution. Image: example of recovered fixed cell stained with Cell Tracker™ Orange (TRITC filter only or merge of TRITC filter and brightfield)

doi:10.1371/journal.pone.0169427.g002

filter (Fig 1C) and its performance was assessed. The Rarecells® Live Cells Buffer solution (ref. 54 0208) was reconstituted according to the manufacturer instructions (Rarecells Diagnostics, France). This solution can be used for up to a week if stored at 4˚C and for up to 6 months if frozen and stored at -20˚C.

Blood was diluted 10 fold with the Rarecells® Live Cells Buffer and kept at room tempera- ture for 5 minutes under gentle constant stirring. The diluted blood (its color becomes bright ruby) was then transferred to the Rarecells® Block and filtered slowly using a minimal depression force (typically -3to -6kPa). When about 200–500 μL of diluted blood remained in the wells, the filtration was stopped. The tubes that contained the diluted blood were rinsed with 13 mL of sterile PBS and the rinse solution was filtered with the device leaving again 500 μL of liquid into the wells. To obtain this, the depression was stopped by closing the tap and turning off the device so that the cells remained in suspension (not attached to the filter). The walls of each well were further rinsed 3 times by filtration with 1 mL of PBS (or culture media) supple- mented with 2% FCS and 3 mM EDTA, again leaving 500 μL of liquid into the well. Finally, the liquid containing the enriched tumor cells (500 μL) was very carefully transferred with a micropipette from the cartridge to a tube or cell culture microplate.

Optionally, live tumor cells enriched from blood by ISET® were concentrated by centrifu- gation for 4 minutes at 300 g. The supernatant was carefully eliminated leaving 20 to 30 μL of

cell suspension, which can be transferred to an 18 well-flat microchamber (Ibidi, Germany) for microscopy evaluation and cell counting or other downstream analyses such as short-term culture.

Optionally, the enriched live cells can be collected with a suitable fixative for downstream analyses or with a storage fixative (Rarecells® Fixcells, Rarecells Diagnostics, France) allowing their storage at + 4˚C for up to 4 weeks.

Optionally, tumor cells can be isolated in suspension as fixed cells (without sticking them to the filter). To this aim, we diluted the blood 1:10 with the Rarecells^{1} Buffer (ref. 54 0203).

After mild agitation for 10 min, we applied the same filtration protocol described for enrichment of live tumor cells and collected the fixed tumor cells.

Counting of residual leukocytes. We assessed the number of remaining leukocytes after live tumor cells enrichment using 2 x 5 mL of blood obtained from 2 distinct healthy donors in 2 separate tests, and using a TC20™ Automated Cell Counter (Bio Rad, USA) after cell staining with Trypan Blue.

Elimination of residual leukocytes after live tumor cells enrichment by ISET®. We tested the feasibility of eliminating the residual leucocytes after live tumor cells enrichment by the ISET® system. To this aim, the live tumor cells samples obtained with the ISET® system were treated with the manual column-free method EasySep™ and the 'Human CD45 Deple- tion kit' (StemCell Technologies, Canada) that contains a combination of monoclonal antibod- ies against the leucocyte marker CD45 [36]. This kit is originally intended for use with whole blood after Ficoll-type density centrifugation, a step that is known to lead to highly significant tumor cells loss [37, 38]. In order to adapt this kit to the protocol for isolation of live tumor cells by ISET®, the amount of antibody and nanoparticles was reduced by 4-fold while the other manufacturer's recommendations were followed. In brief, CD45 positive cells were specifically labeled with dextran-coated magnetic nanoparticles using bispecific Tetrameric Antibody Complexes (TAC). Tumor cells were then recovered after two successive CD45 depletions using the EasySep™ Purple Magnet.

Live tumor cells' number, size and viability after their enrichment by ISET®. Cells were prepared and carefully counted as described in section 6. A fraction of the cell suspension (typically 100 μL) was mixed with 1 mL of blood from a healthy donor, or 1 mL of PBS, diluted tenfold with the Rarecells® Live Cells Buffer and kept at room temperature for 5 minutes, or 3 minutes when cells were treated without blood, under gentle constant stirring. Filtration was then performed with the new protocol as described above. For comparison of cell counts, sizes and viability on the TC20™ Automated Cell Counter (Bio Rad, USA), 10 μL of either the unfil- tered cells or the enriched fraction recovered after filtration were diluted 1:2 with Trypan Blue and loaded into a counting slide (Dual chamber for cell counter, BioRad, USA). Three or more counts were performed to obtain consistent counting values.

Live tumor cells antigen expression assessment before and after their enrichment by ISET®. We assessed the potential impact of this new ISET® filtration protocol on cell surface antigens' expression by fluorescent labeling of the Epithelial Cell Adhesion Marker (EpCAM) on MCF-7 cultured cells before and after live cell enrichment by ISET®. MCF-7 cells in culture were first incubated with 5 μg/mL of Hoechst 33342 (Sigma-Aldrich, USA) for 2 hours before being rinsed twice with PBS, detached from the flask by incubation with trypsin (0.125%) and resuspended in 5 mL of culture media as described in section 6. A fraction of the cell suspension (typically 100 μL) was mixed with 1 mL of blood from a healthy donor, diluted 1:10 with the Rarecells® Live Cells Buffer and kept at room temperature for 5 minutes under gentle con- stant stirring. The enriched fraction recovered after live cells filtration was centrifuged for 2 minutes at 150 g. The supernatant was carefully eliminated leaving 100 μL of suspension. Fluo- rescent labeling of EpCAM was performed on both the unfiltered cells and the enriched

fraction recovered after ISET® filtration. 20 μL of Human FcR binding inhibitor (eBioscience, USA) were added to each 100 μL suspension and kept in the dark at 4˚C for 20 minutes. The Alexa Fluor 488 conjugated anti-EpCAM antibody clone VU1D9 (Cell Signaling Technology, USA) was diluted 1 to 30 in PBS and 20 μL of that dilution were then added to each sample fol- lowed by a 30 minutes incubation in the dark at 4˚C. After washing with 1 mL of PBS, the cells were centrifuged at 300 g for 4 minutes and transferred to a microchamber (Ibidi, Germany). Microscopy evaluation was performed with an epi-fluorescence microscope (Zeiss, Germany). The DAPI filter (emission at 465 nm) and the FITC filter (emission at 525 nm) were used for the detection of the Hoechst and the EpCAM signals, respectively. Images were processed with Image J software. To perform quantitative analysis of EpCAM fluorescence, we analyzed two consecutive optical fields and measured the cell mean fluorescence, the cell area and the inte- grated density (fluorescence per area) for each cell (50 MCF-7 cells before and 50 MCF-7 cells after live cell enrichment). We then calculated the corrected total cell fluorescence (CTCF).

CTCF = Integrated_density–(Area_of _selected_cell x mean_background_fluorescence). Furthermore we applied cutoffs at 91000 units and 200000 units of CTCF based on the calcula- tions of the first and third quartiles of each data set.

Live tumor cells growth after their isolation by ISET®. We performed *in vitro* culture experiments of live tumor cells enriched from blood by ISET®. In two separate tests with 3 replicates, 10^4 A549 cells were added to 1 mL of healthy donor' s blood before treatment with the Rarecells® Live Cells Buffer as described above and in section 6. Samples were incubated for 5 min before filtration as described above.

The enriched cells were recovered and centrifuged for 2 minutes at 150 g. After removal of the supernatant, each pellet was carefully resuspended in 100 μL of complete media, deposited onto a round glass coverslip of 1.2 cm in diameter (MGF-slides, Microscopic Glass Factory) and placed in a 24-wells culture plate (Multiwell™ 24, Becton Dickinson, USA). Cells were left to attach for 2 hours in a culture incubator. Coverslips were then washed with 300 μL of PBS and the cells were either collected for immediate microscopy observation (D0 time points) or supplemented with fresh media and kept in culture for 48 hours (D2 time points) or up to 5 days (D5 time points) before observation.

Confocal microscopy analysis of cytoskeleton markers before enrichment and after enrichment by ISET® and culture for 72 hours. To assess the potential impact of our live tumor cells isolation protocol on cytoskeleton structures, we used cytoskeleton markers and immunofluorescence staining of actin microfilaments and microtubules together with confo- cal microscopy. Live A549 and H2228 tumor cells were seeded onto round glass coverslips and placed in a 24-wells culture plate before and after live cell enrichment from blood by ISET®, as described above. Cells were kept in culture for 72h before fixation by incubating 15 minutes with a 4% paraformaldehyde solution. Cells were then washed twice with PBS and permeabi- lized 15 minutes in PBS containing 0,2% Triton X-100 before washing again twice with PBS. Antigens were then blocked by incubating with PBS containing 10% FCS for 1h at room tem- perature. Primary mouse antibody targeting human actelyl-α-Tubulin (6-11-B1 clone, Ther- mofisher Scientific, USA) was diluted 1:200 in PBS containing 10% FCS and incubated 1h at room temperature. Cells were then washed twice with PBS and incubated 30 minutes in the dark with a 1:200 dilution of the secondary goat anti mouse antibody conjugated to a Dylight 488 fluorophore (Thermofisher Scientific, USA). Without washing, samples were then supple- mented with Alexa Fluor 568 conjugated Phalloidin (Thermofisher Scientific, USA) for F- actin labeling at 20 units/mL and kept in the dark for another 30 minutes at room temperature. Cells were then washed three times in PBS and incubated 15 minutes at room temperature and in the dark with PBS containing 8 μM Hoechst for nuclear staining. After rinsing twice with PBS, coverslips were finally mounted on glass slides using Ultramount permanent mounting

medium (Dako, USA). Microscopy evaluation was performed with an SP5 confocal micro- scope (Leica, Germany) and all images were acquired with identical parameter settings. Images were processed with Image J software and the quantitative analysis of both actin and tubulin fluorescence was performed on 30 cells for each sample evaluated by calculating the corrected total cell fluorescence (CTCF) of each signal as described above.

F- Sensitivity tests and spiking analyses with fluorescent cells

Spiking tests were performed to assess the performance of the ISET® system for isolation and enrichment of fixed and live tumor cells. The sensitivity threshold, also named lower limit of detection (LLOD), is the lowest concentration of tumor cells detectable by a method. It is usu- ally determined by extrapolating a plot of concentration (x) vs measurement unit (y) to the x-axis. The intercept is the lower limit of detection. Sensitivity is the smallest concentration change that a method is capable of detecting. It is determined from the slope of the previously described plot [39]. Since high sensitivity is critical in the rare cells field, we emphasized our work on determining sensitivity in a concentration range close to the LLOD.

Typically, 60–70% confluent cells were cultured and stained in flask with the addition of fluorescent dyes—either 5 μg/mL of Hoechst 33342 (Sigma-Aldrich, USA) or 5 μM of Cell Tracker™ Orange (Life technologies, USA) overnight or for at least two hours. Cells in culture were rinsed twice with PBS to eliminate debris and detached from the flask by incubation with trypsin (0.125%) for 2 minutes at 37˚C. Trypsin reaction was stopped by addition of 2 mL of culture media. Cells were further diluted with PBS, centrifuged at 300 g for 4 minutes, and carefully resuspended in 6 mL of culture media. 10 μL were then diluted 1:2 with Trypan Blue and cells were counted with a manual counting slide (KOVA Glasstic slide 10 with grids, Hycor Biomedical Inc, USA). Three or more counts were performed to obtain consistent counting values. If needed, the cell suspension was mixed again to obtain a homogenous cell dilution. Fluorescent cells can also be resuspended with Rarecells® Cytofix which allows to store them as fixed cells at +4˚C for up to 5 days. The fluorescent staining can decrease or be lost in some cells after this time, implying that fluorescent cells must be counted again before use.

Counted fluorescent cultured cells were added, typically within 1 hour after trypsin treat- ment, to healthy donor blood. Very precise counting of cells used for spiking tests is critical, thus we used two alternative protocols (Fig 2).

1. Completely accurate counting by micropipetting individual fluorescent cells (1 to 10 cells) (Fig 2A and 2B). A 100 μL-drop of PBS containing approximately 10–40 cells was put in a Petri dish and observed under an inverted Olympus CK30-F2000 microscope at the x10 objective. Cells were carefully picked individually using a common micropipette (Gilson P2) and transferred one by one to the blood sample before its dilution with the Rarecells® Buffer solution for fixed or live cells and filtration.

2. Precise counting (two serial counting) by fluorescent cells' dilution (30 to 300 cells) (Fig 2C). After a first accurate manual cell counting performed with Kova counting slides, a first dilution was prepared to reach the desired concentration. For instance, cells were carefully diluted in 10 mL of PBS in order to obtain the target number of cells (from 30 to 300) per 100 μL of solution. The cell count was again verified by depositing 100 μL of that dilution onto a petri dish and by visually identifying the cells using an inverted microscope. We then calculated the average number of cells per μL and this second count was used to deter- mine the amount of diluted cells used in spiking tests. (We note that this type of further control is technically possible with Kova slides only for cell numbers from 100 to 300 per

100 μL). In all spiking experiments, a positive control with 5000-cultured fluorescent tumor cells added to 1 mL of blood was included to check for cell morphology integrity.

Blood samples with spiked-in tumor cells were then processed with one of the ISET® filtration protocols as described above. For spiking tests with 10 mL of blood, we used a 150-mL Falcon-type tube (Dominique Dutscher, France) rather than two 50-mL Falcon-type tubes to dilute the blood (since 50-mL Falcon-type tubes are too small to accommodate 100 mL of diluted blood). After filtration, filters containing isolated fixed cells stained with Cell Tracker™ Orange were optionally stained with 8 μg/mL of nuclear staining Hoechst for 10 min, rinsed with PBS and sterile distilled water and allowed to air dry protected from light. Option- ally, filters were mounted between a slide and a coverslip using the mounting media ProLong® Gold (Life Technologies, USA) before microscopic evaluation.

Fluorescent spiked tumor cells, isolated live and transferred to an 18 well-flat microcham- ber (Ibidi, Germany), or isolated fixed on ISET® filters, were analyzed with an epi-fluores- cence microscope (Zeiss, Germany). The DAPI filter (emission at 465 nm) and the TRITC filter (emission at 576 nm) were used for the detection of the Hoechst and the Cell Tracker™ Orange signals, respectively. Criteria used to identify the spiked-in cells were: i- presence of a cell (defined as round shape with a visible cytoplasm and nucleus) by bright field examination of the filter and ii- detection of a genuine fluorescent signal with the TRITC filter. Presence of auto-fluorescent cell debris was excluded by analyzing the fluorescent image using the 'FITC' filter of the microscope. Images were processed with ImageJ software and reviewed indepen- dently by at least two operators.

For each series of tests, we measured the percentage of recovered cells, the percent coeffi- cient of variation (%CV) and % error as follows:

$$\%CV = \frac{standard\_deviation(measured\_data)}{average(measured\_data)},$$

$$\%Error = absolute\_value(100\% - average\_percentage\_of\_recovered\_cells)$$

G- Next generation sequencing (NGS) molecular characterization of single tumor cells and of cultured tumor cells after their isolation from blood by ISET®

NGS analyses of single tumor cells isolated by ISET®. Live or fixed tumor cells enriched from blood by ISET®, collected without sticking them to the filter as described in section 5, and transferred in suspension to a cell culture plate could be gently picked up manually and individually with a micropipette (Gilson P2) under an inverted Olympus CK30-F2000 micro-scope at the x10 objective and transferred to an individual 0.2 mL PCR tube.

Single cells' proteins were lysed so as to release the DNA using our in house protocol (in 15 μL, 100 mM TrisHCl pH 8 and 400 μg/mL of proteinase K incubated for 2 hours at 60˚C followed by proteinase K inactivation for 5 min at 94˚C). The single-cell DNA was then pre- amplified by combining our lysis protocol and by adapting it to single-cell whole genome amplification (WGA) commercial kits: MALBAC (Yikon Genomics, China); Picoplex (Rubi- con Genomics and New England BioLabs, USA); GenomePlex (Sigma-Aldrich, USA). Ampli- fied DNA was then purified using the DNA Clean & Concentrator™-5 kit (Zymo Research, Germany) and quantified by Quant-iT™ PicoGreen[1] dsDNA Assay Kit (Thermo Fisher Scien- tific, USA). The WGA products' quality was assessed by PCR as described elsewhere [40].

For NGS single-cell analysis using the Illumina approach, 250 ng of the amplified DNA was used to prepare libraries for high-throughput sequencing with the Nextera Exome Enrichment Kit (Illumina, USA) following the supplier's protocol. A fraction of the library DNA from the

pre-capture step was used for whole genome analysis. The libraries were sequenced on a HiSeq2000 (Illumina) in 2 x 100 bp paired-end runs. Data were mapped against the human genome and the number of reads per chromosome was calculated.

In order to perform single-cell targeted theranostic mutations' NGS analysis, we used the ThermoFisher approach, 10 ng of purified WGA DNA was used to generate 207 amplicons libraries including 50 oncogenes and tumor suppressor genes through the use of the optimized primer pool "Hotspot cancer panel v2" and Ion Torrent™ Library Kit V2 (ThermoFisher, USA), according to manufacturer's recommendations. Briefly, Ion adapters and barcodes were added using the "bioanalyzer protocol" (for living single cells and bulk extracted DNA) or the "FFPE protocol" (for fixed single cells), respectively for 17 cycles and 20 cycles of pre-amplica- tion. The quality of purified libraries was verified with the Bioanalyzer (Agilent, USA) and quantified by qPCR using the Ion Library TaqMan™ Quantitation Kit. Libraries were tem- plated using the Ion One-Touch system and sequenced on Ion Torrent™ 318 chips using the Ion Personal Genome Machine™ (ThermoFisher, USA).

Data analysis was performed using the Ion Torrent™ suite (ThermoFisher, USA) and Excel (Microsoft, USA) softwares. Sequencing artifacts in homopolymer regions were filtered out. In theory, when analyzing diploid single cells, only three allele frequencies should be possible: 0% (wild-type), 50% (heterozygous mutant/wild type) and 100% (homozygous mutant). However, WGA and sequencing methods introduce variability and quantitative amplification biases. In consequence, COSMIC hotspot mutations were included in our analysis only if present in at least one single cell WGA sample with a quality score over 100 and 15% allele frequency while using 10X depth amplicon coverage. Venn diagrams were drawn using a public online tool (bioinformatics.psb.ugent.be/webtools/Venn/).

NGS analysis of tumor cells isolated by ISET® and cultured for 72 hours. In order to investigate the feasibility of studying possible tumor cells' genetic changes induced by their iso- lation from blood with our method and culture for 72 hours, we performed NGS analysis on tumor cells before and after isolation by ISET® and culture. Approximately 10^4 live A549 and 10^4 HCT116 live tumor cells were seeded in a 24-wells culture plate before and after their enrichment from blood by ISET®, as described above. Cells were kept in culture for 72h before their collection for DNA extraction by incubating them for 2 minutes with trypsin (0.125%) at 37°C. Trypsin reac- tion was stopped by addition of 2 mL of complete media. Cells were further diluted with PBS, cen- trifuged at 300 g for 4 minutes, and carefully resuspended in 200 μL of PBS for DNA extraction.

We extracted bulk DNA from our samples using the QIAamp DNA Blood Mini Kit (Qiagen, Germany) following the manufacturer's instructions. We then used 10 ng of extracted bulk DNA from unfiltered control tumor cells and from tumor cells cultured for 72 hours after ISET® filtration using the same ThermoFisher protocols with the 'Hotspot Cancer Panel V2' and Ion Torrent™ Library Kit V2 (ThermoFisher, USA) used for single tumor cells.

Data from experiments on tumor cells' populations were further processed with Sophia DDM® software (Sophia Genetics, Switzerland) to calculate variant fraction and coverage. Only variants with more than 5% of allele frequency were reported.

Results

A- Cell size analysis

A comparative cell size analysis of cells from human and mouse tumor cell lines was per- formed to characterize cells used to assess the sensitivity of tumor cells isolation by ISET® (Fig 3A and Table A in S1 File). As detailed in the Methods section 2, at least 100 individual cells from each cell line were analyzed after filtration through standard 8 micron-pores ISET® filters, and MGG staining. The median diameter of cancer cells ranged from 12 μm (mouse

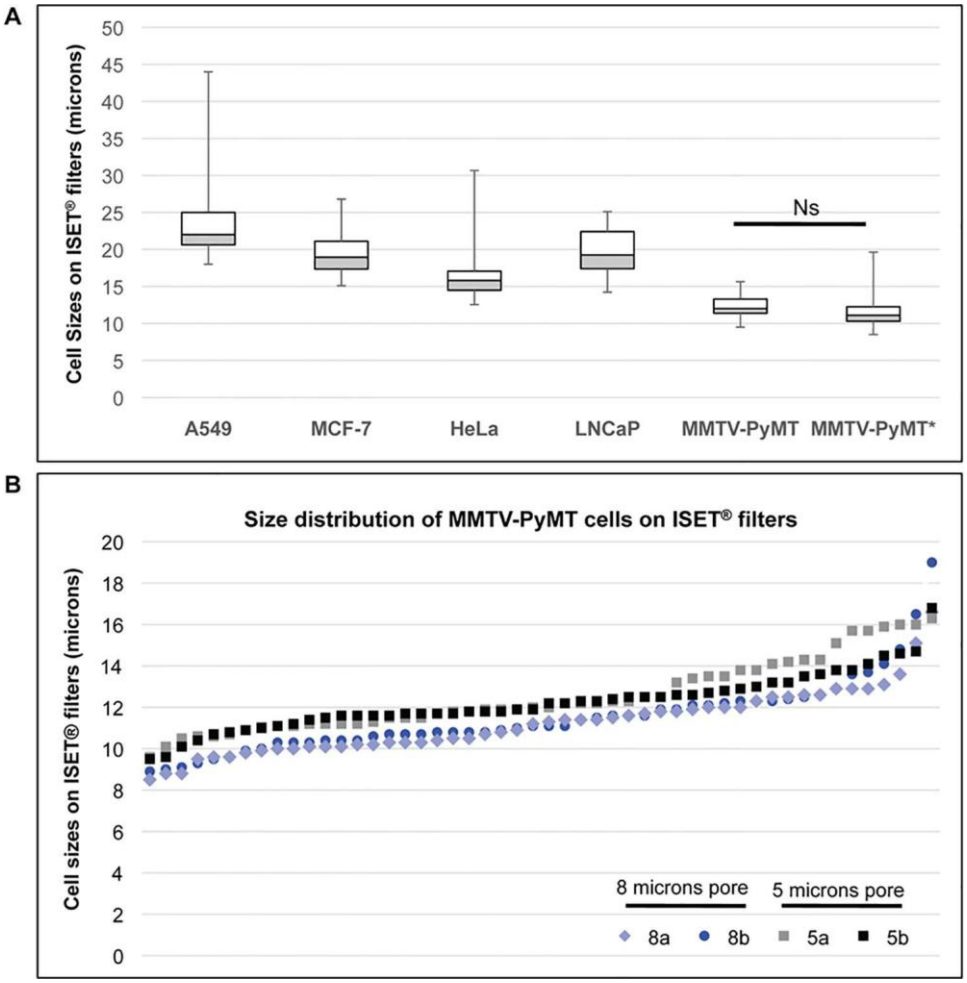

Fig 3. Cell size assessment of tumor cells from human and mouse tumor cell lines. (A) Box plot of cell sizes (diameters) according to each cancer cell line tested. Each box has its ends at the quartiles, and the median of distribution is marked by a line within the box. Error bars indicates maximum and minimum diameters. Cells from human and mouse tumor cell lines were incubated 3 min with the Rarecells® Buffer without blood and recovered on standard (8 micron-pore) ISET® filters. MMTV-PyMT*: values measured for MMTV-PyMT cells isolated using 5 micron-pores ISET® filters. Cells were stained on filters using May-Grünwald Giemsa before analysis by microscopic observation. Ns: Not significant. (B) Size distribution of two series of 50 MMTV-PyMT cells on ISET® filters isolated using 8 micron-pore filters (8a and 8b) and 5 micron-pores filters (5a and 5b).

doi:10.1371/journal.pone.0169427.g003

MMTV-PyMT) to 22 μm (human A549). The mean size ranged from 11.4 μm (MMTV-PyMT, standard deviation [stdev]: 1.6) to 23.2 μm (A549, stdev: 4.4) (Table A in S1 File). LNCaP median diameter measured 19.2 μm which is consistent with previously reported data [10].

We also studied the smallest MMTV-PyMT cells by comparing the range of cell sizes after filtration with the standard 8 micron-pore ISET® filters with those obtained after filtration with 5 micron-pore ISET® filters, in order to assess a possible loss of small cells when using the 8 micron-pore filters. The median and mean diameters of MMTV-PyMT on 5 micron- pore filters were respectively 11.1 μm and 11.4 μm (stdev: 1.7) (Fig 3 and Table A in S1 File). Using the chi^2 test, when comparing the 100 individual data points obtained on the 8 micron- pore and the 5 micron-pore filters, we did not observe a statistical difference. Furthermore, when plotting cell size data for two series of 50 MMTV-PyMT cells for each 8 and 5 micron-

pore filters, we observed a similar distribution throughout all the size ranges (i.e. 8.5 to 16.8 μm) for both types of filters (Fig 3B), indicating that there is no size-selection bias when isolating the small cells from this cell line with the standard pore size of ISET® filters. Fig 3A in fact shows that the MMTV-PyMT median cell size after ISET® filtration through 5-micron pores is slightly greater than that calculated after ISET® filtration through 8-micron pores. However, the difference is not statistically significant and could be related to different batches of cells collected at different times.

These data are consistent with the results described in section C-1 (Table C in S1 File) showing that the size of live MMTV-PyMT cells remains essentially the same before and after ISET® filtration.

A- *In vitro* performance of the ISET® system for isolation of fixed tumor cells

B1. Sensitivity and precision (repeatability and reproducibility) of the ISET® system for isolation of fixed tumor cells from blood. We assessed the analytical sensitivity, sensitiv- ity threshold (or Lower Limit of Detection (LLOD), i.e. the smallest amount of cancer cells which can be detected), repeatability and reproducibility of the ISET® standard system for iso- lation of fixed tumor cells (Fig 1A). Because of the particular clinical relevance of detecting tumor cells in blood when they are very rare, we tested the LLOD and the sensitivity at the LLOD of the ISET® system by performing analyses with very low numbers of fluorescent tumor cells, counted one by one by micropipetting and spiked in blood from healthy donors. Typical "spiking tests" experiments were performed by adding individually micropipetted A549, MCF-7, HeLa or MMTV-PyMT fluorescent tumor cells to one to ten mL of blood and processing the blood by ISET® filtration (Fig 2A). We then analyzed the filter and detected the recovered spiked cells by looking for their fluorescent signal. We only counted fluorescent sig- nals proven to be fluorescent cells (see Methods, section 6). This *in vitro* assay was 100% spe- cific (n = 4 tests with 0 spiked cells in 1 mL of blood).

To assess reproducibility by two different operators using different reagent lots and instru- ments, we performed 12-fold replicate tests with two A549 cells spiked in one mL of blood. We found a total number of 21 and 20 out of 24 spiked cells per operator, respectively (Table 1), with an average recovery success rate of 88% and 83%

Given the structure of the ISET® cartridge (which separates 10 mL of blood in 10 samples of one mL of whole blood i.e. 10 samples of 10 mL of diluted blood) and since the LLOD of one tumor cell per mL of blood had been found by our team and by independent teams [12, 25, 27-29], we thought that the LLOD and physical limit of the ISET® system down to one tumor cell per 10 mL of blood could potentially be achieved and should be tested. Conse- quently we spiked by individual cell counting in 6-fold replicate tests two A549 cells in one mL, five mL and ten mL of blood. We found a total of 10 of 12, 10 of 12 and 12 of 12 spiked cells, respectively, with an average recovery success rate of 83%, 83%, and 100% respectively (Table 2). Similarly, in 10-fold replicate tests with 1 MCF-7, we recovered 9 out 10 spiked MCF-7 cells. In 3-fold replicate tests with 1 and 3 HeLa cells, we recovered 3 out 3 spiked HeLa cells, and 9 out of 9 spiked HeLa cells, respectively (Table 3).

Using the same protocol and workflow, we also spiked the mouse MMTV-PyMT cells which isolation had been studied on 8 micron-pore and 5 micron-pore filters (Fig 3B). In 4-fold replicate tests with two MMTV-PyMT cells, we found a total number of 6 out of 8 spiked cells (Table 3).

Our sensitivity tests with the ISET® System were found to be reproducible and the LLOD was determined as one cancer cell per 10 mL of blood (Tables 1-3). Sensitivity at the closest

Table 1. *In vitro* assay of the repeatability and reproducibility of ISET® sensitivity tests for isolation of fixed cells.

	Operator A	Operator B
Blood processed	**1 mL**	**1 mL**
Spiked tumor cells/test	2	2
Fixed tumor cells detected by ISET® per test (N = 12 tests)	1	2
	2	2
	2	2
	1	1
	2	1
	2	2
	2	2
	2	2
	1	2
	2	0
	2	2
	2	2
Total detected/spiked cells	21/24	20/24
Recovery success rate	88%	83%

doi:10.1371/journal.pone.0169427.t001

concentration to the LLOD was 100%. Importantly, similar average recovery success rates were found with various volumes of blood processed (1 mL, 5 mL or 10 mL of blood) (Table 2) and tumor cells having different sizes (median sizes ranging from 12 to 22 μm) (Tables 1–3, A in S1 File and Fig 3).

B2. Linearity and accuracy of the ISET® System for isolation of fixed tumor cells from blood.

We next assessed the ISET® System' s linearity (i.e. predictability of sample recovery with known dilution factors within an assay range or overall sensitivity) and accuracy (i.e. true- ness as compared to a reference) by using fluorescent A549 cells carefully counted by dilution (see Methods, section 6) and processed with the ISET® fixed cells protocol (Fig 1A and Meth- ods, section 3). Recovery is calculated when cells are spiked into the relevant matrix, blood in our case, at a minimum of five concentration levels covering the linear range of the assay (according to the FDA definition, Docket No. 2004D-0163).

We have assessed linearity by spiking 30, 100 and 300 A549 cells, all counted by dilution, in one mL of blood in 9, 13 and 2 replicates, respectively. We have also plotted the number of observed fluorescent A549 cells on ISET® filters after their counting by micropipetting versus the expected number of A549 (Tables 1 and 2 and Fig 4A). Using a linear regression analysis,

Table 2. *In vitro* assay of ISET® sensitivity threshold for isolation of fixed A549 cells.

Blood processed	1 mL	5 mL	10 mL
Spiked tumor cells/test	2	2	2
Fixed tumor cells detected by ISET® per test (N = 6 tests)	1	1	2
	2	2	2
	2	2	2
	1	2	2
	2	2	2
	2	1	2
Total detected/spiked cells	10/12	10/12	12/12
Recovery success rate	83%	83%	100%

doi:10.1371/journal.pone.0169427.t002

Table 3. *In vitro* assay of ISET® sensitivity using various types of cancer cells.

Cell line	MCF-7		HeLa		MMTV-PyMT
Blood processed	**1 mL**		**1 mL**		**1 mL**
Spiked tumor cells/test	1		1	3	2
Fixed tumor cells detected by ISET® per test (N = 3–5 tests)	1	1	1	3	2
	1	0	1	3	2
	1	1	1	3	1
	1	1			1
	1	1			
Total detected/spiked cells	9/10		3/3	9/9	6/8
Recovery success rate	90%		100%	100%	75%

doi:10.1371/journal.pone.0169427.t003

we found a slope of 0.9991 and correlation coefficient (R^2) of 0.96 (Fig 4A and Table B in S1 File**).** After addition of a number of 2, 30, 100 and 300 cells in 1 mL of blood, we recovered an average number of 1.7 cells per mL (85%, n = 30 replicates), 28 cells per mL (94%, n = 9), 85 cells per mL (85%, n = 13) and 334 cells per mL (111%, n = 2), respectively (Fig 4B and Table B in S1 File). We also obtained similar cell recovery rates by spiking dilutions of 50 and 100 HeLa cells in 1 mL of blood (respectively, 91% n = 14 and 104% n = 9) and 50 MCF-7 cells in 5 mL of blood (105%, n = 5) (S1A Fig).

Since the ISET® cartridge partitions 10 mL of blood in 10 times 1 mL volumes, cell recov- ery in 10 mL of blood has the same efficiency as cell recovery in 1 mL of blood (also demon- strated by our tests (Table 2)). We have thus plotted the equivalent tests in 10 mL of blood (i.e. 2 cells in 1 mL equivalent to 20 cells in 10 mL) and calculated linearity over 6 concentrations of A549 tumor cells ranging from 2 to 3000 CTC in 10 mL equivalent of blood. In this analysis, our average recovery rate (overall sensitivity) was 99.91% (Fig 4C). We observed similar linear- ity (overall sensitivity) with HeLa cells over 4 tumor cell concentrations (Fig 4D), with an aver- age recovery rate of 100% ± 1%.

Finally, we calculated the percent coefficient of variation (%CV), a measure of precision, for each condition tested (cell line, volume of blood, number of spiked cells) (Table B in S1 File). Average %CV was 22% in experiments with spiked cells counted by cell dilution (n = 6 conditions, 52 tests). In experiments with micromanipulated spiked cells, average %CV was also 22% (n = 9 conditions, 62 tests) (Table B in S1 File). As expected, in these tests with an extremely low number of spiked cells, which assess the detection limit, the %CV values are usually higher because of the binary nature of the test results (0 or 1 cell) which has an impact on the readout. Accuracy (measured as recovery error) was below 25% for all conditions (Table B in S1 File). Under the rigorous conditions of our spiking tests and readings (see Methods), tumor cells' recovery obtained using spiked cells counted by dilution was consistent with that obtained using spiked cells counted by micropipetting.

It is worth mentioning that cell spiking with the individually micropipetted cells protocol requires technical skills in single cells' micromanipulation and is a particularly demanding test. One single micropipetted cell added to ten mL of blood (containing on average 50 to 100 million leukocytes and 50 billion erythrocytes) can be lost if it is damaged by the trypsin used to detach cells from the petri dish. In this case, the spiked rare cells can be lost independently from the capability of the ISET® system to capture them from blood.

To verify if the cells are evenly distributed over 5 spots, we used the methodology described by Krebs *et al.* [12] and assessed intra-assay precision and accuracy (Fig 5). We examined the number of tumor cells found on each spot after spiking of 50 A549 cells counted by dilution into 5 mL of blood and filtration on 5 spots (each corresponding to the filtration of 1 mL of

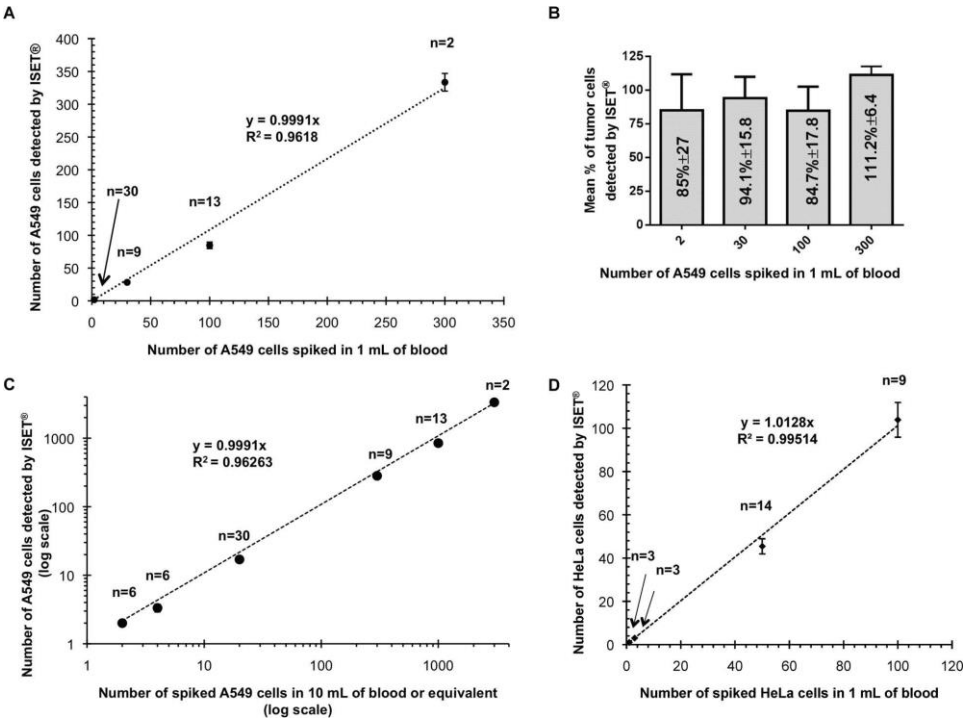

Fig 4. *In vitro* assay of ISET® linearity. (A) Number of tumor cells (A549) detected on ISET® filters plotted against expected number of tumor cells. Cells were spiked into whole blood after counting by dilution (30 to 300 cells) or counting by individual cells micromanipulation (2 cells). 0 cells (n = 4 replicates), 2 cells (n = 30), 30 cells (n = 9), 100 cells (n = 13) or 300 A549 cells (n = 2) were added to 1 mL of blood. Error bars (when visible) indicate standard error. (B) Mean % of tumor cells (A549) detected on ISET® filters plotted against expected number of tumor cells spiked into whole blood. (C) Number of tumor cells (A549) observed on ISET® filters plotted against expected number of tumor cells after extrapolation to 10 mL of blood (log scale). In addition to the test with 2 cells spiked in 10 mL (n = 6 replicates), to facilitate comparison with different volumes of blood, tests in 1 mL or 5 mL were plotted as their equivalent in 10 mL (See Methods). Error bars (when visible) indicate standard error. (D) Number of tumor cells (HeLa) detected on ISET® filters plotted against expected number of tumor cells. Cells were added into the whole blood after their counting by dilution (50 to 100 cells) or after their counting by individual cells micromanipulation (1 or 3 cells). 1 cell (n = 3 replicates), 3 cells (n = 3), 50 cells (n = 14) or 100 cells (n = 9) were added to 1 mL of blood (See Methods). Error bars (when visible) indicate standard error.

doi:10.1371/journal.pone.0169427.g004

blood). To study the impact of tumor cells' distribution on 5 spots, we diluted tumor cells and obtained 43 to 59 cells per 5 mL in three different experiments (on average 8.6 to 11.8 A549 per mL). For each experiment, tumor cells' counts were calculated from all possible combina- tions of spots (i.e. any 1, any 2, any 3, any 4). The average tumor cells' number (± Standard Error) with 95% confidence intervals (CI) was calculated for each experiment and each combi- nation of spots as described by Krebs *et al.* [12]. In an experiment with on average 8.6 tumor cells per mL, analyzing four spots provided an accurate estimation of the true mean (mean ± SE = 8.6 ± 0.13 tumor cells per mL, 95% CI: 8.35–8.85). When analyzing 3 spots or 2 spots, the estimation was less accurate, respectively 8.6 ± 0.14 (CI: 8.33–8.87) and 8.6 ± 0.21 (CI: 8.19– 9.01) tumor cells per mL. Similarly, in an experiment with on average 11.8 tumor cells per mL, analyzing four spots provided an accurate estimation of the true mean (11.8 ± 0.31, 95% CI: 11.41–12.19). When analyzing 3 spots or 2 spots, the estimation was less accurate, respectively 11.8±0.22 (CI: 11.37–12.23) and 11.8±0.33 (CI: 11.16–12.44) (Fig 5).

Altogether, ISET® intra-assay average precision was 4% (range 2.9% to 5.8%) and average accuracy was 2.7% (range 2.5% to 3.1%) when tumor cells were enumerated on 4 spots.

A

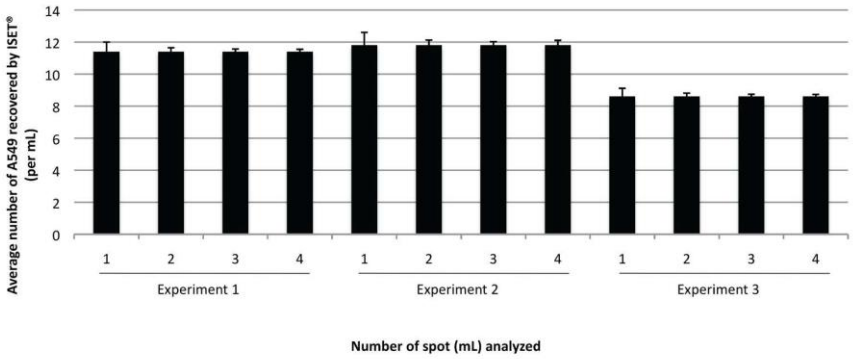

B

	Number of tumor cells detected by ISET® (fixed cells) per mL and per test						95% CI				Intra-assay Accuracy (Error %)				Intra-assay precision (%CV)			
	Spot 1	Spot 2	Spot 3	Spot 4	Spot 5	Average number of tumot cell recovered (per mL)	1 spot	2 spots	3 spots	4 spots	1 spot	2 spots	3 spots	4 spots	1 spot	24.0%	3 spots	4 spots
Exp 1	12	12	10	10	13	11.4	1.2	0.5	0.3	0.3	9.8%	5.3%	3.5%	2.5%	11.8%	6.8%	4.5%	2.9%
Exp 2	13	10	10	12	14	11.8	1.6	0.6	0.4	0.4	12.2%	6.8%	4.5%	3.1%	15.2%	8.8%	5.8%	5.8%
Exp 3	7	9	10	9	8	8.6	1.0	0.4	0.3	0.2	10.2%	6.0%	4.0%	2.6%	13.3%	7.7%	5.1%	3.3%
average	10.7	10.3	10.0	10.3	11.7	10.6	1.2	0.5	0.3	0.3	10.8%	6.0%	4.0%	2.7%	13.4%	7.7%	5.2%	4.0%
stdev	3.2	1.5	0.0	1.5	3.2	1.7	0.3	0.1	0.1	0.1	1.3%	0.8%	0.5%	0.3%	1.7%	1.0%	0.7%	1.6%

Fig 5. Assessment of ISET® intra-assay accuracy and precision. 50 A549 cells were spiked into 5 mL of blood (n = 3 experiments, 43 to 49 cells per 5 mL). The number of tumor cells found on each spot after ISET® filtration (each corresponding to the filtration of 1 mL of blood) was recorded. Experiments were done on 5 spots but for intra-assay precision and accuracy only the assessment of the number of cells found on single spots or randomly grouped spots (any 1, any 2, any 3, any 4 spots) is relevant. The cell counting on the combination of all the 5 spots was used as reference. Results show that cell counting on four spots exhibited a representative mean tumor cells value per mL of blood. (A) Bar chart with the mean tumor cell number per spot and corresponding standard error of the mean (error bars) depending on the number of spots analyzed. Error bars are calculated using the standard deviation in different combinations of any 4 spots, any 3 spots, any 2 spots or any 1 spot, respectively. If only one spot is considered, standard deviation is higher than when counting 4 spots, showing that counting on four spots gives a reliable mean tumor cells' value per mL of blood. (B) Table indicating the number of tumor cells found on each spot for each of the five experiments, the 95% confidence interval (CI), the precision (%CV) and the accuracy (%error) depending on the number of spots analyzed (1 to 4) as compared to the analysis on five spots.

doi:10.1371/journal.pone.0169427.g005

Enumerating tumor cells on 3, 2 and 1 spot(s) leads to a decreased average precision (respectively, 5.2%, 7.7% and 13.4%) and a decreased average accuracy (respectively, 4%, 6% and 10.8%) (Fig 5). We thus found that the ISET® System's intra-assay precision and accuracy related to individual spot's cell counting is consistent when 50 cells are filtered on a total of 5 spots and cells are enumerated on at least 4 spots. We have also performed further analyses showing that intra-assay precision and accuracy is maintained with an extended cell range of 29 to 70 cells in 5 mL of blood (6 to 14 cells per mL) (S2 Fig). These results show that, if the number of tumor cells in 5 mL of blood is comprised between 29 and 70 (between 58 and 140 in 10 mL of blood), counting the tumor cells on 4 spots gives the same number of tumor cells per mL of blood as counting the tumor cells in 5 or 10 mL of blood.

Overall, we found that the ISET® filtration's accuracy, precision and linearity are very high. Furthermore, the average recovery rate from two up to 3000 tumor cells per 10 mL (or equivalent) of blood is close to 100%.

B3. Sensitivity of the ISET® system for isolation of fixed tumor cells from blood after collection of plasma. Since detection of rare circulating tumor cells logically prefers methods

using a non-negligible volume of blood (8 to 10 mL), we checked the feasibility of isolating plasma and tumor cells from the same blood sample. This protocol aims to perform multiple tests using the same sample, in order to make full use of the precious patient's blood sample (Fig 1B). We assessed the *in vitro* sensitivity of this protocol by spiking 10 fluorescent A549 cells, counted one by one by micropipetting, in 5 mL of healthy donor's blood. In 4-fold repli- cate tests, we found 9 cells twice, 10 cells once and 7 cells once (Table 4) with a recovery success rate of 88%. The morphology of the spiked cells was intact as we found by performing MGG cytological staining (S1D Fig). The very high recovery success rate demonstrates that the LLOD and overall sensitivity for dual collection of plasma and tumor cells using the ISET® system are similar to that of the standard ISET® protocol.

B4. Assessment of the number of contaminant leucocytes on filters after isolation of fixed tumor cells. The ISET® system successfully eliminates all red blood cells and the majority of white blood cells, however some of them remain. By using cytopathological stain- ing, we counted the number of residual leucocytes on the filters obtained by filtrating the blood of 4 different healthy donors (see Methods, section 3). With the standard ISET® work- flow for isolation of fixed cells, the number of leucocytes on the filter is variable, ranging from 1208 to 3188 cells per mL (1779 on average). This corresponds to an approximate enrichment factor of 4 logs, in agreement with the data reported by other teams [12].

B- *In vitro* performance of the ISET® system for enrichment of live tumor cells from blood

We then assessed the ISET® system's sensitivity parameters for enrichment of live tumor cells which are relevant for research studies and in particular for molecular characterization of tumor cells, and their culture.

C1 Sensitivity and reproducibility of the ISET® system for enrichment of live tumor cells. Isolating by filtration live cells with no antibody-related bias and no or minimum cell loss is a very challenging goal as live tumor cells are flexible and can more easily slip through the pores. We have concentrated our efforts on developing a new filtration buffer and a variant ISET® protocol allowing enrichment of live tumor cells and their recovery in suspension for molecular analysis, in particular transcripts' analyses, and cell culture (Fig 1C). We have then assessed the *in vitro* sensitivity of this new workflow by spiking various numbers of cultured live A549 and LNCaP fluorescent tumor cells, collected one by one by micropipetting, in 1 mL of healthy donor's blood and performing the new protocol. The enriched cells have been trans- ferred to an Ibidi microchamber and identified under microscope due to their fluorescent sig- nal (Fig 2B), as described in the Methods, section 6.

In 6-fold replicate tests using 1, 3, 5 and 10 spiked live fluorescent A549 cells in 1 mL of blood, we found 6/6, 16/18, 24/30 and 50/60 cells (Table 5), with an overall recovery success

Table 4. *In vitro* assay of ISET® sensitivity with dual collection of tumor cells and plasma.

Blood processed	5 mL
Spiked tumor cells/test	10
Fixed tumor cells detected by ISET® per test (N = 4 tests)	10
	9
	7
	9
Total detected/spiked cells	35/40
Recovery success rate	88%

doi:10.1371/journal.pone.0169427.t004

Table 5. *In vitro* assay of ISET® sensitivity for enrichment of live tumor cells.

Cell line	A549				LNCaP	
Blood processed	**1 mL**				**1 mL**	
Spiked tumor cells/test	1	3	5	10	1	5
Live tumor cells detected by ISET® per test (N = 5–6 tests)	1	3	4	9	1	4
	1	3	5	6	1	4
	1	2	4	8	0	5
	1	3	4	9	1	3
	1	2	3	10	1	5
	1	3	4	8		
Total detected/spiked cells	6/6	16/18	24/30	50/60	4/5	21/25
Recovery success rate	100%	89%	80%	83%	80%	84%

doi:10.1371/journal.pone.0169427.t005

rate of 100%, 89%, 80% and 83%, respectively. Spiking tests were repeated with 5-fold replicate tests using 1 and 5 spiked live fluorescent LNCaP cells in 1 mL of blood. We found a total number of 4/5 and 21/25 cells with an overall recovery success rate of 80 and 84%, respectively (Table 5). Furthermore, using a Trypan blue stain, we found that the viability of the enriched live tumor cells was maintained. The recovery rate and the analytical sensitivity we obtained with live A549 and LNCaP cells are very high. Sensitivity at the closest concentration to the LLOD tested (i.e. 1 tumor cell in 1 mL of blood) was 100% and similar to that obtained with the standard ISET® protocol for isolation of fixed cells (Tables 1-3).

C2 Assessment of cell size and viability before and after enrichment of live tumor cells with the ISET® system. The precise size of at least 200 live A549 and MMTV-PyMT cells has been carefully calculated before and after filtration through 8-micron pores (Table C in S1 File and Fig 6). The median diameter remained essentially the same before and after filtration of live cells from both cell lines (13.6 μm ± 2.6 and 13.9 μm ± 2.6 for A549 cells and 10.0 μm ± 2.2 and 9.9 μm ± 2.2 for MMTV-PyMT cells, n = 3 experiments, respectively). Results demonstrate that filtration does not induce a selection in the cell size, including for the smallest cells (MMTV-PyMT) when they are kept alive (Fig 6). By using Trypan Blue exclu- sion, only the size of living cells has been taken into account. We have also calculated the rate of viability of live cells before and after filtration and found 99% ± 2% and 92.7% ± 2.4% for A549 cells and 97% ± 1.3 and 85% ± 3.4% for MMTV-PyMT cells, respectively (Fig 6 and Table C in S1 File).

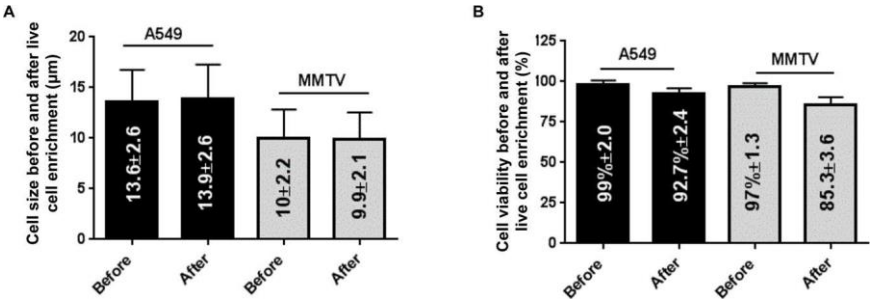

Fig 6. Cell sizes and viability before and after live cell enrichment. Cell sizes (median diameter) (A) or viability (B) according to each cancer cell line tested before or after live cell enrichment (n = 3 experiments). Error bars indicate standard error. Cells from human and mouse tumor cell lines were incubated 5 min with the Rarecells® Live Cells Buffer with blood and recovered on standard (8 micron-pore) ISET® filters. MMTV = MMTV-PyMT. Cell size and viability were analyzed using the TC20™ Automated Cell Counter (Bio Rad) and Trypan Blue stain.

doi:10.1371/journal.pone.0169427.g006

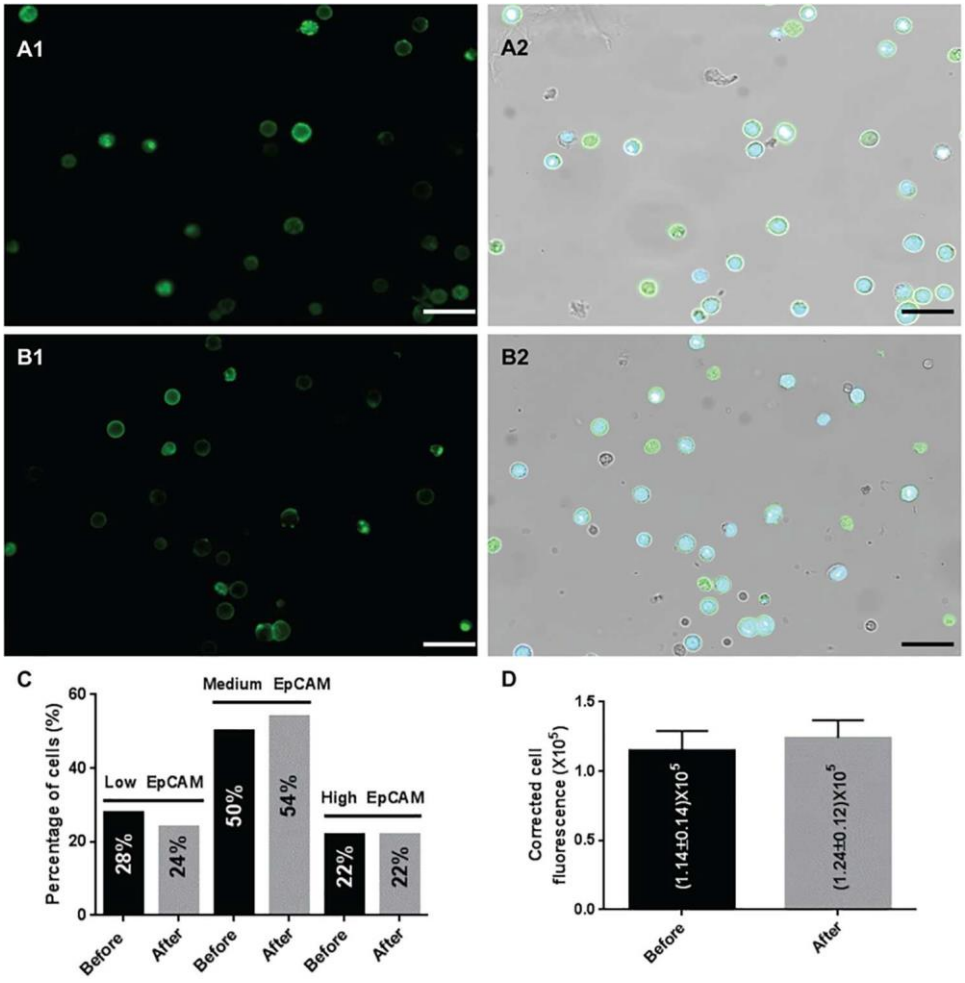

Fig 7. Comparison of EpCAM fluorescence on labeled cells before and after live cell enrichment by ISET®. Representative images of MCF-7 cells before live cell enrichment showing EpCAM fluorescence alone (A1) and merged Hoechst and EpCAM fluorescence with bright field image (A2) are each presented with a scale bar of 50 microns. Representative images of MCF-7 cells after live cell enrichment showing EpCAM fluorescence alone (B1) and merged Hoechst and EpCAM fluorescence with bright field image (B2) are each presented with a scale bar of 50 microns. (C) Comparison of cell distribution across three levels of EpCAM expression for 50 MCF-7 cells before and 50 MCF-7 cells after live cell enrichment. The low EpCAM group comprises cells with corrected total cell fluorescence (CTCF) below 91000 units, the medium EpCAM category regroups cells with CTFC between 91000 and 200000 units and the high EpCAM group contains cells with CTCF above 200000 units. (D) Comparison of median corrected total cell fluorescence (CTCF) calculated on 50 MCF-7 cells before and 50 MCF-7 cells after live cell enrichment. Error bars indicate standard error.

doi:10.1371/journal.pone.0169427.g007

C3 Assessment of cell surface marker expression before and after enrichment of live tumor cells with the ISET® system. As changes in protein expression could potentially occur during filtration, we also tested whether filtration of live tumor cells with our protocol induces a change in antigen expression by using EpCAM antibody immunofluorescence and labeling live MCF-7 cells before and after filtration. The result of our analysis is shown in Fig 7. We did not find any difference in EpCAM expression induced by filtration under the tested filtration conditions. In fact, quantitative analysis of fluorescence using ImageJ (Fig 7D) revealed that the median corrected total cell fluorescence (CTCF) calculated on 50 MCF-7 cells was very similar before (median of 114665 ± 14363 with CTCF ranging from 43754 to

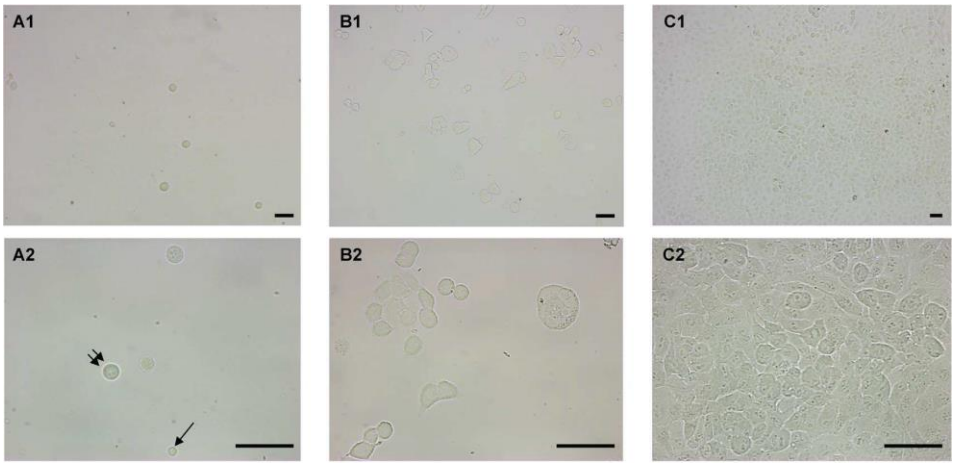

Fig 8. *In vitro* culture of A549 tumor cells after enrichment from blood using ISET®. Representative bright field images of A549 cells after live cell enrichment from blood and *in vitro* culture were obtained at 3 distinct time points. Scale bar of 50 microns. (A1, A2) Images at day zero (D0 = 2h of culture) showing A549 cells after live cell enrichment from blood obtained using the 10X (A1) and the 40X objective (A2). At 40X (A2) a single normal leucocyte is pointed by a single black arrow and a representative tumor cell is pointed by two arrows. (B1, B2) Images at day 2 (D2 = 2 days of culture) showing A549 tumor cells growing after live cell enrichment from blood obtained using the 10X (B1) and the 40X objective (B2). (C1, C2) Images at day 5 (D5 = 5 days of culture) showing A549 tumor cells growing after live cell enrichment from blood obtained using the 10X (C1) and the 40X objective (C2).

doi:10.1371/journal.pone.0169427.g008

494919) and after (median of 124021 ± 12697 with CTCF ranging from 65799 to 594996 units) live cell enrichment. Furthermore, when applying cutoffs of CTCF to distinguish cells with low EpCAM expression from those with medium and high EpCAM expression we found very sim- ilar distributions of cells across all three categories: 28% (low), 50% (medium), 22% (high) before live cell enrichment and 24% (low), 54% (medium), 22% (high) after live cell enrich- ment, respectively (Fig 7C).

C4 *In vitro* culture of live tumor cells enriched from blood with the ISET® system. We tested if cells from cell lines could survive and proliferate *in vitro* after their enrichment from blood using the ISET® System. We spiked A549 cells in blood in duplicate tests and processed the samples with the live cell enrichment protocol as described in the Methods section. We then compared imaging results at day zero (D0) with those obtained after 2 (D2) and 5 days (D5) of *in vitro* culture of enriched A549 cells isolated from blood (Fig 8). In both replicate tests, tumor cells observed at D0 were scattered as individual cells across the surface of the round coverslips (1.2 cm in diameter) used for their culture with an overall similar yet hetero- geneous cell population density (Fig 8A). Tumor cells observed at D2 were mainly present as small clusters with a higher overall cell population density and some mitotic cells, clearly indi- cating cell proliferation (Fig 8B). Tumor cells observed at D5 were present exclusively as large clusters or colonies of proliferating cells with higher density, nearly covering the whole surface of the coverslips (Fig 8C). Interestingly, very few residual leucocytes were found at D0 after the first washing step and none of them were observed at D2 and D5, suggesting that stringent *in vitro* culture conditions can potentially select pure tumor cells populations. These results show that tumor cells' growth in culture is possible after live tumor cells enrichment by the ISET® System.

C5 Assessment of cytoskeleton markers before and after enrichment of live tumor cells with the ISET® system and short term *in vitro* culture. In order to determine the potential impact of filtration on the cytoskeleton of live tumor cells, we performed immunofluorescence

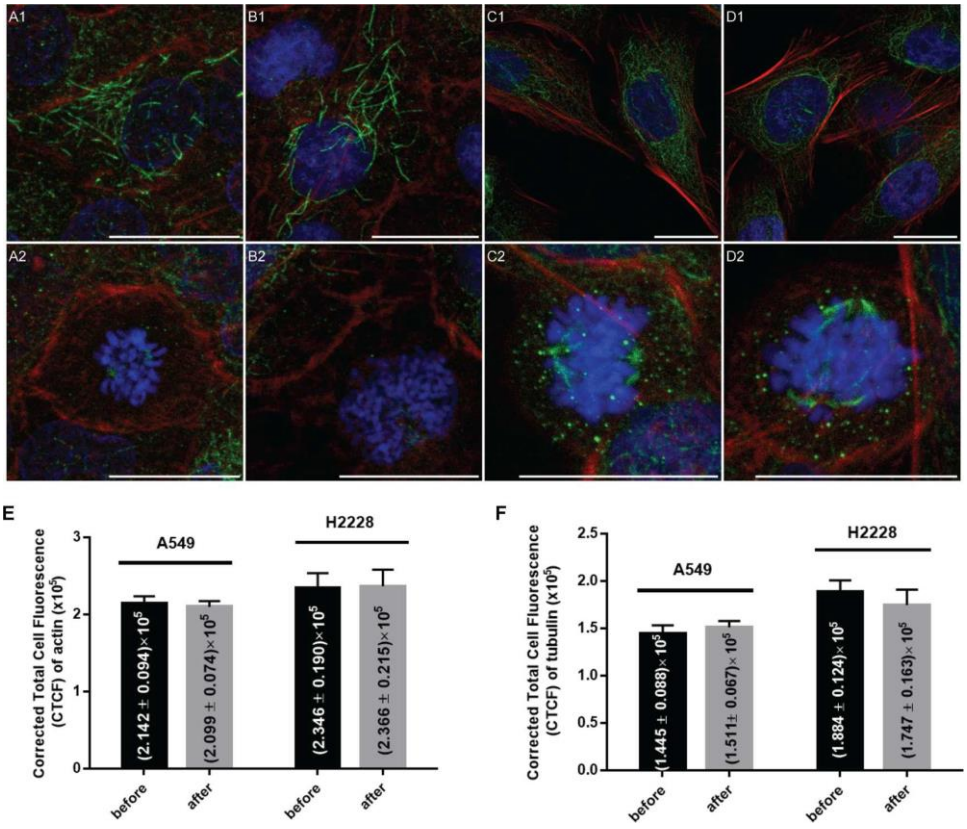

Fig 9. Cytoskeleton analysis of A549 and H2228 cells before and after live cell enrichment by ISET® and *in vitro* culture. Representative images of A549 and H2228 cells showing merged Hoechst (blue), actin (red) and tubulin [41] fluorescence were taken after 72h of *in vitro* culture using the 63X objective and are each presented with a scale bar of 20 microns. Images of A549 cells before filtration show examples of cells in G1/S phase (A1) and during mitosis (A2) for comparison with images showing A549 cells after filtration in G1/S phase (B1) and during mitosis (B2). Images of H2228 cells before filtration show examples of cells in G1/S phase (C1) and during mitosis (C2) for comparison with images showing H2228 cells after filtration in G1/S phase (D1) and during mitosis (D2). Comparisons of median corrected total cell fluorescence (CTCF) of actin (E) and of tubulin (F) calculated on 30 A549 and 30 H2228 cells before and 30 A549 and 30 H2228 cells after live cell enrichment. Error bars indicate standard error.

doi:10.1371/journal.pone.0169427.g009

staining of actin microfilaments and microtubules of A549 and H2228 cells. We compare the profile of cells before enrichment to the one after their enrichment with the ISET® System and short term *in vitro* culture (for 72 hours). For both cell types, key features of cytoskeleton dynamics involved in crucial cellular processes such as proliferation were observed before and after live tumor cells isolation using ISET®. Results are shown in Fig 9.

Microscopy analysis revealed very similar actin and tubulin structures when comparing untreated A549 cells (Fig 9A) to A549 cells enriched live using the ISET® system (Fig 9B) and kept 72h in culture. Importantly, no significant difference was observed in spindle morpho- genesis during mitosis when comparing A549 cells before (Fig 9A2) and after live cell enrich- ment with ISET® (Fig 9B2). In addition, all A549 cells observed at G1/S phase (Fig 9A1 and 9B1) displayed polygonal global shape, uneven distribution and unaligned orientations of F- actin filaments as well as frequent weakening of the peripheral actin cortex colocalized with microtubule-enriched plasma membrane extensions. These observations are consistent with previous literature on A549 cells [42] and correlate with known invasive properties [43] and stiffness' plasticity [44] of A549 cells which are prone to EMT transformation. Similarly,

enrichment followed by 72 hours of *in vitro* culture had no visible impact on the cytoskeleton of H2228 cells (Fig 9D) as compared to untreated H2228 cells (Fig 9C). At G1/S phase, scat- tered microtubules and long straight actin filaments were observed with thicker actin bundles present near attachment sites of the plasma membrane for H2228 cells before (Fig 9C1) and after live cell enrichment (Fig 9D1). Enriched H2228 cells entering mitosis (Fig 9D2) displayed mitotic rounding, chromatin condensation and spindle morphogenesis with no apparent alter- ation compared to untreated controls (Fig 9C2).

Furthermore, global quantitative analysis of actin fluorescence (Fig 9E) performed on 30 randomly picked cells revealed very similar results of median CTCF before (median of 214166 ± 9416 for A549 and 234552 ± 19036 for H2228) and after live cell enrichment and cul- ture (median of 209915 ± 7405 for A549 and 236599 ± 21468 for H2228). Using a Student' s t- test, the differences of actin CTCF before and after live cell enrichment were found to be not significant (p value of Student test = 0.997 for A549 and 0.912 for H228).

Similarly, global quantitative analysis of tubulin fluorescence (Fig 9F) performed on 30 ran- domly picked cells also revealed very similar results of median CTCF before (median of 144482 ± 8824 for A549 and 188390 ± 12406 for H2228) and after live cell enrichment and cul- ture (median of 151118 ± 6732 for A549 and 174672 ± 16327 for H2228). Using a Student test, the differences of tubulin CTCF before and after live cell enrichment were found to be not sig- nificant (p value of Student test = 0.296 for A549 and 0.916 for H2228).

Of note, median CTCF was higher for H2228 as compared to A549, which could be due to the larger size of H2228 cells or a higher expression level of tubulin and actin.

Altogether these results indicate that tumor cells' morphology and cellular functions related to the cytoskeleton distribution of F-actin and acetyl-α-tubulin can be either conserved or restored after 72h of *in vitro* culture following live tumor cells isolation from blood using the ISET® system and protocol.

C6 Estimation of the remaining leukocytes after live tumor cells filtration and their depletion using CD45 magnetic beads. The ISET® System workflow for live cells success- fully eliminates all red blood cells and the majority of white blood cells. The remaining white blood cells (WBC) were counted in 2 tests as described in the Methods section 5. Results showed from 640 to 2485 cells per mL of blood (1563 on average), thus similar to the amount of WBC remaining using the fixed cell protocol, and an approximate enrichment factor of 4 logs.

We next tested the feasibility of eliminating the remaining leucocytes after live cells enrich- ment with the ISET® System using immuno-magnetic beads coated with CD45 antibodies (Fig 1C). We spiked 10 A549 fluorescent cells, counting them one by one by micropipetting, in 1 mL of blood and processed the blood as described in the Methods section 6. In 9 replicate experiments, we found 6 A549 once, 5 A549 once, 4 A549 three times and 3 A549 four times with an average recovery rate of 40%, as shown in Table 6. As compared to the much higher recovery rate obtained after enrichment of live cells (80 to 100%, Table 5), the additional CD45-depletion step causes a loss of 50 to 60% of the enriched cells. However, no remaining leucocytes were identified with this protocol and the morphology of the spiked cells remained intact.

C- Next Generation sequencing analysis of live tumor cells isolated from blood with the ISET® System

D1 Comparative NGS analysis of A549 and HCT116 cells before and after live tumor cell enrichment and 72h *in vitro* culture. In order to further validate the potential clinical interest of our live tumor cells filtration workflow for theranostic applications, we used Next

Table 6. ***In vitro*** **assay of ISET® sensitivity for enrichment of live tumor cells followed by CD45-immunomagnetic mediated leukocytes depletion.**

Blood processed	1 mL
Spiked tumor cells/test	10
Live tumor cells detected by ISET® after CD45-immuno-magnetic depletion per test (N = 9 tests)	4
	3
	3
	6
	4
	5
	4
	3
	3
Total detected/spiked cells	36/90
Recovery success rate	40%

doi:10.1371/journal.pone.0169427.t006

Generation Sequencing (NGS) to study DNA mutations in A549 and HCT116 cells before and after live tumor cells isolation followed by their short term (72h) *in vitro* culture. We used the hotspot cancer panel v2 on the Ion Torrent™ platform as described in the Methods section 7. This amplicon panel can detect 6893 possible COSMIC mutations over 50 oncogenes and tumor suppressor genes [45].

Median coverage ranged from 1423X to 2073X among the different samples (S3 Fig). Median sequencing depth across all variants detected was 2957X and 2357X for A549 DNA extracted before and after live enrichment, respectively and 3103X and 3306X for HCT116 DNA extracted before and after live enrichment, respectively (Table D in S1 File**)**. 17 SNP vari- ants were found in A549 DNA including 11 COSMIC mutations classified as most likely path- ogenic (Fig 10 and Table D in S1 File). Allele frequencies of all variants were concordant in the sample 'before filtration' as compared to the sample 'after filtration' (Fig 10A and 10C).

Similarly, 25 variants were found in HCT116 cells including 23 SNPs and 2 INDELs. 16 of these mutations are classified as most likely pathogenic (Table D in S1 File). Allele frequencies of all variants were concordant in the sample 'before filtration' as compared to the sample 'after filtration' (Fig 10B and 10D). Of note, 4 of these heterozygous mutations were found in the EGFR pathway (PIK3CA H1047R, SMO V404M, ABL1 Y257C and KRAS G13D) in agree- ment with previous literature [46]. Of note, 11 variants were common in A549 and HCT116.

Interestingly, variants were also identified with confidence at a similar low frequency (6 to 10%) in both samples 'before filtration' and 'after filtration' .(STK1 Q37L and FGFR3 P402P in A549, and FGFR3 P402P in HCT116, Fig 10). This reflects a known phenomenon of genetic and phenotypic heterogeneity of cells lines [47-49] that could be identified in our cell populations.

In A549 DNAs, 3 regions had low coverage (under the 500X threshold) (S3 Fig). Two of these regions were in the CDKN2A gene (amplicon coverage 0) which is depleted in A549 [50]. The last low coverage region was the same in all samples (A549 and HCT116); it corre- sponds to a variant in CSF1R 3' UTR identified in all the samples, albeit with a coverage under the 500X threshold (Table D in S1 File).

These results provide a proof of principle that the tumor cells' genetic profile can remain stable after their isolation from blood using our protocol and their short-term culture.

D2 Single-cell genetic analysis after live cell enrichment. Since studying the whole genome of individual CTC when they are very rare is important to explore the CTC

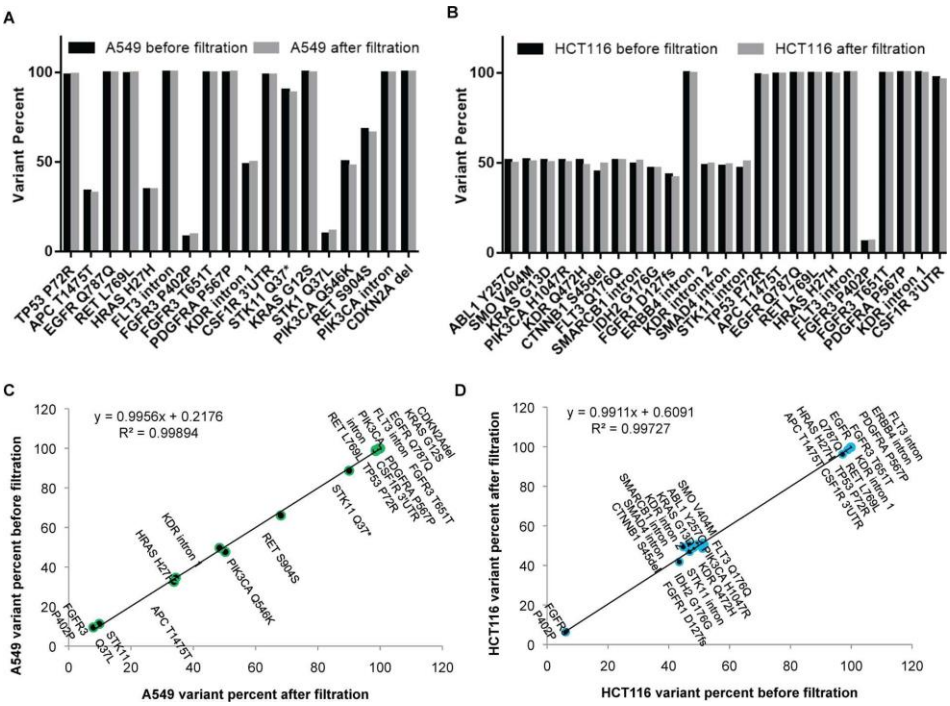

Fig 10. Ion Torrent™ molecular characterization of A549 and HCT116 cells before and after live cell enrichment from blood using ISET®. Comparison of variants' mutant allele frequencies in bulk extracted DNA of approximately 10^4 A549 (A) and 10^4 HCT116 (B) cells at 72h of *in vitro* culture, before and after live cell enrichment. Correlation of variant allele frequencies in bulk extracted DNA of approximately 10^4 A549 (C) and 10^4 HCT116 (D) cells at 72h of *in vitro* culture, before and after live cell enrichment.

doi:10.1371/journal.pone.0169427.g010

heterogeneity at the beginning of tumor invasion, we then assessed if our protocol allows single circulating tumor cells' capture and their NGS analysis.

NGS exome libraries were first prepared using the Illumina technology with purified whole-genome amplified DNA from fresh single cells and fixed (not microdissected) single cells isolated by the ISET® System, and from unamplified human gDNA as control. Respec- tively, we obtained 52, 41, and 44 million reads as well as a genome coverage of 76%, 70%, and 95% with average sequencing depth varying from 20 to 27X. To further assess the quality of our libraries, we next prepared whole genome and exome libraries with whole-genome amplified DNA from 4 fresh single cells and from 4 fixed (not microdissected) cells. The sequencing and mapping results show that we recovered about 70% of the exomes from the analyzed single cells. Since performing NGS analysis of druggable mutations in very rare single CTC may be clin- ically relevant, we studied single tumor cells enriched from blood by the ISET® System using the hotspot cancer panel v2 on the Ion Torrent platform as described in the methods section 7. Overall, we analyzed three live single leucocytes, three live single HCT116 cells, six live single A549 cells, and 3 fixed single A549 cells, isolated by the ISET® System, WGA-amplified bulk DNA from HCT116 and A549 cells, as well as bulk genomic DNA from HCT116, A549 cells and the donor's leukocytes.

We first evaluated standard sequencing quality control parameters of the DNA obtained from the WGA of our single cells (S1 File and S4 Fig). Then, we studied the presence of hotspot mutations registered in the COSMIC database in the WGA DNA from single cells isolated by the ISET® System. We identified the presence of heterozygous mutations in these 4 hotspots

in all HCT116 single cells, WGA-amplified HCT116 DNA and non-amplified HCT116 DNA but not in single leukocytes (Fig 11A). Additionally, when pooling data from three single HCT116 cells, the frequency of mutant allele was consistent with an heterozygous mutation, respectively 56% for KRAS G13D, 50% for PIK3CA H1047R, 45% for SMO V404M, and 51% for ABL1 Y257C (Fig 11A). Furthermore, the coverage for these amplicons ranged from 11 to 2000 (Table E in S1 File). Of note, in HCT116, additional mutations in the APC, FGFR3 and STK11 genes have been described in the literature [46] but are not included in the mutations that can be detected by the hotspot cancer panel v2. A549 cells are known to harbor KRAS G12S homozygous mutation [51] and this mutation was found in all analyzed live A549 single cells (n = 6) as well as fixed A549 single cell (n = 3) (S5 Fig). Furthermore, for all A549 samples, the two amplicons for the *CDKN2A* (p16) gene failed to be detected (Fig 10A and Table D in S1 File), which is consistent with the loss of this locus in this cell line [50]. Interestingly, when analyzing the presence of nonsense COSMIC mutation in leucocytes, we found the presence of heterozygous KIT M541L mutation in all single leucocytes and the matching bulk DNA (Fig 11A and Table E in S1 File). However, although this mutation has been suggested to be associ- ated with leukemia, it is actually a frequent polymorphism among the Caucasian population [52] consistent with our finding.

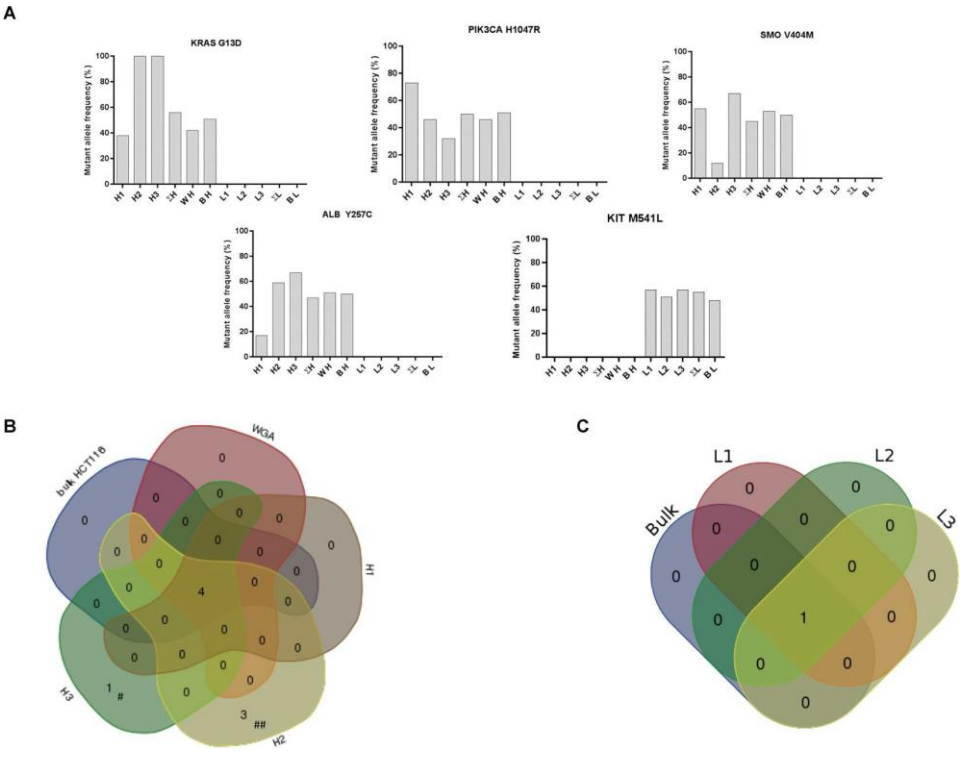

Fig 11. Ion Torrent™ molecular characterization of single HCT116 and leukocytes enriched from blood using ISET®. (A) Non-sense variants mutant allele frequency from Catalogue Of Somatic Mutation In Cancer (COSMIC) database in whole genome amplified DNA from single HCT116 tumor cells (H1 to H3), whole genome amplified DNA single leukocytes (L1 to L3), whole genome amplified bulk HCT116 DNA (WH), unamplified bulk HCT116 DNA (BH) and unamplified bulk extracted DNA from the blood donor (BL). (B) Venn diagram showing the concordance of COSMIC non-sense variants determination in whole genome amplified DNA from single HCT116 tumor cells (H1 to H3) as compared to unamplified bulk HCT116 DNA (bulk HCT116) and whole genome amplified bulk HCT116 DNA (WGA). # indicates SMARCB1 R201* and ## indicate CTNNB1 S45P, NOTCH1 L1574P and RB1 E137*. (C) Venn diagram showing the concordance of COSMIC non-sense variants determination in whole genome amplified DNA from single leukocytes (L1 to L3) as compared to unamplified bulk extracted DNA from the blood donor (bulk).

doi:10.1371/journal.pone.0169427.g011

Finally, we plotted all non-sense COSMIC mutations found in the HCT116 samples and leucocytes and studied personal mutations (i.e. mutations which can only be identified in a single sample). Personal mutations could reflect either heterogeneity (which is not expected among leukocytes) or technical artifacts (error introduced by polymerase during WGA or sequencing) (Fig 11B and 11C). While 0, 1 and 3 personal mutations were identified in the three live single HCT116, personal mutations were not found in single leucocytes (n = 3), nor in WGA-amplified bulk DNA from HCT116, nor in bulk DNA from HCT116 and the donor' s leukocytes. The personal mutations found in HCT116 could represent variants, which are present in less than 5% of the cells (the sensitivity of mutation detection in bulk DNA) or tech- nical artifacts.

Overall, our data suggest that NGS-mediated whole genome analyses, exome analysis and multi-genes panel analyses of tumor cells isolated by the ISET® System are feasible. Of note, we found consistent results with live and fixed tumor cells isolated by the ISET® System, but fixed cells required 3 additional cycles of pre-amplification at the NGS library preparation step (S4A Fig). These data are susceptible to provide reliable and informative results for a deeper understanding of CTC heterogeneity including at the critical early steps of tumor invasion.

Discussion

In this work, we describe new protocols for the study of circulating tumor cells with a particu- lar focus on their isolation when they are extremely rare. We have assessed these protocols using tumor cells from cell lines up to the immune-molecular characterization of the isolated cells including through their culture. We show that the ISET® system consistently isolates 2 cancer cells added to 1, 5 or 10 mL of blood with an average cell-recovery rate ranging from 83 to 100%. This high recovery is reproducible with different operators and with different devices. The ISET® system' s sensitivity threshold (or LLOD, Lower Limit Of Detection) is one tumor cell per 10 mL of blood, which is the physical limit of the method. We also show that this level of sensitivity is maintained when plasma is collected before isolation of tumor cells from blood as well as when tumor cells are isolated from whole blood in a live form using a suitable modi- fied buffer (without fixation). Finally, we show the feasibility of using the isolated live or fixed cells for single-cell NGS analysis.

Our results show that ISET® allows reproducible, accurate and linear detection and enu- meration of cancer cells in blood (Tables 1–5, Figs 4 and 5 and S1 Fig). Our data are consistent with sensitivity and linearity data previously reported by independent teams (S1B and S1C Fig)[12, 27-29]. However, these teams did not extend ISET® s analytical performance and its sensitivity assessment to the extreme limits as we did. Following an independent clinical study which demonstrated the capacity of the ISET® system to detect CTC in patients developing lung cancer years before the detection of tumor nodule by CT-scan [3], we decided to chal- lenge its LLOD by testing it down to a few cells in 10 mL of blood, using an improved and extremely precise protocol. Taken together, our results validate the *in vitro* analytical perfor- mance of the ISET® system.

We have assessed the sensitivity specifications of ISET® with tumor cells having different sizes. The median diameters of cultured tumor cells determined on filters typically range from 12 to 20 μm (Fig 3 and Table A in S1 File), consistently with previously published studies [10, 53, 54]. We have successfully isolated intact fixed mouse tumor cells as small as 8.5 μm in diameter (median size on filter 12 μm) using the standard membrane with a nominal pore size of 8 μm (Table 3, Fig 3 and Table A in S1 File). Furthermore, we could enrich by the ISET® System live cells having a median diameter of 10 μm without bias of selection as shown by size assessment before and after filtration (Fig 6).

Other parameters might affect the performance of blood filtration such as cell fragility and biomechanics of the cytoskeleton. It is unclear whether the spectrum of fragility of primary cells is similar to the one of tumor cells from cell lines. However, by fixating the cells structure, the ISET® buffer makes the cells rigid and eliminates the problem of fragility as demonstrated by the very high recovery of individual spiked cells with our approach. Concerning the fragility of primary versus secondary (from cell lines) live tumor cells, our laboratory experience shows that secondary cells are more malignant, but also more fragile than primary tumor cells during *in vitro* manipulation. This is because secondary tumor cells from solid cancers have to be trypsinized to be manipulated and this step damages the cell membrane making it more fragile. Thus, our sensitivity tests performed with secondary live tumor cells are expected to be reliable.

Since sensitivity is a critical issue in the field of CTC detection, we developed an assay able to provide the maximum reliability for sensitivity assessment using a number of tumor cells under 10, i.e. spiking into blood of individually collected and counted fluorescent tumor cells (Tables 1–6, Fig 2A and 2B). For higher numbers of tumor cells (30 to 300), we counted them by dilution, performing repeated counting to adjust the tumor cells' number (Fig 2C). Then, to assess the number of tumor cells successfully isolated by the ISET® System, we counted very carefully the fluorescent cells to avoid any mistake at the detection level (see Methods and Fig 2).

More than 40 distinct methods developed to isolate CTC have been published, and variable levels of *in vitro* sensitivity have been reported (reviewed in Table 7). However, a substantial difficulty in this domain is related not only to the various isolation methods and systems but also to the different protocols used to assess sensitivity, including how tumor cells are counted before spiking into blood and after their isolation from blood. Therefore, in general, comparing the sensitivity of different methods on the only basis of literature data is not completely informative.

Concerning the different cell-size based methods developed to isolate CTC, they are characterized by different filtration parameters (type of filters, buffer or media used to dilute blood, type of device and filtration pressure . . .) which determine their different performance (summarized in Table F in S1 File). Therefore, despite the fact that the word "filtration" intuitively sounds as an easy and generic approach to separate large and small elements, blood filtration to isolate tumor cells is not at all depending only on the pore size. It is not like filtrating sand (size: 0,2–2 mm) to extract shells (size: few cm). The size difference between white blood cells (8–15 μm) and tumor cells (15–30 μm) is very small, creating a competition of blood cells for the filter's pores and making tumor cells' isolation without cell loss or damage an ambitious technical challenge.

Our *in vitro* data showing the very high sensitivity of ISET® are consistent with *in vivo* data previously published by independent teams, showing the higher *in vivo* sensitivity of ISET® as compared to CellSearch™ [12, 17, 20, 22, 23, 30–32, 97] (Reviewed in [2]).

In vivo sensitivity for circulating cancer cells detection is affected by several factors: 1) how long and how the blood is stored before CTC isolation, 2) the number of steps involved in the isolation process (every step leads to cell loss) and its rapidity, 3) how cells are captured and 4) how cells are enumerated. For instance, the use of markers for CTC capture/enumeration has an impact on how many CTC are detected/counted, depending on the markers' level of expres- sion in cancer cells.

Stabilization of tumor cells in blood for a few days without cell loss and without damage to cell morphology remains an unmet goal. If available, proper stabilization would allow centrali- zation of CTC analysis without loss of sensitivity. CellSave (Veridex, USA) and Streck (Streck, USA) tubes have been used to stabilize tumor cells in blood but analytical reports have shown

Table 7. *In vitro* sensitivity and recovery of various CTC methods.

Method type	Method	Principle of the method	Company or Academic lab	*In vitro* LLOD (overall recovery, concentrations tested)	Method for sensitivity and/ or recovery assessment	Blood Sample size	Ref
Physical—density	Ficoll®	Density separation followed by manual ICC or IF, FACS or RT-PCR	Biochrom, Germany	**10 CTC per 10 mL of blood (42%, 2)**	Spiking of 10 to 1000 cells counted by dilution in 10 mL of blood	variable, typically 10 mL	[38]
Physical—density	OncoQuick®	Density separation followed by manual ICC or IF, FACS or RT-PCR	Greiner BioOne, Germany	**10 CTC per 30 mL of blood (42%, 2)**	Spiking of 10 to 1000 cells counted by dilution in 10 mL of blood	up to 30 mL	[38]
Physical- size	ISET® System	Cell size (filter) followed by manual cytopathology, ICC or ICC, FISH, molecular analysis, culture	Rarecells, France	**1 CTC per 10 mL of blood (99.9%, 6)**	Micromanipulation of 2 fluorescent cells added in 1 to 10 mL, dilution 30 to 300 in 1 mL of blood	10 mL	This study
Physical- size	CTC Membrane Microfilter	Cell size (filter) followed by IF	Cote's lab, USA	**5 CTC in 7.5 mL of blood (89%, 1)**	Micromanipulation (5 cells) in 7.5 mL of blood and detection by immunofluorescence or cell dilution (41 cells) and H stain, spiked in 1 mL of blood	7.5 mL	[54, 55]
Physical- size	Canopus	Cell size and deformability	Canopus Bioscience, Canada	**data not found**	data not found		[56]
Physical- size	3D microfilter	Cell size (filter) followed by IF	Cote's lab, USA	**NA (87%, 1)**	Spiking of 340 cells counted by dilution in 1 mL of blood	1 mL	[57]
Physical- size	Screencell® Cyto, MB,CC	Cell size (filter) followed by cytopathology, IF or ICC, FISH, molecular analysis, culture	Screencell, France	**2 CTC in 1 mL of blood (74%, 2)**	Micromanipulation of 2 non fluorescent cells spiked in 1 mL blood, and detection by HE stain	3 mL (6 mL for MB and CC)	[58, 59]
Physical- size	Captor™ / ClearCell® CX	Cell size (microfluidics) followed by cytopathology, IF	Abnova, Singapore	**data not found**	data not found	1 mL	[60]
Physical- size	ClearCell® FX System	Cell size (microfluidics) followed by IF	Clearbridge Biomedic, Singapore	**NA (84%, 1)**	Spiking of 500 fluorescent cells counted by dilution in 7.5 mL of blood	7.5 mL	[61]
Physical- size	Filtration device	Cell size (track-etched filter) followed by IF, molecular analysis	Terstappen's lab, Netherlands	**2 CTC in 1 mL of blood (67%, 6)**	Micromanipulation (2, 10 cells) and dilutions (up to 100000 cells) of fluorescent cells spiked in 1 mL of blood	1–10 mL	[53, 62]
Physical- size	Filtration device	Cell size (microsieve filter) followed by IF, molecular analysis	Terstappen's lab, Netherlands	**2 CTC in 1 mL of blood (58%, 6)**	Micromanipulation (2, 10 cells) and dilutions (up to 30000 cells) of fluorescent cells spiked in 1 mL of blood	1–10 mL	[53, 62]
Physical- size	CellSieve™	Cell size (filter) followed by cytopathology, IF, FISH, molecular analysis	Creativ Microtech, USA	**NA (89% for unfixed cells and 98% for fixed cells, 1)**	Precouting of 50 fluorescent cultured tumor cell on microscope slide and transfer in 7.5 mL of blood	7.5 mL	[63]
Physical- size	MetaCell®	Cell size (filter) followed by culture	MetaCell, Czech Republic	**data not found**	data not found	8 mL	[64]
Physical- size	Parsortix™	Cell size and deformability (microfluidics) followed by IF, FISH	Angle, UK	**10 CTC in 2 mL of blood (59%, 3)**	Spiking of fluorescent cells counted by dilution (10 to 100 in 2 mL of blood or 25 to 100 cells in 7.5 mL of blood)	4 mL	[65, 66]
Physical- size	VyCap	Cell size (Microsieve filter) followed by IF, molecular analysis	VyCap	**NA, (67%, 3)**	Spiking of 100 to 200 fluorescent cells (counted by dilution) in 1 mL of media	1 mL	[67]

(*Continued*)

Table 7. (*Continued*)

Method type	Method	Principle of the method	Company or Academic lab	*In vitro* LLOD (overall recovery, concentrations tested)	Method for sensitivity and/ or recovery assessment	Blood Sample size	Ref
Physical- size	CelSee	Cell size and deformability (microfluidics) followed by IF, FISH	CelSee Diagnostics	**10 CTC per mL of blood, (84%, 5)**	Spiking of 50 to 2000 cells (counted by dilution) in 2 mL of blood	2 mL	[68]
Physical density or size	Ikoniscope™	Densitiy or Cell size (filter) followed by IF, digital miscroscopy system	Ikonysis, USA	**1 CTC per mL of blood (>90%, 4)**	Micromanipulation (1 to 3 cells) and dilutions (5–1000 cells) in 8 mL of blood	8 mL	[69]
Physical-density and charge	ApoStream™	Density and Cell charge followed by IF	Apocell, USA	**2 CTC in PBMC from 7.5 mL of blood (72%, 4)**	Spiking of 4 to 2600 cells counted by dilution into 1 mL buffer and addition to PBMCs (2 cell lines)	7.5 mL	[70]
Physical-density and size	SmartBiopsy™	Density and cell size followed by IF	Cytogen, Korea	**1 CTC per mL of blood (50%, 3)**	Spiking 10 to 100 fluorescent cell counted by dilution in 3 mL of blood	3 mL	[71]
Marker-based enrichment/ detection	Epithelial Enrich Dynabeads®	Magnetics beads coated with anti-EpCAM antibody with optional density gradient separation, followed by ICC or IF	Life technologies, USA	**10 CTC in PBMC from 15 mL of blood (74%, 3)**	Spiking in PBMC of 10 to 1000 cells counted by dilution	variable up to 15 mL	[72]
Marker-based enrichment/ detection	CellSearch™	Immunomagnetic capture with anti-EpCAM antibody followed by IF (EpCAM, CK, CD45)	Veridex (J&J), USA	**1 CTC per 7.5 mL of blood (85%, 5)**	Spiking of 4 to 1142 cells counted by dilution in 7.5 mL of blood, regression analysis and extrapolation based on Poisson distribution of rare events	7.5 mL	[73]
Marker-based enrichment/ detection	Maintrac™	Density and Milteny anti-EpCAM beads followed by IF (CK, CD45)	Pachmann lab., Germany	**NA (83%, 1)**	Spiking of cells counted by dilution (down to 60 cells) in 1 to 20 mL of blood	1 mL	[74]
Marker-based enrichment/ detection	AdnaTest	Immunocapture (Anti-Epcam Dynabeads) followed by RT-PCR or IF	AdnaGen, Germany	**2 CTC per 5 mL of blood (100%, 1)**	Individual spiking of 2 to 10 cells and 100 cells counted by dilution in 5 mL of blood	5 mL	[75]
Marker-based enrichment/ detection	CTC-Chip	Anti-EpCAM Capture in microfluidic format followed by Cytopathology, IF, FISH, molecular analysis	On-Q-ity, USA	**1 CTC in 1 billion cells (>60%, 6)**	Spiking of 50 to 50,000 cells counted by dilution in 1 mL of blood	1 to 5 mL	[76]
Marker-based enrichment/ detection	Magsweeper	Immunocapture using anti-EpCAM antibody followed by IF, molecular analysis	Illumina, USA	**NA (62%, 1)**	Spiking of 50 fluorescent cells counted by dilution in 3 mL of blood	9 mL	[77]
Marker-based enrichment/ detection	MACS / Carcinoma Cell Enrichment and Detection kit	Ficoll and MACS (EpCAM, HER2, MCSP, NG2, CD45, CKs)	Mitlenyi Biotech, Germany	**2 CTC per 8 mL of blood (61%, 4)**	Spiking of 1 to 10000 cells counted by cell sorter in 8 mL of blood	8 mL	[78]
Marker-based enrichment/ detection	HB Chip	Anti-EpCAM Capture in microfluidic format followed by IF, cytopathology	Toner/harber lab, USA	**NA (92%, 1)**	Spiking of fluorescent 500 fluorescent cells counted by dilution in 1 mL of blood	4 mL	[79]
Marker-based enrichment/ detection	CEE™ platform	Pre-processing with leucosep tubes, Flow-dependant Immuno-capture (antibody cocktail) followed by IF, FISH	Biocept, USA	**NA (70%, 1)**	Spiking of 150 cells counted by cell dilution in 1 mL	10 mL	[80]

(*Continued*)

Table 7. (*Continued*)

Method type	Method	Principle of the method	Company or Academic lab	*In vitro* LLOD (overall recovery, concentrations tested)	Method for sensitivity and/ or recovery assessment	Blood Sample size	Ref
Marker-based enrichment/ detection	Nanovelcro	Anti-Epcam Capture in microfluidic format followed by IF	Tseng's lab, USA	**NA (95%, 5)**	Spiking of 50 to 1000 cells counted by dilution in 1 mL of blood	1 mL	[81]
Marker-based enrichment/ detection	Microtube device	Ficoll+Immunocapture (Anti-EpCAM) + E-selectin	Biocystics, USA	**NA (50%, 5)**	Spiking of 20 to 700 fluorescent cells counted by dilution in 4 mL diluted blood (1:1)	7.5 mL	[41]
Marker-based enrichment/ detection	CTCScope™	Density followed by IF, RNA FISH	ACD, USA	**1 CTC per 5 mL of blood (72%, 17 one replicate)**	Counting under microscope (1–92 cells) and transfer of the drop in to 5 mL of blood	7.5 mL	[82]
Marker-based enrichment/ detection	HDCTC	No enrichment, IF panCK and image analysis	EpicScience, USA	**10 CTC in 2 mL of blood (99%, 4)**	Spiking of 10 to 300 cells counted by dilution in 2 mL of blood and regression analysis	4 mL	[83]
Marker-based enrichment/ detection	CellCollector®	In vivo immunocapture (Anti-EpCAM), IF	Gilupi, Germany	**not evaluated, in vivo assay**	not evaluated, in vivo assay	30 min, *in vivo*	[84]
Marker-based enrichment/ detection	Isoflux	Density gradient (ficoll) and Immunocapture using magnetics beads conjugated with anti-EpCAM followed by IF, molecular analysis	Fluxion Biosciences, USA	**4 CTC in 7 mL of blood (75%, 8)**	Spiking of 4 to 200 fluorescent cells counted by dilution in 7 mL of blood	7 mL	[85]
Marker-based enrichment/ detection	Biofluidica CTC Detection System	Immunocapture using anti-EpCAM antibody followed by IF	Biofluidica, USA	**NA (90%, 1)**	Spiking of 500 fluorescent cells counted by dilution in 7.5 mL of blood	7.5 mL	[86]
Marker-based enrichment/ detection	Cytotrack™	No enrichment, IF, image analysis	Cytotrack, Denmark	**5 CTC in 7.5 mL of blood (68%, 3)**	Spiking of 10 to 100 cells counted by cell sorter in 7.5 mL of blood	7.5 mL	[87]
Marker-based enrichment/ detection	posCTC iChip	Cell size (microfluidics) with positive selection with anti-EpCAM, IF, RT-PCR, cytopathology, culture	Toner/harber lab, USA	**10 cells in 10 mL (91%, 2)**	Spiking of 10, 200 or 1000 fluorescent cells (various cell lines) in 1 mL of blood	variable, up to 10 mL	[88, 89]
Marker-based enrichment/ detection	Liquid Biopsy®	Immunocapture using surface markers (EpCaM, CK. . .) followed by IF, molecular analysis	Cynvenio Biosystems, USA	**3 CTC per mL of blood (74%, 6)**	Spiking of 3 to 900 cells by dilution in 1 mL of blood	8 mL	[90]
Leucocyte Depletion	anti-CD45 Dynabeads®	Magnetics beads coated with anti-CD45 antibody with optional density gradient separation, followed by ICC-IF	Life technologies, USA	**10 CTC in PBMC from 15 mL of blood (65%, 3)**	Spiking of 10 to 1000 cells counted by dilution in PBMC	variable, up to 15 mL	[72]
Leucocyte Depletion	RosetteSep™	Negative selection (gradient and antibody cocktail)	Stem Cell Technologies, Canada	**NA (43%, 2)**	Spiking of 25 to 250 cells counted by dilution in 4 mL of blood	typically 20 mL	[91]
Leucocyte depletion and physical (size)	negCTC iChip	Cell size (microfluidics) with negative selection with anti-CD45, followed by IF, RT-PCR, cytopathology, culture	Toner/harber lab, USA	**NA, (97%, 1)**	Spiking of 1000 fluorescent cells (various cell lines) in 1 mL of blood	variable, up to 10 mL	[88, 89]
Leucocyte depletion and physical (size)	Canpatrol™	Anti-CD45 dynabead, filtration, followed by IF, FISH, DNA mutation analysis	SurExam Bio-Tech, China	**6 CTC in 5 mL of blood (88%, 4)**	Spiking of 10 to 200 fluorescent cells counted by dilution in 5 mL of blood, immunofluorescence and FISH	5 mL	[92]

(*Continued*)

Table 7. (*Continued*)

Method type	Method	Principle of the method	Company or Academic lab	*In vitro* LLOD (overall recovery, concentrations tested)	Method for sensitivity and/ or recovery assessment	Blood Sample size	Ref
Functional	EPISPOT	RosetteSep negative selection followed by secretion assay	Alix-Panabieres, France	**1 CTC per 10 mL of blood (67%, 4)**	Spiking of 100000 to 1 cells counted by dilution in 10 mL of blood	10 mL	[93, 94]
Functional	Telomescan®	No enrichment, telemerase expression (GFP fluorescence)	Oncolys Biopharma, Japan	**10 CTC in 5 mL of blood (60%, 3)**	Spiking of 10 to 1000 Cells by dilution in 5 mL of blood	5 mL	[95]
Functional	CAM	Density (optional), adhesion property and IF	Vitatex, USA	**1 CTC per mL of blood (80%, 3)**	Spiking of 3 to 3000 cells counted by cell sorter in 3 mL of blood	2 to 20 mL	[96]

List of CTC methods and their definitions of sensitivity and/or recovery as shown in peer-reviewed publications. CTC methods are presented according to the principle of the method and per chronological order. Categories include methods based on physical properties (i.e. cell density, cell size or cell charge), enrichment and/or detection with markers (EpCAM, Cytokeratins, etc.), depletion of leucocytes and functional assays (which require the cells to be alive). Recovery is calculated when cells are spiked into the relevant matrix, at a minimum of five concentration levels covering the linear range of the assay (according to the FDA definition). Here, overall recovery is the average recovery for the range of concentration tested and number of concentration tested as indicated in the table (each concentration has n>2 replicates unless specified).

doi:10.1371/journal.pone.0169427.t007

that they lead to the loss of 40 to 60% of tumor cells spiked in blood [98]. In fact, blood cell membranes remain intact for up to 5 hours [99] after blood collection and degrade rapidly and dramatically after that (Dr Carla Ferreri, personal communication). For this reason, the ISET® system manufacturer's guidelines indicate that blood has to be treated by the ISET® System within 5 hours after blood collection.

The exceptional sensitivity of the ISET® System relies on the following aspects: 1) blood is treated soon after collection, 2) blood treatment to prepare blood for ISET® filtration is rapid and efficient 3) the number of steps before the "isolation" step is minimum: blood is just col- lected from the patient, diluted and filtered, 4) fixed cells are collected with no additional steps by the filter and only one additional step is required to collect live cells by pipetting, 5) the filter characteristics avoid losing cells larger than mature lymphocytes, 6) the blood aspiration sys- tem can be modulated and allows to stick large cells to the filter without loss, or concentrate them in a small volume over the filter, 6) the system does not relies on the use of markers for isolation nor for collection not for identification of tumor cells. Combined together, these characteristics play a key role in the ISET® sensitivity for isolation of circulating tumor cells.

Analytical sensitivity cannot be tested by using primary tumor cells as tumor cells from a patient's blood cannot be counted upstream of any further analysis to isolate them. Therefore, we performed precision studies with cells from cell lines made fluorescent, mixed with blood and carefully counted before and after their isolation. However, the clinical sensitivity of ISET® (percentage of patients with CTC in a specific clinical setting) has been studied by inde- pendent authors in comparative and non-comparative studies and shown to be extremely high (Fig 3 in Ref [2] and Table I in S1 File).

We also note that, in the field of CTC, a high sensitivity is clinically relevant only if associ- ated with high specificity. Since circulating rare non-tumor cells may be present in the blood of patients with cancer, high sensitivity with low specificity can lead to mistakes in clinical decisions.

Regarding specificity, ISET® filtration does not perform any detection of CTC *per se*. It is meant to isolate CTC without bias and with a minimum CTC loss. Specificity is brought by the

subsequent step of cytopathology. Since tumor cells are isolated intact without damage, CTC characterization is possible by a variety of downstream approaches (Fig 12). As reported and recognized, cytopathology is the only clinically validated method to diagnose tumor cells [2]. Obtaining intact tumor cell morphology is a key factor for a reliable and diagnostic identification and characterization of CTC. Our team, as well as other authors, have previously emphasized the need of specific markers able to reliably identify the presence of tumor cells in blood. Such markers are not known at present [2, 4, 13-15], and this leaves cytopathology as the only diagnostic approach with regards of the presence of tumor cells in blood. In this set- ting, it is noteworthy that several authors have found similar morphological and immunomorphological characteristics in CTC isolated by ISET® and in tumor cells from the correspondent tumor tissues [10, 12, 32, 103, 104]. Blood cytopathology is diagnostic "per se" and can also be used to study circulating tumor cells after their isolation from blood and cul- ture [105].

The hypothetical loss of small CTC by the indiscriminated filtration approach, mentioned in various literature sources [7, 8, 12, 106, 107] has never been assessed in comparative studies using different filtration approaches, nor clearly related to intact cells or to naked nuclei or cell fragments. In fact, even tumor cells from Small Cell Lung Cancer (SCLC) have been detected by ISET® [11, 104, 108, 109]. These cells have a diameter ranging from 11.2 to 17.7 μm, i.e. 1.4 to 2.2 times larger than the 8 μm lymphocytes [110].

According to cytopathological criteria [16, 30, 111], cancer cells from patients are usually larger than 16 microns. The presence in blood of intact cancer cells smaller than 8 microns, i.e. smaller than mature lymphocytes, has never been diagnosed in patients [13], which comes in support of using ISET® to isolate all types of CTC from blood.

Hofman *et al.* have provided data supporting the key role of cytopathology to identify CTC. They have published a blind multicenter study involving 10 cytopathologists and 808 cases [16] demonstrating that the classical criteria used in standard cytopathology are valid to reliably identify CTC when cells are isolated from blood using the ISET® System. Hofman *et al.* showed that, under these conditions, blood cytopathology has the same advantages and the same limitations as classical cytopathological analyses. In fact, cytopathology is not recom- mended to diagnose cells from parathyroid and thyroid adenoma [16]. Overall, to this date, 475 healthy donor and 211 patients with benign disease have been tested by ISET® setting the *in vivo* specificity of ISET® blood cytopathology at 98.3% (Summarized in Table G in S1 File).

The need for specificity in detection of CTC has prompted us to introduce the term "Circu- lating Cancer Cells" (CCC) [2] referring to tumor cells isolated from blood without loss and without antibody related bias and diagnostically identified by cytopathology. Such cancer cells are expected to be of clinical interest [2, 4] as shown by independent clinical studies using ISET® [3, 17, 18, 22, 24, 26, 35, 103, 111-115] (Reviewed in Table H in S1 File).

Cancer cells isolated by ISET® have been studied across various cancer types and stages, as well as in patients at risk of developing cancer [10-12, 16-27, 29-32, 35, 97, 103, 104, 108, 111-119] (Reviewed in Table I in S1 File). The global number of CCC and CCM has been reported to be higher in patients with advanced disease. For instance, for patients with NSCLC, Krebs *et al.* reported the following median number of CCC per 10 mL: 5.3 in Stage IIIA patients (n = 5), 11.3 in Stage IIIB patients (n = 12) and 50.7 in Stage IV patients (n = 23) [12] (Table I in S1 File).

The detection of CCC by ISET® has been proven by independent teams and studies to have a prognostic value in follow-up prospective studies, in particular in patients with localized lung cancer, liver cancer and uveal melanoma [24, 35, 112] (Table H in S1 File).

Although larger trials are needed, the above mentioned results are consistent with animal studies which have shown that the risk of developing metastases correlates directly with the

number of cancer cells in blood and that a higher risk is associated with the presence of CTM [120-123].

Hofman' s team also brought a conclusive demonstration that the ISET® blood cytopathol- ogy is diagnostic for reliable identification of cancer cells in blood. They showed, in an indepen- dent and prospective study, the ability of this assay to detect "sentinel tumor cells" in patients at risk of developing lung cancer years before the detection of the tumor nodule by CT-scan, thus demonstrating a new way for invasive cancers' early diagnosis and treatment [3].

Early diffusion of tumor cells in blood was first observed in animal models [1, 124, 125]. On average, about one out of 1000 cancer cells from the tumor mass is thought to be able to invade the blood compartment [126]. This data is consistent with earlier work using animal models of fibrosarcoma and breast cancer [127, 128]. If we take this value as a reference, a tumor contain- ing 500 000 cells with a size of about 0.5 mm in diameter (~0.5 mg of tumor [129]) would spread 500 cancer cells into the 5 liters of human blood. Such a small tumor could therefore be detected by the ISET® system which LLOD is 1 tumor cell per 10 mL of blood. Even if these calculations are an estimate and individual cancers have different invasion capabilities, they provide a reference value consistent with the possible detection of tumor cells before an inva- sive tumor reaches the size of a few mm in diameter which makes it detectable by imaging. At this stage, it could spread around 4000 tumor cells in blood, equivalent to 8 tumor cells per 10 mL of blood. However, we do not expect that tumor cells' spreading is continuous and constant through- out the day. As it frequently happens with biological phenomenon, spreading could be variable according to other biological factors such as, for instance, waves of angiogenesis and blood flow. Consistent with this view are preliminary *in vivo* data related to myeloma cells [130] and fetal cells showing circadian rhythms of circulation as well as increased cells' circulation after physical exercise [131]. Although such aspects have not been thoroughly explored yet, they raise the important issue of the best-standardized way to collect blood for the maximum CTC detection and enumeration.

We have reported a new protocol allowing collection of plasma without any loss of intact tumor cells (Fig 1B, Table 4 and S1D Fig). By using this protocol we avoid wasting blood obtained from ill patients. The collection of plasma is useful to detect cell-free DNA, cell-free RNA and exosomes as complementary investigations in cancer patients. While only CTC detection can provide information about the invasive cancer potential, the study of plasma markers may add interesting complementary information [132]. A recent study has compared the presence of tumor cells detected by ISET® and methylated RASSF1A cfDNA in 68 match- ing blood samples from controls and patients with melanoma, allowing to discriminate mela- noma patients from controls. However, 7 out of the 68 healthy controls (10%) were scored positive for the presence of methylated cfDNA in plasma, highlighting the challenge to find specific genetic markers for cfDNA analyses [119].

Cancer cells isolated from blood without antibody-related bias can be further characterized, in a second line of investigation, using immune-molecular approaches (Figs 7, 9 and 12). In this perspective, ISET® allows performing multiplexing tests. In fact, Krebs *et al.* [12] have reported that enumeration of tumor cells on 4 ISET® spots (corresponding to the filtration of 4 mL of blood) is as reliable as enumerating them on 10 spots (corresponding to the filtration of 10 mL of blood). Our data further validate this finding with intra-assay precision and accu- racy below the 15% cutoff when enumerating tumor cells on four spots (Fig 5), showing that it is possible to count tumor cells by ISET® on 4 spots leaving the other 6 spots for CTC immune-molecular characterization. This approach has been demonstrated to be valid for numbers of CTC ranging from 6 to 14 per mL of blood, by our results (Fig 5 and S2 Fig) and for number of CTC ranging from 11 to 26 per mL of blood by Krebs *et al.* [12].

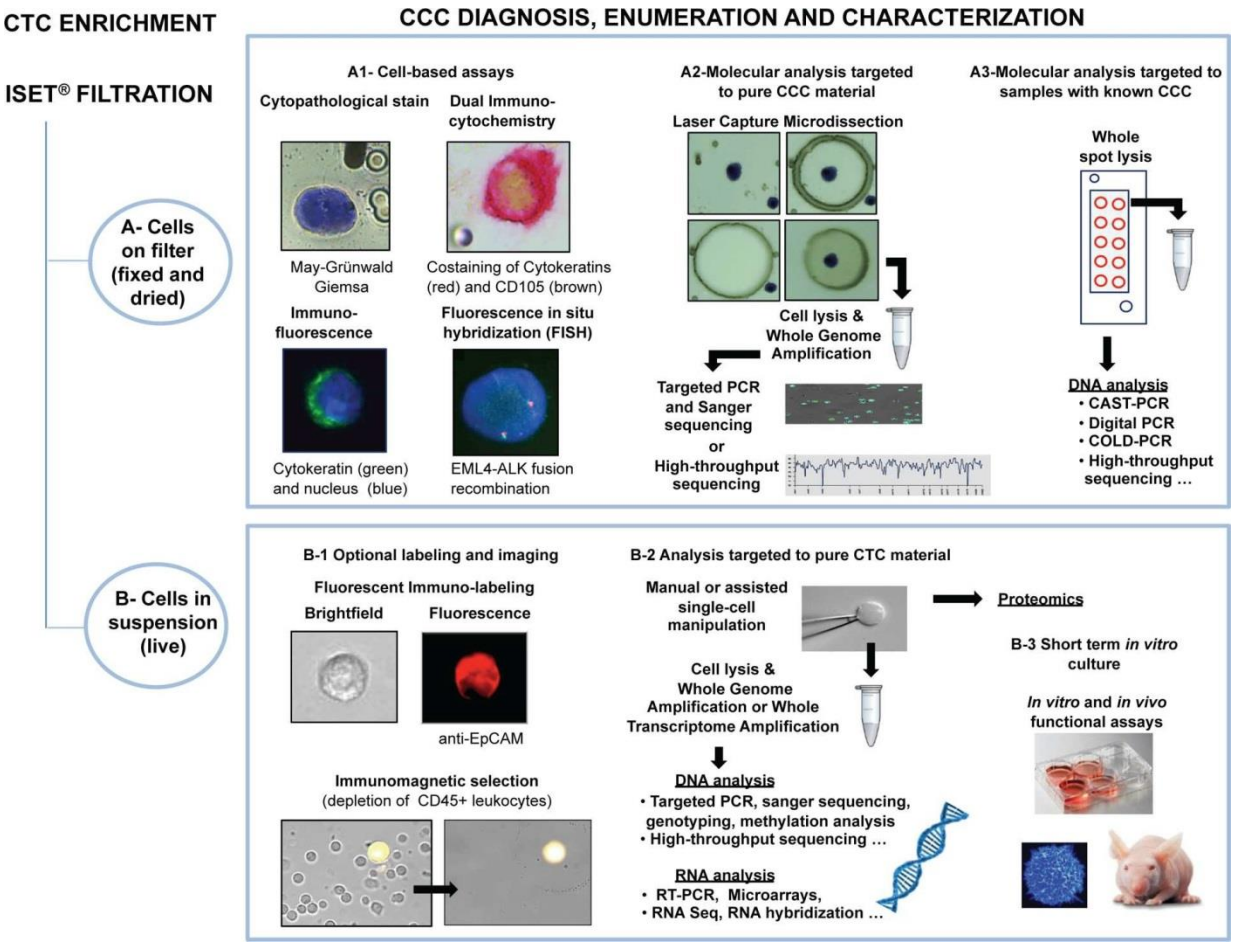

Fig 12. CTC characterization possibFig 12. CTC characterization possibilities after CTC isolation or enrichment by ISET®. (A) CTC characterization possibilities after fixed CTC isolation by ISET®. (A1)-Enriched cells are stained on the filter and CCC can be identified by cytopathology [16] and precisely counted. CTC can also be characterized by simple or multiple immuno-fluorescence-labeling [11, 17, 18], simple or multiple immuno-cytochemistry labeling [10, 12, 19, 20], or FISH [10, 21–23]. (A2) CTC can be characterized by molecular analysis (PCR, next generation sequencing …) after laser microdissection of the filter ([10, 17, 24–26, 100]). (A3) CTC can be characterized by molecular DNA and RNA analyses without microdissection using sensitive methods for detection of mutation such as Competitive Allele-Specific TaqMan® (CAST)-PCR, co-amplification at lower denaturation temperature (COLD)-PCR, Digital PCR, next generation sequencing, or RT-PCR [27]. (B) CTC characterization possibilities after live CTC enrichment by ISET®. (B1) Enriched CTC are collected in suspension and can be optionally immuno-stained or further enriched by CD45 depletion. CTC can be precisely counted after immune-labeling. (B2) Molecular analysis such as PCR and sanger sequencing, next generation sequencing (this study), RNA analysis, DNA methylation analysis [101] and proteomic [102] can be targeted to CTC after single cell isolation by micromanipulation (manual or by robot such as CellCelector™) or dielectrophoresis (DEPArray™). Additionally, mutation detection can be performed without single cell isolation on samples in which CTC have been identified using sensitive mutation-detection methods such as CAST-PCR, COLD-PCR, Digital PCR or next generation sequencing. (B3) Samples can be used for short-term culture, *in vivo* or *in vitro* expansion and functional assays.

doi:10.1371/journal.pone.0169427.g012

The clinical value of ISET® is predictably related to its capacity to isolate all types of tumor cells including tumor cells in Epithelial to Mesenchymal Transition (EMT), expressing mesen- chymal markers such as Vimentin, but not (or barely) expressing epithelial markers (EpCAM or cytokeratin). These cells are lost by methods relying on epithelial markers for CTC isolation and/or detection [12, 20]. The presence of mesenchymal cancer cells in blood has been shown to be relevant in terms of prognostic value in patients with pancreatic cancer [18, 32], and lung cancer [12, 22, 32, 35]. Detection of tumor cells in EMT is also relevant for the development of reliable companion diagnostics tests. For instance, using ISET®, Pailler *et al*. have reported the

presence of a recurrent ALK-rearrangement in CTC which also expressed mesenchymal mark- ers, consistently with a clonal tumor cells' selection [22]. Independent studies have reported the interest of ISET® for *in situ* detection of several theranostic biomarkers including ALK recombination, ROS1 recombination, KRAS mutations, BRAF V600E mutation and HER2 amplification [19, 21–23, 25, 26].

To facilitate further fundamental studies, we have determined that ISET® can isolate cancer cells from mice blood (Fig 3, Table 3 and S6 Fig). The study of animal and human CTC with the same tool (independently from potential antibody related bias and issues of species' cross reactivity) should foster studies in animals in particular for early detection of invasive cancers. ISET® has also been used to isolate tumor cells from rats [133], monkeys and pigs (unpub- lished data).

Fundamental studies need live circulating tumor cells. They are required in particular for culture-based assays allowing drug sensitivity tests and further molecular investigations.

We developed a new protocol to enrich live tumor cells from blood without immune- related bias (Fig 1C) using a dedicated Rarecells® live buffer and using the Rarecells® device and cartridge in a different way. We show that it allows a recovery rate of 80 to 100% of tumor cells and a sensitivity threshold (LLOD) of 1 tumor cells per mL of blood in spiking tests using individually captured single cells (Fig 2B and Table 5). Our results demonstrate that this new protocol for isolation from blood of live tumor cells does not induce a cell-size related bias of selection, including for the smallest cells we tested (MMTV-PyMT, Fig 6).

Biomechanics of the cytoskeleton might affect the performance of the method when using unfixed samples. Articles in the literature indicate that non-malignant tumor cell lines are stiffer in comparison to malignant tumor cell lines (and also less prone to migration and invasion) [43, 134]. Studies with cells obtained from patients' ascites (ovarian cancer) or derived from oral squamous carcinoma have shown that cancer cells from a given tumor cells' population exhibit a varying degree of stiffness, which is similar to the stiffness of cancer cell lines [135, 136]. In addition, stiffness is also correlated to the EMT status of cells: the stiffest/least invasive cell lines expressed more E-Cadherin and less Vimentin, while the compliant/most invasive cell lines expressed less E-Cadherin and more Vimentin [136]. In our tests with live cells, we used both cell lines with epithelial phenotype (LNCaP) and mesenchymal phenotype (A549, H2228, MMTV-PyMT) (details of markers expressed by LNCaP, H2228 and A549 according to the database of DSMZ (Deutsche Sammlung von Mikroorganismen und Zellkulturen) and by MMTV-PyMT according to [137]). Furthermore, our results obtained using quantitative fluorescence analyses show that the level of EpCAM expression of MCF-7 tumor cells is similar before and after their live cell enrichment by ISET® (Fig 7).

In this report, we have also shown that live A549 tumor cells isolated from blood using ISET® can be cultured and expanded *in vitro* for at least 5 days (Fig 8), demonstrating that the buffer and protocol used to isolate live tumor cells from blood allows their growth. Interest- ingly, we noticed that no leucocytes remained alive after 3 days of culture.

In addition, we have assessed cytoskeleton markers by confocal analysis of F-actin and acet- ylated α-tubulin (Fig 9) after live tumor cells isolation and culture for 72h. These markers are known to be therapeutic targets [138, 139]. The microscopy assay we used has been shown to directly correlate with Atomic Force Microscopy, a cell stiffness assay [140]. We have com- pared the profiles of two cell lines, A549 and H2228. Distribution of F-actin and acetyl-α-tubulin were found to be conserved (or restored) after 72h of *in vitro* culture following live tumor cells isolation using the ISET® system.

Furthermore, in the aim of studying theranostic mutations to guide the therapeutic choices, we have demonstrated that, in our model, the basic profile of mutations, assessed with the Hotspot Cancer Panel V2 (Thermofisher, USA) does not change after isolation by ISET® of tumor

cells from blood and their growth in culture (Fig 10, S3 Fig and Table D in S1 File) for 72 hours. This new data may stimulate similar important analyses performed on CTC from can- cer patients.

Taken together, these data suggest that the new ISET® protocol to isolate live tumor cells does not modify the cell phenotype and genotype. Consistently, tumor cells viability after their isolation from blood remained very high (>85%) (Fig 6 and Table C in S1 File).

Since the first report of successful CTC-derived xenografts (CDX) in 2000 [141], several research publications have focused on the *ex vivo* propagation of CTC via short-term *in vitro* culture [64, 142, 143], direct injection into immuno-compromised mice [109, 144, 145] or long-term 3D culture by establishment of prostate and colorectal cancer cell lines derived from CTC [142, 146]. However, long-term *in vitro* culture of CTC remains a technical challenge in the field, with a generally very low percentage of successful growth. Further knowledge about culture conditions is required to obtain *in vitro* growth of heterogeneous and very rare CTC populations. However the first requirement in this aim is the possibility to extract tumor cells from blood without selection bias, keeping their phenotype, genotype viability and growth capabilities potentially unaffected.

The new protocol we have developed for isolation of live tumor cells from blood is highly sensitive, rapid, direct and does not alter their biological characteristics, thus it should help fur- ther studies focused on CTC' *ex vivo* expansion and analysis.

Until now *ex vivo* culture of CTC has been achieved using samples from patients having several hundreds of CTC per 7.5 mL of blood. The success rates of CTC expansion in culture remains low [143, 146, 147] across various isolation methods and culture conditions. CTC from patients with SCLC and NSCLC were successfully implanted into nude mice, creating CTC-derived Xerograph (CDX) for subsequent *in vivo* drug testing [17, 109]. Some data indicate that CTC which are competent for metastasis and able to proliferate in culture are undifferentiated and EpCAM-negative [17, 147]. The excellent sensitivity of the antibody-independent ISET® live CTC isolation protocol (Table 5) and the proof that it allows tumor cell growth in culture (Figs 8 and 9) should help culture assays for fundamental CTC studies and *ex vivo* drug testing (Fig 12).

Very low numbers of live tumor cells can be isolated from blood by ISET® practically with- out loss and with a limited contamination of leukocytes. The number of residual leukocytes, when ISET® is performed with classical filters with pores of 8-micron nominal size, is variable from few hundreds to more than 1000. We did not report results in term of "purity" (defined as the number of target cells divided by the total number of remaining cells) since such calcula- tion is misleading given the variable number of CTC detected *in vivo* (Table I in S1 File) and of tumor cells spiked in blood for *in vitro* sensitivity tests.

Of note, the elimination of leukocytes can be increased by using filters having different parameters, including the pore size, and suitable for maximum elimination of leukocytes while retaining large tumor cells and tumor microemboli.

In order to reduce the number of contaminating leukocytes, we have further developed a protocol using CD45-coated magnetic beads, which was proven to achieve a complete elimina- tion of leukocytes. As a drawback, adding the CD45 selection leads to loss of 50 to 60% of the spiked tumor cells (Table 6). However, given the very high sensitivity of CTC enrichment obtained by ISET® before CD45-depletion, the new protocol remains an interesting option to collect live CTC not contaminated by leukocytes and without antibody-related bias for further RNA, DNA and protein studies and for culture assays (Fig 12).

Single cancer cells capture by their microdissection from the filter has been proven to allow targeted mutation analyses [10, 24, 25]. The new ISET® protocols to enrich live or fixed CTC from blood without sticking them to the filter provide new possibilities for extensive single

tumor cells RNA and DNA molecular studies while avoiding microdissection (Figs 10 and 12). Individual CTC can be simply captured manually after enrichment from blood by micropipetting or by using current commercial approaches (such as CellCelector™ or DEPArray™ or others).

Cancer cells' genetic heterogeneity is increasingly investigated at single cell resolution in tissues [148, 149]. Some studies have reported copy number variation by NGS analysis on single CTC identified by CellSearch™ [109, 150-153], MagSweeper [154] or Epic Sciences [155] but, with these approaches, CTC heterogeneity is predictably underestimated by the EpCAM- related selection bias. An optimized workflow for molecular characterization of individual CTC, which are sensitively isolated from blood without antibody related bias, is expected to be an attractive tool. We reported here an optimized workflow including: 1) highly sensitive isolation of live CTC from blood without bias, 2) capture of individual CTC, 3) single cell whole genome amplification, 4) efficient high throughput sequencing using a multi-gene panel analysis with the Ion Torrent™ approach.

Our results show the feasibility of applying the AmpliSeq hotspot cancer panel V2 on Ion Torrent™ to both live cells and fixed cells enriched from blood by ISET® and recovered in suspension, assessing mutations on a variety of oncogenes including KRAS (Fig 11 and S5 Fig). The study of 3 individual tumor cells allowed the detection of mutations with the same allele frequency detected in the parent cell line (Fig 11B and 11C). To our knowledge these are the first results obtained by NGS analysis on CTC sensitively isolated from blood without bias related to the use of antibodies. The protocol should help discovering theranostic mutations in CTC spread at the early steps of tumor invasion.

Overall, our results demonstrate that ISET® is an open platform which allows a highly sen- sitive and unbiased isolation from blood of fixed tumor cells for reliable identification and immune-molecular study, and of live tumor cells for culture and immune-molecular analyses. We have used cells from cell lines as a model of technical approach with potential to be applied to clinical blood samples. These technical improvements should foster studies targeting circulating cancer cells' detection and characterization, in particular at the early steps of tumor invasion.

Supporting Information

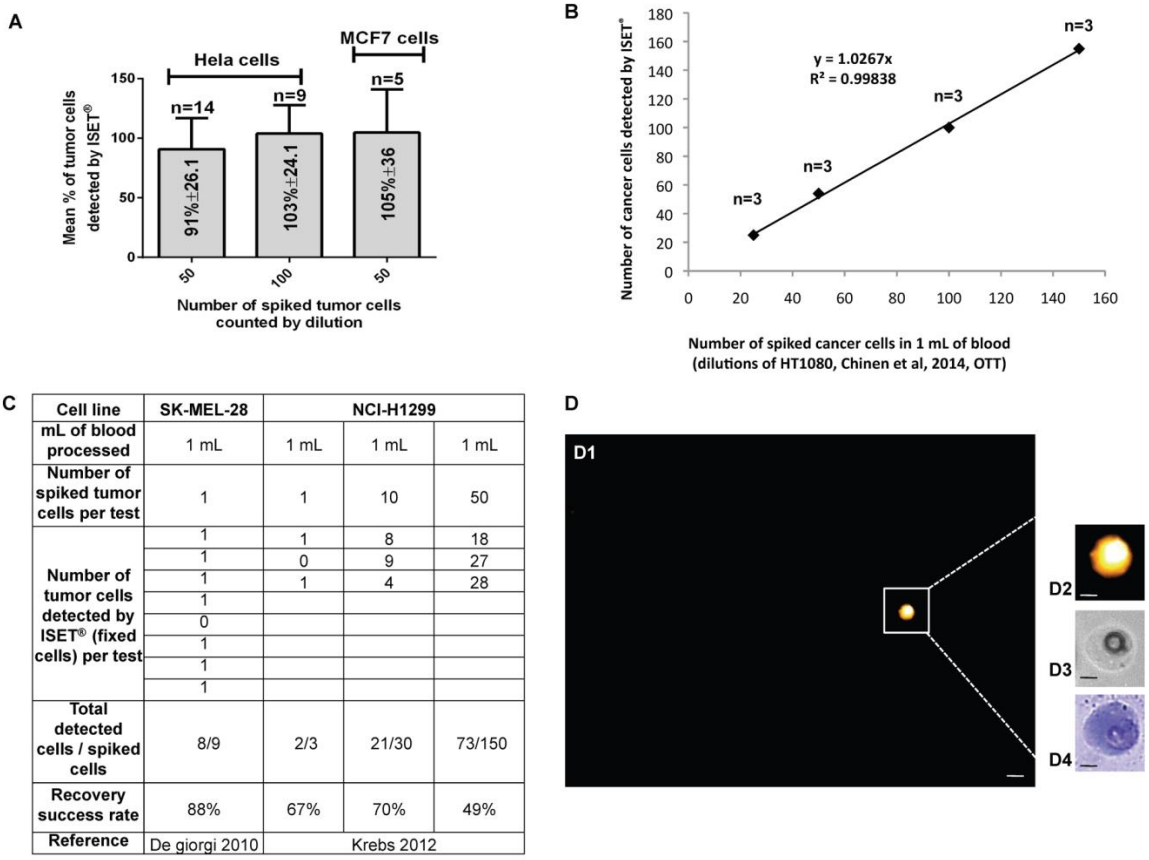

Cell line	SK-MEL-28	NCI-H1299		
mL of blood processed	1 mL	1 mL	1 mL	1 mL
Number of spiked tumor cells per test	1	1	10	50
Number of tumor cells detected by ISET® (fixed cells) per test	1	1	8	18
	1	0	9	27
	1	1	4	28
	1			
	0			
	1			
	1			
	1			
Total detected cells / spiked cells	8/9	2/3	21/30	73/150
Recovery success rate	88%	67%	70%	49%
Reference	De giorgi 2010	Krebs 2012		

S1 Fig. Additional analytical performance data. (A) Recovery experiments with dilutions of HeLa and MCF-7 cells. Mean in % of recovered HeLa and MCF-7 cells observed on ISET® filter. 50 or 100 HeLa cells were added into 1 mL whole blood after counting by dilution. 50 MCF-7 were added to 5 mL of whole blood after counting by dilution. (B) Linearity experi- ment reported by Chinen *et al.* 2014. 25, 50, 100 and 150 HT1080 cells (counted by dilution) were added to 1 blood before processing by ISET® (in triplicates). (C) In vitro sensitivity experiments reported by Krebs *et al.* 2012 and De Giorgi *et al.* 2010. 1 SK-MEL-28 cell isolated by micropipetting was added to 1 mL of blood before processing by ISET® (n = 9 tests). 1, 10 and 50 NCI-H1299 cells isolated by micropipetting were added to 1 mL of blood before pro- cessing by ISET® (in triplicates). (D) Fixed tumor cell isolated in sensitivity test after collection of plasma. Recovered cell (A and B) stained with Cell Tracker™ Orange and observed with the TRITC microscopic filter (A: 20X objective, Scale bar: 4 μm, B: Scale bar: 8 μm) (C) observed with bright field filter, (D) observed with bright field filter after a MGG staining. (TIFF)

A

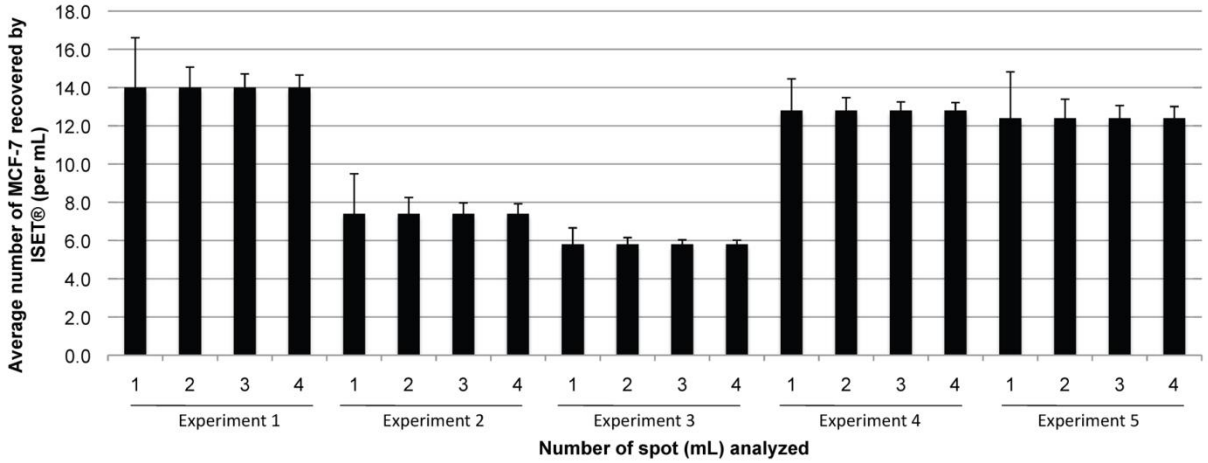

B

	Number of tumor cells detected by ISET® per mL and per test						95% CI				Intra-assay Accuracy (Error %)				Intra-assay precision (%CV)			
	Spot 1	Spot 2	Spot 3	Spot 4	Spot 5	Average number of tumor cell recovered (per mL)	1 spot	2 spots	3 spots	4 spots	1 spot	2 spots	3 spots	4 spots	1 spot	2 spots	3 spots	4 spots
Exp 1	7	19	12	21	11	14.0	5.1	2.1	1.4	1.3	34.3%	18.6%	12.4%	8.6%	41.6%	24.0%	16.0%	10.4%
Exp 2	4	8	14	9	2	7.4	4.1	1.7	1.1	1.0	47.6%	29.7%	19.8%	11.9%	63.1%	36.4%	24.3%	15.8%
Exp 3	6	5	9	5	4	5.8	1.7	0.7	0.5	0.4	23.4%	16.6%	11.0%	5.9%	33.2%	19.1%	12.8%	8.3%
Exp 4	8	18	14	13	11	12.8	3.2	3.0	1.6	0.9	20.6%	13.3%	8.9%	5.2%	28.9%	16.7%	11.1%	7.2%
Exp 5	20	6	15	12	9	12.4	4.7	1.9	1.3	1.2	34.3%	18.6%	12.4%	8.6%	43.7%	25.2%	16.8%	10.9%
average	9.0	11.2	12.8	12.0	7.4	10.5	3.8	1.9	1.2	1.0	32.0%	19.3%	12.9%	8.0%	42.1%	24.3%	16.2%	10.5%
stdev	6.3	6.8	2.4	5.9	4.2	3.6	1.4	0.8	0.4	0.3	10.7%	6.2%	4.1%	2.7%	13.2%	7.6%	5.1%	3.3%

S2 Fig. Assessment of ISET® intra-assay accuracy and precision with dilutions of MCF-7.

About 50 MCF-7 were spiked into 5 mL of blood (n = 5 experiments, 29 to 70 cells per 5 mL).

Cell counting were performed without careful recounting. The number of tumor cells found on each spot after ISET1filtration (each corresponding to the filtration of 1 mL of blood) was recorded. Experiments were done on 5 spots but for intra-assay precision and accuracy only assessment of the comparison of combinations of 1, 2, 3 and 4 spots are relevant. The only combination with the 5 spots was the reference. Four spots exhibited a representative mean tumor cells value. (A) Bar chart with the mean tumor cell number per spot and corresponding standard error of the mean (error bars) depending on the number of spots analyzed. Error bars (which correspond to the Standard Error, i.e. standard deviation divided by the squared root of the number of combinations) are calculated using the standard deviation of different combinations of 4 spots, 3 spots, 2 spots or 1 spot. If only one spot is considered, standard deviation is higher than when counting 4 spots. Thus error bars indicate the increased precision and accuracy when tumor cells are counted on 4 spots as compared to 3, 2 and one spot.

(B) Table indicating the number of tumor cells found on each spot for each of the five experi- ments, the 95% confidence interval (CI), the precision and the accuracy depending on the number of spots analyzed (1 to 4) as compared to the analysis on five spots.

A

Sample ID	Number of reads	On target	Low coverage regions	Coverage 10% quantile	Coverage heterogeneity
A549 control	1,294,171	937,446 (72.44%)	3	2,073x	1.18%
HCT116 control	1,090,391	776,997 (71.26%)	1	1,985x	0.04%
A549 ISET	795,875	706,716 (88,80%)	3	1,423x	1.45%
HCT116 ISET	855,276	834,047 (97.52%)	1	1,936x	0.44%

B

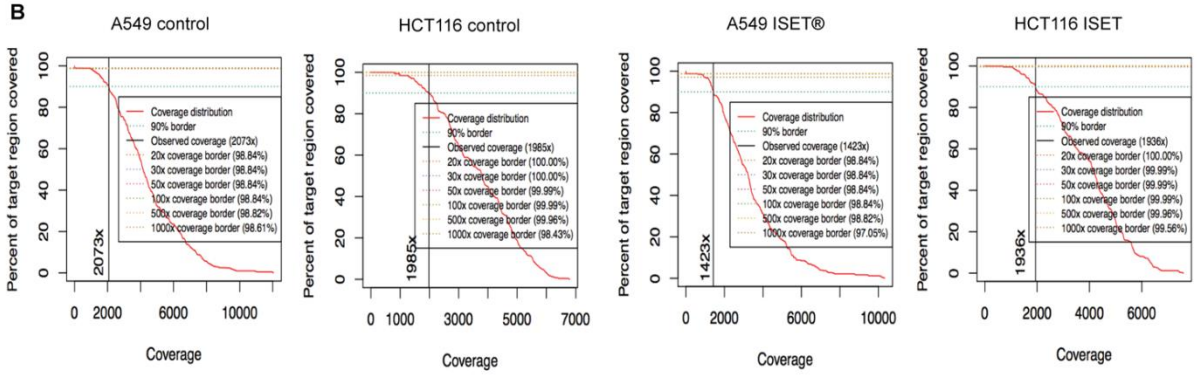

S3 Fig. Ion Torrent™ sequencing quality control parameters of A549 and HCT116 popu- lations before and after live cell ISET® enrichment. (A) Total number of reads, reads on tar- get, low coverage regions, coverage and coverage heterogeneity for each of the 4 bulk DNA samples. (B) Sequencing depth determination (percentage of target region coverage) for each of the 4 bulk DNA samples.

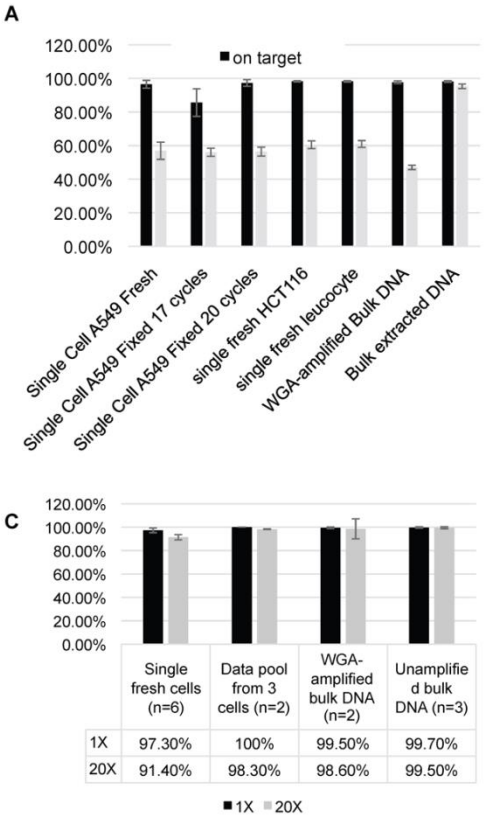

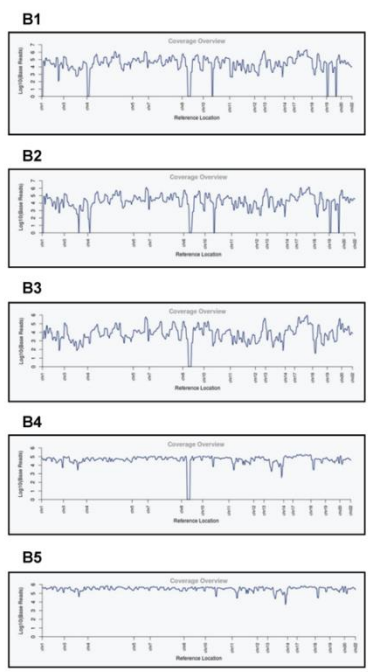

S4 Fig. Ion Torrent™ sequencing quality control parameters of bulk extracted DNA and WGA DNA from single cell enriched from blood using ISET®. (A) Amplicon mapping and sequencing depth uniformity across whole genome amplified single cells and bulk amplified and unamplified DNA controls. (B) Overview coverage plots of sequencing reads obtained from: (B1) whole genome amplified DNA from a single live A549 cell, (B2) whole genome amplified DNA from a single fixed A549 cell, (B3) whole genome amplified from bulk A549 extracted DNA, (B4) control unamplified bulk A549 DNA and (B5) control unamplified bulk DNA extracted from healthy donor blood. (C) Average amplicon coverage on pooled data from whole genome amplified single cells and bulk whole genome amplified and unamplified DNA controls.
(TIFF)

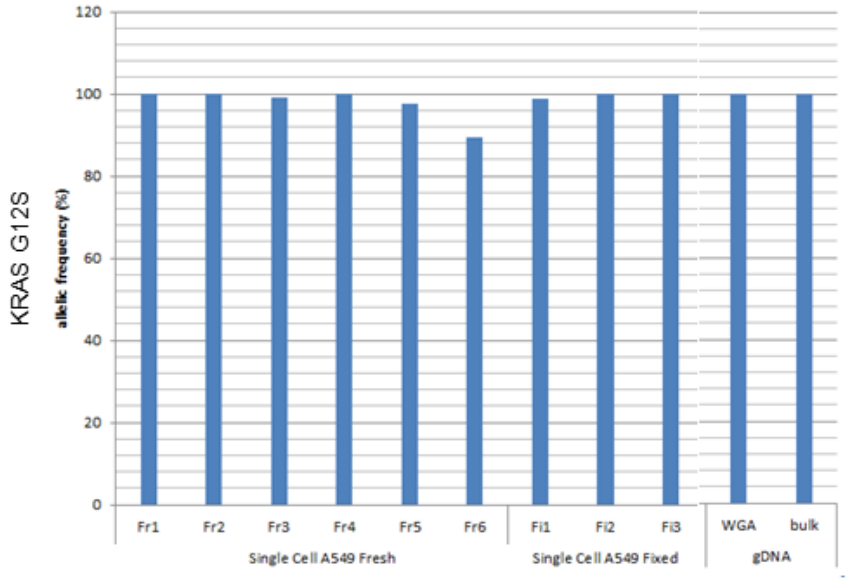

S5 Fig. Mutant KRAS G12S allele frequency by Ion Torrent™ in single cells enriched from blood using ISET®. Mutant KRAS G12S allele frequency was determined by high throughput sequencing of whole genome amplified single A549 cells, both live and fixed, as well as bulk whole genome amplified (WGA) and unamplified (bulk) DNA controls extracted from A549 tumor cells. (TIFF)

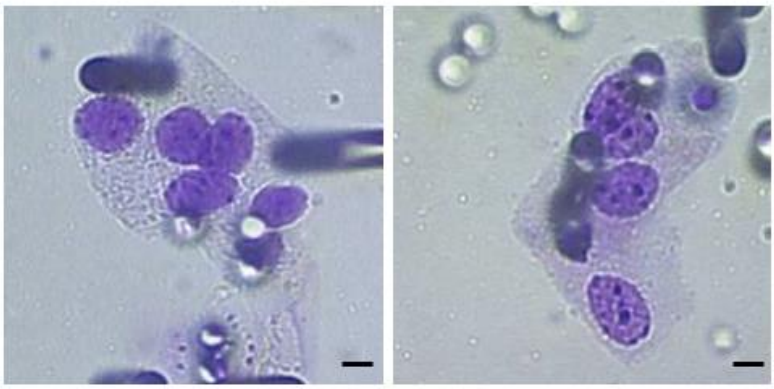

S6 Fig. Isolation of cancer cells from mouse blood. Clusters of cells with malignant features observed in the blood of two MMTV-PyMT mice. Scale bar 8 microns. Mouse blood (200 μL, kind gift of Dr. S. Humbert-Institut Curie, France) was collected, using a 2 mL syringe prefilled with 8 mg of sterile K_3EDTA, from two 14-week old MMTV-PyMT mice under anesthesia by retro-orbital puncture, according to the local ethics rules, transferred to a microcentrifuge tube and kept under gentle agitation before its treatment by ISET® within 3 hours after collec- tion. ISET® was performed by diluting mouse blood 1 to 10 with the buffer and filtering it using the standard protocol in one small compartment of the Rarecells® Block. Up to 10 different mice samples can be processed with the same cartridge. (TIFF)

S1 File. Supplemental text and all supplemental tables.

Supplemental text

We evaluated standard sequencing quality control parameters of the DNA obtained from the WGA of our single cells (S4 Fig.). For all the samples, we obtained sufficient number of mapped reads, on average about 625400 mapped reads (range 238403 to 2149603). Using 17 cycles of pre-amplification for library preparation, most of the reads obtained from the WGA from fresh single cells, WGA-amplified bulk DNA and bulk DNA aligned very well with their targets (>98%). In contrast, the reads obtained from fixed single cells were imperfectly aligned using the standard library protocol preparation with 17 cycles of preamplification (average 86%, n=3). With FFPE protocol using 20 cycles of preamplification, most of the reads from the WGA from fixed single cells were properly aligned (average 97%, n=3) (S4 Fig.). Uniformity of sequencing depth was close to 100% in bulk DNA reflecting the quasi-perfect evenness of coverage. In contrast, for all single cell WGA samples as well as WGA-amplified bulk DNA samples, uniformity was reduced to about 50% (S4A Fig.). This reflects a less uniform sequencing depth after WGA that is expected because of the variability introduced by WGA. Analysis of coverage plots (S4B Fig.) further confirmed that the sequencing of WGA DNA from single cells was noisier than WGA-amplified bulk genomic DNA but with very few amplicon failure. Amplicon coverage in ISET® enriched single-cell WGA DNA was about 97.3 % at 1X depth. At 20X depth, amplicon coverage was still over 90% but lower with the single cell WGA DNAs than with the bulk DNA and WGA-amplified bulk DNA (91.4 %, 99.5% and 98.6% respectively). Amplicon coverage at 20X depth increased to 98.3% when pooling data from 3 single cells (S4C Fig.) suggesting that the analysis of three single cells amplified by WGA could be sufficient to achieve a similar quality as for bulk DNA.

Supplemental tables

Cell line	A549	MCF-7	HeLa	LNCaP	MMTV-PyMT	MMTV-PyMT*
minimum	18.0	15.1	12.5	14.2	9.5	8.5
1st quartile	20.6	17.4	14.5	17.4	11.4	10.3
median	22.0	19.0	15.8	19.2	12.0	11.1
3rd quartile	25.0	21.1	17.1	22.4	13.3	12.3
maximum	44.0	34.7	19.4	29.8	16.8	19.0
Mean	23.2	19.6	15.8	20	12.4	11.4
Standard deviation	4.4	3.3	1.8	3.3	1.6	1.7

Table A in S1 File: Cell size (in microns) on ISET1 filters of various cell lines. Cells from human and mouse tumor cell lines were incubated 3 min with the buffer without blood and collected on standard (8 micron- pore) filters. MMTV-PyMT*: values measured for MMTV-PyMT cells isolated using 5 micron-pore filters.

Cell line	mL of blood analyzed	Number of spiked cells	Total number of tests	Average number of recovered cells	Average percentage of recovered cells	Precision (% CV)	Accuracy (%Error)	Reference
A549	10 mL	2	6	2	100%	0%	0%	Table 2
	5 mL	2	6	1.7	83%	31%	17%	Table 2
	1 mL	0	4	0	0%			Fig 4
	1 mL	2	12	1.75	88%	26%	12%	Table 1
	1 mL	2	12	1.67	83%	39%	17%	Table 1

	1 mL	2	6	1.67	83%	31%	17%	Table 2
	1 mL	2	30	1.7	85%	31%	15%	Overall (Fig 4)
	1 mL	30	9	28.2	94%	17%	6%	Fig 4
	1 mL	100	13	84.7	85%	21%	15%	Fig 4
	1 mL	300	2	333.5	111%	6%	11%	Fig 4
MCF-7	1 mL	1	10	0.9	90%	35%	10%	Table 3
	5 mL	50	5	52.4	105%	35%	5%	Fig S1A
HeLa	1 mL	1	3	1	100%	0%	0%	Table 3
	1 mL	3	3	3	100%	0%	0%	Table 3
	1 mL	50	14	45.4	91%	29%	9%	Fig S1A
	1 mL	100	9	104	104%	23%	4%	Fig S1A
MMTV -PyMT	1 mL	2	4	1.5	75%	38%	25%	Table 3

Table B in S1 File: Percentage of cell Recovery of the ISET1 platform and Precision and Accuracy of spiking tests. A549, MCF-7, MMTV-PyMT and HeLa cells were counted by micromanipulation (for tests with 1 to 3 cells) or dilution (for tests with 30 to 300 cells) and spiked into 1 to 10 mL of blood as indicated. Precision and Accuracy among all these independent tests were calculated as described in the methods. Precision is assessed via calculation of percent coefficient of variation (%CV) that is equal to 0% when data are perfectly precise. Accuracy estimated via %Error that is equal to 0% when data are perfectly accurate.

Cell line	Replicate	Viability	Average Viability	Smallest size (µm)	Largest size (µm)	Median size (µm)	Average of median size (µm)
A549 before filtration	1	95%	**98%**	10	17	14	**14**
	2	100%		10	17	14	
	3	99%		9	17	14	
A549 after filtration	1	95%	**93%**	10	17	14	**14**
	2	89%		11	19	14	
	3	94%		9	17	14	
MMTV-PyMT before filtration	1	99%	**97%**	7	14	10	**9.6**
	2	97%		7	14	10	
	3	95%		7	12	9	
MMTV-PyMT after filtration	1	90%	**85%**	7	12	9	**9.6**
	2	86%		7	13	10	
	3	80%		7	14	10	

Table C in S1 File: Cell size and viability measurement before and after ISET1 filtration of live cells. Cells from human and mouse tumor cell lines were incubated 3 min with the Live Buffer without blood and collected on standard (8 micron-pore) filters.

									A549 control		A549 ISET	
gene	**Overlap Known**	**type**	**Cat**	**Coding Consequence**	**Chrs.**	**Genome position**	**c.DNA**	**protein**	**Depth**	**var_%**	**Depth**	**var_%**
STK11	COSM12925	SNP	A	nonsense	19	1207021	c.109C>T	p.Gln37*	**2956**	**90.05**	**4974**	**88.68**
KRAS	COSM1152506	SNP	A	missense	12	25398285	c.34G>A	p.Gly12Ser	**4777**	**99.9**	**3932**	**99.87**
STK11	COSM48783	SNP	A	missense	19	1207022	c.110A>T	p.Gln37Leu	**2957**	**9.87**	**4974**	**11.24**
PIK3CA	COSM766	SNP	A	missense	3	178936094	c.1636C>A	p.Gln546Lys	**2803**	**50.27**	**1698**	**47.59**
TP53	COSM3766190	SNP	A	missense	17	7579472	c.215C>G	p.Pro72Arg	**7372**	**98.55**	**6875**	**99.07**
APC	COSM3760869	SNP	A	synonymous	5	112175770	c.4425G>A	p.= (p.Thr1475Thr)	**4663**	**33.86**	**5313**	**32.51**
EGFR	COSM1451600	SNP	A	synonymous	7	55249063	c.2361G>A	p.= (p.Gln787Gln)	**3213**	**99.88**	**2357**	**99.79**
RET	COSM4418406	SNP	A	synonymous	10	43613843	c.2307G>T	p.= (p.Leu769Leu)	**6491**	**99.49**	**4304**	**99.77**
RET	COSM3751779	SNP	A	synonymous	10	43615633	c.2712C>G	p.= (p.Ser904Ser)	**6058**	**68.11**	**5237**	**66.05**
HRAS	COSM3752426	SNP	A	synonymous	11	534242	c.81T>C	p.= (p.His27His)	**4320**	**34.42**	**2246**	**34.59**
FLT3	COSM3999060	SNP	A	intronic	13	28610183	c.1310-3T>C		**3872**	**99.92**	**2865**	**100**
FGFR3		SNP	C	synonymous	4	1806187	c.1206C>A	p.= (p.Pro402Pro)	**2369**	**7.94**	**1154**	**9.45**
FGFR3		SNP	C	synonymous	4	1807894	c.1953G>A	p.= (p.Thr651Thr)	**2526**	**99.8**	**2008**	**99.75**
PDGFRA		SNP	C	synonymous	4	55141055	c.1701A>G	p.= (p.Pro567Pro)	**2915**	**99.76**	**1953**	**99.9**
PIK3CA		SNP	C	intronic	3	178917005	c.352+40A>G		**1750**	**99.54**	**918**	**99.89**
KDR		SNP	C	intronic	4	55980239	c.798+54G>A		**2400**	**48.42**	**2153**	**49.65**
CSF1R		SNP	C	3'UTR	5	149433596	c.*35_*36delCAinsTC		**497**	**98.59**	**218**	**98.62**

Tables D in S1 File: Variant list and allele frequency measured by Ion Torrent in cell populations. Cat = Sophia DDM cate- gory of pathogenicity, Chrs = chromosome, var_% = percentage of variant. Table D1: Bulk extracted DNA from A549 control or after ISET® filtration and culture

									HCT-116 control		HCT-116 ISET	
gene	Overlap Known	type	Cat.	Coding Consequence	chrs	Genome position	c.DNA	protein	depth	var_%	depth	var_%
ABL1	COSM1674906	SNP	A	missense	9	133738370	c.827A>G	p.Tyr276Cys	5406	51.17	7492	49.67
SMO	COSM13148	SNP	A	missense	7	128846374	c.1210G>A	p.Val404Met	5094	51.69	5618	50.5
TP53	COSM3766190	SNP	A	missense	17	7579472	c.215C>G	p.Pro72Arg	5273	98.82	4707	98.32
CTNNB1	COSM33668	INDEL	A	inframe_3	3	41266133	c.133_135delTCT	p.Ser45del	3007	44.8	2837	49.35
APC	COSM3760869	SNP	A	synonymous	5	112175770	c.4425G>A	p.= (p.Thr1475Thr)	2751	99.49	3306	99.4
EGFR	COSM1451600	SNP	A	synonymous	7	55249063	c.2361G>A	p.= (p.Gln787Gln)	2644	99.77	2028	99.7
RET	COSM4418406	SNP	A	synonymous	10	43613843	c.2307G>T	p.= (p.Leu769Leu)	4616	99.7	5563	99.53
HRAS	COSM3752426	SNP	A	synonymous	11	534242	c.81T>C	p.= (p.His27His)	3118	99.81	3285	99.45
FLT3	COSM2070142	SNP	A	synonymous	13	28602367	c.2001G>A	p.= (p.Gln667Gln)	3815	51.27	4312	51.39
IDH2	COSM2139738	SNP	A	synonymous	15	90631825	c.528C>T	p.= (p.Gly176Gly)	3839	46.89	3691	47.01
FLT3	COSM3999060	SNP	A	intronic	13	28610183	c.1310-3T>C		4034	100	4984	99.94
SMARCB1	COSM1090	SNP	A	intronic	22	24176287	c.1092-41G>A		4920	49.41	4354	50.71
FGFR1		INDEL	A	frameshift	8	38285932	c.379delG	p.Asp127Metfs*25	2682	43.48	2789	41.77
FGFR3		SNP	C	synonymous	4	1806187	c.1206C>A	p.= (p.Pro402Pro)	2933	6.1	2710	6.31
FGFR3		SNP	C	synonymous	4	1807894	c.1953G>A	p.= (p.Thr651Thr)	2800	99.75	3495	99.89
PDGFRA		SNP	C	synonymous	4	55141055	c.1701A>G	p.= (p.Pro567Pro)	3129	99.9	3033	99.9
ERBB4		SNP	C	intronic	2	212812097	c.421+58A>G		1867	100	1983	99.8
KDR		SNP	C	intronic	4	55946354	c.3849-24C>A		4366	48.31	4843	49.12
KDR		SNP	C	intronic	4	55980239	c.798+54G>A		2159	100	2139	99.58
SMAD4		SNP	C	intronic	18	48586344	c.955+58C>T		4055	48.14	4093	48.99
STK11		SNP	C	intronic	19	1220321	c.465-51T>C		2251	46.82	3325	50.47
CSF1R		SNP	C	3'UTR	5	149433596	c.*35_*36delCAinsTC		384	97.14	238	96.22

Tables D in S1 File: Variant list and allele frequency measured by Ion Torrent in cell populations. Cat = Sophia DDM cate- gory of pathogenicity, Chrs = chromosome, var_% = percentage of variant. Table D2: Bulk extracted DNA from HCT-116 control or after ISET® filtration and culture.

	Sample	Single HCT116 (H1)	Single HCT116 (H2)	Single HCT116 (H3)	Pooled data 3 HCT116	WGA-Amplified HCT116 DNA	Unamplified bulk HCT116 DNA	Single leukocyte (L1)	Single leukocyte (L2)	Single leukocyte (L3)	Pooled data 3 leukocytes	Bulk DNA blood donor
KRAS G13D	**mutant allele frequency**	**38%**	**100%**	**100%**	**56%**	**42%**	**51%**	**0%**	**0%**	**ND**	**0%**	**0%**
	mutant allele coverage	37	11	29	77	59	995	0	0	0	0	0
	amplicon coverage	97	11	29	137	140	1958	13	52	0	65	1942
PIK3CA H1047R	**mutant allele frequency**	**73%**	**46%**	**32%**	**50%**	**46%**	**51%**	**0%**	**0%**	**0%**	**0%**	**0%**
	mutant allele coverage	710	453	312	1475	99	1010	0	0	0	0	0
	amplicon coverage	979	981	986	2946	213	1996	280	524	498	1302	1996
SMO V404M	**mutant allele frequency**	**55%**	**12%**	**67%**	**45%**	**53%**	**50%**	**0%**	**0%**	**0%**	**0%**	**0%**
	mutant allele coverage	1099	245	1346	2690	1064	1009	0	0	0	0	0
	amplicon coverage	2000	1996	2000	5996	1998	2000	1992	1983	1986	5961	1998
KIT M541L	**mutant allele frequency**	**0%**	**0%**	**0%**	**0%**	**0%**	**0%**	**57%**	**51%**	**57%**	**55%**	**48%**
	mutant allele coverage	0	0	0	0	0	0	1141	1009	1132	3282	967
	amplicon coverage	1988	1996	1994	5978	1990	1999	1996	1989	1992	5977	1995
ALB Y257C	**mutant allele frequency**	**17%**	**59%**	**67%**	**47%**	**51%**	**50%**	**0%**	**0%**	**0%**	**0%**	**0%**
	mutant allele coverage	303	1170	1054	2527	1016	999	0	0	0	0	0
	amplicon coverage	1759	1998	1583	5340	2000	2000	1318	990	287	990	2000

Table E in S1 File: Non-sense COSMIC mutant allele coverage, amplicon coverage and allele frequency measured by Ion TorrentTM in WGA-amplified single cells enriched from blood by ISET®.

Method (Company or Academic laboratory)	Pressure type	Pression or Depression	Filter type	Pore size (µm)	Fixation	Sample dilution	Red blood cell lysis	Blood volume (mL)	*In vitro* Sensitivity (overall recovery, number of concentrations tested)*1	Reference
ISET® System (Rarecells Diagnostic France)	Vaccum pump	- 10 kPa	track-etched	8	form.	1:10	yes	10	1 CTC per 10 mL of blood (99.9%, 6)	this study
	Vaccum pump	-3 to - 6 kPa	track-etched	8	none	1:10	yes	10	1 CTC per mL of blood (90%, 4)	this study
CTC Membrane Microfilter (Cote's lab, USA)	Manual Syringe	+ 3.45 kPa	2D parylene	10	form.	1:2	no	7.5	5 CTC in 7.5 mL of blood (89%, 1)	[1, 2]
Screencell® MB or CC (Screencell, France)	Vacutainer tube	- 2.5 kPa	track-etched	6.5	none	1:8	yes	6	NA	[3, 4]
Screencell® Cyto (Screencell, France)	Vacutainer tube	- 2.5 kPa	track-etched	7.5	form.	1:7	yes	3	2 CTC in 1 mL of blood (74%, 2)	[3, 4]
3D microfilter (Cote's lab, USA)	Manual Syringe	+ 3.45 kPa	3D parylene	8 (top) 9 (bottom)	none	1:10	no	1	NA (87%, 1)	[5]
NA (Terstappen's lab, netherlands)	Syringe pump	+ 1 kPa	track-etched	8	none	1:4	no, *2	1 to 10	2 CTC in 1 mL of blood (67%, 6)	[6, 7]
			microsieve	5					2 CTC in 1 mL of blood (58%, 6)	
CellSieve™ (Creativ Microtech, USA)	Vaccum pump	- 1.5 kPa	lithographic	7	optional	1:2	NA	7.5	NA (89 % for unfixed cells and 98% for fixed cells, 1)	[8]
MetaCell® (MetaCell, Czech Republic)	Capillarity	NA	track-etched	8	none	NA	NA	8	NA	[9]

Table F in S1 File: Main parameters and sensitivity of CTC filtration methods. *1 Overall recovery = average recovery for the range of concentration tested, number of concentration tested (n>2 replicates for each concentration unless specified). *2 elimination of red blood cells by centrifugation.

Notes: methods that use Ficoll or equivalent prior to filtration or without any peer reviewed publication are not included in this table. form. = formaldehyde. NA = not available.

Reference	Number of cases	CCC detection	Types
[10]	8	0	healthy
[11]	38	0	healthy
[12]	40	0	healthy
[13]	38	0	healthy
[13]	10	0	nevi
[14]	1	1	benign nevus
[15]	16	0	healthy
[16]	39	0	healthy
[17]	59	0	healthy
[18]	49	0	healthy
[18]	190	10	various benign diseases including parathyroid and thyroid adenoma
[19]	40	0	healthy
[20]	6	0	healthy
[21]	10	0	choroidal nevi
[22]	30	0	healthy
[23]	77	0	healthy
[24]	21	0	Benign nevus
[24]	16	0	healthy
TOTAL	**688**	**11**	**98.4 % Overall specificity**

Table G in S1 File: CCC detection by ISET® in the blood of healthy donors and patients with benign diseases.

Reference	Number of patients	Type	Stage	Percentage of patients with CTC/ CTM	Follow-up	Cut-off	Conclusion	Type (endpoint)
[11]	44	Hepato-Cellular Carcinoma	Localized	52.3%	50 +/- 48 weeks	1 CCC/CCM per 3 mL	Patients without CCCs/CCM: increased survival compared to patients with CCCs/CCM (P =.01, chi2 test), worse prognosis for patients with more than 3 CCCs as compared to those with 1 to 3 CCCs	Prognostic (OS)
[16]	208	Non-Small Cell Lung Cancer	All (I to IV)	36.5%	24 months (12-41)	50 CNHC per 6 mL	Number of CNHCs significantly associated with shorter OS and worse DFS (P= 0.002, and P= 0.001), for both early-stage I+II and later-stage III+IV-resectable NSCLCs (P = 0.05, and P < 0.0001)	Prognostic (OS, DFS)
[19]	210	Non-small cell Lung Cancer	All (I to IV)	49.5%	15 months (1–28)	1 CNHC per 10 mL	Patients without CNHC had a significantly longer DFS compared to patients with CNHC (p < 0.0001; log rank test= 33.07), presence of CNHC was a significant independent prognostic factor for shorter DFS (HR, 1.372; 95% CI, 1.123–3.286; p= 0.006):	Prognostic (OS, DFS)
[25]	1	Non-Small Cell Lung Cancer	IV	-		NA	Longitudinal CCC enumeration by ISET consistent with progression of the disease (while cytokeratin-based CTC enumeration is unrelated)	Longitudinal follow-up
[21]	31	Uveal Melanoma	All (I to IV)	54.8%	55 months (24-180)	>10 CCC and CCM per 10 mL	Significantly different DFS (Log Rank test p = 0.012) and OS (Log Rank test p = 0.017) between subjects with less than 10 CCC/10 mL of blood and subjects with more than 10 CCC/10 mL of blood and CCM.	Prognostic (OS, DFS)
[23]	168	Chronic Obstructive Pulmonary Disease	IA at diagnosis (NSCLC)	3%	4 years	1 CNHC per 10 mL	The five COPD patients with CTCs detected by cytopathology analysis after blood-enrichment at baseline developed a lung cancer that was diagnosed at follow-up, 1 to 4 years after CTCs were first detected.	Prognostic
[26]	52	Colorectal cancer	IV	82.7%	7.9 months (1.2-19.4)	2 CCC/mL	Patients who had CCCs count above cutoff showed more CCC TYMS expression (p=0.02); CCC TYMS positivity was persistent, but not significant in patients who had disease progression (p=0.07),	Prognostic / Predictive (PFS)
[27]	26	Colorectal cancer	IV	88.5%	5-14 months	<3 CTCs/7.5mL	Patients with less CCC (below cutoff) and KRAS wt in tumor: higher PFS and OS than patients with more CCCs and KRAS mutation in tumor (P= 0.001 and P= 0.004)	Prognostic / Predictive (OS, PFS)
[28]	8 (4 ROS1-rearranged)	Non-Small Cell Lung Cancer	Metastatic	100.0%	30-90 days	-	Longitudinal follow-up for 5 patients, heterogeneity of responses to crizotinib in CCC subsets and of FISH patterns	Longitudinal follow-up (resistance)

Reference	Number of patients	Type	Stage	Percentage of patients with CTC/ CTM	Follow-up	Cut-off	Conclusion	Type (endpoint)
[29]	50	Pancreatic cancer	I, II and IV	90.0%	14 months (8.4-16.4)	> 1 mesenchymal CCC in 1 mL	Presence of mesenchymal CCCs was significantly associated with cancer recurrence [HR 2.78, 95% confidence interval (CI) 1.31–5.88, P = 0.01], Shorter time to recurrence (9. vs 13.5 months) in patients with mesenchymal-like CCCs (P = 0.02).	Prognostic (PFS, OS)
						> 1 epithelial CCC in 1 mL	Epithelial CCCs : significantly associated with worse survival compared with patients without CCCs (median survival 13.7 mo vs not reached, P = 0.008)	
[24]	128	Cutaneous Melanoma	IIIB, IIIC, IV	85.2%	12 months (3-18)	> 1 CCM in 10 mL	OS significantly decreased in patients with CCMs alone or CCMs and iCCCs at baseline in comparison to patients with no CCMs or with iCCCs alone independently of the therapeutic strategy Presence of CCMs at baseline (P = 0.022): independent predictor of poor OS	Prognostic (OS)
[30]	34	Colorectal cancer	IV	88.2%	9.1 months (7.2-11)	>1 MRP1 positive CCCs in 1 mL	Among patients treated with irinotecan-based chemotherapy, 4 out of 19 cases with MRP1 positive CCCs showed a worse PFS in comparison to those with MRP1 negative CCCs (2.1 months vs. 9.1 months; P= 0.003).	Prognostic/ Predictive (PFS)
[31]	1	Non-Small Cell Lung Cancer	Metastatic (T1aN2M1b)	100%	2 months	-	Baseline 4 CTC by CellSearch, 0 post-therapy; ISET post-therapy >150 CCCs	Longitudinal follow-up

Table H in S1 File: Studies reporting prognostic value of CCC/CCM detected by ISET® and ISET® longitudinal follow-up studies. CNHC: circulating non-hematological cells include cells with benign, uncertain and malignant features. Overall Survival (OS) is defined by the NIH-NCO as the percentage of patient in a study or treatment group who are still alive for a certain period of time after they were diagnosed with or started treatment for a disease, such as cancer. Progression-free survival (PFS) is defined by the NIH-NCO as length of time during and after the treatment of a disease, such as cancer, that a patient lives with the disease but it does not get worse. Disease-free survival (DFS) is defined by the NIH-NCO as the length of time after primary treatment for a cancer that the patient survives without any signs or symptoms of that cancer. Hazard ratio (HR) is defined by the NIH-NCO as, a measure of how often a particular event happens in one group compared to how often it happens in another group, over time. A hazard ratio of one means that there is no difference in survival between the two groups. A hazard ratio of greater than one or less than one means that survival was better in one of the groups. Prognostic biomarker: biomarker that can be used to estimate the chance of recovery from a disease or the chance of the disease recurring. Predictive bio- marker: biomarker that can be used to help predict whether a person' s cancer will respond to a specific treatment. Predictive factor may also describe something that increases a person' s risk of developing a condition or disease.

Reference	Number of patients	Disease type	Stage	Timing of blood sampling‡	Number of patients with CCC or CCM	% of patients with CCC or CCM	Mean* CCC number (range) per 10 mL	Mean* CCM number (range) per 10 mL
[10]	7	HCC	na	Before and after surgery	3	43 %	0	8.6 (0 to 40)
[11]	44	HCC	M0 (localized or diffuse)	Prior treatment	23	52 %	na	na (3.3 to 33)
[12]	44	BC	I to III	Before surgery	12	27 %	85 (positive patients only) (1 to 300)	
[13]	87	CM	All (I to IV)	Before surgery or during treatment for M1 patients	23	26 %	8 (median) (2.5 to 35)	
	5	non-melanoma skin tumors	na		0	0%	0	0
[15]	16	UM	M0 (small, medium and large)	Before therapy	5	31 %	24 (positive patients only) (7.5 to 58)	
[16]	208	NSCLC	All (I to IV)	Before surgery	76	37 %	na	na
[17]	250	NSCLC	All (I to IV)	Before surgery	102	49 %	na	na
[18]	569	NSCLC, BC, CC, KC, HNC, PM, Sarc, CM, EC	All (I to IV)	Mostly before surgery	245	43 %	na	na
[19]	210	NSCLC	All (I to IV)	Before surgery	104	50 %	34 (positive patients only) (1 to 150)	
[32]	6	3 NSCLC, 3SCLC	IIIB or IV	Unknown	6	100 %	na	na
[33]	20	BC	M1	Unknown	17	85%	5 (0 to 27)	
[33]	20	PrC,	M1	Unknown	20	100%	38 (median) (1 to 331)	
[33]	20	NSCLC	M1	Unknown	20	100%	12.5 (median) (1 to >133)	
[20]	6	NSCLC	M1	Variable after diagnosis	6	100 %	87 (16-190)	18 (0-40)
[34]	40	NSCLC	IIIA to IV	Before therapy	32	80 % (38 % with CCM)	71 (0-1393)	6 (0-13)

Reference	Number of patients	Disease type	Stage	Timing of blood sampling‡	Number of patients with CCC or CCM	% of patients with CCC or CCM	Mean* CCC number (range) per 10 mL	Mean* CCM number (range) per 10 mL
[35]	27	PaC	M1 or inoperable	Variable, 6 weeks off therapy	24	89 %	35 (0-320)	na, 3 patients with CCM
[36]	20	SCLC	Limited and extensive	Before therapy	20	NA	na	34 CTM over 20 patients
[37]	87	NSCLC	All (I to IV)	Before therapy	87	100 %	na	na
[38]	98	CM	IIIB, IIIC, IV	Before surgery	87	89%	na	na
[28]	32	NSCLC	M1	Baseline or under crizotinib	32	100 %	190 (40 to 450)	
[25]	1	NSCLC	IV	Baseline or before new cycle of chemo	1	100 %	735 to 1285 over the course of the disease	
[39]	90	CM	IV	Before therapy	51	57 %	14 (0 to 110)	na, 12 patients with CCM
[21]	31	UM	All (I to IV)	Before therapy	17	55 %	8 (median) (2 to 50)	na, 8 patients with CCM
[40]	8	PrC	All (Gleason 5 to 10)	Before therapy	8	100 %	0 to 300	na
[41]	19	HCC	All (I to IV)	Baseline (4-weeks off therapy)	19	100 %	101 (25 to 271)	na
[22]	11	Sarc	All (I to IV)	Unknown	11	100 %	27 (2.5 to 35)	na
[42]	4	BC	M1, invasive ductal carcinoma	Unknown	4	100 %	na	na
[26]	52	CRC	IV	Before new line of therapy	43	83 %	20 (median) (0 to 310)	na
[27]	26	CRC	IV	Before new line of therapy	23	88 %	20 (median) (0 to 140)	na
[43]	8	NSCLC	M1	Baseline or under crizotinib	4/4 ROS-1 rearranged, 8/8 total	na	123 ROS1 rearranged (median) (80 to 183)	

Reference	Number of patients	Disease type	Stage	Timing of blood sampling‡	Number of patients with CCC or CCM	% of patients with CCC or CCM	Mean* CCC number (range) per 10 mL	Mean* CCM number (range) per 10 mL
[29]	50	PaC	I, II and IV	Before surgery	45	90%	850 (median) (0 to 3000)	na
[44]	68	CM	All (I to IV)	At diagnosis, before surgery and therapy	18	27 %	na	na
[24]	128	CM	IIIB, IIIC, IV	Before first line of therapy	109	85 %	6 (4 to 16)	4 (3 to 9)
[30]	34	CRC	IV	Before new line of therapy	30	88%	20 (median) (0 to 310)	
[31]	1	NSCLC	T1aN2M1b	At diagnosis and after therapy	1	100%	>1500	na
Total	**2347**				**1328**			

Table I in S1 File: CCC/CCM detected by ISET® in the blood of cancer patients. HCC: hepatocellular carcinoma, BC: breast cancer, PrC: prostate can- cer, PaC: pancreatic cancer, NSCLC: Non-Small Cell Lung Cancer, SCLC: Small Cell Lung cancer, CC: Colorectal cancer, KC: Kidney cancer, HNC: Head and Neck carcinoma, Esoph- ageal carcinoma: EC, Pleural Mesothelioma: PM, Sarcoma: Sarc, UM: uveal melanoma, CM: cutaneous melanoma, M0: localized, M1: metastatic, na: not available, ‡ if several blood sam- pling time points are reported, number of patients with CCCs/CCMs and CCC/CTMs number are only indicated for the baseline time point, * if average CCC and CCM numbers are not available, the median or range are provided as indicated in the table. Usually the mean is calcu- lated over the whole population of patients (including patients without CCCs), unless specified otherwise in the table.
(DOCX)

Acknowledgments

The authors greatly acknowledge INSERM (Institut National de Santé et Recherche Médicale), University Paris Descartes and Fondation Lefort-Beaumont de l' Institut de France for their support and the INEM (Institut Necker Enfants Malades) Imaging Facility. We thank Emilie Dugon, Astrid Girard, Karine Prevost, Davide Bréchot and Igor Stzepourginski for their assistance. We thank Gabriela Petkova Campbell for help in reviewing the text.

Author Contributions

Conceptualization: SL PPB.

Data curation: SL KH LB.

Formal analysis: SL LB FBM PPB.

Funding acquisition: PPB LF SJ.

Investigation: SL KH LB TC DMD SJ

MO.

Methodology: SL KH LB FBM TC DMD MO LF SJ PPB.

Project administration: SL

PPB. **Resources:** SL PPB LF

DMD. **Supervision:** SL PPB.

Validation: SL KH LB FBM TC DMD MO LF SJ PPB.

Visualization: SL KH LB FBM TC DMD MO LF SJ PPB.

Writing – original draft: SL PPB.

Writing – review & editing: SL KH LB FBM TC DMD MO LF SJ PPB.

References

1. Rhim AD, Mirek ET, Aiello NM, Maitra A, Bailey JM, McAllister F, et al. EMT and dissemination precede pancreatic tumor formation. Cell. 2012; 148(1–2):349–61. doi: 10.1016/j.cell.2011.11.025 PMID: 22265420
2. Paterlini-Brechot P. Circulating Tumor Cells: Who is the Killer? Cancer Microenviron. 2014; 7(3):161–76. doi: 10.1007/s12307-014-0164-4 PMID: 25527469
3. Ilie M, Hofman V, Long-Mira E, Selva E, Vignaud JM, Padovani B, et al. "Sentinel" circulating tumor cells allow early diagnosis of lung cancer in patients with chronic obstructive pulmonary disease. PLoS One. 2014; 9(10):e111597. doi: 10.1371/journal.pone.0111597 PMID: 25360587
4. Paterlini-Brechot P, Benali NL. Circulating tumor cells (CTC) detection: clinical impact and future directions. Cancer Lett. 2007; 253(2):180–204. doi: 10.1016/j.canlet.2006.12.014 PMID: 17314005

5. Parkinson DR, Dracopoli N, Petty BG, Compton C, Cristofanilli M, Deisseroth A, et al. Considerations in the development of circulating tumor cell technology for clinical use. J Transl Med. 2012; 10:138. doi: 10.1186/1479-5876-10-138 PMID: 22747748

6. Krebs MG, Metcalf RL, Carter L, Brady G, Blackhall FH, Dive C. Molecular analysis of circulating tumour cells-biology and biomarkers. Nat Rev Clin Oncol. 2014; 11(3):129–44. doi: 10.1038/nrclinonc.2013.253 PMID: 24445517

7. Ignatiadis M, Lee M, Jeffrey SS. Circulating Tumor Cells and Circulating Tumor DNA: Challenges and Opportunities on the Path to Clinical Utility. Clin Cancer Res. 2015; 21(21):4786–800. doi: 10.1158/1078-0432.CCR-14-1190 PMID: 26527805

8. Alix-Panabieres C, Pantel K. Technologies for detection of circulating tumor cells: facts and vision. Lab Chip. 2014; 14(1):57–62. doi: 10.1039/c3lc50644d PMID: 24145967

9. Ferreira MM, Ramani VC, Jeffrey SS. Circulating tumor cell technologies. Mol Oncol. 2016; 10 (3):374–94. doi: 10.1016/j.molonc.2016.01.007 PMID: 26897752

10. Vona G, Sabile A, Louha M, Sitruk V, Romana S, Schutze K, et al. Isolation by size of epithelial tumor cells: a new method for the immunomorphological and molecular characterization of circulatingtumor cells. Am J Pathol. 2000; 156(1):57–63. doi: 10.1016/S0002-9440(10)64706-2 PMID: 10623654

11. Lecharpentier A, Vielh P, Perez-Moreno P, Planchard D, Soria JC, Farace F. Detection of circulating tumour cells with a hybrid (epithelial/mesenchymal) phenotype in patients with metastatic non-small cell lung cancer. Br J Cancer. 2011; 105(9):1338–41. doi: 10.1038/bjc.2011.405 PMID: 21970878

12. Krebs MG, Hou JM, Sloane R, Lancashire L, Priest L, Nonaka D, et al. Analysis of circulating tumor cells in patients with non-small cell lung cancer using epithelial marker-dependent and -independent approaches. J Thorac Oncol. 2012; 7(2):306–15. doi: 10.1097/JTO.0b013e31823c5c16 PMID: 22173704

13. Hofman V, Ilie M, Long E, Guibert N, Selva E, Washetine K, et al. Detection of circulating tumor cells from lung cancer patients in the era of targeted therapy: promises, drawbacks and pitfalls. Curr Mol Med. 2014; 14(4):440–56. PMID: 24730524

14. Alix-Panabieres C, Pantel K. Challenges in circulating tumour cell research. Nat Rev Cancer. 2014; 14 (9):623–31. doi: 10.1038/nrc3820 PMID: 25154812

15. Pantel K, Deneve E, Nocca D, Coffy A, Vendrell JP, Maudelonde T, et al. Circulating epithelial cells in patients with benign colon diseases. Clin Chem. 2012; 58(5):936–40. doi: 10.1373/clinchem.2011.175570 PMID: 22205690

16. Hofman VJ, Ilie MI, Bonnetaud C, Selva E, Long E, Molina T, et al. Cytopathologic detection of circulating tumor cells using the isolation by size of epithelial tumor cell method: promises and pitfalls. Am J Clin Pathol. 2011; 135(1):146–56. doi: 10.1309/AJCP9X8OZBEIQVVI PMID: 21173137

17. Morrow CJ, Trapani F, Metcalf RL, Bertolini G, Hodgkinson CL, Khandelwal G, et al. Tumourigenic Non-Small Cell Lung Cancer Mesenchymal Circulating Tumour Cells—A Clinical Case Study. Ann Oncol. 2016.

18. Poruk KE, Valero V 3rd, Saunders T, Blackford AL, Griffin JF, Poling J, et al. Circulating Tumor Cell Phenotype Predicts Recurrence and Survival in Pancreatic Adenocarcinoma. Ann Surg. 2016.

19. Hofman V, Ilie M, Long-Mira E, Giacchero D, Butori C, Dadone B, et al. Usefulness of immunocytochemistry for the detection of the BRAF(V600E) mutation in circulating tumor cells from metastatic melanoma patients. J Invest Dermatol. 2013; 133(5):1378–81. doi: 10.1038/jid.2012.485 PMID: 23303445

20. Hofman V, Ilie MI, Long E, Selva E, Bonnetaud C, Molina T, et al. Detection of circulating tumor cells as a prognostic factor in patients undergoing radical surgery for non-small cell lung carcinoma: Comparison of the efficacy of the CellSearch Assay and the isolation by size of epithelial tumor cell method. Int J Cancer. 2011; 2011.

21. Ilie M, Long E, Butori C, Hofman V, Coelle C, Mauro V, et al. ALK-gene rearrangement: a comparative analysis on circulating tumour cells and tumour tissue from patients with lung adenocarcinoma. Ann Oncol. 2012; 23(11):2907–13. doi: 10.1093/annonc/mds137 PMID: 22735679

22. Pailler E, Adam J, Barthelemy A, Oulhen M, Auger N, Valent A, et al. Detection of circulating tumor cells harboring a unique ALK rearrangement in ALK-positive non-small-cell lung cancer. J Clin Oncol. 2013; 31(18):2273–81. doi: 10.1200/JCO.2012.44.5932 PMID: 23669222

23. Pailler E, Auger N, Lindsay CR, Vielh P, Islas-Morris-Hernandez A, Borget I, et al. High level of chromosomal instability in circulating tumor cells of ROS1-rearranged non-small-cell lung cancer. Ann Oncol. 2015; 26(7):1408–15. doi: 10.1093/annonc/mdv165 PMID: 25846554

24. Vona G, Estepa L, Beroud C, Damotte D, Capron F, Nalpas B, et al. Impact of cytomorphological detection of circulating tumor cells in patients with liver cancer. Hepatology. 2004; 39(3):792–7. doi: 10.1002/hep.20091 PMID: 14999698

25. Pinzani P, Salvadori B, Simi L, Bianchi S, Distante V, Cataliotti L, et al. Isolation by size of epithelial tumor cells in peripheral blood of patients with breast cancer: correlation with real-time reverse transcriptase-polymerase chain reaction results and feasibility of molecular analysis by laser microdissection. Hum Pathol. 2006; 37(6):711–8. doi: 10.1016/j.humpath.2006.01.026 PMID: 16733212

26. Buim ME, Fanelli MF, Souza VS, Romero J, Abdallah EA, Mello CA, et al. Detection of KRAS mutations in circulating tumor cells from patients with metastatic colorectal cancer. Cancer Biol Ther. 2015; 16(9):1289–95. doi: 10.1080/15384047.2015.1070991 PMID: 26252055

27. De Giorgi V, Pinzani P, Salvianti F, Panelos J, Paglierani M, Janowska A, et al. Application of a filtration- and isolation-by-size technique for the detection of circulating tumor cells in cutaneous melanoma. J Invest Dermatol. 2010; 130(10):2440–7. doi: 10.1038/jid.2010.141 PMID: 20535130

28. Kallergi G, Politaki E, Alkahtani S, Stournaras C, Georgoulias V. Evaluation of Isolation Methods for Circulating Tumor Cells (CTCs). Cell Physiol Biochem. 2016; 40(3–4):411–9. doi: 10.1159/000452556 PMID: 27889762

29. Chinen LTD MC, Abdallah EA, Ocea LMM, Buim ME, Breve NM, Gasparini JL Jr, Fanelli MF, Paterlini-Bréchot P. Isolation, detection, and immunomorphological characterization of circulating tumor cells (CTCs) from patients with diffrent types of sarcoma using isolation by size of tumor cells: a window on sarcoma-cell invasion. OncoTargets and Therapy. 2014; 7:1609–17. doi: 10.2147/OTT.S62349 PMID: 25258541

30. Farace F, Massard C, Vimond N, Drusch F, Jacques N, Billiot F, et al. A direct comparison of CellSearch and ISET for circulating tumour-cell detection in patients with metastatic carcinomas. Br J Cancer. 2011; 105(6):847–53. doi: 10.1038/bjc.2011.294 PMID: 21829190

31. Morris KL, Tugwood JD, Khoja L, Lancashire M, Sloane R, Burt D, et al. Circulating biomarkers in hepatocellular carcinoma. Cancer Chemother Pharmacol. 2014; 74(2):323–32. doi: 10.1007/s00280-014-2508-7 PMID: 24923562

32. Khoja L, Backen A, Sloane R, Menasce L, Ryder D, Krebs M, et al. A pilot study to explore circulating tumour cells in pancreatic cancer as a novel biomarker. Br J Cancer. 2012; 106(3):508–16. doi: 10.1038/bjc.2011.545 PMID: 22187035

33. Guy CT, Cardiff RD, Muller WJ. Induction of mammary tumors by expression of polyomavirus middle T oncogene: a transgenic mouse model for metastatic disease. Mol Cell Biol. 1992; 12(3):954–61. PMID: 1312220

34. Jemaa M, Galluzzi L, Kepp O, Castedo M, Rello-Varona S, Vitale I, et al. Transgenerational cell fate profiling: a method for the graphical presentation of complex cell cycle alterations. Cell Cycle. 2013; 12(1):183–90. doi: 10.4161/cc.23046 PMID: 23255111

35. Hofman V, Bonnetaud C, Ilie MI, Vielh P, Vignaud JM, Flejou JF, et al. Preoperative circulating tumor cell detection using the isolation by size of epithelial tumor cell method for patients with lung cancer is a new prognostic biomarker. Clin Cancer Res. 2011; 17(4):827–35. doi: 10.1158/1078-0432.CCR-10-0445 PMID: 21098695

36. Balasubramanian P, Lang JC, Jatana KR, Miller B, Ozer E, Old M, et al. Multiparameter analysis, including EMT markers, on negatively enriched blood samples from patients with squamous cell carcinoma of the head and neck. PLoS One. 2012; 7(7):e42048. doi: 10.1371/journal.pone.0042048 PMID: 22844540

37. Balic M, Dandachi N, Hofmann G, Samonigg H, Loibner H, Obwaller A, et al. Comparison of two methods for enumerating circulating tumor cells in carcinoma patients. Cytometry B Clin Cytom. 2005; 68(1):25–30. doi: 10.1002/cyto.b.20065 PMID: 16142788

38. Rosenberg R, Gertler R, Friederichs J, Fuehrer K, Dahm M, Phelps R, et al. Comparison of two density gradient centrifugation systems for the enrichment of disseminated tumor cells in blood. Cytometry. 2002; 49(4):150–8. doi: 10.1002/cyto.10161 PMID: 12454978

39. Rudy JL. Differentiating between sensitivity and limit of detection. Clin Chem. 1989; 35(3):509.

40. Polzer B, Medoro G, Pasch S, Fontana F, Zorzino L, Pestka A, et al. Molecular profiling of single circulating tumor cells with diagnostic intention. EMBO Mol Med. 2014; 6(11):1371–86. doi: 10.15252/emmm.201404033 PMID: 25358515

41. Hughes AD, Mattison J, Western LT, Powderly JD, Greene BT, King MR. Microtube device for selectin-mediated capture of viable circulating tumor cells from blood. Clin Chem. 2012; 58(5):846–53. doi: 10.1373/clinchem.2011.176669 PMID: 22344286

42. Jeganathan N, Predescu D, Zhang J, Sha F, Bardita C, Patel M, et al. Rac1-mediated cytoskeleton rearrangements induced by intersectin-1s deficiency promotes lung cancer cell proliferation, migration and metastasis. Mol Cancer. 2016; 15(1):59. doi: 10.1186/s12943-016-0543-1 PMID: 27629044

43. Xu W, Mezencev R, Kim B, Wang L, McDonald J, Sulchek T. Cell stiffness is a biomarker of the metastatic potential of ovarian cancer cells. PLoS One. 2012; 7(10):e46609. doi: 10.1371/journal.pone.0046609 PMID: 23056368

44. Matrone MA, Whipple RA, Balzer EM, Martin SS. Microtentacles tip the balance of cytoskeletal forces in circulating tumor cells. Cancer Res. 2010; 70(20):7737–41. doi: 10.1158/0008-5472.CAN-10-1569 PMID: 20924109

45. Lebofsky R, Decraene C, Bernard V, Kamal M, Blin A, Leroy Q, et al. Circulating tumor DNA as a non-invasive substitute to metastasis biopsy for tumor genotyping and personalized medicine in a prospective trial across all tumor types. Mol Oncol. 2015; 9(4):783–90. doi: 10.1016/j.molonc.2014.12.003 PMID: 25579085

46. Klinger B, Sieber A, Fritsche-Guenther R, Witzel F, Berry L, Schumacher D, et al. Network quantification of EGFR signaling unveils potential for targeted combination therapy. Mol Syst Biol. 2013; 9:673. doi: 10.1038/msb.2013.29 PMID: 23752269

47. Masramon L, Vendrell E, Tarafa G, Capella G, Miro R, Ribas M, et al. Genetic instability and divergence of clonal populations in colon cancer cells in vitro. J Cell Sci. 2006; 119(Pt 8):1477–82. doi: 10.1242/jcs.02871 PMID: 16551697

48. Watanabe N, Dickinson DA, Krzywanski DM, Iles KE, Zhang H, Venglarik CJ, et al. A549 subclones demonstrate heterogeneity in toxicological sensitivity and antioxidant profile. Am J Physiol Lung Cell Mol Physiol. 2002; 283(4):L726–36. doi: 10.1152/ajplung.00025.2002 PMID: 12225949

49. Klein CA, Schmidt-Kittler O, Schardt JA, Pantel K, Speicher MR, Riethmuller G. Comparative genomic hybridization, loss of heterozygosity, and DNA sequence analysis of single cells. Proc Natl Acad Sci U S A. 1999; 96(8):4494–9. PMID: 10200290

50. Zhang W, Zhu J, Bai J, Jiang H, Liu F, Liu A, et al. Comparison of the inhibitory effects of three transcriptional variants of CDKN2A in human lung cancer cell line A549. J Exp Clin Cancer Res. 2010; 29:74. doi: 10.1186/1756-9966-29-74 PMID: 20565749

51. Fabbri F, Carloni S, Zoli W, Ulivi P, Gallerani G, Fici P, et al. Detection and recovery of circulating colon cancer cells using a dielectrophoresis-based device: KRAS mutation status in pure CTCs. Cancer Lett. 2013; 335(1):225–31. doi: 10.1016/j.canlet.2013.02.015 PMID: 23419522

52. Kruger S, Emig M, Lohse P, Ehninger G, Hochhaus A, Schackert HK. The c-kit (CD117) sequence variation M541L, but not N564K, is frequent in the general population, and is not associated with CML in Caucasians. Leukemia. 2006; 20(2):354–5; discussion 6–7. doi: 10.1038/sj.leu.2404038 PMID: 16307017

53. Coumans FA, van Dalum G, Beck M, Terstappen LW. Filter characteristics influencing circulating tumor cell enrichment from whole blood. PLoS One. 2013; 8(4):e61770. doi: 10.1371/journal.pone.0061770 PMID: 23626725

54. Lin HK, Zheng S, Williams AJ, Balic M, Groshen S, Scher HI, et al. Portable filter-based microdevice for detection and characterization of circulating tumor cells. Clin Cancer Res. 2010; 16(20):5011–8. doi: 10.1158/1078-0432.CCR-10-1105 PMID: 20876796

55. Zheng S, Lin H, Liu JQ, Balic M, Datar R, Cote RJ, et al. Membrane microfilter device for selective capture, electrolysis and genomic analysis of human circulating tumor cells. J Chromatogr A. 2007; 1162 (2):154–61. doi: 10.1016/j.chroma.2007.05.064 PMID: 17561026

56. Raz RS, inventorMethod for the separation and sorting of different biological objects utilizing differences in their viscoelastic properties2008.

57. Zheng S, Lin HK, Lu B, Williams A, Datar R, Cote RJ, et al. 3D microfilter device for viable circulating tumor cell (CTC) enrichment from blood. Biomed Microdevices. 2011; 13(1):203–13. doi: 10.1007/s10544-010-9485-3 PMID: 20978853

58. Desitter I, Guerrouahen BS, Benali-Furet N, Wechsler J, Janne PA, Kuang Y, et al. A new device for rapid isolation by size and characterization of rare circulating tumor cells. Anticancer Res. 2011; 31 (2):427–41. PMID: 21378321

59. El-Heliebi A, Kroneis T, Zohrer E, Haybaeck J, Fischereder K, Kampel-Kettner K, et al. Are morphological criteria sufficient for the identification of circulating tumor cells in renal cancer? J Transl Med. 2013; 11:214. doi: 10.1186/1479-5876-11-214 PMID: 24044779

60. Lim E, Tay A, Nicholson AG. Antibody independent microfluidic cell capture of circulating tumor cells for the diagnosis of cancer. J Thorac Oncol. 2012; 7(12):e42–3.

61. Warkiani ME, Guan G, Luan KB, Lee WC, Bhagat AA, Chaudhuri PK, et al. Slanted spiral microfluidics for the ultra-fast, label-free isolation of circulating tumor cells. Lab Chip. 2013; 14(1):128–37.

62. Coumans FA, van Dalum G, Beck M, Terstappen LW. Filtration parameters influencing circulating tumor cell enrichment from whole blood. PLoS One. 2013; 8(4):e61774. doi: 10.1371/journal.pone.0061774 PMID: 23658615

63. Adams DL, Zhu P, Makarova OV, Martin SS, Charpentier M, Chumsri S, et al. The systematic study of circulating tumor cell isolation using lithographic microfilters. RSC Adv. 2014; 9:4334–42. doi: 10.1039/C3RA46839A PMID: 25614802

64. Bobek V, Kacprzak G, Rzechonek A, Kolostova K. Detection and cultivation of circulating tumor cells in malignant pleural mesothelioma. Anticancer Res. 2014; 34(5):2565–9. PMID: 24778078

65. Xu L, Mao X, Imrali A, Syed F, Mutsvangwa K, Berney D, et al. Optimization and Evaluation of a Novel Size Based Circulating Tumor Cell Isolation System. PLoS One. 2015; 10(9):e0138032. doi: 10.1371/journal.pone.0138032 PMID: 26397728

66. Hvichia GE, Parveen Z, Wagner C, Janning M, Quidde J, Stein A, et al. A novel microfluidic platform for size and deformability based separation and the subsequent molecular characterization of viable circulating tumor cells. Int J Cancer. 2016; 138(12):2894–904. doi: 10.1002/ijc.30007 PMID: 26789903

67. Swennenhuis JF, Tibbe AG, Stevens M, Katika MR, van Dalum J, Tong HD, et al. Self-seeding microwell chip for the isolation and characterization of single cells. Lab Chip. 2015; 15(14):3039–46. doi: 10.1039/c5lc00304k PMID: 26082273

68. Gogoi P, Sepehri S, Zhou Y, Gorin MA, Paolillo C, Capoluongo E, et al. Development of an Automated and Sensitive Microfluidic Device for Capturing and Characterizing Circulating Tumor Cells (CTCs) from Clinical Blood Samples. PLoS One. 2016; 11(1):e0147400. doi: 10.1371/journal.pone.0147400 PMID: 26808060

69. Ntouroupi TG, Ashraf SQ, McGregor SB, Turney BW, Seppo A, Kim Y, et al. Detection of circulating tumour cells in peripheral blood with an automated scanning fluorescence microscope. Br J Cancer. 2008; 99(5):789–95. doi: 10.1038/sj.bjc.6604545 PMID: 18682708

70. Gupta V, Jafferji I, Garza M, Melnikova VO, Hasegawa DK, Pethig R, et al. ApoStream(), a new dielectrophoretic device for antibody independent isolation and recovery of viable cancer cells from blood. Biomicrofluidics. 2012; 6(2):24133. doi: 10.1063/1.4731647 PMID: 23805171

71. Kim EH, Lee JK, Kim BC, Rhim SH, Kim JW, Kim KH, et al. Enrichment of cancer cells from whole blood using a microfabricated porous filter. Anal Biochem. 2013; 440(1):114–6. doi: 10.1016/j.ab.2013.05.016 PMID: 23747280

72. Naume B, Borgen E, Beiske K, Herstad TK, Ravnas G, Renolen A, et al. Immunomagnetic techniques for the enrichment and detection of isolated breast carcinoma cells in bone marrow and peripheral blood. J Hematother. 1997; 6(2):103–14. doi: 10.1089/scd.1.1997.6.103 PMID: 9131439

73. Allard WJ, Matera J, Miller MC, Repollet M, Connelly MC, Rao C, et al. Tumor cells circulate in the peripheral blood of all major carcinomas but not in healthy subjects or patients with nonmalignant diseases. Clin Cancer Res. 2004; 10(20):6897–904. doi: 10.1158/1078-0432.CCR-04-0378 PMID: 15501967

74. Pachmann K, Heiss P, Demel U, Tilz G. Detection and quantification of small numbers of circulating tumour cells in peripheral blood using laser scanning cytometer (LSC). Clin Chem Lab Med. 2001; 39(9):811–7. doi: 10.1515/CCLM.2001.134 PMID: 11601678

75. Zieglschmid V, Hollmann C, Gutierrez B, Albert W, Strothoff D, Gross E, et al. Combination of immunomagnetic enrichment with multiplex RT-PCR analysis for the detection of disseminated tumor cells. Anticancer Res. 2005; 25(3A):1803–10. PMID: 16033103

76. Nagrath S, Sequist LV, Maheswaran S, Bell DW, Irimia D, Ulkus L, et al. Isolation of rare circulating tumour cells in cancer patients by microchip technology. Nature. 2007; 450(7173):1235–9. doi: 10.1038/nature06385 PMID: 18097410

77. Talasaz AH, Powell AA, Huber DE, Berbee JG, Roh KH, Yu W, et al. Isolating highly enriched populations of circulating epithelial cells and other rare cells from blood using a magnetic sweeper device. Proc Natl Acad Sci U S A. 2009; 106(10):3970–5. doi: 10.1073/pnas.0813188106 PMID: 19234122

78. Pluim D, Devriese LA, Beijnen JH, Schellens JH. Validation of a multiparameter flow cytometry method for the determination of phosphorylated extracellular-signal-regulated kinase and DNA in circulating tumor cells. Cytometry A. 2012; 81(8):664–71. doi: 10.1002/cyto.a.22049 PMID: 22499242

79. Stott SL, Hsu CH, Tsukrov DI, Yu M, Miyamoto DT, Waltman BA, et al. Isolation of circulating tumor cells using a microvortex-generating herringbone-chip. Proc Natl Acad Sci U S A. 2010; 107(43):18392–7. doi: 10.1073/pnas.1012539107 PMID: 20930119

80. Nora Dickson M, Tsinberg P, Tang Z, Bischoff FZ, Wilson T, Leonard EF. Efficient capture of circulating tumor cells with a novel immunocytochemical microfluidic device. Biomicrofluidics. 2011; 5(3):34119–3411915. doi: 10.1063/1.3623748 PMID: 22662044

81. Wang S, Liu K, Liu J, Yu ZT, Xu X, Zhao L, et al. Highly efficient capture of circulating tumor cells by using nanostructured silicon substrates with integrated chaotic micromixers. Angew Chem Int Ed Engl. 2011; 50(13):3084–8. doi: 10.1002/anie.201005853 PMID: 21374764

82. Payne RE, Wang F, Su N, Krell J, Zebrowski A, Yague E, et al. Viable circulating tumour cell detection using multiplex RNA in situ hybridisation predicts progression-free survival in metastatic breast cancer patients. Br J Cancer. 2012; 106(11):1790–7. doi: 10.1038/bjc.2012.137 PMID: 22538972

83. Marrinucci D, Bethel K, Kolatkar A, Luttgen MS, Malchiodi M, Baehring F, et al. Fluid biopsy in patients with metastatic prostate, pancreatic and breast cancers. Phys Biol. 2012; 9(1):016003. doi: 10.1088/1478-3975/9/1/016003 PMID: 22306768

84. Saucedo-Zeni N, Mewes S, Niestroj R, Gasiorowski L, Murawa D, Nowaczyk P, et al. A novel method for the in vivo isolation of circulating tumor cells from peripheral blood of cancer patients using a functionalized and structured medical wire. Int J Oncol. 2012; 41(4):1241–50. doi: 10.3892/ijo.2012.1557 PMID: 22825490

85. Harb W, Fan A, Tran T, Danila DC, Keys D, Schwartz M, et al. Mutational Analysis of Circulating Tumor Cells Using a Novel Microfluidic Collection Device and qPCR Assay. Transl Oncol. 2013; 6 (5):528–38. PMID: 24151533

86. Kamande JW, Hupert ML, Witek MA, Wang H, Torphy RJ, Dharmasiri U, et al. Modular microsystem for the isolation, enumeration, and phenotyping of circulating tumor cells in patients with pancreatic cancer. Anal Chem. 2013; 85(19):9092–100. doi: 10.1021/ac401720k PMID: 23947293

87. Hillig T, Nygaard AB, Nekiunaite L, Klingelhofer J, Soletormos G. In vitro validation of an ultra-sensitive scanning fluorescence microscope for analysis of circulating tumor cells. APMIS. 2013; 122(6):545–51. doi: 10.1111/apm.12183 PMID: 24164622

88. Ozkumur E, Shah AM, Ciciliano JC, Emmink BL, Miyamoto DT, Brachtel E, et al. Inertial focusing for tumor antigen-dependent and -independent sorting of rare circulating tumor cells. Sci Transl Med. 2013; 5(179):179ra47. doi: 10.1126/scitranslmed.3005616 PMID: 23552373

89. Karabacak NM, Spuhler PS, Fachin F, Lim EJ, Pai V, Ozkumur E, et al. Microfluidic, marker-free isolation of circulating tumor cells from blood samples. Nat Protoc. 2014; 9(3):694–710. doi: 10.1038/nprot.2014.044 PMID: 24577360

90. Winer-Jones JP, Vahidi B, Arquilevich N, Fang C, Ferguson S, Harkins D, et al. Circulating tumor cells: clinically relevant molecular access based on a novel CTC flow cell. PLoS One. 2014; 9(1): e86717. doi: 10.1371/journal.pone.0086717 PMID: 24489774

91. Naume B, Borgen E, Tossvik S, Pavlak N, Oates D, Nesland JM. Detection of isolated tumor cells in peripheral blood and in BM: evaluation of a new enrichment method. Cytotherapy. 2004; 6(3):244–52. doi: 10.1080/14653240410006086 PMID: 15203981

92. Wu S, Liu Z, Liu S, Lin L, Yang W, Xu J. Enrichment and enumeration of circulating tumor cells by efficient depletion of leukocyte fractions. Clin Chem Lab Med. 2013; 52(2):243–51.

93. Alix-Panabieres C, Brouillet JP, Fabbro M, Yssel H, Rousset T, Maudelonde T, et al. Characterization and enumeration of cells secreting tumor markers in the peripheral blood of breast cancer patients. J Immunol Methods. 2005; 299(1–2):177–88. doi: 10.1016/j.jim.2005.02.007 PMID: 15914200

94. Alix-Panabieres C, Rebillard X, Brouillet JP, Barbotte E, Iborra F, Segui B, et al. Detection of circulating prostate-specific antigen-secreting cells in prostate cancer patients. Clin Chem. 2005; 51(8):1538–41. doi: 10.1373/clinchem.2005.049445 PMID: 16040853

95. Kojima T, Hashimoto Y, Watanabe Y, Kagawa S, Uno F, Kuroda S, et al. A simple biological imaging system for detecting viable human circulating tumor cells. J Clin Invest. 2009; 119(10):3172–81. doi: 10.1172/JCI38609 PMID: 19729837

96. Paris PL, Kobayashi Y, Zhao Q, Zeng W, Sridharan S, Fan T, et al. Functional phenotyping and genotyping of circulating tumor cells from patients with castration resistant prostate cancer. Cancer Lett. 2009; 277(2):164–73. doi: 10.1016/j.canlet.2008.12.007 PMID: 19162393

97. Khoja L, Shenjere P, Hodgson C, Hodgetts J, Clack G, Hughes A, et al. Prevalence and heterogeneity of circulating tumour cells in metastatic cutaneous melanoma. Melanoma Res. 2014; 24(1):40–6. doi: 10.1097/CMR.0000000000000025 PMID: 24201293

98. Qin J, Alt JR, Hunsley BA, Williams TL, Fernando MR. Stabilization of circulating tumor cells in blood using a collection device with a preservative reagent. Cancer Cell Int. 2014; 14(1):23. doi: 10.1186/1475-2867-14-23 PMID: 24602297

99. Conti M, Scanferlato R, Louka M, Sansone A, Marzetti C, Ferreri C. Building up spectral libraries for mapping erythrocytes by hyperspectral dark field microscopy. Biomedical Spectroscopy and Imaging. 2016; 5(2):175–84.

100. Mouawia H, Saker A, Jais JP, Benachi A, Bussieres L, Lacour B, et al. Circulating trophoblastic cells provide genetic diagnosis in 63 fetuses at risk for cystic fibrosis or spinal muscular atrophy. Reprod Biomed Online. 2012; 25(5):508–20. doi: 10.1016/j.rbmo.2012.08.002 PMID: 23000084

101. Smallwood SA, Lee HJ, Angermueller C, Krueger F, Saadeh H, Peat J, et al. Single-cell genome-wide bisulfite sequencing for assessing epigenetic heterogeneity. Nat Methods. 2014; 11(8):817–20. doi: 10.1038/nmeth.3035 PMID: 25042786

102. Zhang Y, Tang Y, Sun S, Wang Z, Wu W, Zhao X, et al. Single-cell codetection of metabolic activity, intracellular functional proteins, and genetic mutations from rare circulating tumor cells. Anal Chem. 2015; 87(19):9761–8. doi: 10.1021/acs.analchem.5b01901 PMID: 26378744

103. Hofman V, Long E, Ilie M, Bonnetaud C, Vignaud JM, Flejou JF, et al. Morphological analysis of circulating tumour cells in patients undergoing surgery for non-small cell lung carcinoma using the isolation by size of epithelial tumour cell (ISET) method. Cytopathology. 2011.

104. Hou JM, Krebs M, Ward T, Sloane R, Priest L, Hughes A, et al. Circulating tumor cells as a window on metastasis biology in lung cancer. Am J Pathol. 2011; 178(3):989–96. doi: 10.1016/j.ajpath.2010.12.003 PMID: 21356352

105. Malara N, Guzzi G, Mignogna C, Trunzo V, Camastra C, Della Torre A, et al. Non-invasive real-time biopsy of intracranial lesions using short time expanded circulating tumor cells on glass slide: report of two cases. BMC Neurol. 2016; 16:127. doi: 10.1186/s12883-016-0652-x PMID: 27502239

106. Pantel K, Alix-Panabieres C. Functional Studies on Viable Circulating Tumor Cells. Clin Chem. 2016; 62(2):328–34. doi: 10.1373/clinchem.2015.242537 PMID: 26637479

107. Ligthart ST, Coumans FA, Bidard FC, Simkens LH, Punt CJ, de Groot MR, et al. Circulating Tumor Cells Count and Morphological Features in Breast, Colorectal and Prostate Cancer. PLoS One. 2013; 8(6):e67148. doi: 10.1371/journal.pone.0067148 PMID: 23826219

108. Hou JM, Krebs MG, Lancashire L, Sloane R, Backen A, Swain RK, et al. Clinical significance and molecular characteristics of circulating tumor cells and circulating tumor microemboli in patients with small-cell lung cancer. J Clin Oncol. 2012; 30(5):525–32. doi: 10.1200/JCO.2010.33.3716 PMID: 22253462

109. Hodgkinson CL, Morrow CJ, Li Y, Metcalf RL, Rothwell DG, Trapani F, et al. Tumorigenicity and genetic profiling of circulating tumor cells in small-cell lung cancer. Nat Med. 2014; 20(8):897–903. doi: 10.1038/nm.3600 PMID: 24880617

110. Lee TK, Esinhart JD, Blackburn LD, Silverman JF. The size of small cell lung carcinoma cells. Ratio to lymphocytes and correlation with specimen size and crush artifact. Anal Quant Cytol Histol. 1992; 14 (1):32–4. PMID: 1313679

111. Long E, Ilie M, Bence C, Butori C, Selva E, Lalvee S, et al. High expression of TRF2, SOX10, and CD10 in circulating tumor microemboli detected in metastatic melanoma patients. A potential impact for the assessment of disease aggressiveness. Cancer Med. 2016.

112. Mazzini C, Pinzani P, Salvianti F, Scatena C, Paglierani M, Ucci F, et al. Circulating tumor cells detection and counting in uveal melanomas by a filtration-based method. Cancers (Basel). 2014; 6(1):323–32.

113. Chinen LT, de Carvalho FM, Rocha BM, Aguiar CM, Abdallah EA, Campanha D, et al. Cytokeratin-based CTC counting unrelated to clinical follow up. J Thorac Dis. 2013; 5(5):593–9. doi: 10.3978/j.issn.2072-1439.2013.09.18 PMID: 24255771

114. Abdallah EA, Fanelli MF, Buim ME, Machado Netto MC, Gasparini Junior JL, Souza ESV, et al. Thymidylate synthase expression in circulating tumor cells: a new tool to predict 5-fluorouracil resistance in metastatic colorectal cancer patients. Int J Cancer. 2015; 137(6):1397–405. doi: 10.1002/ijc.29495 PMID: 25721610

115. Abdallah EA, Fanelli MF, Souza ESV, Machado Netto MC, Gasparini Junior JL, Vilarim Araujo D, et al. MRP1 expression in CTCs confers resistance to irinotecan-based treatment in metastatic colorectal cancer. Int J Cancer. 2016.

116. Pinzani P, Mazzini C, Salvianti F, Massi D, Grifoni R, Paoletti C, et al. Tyrosinase mRNA levels in the blood of uveal melanoma patients: correlation with the number of circulating tumor cells and tumor progression. Melanoma Res. 2010; 20(4):303–10. doi: 10.1097/CMR.0b013e32833906e3 PMID: 20442676

117. Cummings J, Sloane R, Morris K, Zhou C, Lancashire M, Moore D, et al. Optimisation of an immunohistochemistry method for the determination of androgen receptor expression levels in circulating tumour cells. BMC Cancer. 2014; 14:226. doi: 10.1186/1471-2407-14-226 PMID: 24674711

118. LeBleu VS, O'Connell JT, Gonzalez Herrera KN, Wikman H, Pantel K, Haigis MC, et al. PGC-1alpha mediates mitochondrial biogenesis and oxidative phosphorylation in cancer cells to promote metastasis. Nat Cell Biol. 2014; 16(10):992–1003, 1–15. doi: 10.1038/ncb3039 PMID: 25241037

119. Salvianti F, Orlando C, Massi D, De Giorgi V, Grazzini M, Pazzagli M, et al. Tumor-Related Methylated Cell-Free DNA and Circulating Tumor Cells in Melanoma. Front Mol Biosci. 2016; 2:76. doi: 10.3389/fmolb.2015.00076 PMID: 26779490

120. Fidler IJ. Metastasis: quantitative analysis of distribution and fate of tumor emboli labeled with 125 I-5-iodo-2'-deoxyuridine. J Natl Cancer Inst. 1970; 45(4):773–82. PMID: 5513503

121. Liotta LA, Saidel MG, Kleinerman J. The significance of hematogenous tumor cell clumps in the metastatic process. Cancer Res. 1976; 36(3):889–94. PMID: 1253177

122. Duda DG, Duyverman AM, Kohno M, Snuderl M, Steller EJ, Fukumura D, et al. Malignant cells facilitate lung metastasis by bringing their own soil. Proc Natl Acad Sci U S A. 2010; 107(50):21677–82. doi: 10.1073/pnas.1016234107 PMID: 21098274

123. Aceto N, Bardia A, Miyamoto DT, Donaldson MC, Wittner BS, Spencer JA, et al. Circulating tumor cell clusters are oligoclonal precursors of breast cancer metastasis. Cell. 2014; 158(5):1110–22. doi: 10.1016/j.cell.2014.07.013 PMID: 25171411

124. Magnon C, Hall SJ, Lin J, Xue X, Gerber L, Freedland SJ, et al. Autonomic nerve development contributes to prostate cancer progression. Science. 2013; 341(6142):1236361. doi: 10.1126/science.1236361 PMID: 23846904

125. Husemann Y, Geigl JB, Schubert F, Musiani P, Meyer M, Burghart E, et al. Systemic spread is an early step in breast cancer. Cancer Cell. 2008; 13(1):58–68. doi: 10.1016/j.ccr.2007.12.003 PMID: 18167340

126. Chang YS, di Tomaso E, McDonald DM, Jones R, Jain RK, Munn LL. Mosaic blood vessels in tumors: frequency of cancer cells in contact with flowing blood. Proc Natl Acad Sci U S A. 2000; 97(26):14608–13. doi: 10.1073/pnas.97.26.14608 PMID: 11121063

127. Liotta LA, Kleinerman J, Saidel GM. Quantitative relationships of intravascular tumor cells, tumor vessels, and pulmonary metastases following tumor implantation. Cancer Res. 1974; 34(5):997–1004. PMID: 4841969

128. Butler TP, Gullino PM. Quantitation of cell shedding into efferent blood of mammary adenocarcinoma. Cancer Res. 1975; 35(3):512–6. PMID: 1090362

129. Klein CA. Parallel progression of primary tumours and metastases. Nat Rev Cancer. 2009; 9(4):302–12. doi: 10.1038/nrc2627 PMID: 19308069

130. Paiva B, Paino T, Sayagues JM, Garayoa M, San-Segundo L, Martin M, et al. Detailed characterization of multiple myeloma circulating tumor cells shows unique phenotypic, cytogenetic, functional, and circadian distribution profile. Blood. 2013; 122(22):3591–8. doi: 10.1182/blood-2013-06-510453 PMID: 24072855

131. Schlutter JM, Kirkegaard I, Ferreira AS, Hatt L, Christensen B, Kolvraa S, et al. The Number of Endovascular Trophoblasts in Maternal Blood Increases Overnight and after Physical Activity: An Experimental Study. Fetal Diagn Ther. 2015.

132. Pantel K, Alix-Panabieres C. Liquid biopsy: Potential and challenges. Mol Oncol. 2015; 10(3):371–3.

133. Lelievre L, Paterlini-Brechot P, Camatte S, Tartour E, Aggerbeck M, Vilde F, et al. Effect of laparoscopy versus laparotomy on circulating tumor cells using isolation by size of epithelial tumor cells. Int J Gynecol Cancer. 2004; 14(2):229–33. doi: 10.1111/j.1048-891X.2004.014205.x PMID: 15086721

134. Harouaka RA, Nisic M, Zheng SY. Circulating tumor cell enrichment based on physical properties. J Lab Autom. 2013; 18(6):455–68. doi: 10.1177/2211068213494391 PMID: 23832928

135. Runge J, Reichert TE, Fritsch A, Kas J, Bertolini J, Remmerbach TW. Evaluation of single-cell biomechanics as potential marker for oral squamous cell carcinomas: a pilot study. Oral Dis. 2014; 20(3): e120–7. doi: 10.1111/odi.12171 PMID: 24006964

136. Swaminathan V, Mythreye K, O'Brien ET, Berchuck A, Blobe GC, Superfine R. Mechanical stiffness grades metastatic potential in patient tumor cells and in cancer cell lines. Cancer Res. 2011; 71 (15):5075–80. doi: 10.1158/0008-5472.CAN-11-0247 PMID: 21642375

137. Qin L, Liao L, Redmond A, Young L, Yuan Y, Chen H, et al. The AIB1 oncogene promotes breast cancer metastasis by activation of PEA3-mediated matrix metalloproteinase 2 (MMP2) and MMP9 expression. Mol Cell Biol. 2008; 28(19):5937–50. doi: 10.1128/MCB.00579-08 PMID: 18644862

138. Wang X, Tanaka M, Krstin S, Peixoto HS, Moura CC, Wink M. Cytoskeletal interference—A new mode of action for the anticancer drugs camptothecin and topotecan. Eur J Pharmacol. 2016; 789:265–74. doi: 10.1016/j.ejphar.2016.07.044 PMID: 27474470

139. Dumontet C, Jordan MA. Microtubule-binding agents: a dynamic field of cancer therapeutics. Nat Rev Drug Discov. 2010; 9(10):790–803. doi: 10.1038/nrd3253 PMID: 20885410

140. Calzado-Martin A, Encinar M, Tamayo J, Calleja M, San Paulo A. Effect of Actin Organization on the Stiffness of Living Breast Cancer Cells Revealed by Peak-Force Modulation Atomic Force Microscopy. ACS Nano. 2016; 10(3):3365–74. doi: 10.1021/acsnano.5b07162 PMID: 26901115

141. Pretlow TG, Schwartz S, Giaconia JM, Wright AL, Grimm HA, Edgehouse NL, et al. Prostate cancer and other xenografts from cells in peripheral blood of patients. Cancer Res. 2000; 60(15):4033–6. PMID: 10945604

142. Gao D, Vela I, Sboner A, Iaquinta PJ, Karthaus WR, Gopalan A, et al. Organoid cultures derived from patients with advanced prostate cancer. Cell. 2014; 159(1):176–87. doi: 10.1016/j.cell.2014.08.016 PMID: 25201530

143. Yu M, Bardia A, Aceto N, Bersani F, Madden MW, Donaldson MC, et al. Cancer therapy. Ex vivo cul- ture of circulating breast tumor cells for individualized testing of drug susceptibility. Science. 2014; 345 (6193):216–20. doi: 10.1126/science.1253533 PMID: 25013076

144. Baccelli I, Schneeweiss A, Riethdorf S, Stenzinger A, Schillert A, Vogel V, et al. Identification of a pop- ulation of blood circulating tumor cells from breast cancer patients that initiates metastasis in a xeno- graft assay. Nat Biotechnol. 2013; 31(6):539–44. doi: 10.1038/nbt.2576 PMID: 23609047

145. Kolostova K, Zhang Y, Hoffman RM, Bobek V. In vitro culture and characterization of human lung can- cer circulating tumor cells isolated by size exclusion from an orthotopic nude-mouse model expressing fluorescent protein. J Fluoresc. 2014; 24(5):1531–6. doi: 10.1007/s10895-014-1439-3 PMID: 25141982

146. Cayrefourcq L, Mazard T, Joosse S, Solassol J, Ramos J, Assenat E, et al. Establishment and charac- terization of a cell line from human circulating colon cancer cells. Cancer Res. 2015; 75(5):892–901. doi: 10.1158/0008-5472.CAN-14-2613 PMID: 25592149

147. Zhang L, Ridgway LD, Wetzel MD, Ngo J, Yin W, Kumar D, et al. The identification and characteriza- tion of breast cancer CTCs competent for brain metastasis. Sci Transl Med. 2013; 5(180):180ra48. doi: 10.1126/scitranslmed.3005109 PMID: 23576814

148. Klein CA, Blankenstein TJ, Schmidt-Kittler O, Petronio M, Polzer B, Stoecklein NH, et al. Genetic het- erogeneity of single disseminated tumour cells in minimal residual cancer. Lancet. 2002; 360 (9334):683–9. doi: 10.1016/S0140-6736(02)09838-0 PMID: 12241875

149. Navin N, Kendall J, Troge J, Andrews P, Rodgers L, McIndoo J, et al. Tumour evolution inferred by sin- gle-cell sequencing. Nature. 2011; 472(7341):90–4. doi: 10.1038/nature09807 PMID: 21399628

150. Swennenhuis JF, Reumers J, Thys K, Aerssens J, Terstappen LW. Efficiency of whole genome ampli- fication of single circulating tumor cells enriched by CellSearch and sorted by FACS. Genome Med. 2013; 5(11):106. doi: 10.1186/gm510 PMID: 24286536

151. Ni X, Zhuo M, Su Z, Duan J, Gao Y, Wang Z, et al. Reproducible copy number variation patterns among single circulating tumor cells of lung cancer patients. Proc Natl Acad Sci U S A. 2013; 110 (52):21083–8. doi: 10.1073/pnas.1320659110 PMID: 24324171

152. De Luca F, Rotunno G, Salvianti F, Galardi F, Pestrin M, Gabellini S, et al. Mutational analysis of single circulating tumor cells by next generation sequencing in metastatic breast cancer. Oncotarget. 2016.

153. Neumann MH, Schneck H, Decker Y, Schomer S, Franken A, Endris V, et al. Isolation and characteri- zation of circulating tumor cells using a novel workflow combining the CellSearch(R) system and the CellCelector. Biotechnol Prog. 2016.

154. Lohr JG, Adalsteinsson VA, Cibulskis K, Choudhury AD, Rosenberg M, Cruz-Gordillo P, et al. Whole- exome sequencing of circulating tumor cells provides a window into metastatic prostate cancer. Nat Biotechnol. 2014; 32(5):479–84. doi: 10.1038/nbt.2892 PMID: 24752078

155. Dago AE, Stepansky A, Carlsson A, Luttgen M, Kendall J, Baslan T, et al. Rapid phenotypic and geno- mic change in response to therapeutic pressure in prostate cancer inferred by high content analysis of single circulating tumor cells. PLoS One. 2014; 9(8):e101777. doi: 10.1371/journal.pone.0101777 PMID: 25084170

Discussion

Single-cell analysis has revolutionized modern biology. The study of life's most basic elements promise to improve diganostics and therapies and provide insights into some of the most fundamental processes. Studies are showing that the diversity of individual cell types are much greater than what we could imagine (Perkel, 2017; Wagner and Klein, 2017; 2017). However, if more and more researches are directed to single-cell analysis in so many differet and diverse fields of cell biology, including developmental biology, immunology and oncology, among others, fewer studies have faced the double challenge of exploring circulating rare cells (CRC) at single-cell level. My Ph.D. thesis work has been focused on the study of single rare cells extracted from blood (and other biological fluids) using a technology previously developed in my team, called the ISET® technology. This particular method has been developed to isolate from blood circulating tumor cells without using antibodies, after the demonstration had been obtained that specific antigens expressed only on tumor cells and not expressed at all on blood cells do not exist. Thus, ISET® avoids the use of antibodies and still isolates from blood, practically without loss, the very rare non-hematological cells, based on their size and following the observation that blood cells are the smallest cells in the body. Since ISET® does not use antibodies and since all the rare non-hematological cells are larger than the majority of leukocytes, ISET® potentially isolates nearly all types of circulating rare cells (CRC) such as stem cells derived from the bone marrow (Fadini *et al.*, 2017) or other stem cell niches (Heise *et al.*, 2016), endothelial cells which are essential components of the human vasculature (Medina *et al.*, 2017), but also cancer cells in patients bearing invasive malignant neoplasms (Paterlini-Bréchot, 2014) as well as cells of fetal and placental origins in pregnant mothers (Oudejans *et al.*, 2003). The method appears as a plateform which offers the opportunity to capture those rare cells through the minimally invasive procedure of venipuncture, and analyze them in order to achieve their accurate identification and characterization.

During the course of my doctoral research, as part of a collaborative effort between private and public research entities, I have focused on the development and validation of innovative methodologies for the genetic analysis of ISET®-enriched CRC, both trophoblastic cells in the context of non-invasive prenatal diagnosis (NIPD), and circulating cancer cells in the context of predictive oncology. My work has been focused on developing new tools and strategies to explore the genome of CRC as a means to improve diagnostic approaches in the fileds of non-invasive predictive oncology and non-invasive prenatal diagnosis.

1. Single-cell genetic analysis for prenatal diagnosis

1.1. Reliable capture and identification of fetal trophoblastic cells

In order to produce reliable NIPD results based on analysis of ISET®-enriched trophoblastic cells, molecular analysis must be applied to single cells because the fetal nature of each cell analyzed needs to be accurately confirmed before further analysis is performed. Previous work from my collaborators has shown that the amplification of short tandem repeat (STR) markers by PCR following laser capture microdissection (LCM) of putative fetal cells recovered by ISET® filtration enables a reliable identification of fetal cells suitable for use in NIPD of recessive genetic disorders (Mouawia *et al.*, 2012). Based on findings of the latter study, the detection of immunological markers such as cytokeratin staining (KL1 antibody) was not considered for this subsequent proof of concept study aiming at reliable NIPD based on analysis of cervical trophoblasts. More precisely, Mouawia et al. determined that selecting cells for microdissection on the basis of a cell size equal to or greater than 15 microns (for fixed cells) correlated to the specific selection of cytokeratin-positive cells, approximately half of which were of genetically confirmed fetal origin (Mouawia *et al.*, 2012).

Importantly, at the time this study was performed, no unique cell-surface marker had been demonstrated to be specific to fetal trophoblasts in the available literature. Since then, several reports following our own provided interesting results concerning the identification of potentially specific molecules in various populations of human trophoblasts.

For example, Weber and colleagues characterized first trimester placentae regarding expression of the trophoblastic stem cell marker CDX2 (caudal type homeobox 2 transcription factor, specific of trophectoderm differentiation) and determined that villous SynT were strongly positive for nuclear staining of CDX2 during the first trimester (Weber *et al.*, 2016). Interestingly, placentae from preeclamptic pregnancies exhibited even stronger nuclear staining of CDX2 in villous structures. However, the scarce expression of CDX2 in extravillous trophoblasts (EVT) and its complete disappearance in placentae from pregnancies suffering further complications of both preeclampsia and intrauterine growth retardation (IUGR) preclude the use of this marker for NIPD purposes

(Weber *et al.*, 2016).

Likewise, identification of the placentation-restricted and -necessary expression of Syncytins (human endogenous retrovirus) by trophectodermal cells and their progenies, especially by SynT, during the first trimester of pregnancy provides interesting conceptual opportunities to specifically identify trophoblastic cells during the first 12 WG (Soygur and Moore, 2016), but the specificity and sensitivity of potential future methods targeting Syncytins for trophoblast recovery still awaits investigation.

Around the same time, Schlutter et al. performed immunomagnetic selection of putative CFTC from the blood of pregnant mothers using combined antibodies targeting CD105 (also called endoglin, a transmembrane protein and receptor component of TGFβ signaling) and CD141 (also known as thrombomodulin, a thrombin-binding membranous receptor) to determine an increased level of CFTC in 30 mL blood samples from pregnant mothers following a short period of increased physical activity (Schlütter *et al.*, 2016). However, putative CFTC recovered by this method were not genetically validated as fetal cells.

Meanwhile, Breman and colleagues provided a first evidence of the feasibility of combining array CGH and high throughput whole genome sequencing (WGS) analyses of single CFTC to simultaneously detect chromosomal and subchromosomal copy-number abnormalities (CNA) for NIPT purposes (Breman *et al.*, 2016). In this study, putative CFTC were enriched from 30 mL of maternal blood at 10-16 WG by density gradient separation with further immune-magnetic depletion of CD45- and/or CD36-presenting leukocytes. Individual selection of putative fetal cells was then carried out based on both negativity of CD45 and positivity of cytokeratin immunomolecular stainings following cytological fixation and layering on glass slides for microscopic examination. Multiplex targeted analysis of 11 polymorphic STR loci allowed Breman *et al.* to verify the fetal nature of an average of 0.36 CFTC per milliliter of maternal blood, using the above-mentionned selection method. This proof-of-concept study provides important preliminary data regarding the feasibility of reliably identifying smaller subchromosomal CNA and possibly detecting placental mosaicism through a cell-based NIPT approach combining array CGH and NGS analyses. Such validation opens important investigative avenues, especially considering the poor reliability of current cffDNA-targeted methods

in detecting subchromosomal aberrations (Zhao *et al.*, 2015) together with their documented inability to diagnose cases of confined placental mosaicism (Pan *et al.*, 2014). However, the relatively low CFTC recovery rate reported by Breman *et al.* from maternal blood at 10-16 WG constitutes a non-negligeable limitation to this study as far as diagnosis of confined placental mosaicism is concerned. In fact, these same authors determined that, depending on the extent of mosaic confinement in placental tissues, accurate diagnosis of mosaicism would likely require consecutive analysis of at least ten and up to 20 single CFTC per case (Breman *et al.*, 2016).

Previous investigations from my team allowed estimating the average rate of ISET®-detectable CFTC in maternal blood at 4-12 WG by performing weekly blood draws on 14 mothers that became pregnant through *in vitro* fecundation (IVF) (Mouawia *et al.*, 2012). To that aim, CFTC from each weakly 10 mL blood sample were enriched by ISET®, morphologically selected for LCM and genetically analyzed to reliably establish their fetal nature. Whereas only half of the mothers tested at 4 WG presented with very low levels of CFTC (0.3 per mL), all 14 mothers harbored consistently detectable CFTC in all blood samples obtained weekly from 5 to 12 WG. More precisely, average CFTC levels exhibited a steady increase from 1.19 CFTC per mL at 5 WG to 2.0 CFTC per mL at 11 WG with an observed (although not statistically significant) decrease to 1.66 CFTC per mL at 12 WG (Mouawia *et al.*, 2012).

1.2. Completely safe recovery of trophoblastic cells from the cervix: why and how?

Although ISET® methodology enables sufficient CFTC recovery for targeted NIPD of single-gene disorders and chromosomal aneuploidies, even when considering theoretical cases of placental mosaicism confined to as little as 5% of the placental tissue (either from a single 10 mL blood sample in pregnancies allowing for the recovery of 2 CFTC per mL or from multiple consecutive blood samples in cases where CFTC recovery rates fall to 1 fetal cell per mL of blood and lower), recovering trophoblastic cells solely from the maternal blood circulation has potential pitfalls. For instance, singleton pregnancies occurring closely after spontaneous miscarriage of a previous conceptus could

result in substancial technical difficulties and potentially biased results of CFTC-based NIPT due to the persistence in maternal circulation of trophoblastic cells originated from the previous conceptus after spontaneous termination of pregnancy. In fact, specific types of CFTC (expressing CD34) have been described to persist in maternal circulation for years and up to several decades after child birth or premature termination of pregnancy (Bianchi *et al.*, 1996). By contrast, shedding of trophoblasts down from the uterine cavity through the endocervical canal is thought to coincide specifically with first-trimester placentation and presence of trophoblastic cells in the cervix has been described as an early and transient event lasting on average 2 months and remaining strictly confined to the 5-15 WG timeframe (Adinolfi and Sherlock, 2001; Sifakis *et al.*, 2010). In such context, combining single-cell analyses of cervical trophoblasts with that of CFTC for NIPD purposes offers an opportunity to increase fetal cell recovery while providing a unique perspective on molecular features of multiple distinct populations of fetal cells.

In an attempt to diversify and maximize the recovery of trophoblastic cells through a completely safe method, we sought to introduce the collection of cervical trophoblasts by a minimally intrusive method largely inspired by the Papanicolaou (PAP) test (McCRACKEN, 1948; Reed and Chesley, 1948). Following transfer to ISET® filters, 2 mL from each 10 mL sample of fixative buffer containing the sampling cytobrush enabled LCM-mediated recovery of at least 2 and up to 12 genetically diagnosed trophoblasts in all 21 mothers tested between 8 and 12 WG. This completely safe sampling method thereby allowed identifying at least 1.0 trophoblastic cell per mL and up to 6.0 cytotrophoblasts per mL of sample, thus extending the maximum recovery of 20 CFTC from 10 mL blood samples to a maximum of 60 cytotrophoblasts recovered from our 10 mL cervical samples. Furthermore, applying genetic analysis to the cervical trophoblasts recovered via this method enabled conducting accurate NIPD of CF or SMA in 6 mothers at risk of carrying a fetus affected by either one of those two recessive genetic disorders.

Trophoblast collection from the cervix had been previously investigated by other groups (Imudia *et al.*, 2009; Bolnick *et al.*, 2014), as stated in our own publication, but differed from the method presented here since our protocol did not require cytobrush incertion into the endocervical canal but

rather instructed rotation of the cytobrush at the external os without full incertion into the cervix, contrary to the sampling methods previously reported.

Subsequently, following publication of our study, Jain *et al.* also reported trophoblastic cell isolation from the endocervical canal, using the collection method previously introduced by Imudia and colleagues (Imudia *et al.*, 2009), followed by immune-magnetic selection of HLA-G-presenting cells and nuclear isolation to apply targeted multiplex high throughput sequencing to the isolated DNA for simultaneous NIPT of multiple genetic disorders (Jain *et al.*, 2016). Although employing an interesting molecular approach to enable the simultaneous interrogation of 94 SNV and 59 STR loci throughout the human genome, this study could not analyze pure fetal DNA since magnetic depletion and nuclear isolation of HLA-G-presenting cells yielded an average fetal DNA fraction of 91.5 % across the 20 consecutive endocervical specimens (Jain *et al.*, 2016).

In contrast, investigations from my team remained focused on single-cell analysis of trophoblasts recovered from our 21 cervical samples, thereby allowing to address molecular characterization to completely pure fetal DNA by first interrogating up to 10 polymorphic STR loci scattered across 4 chromosomes for genetic validation of fetoplacental origin of each individual cell collected (Pfeifer *et al.*, 2016). Moreover, our collection method proved successful in enhancing trophoblast recovery rates when compared to CFTC extraction from maternal blood while still enabling accurate NIPD of single-gene disorders and remaining minimally intrusive to insure fetal health safety.

1.3. Perspectives and potential limitations of our study

Our proof of concept study did provide encouraging preliminary results on collection of cervical trophoblasts for use in NIPD of recessive genetic disorders (Pfeifer *et al.*, 2016). However, further validation of this method is warranted to confirm those results on larger casistics of pregnant women. Additionally, like all other NIPD/NIPT strategies that are currently under scientific investigation as well as the only non-invasive method that has already reached clinical implementation (i.e. based on cffDNA analysis), our method could encounter substantial difficulties in providing an accurate

diagnosis of fetal disorders in some cases of placental mosaicism with acute unbalanced confinement (Pan *et al.*, 2014) as well as for twin pregnancies in cases presenting with an early vanishing twin (Mantzaris and Cram, 2015). Indeed, because trophoblasts have been shown to constitute the primary source of cffDNA release during pregnancy (Faas *et al.*, 2012), placental mosaicism could constitute a non-negligeable source of misdiagnosis for all NIPD/NIPT methods developed up to now, depending on the extent of the mosaicism and the relative differences between the cellular genotypes contributing to placentation. Moreover, the rarely documented occurrence of a vanishing twin in dizygotic and dichorionic pregnancies has been recently evidenced as a potential source of misdiagnosis caused by excessive shedding of fetal cells and placental DNA from the resorbing conceptus (Mantzaris and Cram, 2015).

Despite this rather global limitation affecting NIPD/NIPT in general, our study fulfilled our initial expectations by validating the concept of retrieving cervical trophoblasts from 8-12 WG pregnancies and using ISET® without drawing blood for NIPD of recessive genetic disorders by a completely safe approach. Combining this strategy to that of CFTC collection from maternal blood samples would likely be very advantageous for several reasons, such as for reaching and maintaining maximum accuracy of NIPD results in cases of genetically complex pregnancies and/or cases with artefactual bias influencing molecular data.

For instance, multiple blood and cervical samplings distributed across the second half of the first trimester of pregnancy could potentially provide sufficient data to identify and distinguish cases of early vanishing twins from mosaic pregnancies with extremely unbalanced confinement and from cases with persistence of multiple fetal genomes from previous successful conceptions and/or aborted pregnancies. Such accurate distinctions between genetically complex cases currently remain out of reach for cffDNA-targeted NIPT (Pan *et al.*, 2014; Mantzaris and Cram, 2015).

Furthermore, despite continuous technical progress, cffDNA-based NIPT methods still struggle with detection of maternally inherited disorders, subchromosomal CNA smaller than 9 Mb (Zhao *et al.*, 2015) and *de novo* mutations (de Ligt *et al.*, 2013) due to the large portion of maternal cfDNA in blood. High throughput sequencing applied to single trophoblastic cells recovered non-invasively

appears as best suited to overcome those limitations if false positive results arising from single-cell whole genome amplification biases are distinguished from actual *de novo* mutations by comparing data from several trophoblasts from each pregnancy after single-cell analysis (Beaudet, 2016).

Consequently, maximizing trophoblastic cell recovery at early gestational ages by completely safe sampling methods and addressing high throuput molecular analysis to multiple fetal cells at single-cell level both constitute important experimental endevours in the field of prenatal diagnosis. In 2016, whole genome sequencing of individual CFTC was successfully conducted by Breman and colleagues, albeit limited to a low number of cells per case (1-15 CFTC recovered from 30 mL blood samples) due to the rarity of CFTC in blood and the relative difficulty to efficiently isolate them without loss (Breman *et al.*, 2016).

As previously reported by my team (Mouawia *et al.*, 2012), ISET® enables high CFTC recovery rates, providing up to 20 genetically diagnosed CFTC per 10 mL blood samples and enabling accurate NIPD of recessive single-gene disorders, as demonstrated for cystic fibrosis and spinal muscular atrophy. In 2016, we reported further investigation of cervical trophoblast recovery through a minimally intrusive sampling strategy inspired by Papanicolaou (Pfeifer *et al.*, 2016). Our results demonstrate that ISET® enables improved recovery rates of trophoblastic cells from the cervix compared with that of CFTC isolation from blood, providing up to 60 genetically diagnosed fetal cells per cervical sample. Based on this proof of concept, future invrestigations of my team will focus on addressing the technical challenges that remain inherent to whole genome or whole exome sequencing application to fixed and microdissected single cells, as evidenced by other scientists in the field of NIPD/NIPT (Breman *et al.*, 2016; Kølvraa *et al.*, 2016). Furthermore, in addition to single-gene disorders, detecting chromosomal aneuploidy and subchromosomal CNA by high throughput sequencing of ISET®-enriched single cells is currently under investigation in our lab and will further be pursued by my team in the coming years.

In the long run, clinical applicability of an ISET®-based NIPD test combining cervical and circulating trophoblast analyses at single-cell level would require additional considerations such as reducing costs and hands-on time to a minimal, possibly by implementing automated or semi-automated

analytical strategies that we are also currently developing. And finally, large-scale clinical validation of our methodological developments will be a strict prior requirement for the commercial introduction of this potential fucture ISET®-based NIPD test.

2. Single-cell genetic analysis for predictive oncology

2.1. The present work

As shown in previous sections, results obtained by my co-authors and I on a cohort of 30 ccRCC patients allowed us to identify VHL mutations in 83% of tumor samples, which correlates to some of the previous findings reported by other researchers in the literature (Sato *et al.*, 2013). It should be noted that a great variability in reported incidences of VHL mutations, up to 83% of patients (Nickerson *et al.*, 2008), can be found in the literature (Shuin *et al.*, 1994; Kanno *et al.*, 1997; Béroud *et al.*, 1998; Gallou *et al.*, 1999, 2001; Kondo *et al.*, 2002a; Schraml *et al.*, 2002; Banks *et al.*, 2006; Cheng *et al.*, 2009b; Cowey and Rathmell, 2009; Varela *et al.*, 2011; Cancer Genome Atlas Research Network, 2013; Sato *et al.*, 2013; Razafinjatovo *et al.*, 2016; Kim *et al.*, 2017; Li *et al.*, 2017b; Razafinjatovo *et al.*, 2017; Tennenbaum *et al.*, 2017), possibly owing to differential geographic provenances along with the great variability in sizes of the respective cohorts studied and the inherent intratumor heterogeneity (ITH) of ccRCC tumors.

In our own study, VHL mutational status found in all CCC identified by cytopathology correlated exactly with corresponding VHL status in primary tumors. This is consistent with previous studies having demonstrated the diagnostic character of cytopathology based on Hofman's classification of morphological criteria, which enables reliable identification of cancer cells in the blood of cancer patients while healthy individuals do not present CRC with malignant morphology (Hofman *et al.*, 2011c, 2012, 2016). However, cytopathological criteria are not always clear cut and when the doubt persists concerning the cancerous nature of circulating cells they are classified as circulating rare cells with uncertain malignant features (CRC-UMF). Those cells present with an atypical morphology, displaying at least one and up to three of Hofman's five morphological criteria (anisonucleosis (ratio >0.5), nuclei larger than three times the calibrated pore size (i.e., >24 µm), irregular nuclei, presence of tridimensional sheets, and a high nuclear/cytoplasmic ratio), whereas malignant CRC (CCC) are defined by the presence of at least four of those criteria. Therefore, CRC-UMF do not fit the stringent requirements for cytopathological diagnosis of cancer cells. Yet, in our study of ccRCC

patients, 104 CRC-UMF exhibited concordant VHL mutational profiles compared to those found in the corresponding tumor samples. It is important to note that if identical VHL mutational profiles found in single CRC and paired tumor samples can be considered a diagnostic marker of the cancerous nature of those CRC then combining molecular and morphological analyses would provide a more sensitive diagnosis of CCC then cytopathology alone.

The aim of this study being the comparison of VHL mutational data with morphological assessment of each circulating individual cell analyzed, the observed correlations would validate a 100% specificity of cytopathological diagnosis while suggesting that molecular data could potentially complement cytopathology by enhancing its clinical sensitivity. In order to conclude on those results, the diagnostic character of the presence of identical VHL mutations in CRC and corresponding primary tumors must be assessed based on previous literature from other goups.

2.2. Classification and pathological features of renal cell carcinomas (RCC)

Renal carcinomas do not constitute a single cancer entity but rather encompass a broad range of phenotypically and genetically distinct kidney neoplasms among which the three most common subtypes are clear cell (ccRCC) accounting for an estimated 75% of cases, papillary (pRCC) accounting for approximately 10% and chromophobe carcinomas (chRCC), found in roughly 5% of cases (Lopez-Beltran *et al.*, 2006). There are however several other subtypes, such as the rarer collecting duct RCC, and the continually evolving classification of renal tumors from the world health organization (WHO) was recently reformed by the 2016 update to add 5 new entities to the 10 previously established subtypes (Kuthi *et al.*, 2017).

RCC tumors of the common (clear cell) type often present with areas of necrosis and are associated with shorter survival times when exhibiting intravascular tumor embolization extending to the inferior vena cava (Park and Eisen, 2007). The complexity of the current classification of renal tumors, now also acknowledging ccRCC development in end stage renal diseases, accounts for ccRCC cases without morphological evidence of clear cell content as well as for renal tumors displaying a clear

cell morphology while not qualifying for ccRCC subtype classification, including the pathologically ambiguous clear cell papillary RCC (López, 2013). Despite increasingly precise and complex subtype classification guidelines, approximately 4% of RCC remain unclassified and those uRCC tumors are currently emerging as particularly aggressive types of renal malignancies (Hsieh *et al.*, 2017). The biological behavior of renal tumors remains largely unpredictable by histology alone. In this particular context, there seems to be a need for molecular markers to complement our current methods for RCC subtyping, grading and staging, which up to now have relied exclusively on histopathological features (Moch, 2013). In fact, accumulating evidence reported throughout the last decades suggests that specific genetic alterations could further stratify our current classification of RCC tumors.

2.3. Some molecular features of ccRCC

Studies focusing on familial cancer syndromes to identify genetic alterations responsible, at least in part, for the multiple malignant manifestations of each disease have greatly contributed to broaden our understanding of the molecular components of RCC. For example, while mutations of the MET (also called c-met) proto-oncogene located on the long arm of chromosome seven (7q31) and coding for a receptor to the hepatocyte growth factor (HGF) can be found in both sporadic and familial type 1 pRCC (Lubensky *et al.*, 1999), the conventional RCC subtype (ccRCC) can also arise sporadically or as part of the hereditary Von Hippel-Lindau (VHL) disease. Identification of the VHL gene by Latif and colleagues in 1993 marked an essential cornerstone in our ever evolving understanding of ccRCC pathogenesis (Latif *et al.*, 1993). Indeed, subsequent studies identified VHL mutations in 35-85% of sporadic ccRCC (Schraml *et al.*, 2002; Sato *et al.*, 2013) and deletion on one allele of the short arm of chromosome three harboring the VHL locus (3p25) has been described to occur at exceptionally high rates in large ccRCC cohorts, characterizing up to 94% of cases (Sato *et al.*, 2013). Considering that pVHL has been shown to restrain genomic instability during DNA replication (Roe *et al.*, 2006), it is not surprising to learn that additional genetic alterations accumulate in ccRCC cells lacking

functional pVHL expression.

Of particular interest are some of the recent high throughput molecular studies using phylogenetic clustering algorithms to sort molecular data obtained on ccRCC tumor samples in order to produce an estimated timeline of the occurrence of each specific oncogenic aberration. For instance, Gerstung and colleagues employed deep sequencing of single nucleotides variants (SNV) to infer the evolutionary pattern of 4 ccRCC tumors (Gerstung *et al.*, 2012). This study used deep sequencing analysis of SNV to investigate mutations of the VHL, TP53 (coding for p53), PTEN (coding for the phosphatase and tensin homolog protein) and CDKN1B (coding for the cyclin-dependent kinase inhibitor protein 1B) tumor suppressor genes in four ccRCC patients, three of which displayed biallelic inactivation of the VHL gene. For a single patient, allele frequencies recorded by deep sequencing of those tumor suppressor genes in a paired metastatic site together with two distinct sites of the primary tumor further allowed the authors to propose a model of tumor evolution in which VHL alterations were placed as the earliest events in tumorigenesis, representing the initial "trunk" mutations on the evolutionary tree of the tumor (Gerstung *et al.*, 2012).

This was paralleled by another study from a different group who used multiregion sampling to uncover intratumor heterogeneity (ITH) at both genetic and transcriptomic levels in 4 metastatic ccRCC patients and determined that VHL truncating mutations and loss of 3p on the concomitant allele were the only two ubiquitous events found to be identical in all 30 tumor/metastatic regions sampled from all four patients (Gerlinger *et al.*, 2012). Additionally, the same authors later determined in a cohort of 10 ccRCC that up to 75% of all driver aberrations found in each patient were subclonal and yet VHL alterations together with LOH at 3p were again found to represent the only ubiquitous events across the multiple tumor sites sampled (Gerlinger *et al.*, 2014).

2.4. VHL loss-driven tumorigenesis

For the purpose of the present study, understanding VHL loss-driven tumorigenesis appears essential to correctly interpret the genetic data obtained on single CRC isolated by ISET® and in particular to

understand if the mutations may be "diagnostic" of their tumor nature.

pVHL is a multipurpose protein with many important regulatory functions, the most studied of which involves regulation of hypoxia inducible factors (HIF). In the presence of sufficient oxygen levels (21%) and with functional pVHL, the VCB complex forms between pVHL, Cullin 2 (Cul2) and both elongins B and C (EloB & EloC) to perform ubiquitination of HIF-α subunits, ultimately leading to their proteasomal degradation (Stebbins *et al.*, 1999). HIF-1α and HIF-2α are potent transcription factors which are stabilized and accumulate during both developmental and pathological hypoxia, when oxygen levels are below 1% for HIF-1α and below 5% for HIF-2α, the latter accumulating slightly faster in prolonged periods of hypoxia (Keith *et al.*, 2011). Involvement of HIFs in the physiological responses to hypoxia and hypoglycemia, together with a role of HIF-2α in iron sensing, confer to ccRCC features of a metabolic disease (Linehan *et al.*, 2010). HIFs are potent transcription factors currently known to target over 800 genes (Gossage *et al.*, 2015) by binding promoter regions containing hypoxia response elements (HRE) (Lau *et al.*, 2007; Yu and Kodadek, 2007). However, despite presenting some overlapping functions, HIF-1α and HIF-2α also activate target genes that are specific to each one of those transcription factors (Brusselmans *et al.*, 2001; Maina *et al.*, 2005; Petrella *et al.*, 2005; Gordan *et al.*, 2008; Patel and Simon, 2008; Rankin and Giaccia, 2008). For a detailed depiction of HIF target genes, please refer to **Figure 10**.

It should however be noted that HIF-regulated expression of target genes is highly cell type-specific and that a portion of the mechanisms depicted in **Figure 10** have been described to occur specifically in pVHL-deficient ccRCC cell lines *in vitro* and not in any other cell type (Raval *et al.*, 2005).

Figure 10: *HIF-regulated genes during hypoxia or in absence of functional pVHL (see legend on the following page)*

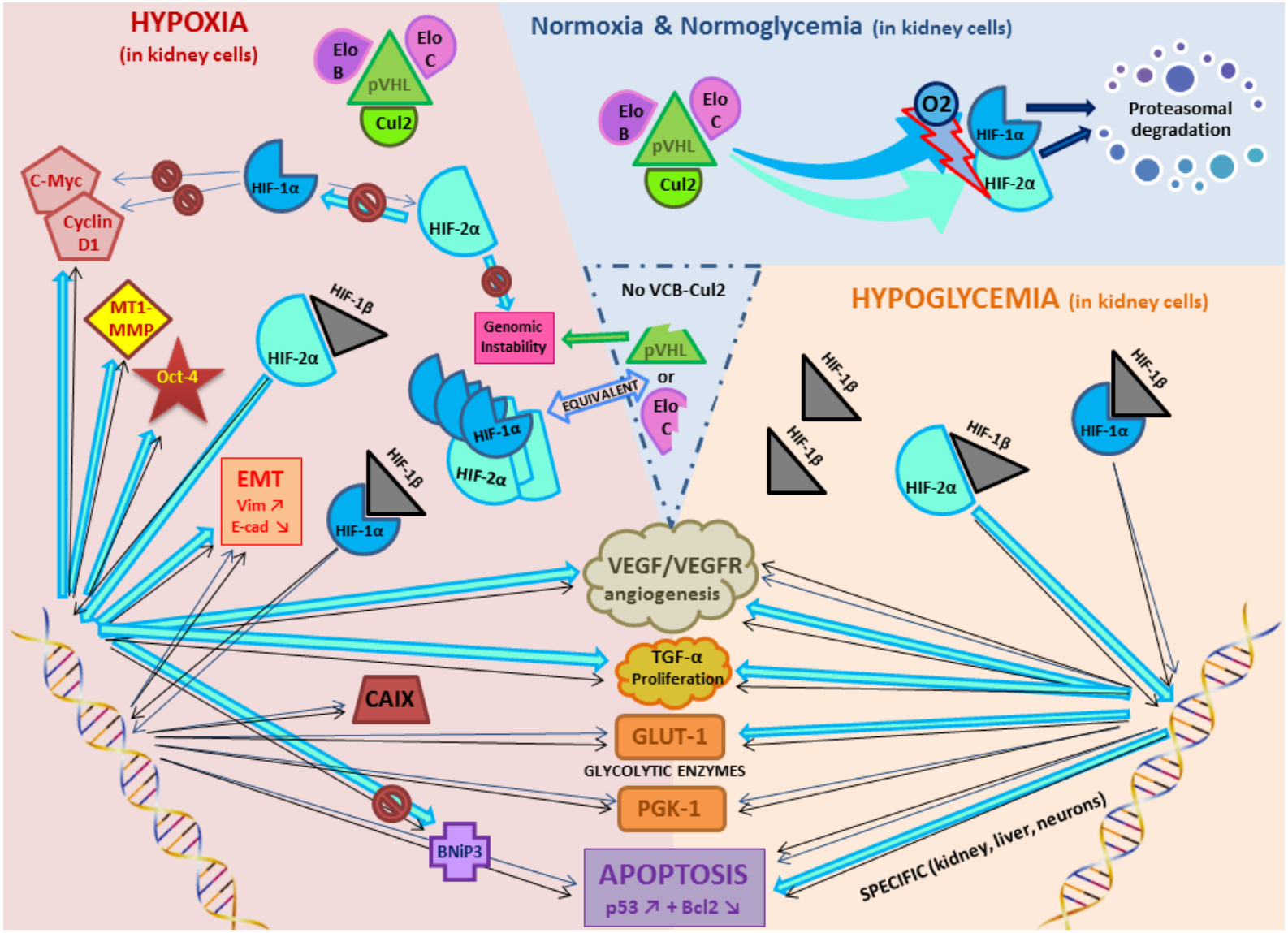

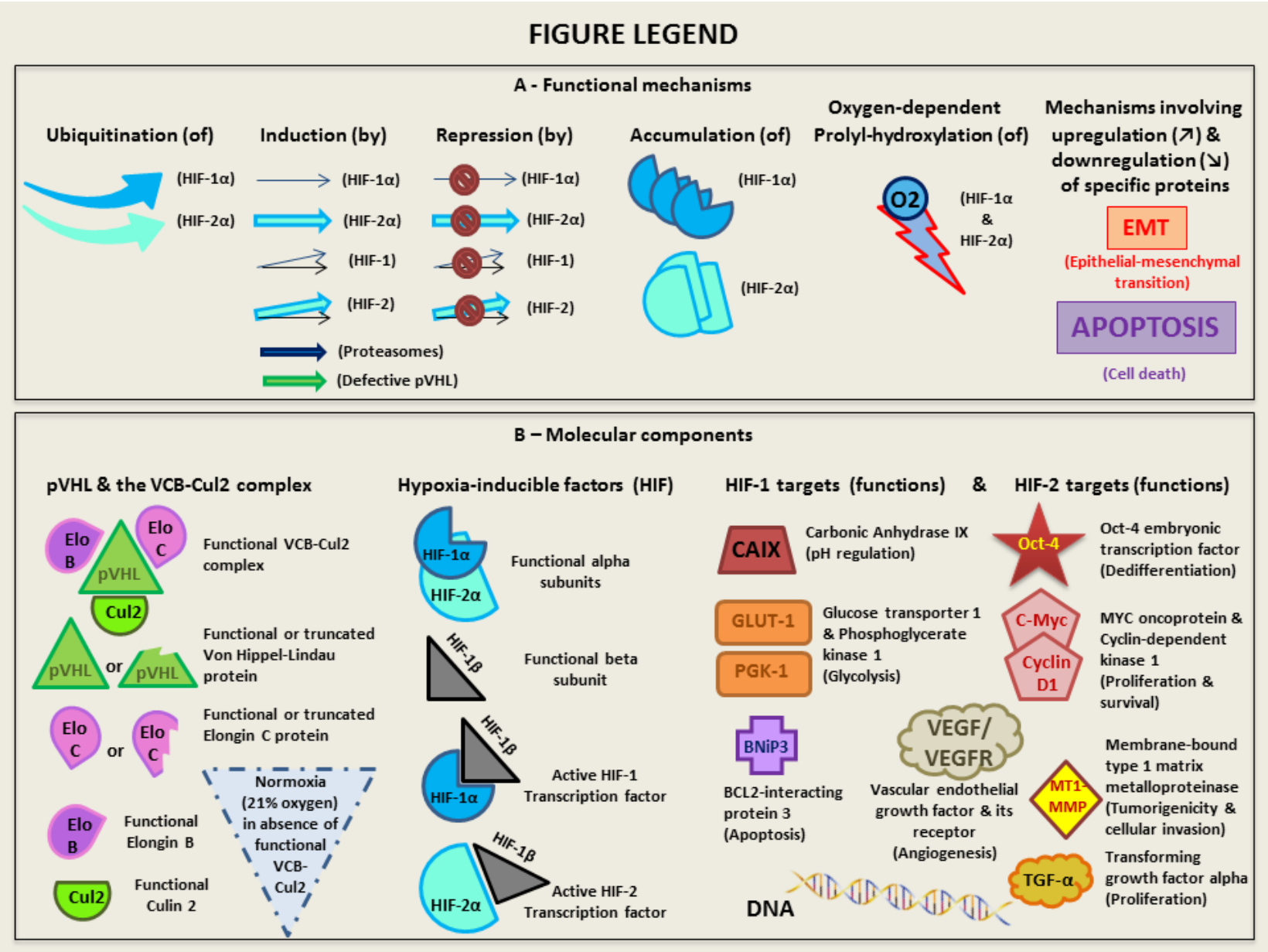
FIGURE LEGEND
A - Functional mechanisms
Ubiquitination (of)
(HIF-1α)
(HIF-2α)
Induction (by)
(HIF-1α)
(HIF-2α)
(HIF-1)
(HIF-2)
Repression (by)
(HIF-1α)
(HIF-2α)
(HIF-1)
(HIF-2)
(Proteasomes)
(Defective pVHL)
Accumulation (of)
(HIF-1α)
(HIF-2α)
Oxygen-dependent Prolyl-hydroxylation (of)
O2
(HIF-1α & HIF-2α)
Mechanisms involving upregulation (↗) & downregulation (↘) of specific proteins
EMT
(Epithelial-mesenchymal transition)
APOPTOSIS
(Cell death)
B – Molecular components
pVHL & the VCB-Cul2 complex
Elo B
Elo C
pVHL
Cul2
Functional VCB-Cul2 complex
pVHL
or
pVHL
Functional or truncated Von Hippel-Lindau protein
Elo C
or
Elo C
Functional or truncated Elongin C protein
Elo B
Functional Elongin B
Cul2
Functional Culin 2
Normoxia (21% oxygen) in absence of functional VCB-Cul2
Hypoxia-inducible factors (HIF)
HIF-1α
HIF-2α
Functional alpha subunits
HIF-1β
Functional beta subunit
HIF-1β
HIF-1α
Active HIF-1 Transcription factor
HIF-1β
HIF-2α
Active HIF-2 Transcription factor
HIF-1 targets (functions) & HIF-2 targets (functions)
CAIX
Carbonic Anhydrase IX (pH regulation)
GLUT-1
PGK-1
Glucose transporter 1 & Phosphoglycerate kinase 1 (Glycolysis)
BNiP3
BCL2-interacting protein 3 (Apoptosis)
VEGF/ VEGFR
Vascular endothelial growth factor & its receptor (Angiogenesis)
DNA
Oct-4
Oct-4 embryonic transcription factor (Dedifferentiation)
C-Myc
Cyclin D1
MYC oncoprotein & Cyclin-dependent kinase 1 (Proliferation & survival)
MT1-MMP
Membrane-bound type 1 matrix metalloproteinase (Tumorigenicity & cellular invasion)
TGF-α
Transforming growth factor alpha (Proliferation)

In addition to the previously mentioned regulation of HIF, pVHL also contributes to many other aspects of cellular biology independently of its hypoxia-related functions (Frew and Moch, 2015). Details regarding important pVHL functions are depicted in **Figure 11**. Since pVHL has more than 35 interacting protein partners but contains only three major interacting domains, some interactions are mutually exclusive while others can occur simultaneously (Leonardi *et al.*, 2009).

Figure 11: *pVHL functions in human kidney cells*

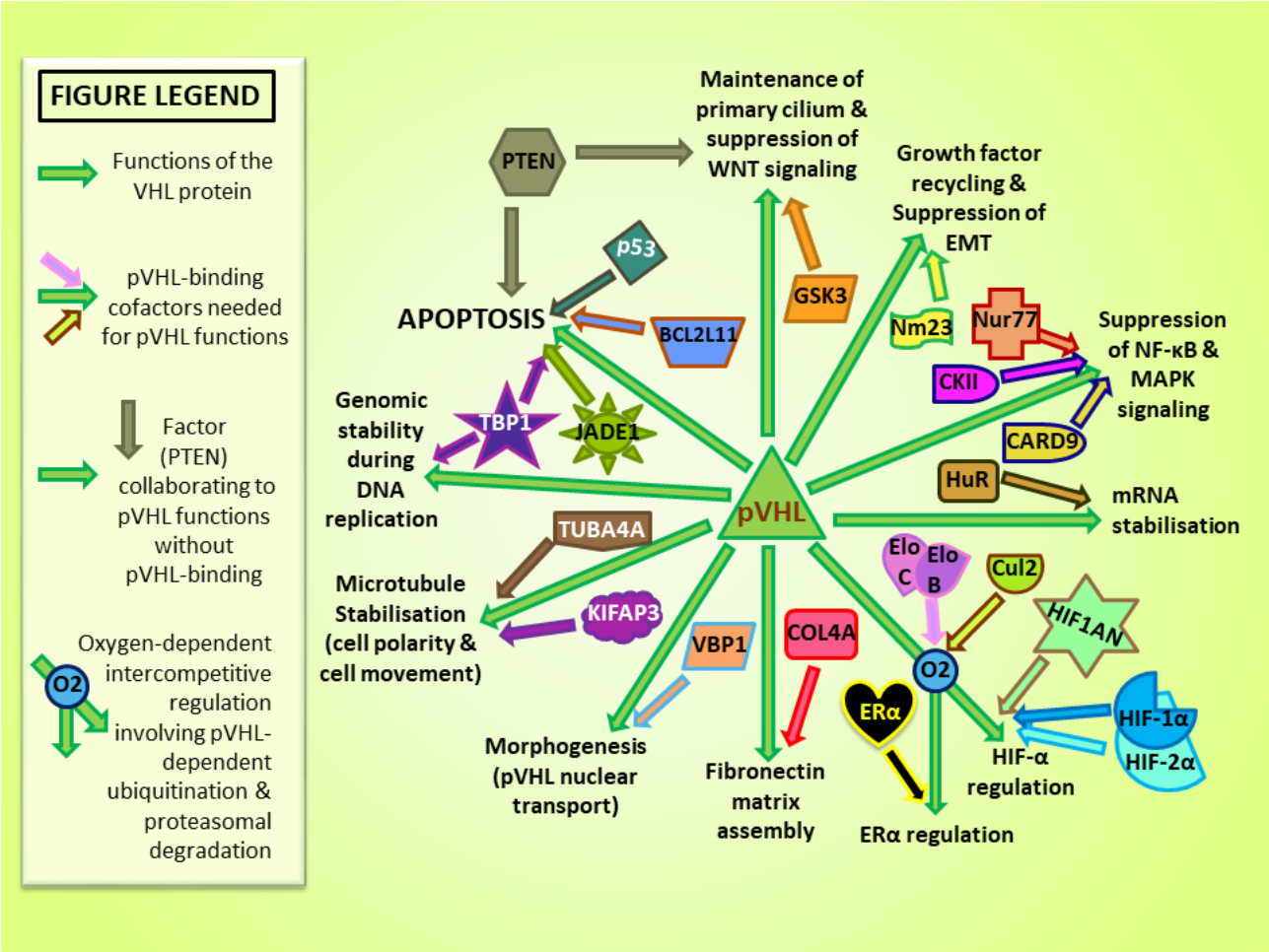

2.5. Is loss of functional pVHL expression sufficient for ccRCC tumorigenesis?

Complete loss of functional pVHL has been described to play a pivotal role in the tumorigenesis of ccRCC (Li *et al.*, 2017b). If mutational profiles of the VHL gene can be used as markers of ccRCC presence, and thus bear diagnostic significance, the sole presence of VHL biallelic inactivation should invariably correlate with the presence of ccRCC. However, this is not always the case.

On the one hand, efforts to obtain a representative animal model for the VHL disease have suffered some major limitations. The observation that double knockdown of the murine *Vhl* gene (formerly known as *Vhlh*) results in embryonic lethality prompted scientists to use conditional knockdown of *Vhl* in kidney cells in an attempt to recreate in adult mice the adverse effects of the VHL disease observed in human kidney cells. Despite application of several strategies, including the conditional knockdown of *Vhl* in specific kidney cell types, ccRCC growth was never observed following biallelic inactivation of *Vhl* in mice (Mack *et al.*, 2003; Rankin *et al.*, 2006; Pritchett *et al.*, 2015). *Vhl*-null mice did develop abnormal cystic lesions with severe concomitant renal fibrosis that were characterized by abnormal nuclear accumulation of HIF-1α (Mack *et al.*, 2003). Interstitial fibrosis observed in kidneys of *Vhl*-null mice was caused by an overall ninefold increase in collagen deposition and a sixfold increase in expression of the proliferative marker Ki67 was observed in disorganized tubular architectures of *Vhl*-null nephrons compared to normal mice controls (Pritchett *et al.*, 2015). In the latter study, the presence of hyperplastic epithelia lining cystic lesions along with a marked increase in infiltrating stromal cells (myofibroblasts) were noted and considered as indicators of a sustained inflammatory microenvironment. Together these experiments suggest that the biallelic inactivation of *Vhl* is not sufficient to elicit malignant tumor growth in mice kidneys but could prove instrumental in preparing the organ for ccRCC tumorigenesis, implying that additional genetic alterations may be required for ccRCC tumorigenesis.

On the other hand, studies analyzing resected kidneys from human patients affected by the hereditary VHL disease identified a multitude of isolated kidney cells, small multicellular clusters, cystic lesions of both benign and malignant nature, as well as solid ccRCC that all exhibit loss of functional pVHL (Lubensky *et al.*, 1996; Mandriota *et al.*, 2002; Montani *et al.*, 2010). Mandriota and colleagues performed immune-histochemical (IHC) labeling of thin consecutive kidney sections to reveal the presence of pVHL, HIF-1α and HIF-2α in distinct lesions of VHL-diseased kidneys. These authors reported that, in contrast to the observed patterns of VHL loss, patterns of HIF-2α expression were strikingly specific to malignant lesions found in kidneys of patients affected by the hereditary VHL disease (Mandriota *et al.*, 2002). More precisely, HIF-1α-positive staining was faintly observed

in benign lesions without concomitant pVHL expression and was noted to gradually gain stronger positivity in atypical and then malignant cystic lesions respectively. Conversely HIF-2α-positive staining was never present in benign lesions but sometimes faintly observed in hyperplastic cells lining atypical cysts whereas all microscopic foci of ccRCC in VHL-diseased kidneys from all ten patients studied were strongly positive for HIF-2α (Mandriota *et al.*, 2002).

Furthermore, analysis of mRNA expression in paired tumor samples and adjacent normal renal tissue from 17 whole nephrectomy specimens of sporadic ccRCC revealed that all 17 tumors presented significantly higher HIF-2α mRNA compared to their normal counterpart, corresponding on average to a 5.2 fold induction, which correlated well with HIF-2α protein levels measured (Turner *et al.*, 2002). Concerning HIF-1α mRNA and protein levels, only 12 tumors showed slight induction when compared to normal tissues but the difference was not statistically significant. Interestingly, among cases harboring a mutated VHL gene, 94% of ccRCC tumors showed strong induction of HIF-2α with regards to paired normal kidneys while none of the rarer RCC subtypes tested in humans (papillary, chromophobe and collecting duct RCC) showed induction of HIF-2α (Turner *et al.*, 2002).

So it seams that HIF-2α overexpression and protein accumulation are a common denominator among human ccRCC, whether sporadic or VHL disease-associated. Looking back at rodent models, I find very interesting that both carcinogen-induced RCC in mice and the hereditary form of RCC found in the Eker rat strain are also characterized by extensive vascularization and upregulation of HIF-2α (Liu *et al.*, 2003). Yet in rodents the tumor suppressor gene involved in the large majority of both hereditary and carcinogen-induced forms of sporadic RCC is not VHL but TSC-2 (Tuberous Sclerosis gene 2) which encodes the tuberin tumor suppressor protein. Loss of tuberin function in rodents predisposes to a form of tubulo-papillary RCC with prominent cystic features that accounts for the majority of RCC cases in these animals and they only very rarely develop tumors of the clear cell subtype.These cross-species observations suggest that RCC is rather a disease of whole pathway deregulation that appears to converge towards HIF-2α rather than HIF-1α activationi in both humans and rodents regardless of the specific tumor suppressor gene that predisposes to RCC upon biallelic inactivation..

Other groups have reported that expression of a normoxically stable HIF-1α (unrecognized by wild type pVHL in presence of oxygen) in pVHL-rescued ccRCC xenografts inhibits tumor growth (Maranchie and Zhan, 2005) while expression of a normoxically stable variant of HIF-2α promotes xenograft tumor growth in the presence of pVHL (Kondo *et al.*, 2002b). Looking back at **Figure 10**, the latter results fully concord with the specific functions reported for HIF-1α and HIF-2α respectively. Indeed, in the absence of HIF-2α stabilization, activation of HIF-1-specific transcriptional targets would induce apoptotic mechanisms resulting in cell death. Conversely, accumulation of both transcription factors results in a more balanced regulation of hypoxia responsive genes, with each HIF transcription factor exerting opposing effects on both apoptotic an proliferative signals (Keith *et al.*, 2011).

The subsequent observation in resected ccRCC samples that loss of functional pVHL leads either to stabilization of both HIF alpha subunits or to the sole accumulation of HIF-2α demonstrates that HIF-2α is the necessary and sufficient hypoxia-related component of VHL loss-driven ccRCC tumorigenesis (Bertout *et al.*, 2009). Furthermore, gene expression analysis comparing VHL-deficient ccRCC tumors expressing HIF-2α only versus those expressing both HIF-α subunits has shown that the latter group achieves proliferation mainly through Akt/ERK signaling while the former HIF-2α-restricted group relies mostly on MYC-driven proliferation (Gordan *et al.*, 2008). Interestingly, it appears that the MYC-driven group defines a therapy-resistant subtype of ccRCC while tumors expressing both HIF-α subunits associate with lower grade and better outcome after cytotoxic therapy (Gordan *et al.*, 2008).

Altogether, observations drawn from the literature suggest that the specific features of metabolic deregulation that arise from genetic or epigenetic alterations of the VHL locus depend on the functional impact on pVHL carried by those alterations. Therefore, it is not surprising that the binary mode of assessing VHL mutational status (altered or not) has been shown to lack significant association with prognosis on large cohorts of ccRCC patients (Kim *et al.*, 2017). Considering the multitude of VHL mutations reported in the literature, and more importantly the multitude of distinct phenotypic results verified to correlate with those mutations, it appears essential to determine the

phenotypic consequence of each VHL mutation found in our cohort of ccRCC patients in order to better understand our own results.

2.6. Analysis of VHL mutations found and genotype-phenotype correlations

In our cohort of 30 ccRCC patients, 25 patients had VHL mutations, including 3 patients bearing double mutations in their tumor samples as well as in all the corresponding CRC analyzed. In total, 18 distinct VHL gene sequence alterations were found, including 7 homozygous deletions causing frameshifts and affecting 10 patients. Among those 10 patients, one had both c.205-206delCG and c.548C>A truncating mutations simultaneously detected as homozygous in each one of the single CRC analyzed as well as in the corresponding primary tumor. Three additional patients also carried the nonsense truncating mutation c.548C>A (S183X) found as homozygous in all CRC as well as corresponding primary tumor samples. These results clearly show that those 13 patients suffered from biallelic inactivation of the VHL gene because any aberrantly truncated form of pVHL would rapidly be degraded following translation (Yang *et al.*, 2013).

Considering that the VHL tumor suppressor gene has been shown to follow the two-hit Knudson model of tumorigenesis (Cowey and Rathmell, 2009) and without further data from copy number analysis of the VHL gene locus, several possible genetic mechanisms can be proposed to explain our results.

For the 12 patients bearing single truncating VHL mutations found as homozygous, it appears likely that only one VHL allele acquired the truncating mutation while the remaining functional allele was deleted by LOH at 3p. The latter hypothesis appears more likely to occur then a scenario in which each of the two VHL alleles would suffer identical alterations in a sequential manner since more than 500 distinct mutations have already been evidenced across all three VHL exons in past literature (http://www.umd.be/VHL/), and especially considering the very high occurrence rate of LOH at 3p reported for sporadic ccRCC (Cheng *et al.*, 2009b). However, the presence of two identically mutated copies of the VHL gene cannot be ruled out for those patients because, owing to the role of pVHL

in preventing genomic instability during DNA replication, loss of functional pVHL caused by both LOH at 3p and inactivation of the remaining allele by truncating mutation could subsequently give rise to an aberrant duplication of the mutated allele, sometimes referred to as uniparental disomy (Pei *et al.*, 2010). In any case, a minimum of two genetic hits can be postulated to explain biallelic inactivation of the VHL gene for those 12 patients. Additionally, regarding the single patient carrying double truncating mutations detected as homozygous in the tumor sample as well as in all of the single CRC analyzed, similar reasoning would deduce that a minimum of three distinct genetic hits could explain such results (with a possible fourth hit consisting in duplication of the doubly mutated allele either prior to or following deletion of the wild type allele by LOH at 3p).

While nonsense mutations and frameshifts generally induce loss of all pVHL functions, and thus stabilization of both HIF-α subunits, the significance of missense mutations requires further investigation because single amino acid changes affecting specific regions of pVHL may impact distinct functions of the protein and result in distinct biological significances. Just like the remaining two nonsense mutations (c.194C>A and c.263G>A) found in 3 patients, all missense mutations were found as heterozygous in our cohort, which does not rule out the biallelic inactivation of the VHL gene since the remaining wild-type allele might be epigenetically silenced or affected by intronic alterations giving rise to aberrant splicing of VHL mRNA. However, our results simply cannot confirm the biallelic inactivation of VHL for those 12 patients bearing heterozygous VHL alterations since the methylation status of the VHL gene promoter and intronic sequences of the VHL gene could not be assessed in single CRC following microdissection.

Moreover, one of those patients was found to bear the silent mutation c.183C>G (P61P) on one allele while another patient presented with a heterozygous manifestation of c.526A>T (R176W). Considering that the pVHL variant bearing a R176W amino acid change has been described to retain all the functions attributed to the wild type pVHL (Gossage *et al.*, 2014b), those two patients are thus expected to retain functional pVHL expression if not affected by additional intronic or promoter alteration of the VHL gene. For the remaining 4 patients of our cohort bearing wild type VHL gene sequences in all single CRC and corresponding tumor samples analyzed, comparing results of

cytomorphological assessment with those of VHL mutational analysis would not provide any substantial added value over the sole cytopathological classification of circulating cells.

Interestingly though, our cohort also contained two patients who each harbored two simultaneous missense mutations in their tumor samples as well as in each of the corresponding circulating cells analyzed. One of them exhibited mutations coding for both A18E (c.53C>A) and L116V variants (c.346C>G) while the other had both D9Y (c.27G>T) and Q145H (c.435G>T).

To my knowledge, the A18E variant was reported in a single past study and, although the precise mechanism of its functional impact on pVHL remains poorly characterized, it was hypothesized to carry some degree of pathogenicity based on its disruption of pVHL binding to a specific protein of unknown identity and unidentified function at the time this particular study was published (Kishida *et al.*, 1995). Considering the plethora of pVHL interactors that were subsequently identified in recent years, the proper characterization of this putative pVHL interactor is warranted for future research in order to better understand the reported impact of A18E on pVHL functions.

Surprisingly, Forman and colleagues reported that the variant referred to as L116V was more commonly associated to retinal angioma than to RCC, although both pathologies are known to manifest in patients bearing this mutation (c.346C>G) as part of a hereditary VHL disease (Forman *et al.*, 2009). In the latter study, L116V was revealed to influence the 3D conformation of pVHL, specifically by altering the packing of the C-terminal helix of pVHL, thereby disrupting the binding of Elongin C. Since Elongin C is one of the main stabilizing cofactors of pVHL, their disrupted interaction was predicted to result in the immediate degradation of pVHL following translation (Forman *et al.*, 2009).

Conversely, the missense mutation Q145H was described by Miller and colleagues to result in an altered specificity of pVHL to bind and regulate HIF-α. More precisely, formation of the complex involving this Q145H variant of pVHL and HIF-1α was stably observed, thus not impacting HIF-1α degradation, whereas HIF-2α binding and degradation were both dramatically impaired (Miller *et al.*, 2005). This study classified the Q145H variant as likely to drive kidney cells towards RCC tumorigenesis by switching the function of pVHL from the degradation of both HIF-α subunits to the

sole stabilization of HIF-2α.

Considering the previously mentioned critical role of HIF-2α in ccRCC tumorigenesis (Mandriota *et al.*, 2002), there would be very little doubt concerning the diagnostic character of this Q145H mutation if it had been detected at consistently homozygous states across all CRC and in the corresponding tumor sample derived from the affected patient.

The remaining missense VHL mutation c.27G>T (D9Y) found in patients bearing double missense mutations has, to my knowledge, never been reported in previous publications and exerts unknown effects on pVHL functions. However, this D9Y variant corresponds to a missense mutation depleting a Guanine nucleotide from the initial CpG Island of the first VHL exon and could therefore impact the initiation of VHL transcription.

On the basis of L116V, A18E and Q145H having all been shown to alter pVHL function in past studies and further considering that all missense mutations were found at heterozygous states in our cohort, it is tempting to speculate that our pair of patients displaying double missense mutations harbored biallelic inactivation of VHL, with each allele bearing a distinct missense mutation. Such speculation would imply that D9Y significantly impairs pVHL functions; however, this cannot be verified strictly on the basis of our results. Therefore, further studies are warranted to establish the functional significance of this D9Y variant.

2.7. Comparing cytopathological classification with VHL mutational profiles of single CRC

Among the 25 patients found to harbor VHL mutations in their primary tumor, 18 patients had CCC diagnosed by cytopathology while all 25 patients had CRC-UMF bearing identical VHL mutations as the corresponding tumor samples. Importantly, VHL mutational profiles of all CCC diagnosed by cytopathology from 20 patients (including 2 patients with wild type VHL tumors) correlated exactly with the molecular profiles determined from corresponding tumor samples. If we considered that all of the single CRC found to bear identical VHL mutations as those found in corresponding tumor samples represent cancer cells derived from said tumor, then analysis of VHL mutational profiles

would indeed prove adequate in reliably complementing the cytopathological diagnosis of CCC in ccRCC patients. In fact, molecular analysis would then allow validating the 100% specificity of the cytopathological diagnosis of all CCC while proving useful in identifying an additional 104 single cells initially classified as CRC-UMF by cytopathology and derived from all 25 patients bearing VHL mutations in their tumor samples.

For those 25 patients bearing VHL mutations in their tumor samples (referred to as **group C in Table 1**), cytopathology would have identified 72% of patients found to harbor cancer cells by combining mutational analysis to morphological assessment (18/25 patients).This analytical strategy would imply that combining molecular analysis of the VHL gene with the reference cytomorphological approach would prove beneficial to enhance the respective analytical (number of cancer cells found) and clinical (number of patients presenting cancer cells) sensitivities of cytopathology.

Considering that, despite substantial evidence of ITH in ccRCC tumors, alterations of the VHL locus (including VHL mutations, silencing promoter hypermethylation and LOH at 3p) were found in several studies to be the only ubiquitous events characterizing all tumor subclones in ccRCC patients (Gerlinger *et al.*, 2012, 2014; Gerstung *et al.*, 2012; Gulati *et al.*, 2014; Voss *et al.*, 2014; Dagher *et al.*, 2017), it is hard to imagine how non-neoplastic cells bearing the exact same VHL mutation as the primary tumor could disseminate in the bloodstream.

In this context, our finding that 21 CRC-UMF from 11 patients exhibited discordant VHL mutational profiles when compared to corresponding tumor samples raises questions concerning the origin of those cells. Several hypotheses can be proposed to explain such results. It must be noted that up to 25% of patients present with multifocal RCC at diagnosis and that genetic analyses performed on a cohort of 26 multifocal ccRCC cases revealed that 46% of those patients were in fact carrying several coexisting tumors of distinct genetic origins and separate intra-organ localization (Cheng *et al.*, 2008). Thus, multifocal ccRCC tumors of distinct origins could in part explain a discordance of VHL mutational profiles found in CRC-UMF with respect to the specific tumor sample analysed.

Moreover, those CRC exhibiting uncertain morphology and distinct genetic profiles from that of the tumor could also represent hyperplastic non-neoplastic cells derived from distinct precursor lesions

of the kidney, since those can coexist with ccRCC and have been shown to directly result from VHL inactivation (Mandriota *et al.*, 2002; Montani *et al.*, 2010). Therefore, the tumorous nature of these 21 CRC-UMF could not be proven by either cytopathology or VHL genetic analysis.

From a statistical viewpoint, correlating the concordance of molecular profiles of CRC and paired primary tumors with a corresponding clonal identity of tumor cells would bear a less significant risk of bias if based on the detection of several identical genetic hits. According to previously discussed genotype-phenotype correlations, only a single patient from our cohort exhibited a mutational profile which could arise from at least three separate but converging genetic hits affecting the VHL locus. When further considering all cases in which biallelic inactivation of the VHL gene could be identified, thus considering only cases where at least two genetic hits occurred to result in undeniable loss of all functional pVHL expression, 13 of the 25 patients with VHL mutated tumors can be selected (reffered to as **group A in Table 1**). When applied strictly within this selection of patients, concordance of mutational profiles between single CRC and corresponding primary tumors would more likely reflect the accurate identification of cancer cells derived from the same initial clonal population as the primary tumor. As presesented in **Table 1**, such selected results show a lower clinical sensitivity being attributed to cytopathology as compared to the mutation analysis.

Slightly damping the stringency of this selection could further include 2 patients bearing double missense heterozygous mutations found identically in all CRC and corresponding tumors because two genetic hits would also be required for this profile to appear, although biallelic inactivation of the VHL gene cannot be unequivocally determined for those patients on the simple basis of our results. This method would consider concordant VHL mutational profiles between the tumor and the CRC as likely to bear diagnostic significance in (13 + 2 =) 15 patients (reffered to as **group B in Table 1**).

Table 1: *Comparing VHL mutations and cytopathology for cancer cell diagnosis*

If concordant VHL mutational profiles are considered to be diagnostic in:	Group A only (n=13)	Group B only (n=15)	Group C only (n=25)
Number of CCC diagnosed by cytopathology	21	28	57
Number of CRC-UMF diagnosed by VHL mutational analysis	59	73	161
Total number of cancer cells diagnosed by either methods or both	59	73	161
Number of patients with CCC diagnosed by cytopathology	8	10	18
Number of patients with CRC-UMF diagnosed by VHL mutational analysis	13	15	25
Total number of patients with cancer cells diagnosed by either methods or both	13	15	25
Clinical sensitivity of cytopathology	61.5%	66.7%	72.0%

In the future, it will be important to evaluate the possible presence in the circulation of non-neoplastic VHL-null cells derived from precursor lesions of the kidney. Investigating patients without ccRCC but bearing benign renal tumors such as oncocytomas or multilocular cystic nephromas would allow to clarify the extent to which hyperplastic VHL-null cells from benign renal lesions may circulate in blood (Stamatiou *et al.*, 2008).

2.8. Could molecular analysis of single CRC from ccRCC further complement cytopathology?

It will be important to broaden the scope of future molecular characterization of CRC in ccRCC by analyzing additional molecular markers implicated in ccRCC tumorigenesis in order to achieve diagnostic significance of said molecular results. As a matter of fact, recent genetic data obtained on ccRCC through the use of high throughput molecular platforms suggest that specific genetic abberations can cooperate with the initial biallelic inactivation of VHL to drive ccRCC tumorigenesis. Aside from the biallelic inactivation of VHL, according to recent studies, common genetic alterations that are most recurrently found in ccRCC patients often target genes controlling the expression of epigenetic regulator proteins involved in modulating chromatin conformation and accessibility to transcription, such as PBRM1, SETD2, BAP1, ARID1A, KDM5C and KDM6A (Gao *et al.*, 2017a).

Interestingly, studying human biology has revealed that PBRM1, BAP1 and SETD2 are all located in proximity of the VHL locus on the short arm of chromosome 3 and represent simultaneous targets of depletion by LOH at 3p (Sato *et al.*, 2013). Conversely, when looking at the mouse genome, those three tumor suppressor genes coding for chromatin regulators are well conserved but are also located on distinct chromosomes compared to the VHL locus, meaning they would not suffer simultaneous allele deletion from a single genetic hit, as can be observed in humans affected by LOH at 3p (Wang *et al.*, 2014b). The differential chromosomal location of VHL, PBRM1, BAP1 and SETD2 in the mouse genome compared to the features of human genetics provides a potential explanation for the struggle initially encountered by researchers in trying to create a representative murine model for the human VHL disease.

Moreover, while conditional inactivation of either *Vhl* alone or *Pbrm1* alone in mice kidneys fails to elicit malignant tumor growth, simultaneous inactivation of both *Vhl* and *Pbrm1* has been shown to result in the development of multifocal ccRCC tumors in mice (Nargund *et al.*, 2017). The PBRM1 gene codes for the BRG1-associated factor 180 (BAF180), a protein that forms a complex with other polybromo- and BRG1-associated factors (which also include the protein product of ARID1A) to regulate the position of nucleosomes throughout the genome (Gao *et al.*, 2017a). Interestingly, concomitant loss of PBRM1 and VHL has been shown to amplify HIF responses when compared to VHL loss alone (Nargund *et al.*, 2017), although with different implications for HIF-1α and HIF-2α depending on other components of the genetic background in ccRCC cell lines *in vitro* (Gao *et al.*, 2017a). For example, approximately 40% of ccRCC patients display inactivating mutations of the HIF1A gene encoding HIF-1α together with deletion of its 14q31 locus by LOH, thereby identifying a particular subset of ccRCC expressing only HIF-2α in the absence of functional pVHL (Li *et al.*, 2017b).

While PBRM1 is mutated in 30-40% of ccRCC, those alterations are mutually exclusive with mutations of BAP1 (coding for a BRCA1-associated protein) that are detected in 5-20% of ccRCC (Tennenbaum *et al.*, 2017). Importantly, heterozygous inactivation of *Bap1* together with homozygous inactivation of *Vhl* is sufficient to cause tumors in mice (Wang *et al.*, 2014b; Hsieh *et al.*, 2017). The mutual

exclusivity of mutations in PBRM1 and BAP1 defines two distinct subtypes of ccRCC with BAP1 mutations being significantly associated with poor survival for ccRCC pateints (Gulati *et al.*, 2014). In contrast, mutations in SETD2 (encoding a SET domain-containing protein) can be found in conjunction with either PBRM1 or BAP1 alterations and rather predict shorter progression free survival (PFS) and higher reccurence rates for ccRCC patients (Sato *et al.*, 2013).

Additionally, although VHL alterations are commonly found in a large portion of ccRCC patients, other ccRCC subtypes do not arise from loss of functional pVHL, as exemplified by the 4 patients in our cohort displaying wild type VHL sequences in their tumor samples and in all the corresponding single CRC analyzed. For those patients, VHL mutational analysis failed to provide additional information on the nature of CRC when compared to cytopathology alone, emphasizing the need to interrogate other genetic markers for a broader utility of combining molecular and cytomorphological assessments of CRC in ccRCC.

Thanks to the substancial technological improvements achieved for sequencing analyses, additional ccRCC molecular subtypes have recently emerged. For instance, by combining whole genome and/or whole exome sequencing with microarray-based gene expression, DNA methylation and genomic copy number analyses of 106 ccRCC samples, Sato and colleagues found that 40% of ccRCC samples with functional pVHL expression harbored biallelic inactivation of the ELOC gene (also called TCEB1) encoding one of pVHL's stabilizing cofactors, Elongin C, by concomitant mutations and loss of chromosome 8 deleting the ELOC locus (8q21) on the contralateral allele (Sato *et al.*, 2013). Interestingly, loss of functional Elongin C and inactivation of VHL were found to be mutually exclusive, highlighting the critical role in ccRCC of the VCB-Cul2 complex regulating HIF-α subunits (Stebbins *et al.*, 1999). However, hypoxia regulation is a complex pathway involving other regulators in addition to functional pVHL. Concomittant loss (through loss of whole chromosome arms or smaller aneuploidies) of several factors converging towards (de)regulation of the physiological response to hypoxia has been implicated in ccRCC tumorigenesis and subsequent disease progression, as shown in **Figure 12**.

Figure 12: *Regulation of hypoxia inducible factors in humans*

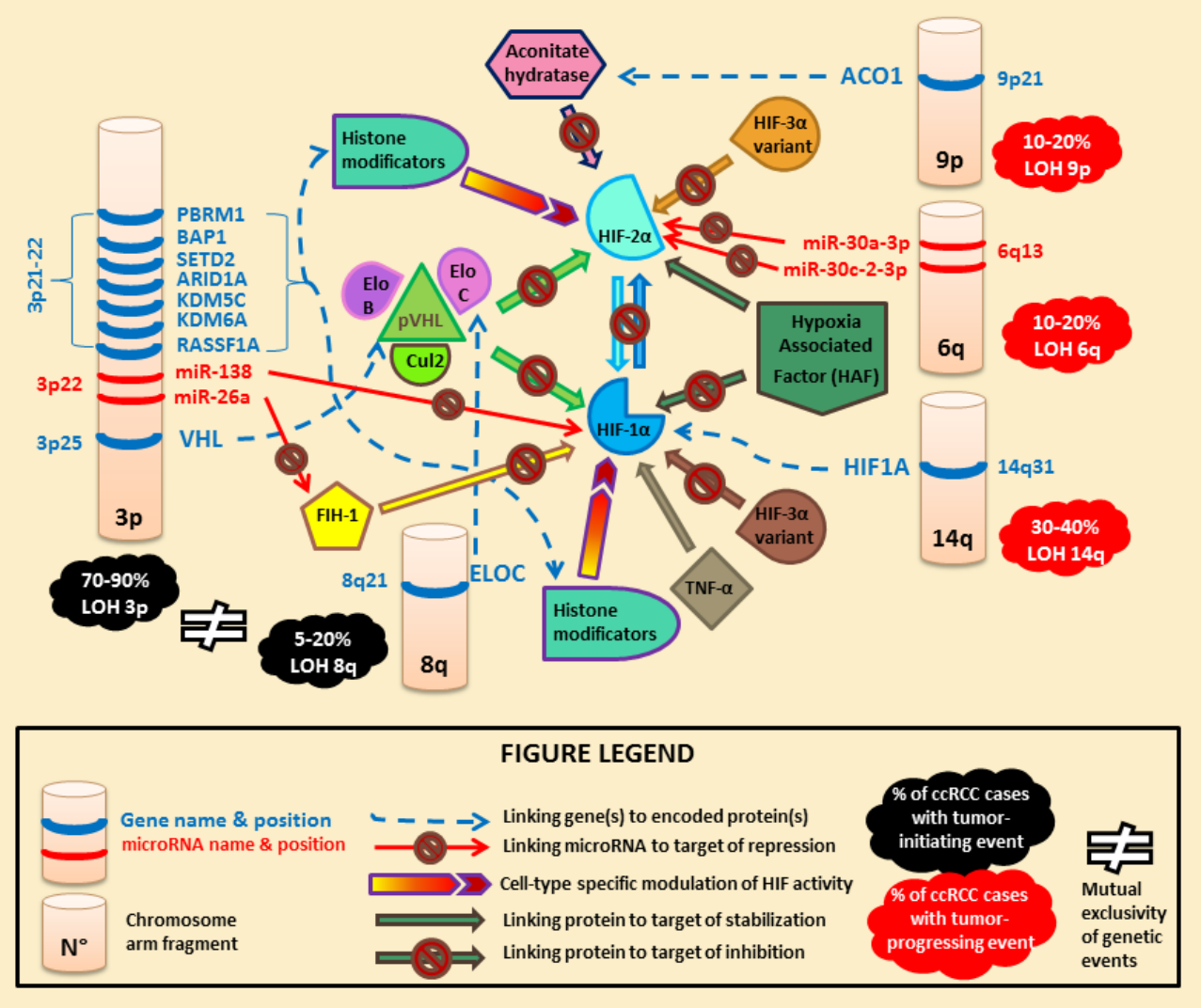

Importantly, several recent reports (Cancer Genome Atlas Research Network, 2013; Sato *et al.*, 2013; Czarnecka *et al.*, 2014; Li *et al.*, 2017b) have clearly demonstrated that combining multiple strategies for molecular characterization of ccRCC, such as analyses of genomic sequence and copy number alterations with gene expression profiling and DNA methylation assessment, offers a unique opportunity to deepen our understanding of the differential molecular contributions relative to the wide array of pathogical phenotypes observed in cancer patients. However, few studies have addressed molecular characterization of ccRCC to single cells, whether recovered from the blood circulation (Nel *et al.*, 2016) or dissociated from the primary tumor tissue (Xu *et al.*, 2012b). The latter example, through single-cell whole exome sequencing (WES) of a single ccRCC tumor

exhibiting wild type gene sequences on both VHL and PBRM1 loci, depicts the particular complexity of ccRCC molecular architecture which is reflected in the extensive genetic heterogeneity that can be found both within individual tumors and at population level. These observations suggest that single-cell molecular characterization may be crutial to unravel the complexity of cancer and especially in the context of pathway-regulated diseases such as ccRCC.

In summary, considering the whole literature data, assessment of the diagnostic role of VHL mutations suffers from a lack of extensive mutational analysis of the whole genome at single-cell level in patients with and without ccRCC. These technical aspects and partial information also limit the interpretation of the detection of VHL mutations in circulating rare cells with certain and uncertain malignant features. However, despite these limitations and considerations, by performing a parallel and blind VHL genetic analysis in the tumorous tissue and CRC, our work strongly suggests a possible role of mutation analysis to confirm and extend the diagnostic identification of circulating cancer cells by cytopathology.

3. ISET®-related methodological developments for single cells CRC analysis

3.1. Assessing ISET® performances

More than 40 distinct methods developed to isolate CTC have been published (Song *et al.*, 2017) and among those several size-based enrichment methods. Filtration methods are characterized by different filtration parameters (type of filters, buffer or media used to dilute blood, type of device and filtration pressure…) that determine their different performances. Therefore, despite the fact that the word "filtration" intuitively sounds as an easy and generic approach to separate large and small elements, blood filtration to isolate circulating rare cells (CRC) is not at all depending only on the pore size. Additionally, the size difference between white blood cells (8–15 µm) and tumor/trophoblastic cells (15–30 µm) is very small, creating a competition of blood cells for the filter's pores and making tumor/trophoblastic cells' isolation without cell loss or damage an ambitious technical challenge. Sensitivity and specificity are crucial parameters to define the performance of a given methodological approach for selection/detection and sensitivity is of particular importance for the detection and analysis of rare cells.

In an effort to extend our methodological tools for the study of individual CRC, we have first assessed the sensitivity specifications of ISET® using cells having different sizes from human and mouse cancer cell lines grown *in vitro*. Since sensitivity is a critical issue, we developed an assay able to provide the maximum reliability for sensitivity assessment using a number of tumor cells under 10, i.e. spiking into blood of individually collected and counted fluorescent tumor cells. For higher numbers of tumor cells (30 to 300), we counted them by dilution, performing repeated counting to adjust the tumor cells' number. Then, to assess the number of tumor cells successfully isolated by the ISET® System, we counted very carefully the fluorescent cells to avoid any mistake at the detection level.

An overview of ISET®'s average recovery success rates of cancer cells spiked in blood can be found in **Figure 13**.

Figure 13: *ISET® mean recovery success rates*

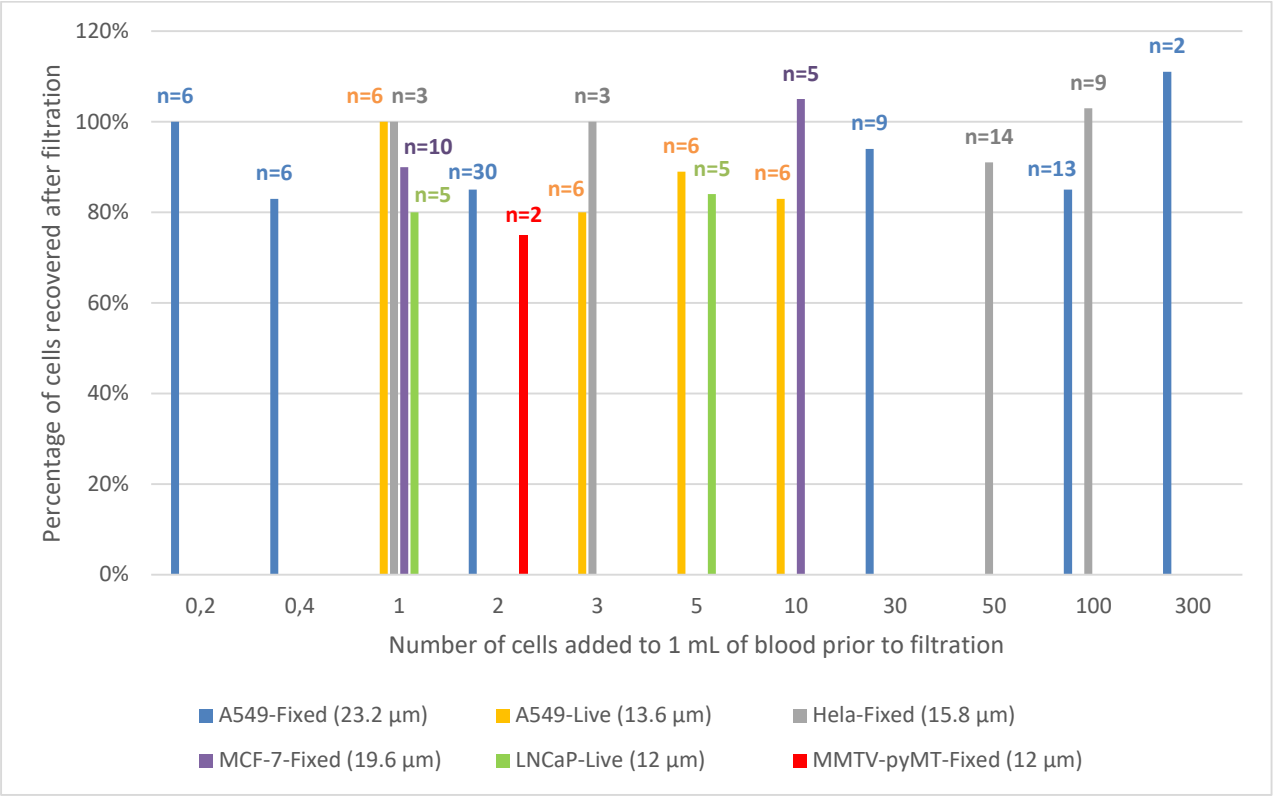

The median diameters of cultured tumor cells that we determined on filters typically range from 12 to 20 µm, consistently with previously published studies (Lin *et al.*, 2010; Coumans *et al.*, 2013). Moreover, we have successfully isolated intact fixed mouse tumor cells as small as 8.5 µm in diameter (median size on filter 12 µm) using the standard membrane with a nominal pore size of 8 µm.

Our *in vitro* data showing the very high sensitivity of ISET® are consistent with in vivo data previously published by independent teams, showing the higher in vivo sensitivity of ISET® as compared to CellSearchTM (Farace *et al.*, 2011; Hofman *et al.*, 2011b; Khoja *et al.*, 2012; Krebs *et al.*, 2012; Pailler *et al.*, 2013; Khoja *et al.*, 2014; Morris *et al.*, 2014; Pailler *et al.*, 2015; Morrow *et al.*, 2016). ISET® performances rely crutially on the following aspects: 1) blood is treated soon after collection, 2) treatment to prepare blood for ISET® filtration is rapid and efficient 3) the number of steps before the "isolation" step is minimum: blood is just collected from the patient, diluted and filtered, 4) fixed cells are collected with no additional steps by the filter and only one additional step is required to

collect live cells by pipetting, 5) the filter characteristics avoid losing cells larger than mature lymphocytes, 6) the blood aspiration system can be modulated and allows to stick large cells to the filter without loss, or concentrate them in a small volume over the filter, 6) the system does not relies on the use of markers for isolation nor for collection not for identification of tumor cells. Combined together, these characteristics play a key role in setting the sensitivity of ISET® for isolation of CRC.

We also note that, in the field of CTC, a high sensitivity is clinically relevant only if associated with high specificity. Since circulating rare non-tumor cells may be present in the blood of patients with cancer, high sensitivity with low specificity can lead to mistakes in clinical decisions.

Regarding specificity, ISET® filtration does not perform any detection of CTC per se. It is meant to isolate CRC without bias and with a minimum CRC loss. Specificity is brought by the subsequent step of cytopathology. Since tumor cells are isolated intact without damage, CRC characterization is possible by a variety of downstream approaches. As reported and recognized, cytopathology is the only clinically validated method to diagnose tumor cells (Paterlini-Bréchot, 2014).According to cytopathological criteria (Long *et al.*, 2016), cancer cells from patients are usually larger than 16 microns. The presence in blood of intact cancer cells smaller than 8 microns, i.e. smaller than mature lymphocytes, has never been diagnosed in patients (Hofman *et al.*, 2014), which comes in support of using ISET® to isolate all types of CTC from blood.

Hofman's team also brought a conclusive demonstration that the ISET® blood cytopathology is diagnostic for reliable identification of cancer cells in blood. They showed, in an independent and prospective study, the ability of this assay to detect "sentinel tumor cells" in patients at risk of developing lung cancer years before the detection of the tumor nodule by CT-scan, thus demonstrating a new way for invasive cancers' early diagnosis and treatment (Ilie *et al.*, 2014).

The clinical value of ISET® is predictably related to its capacity to isolate all types of tumor cells including tumor cells in Epithelial to Mesenchymal Transition (EMT), expressing mesenchymal markers such as Vimentin, but not (or barely) expressing epithelial markers (EpCAM or cytokeratin). The presence of mesenchymal cancer cells in blood has been shown to be relevant in terms of

prognostic value in patients with pancreatic cancer (Khoja *et al.*, 2012; Poruk *et al.*, 2016), and lung cancer (Hofman *et al.*, 2011a; Krebs *et al.*, 2012; Pailler *et al.*, 2013). Detection of tumor cells in EMT is also relevant for the development of reliable companion diagnostics tests. For instance, using ISET®, Pailler *et al.* have reported the presence of a recurrent ALK-rearrangement in CTC which also expressed mesenchymal markers, consistently with a clonal selection of tum or cells (Pailler *et al.*, 2013). Regarding molecular interrogation of CRC, independent studies have reported the interest of ISET® for *in situ* detection of several theranostic biomarkers including ALK recombination, ROS1 recombination, KRAS mutations, BRAF V600E mutation and HER2 amplification (Pinzani *et al.*, 2006; Ilie *et al.*, 2012; Hofman *et al.*, 2013; Buim *et al.*, 2015; Pailler *et al.*, 2015). .

Despite those results and ISET®' s impressive performances in terms of sensitivity and specificity of CCC diagnosis, the requirement of using cytological fixatives prior to filtration in order to permenantly attach cells to the filter constitute a substantial limitation for molecular characterization since the possibilities for molecular analyses of fixed cells at single-cell level remain limited. Therefore, it seemed important to develop and optimize a new process by which ISET® filtration could ensure the recovery of viable CRC.

When it comes to viable cells, other parameters might affect the performance of blood filtration such as cell fragility and biomechanics of the cytoskeleton (Zemła *et al.*, 2017). It is unclear whether the spectrum of fragility of primary cells is similar to the one of tumor cells from cell lines. By fixating the cells structure, the standard buffer for fixed cell recovery makes the cells rigid and eliminates the problem of fragility as demonstrated by the very high recovery of individually-spiked fixed cells. Concerning live cells, our laboratory experience shows that secondary (from cell lines) cells are more malignant, but also more fragile than primary tumor cells during in vitro manipulation. This is because secondary tumor cells from solid cancers have to be trypsinized to be manipulated and this step damages the cell membrane making it more fragile. Thus, our sensitivity tests performed with secondary live tumor cells are expected to be reliable.

3.2. Methodological developments

We developed a new protocol to enrich live tumor cells from blood without immune-related bias using a dedicated buffer and using the filtration device and consummables in a different way. We show that it allows a recovery rate of 80 to 100% of tumor cells and a sensitivity threshold (LLOD) of 1 tumor cells per mL of blood in spiking tests using individually captured single cells. Our results demonstrate that this new protocol for isolation from blood of live tumor cells does not induce a cell-size related bias of selection, including for the smallest cells we tested (MMTV-PyMT).

Biomechanics of the cytoskeleton might affect the performance of the method when using unfixed samples. Articles in the literature indicate that non-malignant tumor cell lines are stiffer in comparison to malignant tumor cell lines (and also less prone to migration and invasion) (Xu *et al.*, 2012a; Harouaka *et al.*, 2013). Studies with cells obtained from patients' ascites (ovarian cancer) or derived from oral squamous carcinoma have shown that cancer cells from a given tumor cells' population exhibit a varying degree of stiffness, which is similar to the stiffness of cancer cell lines (Swaminathan *et al.*, 2011; Runge *et al.*, 2014). In addition, stiffness is also correlated to the EMT status of cells: the stiffest/least invasive cell lines expressed more E-Cadherin and less Vimentin, while the compliant/most invasive cell lines expressed less E-Cadherin and more Vimentin (Swaminathan *et al.*, 2011). In our tests with live cells, we used both cell lines with epithelial phenotype (LNCaP) and mesenchymal phenotype (A549, H2228, MMTV-PyMT)

In this report, we have also shown that live A549 tumor cells isolated from blood can be cultured and expanded in vitro for at least 5 days, demonstrating that the buffer and protocol used to isolate live tumor cells from blood allows their growth. Interestingly, we noticed that no leucocytes remained alive after 3 days of culture.

In addition, we have assessed cytoskeleton markers by confocal analysis of F-actin and acet- ylated α-tubulin after live tumor cells isolation and culture for 72h. These markers are known to be therapeutic targets (Dumontet and Jordan, 2010; Wang *et al.*, 2016). The microscopy assay we used has been shown to directly correlate with Atomic Force Microscopy, a cell stiffness assay (Calzado-Martín *et al.*, 2016). We have compared the profiles of two cell lines, A549 and H2228. Distribution

of F-actin and acetyl-α-tubulin were found to be conserved (or restored) after 72h of in vitro culture following live tumor cells isolation using the ISET® system.

Furthermore, in the aim of studying theranostic mutations to guide the therapeutic choices, we have demonstrated that, in our model, the basic profile of mutations, assessed with the Hotspot Cancer Panel V2 (Thermofisher, USA) does not change after isolation by ISET® of tumor cells from blood and their growth in culture for 72 hours. This new data may stimulate similar important analyses performed on CTC from cancer patients.

Taken together, these data suggest that the new ISET® protocol to isolate live tumor cells does not modify the cell phenotype and genotype. Consistently, tumor cells viability after their isolation from blood remained very high (>85%).

Since the first report of successful CTC-derived xenografts (CDX) in 2000 (Pretlow *et al.*, 2000), several research publications have focused on the ex vivo propagation of CTC via short-term in vitro culture (Bobek *et al.*, 2014; Gao *et al.*, 2014; Yu *et al.*, 2014), direct injection into immuno-compromised mice (Baccelli *et al.*, 2013; Hodgkinson *et al.*, 2014; Kolostova *et al.*, 2014) or long-term 3D culture by establishment of prostate and colorectal cancer cell lines derived from CTC (Cayrefourcq *et al.*, 2015). However, long-term in vitro culture of CTC remains a technical challenge in the field, with a generally very low percentage of successful growth. Further knowledge about culture conditions is required to obtain in vitro growth of heterogeneous and very rare CTC populations. However the first requirement in this aim is the possibility to extract tumor cells from blood without selection bias, keeping their phenotype, genotype viability and growth capabilities potentially unaffected. The new protocol we have developed for isolation of live tumor cells from blood is highly sensitive, rapid, direct and does not alter their biological characteristics, thus it should help further studies focused on ex vivo expansion and analysis of CTC.

Until now ex vivo culture of CTC has been achieved using samples from patients having several hundreds of CTC per 7.5 mL of blood. The success rates of CTC expansion in culture remains low across various isolation methods and culture conditions. A possible explanation for this low culture success rate was suggested by Grillet and colleagues who demonstrated the presence of CTC with

all the functional attributes of cancer stem cells (CSC) in the blood of colorectal cancer patients (Grillet *et al.*, 2016). CSC have crutial self-reniewal properties (Abbaszadegan *et al.*, 2017) which make them best suited to initiate long term growth *in vitro* and Grillet *et al.* were able to establish several cell lines by selecting the CSC subpopulation among CTC from colorectal cancer patients. This allowed assessing CSC and CTC molecular features among CTC lines to determine that drug metabolism is upregulated in these cells, consistently with their observed resistance to cytotoxic compounds (Grillet *et al.*, 2016). CSC are even rarer than CTC in the bloodstream and improving the sensitivity of CSC recovery may prove useful to enhance success rates of long term ex vivo culture of CTC. The excellent sensitivity of the ISET® live cell isolation protocol and the proof that it allows tumor cell growth in culture should help culture assays for fundamental CTC studies and *ex vivo* drug testing (Yu *et al.*, 2014; Malara *et al.*, 2016; Wenjun *et al.*, 2017).

3.3. Perspectives for future applications

Considering the currently ongoing switch from systemic cytotoxic anticancer treatments towards personalized molecular-targeted therapy, it is becoming evident that bulk molecular characterization of the primary tumor cannot recapitulate the highly heterogeneous molecular features of all the individual cancer cells that together constitute the cancer burden of a given patient (Qian *et al.*, 2017). Therefore, because molecular markers are currently assessed on a bulk collection of cells extracted from the primary tumor for theranostic purposes, therapeutic strategies only target the predominant tumor subclones that characterize a given tumor mass at a given timepoint in its development (i.e. at the time of biopsy or whenever other tumor sampling methods are performed). This "bulk" strategy has been shown to pose significant limitations whith regards to the detection of minoritarily preexisting therapy-resistant subclones of cancer cells as well as to distinguish preexisting from acquired resistance to anti-cancer therapy (Tirosh *et al.*, 2016). Cancer cells are genetically unstable and prone to mutational events due to frequent mitosis in proliferating cells and DNA replication errors along with an altered machinery of DNA damage response mechanisms (Shan

et al., 2017). Such genetic instability promotes the generation of highly heterogeneous populations of cancer cells within a given tumor (ITH) and our current technologies for "bulk" molecular analysis of the tumor do not allow for an accurate vizualisation of the less abundant subclones of cancer cells (Mroz and Rocco, 2017). However, recent technological developments have fostered interesting studies using single-cell molecular characterization to improve both our understanding of cancer biology and our current medical practices for cancer treatment.

High throughput sequencing technologies for genetic characterization have emerged as a powerful tool to probe the genetic landscape of a given sample. On the one hand, advances in high throughput deep sequencing have largely contributed to the clinical implementation of NIPT based on cfDNA analysis (Faas *et al.*, 2012). On the other hand, high throughput single-cell sequencing methodologies have greatly improved our understanding of cancer biology, including our conception of the metastatic process (Gao *et al.*, 2017b). Moreover, those recent technological developments have fostered a growing interest of the scientific community for applications of single-cell RNA sequencing (RNAseq) in predictive oncology (Zhu *et al.*, 2017). Although recent studies have emphasized the need for additional technical improvements to be achieved before single-cell RNAseq methodologies can be reliably implemented in clinical settings (Yan *et al.*, 2017), others have already highlighted the tremendous potential held by single-cell RNA-seq methods to infer therapeutic strategies for personalized medicine (Kim *et al.*, 2016) as well as to retrace the evolutionary journey of a given cell to determine its exact nature (Trapnell, 2015). Such transcriptomic analyses pose the necessary restriction of being applied to intact and viable cells, a requirement which applies to all functional studies.

With the advent of single-cell technologies (Khoo *et al.*, 2016), including the emerging fields of single cell proteomics (Lu *et al.*, 2017; Sinkala *et al.*, 2017) and single-cell methylomics (Yu *et al.*, 2017), new methodological strategies are becoming increasingly available for application in the field of rare cells. In order to enable combining ISET® filtration with any one of those emerging strategies for single-cell analysis, alternatives to the standard ISET® workflow were developed and a full assessment of optimal technical parameters was performed. Our results validate the feasibility of

next generation sequencing (NGS) to interrogate the genetic heterogeneity of ISET®-enriched CRC at single-cell level. Indeed, single-cell analysis of CTC has recently opened a new window into the complexity of tumor heterogeneity, since CTC are thought to recapitulate the invasive population of tumor cells derived from all tumor sites, including from distant metastatic sites (Miyamoto *et al.*, 2016). Although analysis of cell-free tumor DNA (ctDNA) presents as a straightforward approach for genetic analysis of the tumor burden, CTC are uniquely suited to interrogate functional heterogeneity by combining genetic and transcriptomic assessment of single CTC (Klein *et al.*, 2002) or by parallel single-cell transcriptome and epigenome analysis (Zhao *et al.*, 2017a). Therefore, our methodological developments should foster exciting research to uncover the metastastatic process in further detail and to interrogate the biology of cancer in general.

The new ISET® protocol to enrich live CTC from blood without sticking them to the filter provides new possibilities for extensive single tumor cells RNA and DNA molecular studies while avoiding microdissection. Individual CTC can be simply captured manually after enrichment from blood by micropipetting or by using current commercial approaches (such as CellCelector™ (ALS) or DEPArray™ (Silicon Biosystems) or QiaScout (Qiagen)). An optimized workflow for molecular characterization of individual CTC, which are sensitively isolated from blood without antibody related bias, is expected to be an attractive tool. We reported here an optimized workflow including: 1) highly sensitive isolation of live CTC from blood without bias, 2) capture of individual CTC, 3) single cell whole genome amplification, 4) efficient high throughput sequencing using a multi-gene panel analysis with the Ion Torrent™ approach. An overview of possible downstream applications of ISET® is presented in **Figure 14**.

Our results show the feasibility of applying next generation sequencing to both live and fixed single cells enriched from blood by ISET® and recovered in suspension, assessing mutations on a variety of oncogenes including KRAS and PIK3CA. Those are important to screen for theranostic purposes since mutations in those genes can be predictive of treatment resistance. Diagnostic and theranostic applications of single-cell molecular analysis of CTC or CTC-derived cell lines could help bringing increasingly precise personalized medicine to cancer patients (Polzer *et al.*, 2014; Grillet *et al.*, 2016).

Figure 14: *Overview of possible downstream applications of ISET®*

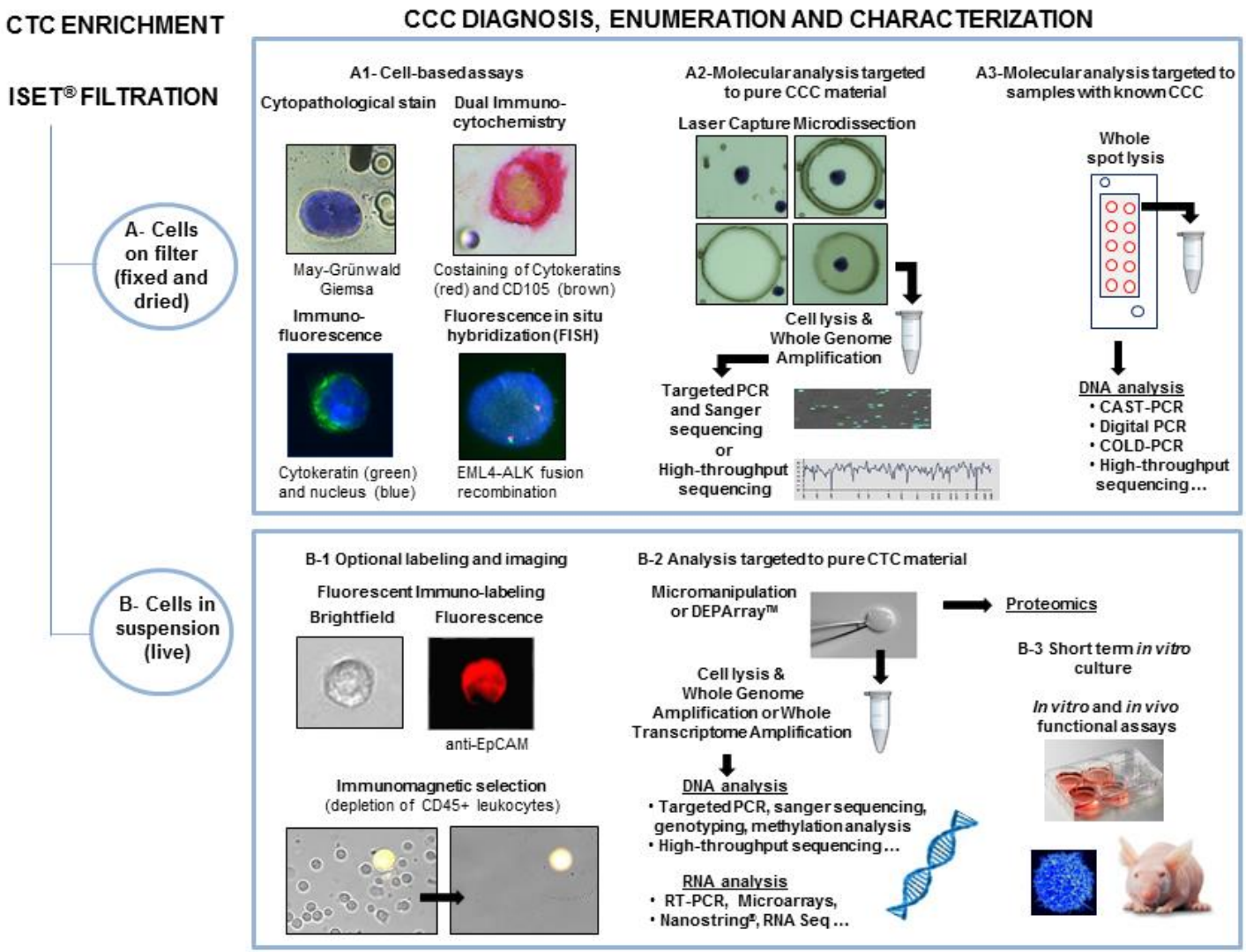

Conclusion

The work presented here aimed at proposing methodological solutions for the study of circulating rare cells (CRC) using ISET®, with applications in both predictive oncology and prenatal diagnosis.

For prenatal diagnosis, the concept of retrieving cervical trophoblasts from 8-12 WG pregnancies using ISET® for NIPD of recessive genetic disorders was validated by a completely safe approach and without drawing blood. Combining this strategy with fetal trophoblastic cell collection from maternal blood samples would likely be very advantageous considering the extreme rarity of those cells. By allowing recovery of three times more fetal cells per sample volume, external cervical sampling followed by filtration provides additional material for NIPD of genetic disorders. In the future, NIPD can be envisioned at early gestanional age for multiple disorders simultaneously by applying high throughput sequencing (NGS) to single trophoblastic cells (Breman *et al.*, 2016).

In the field of oncology, circulating cancer cells (CCC) and microemboli are important populations to study since they potentially create metastasis to distant organs and are therefore responsible for approximately 90% of cancer-related deaths (Siegel *et al.*, 2015). Single-cell molecular analysis of CRC is not required for CCC diagnosis since cytopathology provides reliable diagnosis, however our experimental data suggest that both approaches could prove complementary. To go further, methodological developments were performed to enable the simultaneous interrogation of multiple genetic targets from a single circulating cell using next generation sequencing. If further validated on clinical cases, those methodologies would find clinical usefulness for theranostic purposes by providing guidance for adequate targeted therapy, monitoring of response and early detection of acquired resistance to treatment (Alix-Panabières and Pantel, 2016). Further development and clinical validation of single-cell whole genome and whole transcriptome analyses on ISET®-enriched CRC would certainly prove interesting for research purposes. Indeed, this multimodal approach may help identifying specific sets of true molecular markers of cancer in distinct types of solid malignant

neoplasms, similarly to the knowledge already acquired for molecular diagnosis of leukemia (Onaindia *et al.*, 2017). And finally, the emerging field of single-cell epigenomics (Miyamoto *et al.*, 2016) promises to unlock understanding of heterogeneity and cellular plasticity at a more in deep level which would allow to stratify CRC populations for their clinical use. Our work aims to contribute to set the basis for this exciting route toward using CRC for relevant clinical applicatons.

References

Abbaszadegan, M. R., Bagheri, V., Razavi, M. S., Momtazi, A. A., Sahebkar, A., and Gholamin, M. (2017). Isolation, identification, and characterization of cancer stem cells: A review. J. Cell. Physiol. *232*, 2008–2018.

Abbosh, C. *et al.* (2017). Phylogenetic ctDNA analysis depicts early-stage lung cancer evolution. Nature *545*, 446–451.

Abdallah, E. A. *et al.* (2015). Thymidylate synthase expression in circulating tumor cells: a new tool to predict 5-fluorouracil resistance in metastatic colorectal cancer patients. Int. J. Cancer *137*, 1397–1405.

Abdallah, E. A. *et al.* (2016). MRP1 expression in CTCs confers resistance to irinotecan-based chemotherapy in metastatic colorectal cancer. Int. J. Cancer *139*, 890–898.

Abdolahad, M., Taghinejad, M., Taghinejad, H., Janmaleki, M., and Mohajerzadeh, S. (2012). A vertically aligned carbon nanotube-based impedance sensing biosensor for rapid and high sensitive detection of cancer cells. Lab. Chip *12*, 1183–1190.

Abrahamsson, A., and Dabrosin, C. (2015). Tissue specific expression of extracellular microRNA in human breast cancers and normal human breast tissue in vivo. Oncotarget *6*, 22959–22969.

Aceto, N. *et al.* (2014). Circulating tumor cell clusters are oligoclonal precursors of breast cancer metastasis. Cell *158*, 1110–1122.

Adam, A. P., George, A., Schewe, D., Bragado, P., Iglesias, B. V., Ranganathan, A. C., Kourtidis, A., Conklin, D. S., and Aguirre-Ghiso, J. A. (2009). Computational identification of a p38SAPK-regulated transcription factor network required for tumor cell quiescence. Cancer Res. *69*, 5664–5672.

Adinolfi, M., and Sherlock, J. (2001). Fetal cells in transcervical samples at an early stage of gestation. J. Hum. Genet. *46*, 99–104.

Afik, R. *et al.* (2016). Tumor macrophages are pivotal constructors of tumor collagenous matrix. J. Exp. Med. *213*, 2315–2331.

Aguirre-Ghiso, J. A. (2007). Models, mechanisms and clinical evidence for cancer dormancy. Nat. Rev. Cancer *7*, 834–846.

Alexandrova, A. Y., Arnold, K., Schaub, S., Vasiliev, J. M., Meister, J.-J., Bershadsky, A. D., and Verkhovsky, A. B. (2008). Comparative dynamics of retrograde actin flow and focal adhesions: formation of nascent adhesions triggers transition from fast to slow flow. PloS One *3*, e3234.

Al-Hajj, M., Wicha, M. S., Benito-Hernandez, A., Morrison, S. J., and Clarke, M. F. (2003). Prospective identification of tumorigenic breast cancer cells. Proc. Natl. Acad. Sci. U. S. A. *100*, 3983–3988.

Alitalo, K., Tammela, T., and Petrova, T. V. (2005). Lymphangiogenesis in development and human disease. Nature *438*, 946–953.

Alix-Panabières, C., and Pantel, K. (2016). Clinical Applications of Circulating Tumor Cells and Circulating Tumor DNA as Liquid Biopsy. Cancer Discov. *6*, 479–491.

Almog, N. *et al.* (2006). Prolonged dormancy of human liposarcoma is associated with impaired tumor angiogenesis. FASEB J. Off. Publ. Fed. Am. Soc. Exp. Biol. *20*, 947–949.

Almog, N. *et al.* (2009). Transcriptional switch of dormant tumors to fast-growing angiogenic phenotype. Cancer Res. *69*, 836–844.

Alves, C. S., Burdick, M. M., Thomas, S. N., Pawar, P., and Konstantopoulos, K. (2008). The dual role of CD44 as a functional P-selectin ligand and fibrin receptor in colon carcinoma cell adhesion. Am. J. Physiol. Cell Physiol. *294*, C907-916.

Andor, N., Graham, T. A., Jansen, M., Xia, L. C., Aktipis, C. A., Petritsch, C., Ji, H. P., and Maley, C. C. (2016). Pan-cancer analysis of the extent and consequences of intratumor heterogeneity. Nat. Med. *22*, 105–113.

Antonarakis, E. S. *et al.* (2014). AR-V7 and resistance to enzalutamide and abiraterone in prostate cancer. N. Engl. J. Med. *371*, 1028–1038.

Arima, S., Nishiyama, K., Ko, T., Arima, Y., Hakozaki, Y., Sugihara, K., Koseki, H., Uchijima, Y., Kurihara, Y., and Kurihara, H. (2011). Angiogenic morphogenesis driven by dynamic and heterogeneous collective endothelial cell movement. Dev. Camb. Engl. *138*, 4763–4776.

Ashworth, T. R. (1869). A case of cancer in which cells similar to those in the tumors were seen in the blood after death. Aus Med J, 146–9.

Au, S. H. *et al.* (2016). Clusters of circulating tumor cells traverse capillary-sized vessels. Proc. Natl. Acad. Sci. U. S. A. *113*, 4947–4952.

Baccelli, I. *et al.* (2013). Identification of a population of blood circulating tumor cells from breast cancer patients that initiates metastasis in a xenograft assay. Nat. Biotechnol. *31*, 539–544.

Bai, Y.-P., Shang, K., Chen, H., Ding, F., Wang, Z., Liang, C., Xu, Y., Sun, M.-H., and Li, Y.-Y. (2015). FGF-1/-3/FGFR4 signaling in cancer-associated fibroblasts promotes tumor progression in colon cancer through Erk and MMP-7. Cancer Sci. *106*, 1278–1287.

Balko, J. M. *et al.* (2014). Molecular profiling of the residual disease of triple-negative breast cancers after neoadjuvant chemotherapy identifies actionable therapeutic targets. Cancer Discov. *4*, 232–245.

Banks, R. E. *et al.* (2006). Genetic and epigenetic analysis of von Hippel-Lindau (VHL) gene alterations and relationship with clinical variables in sporadic renal cancer. Cancer Res. *66*, 2000–2011.

Barkan, D. *et al.* (2010). Metastatic growth from dormant cells induced by a col-I-enriched fibrotic environment. Cancer Res. *70*, 5706–5716.

Barnhill, R. L. *et al.* (2017). The biological and prognostic significance of angiotropism in uveal melanoma. Lab. Investig. J. Tech. Methods Pathol.

Barondes, S. H., Cooper, D. N., Gitt, M. A., and Leffler, H. (1994). Galectins. Structure and function of a large family of animal lectins. J. Biol. Chem. *269*, 20807–20810.

Barreiro, E., Bustamante, V., Curull, V., Gea, J., López-Campos, J. L., and Muñoz, X. (2016). Relationships between chronic obstructive pulmonary disease and lung cancer: biological insights. J. Thorac. Dis. *8*, E1122–E1135.

Bayarri-Lara, C. *et al.* (2016). Circulating Tumor Cells Identify Early Recurrence in Patients with Non-Small Cell Lung Cancer Undergoing Radical Resection. PloS One *11*, e0148659.

Bazellières, E., Conte, V., Elosegui-Artola, A., Serra-Picamal, X., Bintanel-Morcillo, M., Roca-Cusachs, P., Muñoz, J. J., Sales-Pardo, M., Guimerà, R., and Trepat, X. (2015). Control of cell-cell forces and collective cell dynamics by the intercellular adhesome. Nat. Cell Biol. *17*, 409–420.

Beaudet, A. L. (2016). Using fetal cells for prenatal diagnosis: History and recent progress. Am. J. Med. Genet. C Semin. Med. Genet. *172*, 123–127.

Bergsmedh, A., Szeles, A., Henriksson, M., Bratt, A., Folkman, M. J., Spetz, A. L., and Holmgren, L. (2001). Horizontal transfer of oncogenes by uptake of apoptotic bodies. Proc. Natl. Acad. Sci. U. S. A. *98*, 6407–6411.

Béroud, C., Joly, D., Gallou, C., Staroz, F., Orfanelli, M. T., and Junien, C. (1998). Software and database for the analysis of mutations in the VHL gene. Nucleic Acids Res. *26*, 256–258.

Béroud, C., Karliova, M., Bonnefont, J. P., Benachi, A., Munnich, A., Dumez, Y., Lacour, B., and Paterlini-Bréchot, P. (2003). Prenatal diagnosis of spinal muscular atrophy by genetic analysis of circulating fetal cells. Lancet Lond. Engl. *361*, 1013–1014.

Bertout, J. A., Majmundar, A. J., Gordan, J. D., Lam, J. C., Ditsworth, D., Keith, B., Brown, E. J., Nathanson, K. L., and Simon, M. C. (2009). HIF2alpha inhibition promotes p53 pathway activity, tumor cell death, and radiation responses. Proc. Natl. Acad. Sci. U. S. A. *106*, 14391–14396.

Bianchi, D. W., Zickwolf, G. K., Weil, G. J., Sylvester, S., and DeMaria, M. A. (1996). Male fetal progenitor cells persist in maternal blood for as long as 27 years postpartum. Proc. Natl. Acad. Sci. U. S. A. *93*, 705–708.

Bidard, F.-C. *et al.* (2014). Clinical validity of circulating tumour cells in patients with metastatic breast cancer: a pooled analysis of individual patient data. Lancet Oncol. *15*, 406–414.

Bidard, F.-C., Weigelt, B., and Reis-Filho, J. S. (2013). Going with the flow: from circulating tumor cells to DNA. Sci. Transl. Med. *5*, 207ps14.

Bobek, V., Kacprzak, G., Rzechonek, A., and Kolostova, K. (2014). Detection and cultivation of circulating tumor cells in malignant pleural mesothelioma. Anticancer Res. *34*, 2565–2569.

Boiko, A. D. (2013). Isolation of melanoma tumor-initiating cells from surgical tissues. Methods Mol. Biol. Clifton NJ *961*, 253–259.

Bolnick, J. M., Kilburn, B. A., Bajpayee, S., Reddy, N., Jeelani, R., Crone, B., Simmerman, N., Singh, M., Diamond, M. P., and Armant, D. R. (2014). Trophoblast retrieval and isolation from the cervix (TRIC) for noninvasive prenatal screening at 5 to 20 weeks of gestation. Fertil. Steril. *102*, 135–142.e6.

Bonnet, D., and Dick, J. E. (1997). Human acute myeloid leukemia is organized as a hierarchy that originates from a primitive hematopoietic cell. Nat. Med. *3*, 730–737.

Boyle, W., and Chow, A. (1969). Isolation of human lymphocytes by a Ficoll barrier method. Transfusion (Paris) *9*, 151–155.

Brabletz, T. (2012). To differentiate or not--routes towards metastasis. Nat. Rev. Cancer *12*, 425–436.

Brabletz, T., Jung, A., Spaderna, S., Hlubek, F., and Kirchner, T. (2005). Opinion: migrating cancer stem cells - an integrated concept of malignant tumour progression. Nat. Rev. Cancer *5*, 744–749.

Braun, S. *et al.* (2005). A pooled analysis of bone marrow micrometastasis in breast cancer. N. Engl. J. Med. *353*, 793–802.

Bredfeldt, J. S., Liu, Y., Conklin, M. W., Keely, P. J., Mackie, T. R., and Eliceiri, K. W. (2014). Automated quantification of aligned collagen for human breast carcinoma prognosis. J. Pathol. Inform. *5*, 28.

Breman, A. M. *et al.* (2016). Evidence for feasibility of fetal trophoblastic cell-based noninvasive prenatal testing. Prenat. Diagn. *36*, 1009–1019.

Brenner, D. A., Waterboer, T., Choi, S. K., Lindquist, J. N., Stefanovic, B., Burchardt, E., Yamauchi, M., Gillan, A., and Rippe, R. A. (2000). New aspects of hepatic fibrosis. J. Hepatol. *32*, 32–38.

Brusselmans, K., Bono, F., Maxwell, P., Dor, Y., Dewerchin, M., Collen, D., Herbert, J. M., and Carmeliet, P. (2001). Hypoxia-inducible factor-2alpha (HIF-2alpha) is involved in the apoptotic response to hypoglycemia but not to hypoxia. J. Biol. Chem. *276*, 39192–39196.

Buenrostro, J. D., Wu, B., Litzenburger, U. M., Ruff, D., Gonzales, M. L., Snyder, M. P., Chang, H. Y., and Greenleaf, W. J. (2015). Single-cell chromatin accessibility reveals principles of regulatory variation. Nature *523*, 486–490.

Buim, M. E. *et al.* (2015). Detection of KRAS mutations in circulating tumor cells from patients with metastatic colorectal cancer. Cancer Biol. Ther. *16*, 1289–1295.

Bulfoni, M. *et al.* (2016). In patients with metastatic breast cancer the identification of circulating tumor cells in epithelial-to-mesenchymal transition is associated with a poor prognosis. Breast Cancer Res. BCR *18*, 30.

Burk, U., Schubert, J., Wellner, U., Schmalhofer, O., Vincan, E., Spaderna, S., and Brabletz, T. (2008). A reciprocal repression between ZEB1 and members of the miR-200 family promotes EMT and invasion in cancer cells. EMBO Rep. *9*, 582–589.

Bussard, K. M., Mutkus, L., Stumpf, K., Gomez-Manzano, C., and Marini, F. C. (2016). Tumor-associated stromal cells as key contributors to the tumor microenvironment. Breast Cancer Res. BCR *18*, 84.

Cabel, L., Proudhon, C., Gortais, H., Loirat, D., Coussy, F., Pierga, J.-Y., and Bidard, F.-C. (2017). Circulating tumor cells: clinical validity and utility. Int. J. Clin. Oncol. *22*, 421–430.

Cairns, J. (1975). Mutation selection and the natural history of cancer. Nature *255*, 197–200.

Calzado-Martín, A., Encinar, M., Tamayo, J., Calleja, M., and San Paulo, A. (2016). Effect of Actin Organization on the Stiffness of Living Breast Cancer Cells Revealed by Peak-Force Modulation Atomic Force Microscopy. ACS Nano *10*, 3365–3374.

Campbell, P. J. *et al.* (2010). The patterns and dynamics of genomic instability in metastatic pancreatic cancer. Nature *467*, 1109–1113.

Cancer Genome Atlas Research Network (2013). Comprehensive molecular characterization of clear cell renal cell carcinoma. Nature *499*, 43–49.

Cao, Z., Bao, M., Miele, L., Sarkar, F. H., Wang, Z., and Zhou, Q. (2013). Tumour vasculogenic mimicry is associated with poor prognosis of human cancer patients: a systemic review and meta-analysis. Eur. J. Cancer Oxf. Engl. 1990 *49*, 3914–3923.

Cayrefourcq, L. *et al.* (2015). Establishment and characterization of a cell line from human circulating colon cancer cells. Cancer Res. *75*, 892–901.

Celià-Terrassa, T. *et al.* (2012). Epithelial-mesenchymal transition can suppress major attributes of human epithelial tumor-initiating cells. J. Clin. Invest. *122*, 1849–1868.

Chaffer, C. L., Brennan, J. P., Slavin, J. L., Blick, T., Thompson, E. W., and Williams, E. D. (2006). Mesenchymal-to-epithelial transition facilitates bladder cancer metastasis: role of fibroblast growth factor receptor-2. Cancer Res. *66*, 11271–11278.

Chang, M.-C. *et al.* (2016). Clinical Significance of Circulating Tumor Microemboli as a Prognostic Marker in Patients with Pancreatic Ductal Adenocarcinoma. Clin. Chem. *62*, 505–513.

Chapman, J. R., Webster, A. C., and Wong, G. (2013). Cancer in the transplant recipient. Cold Spring Harb. Perspect. Med. *3*.

Chen, Z. *et al.* (2017). Cellular and Molecular Identity of Tumor-Associated Macrophages in Glioblastoma. Cancer Res. *77*, 2266–2278.

Cheng, G., Tse, J., Jain, R. K., and Munn, L. L. (2009a). Micro-environmental mechanical stress controls tumor spheroid size and morphology by suppressing proliferation and inducing apoptosis in cancer cells. PloS One *4*, e4632.

Cheng, L., MacLennan, G. T., Zhang, S., Wang, M., Zhou, M., Tan, P.-H., Foster, S., Lopez-Beltran, A., and Montironi, R. (2008). Evidence for polyclonal origin of multifocal clear cell renal cell carcinoma. Clin. Cancer Res. Off. J. Am. Assoc. Cancer Res. *14*, 8087–8093.

Cheng, L., Zhang, S., MacLennan, G. T., Lopez-Beltran, A., and Montironi, R. (2009b). Molecular and cytogenetic insights into the pathogenesis, classification, differential diagnosis, and prognosis of renal epithelial neoplasms. Hum. Pathol. *40*, 10–29.

Cheung, T. H., and Rando, T. A. (2013). Molecular regulation of stem cell quiescence. Nat. Rev. Mol. Cell Biol. *14*, 329–340.

Cima, I. *et al.* (2016). Tumor-derived circulating endothelial cell clusters in colorectal cancer. Sci. Transl. Med. *8*, 345ra89.

Cohen, S. J. *et al.* (2008). Relationship of circulating tumor cells to tumor response, progression-free survival, and overall survival in patients with metastatic colorectal cancer. J. Clin. Oncol. Off. J. Am. Soc. Clin. Oncol. *26*, 3213–3221.

Collins, A. T., Berry, P. A., Hyde, C., Stower, M. J., and Maitland, N. J. (2005). Prospective identification of tumorigenic prostate cancer stem cells. Cancer Res. *65*, 10946–10951.

Collins, V. P., Loeffler, R. K., and Tivey, H. (1956). Observations on growth rates of human tumors. Am. J. Roentgenol. Radium Ther. Nucl. Med. *76*, 988–1000.

Corrò, C. *et al.* (2017). Detecting circulating tumor DNA in renal cancer: An open challenge. Exp. Mol. Pathol. *102*, 255–261.

Coumans, F. A. W., van Dalum, G., Beck, M., and Terstappen, L. W. M. M. (2013). Filter characteristics influencing circulating tumor cell enrichment from whole blood. PloS One *8*, e61770.

Cowey, C. L., and Rathmell, W. K. (2009). VHL gene mutations in renal cell carcinoma: role as a biomarker of disease outcome and drug efficacy. Curr. Oncol. Rep. *11*, 94–101.

Cristofanilli, M. *et al.* (2004). Circulating tumor cells, disease progression, and survival in metastatic breast cancer. N. Engl. J. Med. *351*, 781–791.

Cristofanilli, M. *et al.* (2005). Circulating tumor cells: a novel prognostic factor for newly diagnosed metastatic breast cancer. J. Clin. Oncol. Off. J. Am. Soc. Clin. Oncol. *23*, 1420–1430.

Curley, M. D. *et al.* (2009). CD133 expression defines a tumor initiating cell population in primary human ovarian cancer. Stem Cells Dayt. Ohio *27*, 2875–2883.

Czarnecka, A. M., Kornakiewicz, A., Kukwa, W., and Szczylik, C. (2014). Frontiers in clinical and molecular diagnostics and staging of metastatic clear cell renal cell carcinoma. Future Oncol. Lond. Engl. *10*, 1095–1111.

Dagher, J., Kammerer-Jacquet, S.-F., Dugay, F., Beaumont, M., Lespagnol, A., Cornevin, L., Verhoest, G., Bensalah, K., Rioux-Leclercq, N., and Belaud-Rotureau, M.-A. (2017). Clear cell renal cell carcinoma: a comparative study of histological and chromosomal characteristics between primary tumors and their corresponding metastases. Virchows Arch. Int. J. Pathol.

Danila, D. C. *et al.* (2007). Circulating tumor cell number and prognosis in progressive castration-resistant prostate cancer. Clin. Cancer Res. Off. J. Am. Assoc. Cancer Res. *13*, 7053–7058.

Denève, E., Riethdorf, S., Ramos, J., Nocca, D., Coffy, A., Daurès, J.-P., Maudelonde, T., Fabre, J.-M., Pantel, K., and Alix-Panabières, C. (2013). Capture of viable circulating tumor cells in the liver of colorectal cancer patients. Clin. Chem. *59*, 1384–1392.

Derynck, R., Akhurst, R. J., and Balmain, A. (2001). TGF-beta signaling in tumor suppression and cancer progression. Nat. Genet. *29*, 117–129.

Deryugina, E. I., and Quigley, J. P. (2015). Tumor angiogenesis: MMP-mediated induction of intravasation- and metastasis-sustaining neovasculature. Matrix Biol. J. Int. Soc. Matrix Biol. *44–46*, 94–112.

Dexter, D. L., Kowalski, H. M., Blazar, B. A., Fligiel, Z., Vogel, R., and Heppner, G. H. (1978). Heterogeneity of tumor cells from a single mouse mammary tumor. Cancer Res. *38*, 3174–3181.

Doridot, L., Houry, D., Gaillard, H., Chelbi, S. T., Barbaux, S., and Vaiman, D. (2014). miR-34a expression, epigenetic regulation, and function in human placental diseases. Epigenetics *9*, 142–151.

Doridot, L., Miralles, F., Barbaux, S., and Vaiman, D. (2013). Trophoblasts, invasion, and microRNA. Front. Genet. *4*, 248.

Drummond, C. A. *et al.* (2016). Cigarette smoking causes epigenetic changes associated with cardiorenal fibrosis. Physiol. Genomics *48*, 950–960.

Dumontet, C., and Jordan, M. A. (2010). Microtubule-binding agents: a dynamic field of cancer therapeutics. Nat. Rev. Drug Discov. *9*, 790–803.

Easwaran, H., Tsai, H.-C., and Baylin, S. B. (2014). Cancer epigenetics: tumor heterogeneity, plasticity of stem-like states, and drug resistance. Mol. Cell *54*, 716–727.

El-Heliebi, A. *et al.* (2013). Are morphological criteria sufficient for the identification of circulating tumor cells in renal cancer? J. Transl. Med. *11*, 214.

Erdogan, B., and Webb, D. J. (2017). Cancer-associated fibroblasts modulate growth factor signaling and extracellular matrix remodeling to regulate tumor metastasis. Biochem. Soc. Trans. *45*, 229–236.

Faas, B. H. W., de Ligt, J., Janssen, I., Eggink, A. J., Wijnberger, L. D. E., van Vugt, J. M. G., Vissers, L., and Geurts van Kessel, A. (2012). Non-invasive prenatal diagnosis of fetal aneuploidies using massively parallel sequencing-by-ligation and evidence that cell-free fetal DNA in the maternal plasma originates from cytotrophoblastic cells. Expert Opin. Biol. Ther. *12 Suppl 1*, S19-26.

Fabbri, F. *et al.* (2013). Detection and recovery of circulating colon cancer cells using a dielectrophoresis-based device: KRAS mutation status in pure CTCs. Cancer Lett. *335*, 225–231.

Fadini, G. P., Ciciliot, S., and Albiero, M. (2017). Concise Review: Perspectives and Clinical Implications of Bone Marrow and Circulating Stem Cell Defects in Diabetes. Stem Cells Dayt. Ohio *35*, 106–116.

Farace, F. *et al.* (2011). A direct comparison of CellSearch and ISET for circulating tumour-cell detection in patients with metastatic carcinomas. Br. J. Cancer *105*, 847–853.

Faugeroux, V., Pailler, E., Auger, N., Taylor, M., and Farace, F. (2014). Clinical Utility of Circulating Tumor Cells in ALK-Positive Non-Small-Cell Lung Cancer. Front. Oncol. *4*, 281.

Fidler, I. J. (1975). Biological behavior of malignant melanoma cells correlated to their survival in vivo. Cancer Res. *35*, 218–224.

Fidler, I. J. (2003). The pathogenesis of cancer metastasis: the "seed and soil" hypothesis revisited. Nat. Rev. Cancer *3*, 453–458.

Fischer, A. N. M., Fuchs, E., Mikula, M., Huber, H., Beug, H., and Mikulits, W. (2007). PDGF essentially links TGF-beta signaling to nuclear beta-catenin accumulation in hepatocellular carcinoma progression. Oncogene *26*, 3395–3405.

Fong, M. Y. *et al.* (2015). Breast-cancer-secreted miR-122 reprograms glucose metabolism in premetastatic niche to promote metastasis. Nat. Cell Biol. *17*, 183–194.

Forman, J. R., Worth, C. L., Bickerton, G. R. J., Eisen, T. G., and Blundell, T. L. (2009). Structural bioinformatics mutation analysis reveals genotype-phenotype correlations in von Hippel-Lindau disease and suggests molecular mechanisms of tumorigenesis. Proteins *77*, 84–96.

Franco, D. L., Mainez, J., Vega, S., Sancho, P., Murillo, M. M., de Frutos, C. A., Del Castillo, G., López-Blau, C., Fabregat, I., and Nieto, M. A. (2010). Snail1 suppresses TGF-beta-induced apoptosis and is sufficient to trigger EMT in hepatocytes. J. Cell Sci. *123*, 3467–3477.

Frew, I. J., and Moch, H. (2015). A clearer view of the molecular complexity of clear cell renal cell carcinoma. Annu. Rev. Pathol. *10*, 263–289.

Friedl, P., and Wolf, K. (2010). Plasticity of cell migration: a multiscale tuning model. J. Cell Biol.

188, 11–19.

Furuse, M. (2010). Molecular basis of the core structure of tight junctions. Cold Spring Harb. Perspect. Biol. *2*, a002907.

Gaggioli, C., Hooper, S., Hidalgo-Carcedo, C., Grosse, R., Marshall, J. F., Harrington, K., and Sahai, E. (2007). Fibroblast-led collective invasion of carcinoma cells with differing roles for RhoGTPases in leading and following cells. Nat. Cell Biol. *9*, 1392–1400.

Gallou, C. *et al.* (1999). Mutations of the VHL gene in sporadic renal cell carcinoma: definition of a risk factor for VHL patients to develop an RCC. Hum. Mutat. *13*, 464–475.

Gallou, C. *et al.* (2001). Association of GSTT1 non-null and NAT1 slow/rapid genotypes with von Hippel-Lindau tumour suppressor gene transversions in sporadic renal cell carcinoma. Pharmacogenetics *11*, 521–535.

Gama-Sosa, M. A., Slagel, V. A., Trewyn, R. W., Oxenhandler, R., Kuo, K. C., Gehrke, C. W., and Ehrlich, M. (1983). The 5-methylcytosine content of DNA from human tumors. Nucleic Acids Res. *11*, 6883–6894.

Gao, D. *et al.* (2014). Organoid cultures derived from patients with advanced prostate cancer. Cell *159*, 176–187.

Gao, H., Chakraborty, G., Lee-Lim, A. P., Mo, Q., Decker, M., Vonica, A., Shen, R., Brogi, E., Brivanlou, A. H., and Giancotti, F. G. (2012). The BMP inhibitor Coco reactivates breast cancer cells at lung metastatic sites. Cell *150*, 764–779.

Gao, W., Li, W., Xiao, T., Liu, X. S., and Kaelin, W. G. (2017a). Inactivation of the PBRM1 tumor suppressor gene amplifies the HIF-response in VHL-/- clear cell renal carcinoma. Proc. Natl. Acad. Sci. U. S. A. *114*, 1027–1032.

Gao, Y. *et al.* (2017b). Single-cell sequencing deciphers a convergent evolution of copy number alterations from primary to circulating tumour cells. Genome Res.

Gasic, G. J., Gasic, T. B., and Stewart, C. C. (1968). Antimetastatic effects associated with platelet reduction. Proc. Natl. Acad. Sci. U. S. A. *61*, 46–52.

Gatenby, R. A., and Vincent, T. L. (2003). An evolutionary model of carcinogenesis. Cancer Res. *63*, 6212–6220.

Gay, L. J., and Felding-Habermann, B. (2011). Contribution of platelets to tumour metastasis. Nat. Rev. Cancer *11*, 123–134.

Georgoulias, V., Bozionelou, V., Agelaki, S., Perraki, M., Apostolaki, S., Kallergi, G., Kalbakis, K., Xyrafas, A., and Mavroudis, D. (2012). Trastuzumab decreases the incidence of clinical relapses in patients with early breast cancer presenting chemotherapy-resistant CK-19mRNA-positive circulating tumor cells: results of a randomized phase II study. Ann. Oncol. Off. J. Eur. Soc. Med. Oncol. *23*, 1744–1750.

Gerlinger, M. *et al.* (2012). Intratumor heterogeneity and branched evolution revealed by multiregion sequencing. N. Engl. J. Med. *366*, 883–892.

Gerlinger, M. *et al.* (2014). Genomic architecture and evolution of clear cell renal cell carcinomas defined by multiregion sequencing. Nat. Genet. *46*, 225–233.

Gerstung, M., Beisel, C., Rechsteiner, M., Wild, P., Schraml, P., Moch, H., and Beerenwinkel, N. (2012). Reliable detection of subclonal single-nucleotide variants in tumour cell populations. Nat. Commun. *3*, 811.

Ghajar, C. M. *et al.* (2013). The perivascular niche regulates breast tumour dormancy. Nat. Cell Biol. *15*, 807–817.

Giampieri, S., Manning, C., Hooper, S., Jones, L., Hill, C. S., and Sahai, E. (2009). Localized and reversible TGFbeta signalling switches breast cancer cells from cohesive to single cell motility. Nat. Cell Biol. *11*, 1287–1296.

Godinho, S. A., Picone, R., Burute, M., Dagher, R., Su, Y., Leung, C. T., Polyak, K., Brugge, J. S., Théry, M., and Pellman, D. (2014). Oncogene-like induction of cellular invasion from centrosome amplification. Nature *510*, 167–171.

Goelz, S. E., Vogelstein, B., Hamilton, S. R., and Feinberg, A. P. (1985). Hypomethylation of DNA from benign and malignant human colon neoplasms. Science *228*, 187–190.

Gordan, J. D. *et al.* (2008). HIF-alpha effects on c-Myc distinguish two subtypes of sporadic VHL-deficient clear cell renal carcinoma. Cancer Cell *14*, 435–446.

Gossage, L., Eisen, T., and Maher, E. R. (2015). VHL, the story of a tumour suppressor gene. Nat. Rev. Cancer *15*, 55–64.

Gossage, L., Pires, D. E. V., Olivera-Nappa, Á., Asenjo, J., Bycroft, M., Blundell, T. L., and Eisen, T. (2014a). An integrated computational approach can classify VHL missense mutations according to risk of clear cell renal carcinoma. Hum. Mol. Genet. *23*, 5976–5988.

Gossage, L., Pires, D. E. V., Olivera-Nappa, Á., Asenjo, J., Bycroft, M., Blundell, T. L., and Eisen, T. (2014b). An integrated computational approach can classify VHL missense mutations according to risk of clear cell renal carcinoma. Hum. Mol. Genet. *23*, 5976–5988.

Goswami, S., Sahai, E., Wyckoff, J. B., Cammer, M., Cox, D., Pixley, F. J., Stanley, E. R., Segall, J. E., and Condeelis, J. S. (2005). Macrophages promote the invasion of breast carcinoma cells via a colony-stimulating factor-1/epidermal growth factor paracrine loop. Cancer Res. *65*, 5278–5283.

Gradilone, A. *et al.* (2011). Circulating tumor cells and "suspicious objects" evaluated through CellSearch® in metastatic renal cell carcinoma. Anticancer Res. *31*, 4219–4221.

Grange, C., Tapparo, M., Collino, F., Vitillo, L., Damasco, C., Deregibus, M. C., Tetta, C., Bussolati, B., and Camussi, G. (2011). Microvesicles released from human renal cancer stem cells stimulate angiogenesis and formation of lung premetastatic niche. Cancer Res. *71*, 5346–5356.

Greenberg, J. I. *et al.* (2008). A role for VEGF as a negative regulator of pericyte function and vessel maturation. Nature *456*, 809–813.

Grillet, F. *et al.* (2016). Circulating tumour cells from patients with colorectal cancer have cancer stem cell hallmarks in ex vivo culture. Gut.

Grosse-Gehling, P., Fargeas, C. A., Dittfeld, C., Garbe, Y., Alison, M. R., Corbeil, D., and Kunz-Schughart, L. A. (2013). CD133 as a biomarker for putative cancer stem cells in solid tumours: limitations, problems and challenges. J. Pathol. *229*, 355–378.

Grozovsky, R., Giannini, S., Falet, H., and Hoffmeister, K. M. (2015). Regulating billions of blood

platelets: glycans and beyond. Blood *126*, 1877–1884.

Guck, J. *et al.* (2005). Optical deformability as an inherent cell marker for testing malignant transformation and metastatic competence. Biophys. J. *88*, 3689–3698.

Gulati, S. *et al.* (2014). Systematic evaluation of the prognostic impact and intratumour heterogeneity of clear cell renal cell carcinoma biomarkers. Eur. Urol. *66*, 936–948.

Hadfield, G. (1954). The dormant cancer cell. Br. Med. J. *2*, 607–610.

Hahn, S., Huppertz, B., and Holzgreve, W. (2005). Fetal cells and cell free fetal nucleic acids in maternal blood: new tools to study abnormal placentation? Placenta *26*, 515–526.

Han, W. *et al.* (2016). Oriented collagen fibers direct tumor cell intravasation. Proc. Natl. Acad. Sci. U. S. A. *113*, 11208–11213.

Han, X., Wang, J., and Sun, Y. (2017). Circulating Tumor DNA as Biomarkers for Cancer Detection. Genomics Proteomics Bioinformatics *15*, 59–72.

Hannan, N. J., Jones, R. L., White, C. A., and Salamonsen, L. A. (2006). The chemokines, CX3CL1, CCL14, and CCL4, promote human trophoblast migration at the feto-maternal interface. Biol. Reprod. *74*, 896–904.

Harney, A. S., Arwert, E. N., Entenberg, D., Wang, Y., Guo, P., Qian, B.-Z., Oktay, M. H., Pollard, J. W., Jones, J. G., and Condeelis, J. S. (2015). Real-Time Imaging Reveals Local, Transient Vascular Permeability, and Tumor Cell Intravasation Stimulated by TIE2hi Macrophage-Derived VEGFA. Cancer Discov. *5*, 932–943.

Harouaka, R. A., Nisic, M., and Zheng, S.-Y. (2013). Circulating tumor cell enrichment based on physical properties. J. Lab. Autom. *18*, 455–468.

Harouaka, R., Kang, Z., Zheng, S.-Y., and Cao, L. (2014). Circulating tumor cells: advances in isolation and analysis, and challenges for clinical applications. Pharmacol. Ther. *141*, 209–221.

Hayata, K., Hiramatsu, Y., Masuyama, H., Eto, E., Mitsui, T., and Tamada, S. (2017). Discrepancy between Non-invasive Prenatal Genetic Testing (NIPT) and Amniotic Chromosomal Test due to Placental Mosaicism: A Case Report and Literature Review. Acta Med. Okayama *71*, 181–185.

Heise, R. L., Link, P. A., and Farkas, L. (2016). From Here to There, Progenitor Cells and Stem Cells Are Everywhere in Lung Vascular Remodeling. Front. Pediatr. *4*, 80.

Hiratsuka, S., Watanabe, A., Aburatani, H., and Maru, Y. (2006). Tumour-mediated upregulation of chemoattractants and recruitment of myeloid cells predetermines lung metastasis. Nat. Cell Biol. *8*, 1369–1375.

Hobor, S., Van Emburgh, B. O., Crowley, E., Misale, S., Di Nicolantonio, F., and Bardelli, A. (2014). TGFα and amphiregulin paracrine network promotes resistance to EGFR blockade in colorectal cancer cells. Clin. Cancer Res. Off. J. Am. Assoc. Cancer Res. *20*, 6429–6438.

Hodgkinson, C. L. *et al.* (2014). Tumorigenicity and genetic profiling of circulating tumor cells in small-cell lung cancer. Nat. Med. *20*, 897–903.

Hofman, V. *et al.* (2011a). Preoperative circulating tumor cell detection using the isolation by size of epithelial tumor cell method for patients with lung cancer is a new prognostic biomarker. Clin.

Cancer Res. Off. J. Am. Assoc. Cancer Res. *17*, 827–835.

Hofman, V. *et al.* (2012). Morphological analysis of circulating tumour cells in patients undergoing surgery for non-small cell lung carcinoma using the isolation by size of epithelial tumour cell (ISET) method. Cytopathol. Off. J. Br. Soc. Clin. Cytol. *23*, 30–38.

Hofman, V. *et al.* (2013). Usefulness of immunocytochemistry for the detection of the BRAF(V600E) mutation in circulating tumor cells from metastatic melanoma patients. J. Invest. Dermatol. *133*, 1378–1381.

Hofman, V. *et al.* (2014). Detection of circulating tumor cells from lung cancer patients in the era of targeted therapy: promises, drawbacks and pitfalls. Curr. Mol. Med. *14*, 440–456.

Hofman, V., Ilie, M. I., Long, E., Selva, E., Bonnetaud, C., Molina, T., Vénissac, N., Mouroux, J., Vielh, P., and Hofman, P. (2011b). Detection of circulating tumor cells as a prognostic factor in patients undergoing radical surgery for non-small-cell lung carcinoma: comparison of the efficacy of the CellSearch Assay™ and the isolation by size of epithelial tumor cell method. Int. J. Cancer *129*, 1651–1660.

Hofman, V. J. *et al.* (2011c). Cytopathologic detection of circulating tumor cells using the isolation by size of epithelial tumor cell method: promises and pitfalls. Am. J. Clin. Pathol. *135*, 146–156.

Hofman, V. J., Ilie, M., and Hofman, P. M. (2016). Detection and characterization of circulating tumor cells in lung cancer: Why and how? Cancer Cytopathol. *124*, 380–387.

Holmgren, L., Szeles, A., Rajnavölgyi, E., Folkman, J., Klein, G., Ernberg, I., and Falk, K. I. (1999). Horizontal transfer of DNA by the uptake of apoptotic bodies. Blood *93*, 3956–3963.

Hoshino, A. *et al.* (2015). Tumour exosome integrins determine organotropic metastasis. Nature *527*, 329–335.

Hou, J.-M. *et al.* (2012). Clinical significance and molecular characteristics of circulating tumor cells and circulating tumor microemboli in patients with small-cell lung cancer. J. Clin. Oncol. Off. J. Am. Soc. Clin. Oncol. *30*, 525–532.

Hsieh, J. J., Purdue, M. P., Signoretti, S., Swanton, C., Albiges, L., Schmidinger, M., Heng, D. Y., Larkin, J., and Ficarra, V. (2017). Renal cell carcinoma. Nat. Rev. Dis. Primer *3*, 17009.

Hu, W., Wang, T., Yang, Y., and Zheng, S. (2015). Tumor heterogeneity uncovered by dynamic expression of long noncoding RNA at single-cell resolution. Cancer Genet. *208*, 581–586.

Huang, X., Gao, P., Song, Y., Sun, J., Chen, X., Zhao, J., Xu, H., and Wang, Z. (2015). Meta-analysis of the prognostic value of circulating tumor cells detected with the CellSearch System in colorectal cancer. BMC Cancer *15*, 202.

Hughes, R. C. (2001). Galectins as modulators of cell adhesion. Biochimie *83*, 667–676.

Hunkapiller, N. M., and Fisher, S. J. (2008). Chapter 12. Placental remodeling of the uterine vasculature. Methods Enzymol. *445*, 281–302.

Hüsemann, Y. *et al.* (2008). Systemic spread is an early step in breast cancer. Cancer Cell *13*, 58–68.

Hwang, I., Kim, J., and Jeong, S. (2012). β-Catenin and peroxisome proliferator-activated

receptor-δ coordinate dynamic chromatin loops for the transcription of vascular endothelial growth factor A gene in colon cancer cells. J. Biol. Chem. *287*, 41364–41373.

Ilie, M. *et al.* (2012). ALK-gene rearrangement: a comparative analysis on circulating tumour cells and tumour tissue from patients with lung adenocarcinoma. Ann. Oncol. Off. J. Eur. Soc. Med. Oncol. *23*, 2907–2913.

Ilie, M., Hofman, V., Long-Mira, E., Selva, E., Vignaud, J.-M., Padovani, B., Mouroux, J., Marquette, C.-H., and Hofman, P. (2014). "Sentinel" circulating tumor cells allow early diagnosis of lung cancer in patients with chronic obstructive pulmonary disease. PloS One *9*, e111597.

Imudia, A. N., Suzuki, Y., Kilburn, B. A., Yelian, F. D., Diamond, M. P., Romero, R., and Armant, D. R. (2009). Retrieval of trophoblast cells from the cervical canal for prediction of abnormal pregnancy: a pilot study. Hum. Reprod. Oxf. Engl. *24*, 2086–2092.

Inda, M.-M. *et al.* (2010). Tumor heterogeneity is an active process maintained by a mutant EGFR-induced cytokine circuit in glioblastoma. Genes Dev. *24*, 1731–1745.

Islam, F., Gopalan, V., Smith, R. A., and Lam, A. K.-Y. (2015). Translational potential of cancer stem cells: A review of the detection of cancer stem cells and their roles in cancer recurrence and cancer treatment. Exp. Cell Res. *335*, 135–147.

Jacobsen, B. M., Harrell, J. C., Jedlicka, P., Borges, V. F., Varella-Garcia, M., and Horwitz, K. B. (2006). Spontaneous fusion with, and transformation of mouse stroma by, malignant human breast cancer epithelium. Cancer Res. *66*, 8274–8279.

Jain, C. V. *et al.* (2016). Fetal genome profiling at 5 weeks of gestation after noninvasive isolation of trophoblast cells from the endocervical canal. Sci. Transl. Med. *8*, 363re4.

Janatpour, M. J., McMaster, M. T., Genbacev, O., Zhou, Y., Dong, J., Cross, J. C., Israel, M. A., and Fisher, S. J. (2000). Id-2 regulates critical aspects of human cytotrophoblast differentiation, invasion and migration. Dev. Camb. Engl. *127*, 549–558.

Jolly, M. K., Tripathi, S. C., Jia, D., Mooney, S. M., Celiktas, M., Hanash, S. M., Mani, S. A., Pienta, K. J., Ben-Jacob, E., and Levine, H. (2016). Stability of the hybrid epithelial/mesenchymal phenotype. Oncotarget *7*, 27067–27084.

Joosse, S. A., Gorges, T. M., and Pantel, K. (2015). Biology, detection, and clinical implications of circulating tumor cells. EMBO Mol. Med. *7*, 1–11.

Joyce, J. A., and Pollard, J. W. (2009). Microenvironmental regulation of metastasis. Nat. Rev. Cancer *9*, 239–252.

Kanno, H., Shuin, T., Kondo, K., Yamamoto, I., Ito, S., Shinonaga, M., Yoshida, M., and Yao, M. (1997). Somatic mutations of the von Hippel-Lindau tumor suppressor gene and loss of heterozygosity on chromosome 3p in human glial tumors. Cancer Res. *57*, 1035–1038.

Kaplan, R. N. *et al.* (2005). VEGFR1-positive haematopoietic bone marrow progenitors initiate the pre-metastatic niche. Nature *438*, 820–827.

Karpinich, N. O., and Caron, K. M. (2015). Gap junction coupling is required for tumor cell migration through lymphatic endothelium. Arterioscler. Thromb. Vasc. Biol. *35*, 1147–1155.

Karrison, T. G., Ferguson, D. J., and Meier, P. (1999). Dormancy of mammary carcinoma after

mastectomy. J. Natl. Cancer Inst. *91*, 80–85.

Kartenbeck, J., Schmelz, M., Franke, W. W., and Geiger, B. (1991). Endocytosis of junctional cadherins in bovine kidney epithelial (MDBK) cells cultured in low Ca2+ ion medium. J. Cell Biol. *113*, 881–892.

Kats-Ugurlu, G. *et al.* (2009). Circulating tumour tissue fragments in patients with pulmonary metastasis of clear cell renal cell carcinoma. J. Pathol. *219*, 287–293.

Keith, B., Johnson, R. S., and Simon, M. C. (2011). HIF1α and HIF2α: sibling rivalry in hypoxic tumour growth and progression. Nat. Rev. Cancer *12*, 9–22.

Kervancioglu Demirci, E., Salamonsen, L. A., and Gauster, M. (2016). The role of CX3CL1 in fetal-maternal interaction during human gestation. Cell Adhes. Migr. *10*, 189–196.

Khoja, L. *et al.* (2012). A pilot study to explore circulating tumour cells in pancreatic cancer as a novel biomarker. Br. J. Cancer *106*, 508–516.

Khoja, L., Shenjere, P., Hodgson, C., Hodgetts, J., Clack, G., Hughes, A., Lorigan, P., and Dive, C. (2014). Prevalence and heterogeneity of circulating tumour cells in metastatic cutaneous melanoma. Melanoma Res. *24*, 40–46.

Khoo, B. L., Chaudhuri, P. K., Ramalingam, N., Tan, D. S. W., Lim, C. T., and Warkiani, M. E. (2016). Single-cell profiling approaches to probing tumor heterogeneity. Int. J. Cancer *139*, 243–255.

Khoo, B. L., Lee, S. C., Kumar, P., Tan, T. Z., Warkiani, M. E., Ow, S. G. W., Nandi, S., Lim, C. T., and Thiery, J. P. (2015). Short-term expansion of breast circulating cancer cells predicts response to anti-cancer therapy. Oncotarget *6*, 15578–15593.

Kienast, Y., von Baumgarten, L., Fuhrmann, M., Klinkert, W. E. F., Goldbrunner, R., Herms, J., and Winkler, F. (2010). Real-time imaging reveals the single steps of brain metastasis formation. Nat. Med. *16*, 116–122.

Kim, B. J., Kim, J. H., Kim, H. S., and Zang, D. Y. (2017). Prognostic and predictive value of VHL gene alteration in renal cell carcinoma: a meta-analysis and review. Oncotarget *8*, 13979–13985.

Kim, K.-T. *et al.* (2016). Application of single-cell RNA sequencing in optimizing a combinatorial therapeutic strategy in metastatic renal cell carcinoma. Genome Biol. *17*, 80.

Kim, M.-Y., Oskarsson, T., Acharyya, S., Nguyen, D. X., Zhang, X. H.-F., Norton, L., and Massagué, J. (2009). Tumor self-seeding by circulating cancer cells. Cell *139*, 1315–1326.

Kim, N. H. *et al.* (2011). p53 and microRNA-34 are suppressors of canonical Wnt signaling. Sci. Signal. *4*, ra71.

Kim, T.-J., Zheng, S., Sun, J., Muhamed, I., Wu, J., Lei, L., Kong, X., Leckband, D. E., and Wang, Y. (2015). Dynamic visualization of α-catenin reveals rapid, reversible conformation switching between tension states. Curr. Biol. CB *25*, 218–224.

Kim, W.-T., and Ryu, C. J. (2017). Cancer stem cell surface markers on normal stem cells. BMB Rep. *50*, 285–298.

Kishida, T., Stackhouse, T. M., Chen, F., Lerman, M. I., and Zbar, B. (1995). Cellular proteins that

bind the von Hippel-Lindau disease gene product: mapping of binding domains and the effect of missense mutations. Cancer Res. *55*, 4544–4548.

Klein, C. A. *et al.* (2002). Combined transcriptome and genome analysis of single micrometastatic cells. Nat. Biotechnol. *20*, 387–392.

Klein, C. A. (2009). Parallel progression of primary tumours and metastases. Nat. Rev. Cancer *9*, 302–312.

Klein, C. A. (2011). Framework models of tumor dormancy from patient-derived observations. Curr. Opin. Genet. Dev. *21*, 42–49.

Kleinsmith, L. J., and Pierce, G. B. (1964). MULTIPOTENTIALITY OF SINGLE EMBRYONAL CARCINOMA CELLS. Cancer Res. *24*, 1544–1551.

Kolostova, K., Zhang, Y., Hoffman, R. M., and Bobek, V. (2014). In vitro culture and characterization of human lung cancer circulating tumor cells isolated by size exclusion from an orthotopic nude-mouse model expressing fluorescent protein. J. Fluoresc. *24*, 1531–1536.

Kølvraa, S. *et al.* (2016). Genome-wide copy number analysis on DNA from fetal cells isolated from the blood of pregnant women. Prenat. Diagn. *36*, 1127–1134.

Kondo, K. *et al.* (2002a). Comprehensive mutational analysis of the VHL gene in sporadic renal cell carcinoma: relationship to clinicopathological parameters. Genes. Chromosomes Cancer *34*, 58–68.

Kondo, K., Klco, J., Nakamura, E., Lechpammer, M., and Kaelin, W. G. (2002b). Inhibition of HIF is necessary for tumor suppression by the von Hippel-Lindau protein. Cancer Cell *1*, 237–246.

Kong, D., Wang, Z., Sarkar, S. H., Li, Y., Banerjee, S., Saliganan, A., Kim, H.-R. C., Cher, M. L., and Sarkar, F. H. (2008). Platelet-derived growth factor-D overexpression contributes to epithelial-mesenchymal transition of PC3 prostate cancer cells. Stem Cells Dayt. Ohio *26*, 1425–1435.

Kopp, H.-G., Placke, T., and Salih, H. R. (2009). Platelet-derived transforming growth factor-beta down-regulates NKG2D thereby inhibiting natural killer cell antitumor reactivity. Cancer Res. *69*, 7775–7783.

Koury, J., Zhong, L., and Hao, J. (2017). Targeting Signaling Pathways in Cancer Stem Cells for Cancer Treatment. Stem Cells Int. *2017*, 2925869.

Krabchi, K., Gadji, M., Samassekou, O., Grégoire, M.-C., Forest, J.-C., and Drouin, R. (2006). Quantification of fetal nucleated cells in maternal blood of pregnant women with a male trisomy 21 fetus using molecular cytogenetic techniques. Prenat. Diagn. *26*, 28–34.

Krawczyk, W. S. (1971). A pattern of epidermal cell migration during wound healing. J. Cell Biol. *49*, 247–263.

Krebs, M. G. *et al.* (2011). Evaluation and prognostic significance of circulating tumor cells in patients with non-small-cell lung cancer. J. Clin. Oncol. Off. J. Am. Soc. Clin. Oncol. *29*, 1556–1563.

Krebs, M. G. *et al.* (2012). Analysis of circulating tumor cells in patients with non-small cell lung cancer using epithelial marker-dependent and -independent approaches. J. Thorac. Oncol. Off. Publ. Int. Assoc. Study Lung Cancer *7*, 306–315.

Krebs, M. G. *et al.* (2015). Circulating Tumor Cell Enumeration in a Phase II Trial of a Four-Drug Regimen in Advanced Colorectal Cancer. Clin. Colorectal Cancer *14*, 115-122.e1-2.

Krivacic, R. T. *et al.* (2004). A rare-cell detector for cancer. Proc. Natl. Acad. Sci. U. S. A. *101*, 10501–10504.

Kubo, N., Araki, K., Kuwano, H., and Shirabe, K. (2016). Cancer-associated fibroblasts in hepatocellular carcinoma. World J. Gastroenterol. *22*, 6841–6850.

Kudo-Saito, C., Shirako, H., Takeuchi, T., and Kawakami, Y. (2009). Cancer metastasis is accelerated through immunosuppression during Snail-induced EMT of cancer cells. Cancer Cell *15*, 195–206.

Kukulski, F., Ben Yebdri, F., Bahrami, F., Fausther, M., Tremblay, A., and Sévigny, J. (2010). Endothelial P2Y2 receptor regulates LPS-induced neutrophil transendothelial migration in vitro. Mol. Immunol. *47*, 991–999.

Kuperwasser, C., Chavarria, T., Wu, M., Magrane, G., Gray, J. W., Carey, L., Richardson, A., and Weinberg, R. A. (2004). Reconstruction of functionally normal and malignant human breast tissues in mice. Proc. Natl. Acad. Sci. U. S. A. *101*, 4966–4971.

Kurrey, N. K., Jalgaonkar, S. P., Joglekar, A. V., Ghanate, A. D., Chaskar, P. D., Doiphode, R. Y., and Bapat, S. A. (2009). Snail and slug mediate radioresistance and chemoresistance by antagonizing p53-mediated apoptosis and acquiring a stem-like phenotype in ovarian cancer cells. Stem Cells Dayt. Ohio *27*, 2059–2068.

Küsters, B., Kats, G., Roodink, I., Verrijp, K., Wesseling, P., Ruiter, D. J., de Waal, R. M. W., and Leenders, W. P. J. (2007). Micronodular transformation as a novel mechanism of VEGF-A-induced metastasis. Oncogene *26*, 5808–5815.

Kuthi, L., Jenei, A., Hajdu, A., Németh, I., Varga, Z., Bajory, Z., Pajor, L., and Iványi, B. (2017). Prognostic Factors for Renal Cell Carcinoma Subtypes Diagnosed According to the 2016 WHO Renal Tumor Classification: a Study Involving 928 Patients. Pathol. Oncol. Res. POR *23*, 689–698.

Labelle, M., Begum, S., and Hynes, R. O. (2011). Direct signaling between platelets and cancer cells induces an epithelial-mesenchymal-like transition and promotes metastasis. Cancer Cell *20*, 576–590.

Labernadie, A. *et al.* (2017). A mechanically active heterotypic E-cadherin/N-cadherin adhesion enables fibroblasts to drive cancer cell invasion. Nat. Cell Biol. *19*, 224–237.

Laget, S., Broncy, L., Hormigos, K., Dhingra, D. M., BenMohamed, F., Capiod, T., Osteras, M., Farinelli, L., Jackson, S., and Paterlini-Bréchot, P. (2017). Technical Insights into Highly Sensitive Isolation and Molecular Characterization of Fixed and Live Circulating Tumor Cells for Early Detection of Tumor Invasion. PloS One *12*, e0169427.

Latif, F., Tory, K., Gnarra, J., Yao, M., Duh, F. M., Orcutt, M. L., Stackhouse, T., Kuzmin, I., Modi, W., and Geil, L. (1993). Identification of the von Hippel-Lindau disease tumor suppressor gene. Science *260*, 1317–1320.

Lau, K. W., Tian, Y.-M., Raval, R. R., Ratcliffe, P. J., and Pugh, C. W. (2007). Target gene selectivity of hypoxia-inducible factor-alpha in renal cancer cells is conveyed by post-DNA-binding mechanisms. Br. J. Cancer *96*, 1284–1292.

Lawson, M. A. *et al.* (2015). Osteoclasts control reactivation of dormant myeloma cells by remodelling the endosteal niche. Nat. Commun. *6*, 8983.

Lecharpentier, A., Vielh, P., Perez-Moreno, P., Planchard, D., Soria, J. C., and Farace, F. (2011). Detection of circulating tumour cells with a hybrid (epithelial/mesenchymal) phenotype in patients with metastatic non-small cell lung cancer. Br. J. Cancer *105*, 1338–1341.

Lee, H.-O., Mullins, S. R., Franco-Barraza, J., Valianou, M., Cukierman, E., and Cheng, J. D. (2011). FAP-overexpressing fibroblasts produce an extracellular matrix that enhances invasive velocity and directionality of pancreatic cancer cells. BMC Cancer *11*, 245.

Lench, N., Barrett, A., Fielding, S., McKay, F., Hill, M., Jenkins, L., White, H., and Chitty, L. S. (2013). The clinical implementation of non-invasive prenatal diagnosis for single-gene disorders: challenges and progress made. Prenat. Diagn. *33*, 555–562.

Leonardi, E., Murgia, A., and Tosatto, S. C. E. (2009). Adding structural information to the von Hippel-Lindau (VHL) tumor suppressor interaction network. FEBS Lett. *583*, 3704–3710.

Li, C., Heidt, D. G., Dalerba, P., Burant, C. F., Zhang, L., Adsay, V., Wicha, M., Clarke, M. F., and Simeone, D. M. (2007). Identification of pancreatic cancer stem cells. Cancer Res. *67*, 1030–1037.

Li, H., Ma, S.-Q., Huang, J., Chen, X.-P., and Zhou, H.-H. (2017a). Roles of long noncoding RNAs in colorectal cancer metastasis. Oncotarget *8*, 39859–39876.

Li, J., Guo, L., and Ai, Z. (2017b). An integrated analysis of cancer genes in clear cell renal cell carcinoma. Future Oncol. Lond. Engl. *13*, 715–725.

Li, L. *et al.* (2016). Exosomes Derived from Hypoxic Oral Squamous Cell Carcinoma Cells Deliver miR-21 to Normoxic Cells to Elicit a Prometastatic Phenotype. Cancer Res. *76*, 1770–1780.

Li, Q.-Q., Xu, J.-D., Wang, W.-J., Cao, X.-X., Chen, Q., Tang, F., Chen, Z.-Q., Liu, X.-P., and Xu, Z.-D. (2009). Twist1-mediated adriamycin-induced epithelial-mesenchymal transition relates to multidrug resistance and invasive potential in breast cancer cells. Clin. Cancer Res. Off. J. Am. Assoc. Cancer Res. *15*, 2657–2665.

Liang, Y.-C., Lin, W.-C., Lin, Y.-J., and Lin, J.-C. (2015). The impact of RNA binding motif protein 4-regulated splicing cascade on the progression and metabolism of colorectal cancer cells. Oncotarget *6*, 38046–38060.

Ligon, L. A., and Holzbaur, E. L. F. (2007). Microtubules tethered at epithelial cell junctions by dynein facilitate efficient junction assembly. Traffic Cph. Den. *8*, 808–819.

de Ligt, J., Veltman, J. A., and Vissers, L. E. L. M. (2013). Point mutations as a source of de novo genetic disease. Curr. Opin. Genet. Dev. *23*, 257–263.

Lin, H. K. *et al.* (2010). Portable filter-based microdevice for detection and characterization of circulating tumor cells. Clin. Cancer Res. Off. J. Am. Assoc. Cancer Res. *16*, 5011–5018.

Linde, N., Fluegen, G., and Aguirre-Ghiso, J. A. (2016). The Relationship Between Dormant Cancer Cells and Their Microenvironment. Adv. Cancer Res. *132*, 45–71.

Linehan, W. M., Srinivasan, R., and Schmidt, L. S. (2010). The genetic basis of kidney cancer: a metabolic disease. Nat. Rev. Urol. *7*, 277–285.

Liu, M. Y., Poellinger, L., and Walker, C. L. (2003). Up-regulation of hypoxia-inducible factor 2alpha in renal cell carcinoma associated with loss of Tsc-2 tumor suppressor gene. Cancer Res. *63*, 2675–2680.

Liu, Z.-L., Wang, C., Chen, H.-J., Li, X., Dai, L.-J., and Ding, Z.-Y. (2017). Bone metastasis from lung cancer identified by genetic profiling. Oncol. Lett. *13*, 847–850.

Lo, Y. M., Corbetta, N., Chamberlain, P. F., Rai, V., Sargent, I. L., Redman, C. W., and Wainscoat, J. S. (1997). Presence of fetal DNA in maternal plasma and serum. Lancet Lond. Engl. *350*, 485–487.

Lobastova, L., Kraus, D., Glassmann, A., Khan, D., Steinhäuser, C., Wolff, C., Veit, N., Winter, J., and Probstmeier, R. (2017). Collective cell migration of thyroid carcinoma cells: a beneficial ability to override unfavourable substrates. Cell. Oncol. Dordr. *40*, 63–76.

Long, E. *et al.* (2016). High expression of TRF2, SOX10, and CD10 in circulating tumor microemboli detected in metastatic melanoma patients. A potential impact for the assessment of disease aggressiveness. Cancer Med. *5*, 1022–1030.

López, J. I. (2013). Renal tumors with clear cells. A review. Pathol. Res. Pract. *209*, 137–146.

Lopez-Beltran, A., Scarpelli, M., Montironi, R., and Kirkali, Z. (2006). 2004 WHO classification of the renal tumors of the adults. Eur. Urol. *49*, 798–805.

Lou, X.-L., Sun, J., Gong, S.-Q., Yu, X.-F., Gong, R., and Deng, H. (2015). Interaction between circulating cancer cells and platelets: clinical implication. Chin. J. Cancer Res. Chung-Kuo Yen Cheng Yen Chiu *27*, 450–460.

Lu, X., Yan, C. H., Yuan, M., Wei, Y., Hu, G., and Kang, Y. (2010). In vivo dynamics and distinct functions of hypoxia in primary tumor growth and organotropic metastasis of breast cancer. Cancer Res. *70*, 3905–3914.

Lu, Y., Yang, L., Wei, W., and Shi, Q. (2017). Microchip-based single-cell functional proteomics for biomedical applications. Lab. Chip *17*, 1250–1263.

Lu, Z., Ghosh, S., Wang, Z., and Hunter, T. (2003). Downregulation of caveolin-1 function by EGF leads to the loss of E-cadherin, increased transcriptional activity of beta-catenin, and enhanced tumor cell invasion. Cancer Cell *4*, 499–515.

Lu, Z., Jiang, G., Blume-Jensen, P., and Hunter, T. (2001). Epidermal growth factor-induced tumor cell invasion and metastasis initiated by dephosphorylation and downregulation of focal adhesion kinase. Mol. Cell. Biol. *21*, 4016–4031.

Lubensky, I. A., Gnarra, J. R., Bertheau, P., Walther, M. M., Linehan, W. M., and Zhuang, Z. (1996). Allelic deletions of the VHL gene detected in multiple microscopic clear cell renal lesions in von Hippel-Lindau disease patients. Am. J. Pathol. *149*, 2089–2094.

Lubensky, I. A., Schmidt, L., Zhuang, Z., Weirich, G., Pack, S., Zambrano, N., Walther, M. M., Choyke, P., Linehan, W. M., and Zbar, B. (1999). Hereditary and sporadic papillary renal carcinomas with c-met mutations share a distinct morphological phenotype. Am. J. Pathol. *155*, 517–526.

Mack, F. A., Rathmell, W. K., Arsham, A. M., Gnarra, J., Keith, B., and Simon, M. C. (2003). Loss of pVHL is sufficient to cause HIF dysregulation in primary cells but does not promote tumor growth.

Cancer Cell *3*, 75–88.

Mackie, F. L., Hemming, K., Allen, S., Morris, R. K., and Kilby, M. D. (2017). The accuracy of cell-free fetal DNA-based non-invasive prenatal testing in singleton pregnancies: a systematic review and bivariate meta-analysis. BJOG Int. J. Obstet. Gynaecol. *124*, 32–46.

Maina, E. N., Morris, M. R., Zatyka, M., Raval, R. R., Banks, R. E., Richards, F. M., Johnson, C. M., and Maher, E. R. (2005). Identification of novel VHL target genes and relationship to hypoxic response pathways. Oncogene *24*, 4549–4558.

Makino, S. (1956). Further evidence favoring the concept of the stem cell in ascites tumors of rats. Ann. N. Y. Acad. Sci. *63*, 818–830.

Malara, N. *et al.* (2016). Ex-vivo characterization of circulating colon cancer cells distinguished in stem and differentiated subset provides useful biomarker for personalized metastatic risk assessment. J. Transl. Med. *14*, 133.

Maltepe, E., Bakardjiev, A. I., and Fisher, S. J. (2010). The placenta: transcriptional, epigenetic, and physiological integration during development. J. Clin. Invest. *120*, 1016–1025.

Manca, P., Pantano, F., Iuliani, M., Ribelli, G., De Lisi, D., Danesi, R., Del Re, M., Vincenzi, B., Tonini, G., and Santini, D. (2017). Determinants of bone specific metastasis in prostate cancer. Crit. Rev. Oncol. Hematol. *112*, 59–66.

Mandriota, S. J. *et al.* (2002). HIF activation identifies early lesions in VHL kidneys: evidence for site-specific tumor suppressor function in the nephron. Cancer Cell *1*, 459–468.

Maniotis, A. J., Folberg, R., Hess, A., Seftor, E. A., Gardner, L. M., Pe'er, J., Trent, J. M., Meltzer, P. S., and Hendrix, M. J. (1999). Vascular channel formation by human melanoma cells in vivo and in vitro: vasculogenic mimicry. Am. J. Pathol. *155*, 739–752.

Mantovani, A., Allavena, P., Sica, A., and Balkwill, F. (2008). Cancer-related inflammation. Nature *454*, 436–444.

Mantzaris, D., and Cram, D. S. (2015). Potential of syncytiotrophoblasts isolated from the cervical mucus for early non-invasive prenatal diagnosis: evidence of a vanishing twin. Clin. Chim. Acta Int. J. Clin. Chem. *438*, 309–315.

Maranchie, J. K., and Zhan, Y. (2005). Nox4 is critical for hypoxia-inducible factor 2-alpha transcriptional activity in von Hippel-Lindau-deficient renal cell carcinoma. Cancer Res. *65*, 9190–9193.

Martello, G. *et al.* (2010). A MicroRNA targeting dicer for metastasis control. Cell *141*, 1195–1207.

Marusyk, A., Tabassum, D. P., Altrock, P. M., Almendro, V., Michor, F., and Polyak, K. (2014). Non-cell-autonomous driving of tumour growth supports sub-clonal heterogeneity. Nature *514*, 54–58.

Mazor, T., Pankov, A., Song, J. S., and Costello, J. F. (2016). Intratumoral Heterogeneity of the Epigenome. Cancer Cell *29*, 440–451.

McCRACKEN, W. J. (1948). On the diagnosis of various malignancies by Papanicolaou smear. Can. J. Med. Technol. *10*, 114–117.

Medina, R. J. *et al.* (2017). Endothelial Progenitors: A Consensus Statement on Nomenclature.

Stem Cells Transl. Med. *6*, 1316–1320.

Mego, M. *et al.* (2012). Expression of epithelial-mesenchymal transition-inducing transcription factors in primary breast cancer: The effect of neoadjuvant therapy. Int. J. Cancer *130*, 808–816.

Meinhardt, G., Husslein, P., and Knöfler, M. (2005). Tissue-specific and ubiquitous basic helix-loop-helix transcription factors in human placental trophoblasts. Placenta *26*, 527–539.

Mejlvang, J., Kriajevska, M., Vandewalle, C., Chernova, T., Sayan, A. E., Berx, G., Mellon, J. K., and Tulchinsky, E. (2007). Direct repression of cyclin D1 by SIP1 attenuates cell cycle progression in cells undergoing an epithelial mesenchymal transition. Mol. Biol. Cell *18*, 4615–4624.

Miettinen, M., and Fetsch, J. F. (2000). Distribution of keratins in normal endothelial cells and a spectrum of vascular tumors: implications in tumor diagnosis. Hum. Pathol. *31*, 1062–1067.

Miller, F., Kentsis, A., Osman, R., and Pan, Z.-Q. (2005). Inactivation of VHL by tumorigenic mutations that disrupt dynamic coupling of the pVHL.hypoxia-inducible transcription factor-1alpha complex. J. Biol. Chem. *280*, 7985–7996.

Mirzaei, A., Tavoosidana, G., Modarressi, M. H., Rad, A. A., Fazeli, M. S., Shirkoohi, R., Tavakoli-Yaraki, M., and Madjd, Z. (2015). Upregulation of circulating cancer stem cell marker, DCLK1 but not Lgr5, in chemoradiotherapy-treated colorectal cancer patients. Tumour Biol. J. Int. Soc. Oncodevelopmental Biol. Med. *36*, 4801–4810.

Miteva, D. O., Rutkowski, J. M., Dixon, J. B., Kilarski, W., Shields, J. D., and Swartz, M. A. (2010). Transmural flow modulates cell and fluid transport functions of lymphatic endothelium. Circ. Res. *106*, 920–931.

Miyamoto, D. T., Ting, D. T., Toner, M., Maheswaran, S., and Haber, D. A. (2016). Single-Cell Analysis of Circulating Tumor Cells as a Window into Tumor Heterogeneity. Cold Spring Harb. Symp. Quant. Biol. *81*, 269–274.

Moch, H. (2013). An overview of renal cell cancer: pathology and genetics. Semin. Cancer Biol. *23*, 3–9.

Montani, M., Heinimann, K., von Teichman, A., Rudolph, T., Perren, A., and Moch, H. (2010). VHL-gene deletion in single renal tubular epithelial cells and renal tubular cysts: further evidence for a cyst-dependent progression pathway of clear cell renal carcinoma in von Hippel-Lindau disease. Am. J. Surg. Pathol. *34*, 806–815.

Morales-Prieto, D. M., Chaiwangyen, W., Ospina-Prieto, S., Schneider, U., Herrmann, J., Gruhn, B., and Markert, U. R. (2012). MicroRNA expression profiles of trophoblastic cells. Placenta *33*, 725–734.

Morris, K. L. *et al.* (2014). Circulating biomarkers in hepatocellular carcinoma. Cancer Chemother. Pharmacol. *74*, 323–332.

Morrow, C. J. *et al.* (2016). Tumourigenic non-small-cell lung cancer mesenchymal circulating tumour cells: a clinical case study. Ann. Oncol. Off. J. Eur. Soc. Med. Oncol. *27*, 1155–1160.

Mouawia, H., Saker, A., Jais, J.-P., Benachi, A., Bussières, L., Lacour, B., Bonnefont, J.-P., Frydman, R., Simpson, J. L., and Paterlini-Brechot, P. (2012). Circulating trophoblastic cells provide genetic diagnosis in 63 fetuses at risk for cystic fibrosis or spinal muscular atrophy. Reprod. Biomed. Online *25*, 508–520.

Mroz, E. A., and Rocco, J. W. (2017). The challenges of tumor genetic diversity. Cancer *123*, 917–927.

Nabeshima, K., Inoue, T., Shimao, Y., and Sameshima, T. (2002). Matrix metalloproteinases in tumor invasion: role for cell migration. Pathol. Int. *52*, 255–264.

Nakayama, M., and Berger, P. (2013). Coordination of VEGF receptor trafficking and signaling by coreceptors. Exp. Cell Res. *319*, 1340–1347.

Nargund, A. M. *et al.* (2017). The SWI/SNF Protein PBRM1 Restrains VHL-Loss-Driven Clear Cell Renal Cell Carcinoma. Cell Rep. *18*, 2893–2906.

Nekrasova, O. E., Amargo, E. V., Smith, W. O., Chen, J., Kreitzer, G. E., and Green, K. J. (2011). Desmosomal cadherins utilize distinct kinesins for assembly into desmosomes. J. Cell Biol. *195*, 1185–1203.

Nel, I., Gauler, T. C., Bublitz, K., Lazaridis, L., Goergens, A., Giebel, B., Schuler, M., and Hoffmann, A.-C. (2016). Circulating Tumor Cell Composition in Renal Cell Carcinoma. PloS One *11*, e0153018.

Nickerson, M. L. *et al.* (2008). Improved identification of von Hippel-Lindau gene alterations in clear cell renal tumors. Clin. Cancer Res. Off. J. Am. Assoc. Cancer Res. *14*, 4726–4734.

Nieto, M. A. (2011). The ins and outs of the epithelial to mesenchymal transition in health and disease. Annu. Rev. Cell Dev. Biol. *27*, 347–376.

Nieva, J. *et al.* (2012). High-definition imaging of circulating tumor cells and associated cellular events in non-small cell lung cancer patients: a longitudinal analysis. Phys. Biol. *9*, 016004.

Nowell, P. C. (1976). The clonal evolution of tumor cell populations. Science *194*, 23–28.

O'Brien, C. A., Pollett, A., Gallinger, S., and Dick, J. E. (2007). A human colon cancer cell capable of initiating tumour growth in immunodeficient mice. Nature *445*, 106–110.

Onaindia, A., Medeiros, L. J., and Patel, K. P. (2017). Clinical utility of recently identified diagnostic, prognostic, and predictive molecular biomarkers in mature B-cell neoplasms. Mod. Pathol. Off. J. U. S. Can. Acad. Pathol. Inc.

Oudejans, C. B. M., Tjoa, M. L., Westerman, B. A., Mulders, M. A. M., Van Wijk, I. J., and Van Vugt, J. M. G. (2003). Circulating trophoblast in maternal blood. Prenat. Diagn. *23*, 111–116.

Ouyang, W., Yu, Z., Zhao, X., Lu, S., and Wang, Z. (2016). Aptamers in hematological malignancies and their potential therapeutic implications. Crit. Rev. Oncol. Hematol. *106*, 108–117.

Paget, S. (1889). THE DISTRIBUTION OF SECONDARY GROWTHS IN CANCER OF THE BREAST. The Lancet *133*, 571–573.

Paguirigan, A. L., Smith, J., Meshinchi, S., Carroll, M., Maley, C., and Radich, J. P. (2015). Single-cell genotyping demonstrates complex clonal diversity in acute myeloid leukemia. Sci. Transl. Med. *7*, 281re2.

Pailler, E. *et al.* (2013). Detection of circulating tumor cells harboring a unique ALK rearrangement in ALK-positive non-small-cell lung cancer. J. Clin. Oncol. Off. J. Am. Soc. Clin. Oncol. *31*, 2273–2281.

Pailler, E. *et al.* (2015). High level of chromosomal instability in circulating tumor cells of ROS1-rearranged non-small-cell lung cancer. Ann. Oncol. Off. J. Eur. Soc. Med. Oncol. *26*, 1408–1415.

Pan, M.-R., Chang, H.-C., Wu, Y.-C., Huang, C.-C., and Hung, W.-C. (2009). Tubocapsanolide A inhibits transforming growth factor-beta-activating kinase 1 to suppress NF-kappaB-induced CCR7. J. Biol. Chem. *284*, 2746–2754.

Pan, Q. *et al.* (2014). A prenatal case with discrepant findings between non-invasive prenatal testing and fetal genetic testings. Mol. Cytogenet. *7*, 48.

Pantel, K., Denève, E., Nocca, D., Coffy, A., Vendrell, J.-P., Maudelonde, T., Riethdorf, S., and Alix-Panabières, C. (2012). Circulating epithelial cells in patients with benign colon diseases. Clin. Chem. *58*, 936–940.

Park, S., Ang, R. R., Duffy, S. P., Bazov, J., Chi, K. N., Black, P. C., and Ma, H. (2014). Morphological differences between circulating tumor cells from prostate cancer patients and cultured prostate cancer cells. PloS One *9*, e85264.

Park, W.-H., and Eisen, T. (2007). Prognostic factors in renal cell cancer. BJU Int. *99*, 1277–1281.

Parmar, H., and Cunha, G. R. (2004). Epithelial-stromal interactions in the mouse and human mammary gland in vivo. Endocr. Relat. Cancer *11*, 437–458.

Patel, S. A., and Simon, M. C. (2008). Biology of hypoxia-inducible factor-2alpha in development and disease. Cell Death Differ. *15*, 628–634.

Paterlini-Bréchot, P. (2014). Circulating Tumor Cells: Who is the Killer? Cancer Microenviron. Off. J. Int. Cancer Microenviron. Soc. *7*, 161–176.

Pawelek, J. M., and Chakraborty, A. K. (2008). Fusion of tumour cells with bone marrow-derived cells: a unifying explanation for metastasis. Nat. Rev. Cancer *8*, 377–386.

Peglion, F., Llense, F., and Etienne-Manneville, S. (2014). Adherens junction treadmilling during collective migration. Nat. Cell Biol. *16*, 639–651.

Pei, J., Feder, M. M., Al-Saleem, T., Liu, Z., Liu, A., Hudes, G. R., Uzzo, R. G., and Testa, J. R. (2010). Combined classical cytogenetics and microarray-based genomic copy number analysis reveal frequent 3;5 rearrangements in clear cell renal cell carcinoma. Genes. Chromosomes Cancer *49*, 610–619.

Peinado, H. *et al.* (2012). Melanoma exosomes educate bone marrow progenitor cells toward a pro-metastatic phenotype through MET. Nat. Med. *18*, 883–891.

Peitzsch, C., Tyutyunnykova, A., Pantel, K., and Dubrovska, A. (2017). Cancer stem cells: The root of tumor recurrence and metastases. Semin. Cancer Biol. *44*, 10–24.

Penet, M.-F., Kakkad, S., Pathak, A. P., Krishnamachary, B., Mironchik, Y., Raman, V., Solaiyappan, M., and Bhujwalla, Z. M. (2017). Structure and Function of a Prostate Cancer Dissemination-Permissive Extracellular Matrix. Clin. Cancer Res. Off. J. Am. Assoc. Cancer Res. *23*, 2245–2254.

Perkel, J. M. (2017). Single-cell sequencing made simple. Nature *547*, 125–126.

Petrella, B. L., Lohi, J., and Brinckerhoff, C. E. (2005). Identification of membrane type-1 matrix

metalloproteinase as a target of hypoxia-inducible factor-2 alpha in von Hippel-Lindau renal cell carcinoma. Oncogene *24*, 1043–1052.

Pfeifer, I. *et al.* (2016). Cervical trophoblasts for non-invasive single-cell genotyping and prenatal diagnosis. Placenta *37*, 56–60.

Phillips, K. G. *et al.* (2015). The thrombotic potential of circulating tumor microemboli: computational modeling of circulating tumor cell-induced coagulation. Am. J. Physiol. Cell Physiol. *308*, C229-236.

Pierga, J.-Y., Bonneton, C., Magdelénat, H., Vincent-Salomon, A., Nos, C., Pouillart, P., and Thiery, J.-P. (2003). Clinical significance of proliferative potential of occult metastatic cells in bone marrow of patients with breast cancer. Br. J. Cancer *89*, 539–545.

Pinzani, P. *et al.* (2013). Detection of circulating tumor cells in patients with adrenocortical carcinoma: a monocentric preliminary study. J. Clin. Endocrinol. Metab. *98*, 3731–3738.

Pinzani, P., Salvadori, B., Simi, L., Bianchi, S., Distante, V., Cataliotti, L., Pazzagli, M., and Orlando, C. (2006). Isolation by size of epithelial tumor cells in peripheral blood of patients with breast cancer: correlation with real-time reverse transcriptase-polymerase chain reaction results and feasibility of molecular analysis by laser microdissection. Hum. Pathol. *37*, 711–718.

Pisano, M., Triacca, V., Barbee, K. A., and Swartz, M. A. (2015). An in vitro model of the tumor-lymphatic microenvironment with simultaneous transendothelial and luminal flows reveals mechanisms of flow enhanced invasion. Integr. Biol. Quant. Biosci. Nano Macro *7*, 525–533.

Placke, T., Örgel, M., Schaller, M., Jung, G., Rammensee, H.-G., Kopp, H.-G., and Salih, H. R. (2012). Platelet-derived MHC class I confers a pseudonormal phenotype to cancer cells that subverts the antitumor reactivity of natural killer immune cells. Cancer Res. *72*, 440–448.

Podsypanina, K., Du, Y.-C. N., Jechlinger, M., Beverly, L. J., Hambardzumyan, D., and Varmus, H. (2008). Seeding and propagation of untransformed mouse mammary cells in the lung. Science *321*, 1841–1844.

Pollard, T. D., and Borisy, G. G. (2003). Cellular motility driven by assembly and disassembly of actin filaments. Cell *112*, 453–465.

Pollard, T. D., and Cooper, J. A. (2009). Actin, a central player in cell shape and movement. Science *326*, 1208–1212.

Polzer, B. *et al.* (2014). Molecular profiling of single circulating tumor cells with diagnostic intention. EMBO Mol. Med. *6*, 1371–1386.

Ponting, C. P., Oliver, P. L., and Reik, W. (2009). Evolution and functions of long noncoding RNAs. Cell *136*, 629–641.

Poruk, K. E. *et al.* (2016). Circulating Tumor Cell Phenotype Predicts Recurrence and Survival in Pancreatic Adenocarcinoma. Ann. Surg. *264*, 1073–1081.

Pretlow, T. G. *et al.* (2000). Prostate cancer and other xenografts from cells in peripheral blood of patients. Cancer Res. *60*, 4033–4036.

Principe, D. R., Doll, J. A., Bauer, J., Jung, B., Munshi, H. G., Bartholin, L., Pasche, B., Lee, C., and Grippo, P. J. (2014). TGF-β: duality of function between tumor prevention and carcinogenesis. J.

Natl. Cancer Inst. *106*, djt369.

Pritchett, T. L., Bader, H. L., Henderson, J., and Hsu, T. (2015). Conditional inactivation of the mouse von Hippel-Lindau tumor suppressor gene results in wide-spread hyperplastic, inflammatory and fibrotic lesions in the kidney. Oncogene *34*, 2631–2639.

Provenzano, P. P., Eliceiri, K. W., Campbell, J. M., Inman, D. R., White, J. G., and Keely, P. J. (2006). Collagen reorganization at the tumor-stromal interface facilitates local invasion. BMC Med. *4*, 38.

Provenzano, P. P., Inman, D. R., Eliceiri, K. W., Knittel, J. G., Yan, L., Rueden, C. T., White, J. G., and Keely, P. J. (2008). Collagen density promotes mammary tumor initiation and progression. BMC Med. *6*, 11.

Punnoose, E. A. *et al.* (2012). Evaluation of circulating tumor cells and circulating tumor DNA in non-small cell lung cancer: association with clinical endpoints in a phase II clinical trial of pertuzumab and erlotinib. Clin. Cancer Res. Off. J. Am. Assoc. Cancer Res. *18*, 2391–2401.

Qian, M., Wang, D. C., Chen, H., and Cheng, Y. (2017). Detection of single cell heterogeneity in cancer. Semin. Cell Dev. Biol. *64*, 143–149.

Qiao, A., Gu, F., Guo, X., Zhang, X., and Fu, L. (2016). Breast cancer-associated fibroblasts: their roles in tumor initiation, progression and clinical applications. Front. Med. *10*, 33–40.

Rack, B. *et al.* (2014). Circulating tumor cells predict survival in early average-to-high risk breast cancer patients. J. Natl. Cancer Inst. *106*.

Ramos, G. de O., Bernardi, L., Lauxen, I., Sant'Ana Filho, M., Horwitz, A. R., and Lamers, M. L. (2016). Fibronectin Modulates Cell Adhesion and Signaling to Promote Single Cell Migration of Highly Invasive Oral Squamous Cell Carcinoma. PloS One *11*, e0151338.

Rankin, E. B., and Giaccia, A. J. (2008). The role of hypoxia-inducible factors in tumorigenesis. Cell Death Differ. *15*, 678–685.

Rankin, E. B., Tomaszewski, J. E., and Haase, V. H. (2006). Renal cyst development in mice with conditional inactivation of the von Hippel-Lindau tumor suppressor. Cancer Res. *66*, 2576–2583.

Raval, R. R., Lau, K. W., Tran, M. G. B., Sowter, H. M., Mandriota, S. J., Li, J.-L., Pugh, C. W., Maxwell, P. H., Harris, A. L., and Ratcliffe, P. J. (2005). Contrasting properties of hypoxia-inducible factor 1 (HIF-1) and HIF-2 in von Hippel-Lindau-associated renal cell carcinoma. Mol. Cell. Biol. *25*, 5675–5686.

Razafinjatovo, C., Bihr, S., Mischo, A., Vogl, U., Schmidinger, M., Moch, H., and Schraml, P. (2016). Characterization of VHL missense mutations in sporadic clear cell renal cell carcinoma: hotspots, affected binding domains, functional impact on pVHL and therapeutic relevance. BMC Cancer *16*, 638.

Razafinjatovo, C. F., Stiehl, D., Deininger, E., Rechsteiner, M., Moch, H., and Schraml, P. (2017). VHL missense mutations in the p53 binding domain show different effects on p53 signaling and HIFα degradation in clear cell renal cell carcinoma. Oncotarget *8*, 10199–10212.

Reed, J. D., and Chesley, R. F. (1948). The routine use of Papanicolaou vaginal smears in gynecologic practice. Bull. Margaret Hague Matern. Hosp. Jersey City NJ *1*, 104–106.

Reffay, M., Parrini, M. C., Cochet-Escartin, O., Ladoux, B., Buguin, A., Coscoy, S., Amblard, F., Camonis, J., and Silberzan, P. (2014). Interplay of RhoA and mechanical forces in collective cell migration driven by leader cells. Nat. Cell Biol. *16*, 217–223.

Reymond, N., d'Água, B. B., and Ridley, A. J. (2013). Crossing the endothelial barrier during metastasis. Nat. Rev. Cancer *13*, 858–870.

Rhim, A. D. *et al.* (2012). EMT and dissemination precede pancreatic tumor formation. Cell *148*, 349–361.

Ricci-Vitiani, L. *et al.* (2010). Tumour vascularization via endothelial differentiation of glioblastoma stem-like cells. Nature *468*, 824–828.

Roe, J.-S., Kim, H., Lee, S.-M., Kim, S.-T., Cho, E.-J., and Youn, H.-D. (2006). p53 stabilization and transactivation by a von Hippel-Lindau protein. Mol. Cell *22*, 395–405.

Rossant, J., and Cross, J. C. (2001). Placental development: lessons from mouse mutants. Nat. Rev. Genet. *2*, 538–548.

Roth, A. *et al.* (2016). Clonal genotype and population structure inference from single-cell tumor sequencing. Nat. Methods *13*, 573–576.

Ruggeri, Z. M. (2009). Platelet adhesion under flow. Microcirc. N. Y. N 1994 *16*, 58–83.

Runge, J., Reichert, T. E., Fritsch, A., Käs, J., Bertolini, J., and Remmerbach, T. W. (2014). Evaluation of single-cell biomechanics as potential marker for oral squamous cell carcinomas: a pilot study. Oral Dis. *20*, e120-127.

Sabeh, F., Shimizu-Hirota, R., and Weiss, S. J. (2009). Protease-dependent versus -independent cancer cell invasion programs: three-dimensional amoeboid movement revisited. J. Cell Biol. *185*, 11–19.

Saker, A., Benachi, A., Bonnefont, J. P., Munnich, A., Dumez, Y., Lacour, B., and Paterlini-Brechot, P. (2006). Genetic characterisation of circulating fetal cells allows non-invasive prenatal diagnosis of cystic fibrosis. Prenat. Diagn. *26*, 906–916.

Salsbury, A. J. (1975). The significance of the circulating cancer cell. Cancer Treat. Rev. *2*, 55–72.

Sato, Y. *et al.* (2013). Integrated molecular analysis of clear-cell renal cell carcinoma. Nat. Genet. *45*, 860–867.

Saucedo-Zeni, N. *et al.* (2012). A novel method for the in vivo isolation of circulating tumor cells from peripheral blood of cancer patients using a functionalized and structured medical wire. Int. J. Oncol. *41*, 1241–1250.

Scher, H. I. *et al.* (2015). Circulating tumor cell biomarker panel as an individual-level surrogate for survival in metastatic castration-resistant prostate cancer. J. Clin. Oncol. Off. J. Am. Soc. Clin. Oncol. *33*, 1348–1355.

Scher, H. I. *et al.* (2016). Association of AR-V7 on Circulating Tumor Cells as a Treatment-Specific Biomarker With Outcomes and Survival in Castration-Resistant Prostate Cancer. JAMA Oncol. *2*, 1441–1449.

Schlütter, J. M., Kirkegaard, I., Ferreira, A. S., Hatt, L., Christensen, B., Kølvraa, S., and Uldbjerg,

N. (2016). The Number of Endovascular Trophoblasts in Maternal Blood Increases Overnight and after Physical Activity: An Experimental Study. Fetal Diagn. Ther. *40*, 54–58.

Schrader, J., Gordon-Walker, T. T., Aucott, R. L., van Deemter, M., Quaas, A., Walsh, S., Benten, D., Forbes, S. J., Wells, R. G., and Iredale, J. P. (2011). Matrix stiffness modulates proliferation, chemotherapeutic response, and dormancy in hepatocellular carcinoma cells. Hepatol. Baltim. Md *53*, 1192–1205.

Schraml, P., Struckmann, K., Hatz, F., Sonnet, S., Kully, C., Gasser, T., Sauter, G., Mihatsch, M. J., and Moch, H. (2002). VHL mutations and their correlation with tumour cell proliferation, microvessel density, and patient prognosis in clear cell renal cell carcinoma. J. Pathol. *196*, 186–193.

Schumacher, D., Strilic, B., Sivaraj, K. K., Wettschureck, N., and Offermanns, S. (2013). Platelet-derived nucleotides promote tumor-cell transendothelial migration and metastasis via P2Y2 receptor. Cancer Cell *24*, 130–137.

Seal, S. H. (1956). A method for concentrating cancer cells suspended in large quantities of fluid. Cancer *9*, 866–868.

Seal, S. H. (1959). Silicone flotation: a simple quantitative method for the isolation of free-floating cancer cells from the blood. Cancer *12*, 590–595.

Seal, S. H. (1964). A SIEVE FOR THE ISOLATION OF CANCER CELLS AND OTHER LARGE CELLS FROM THE BLOOD. Cancer *17*, 637–642.

Shan, W., Jiang, Y., Yu, H., Huang, Q., Liu, L., Guo, X., Li, L., Mi, Q., Zhang, K., and Yang, Z. (2017). HDAC2 overexpression correlates with aggressive clinicopathological features and DNA-damage response pathway of breast cancer. Am. J. Cancer Res. *7*, 1213–1226.

Shimono, Y. *et al.* (2009). Downregulation of miRNA-200c links breast cancer stem cells with normal stem cells. Cell *138*, 592–603.

Shuin, T., Kondo, K., Torigoe, S., Kishida, T., Kubota, Y., Hosaka, M., Nagashima, Y., Kitamura, H., Latif, F., and Zbar, B. (1994). Frequent somatic mutations and loss of heterozygosity of the von Hippel-Lindau tumor suppressor gene in primary human renal cell carcinomas. Cancer Res. *54*, 2852–2855.

Siegel, R. L., Miller, K. D., and Jemal, A. (2015). Cancer statistics, 2015. CA. Cancer J. Clin. *65*, 5–29.

Sifakis, S., Ghatpande, S., Seppo, A., Kilpatrick, M. W., Tafas, T., Tsipouras, P., Fejgin, M., and Amiel, A. (2010). Prenatal diagnosis of trisomy 21 through detection of trophoblasts in cervical smears. Early Hum. Dev. *86*, 311–313.

Singh, S. K., Hawkins, C., Clarke, I. D., Squire, J. A., Bayani, J., Hide, T., Henkelman, R. M., Cusimano, M. D., and Dirks, P. B. (2004). Identification of human brain tumour initiating cells. Nature *432*, 396–401.

Sinkala, E. *et al.* (2017). Profiling protein expression in circulating tumour cells using microfluidic western blotting. Nat. Commun. *8*, 14622.

Sluysmans, S., Vasileva, E., Spadaro, D., Shah, J., Rouaud, F., and Citi, S. (2017). The role of apical cell-cell junctions and associated cytoskeleton in mechanotransduction. Biol. Cell *109*, 139–

161.

Söhl, G., and Willecke, K. (2004). Gap junctions and the connexin protein family. Cardiovasc. Res. *62*, 228–232.

Song, Y., Tian, T., Shi, Y., Liu, W., Zou, Y., Khajvand, T., Wang, S., Zhu, Z., and Yang, C. (2017). Enrichment and single-cell analysis of circulating tumor cells. Chem. Sci. *8*, 1736–1751.

Sosa, M. S., Bragado, P., and Aguirre-Ghiso, J. A. (2014). Mechanisms of disseminated cancer cell dormancy: an awakening field. Nat. Rev. Cancer *14*, 611–622.

Soygur, B., and Moore, H. (2016). Expression of Syncytin 1 (HERV-W), in the preimplantation human blastocyst, embryonic stem cells and trophoblast cells derived in vitro. Hum. Reprod. Oxf. Engl. *31*, 1455–1461.

Stacker, S. A., Achen, M. G., Jussila, L., Baldwin, M. E., and Alitalo, K. (2002). Lymphangiogenesis and cancer metastasis. Nat. Rev. Cancer *2*, 573–583.

Stamatiou, K., Polizois, K., Kollaitis, G., Dahanis, S., Zafeiropoulos, G., Leventis, C., and Lambou, T. (2008). Cystic nephroma: a case report and review of the literature. Cases J. *1*, 267.

Stebbins, C. E., Kaelin, W. G., and Pavletich, N. P. (1999). Structure of the VHL-ElonginC-ElonginB complex: implications for VHL tumor suppressor function. Science *284*, 455–461.

Stillman, B. N., Hsu, D. K., Pang, M., Brewer, C. F., Johnson, P., Liu, F.-T., and Baum, L. G. (2006). Galectin-3 and galectin-1 bind distinct cell surface glycoprotein receptors to induce T cell death. J. Immunol. Baltim. Md 1950 *176*, 778–789.

Strell, C., and Entschladen, F. (2008). Extravasation of leukocytes in comparison to tumor cells. Cell Commun. Signal. CCS *6*, 10.

Strell, C., Lang, K., Niggemann, B., Zaenker, K. S., and Entschladen, F. (2007). Surface molecules regulating rolling and adhesion to endothelium of neutrophil granulocytes and MDA-MB-468 breast carcinoma cells and their interaction. Cell. Mol. Life Sci. CMLS *64*, 3306–3316.

Sugino, T., Yamaguchi, T., Ogura, G., Saito, A., Hashimoto, T., Hoshi, N., Yoshida, S., Goodison, S., and Suzuki, T. (2004). Morphological evidence for an invasion-independent metastasis pathway exists in multiple human cancers. BMC Med. *2*, 9.

Sun, H. *et al.* (2017). Anti-angiogenic treatment promotes triple-negative breast cancer invasion via vasculogenic mimicry. Cancer Biol. Ther. *18*, 205–213.

Suvà, M. L. *et al.* (2014). Reconstructing and reprogramming the tumor-propagating potential of glioblastoma stem-like cells. Cell *157*, 580–594.

Swaminathan, V., Mythreye, K., O'Brien, E. T., Berchuck, A., Blobe, G. C., and Superfine, R. (2011). Mechanical stiffness grades metastatic potential in patient tumor cells and in cancer cell lines. Cancer Res. *71*, 5075–5080.

Tabor, A., and Alfirevic, Z. (2010). Update on procedure-related risks for prenatal diagnosis techniques. Fetal Diagn. Ther. *27*, 1–7.

Takahashi, K., and Yamanaka, S. (2006). Induction of pluripotent stem cells from mouse embryonic and adult fibroblast cultures by defined factors. Cell *126*, 663–676.

Takaishi, S., Okumura, T., Tu, S., Wang, S. S. W., Shibata, W., Vigneshwaran, R., Gordon, S. A. K., Shimada, Y., and Wang, T. C. (2009). Identification of gastric cancer stem cells using the cell surface marker CD44. Stem Cells Dayt. Ohio *27*, 1006–1020.

Talasaz, A. H. *et al.* (2009). Isolating highly enriched populations of circulating epithelial cells and other rare cells from blood using a magnetic sweeper device. Proc. Natl. Acad. Sci. U. S. A. *106*, 3970–3975.

Teng, F., Tian, W.-Y., Wang, Y.-M., Zhang, Y.-F., Guo, F., Zhao, J., Gao, C., and Xue, F.-X. (2016). Cancer-associated fibroblasts promote the progression of endometrial cancer via the SDF-1/CXCR4 axis. J. Hematol. Oncol.J Hematol Oncol *9*, 8.

Tennenbaum, D. M. *et al.* (2017). Genomic alterations as predictors of survival among patients within a combined cohort with clear cell renal cell carcinoma undergoing cytoreductive nephrectomy. Urol. Oncol.

Terris, B., Cavard, C., and Perret, C. (2010). EpCAM, a new marker for cancer stem cells in hepatocellular carcinoma. J. Hepatol. *52*, 280–281.

Tewes, M., Aktas, B., Welt, A., Mueller, S., Hauch, S., Kimmig, R., and Kasimir-Bauer, S. (2009). Molecular profiling and predictive value of circulating tumor cells in patients with metastatic breast cancer: an option for monitoring response to breast cancer related therapies. Breast Cancer Res. Treat. *115*, 581–590.

Thapa, R., and Wilson, G. D. (2016). The Importance of CD44 as a Stem Cell Biomarker and Therapeutic Target in Cancer. Stem Cells Int. *2016*, 2087204.

Thiele, J.-A., Bethel, K., Králíčková, M., and Kuhn, P. (2017). Circulating Tumor Cells: Fluid Surrogates of Solid Tumors. Annu. Rev. Pathol. *12*, 419–447.

Thiery, J. P., Acloque, H., Huang, R. Y. J., and Nieto, M. A. (2009). Epithelial-mesenchymal transitions in development and disease. Cell *139*, 871–890.

Thijssen, V. L. J. L., Poirier, F., Baum, L. G., and Griffioen, A. W. (2007). Galectins in the tumor endothelium: opportunities for combined cancer therapy. Blood *110*, 2819–2827.

Tinhofer, I., Saki, M., Niehr, F., Keilholz, U., and Budach, V. (2014). Cancer stem cell characteristics of circulating tumor cells. Int. J. Radiat. Biol. *90*, 622–627.

Tirosh, I. *et al.* (2016). Dissecting the multicellular ecosystem of metastatic melanoma by single-cell RNA-seq. Science *352*, 189–196.

Trapnell, C. (2015). Defining cell types and states with single-cell genomics. Genome Res. *25*, 1491–1498.

Tremblay, P.-L., Huot, J., and Auger, F. A. (2008). Mechanisms by which E-selectin regulates diapedesis of colon cancer cells under flow conditions. Cancer Res. *68*, 5167–5176.

Tsuji, T., Ibaragi, S., Shima, K., Hu, M. G., Katsurano, M., Sasaki, A., and Hu, G. (2008). Epithelial-mesenchymal transition induced by growth suppressor p12CDK2-AP1 promotes tumor cell local invasion but suppresses distant colony growth. Cancer Res. *68*, 10377–10386.

Turner, K. J. *et al.* (2002). Expression of hypoxia-inducible factors in human renal cancer: relationship to angiogenesis and to the von Hippel-Lindau gene mutation. Cancer Res. *62*, 2957–

2961.

Uechi, H., and Kuranaga, E. (2017). Mechanisms of collective cell movement lacking a leading or free front edge in vivo. Cell. Mol. Life Sci. CMLS.

Uga, S., Ikeda, S., Matsukage, S., and Hamada, M. (2012). An autopsy case of acute cor pulmonale and paradoxical systemic embolism due to tumour cell microemboli in a patient with breast cancer. BMJ Case Rep. *2012*.

Vallenius, T. (2013). Actin stress fibre subtypes in mesenchymal-migrating cells. Open Biol. *3*, 130001.

Varela, I. *et al.* (2011). Exome sequencing identifies frequent mutation of the SWI/SNF complex gene PBRM1 in renal carcinoma. Nature *469*, 539–542.

Vega, S., Morales, A. V., Ocaña, O. H., Valdés, F., Fabregat, I., and Nieto, M. A. (2004). Snail blocks the cell cycle and confers resistance to cell death. Genes Dev. *18*, 1131–1143.

Velez, J. *et al.* (2014). Platelets promote mitochondrial uncoupling and resistance to apoptosis in leukemia cells: a novel paradigm for the bone marrow microenvironment. Cancer Microenviron. Off. J. Int. Cancer Microenviron. Soc. *7*, 79–90.

Viadana, E., Cotter, R., Pickren, J. W., and Bross, I. D. (1973). An autopsy study of metastatic sites of breast cancer. Cancer Res. *33*, 179–181.

Vona, G. *et al.* (2000). Isolation by size of epithelial tumor cells : a new method for the immunomorphological and molecular characterization of circulatingtumor cells. Am. J. Pathol. *156*, 57–63.

Vonach, C. *et al.* (2011). NF-κB mediates the 12(S)-HETE-induced endothelial to mesenchymal transition of lymphendothelial cells during the intravasation of breast carcinoma cells. Br. J. Cancer *105*, 263–271.

Voss, M. H. *et al.* (2014). Tumor genetic analyses of patients with metastatic renal cell carcinoma and extended benefit from mTOR inhibitor therapy. Clin. Cancer Res. Off. J. Am. Assoc. Cancer Res. *20*, 1955–1964.

Wagner, D. E., and Klein, A. M. (2017). Genetic screening enters the single-cell era. Nat. Methods *14*, 237–238.

Wang, J.-R., Gan, W.-J., Li, X.-M., Zhao, Y.-Y., Li, Y., Lu, X.-X., Li, J.-M., and Wu, H. (2014a). Orphan nuclear receptor Nur77 promotes colorectal cancer invasion and metastasis by regulating MMP-9 and E-cadherin. Carcinogenesis *35*, 2474–2484.

Wang, Q., Uhlirova, M., and Bohmann, D. (2010). Spatial restriction of FGF signaling by a matrix metalloprotease controls branching morphogenesis. Dev. Cell *18*, 157–164.

Wang, S. *et al.* (2009). Three-dimensional nanostructured substrates toward efficient capture of circulating tumor cells. Angew. Chem. Int. Ed Engl. *48*, 8970–8973.

Wang, S.-S. *et al.* (2014b). Bap1 is essential for kidney function and cooperates with Vhl in renal tumorigenesis. Proc. Natl. Acad. Sci. U. S. A. *111*, 16538–16543.

Wang, T. N., Albo, D., and Tuszynski, G. P. (2002). Fibroblasts promote breast cancer cell invasion

by upregulating tumor matrix metalloproteinase-9 production. Surgery *132*, 220–225.

Wang, X., Tanaka, M., Krstin, S., Peixoto, H. S., Moura, C. C. de M., and Wink, M. (2016). Cytoskeletal interference - A new mode of action for the anticancer drugs camptothecin and topotecan. Eur. J. Pharmacol. *789*, 265–274.

Webb, D. J., Brown, C. M., and Horwitz, A. F. (2003). Illuminating adhesion complexes in migrating cells: moving toward a bright future. Curr. Opin. Cell Biol. *15*, 614–620.

Weber, M., Göhner, C., San Martin, S., Vattai, A., Hutter, S., Parraga, M., Jeschke, U., Schleussner, E., Markert, U. R., and Fitzgerald, J. S. (2016). Unique trophoblast stem cell- and pluripotency marker staining patterns depending on gestational age and placenta-associated pregnancy complications. Cell Adhes. Migr. *10*, 56–65.

Weitz, J., Kienle, P., Lacroix, J., Willeke, F., Benner, A., Lehnert, T., Herfarth, C., and von Knebel Doeberitz, M. (1998). Dissemination of tumor cells in patients undergoing surgery for colorectal cancer. Clin. Cancer Res. Off. J. Am. Assoc. Cancer Res. *4*, 343–348.

Wenjun, W., Zhihua, W., Zhuo, W., Yuliang, D., and Qihui, S. (2017). Fast isolation and ex vivo culture of circulating tumor cells from the peripheral blood of lung cancer patients. Yi Chuan Hered. *39*, 66–74.

Wong, C. W., Song, C., Grimes, M. M., Fu, W., Dewhirst, M. W., Muschel, R. J., and Al-Mehdi, A.-B. (2002). Intravascular location of breast cancer cells after spontaneous metastasis to the lung. Am. J. Pathol. *161*, 749–753.

Wyckoff, J. B., Wang, Y., Lin, E. Y., Li, J., Goswami, S., Stanley, E. R., Segall, J. E., Pollard, J. W., and Condeelis, J. (2007). Direct visualization of macrophage-assisted tumor cell intravasation in mammary tumors. Cancer Res. *67*, 2649–2656.

Xu, W., Mezencev, R., Kim, B., Wang, L., McDonald, J., and Sulchek, T. (2012a). Cell stiffness is a biomarker of the metastatic potential of ovarian cancer cells. PloS One *7*, e46609.

Xu, X. *et al.* (2012b). Single-cell exome sequencing reveals single-nucleotide mutation characteristics of a kidney tumor. Cell *148*, 886–895.

Yadav, A., Kumar, B., Yu, J.-G., Old, M., Teknos, T. N., and Kumar, P. (2015). Tumor-Associated Endothelial Cells Promote Tumor Metastasis by Chaperoning Circulating Tumor Cells and Protecting Them from Anoikis. PloS One *10*, e0141602.

Yadavalli, S. *et al.* (2017). Data-Driven Discovery of Extravasation Pathway in Circulating Tumor Cells. Sci. Rep. *7*, 43710.

Yan, B. *et al.* (2017). Single-cell genomic profiling of acute myeloid leukemia for clinical use: A pilot study. Oncol. Lett. *13*, 1625–1630.

Yan, H. H., Pickup, M., Pang, Y., Gorska, A. E., Li, Z., Chytil, A., Geng, Y., Gray, J. W., Moses, H. L., and Yang, L. (2010). Gr-1+CD11b+ myeloid cells tip the balance of immune protection to tumor promotion in the premetastatic lung. Cancer Res. *70*, 6139–6149.

Yang, C., Huntoon, K., Ksendzovsky, A., Zhuang, Z., and Lonser, R. R. (2013). Proteostasis modulators prolong missense VHL protein activity and halt tumor progression. Cell Rep. *3*, 52–59.

Yang, Y. H., Kim, S. H., Yang, E. S., Kim, S. K., Kim, I. K., Park, Y. W., Cho, J. S., and Lee, Y. H.

(2003). Prenatal diagnosis of fetal trisomy 21 from maternal peripheral blood. Yonsei Med. J. *44*, 181–186.

Yang, Y. H., Yang, E. S., Kwon, J. Y., Kim, I. K., and Park, Y. W. (2006). Prenatal diagnosis of trisomy 21 with fetal cells in maternal blood using comparative genomic hybridization. Fetal Diagn. Ther. *21*, 125–133.

Yao, X., Williamson, C., Adalsteinsson, V. A., D'Agostino, R. S., Fitton, T., Smaroff, G. G., William, R. T., Wittrup, K. D., and Love, J. C. (2014). Tumor cells are dislodged into the pulmonary vein during lobectomy. J. Thorac. Cardiovasc. Surg. *148*, 3224-3231.e1-5.

Ye, Y., Liu, S., Wu, C., and Sun, Z. (2015). TGFβ modulates inflammatory cytokines and growth factors to create premetastatic microenvironment and stimulate lung metastasis. J. Mol. Histol. *46*, 365–375.

Yin, J. *et al.* (2015). Circulating Tumor Cells Enriched by the Depletion of Leukocytes with Bi-Antibodies in Non-Small Cell Lung Cancer: Potential Clinical Application. PloS One *10*, e0137076.

Yu, B., Dong, X., Gravina, S., Kartal, Ö., Schimmel, T., Cohen, J., Tortoriello, D., Zody, R., Hawkins, R. D., and Vijg, J. (2017). Genome-wide, Single-Cell DNA Methylomics Reveals Increased Non-CpG Methylation during Human Oocyte Maturation. Stem Cell Rep.

Yu, L.-G. *et al.* (2007). Galectin-3 interaction with Thomsen-Friedenreich disaccharide on cancer-associated MUC1 causes increased cancer cell endothelial adhesion. J. Biol. Chem. *282*, 773–781.

Yu, M. *et al.* (2013). Circulating breast tumor cells exhibit dynamic changes in epithelial and mesenchymal composition. Science *339*, 580–584.

Yu, M. *et al.* (2014). Cancer therapy. Ex vivo culture of circulating breast tumor cells for individualized testing of drug susceptibility. Science *345*, 216–220.

Yu, P., and Kodadek, T. (2007). Dynamics of the hypoxia-inducible factor-1-vascular endothelial growth factor promoter complex. J. Biol. Chem. *282*, 35035–35045.

Yu, T., Guo, Z., Fan, H., Song, J., Liu, Y., Gao, Z., and Wang, Q. (2016). Cancer-associated fibroblasts promote non-small cell lung cancer cell invasion by upregulation of glucose-regulated protein 78 (GRP78) expression in an integrated bionic microfluidic device. Oncotarget *7*, 25593–25603.

Zamay, G. S. *et al.* (2015). Aptamers Selected to Postoperative Lung Adenocarcinoma Detect Circulating Tumor Cells in Human Blood. Mol. Ther. J. Am. Soc. Gene Ther. *23*, 1486–1496.

Zemła, J., Danilkiewicz, J., Orzechowska, B., Pabijan, J., Seweryn, S., and Lekka, M. (2017). Atomic force microscopy as a tool for assessing the cellular elasticity and adhesiveness to identify cancer cells and tissues. Semin. Cell Dev. Biol.

Zhang, D., Zhao, L., Zhou, P., Ma, H., Huang, F., Jin, M., Dai, X., Zheng, X., Huang, S., and Zhang, T. (2017a). Circulating tumor microemboli (CTM) and vimentin+ circulating tumor cells (CTCs) detected by a size-based platform predict worse prognosis in advanced colorectal cancer patients during chemotherapy. Cancer Cell Int. *17*, 6.

Zhang, J., Qiao, X., Shi, H., Han, X., Liu, W., Tian, X., and Zeng, X. (2016). Circulating tumor-associated neutrophils (cTAN) contribute to circulating tumor cell survival by suppressing peripheral leukocyte activation. Tumour Biol. J. Int. Soc. Oncodevelopmental Biol. Med. *37*, 5397–

5404.

Zhang, L., Ridgway, L. D., Wetzel, M. D., Ngo, J., Yin, W., Kumar, D., Goodman, J. C., Groves, M. D., and Marchetti, D. (2013a). The identification and characterization of breast cancer CTCs competent for brain metastasis. Sci. Transl. Med. *5*, 180ra48.

Zhang, W. C. *et al.* (2012). Glycine decarboxylase activity drives non-small cell lung cancer tumor-initiating cells and tumorigenesis. Cell *148*, 259–272.

Zhang, X. H.-F., Jin, X., Malladi, S., Zou, Y., Wen, Y. H., Brogi, E., Smid, M., Foekens, J. A., and Massagué, J. (2013b). Selection of bone metastasis seeds by mesenchymal signals in the primary tumor stroma. Cell *154*, 1060–1073.

Zhang, Y., Tao, Y., and Liao, Q. (2017b). Long noncoding RNA: a crosslink in biological regulatory network. Brief. Bioinform.

Zhang, Y., Thayele Purayil, H., Black, J. B., Fetto, F., Lynch, L. D., Masannat, J. N., and Daaka, Y. (2017c). Prostaglandin E2 receptor 4 mediates renal cell carcinoma intravasation and metastasis. Cancer Lett. *391*, 50–58.

Zhao, C., Hu, S. 'en, Huo, X., and Zhang, Y. (2017a). Dr.seq2: A quality control and analysis pipeline for parallel single cell transcriptome and epigenome data. PloS One *12*, e0180583.

Zhao, C., Tynan, J., Ehrich, M., Hannum, G., McCullough, R., Saldivar, J.-S., Oeth, P., van den Boom, D., and Deciu, C. (2015). Detection of fetal subchromosomal abnormalities by sequencing circulating cell-free DNA from maternal plasma. Clin. Chem. *61*, 608–616.

Zhao, L. *et al.* (2013). High-purity prostate circulating tumor cell isolation by a polymer nanofiber-embedded microchip for whole exome sequencing. Adv. Mater. Deerfield Beach Fla *25*, 2897–2902.

Zhao, M., Ang, L., Huang, J., and Wang, J. (2017b). MicroRNAs regulate the epithelial-mesenchymal transition and influence breast cancer invasion and metastasis. Tumour Biol. J. Int. Soc. Oncodevelopmental Biol. Med. *39*, 1010428317691682.

Zhou, C., Liu, J., Tang, Y., and Liang, X. (2012). Inflammation linking EMT and cancer stem cells. Oral Oncol. *48*, 1068–1075.

Zhou, M. I., Wang, H., Foy, R. L., Ross, J. J., and Cohen, H. T. (2004). Tumor suppressor von Hippel-Lindau (VHL) stabilization of Jade-1 protein occurs through plant homeodomains and is VHL mutation dependent. Cancer Res. *64*, 1278–1286.

Zhu, S., Qing, T., Zheng, Y., Jin, L., and Shi, L. (2017). Advances in single-cell RNA sequencing and its applications in cancer research. Oncotarget.

Zhuang, Z., Gnarra, J. R., Dudley, C. F., Zbar, B., Linehan, W. M., and Lubensky, I. A. (1996). Detection of von Hippel-Lindau disease gene mutations in paraffin-embedded sporadic renal cell carcinoma specimens. Mod. Pathol. Off. J. U. S. Can. Acad. Pathol. Inc *9*, 838–842.

Zuo, J.-H. *et al.* (2011). Activation of EGFR promotes squamous carcinoma SCC10A cell migration and invasion via inducing EMT-like phenotype change and MMP-9-mediated degradation of E-cadherin. J. Cell. Biochem. *112*, 2508–2517.

(2017). Single-cell biology. Nature *547*, 19.

NNT : 2017SACLS391

Résumé en français de thèse de doctorat de l'Université Paris-Saclay préparée à l'Université Paris Sud

Ecole Doctorale n° 577
Structure et dynamique des systèmes vivants (SDSV)
Spécialité de doctorat : sciences de la vie et de la santé

Par

Lucile Broncy

Isolement et caractérisation moléculaire de cellules rares circulantes individuelles : développement de nouvelles approches méthodologiques en oncologie prédictive et diagnostic prénatal.

Thèse présentée et soutenue à Paris, le 7 novembre 2017

Composition du Jury :

M. Saule, Simon	Professeur, Université Paris-Sud	Président
Mme Taly, Valérie	Directeur de recherche, Université Paris-Descartes	Rapporteur
Mme Brevet, Marie	Professeur, Centre de biologie et pathologie EST Lyon	Rapporteur
M. Cussenot, Olivier	Professeur, Centre de recherche sur les pathologies prostatiques	Examinateur
Mme Paterlini-Bréchot, Patrizia	Professeur, Université Paris-Descartes	Directeur de thèse
Mme Ezine, Sophie	Directeur de recherche, Université Paris-Descartes	Co-directeur de thèse

Sommaire

Introduction

1. Invasion tumorale, dormance et métastases

L'invasion tumorale et la propagation métastatique du cancer sont responsables de 90% des décès humains liés au cancer dans le monde (Siegel *et al.*, 2015). L'invasion tumorale était à l'origine considérée comme un processus linéaire où la tumeur primaire se développe en acquérant une série de caractéristiques génétiques et épigénétiques jusqu'à l'apparition d'un profil malin de cellules cancéreuses (Fidler, 2003). La vascularisation tumorale se développe par néoangiogenèse et les cellules cancéreuses invasives peuvent exploiter le système vasculaire existant pour se disséminer à la fois dans le système lymphatique et dans la circulation sanguine. Ces cellules sont donc nommées cellules tumorales circulantes (CTC). La survie dans la circulation est cependant difficile même pour les CTC invasives et la plupart d'entre elles meurent pendant le voyage (Fidler, 1975). Mais pour celles qui survivent, l'arrivée au sein d'organes distants ou dans les ganglions lymphatiques régionaux représente une dissémination effective et ces cellules sont donc appelées cellules tumorales disséminées (CTD).

Des preuves substantielles soutiennent maintenant le modèle d'une progression parallèle des tumeurs primaires et des métastases. Par exemple, l'étude des modèles murins de cancer du sein suggère que la dissémination des cellules cancéreuses intervient à des stades très précoces du développement tumoral (Hüsemann *et al.*, 2008) et que même les cellules épithéliales mammaires non transformées (non cancéreuses) peuvent survivre à l'injection dans la circulation sanguine, se diffuser dans les poumons et adopter un état quiescent de dormance jusqu'à ce que l'activation d'oncogènes déclenche une prolifération maligne (Podsypanina *et al.*, 2008). En outre, la présence de cellules épithéliales circulant dans le sang de patients atteints de maladies intestinales inflammatoires bénignes et leur complète absence chez des sujets témoins sains (Pantel *et al.*, 2012) démontre clairement que la transformation néoplasique n'est pas une nécessité stricte pour que des cellules épithéliales envahissent la circulation sanguine, particulièrement lorsqu'un état d'inflammation chronique gouverne leur microenvironnement. Le modèle de progression parallèle des tumeurs et des métastases postule que la dissémination des cellules dans tout le corps commence très tôt dans l'histoire naturelle du cancer et peut même être antérieure à l'acquisition complète de caractères malins (Klein, 2009). Ce modèle est beaucoup plus à même d'expliquer le niveau d'hétérogénéité génétique observé entre les cellules cancéreuses provenant d'emplacements biologiques distincts au sein d'un même individu. La transition vers un phénotype mésenchymateux confère des capacités motiles aux cellules épithéliales, notamment grâce à la transformation de leur polarité apico-basale en polarité avant-arrière (caractéristique du mode de migration mésenchymateux) ainsi qu'à la répression des adhésions intercellulaires, un phénomène que l'on retrouve également à certaines étapes du développement embryonnaire normal (Nieto, 2011). Cependant, dans le contexte du cancer, cette transition s'associe également à la réduction des capacités de prolifération et à la quiescence des cellules tumorales (Mejlvang *et al.*, 2007), les protégeant ainsi des mécanismes d'apoptose qui induisent la mort cellulaire (Vega *et al.*, 2004). Notamment, la présence de CTC mésenchymateuses dans le sang de patients a été corrélée de manière significative à la progression de la

maladie et à la résistance aux traitements chimiothérapeutiques (Mego *et al.*, 2012; Yu *et al.*, 2013).
Le concept émergent de cellules souches cancéreuses postule qu'une petite fraction des cellules cancéreuses possèdent des propriétés intrinsèques initiatrices de tumeur qui leur permettent de remodeler leur microenvironnement et de repeupler un compartiment biologique par de nouvelles cellules cancéreuses (Brabletz *et al.*, 2005). La plasticité phénotypique est maintenant considérée comme une caractéristique majeure de l'invasion tumorale ainsi qu'un phénomène intrinsèquement lié à la génération de cellules souches cancéreuses.
Au front invasif de la tumeur, les interactions entre les cellules cancéreuses et le stroma tumoral induisent une transition partielle ou complète des cellules épithéliales vers un phénotype mésenchymateux, ce qui leur permet d'acquérir des capacités migratoires. Le processus de la transition epithelio-mésenchymateuse (TEM) peut être défini par la perte de marqueurs épithéliaux tels que les kératines, la cadhérine épithéliale (E-cadhérine), la claudine et l'occludine accompagnées d'une augmentation de l'expression des marqueurs mésenchymateux tels que la vimentine, la cadhérine neuronale (N-cadhérine), la fibronectine et les enzymes de remodelage de la matrice extracellulaire telles que les métalloprotéases sécrétées (MMP2 et MMP9 par exemple) et les métalloprotéases membranaires (MT1-MMP par exemple).
L'induction de l'angiogenèse est une étape importante dans le développement de la tumeur primaire et le phénomène de néoangiogénèse est considéré comme un tremplin majeur dans la transformation des tumeurs localisées en carcinomes invasifs. L'activation au sein de la tumeur des voies de signalisation en lien avec l'hypoxie déclenche la sécrétion de facteurs de croissance vasculaires (VEGF) par des cellules tumorales et des niveaux élevés de VEGF actif induisent une germination de vaisseaux désorganisés et une couverture réduite de péricites conduisant à un réseau vasculaire immature (Greenberg *et al.*, 2008).
De plus, il est intéressant de noter que les tumeurs hautement vasculaires comportant des vaisseaux sinusoïdaux, comme dans le cas des carcinomes rénaux et hépatocellulaires, tendent à libérer des fragments de tumeurs organisés en grappes hétérocellulaires contenant des péricites, des cellules endothéliales, stromales et cancéreuses, comme en témoignent plusieurs études (Sugino *et al.*, 2004; Küsters *et al.*, 2007; Kats-Ugurlu *et al.*, 2009), illustrant ainsi un mode d'invasion tumorale indépendant des mécanismes de la TEM.
Malgré la multitude des stratégies de dissémination adoptées par les cellules cancéreuses, le compartiment sanguin est encore aujourd'hui considéré comme la voie principale de dissémination des cellules tumorales et représente la source de CTC la plus facilement accessible.

2. Les cellules tumorales circulantes (CTC)

2.1. Définition

Les cellules tumorales circulantes (CTC) sont des cellules qui se sont détachées d'une masse tumorale donnée pour envahir la circulation sanguine ou lymphatique. Dans le sang, ces cellules sont très rares par rapport à la population de cellules sanguines. En moyenne, 1 cellule tumorale se trouve mélangée à 10 millions de leucocytes et 5 milliards d'érythrocytes dans chaque millilitre de sang (Paterlini-Bréchot, 2014). Les CTC

représentent une population très hétérogène de cellules, récapitulant l'ensemble des clones et des phénotypes tumoraux distincts qui ont permis une invasion passive ou active de cellules cancéreuses, y compris des cellules cancéreuses issues de la tumeur primaire et des métastases coexistantes, des cellules cancéreuses viables et d'autres apoptotiques, des cellules tumorales épithéliales, mésenchymateuses ou bien présentant des phénotypes hybrides. Malgré leur hétérogénéité en terme de déformabilité et de taille cellulaire, les CTC sont généralement plus grandes que la plupart des cellules sanguines normales, allant de 10 µm dans le cancer du poumon à petites cellules jusqu'à 70 µm dans le cancer du sein, tandis que les lymphocytes et les monocytes comprennent des cellules de 6 à 20 µm de diamètre (Thiele *et al.*, 2017). Avec une augmentation du potentiel tumorigène, les CTC présentent également une déformabilité accrue du cytosquelette (Guck *et al.*, 2005). Et avec une déformation accrue du cytosquelette, les variations de la taille mesurable des cellules sont plus importantes (Park *et al.*, 2014), et se trouvent également influencées par les techniques d'isolement des CTC. Le défi technique important que l'isolement et l'analyse des CTC représente, en raison de leur hétérogénéité et de leur rareté relative dans les échantillons de sang, a entravé le transfert des analyses des CTC vers les applications cliniques de routine. En effet, la plateforme CellSearch® (Veridex, États-Unis), en tant que premier et unique test clinique approuvé par la l'instance médicale réglementaire américaine (FDA) comme test pronostique pour les cancers métastatiques mammaires (Cristofanilli *et al.*, 2004), colorectaux (Cohen *et al.*, 2008) et prostatiques (Danila *et al.*, 2007). Pourtant, l'approche de CellSearch® ainsi que des autres techniques basées sur l'utilisation de marqueurs épithéliaux tels que le marqueur d'adhésion épithéliale (EpCAM) et les cytokératines pour la sélection et/ou l'identification des CTC manquent vraiment de spécificité car une partie significative des CTC ne retient pas l'expression des marqueurs épithéliaux et davantage car des cellules épithéliales non malignes peuvent également circuler dans la circulation sanguine en réponse à une inflammation chronique (Pantel *et al.*, 2012).

2.2. Intérêt Clinique de l'étude des CTC

Compte tenu des aspects coûteux, hautement invasifs et peu répétables de l'échantillonnage des tumeurs par des méthodes chirurgicales telles que les biopsies, l'utilisation de biomarqueurs sanguins fiables permettant une «biopsie liquide» du cancer aurait d'énormes répercussions sur les soins des patients s'ils étaient mis en œuvre avec succès en milieu clinique. Notamment, les développements récents dans l'analyse de l'ADN tumoral circulant (ADNtc) ont complémenté l'analyse des variations de nucléotides dans les CTC pour les patients avec cancers localement avancés et métastatiques (Bidard *et al.*, 2013). Cependant, la détection des altérations complexes de l'ADN telles que les translocations chromosomiques reste difficile à réaliser sur l'ADNtc (Cabel *et al.*, 2017) et les méthodes actuelles les plus sensibles basées sur l'ADNtc ne sont pas en mesure de fournir un diagnostic fiable des cancers au stade précoce (Alix-Panabières and Pantel, 2016; Abbosh *et al.*, 2017). En revanche, les CTC peuvent servir de substitut de tumeur et être collectées de façon non invasive pour une gamme beaucoup plus large d'analyses biologiques, y compris la caractérisation génétique, épigénétique, transcriptomique et protéomique. Notamment, l'enrichissement des CTC basé sur la taille a déjà prouvé son utilité pour le diagnostic précoce (Ilie *et al.*, 2014), le pronostic (Hofman *et al.*, 2011), le choix thérapeutique (Faugeroux *et al.*, 2014), le suivi et la détection de récurrence (Abdallah *et al.*, 2016; Poruk *et al.*, 2016) du

cancer.

3. Diagnostic prénatal et cellules fœtales trophoblastiques circulantes

3.1. Cellules fœtales trophoblastiques circulantes (CFTC)

Les cellules fœtales peuvent pénétrer la circulation sanguine maternelle de manière précoce et persistante durant la grossesse. Dans le sang des femmes enceintes, les cellules fœtales trophoblastiques circulantes (CFTC) font partie de la population de cellules rares car environ 1-2 CFTC peu(ven)t être trouvée(s) dans un millilitre de sang maternel, selon le moment de la collecte pendant la grossesse.

Le placenta humain est un organe chimérique complexe composé de structures cellulaires maternelles et fœtales et le premier trimestre de la grossesse est principalement consacré à la placentation (Maltepe *et al.*, 2010). En acquérant des capacités invasives par différenciation, les cytotrophoblastes peuvent migrer loin des villosités placentaires pour former des trophoblastes extraviliens (TEV). Un sous-type particulier de TEV appelé TEV endovasculaire (vTEV) migre spécifiquement vers les artères maternelles pour former des bouchons, obstruant localement la circulation maternelle et permettant un remodelage efficace des artères maternelles (Hunkapiller and Fisher, 2008). Dès 15 jours après la fécondation, les cytotrophoblastes commencent à migrer pour devenir des TEV. Alors que les vTEV envahissent la circulation maternelle, les TEV interstitiels (iTEV) migrent à travers le tissu maternel de la décidua (Kervancioglu Demirci *et al.*, 2016) et jusqu'à la 11ème ou la 12ème semaine d'aménorrhée (SA) marquant la fin du premier trimestre, lorsque les bouchons de vTEV se dissolvent naturellement après remodelage vasculaire pour laisser le sang maternel irriguer complètement l'espace intervillaire du placenta, l'invasion de trophoblastes est considérée comme la principale source de cellules foetales dans la circulation maternelle.

3.2. Diagnostic prénatal

Historiquement, le diagnostic prénatal des troubles génétiques a reposé principalement sur l'utilisation de procédures invasives pour récupérer le matériel génétique fœtal comme l'amniocentèse ou le prélèvement de villosités choriales (CVS). Pourtant, ces techniques invasives comportent des risques bien connus de fausse couche dans jusqu'à 1% des cas lorsque les procédures invasives sont effectuées à des périodes gestationnelles précoces, soit avant 10 SA pour le CVS et avant 15 SA pour l'amniocentèse (Tabor and Alfirevic, 2010). Dans ce contexte, l'application de méthodes non invasives de diagnostic prénatal constitue un objectif de longue date dans le domaine.

Les stratégies appliquées cliniquement pour les tests prénataux non-invasifs de routine (TPNI) reposent exclusivement sur la détection et l'analyse de l'ADN fœtal circulant (ADNfc) qui peut être trouvé dans les échantillons de sang maternel. Pour assurer l'absence de faux négatifs dans les résultats du TPNI, les niveaux d'ADNfc dans le sang maternel doivent dépasser 4% de la quantité totale d'ADN circulant (ADNc) qui contient une grande majorité d'ADN maternel. En conséquence, le TPNI est actuellement limité aux tests effectués à partir de 10 SA, lorsque les niveaux d'ADNfc représentent de 4 à 10% de la quantité totale d'ADNc des échantillons de plasma (Jain *et al.*, 2016). Il est également important de noter que, malgré les progrès

technologiques énormes déjà réalisés, les méthodes actuelles pour l'analyse de l'ADNfc ne permettent pas une détection précise des maladies monogéniques récessives ou dominantes héritées de la mère, ni celle des réarrangements chromosomiques complexes tels que les grandes délétions chromosomiques ou les duplications, les inversions, les translocations équilibrées ou non équilibrées et se trouvent également limitées par la présence de mosaïcisme placentaire confiné provoquant des résultats faux positifs (Hayata *et al.*, 2017). En revanche, les cellules fœtales intactes collectées de façon non-invasive représentent une source d'ADN fœtal pur qui pourrait informer sur une variété étendue de troubles génétiques et ce dès la 5ème SA (Mouawia *et al.*, 2012). Une publication récente de Breman *et al.* a permi d'établir une preuve de concept que les grandes délétions chromosomiques et le mosaïcisme confiné au placenta peuvent être détectés avec précision par des analyses à haut débit (séquençage de nouvelle génération, SNG) effectuées sur CFTC après séparation par gradient de densité (Breman *et al.*, 2016). En effet, l'analyse des CFTC a un grand potentiel pour aider à développer les applications cliniques du diagnostic prénatal non-invasif (DPNI).

4. Le présent travail

Mon travail doctoral a été axé sur l'étude de cellules rares circulantes uniques extraites du sang (et d'autres fluides biologiques) en utilisant une technologie développée précédemment dans mon équipe, appelée ISET® (Isolation by SizE of Tumor/Trophoblastic cells). Cette méthode de filtration particulière a été développée pour isoler les cellules tumorales circulant dans le sang sans utiliser d'anticorps, car on ne connait pas à l'heure actuelle d'antigènes spécifiques exprimés uniquement par les cellules tumorales et qui ne soient pas présents sur les cellules sanguines normales. Étant donné qu'ISET® n'utilise pas d'anticorps et que toutes les cellules non hématologiques rares sont plus grandes que la majorité des leucocytes, ISET® isole par la taille presque tous les types de cellules rares circulantes (CRC) telles que les cellules souches dérivées de la moelle osseuse (Fadini *et al.*, 2017) ou d'autres niches de cellules souches (Heise *et al.*, 2016), les cellules endothéliales qui sont des composants essentiels de la vascularisation humaine (Medina *et al.*, 2017) mais aussi les cellules cancéreuses chez des patients porteurs de néoplasmes malins invasifs (Paterlini-Bréchot, 2014) ainsi que les cellules d'origine fœtale et placentaire chez les femmes enceintes (Oudejans *et al.*, 2003).

Résultats

1. Résultats de l'application d'ISET® pour le diagnostic prénatal

Dans le contexte du diagnostic prénatal, l'analyse moléculaire individuelle constitue une condition préalable requise pour l'identification fiable des cellules trophoblastiques fœtales car il n'existe actuellement aucun marqueur cytologique unique connu pour être spécifique à tous les trophoblastes humains. Les travaux antérieurs de notre équipe scientifique ont démontré que l'amplification du génome suivi par celle des marqueurs de polymorphismes informatifs à partir d'une CFTC unique enrichie par ISET® permet à la fois la validation moléculaire de sa nature fœtale et un diagnostic précis des troubles génétiques récessifs tels que la mucoviscidose et l'amyotrophie spinale (AS) (Mouawia *et al.*, 2012). L'amyotrophie spinale est une maladie héréditaire autosomique récessive causée par des mutations du gène codant pour le régulateur transmembranaire de la mucoviscidose (CFTR) et portant des implications létales fréquentes pour les individus affectés (Saker *et al.*, 2006). Après la mucoviscidose, l'AS est la deuxième maladie génétique récessive mortelle la plus fréquente qui survient dans la plupart des cas à partir de mutations homozygotes du gène moteur des neurones spinaux (SMN): SMN1, tandis que 4% des cas sont causés par des mutations hétérozygotes avec délétion concommittante du second allèle SMN1 (Béroud *et al.*, 2003).

Le principal défi concernant l'analyse des CFTC est lié à leur extrême rareté dans le flux sanguin, une caractéristique particulière qui est commune à toutes les CRC. Les enquêtes antérieures de mon équipe ont permis d'estimer le taux moyen de CFTC détectable par ISET® dans le sang maternel à 4-12 SA en effectuant des prélèvements sanguins hebdomadaires sur 14 femmes enceintes ayant choisi la fécondation *in* vitro (FIV) (Mouawia *et al.*, 2012). Dans ce but, les CFTC de chaque échantillon de sang de 10 ml ont été enrichies par ISET®, sélectionnées morphologiquement pour microdissection laser et analyse génétique individuelle afin d'établir de manière fiable leur nature fœtale. Tandis que seulement la moitié des femmes enceintes testées à 4 SA présentaient des taux très faibles de CFTC (0,3 par mL), les 14 mères présentaient des CFTC détectables dans tous les échantillons de sang obtenus chaque semaine de 5 à 12 SA. Plus précisément, les taux moyens de CFTC ont montré une augmentation régulière de 1,19 CFTC par mL à 5 SA jusqu'à 2,0 CFTC par mL à 11 SA avec une diminution observée (bien que non statistiquement significative) à 1,66 CFTC par mL à 12 SA (Mouawia *et al.*, 2012).

Dans le but de diversifier et de maximiser la récupération des cellules trophoblastiques par une méthode complètement sûre, nous avons cherché à introduire la collecte des trophoblastes à partir du col de l'utérus par une méthode non-invasive largement inspirée du test Papanicolaou (PAP) (McCRACKEN, 1948; Reed and Chesley, 1948). Après le transfert sur filtres ISET®, 2 mL de chaque échantillon de 10 ml de tampon fixateur contenant l'écouvillon d'échantillonnage ont permis la récupération par microdissection d'au moins 2 et jusqu'à 12 trophoblastes génétiquement diagnostiqués chez les 21 femmes enceintes testées entre 8 et 12 SA. Cette méthode d'échantillonnage complètement sécurisée permettait ainsi d'identifier au moins 1,0 cellule trophoblastique par mL et jusqu'à 6,0 totrophoblastes par mL d'échantillon, permettant ainsi d'augmenter la récupération maximale de CFTC de 20 jusqu'à 60 cellules à partir de 10 mL d'échantillons biologiques. En

outre, l'application de l'analyse génétique aux trophoblastes récupérés via cette méthode a permis de mener avec succès un DPNI de la mucoviscidose et l'AS chez 6 mères à risque de porter un fœtus affecté par l'un ou l'autre de ces deux troubles génétiques récessifs.

2. Application d'ISET® en oncologie prédictive : cancer du rein à cellules claires

Malgré les améliorations évidentes aux soins de la mère et de l'enfant que le DPNI promettent, mon intérêt scientifique personnel s'est d'abord porté sur l'oncologie prédictive, car l'analyse moléculaire de CTC à l'échelle de la cellule unique présente un potentiel énorme, à mon avis, pour améliorer les pratiques médicales actuelles grâce à des stratégies raffinées de thérapie anticancéreuse personnalisée et permettre un suivi non invasif en temps réel de la maladie ainsi que la découverte de nouveaux aspects concernant la biologie du cancer, des objectifs concomitants qui sont fondamentalement liés.

L'application des analyses moléculaires au carcinome rénal à cellules claires (CRCC) et aux cellules rares circulantes uniques isolées par ISET® et analysées par cytopathologie a été axée sur la détection des altérations génétiques du gène suppresseur de tumeur von Hippel-Lindau (VHL).

Les résultats obtenus par mes co-auteurs et moi-même sur une cohorte de 30 patients atteints de CRCC nous ont permis d'identifier des mutations du gène VHL dans 83% des échantillons de tumeurs, ce qui correspond à certains des résultats précédents rapportés par d'autres chercheurs dans la littérature (Sato *et al.*, 2013). Dans notre propre étude, le statut VHL trouvé dans toutes les cellules cancéreuses circulantes (CCC) identifiées par cytopathologie concorde exactement avec le statut VHL correspondant dans les tumeurs primaires. Ceci est cohérent avec des études antérieures ayant démontré le caractère diagnostique de la cytopathologie basée sur la classification de critères morphologiques de Hofman, qui permet une identification fiable des cellules rares circulantes présentant des caractéristiques malignes (CRC-MF = CCC) dans le sang des patients avec cancer tandis que les individus en bonne santé ne présentent pas de CRC avec une morphologie maligne (Hofman *et al.*, 2011c, 2012, 2016). Cependant, les critères cytopathologiques ne sont pas toujours conclusifs et, lorsque le doute persiste concernant la nature cancéreuse des cellules circulantes, celles-ci sont classéss comme des cellules rares circulantes présentant des caractéristiques malignes incertaines (CRC-UMF). Ces cellules présentent une morphologie atypique, et réunissent au moins un et jusqu'à trois des cinq critères cytopathologiques de Hofman (anisonucléose (ratio> 0,5), noyaux supérieurs à trois fois la taille des pores calibrés (c'est-à-dire> 24 µm), noyaux irréguliers, présence de feuillets tridimensionnels et un ratio nucléocytoplasmique élevé), alors que les CRC malignes (CCC) sont définies par la présence d'au moins quatre de ces cinq critères. Par conséquent, les CRC-UMF ne répondent pas aux exigences strictes du diagnostic cytopathologique des cellules cancéreuses. Pourtant, dans notre étude sur les patients atteints de CRCC, 104 CRC-UMF ont présenté des profils de mutation VHL concordants par rapport à ceux trouvés dans les échantillons de tumeurs correspondants.

Parmi nos 25 patients porteurs de mutations du gène VHL dans leur tumeur primaire, 18 patients ont présenté des CCC diagnostiquées par cytopathologie tandis que les 25 patients présentaient tous des CRC-UMF portant

des mutations de VHL identiques à celles trouvées dans les échantillons de tumeurs correspondants. Il est important de noter que les profils VHL de toutes les CCC diagnostiquées par cytopathologie chez 20 patients (dont 2 patients porteurs de tumeurs à profil VHL non muté) se sont avérés identiques aux profils moléculaires déterminés à partir des échantillons de tumeurs correspondants. Si l'on considère que toutes les CRC uniques portant des mutations de VHL identiques à celles trouvées dans les échantillons de tumeurs correspondants représentent des cellules cancéreuses dérivées de ladite tumeur, alors l'analyse des profils mutationnels de VHL s'avérerait adaptée pour compléter de manière fiable le diagnostic cytopathologique des CCC dans le contexte du CRCC. En fait, l'analyse moléculaire permettrait alors de valider une spécificité de 100% du diagnostic cytopathologique des CCC tout en s'avérant utiles pour identifier 104 cellules individuelles classées initialement comme CRC-UMF par cytopathologie et dérivant de l'ensemble des 25 patients porteurs de mutations VHL dans leur tumeur.

D'un point de vue statistique, corréler la concordance des profils moléculaires des CRC et des tumeurs primaires correspondantes avec une identité clonale convergente des cellules tumorales serait moins sujet à erreur si plusieurs altérations génétiques identiques sont détectées. En examinant de plus près tous les cas où l'inactivation bialélique du gène VHL pouvait être identifiée, et en considérant uniquement les cas où au moins deux altérations génétiques se sont produites pour entraîner une perte indéniable de toute expression fonctionnelle de pVHL, 13 des 25 patients atteints de tumeur mutée pour VHL peuvent être sélectionnés (désigné comme groupe A dans la **Table 1**).

Un élargissement de cette sélection pourrait inclure 2 patients portant des doubles mutations hétérozygotes trouvées de manière identique dans toutes les CRC et les tumeurs correspondantes, car deux altérations génétiques successives sont nécessaires pour que ce profil apparaisse (désignés comme groupe B dans la **Table 1** : 13+2=15). Par analogie, il est plausible de considérer que les profils VHL concordants entre la tumeur et les CRC auraient une signification diagnostique tumorale chez 10 patients restants (désignés comme groupe C dans la **Table 1** : 15+10=25).

Table 1: *Profils VHL et diagnostic cytopathologique des CRC*

Si les profils VHL concordants sont considérés comme indicateurs diagnostiques de la nature cancéreuse des CRC seulement pour :	**Le groupe A (n=13)**	**Le groupe B (n=15)**	**Le groupe C (n=25)**
Nombre de CCC diagnostiquées par cytopathologie	21	28	57
Nombre de CRC-UMF correspondant à des cellules cancéreuses selon l'analyse du gène VHL	59	73	161
Nombre total de cellules cancéreuses identifiées par les deux methodes (moléculaire et morphologique)	59	73	161
Nombre de patients avec CCC diagnostiquées par cytopathologie	8	10	18
Nombre de patients avec CRC-UMF correspondant à des cellules cancéreuses selon l'analyse du gène VHL	13	15	25
Nombre total de patients avec cellules cancéreuses identifiées par les deux methodes	13	15	25
Sensibilité de la cytopathologie	61.5%	66.7%	72.0%

3. Développements méthodologiques appliqués à ISET®

Compte-tenu de l'hétérogénéité intratumorale mise en évidence par les récentes études moléculaires à haut débit dans pratiquement tous les types de cancers solides, il est crucial de développer des méthodes fiables pour obtenir les données génomiques de manière globale à partir de CRC isolées par ISET®.

Nous avons développé un nouveau protocole pour enrichir les cellules tumorales vivantes du sang sans biais lié à la sélection d'antigènes en utilisant un tampon dédié et en adaptant le protocole sur le dispositif de filtration. Nous avons montré que ce protocole permet un taux de récupération de 80 à 100% des cellules tumorales et un seuil de sensibilité évalué à 1 cellule tumorale par millilitre de sang dans les tests de spiking utilisant des cellules capturées individuellement.

Plus de 40 méthodes distinctes développées pour isoler les CTC ont été publiées (Song *et al.*, 2017) et parmi ces méthodes, l'enrichissement basé sur la taille peut être réalisé selon plusieurs techniques. Les méthodes de filtration sont caractérisées par différents paramètres de filtration (type de filtres, tampon ou supports utilisés pour diluer le sang, type de dispositif et pression de filtration ...) qui déterminent leurs différentes performances. Par conséquent, en dépit du fait que le mot «filtration» semble intuitivement être une approche simple et générique pour séparer les éléments de grande taille et ceux de petite taille, la filtration du sang pour isoler les cellules rares circulantes (CRC) ne dépend pas uniquement de la taille des pores. En outre, la différence de taille entre les leucocytes (8-15 µm) et les cellules tumorales/trophoblastiques (15-30 µm) est relativement faible, créant une compétition des cellules sanguines pour les pores du filtre et faisant de l'isolement sans perte des cellules tumorales/trophoblastiques morphologiquement intactes un défi technique ambitieux.

Étant donné que la sensibilité est un élément critique, nous avons développé un protocole capable de fournir une fiabilité maximale pour l'évaluation de la sensibilité à l'aide d'un certain nombre de cellules tumorales inférieures à 10, c'est-à-dire en ajoutant au sang des cellules tumorales fluorescentes recueillies et comptées individuellement. Pour un nombre plus élevé de cellules tumorales (30 à 300), nous les avons comptées par dilution, en effectuant des comptages répétés pour ajuster le nombre effectif de cellules. Un aperçu des taux de réussite de la récupération des cellules par ISET® est présenté dans la **Figure 1**.

Figure 1: *Performances de la méthode ISET®*

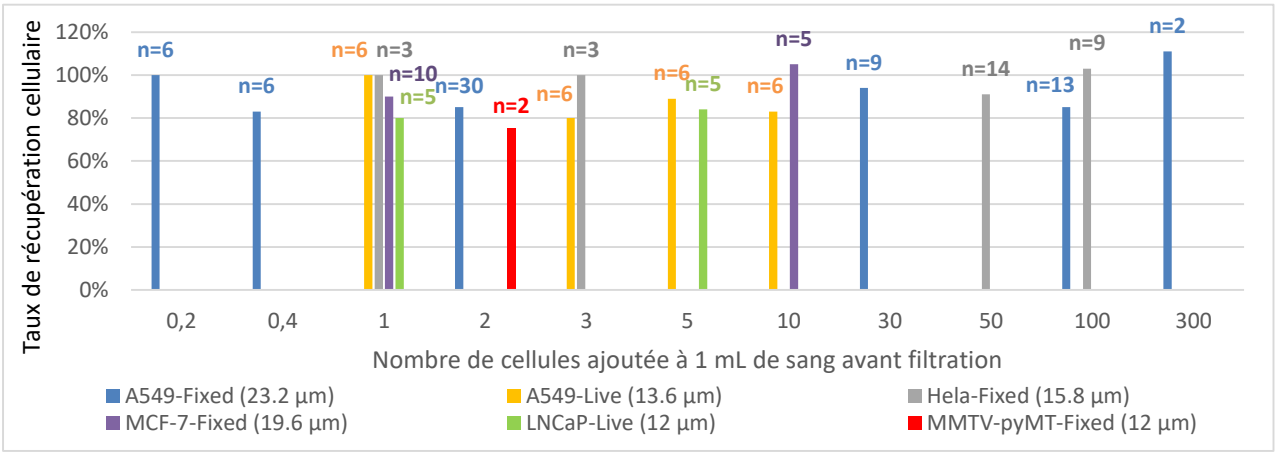

Discussion

1. Analyse génétique de cellules uniques pour le diagnostic prénatal

1.1. Pourquoi et comment récupérer non-invasivement les cellules trophoblastiques du col ?

La récupération des cellules trophoblastiques uniquement à partir de la circulation sanguine maternelle présente des pièges potentiels. Par exemple, les grossesses qui pourraient commencer peu après une fausse couche spontanée pourraient théoriquement entraîner des résultats potentiellement biaisés du DPNI en raison de la possible persistance transitoire dans la circulation maternelle de cellules trophoblastiques issues du conceptus précédent. Des types spécifiques de CFC (Cellules Fœtales Circulantes), lymphoides et myeloydes, ont été décrits comme pouvant persister dans la circulation maternelle pendant des années et jusqu'à plusieurs décennies après la naissance de l'enfant ou la fin de la grossesse prématurée (Bianchi *et al.*, 1996), ce qui n'est pas le cas des CFTC qui sont éliminées du sang après quelques semaines dès la fin de la grossesse. La diffusion des trophoblastes vers le bas de la cavité utérine à travers le canal endocervical est censée coïncider spécifiquement avec la placentation lors du premier trimestre et la présence de cellules trophoblastiques dans le col de l'utérus a été décrite comme un événement précoce et transitoire d'une durée moyenne de 2 mois, restant strictement limitée au délai de 5 à 15 SA (Adinolfi and Sherlock, 2001; Sifakis *et al.*, 2010). Ces cellules ne sont plus présentes ou disparaissent très rapidement après la fin de la grossesse. Dans ce contexte, la combinaison des analyses individuelles des trophoblastes du col avec celles des CFTC à des fins diagnostiques offre une opportunité importante d'augmenter la récupération des cellules fœtales tout en fournissant une perspective non biaisée sur les caractéristiques moléculaires des cellules fœtales trophoblastiques.

La collecte de trophoblastes du col de l'utérus avait déjà été étudiée par d'autres groupes (Imudia *et al.*, 2009; Bolnick *et al.*, 2014), mais les approches différaient de la méthode présentée ici puisque notre protocole ne nécessite pas d'insérer l'écouvillon dans le canal endocervical ni un lavage endocervical, mais se base plutôt sur la rotation de l'écouvillon à la jonction externe du canal sans réelle insertion dans le col de l'utérus, contrairement aux méthodes d'échantillonnage précédemment rapportées.

Suite à la publication de notre étude, Jain *et al.* ont également rapporté l'isolement de cellules trophoblastiques à partir du canal endocervical, en utilisant la méthode de collecte précédemment introduite par Imudia et ses collègues (Imudia *et al.*, 2009), suivie d'une sélection immunologique des cellules présentant le marqueur HLA-G et d'un isolement nucléaire pour appliquer un séquençage ciblé multiplexe à haut débit de l'ADN isolé pour l'interrogation simultanée de multiples marqueurs génétiques (Jain *et al.*, 2016). Malgré l'utilisation d'une approche moléculaire intéressante, cette étude n'a pas pu analyser l'ADN fœtal pur puisque l'isolement nucléaire des cellules présentatrices de HLA-G a donné une fraction moyenne d'ADN fœtal de 91,5% dans les 20 spécimens endocervicaux consécutifs (Jain *et al.*, 2016).

En revanche, les recherches menées par mon équipe sont restées concentrées sur l'analyse individuelle des trophoblastes récupérés à partir de nos 21 échantillons cervicaux, ce qui permet d'aborder la caractérisation moléculaire de l'ADN fœtal complètement pur en interrogeant jusqu'à 10 loci polymorphes répartis sur 4 chromosomes pour la validation génétique de l'origine fetoplacentale de chaque cellule individuelle collectée

(Pfeifer *et al.*, 2016). Notre méthode de collecte s'est révélée efficace pour améliorer les taux de récupération de trophoblastes par rapport à l'extraction de CFTC du sang maternel tout en permettant un DPNI précis de troubles monogéniques et restant complètement non-invasif pour assurer la sécurité du fœtus.

1.2. Perspectives et limites potentielles à cette étude

Notre étude a fourni des résultats préliminaires encourageants sur la collecte des trophoblastes cervicaux à utiliser dans le DPNI des troubles génétiques (Pfeifer *et al.*, 2016). Une validation supplémentaire de cette méthode est justifiée pour confirmer ces résultats sur des plus larges groupes de femmes enceintes.

De plus, comme toutes les autres stratégies de DPNI/TPNI qui font actuellement l'objet d'une investigation scientifique ainsi que la seule méthode non invasive qui a déjà atteint la mise en œuvre clinique (c'est-à-dire basée sur l'analyse de l'ADNc), notre méthode pourrait rencontrer des difficultés importantes pour fournir un diagnostic précis dans certains cas de mosaïcisme placentaire avec un confinement aigu (Pan *et al.*, 2014) ainsi que pour les grossesses gémellaires dans les cas présentant un jumeau qui disparait spontanément de manière précoce (Mantzaris and Cram, 2015). En effet, étant donné que les trophoblastes placentaires ont été considérés comme la principale source de libération de l'ADNfc pendant la grossesse (Faas *et al.*, 2012), le mosaïcisme placentaire pourrait constituer une source non négligeable de faux résultats.

Malgré cette limitation plutôt globale qui affecte le DPNI/TPNI en général, notre étude a répondu à nos attentes initiales en validant la notion de la récupération de trophoblastes à partir du col de l'uterus entre 8 et 12 semaines de grossesse et l'utilisation d'ISET® sans prélèvement de sang pour le DPNI de troubles génétiques récessifs par une approche sans danger pour la mère ni pour l'enfant. La combinaison de cette stratégie par rapport à la collecte de CFTC à partir d'échantillons de sang maternel serait probablement très avantageuse pour plusieurs raisons, par exemple pour atteindre et maintenir la précision maximale des résultats du DPNI dans les cas de grossesses génétiquement complexes où un biais pourrait influencer les données moléculaires. Les prélèvements multiples de sang et d'échantillons cervicaux répartis tout au long de la deuxième moitié du premier trimestre de grossesse pourraient aider les cas génétiquement complexes qui restent actuellement hors de portée du TPNI ciblant l'ADNc (Pan *et al.*, 2014; Mantzaris and Cram, 2015).

De plus, malgré des progrès techniques constants, les méthodes de TPNI basées sur l'ADNc ne sont toujours pas adaptées à la détection de troubles hérités de la mère, les délétions et translocations sous-chromosomiques concernant des fragments inférieurs à 9 Mb (Zhao *et al.*, 2015) et les mutations *de novo* (de Ligt *et al.*, 2013) en raison de la large portion d'ADNc maternel dans le sang. Le séquençage à haut débit appliqué aux cellules trophoblastiques individuelles récupérées de manière non-invasive apparaît comme le mieux adapté pour surmonter ces limitations. Il faut toutefois que les possibles faux-positifs résultant des biais d'amplification du génome entier d'une cellule unique soient distingués des réelles mutations *de novo* en comparant les données de plusieurs trophoblastes de chaque grossesse (Beaudet, 2016). Ainsi, la collecte d'un nombre suffisant de cellules trophoblastiques est essentielle pour le débeloppement d'un test fiable.

Comme indiqué précédemment (Mouawia *et al.*, 2012), ISET® permet des taux élevés de récupération de CFTC, fournissant jusqu'à 20 CFTC par prélèvement de 10 ml et permettant un DPNI précis de troubles récessifs monogéniques, comme cela a été démontré pour la mucoviscidose et l'amyotrophie spinale. Mon

travail a permis de réaliser une étude plus approfondie de la récupération du trophoblaste cervical grâce à une stratégie d'échantillonnage minimalement intrusive inspirée de Papanicolaou (Pfeifer *et al.*, 2016). Nos résultats démontrent qu'ISET® permet des taux de récupération améliorés des cellules trophoblastiques du col de l'utérus par rapport à l'isolement du CFTC par le sang, fournissant jusqu'à 60 cellules du foetus génétiquement diagnostiquées par échantillon cervical. Sur la base de cette preuve de concept, les approches futures de mon équipe porteront sur les améliorations techniques qui restent inhérentes à l'amplification du génome entier ou à de l'exome de cellules individuelles isolées par ISET®. Ces aspects techniques sont communs à d'autres approches scientifiques dans le domaine du DPNI/TPNI qui toutefois isolent un nombre très inferieur de CFC par rapport à ISET® (Breman *et al.*, 2016; Kølvraa *et al.*, 2016).

À long terme, l'applicabilité clinique d'un test de DPNI basé sur ISET® combinant des analyses de trophoblastes issus du col et du sang au niveau de la cellule unique nécessitera des considérations supplémentaires telles que la réduction des coûts et du temps d'exécution, en mettant en œuvre des stratégies analytiques automatisées ou semi-automatisées que nous développons actuellement. Et enfin, la validation clinique de nos développements méthodologiques sera une exigence préalable pour l'introduction commerciale de ce test de DPNI basé sur ISET®.

2. Analyse génétique de cellules uniques pour l'oncologie prédictive (CRCC)

Les carcinomes rénaux (CR) ne constituent pas une seule entité cancéreuse, mais englobent une large gamme de néoplasmes rénaux phénotypiquement et génétiquement distincts parmi lesquels le sous-type le plus commun est celui à cellules claires (CRCC) représentant environ 75% des cas. Les tumeurs du type CRCC présentent souvent des zones de nécrose et sont associées à des temps de survie plus courts lorsqu'elles présentent une embolisation tumorale intravasculaire s'étendant jusqu'à la veine cave inférieure (Park and Eisen, 2007). La complexité de la classification actuelle des tumeurs rénales, comprenant également le développement du CRCC dans les maladies rénales en phase terminale, inclue des cas de CRCC sans évidence morphologique de cellules claires ainsi que des tumeurs rénales présentant une morphologie de cellules claires sans être admissibles dans la classification du CRCC, y compris notamment le sous-type pathologiquement ambigu du CR papillaire à cellules claires (López, 2013). Le comportement biologique des tumeurs rénales reste largement imprévisible si l'on se base uniquement sur l'histologie.

2.1. Les paramètres moléculaires du carcinoma renal à cellules claires

Les études portant sur les syndromes de cancer familial pour identifier les altérations génétiques responsables, au moins en partie, des multiples manifestations malignes de chaque maladie ont largement contribué à élargir notre compréhension des composants moléculaires du CR. Par exemple, les mutations du proto-oncogène MET (également appelé c-met) situé sur le bras long du chromosome sept (7q31) et codant pour un récepteur au facteur de croissance des hépatocytes (HGF) peuvent être trouvées à la fois dans les cancers rénaux papillaires sporadiques et familiaux (Lubensky *et al.*, 1999) ; le CRCC peut également apparaître sporadiquement ou dans le cadre de la maladie héréditaire de Von Hippel-Lindau (VHL). L'identification du gène VHL par Latif et ses

collègues en 1993 a marqué une progression essentielle dans notre compréhension de la pathogenèse du CRCC (Latif *et al.*, 1993). En effet, des études ultérieures ont identifié des mutations de VHL dans 35 à 85% des CRCC sporadiques (Schraml *et al.*, 2002; Sato *et al.*, 2013) et la suppression d'un allèle du bras court du chromosome trois abritant le locus de VHL (3p25) a été décrite à des taux exceptionnellement élevés dans de larges cohortes de CRCC, caractérisant jusqu'à 94% des cas (Sato *et al.*, 2013). Malgré des preuves substantielles de l'hétérogénéité des tumeurs CRCC, des altérations du locus de VHL (y compris les mutations de VHL, l'hyperméthylation du promoteur et la perte d'hétérozygotie du chromosome 3p) ont été décrites dans plusieurs études comme étant les seuls événements omniprésents caractérisant tous les sous-clones tumoraux chez les patients atteints de CRCC (Gerlinger *et al.*, 2012, 2014; Gerstung *et al.*, 2012; Gulati *et al.*, 2014; Voss *et al.*, 2014; Dagher *et al.*, 2017). Ainsi, il est difficile d'imaginer comment des cellules non néoplasiques qui porteraient exactement la même mutation de VHL que la tumeur primaire pourraient se disséminer dans le sang. Par conséquent, les CRC-UMF, donc les cellules rares circulantes avec cytomorphologie incertaine, identifiées chez les 25 patients ayant une mutation VHL dans la tumeur, qui portent la même mutation VHL identifiée dans la tumeur (**Table 1**) sont à considérer comme cellules tumorales circulantes, c'est à dire comme CCC. Notre travail a demontré que la cytopathologie, dans le domaine des CRC issues de CRCC, est complètement spécifique mais pas complètement sensible, l'analyse moléculaire ciblée pouvant permettre d'apporter la preuve du « caractère tumoral » en cas de doute morphologique.

Par contre, l'observation de 21 CRC-UMF provenant de 11 patients et présentant des profils mutationnels VHL discordants par rapport aux échantillons tumoraux correspondants soulève des questions concernant l'origine de ces cellules. Plusieurs hypothèses peuvent être proposées pour expliquer ces résultats. Il convient tout d'abord de noter que jusqu'à 25% des patients présentent un CR multifocal au moment du diagnostic et que les analyses génétiques effectuées dans une cohorte de 26 tumeurs CRCC multifocales ont révélé que 46% de ces patients portaient en fait plusieurs tumeurs coexistantes d'origines génétiques distinctes (Cheng *et al.*, 2008). Ainsi, les tumeurs CRCC multifocales avec multiples origines distinctes pourraient en partie expliquer une discordance des profils mutationnels de VHL trouvés dans les CRC-UMF par rapport à l'échantillon tumoral spécifique analysé.

Par ailleurs, ces CRC présentant une morphologie incertaine et des profils génétiques distincts de ceux de la tumeur pourraient également représenter des cellules hyperplasiques non néoplasiques dérivées de lésions rénales distinctes et précurseurs car celles-ci peuvent coexister avec le CRCC et résultent directement de l'inactivation de VHL (Mandriota *et al.*, 2002; Montani *et al.*, 2010). Par conséquent, dans le doute, ces cellules n'ont pas été considérées comme tumorales. Néanmoins, nos analyses dans leur ensemble montrent la présence de cellules tumorales identifiées soit par cytomorphologie et analyse moléculaire soit par analyse moléculaire dans tous les patients probants pour l'étude, c'est à dire ayant une mutation VHL dans la tumeur.

Il sera important dans le futur d'élargir la portée de la caractérisation moléculaire des CRC dans le CRCC en analysant des marqueurs moléculaires supplémentaires impliqués dans la tumorigénèse du CRCC. En effet, les données génétiques récentes obtenues sur le CRCC par l'utilisation de plateformes moléculaires à haut débit suggèrent que des abbérations génétiques spécifiques peuvent coopérer avec l'inactivation bialélique initiale

de VHL pour orchestrer la tumorigénèse du CRCC. Mise à part l'inactivation bialélique de VHL, selon des études récentes, des altérations génétiques courantes qui se retrouvent le plus fréquemment chez les patients atteints de CRCC visent souvent des gènes contrôlant l'expression de protéines régulatrices épigénétiques impliquées dans la modulation de la conformation de la chromatine et l'accessibilité à la transcription, comme PBRM1, SETD2, BAP1, ARID1A, KDM5C et KDM6A (Gao *et al.*, 2017a). Fait intéressant, les études ont révélé que PBRM1, BAP1 et SETD2 sont tous situés à proximité du locus de VHL sur le bras court du chromosome 3 et représentent des cibles simultanées de délétion par perte d'hétérozygotie sur 3p (Sato *et al.*, 2013).

En outre, bien que les altérations de VHL soient couramment identifiées chez une grande partie des patients atteints de CRCC, d'autres sous-types de CRCC ne sont pas associés à la perte de fonctionalité de la protéine VHL (pVHL), comme en témoignent les 4 patients de notre cohorte présentant des séquences de VHL de type sauvage dans leurs échantillons de tumeurs et dans toutes leurs CRC uniques analysées. Pour ces patients, l'analyse mutationnelle de VHL n'a pas fourni d'informations supplémentaires sur la nature des CRC par rapport à la cytopathologie seule, soulignant la nécessité d'interroger d'autres marqueurs génétiques.

Grâce aux améliorations technologiques substantielles réalisées pour les analyses de séquençage, des sous-types moléculaires supplémentaires de CRCC ont récemment émergé. Par exemple, en combinant le séquençage du génome entier et/ou de l'exome entier avec des analyses de méthylation d'ADN et des analyses génomiques quantitatives sur 106 échantillons de CRCC, Sato et ses collègues ont constaté que 40% des échantillons de CRCC avec une expression fonctionnelle de pVHL présentaient une inactivation bialélique du gène ELOC (également appelé TCEB1) encodant l'un des cofacteurs stabilisants de pVHL, l'élongine C, par des mutations concomitantes à la perte du chromosome 8 supprimant le locus ELOC (8q21) sur l'allèle contralatéral (Sato *et al.*, 2013).

2.3. Perspectives futures

Il est important de noter que des travaux récents (Cancer Genome Atlas Research Network, 2013; Sato *et al.*, 2013; Czarnecka *et al.*, 2014; Li *et al.*, 2017) ont clairement démontré que la combinaison de multiples stratégies de caractérisation moléculaire de CRCC, telles que les analyses de séquences génomiques et les modifications des nombres de copies avec le profilage de l'expression des gènes et l'évaluation de la méthylation de l'ADN offrent une occasion unique d'approfondir notre compréhension des contributions moléculaires différentielles par rapport au large éventail de phénotypes pathogènes observés chez les patients cancéreux. Cependant, peu d'études ont abordé la caractérisation moléculaire de cellules individuelles issues de CRCC, qu'elles soient récupérées à partir de la circulation sanguine (Nel *et al.*, 2016) ou dissociées du tissu tumoral (Xu *et al.*, 2012b). Ce dernier exemple, à travers le séquençage d'exome complet d'une seule cellule (WES) d'une tumeur CRCC présentant des séquences de gènes de type sauvage sur les loci de VHL et PBRM1, a permis d'illustrer la complexité particulière de l'architecture moléculaire du CRCC qui se reflète dans l'hétérogénéité génétique qui peut être identifiée à la fois dans les tumeurs individuelles et au niveau de la population. Ces observations suggèrent que la caractérisation moléculaire de cellules uniques peut être cruciale pour démêler la complexité du cancer surtout dans le contexte de dérèglements métaboliques tels que ceux observés chez les patients atteints de CRCC.

En résumé, malgré le besoin d'analyses mutationnelles étendues du génome entier au niveau des CRC chez les patients avec CRCC, notre travail a permis de fournir des éléments clé demontrant que la cytopathologie est complètement spécifique mais sa sensibilité est limitée et que l'analyse moléculaire ciblée peut apporter la preuve du « caractère tumoral » en cas de doute morphologique.

3. Développements méthodologiques en lien avec ISET®

3.1. Les performances de la technique ISET®

Nos données in vitro montrant la très grande sensibilité d'ISET® sont compatibles avec les données in vivo précédemment publiées par des équipes indépendantes, montrant la plus grande sensibilité in vivo d'ISET® par rapport à CellSearch™ (Farace *et al.*, 2011; Hofman *et al.*, 2011b; Khoja *et al.*, 2012; Krebs *et al.*, 2012; Pailler *et al.*, 2013; Khoja *et al.*, 2014; Morris *et al.*, 2014; Pailler *et al.*, 2015; Morrow *et al.*, 2016). Les performances d'ISET® dépendent des aspects suivants: 1) le sang est traité peu de temps après la collecte, 2) le traitement pour préparer le sang pour la filtration ISET® est rapide et efficace 3) le nombre d'étapes avant l'étape "isolement" est minimum: le sang du patient est recueilli, dilué et filtré, 4) les cellules fixes sont collectées sans étapes supplémentaires par le filtre et une seule étape supplémentaire est nécessaire pour collecter des cellules vivantes en pipettant, 5) les caractéristiques du filtre évitent de perdre des cellules plus grandes que les lymphocytes matures, 6) le système d'aspiration sanguine peut être modulé et permet de coller de grandes cellules au filtre sans perte, ou de les concentrer dans un petit volume à la surface du filtre, 6) le système ne repose pas sur l'utilisation de marqueurs pour l'isolement ni pour l'identification des cellules tumorales. Ensemble, ces caractéristiques jouent un rôle clé dans la détermination de la sensibilité d'ISET® pour l'isolement des CRC.

Nous notons également que, dans le domaine des CTC, une sensibilité élevée n'est pertinente cliniquement que si elle est associée à une spécificité élevée. Puisque la circulation de cellules rares non tumorales peut être présente dans le sang de patients atteints de cancer, une sensibilité élevée avec une faible spécificité peut entraîner des erreurs dans les décisions cliniques.

En ce qui concerne la spécificité, la filtration ISET® n'effectue aucune détection de CTC en tant que telle. La technique est destinée à isoler les CRC sans biais et avec une perte minimale. La spécificité est apportée par l'étape suivante de la cytopathologie. Comme les cellules tumorales sont isolées intactes sans dommage, la caractérisation des CRC est possible grâce à diverses approches en aval. Comme indiqué et reconnu, la cytopathologie est la seule méthode cliniquement validée pour diagnostiquer les cellules tumorales (Paterlini-Bréchot, 2014). Selon les critères cytopathologiques (Long *et al.*, 2016), les cellules cancéreuses des patients sont habituellement supérieures à 16 microns. La présence dans le sang de cellules cancéreuses intactes de moins de 8 microns, c'est-à-dire plus petites que les lymphocytes matures, n'a jamais été diagnostiquée chez les patients (Hofman *et al.*, 2014), en accord avec l'utilisation d'ISET® pour isoler tous les types de CTC du sang. L'équipe de Paul Hofman a également démontré avec certitude que la cytopathologie sanguine ISET® est diagnostique pour une identification fiable des cellules cancéreuses dans le sang.

La valeur clinique d'ISET® est prévisiblement liée à sa capacité à isoler tous les types de cellules tumorales, y compris les cellules tumorales en transition épithélio-mesenchymateuse (TEM), exprimant des marqueurs mésenchymateux tels que la Vimentin, mais pas (ou très peu) exprimant des marqueurs épithéliaux (EpCAM ou Cytokératine). La présence de cellules cancéreuses mésenchymateuses dans le sang s'est révélée pertinente en termes de valeur pronostique chez les patients atteints de cancer du pancréas (Khoja *et al.*, 2012; Poruk *et al.*, 2016), et des poumons (Hofman *et al.*, 2011a; Krebs *et al.*, 2012; Pailler *et al.*, 2013). La détection des cellules tumorales en TEM est également pertinente pour le développement de tests de diagnostic fiables. Par exemple, en utilisant ISET®, Pailler et al. ont signalé la présence d'un réarrangement récurrent de l'ALK dans les CTC qui exprimaient également des marqueurs mésenchymateux, en accord avec une sélection clonale de cellules tumorales (Pailler *et al.*, 2013). En ce qui concerne l'interrogation moléculaire des CRC, des études indépendantes ont révélé l'intérêt d'ISET® pour la détection *in situ* de plusieurs biomarqueurs théranostiques, y compris la recombinaison d'ALK, la recombinaison ROS1, les mutations KRAS, la mutation BRAF V600E et l'amplification HER2 (Pinzani *et al.*, 2006; Ilie *et al.*, 2012; Hofman *et al.*, 2013; Buim *et al.*, 2015; Pailler *et al.*, 2015).

Malgré ces résultats et les performances exceptionnelles d'ISET® en termes de sensibilité et de spécificité du diagnostic, la nécessité d'utiliser des fixateurs cytologiques avant la filtration afin de fixer de manière permanente les cellules au filtre constitue une limitation substantielle pour la caractérisation moléculaire puisque les possibilités d'analyses moléculaires de cellules fixées au niveau de la cellule unique restent limitées. Par conséquent, il semblait important de développer et d'optimiser un nouveau processus par lequel la filtration ISET® pourrait assurer la récupération de CRC viable.

3.2. Développements méthodologiques

La biomécanique du cytosquelette peut affecter la performance de la méthode lors de l'utilisation d'échantillons non fixés. Les articles dans la littérature indiquent que les lignées de cellules tumorales non malignes sont plus rigides par rapport aux lignées de cellules tumorales malignes (et moins sujettes à la migration et à l'invasion) (Xu *et al.*, 2012a; Harouaka *et al.*, 2013). Les études avec des cellules obtenues à partir d'ascite des patients (cancer de l'ovaire) ou dérivées du carcinome squameux oral ont montré que les cellules cancéreuses provenant d'une population de cellules tumorales donnée présentent un degré de rigidité variable, similaire à la rigidité des lignées cellulaires cancéreuses (Swaminathan *et al.*, 2011; Runge *et al.*, 2014).

Dans ce rapport nous avons également montré que les cellules tumorales vivantes A549 isolées du sang peuvent être cultivées et croître *in vitro* pendant au moins 5 jours, ce qui démontre que le tampon et le protocole utilisés pour isoler les cellules tumorales vivantes du sang permettent leur croissance. Fait intéressant, nous avons remarqué qu'aucun leucocyte n'est resté vivant après 3 jours de culture.

De plus, nous avons évalué les marqueurs du cytosquelette par analyse en microscopie confocale de la F-actine et de l'acetyl-α-tubuline après l'isolement et la culture des cellules tumorales vivantes pendant 72 heures. Ces marqueurs sont connus pour être des cibles thérapeutiques (Dumontet and Jordan, 2010; Wang *et al.*, 2016). La méthode de microscopie que nous avons utilisée a été prouvée comme ayant une corrélation directe avec la microscopie de force atomique, un test de rigidité cellulaire (Calzado-Martín *et al.*, 2016). Nous

avons comparé les profils de deux lignes cellulaires, A549 et H2228. Après l'isolement des cellules tumorales vivantes à l'aide du système ISET®, l a distribution de la F-actine et de l'acétyl-α-tubuline a été conservée (ou restaurée) après 72 heures de culture *in vitro*. De plus, pour étudier les mutations théranostiques capables de guider les choix thérapeutiques, nous avons démontré que dans notre modèle, le profil des mutations, évalué avec le Hotspot Cancer Panel V2 (Thermofisher, USA), n'est pas modifié après l'isolement des cellules tumorales par ISET® et leur croissance en culture pendant 72 heures. Ces nouvelles données peuvent stimuler des analyses importantes similaires effectuées sur les CTC des patients cancéreux.

Ensemble, ces données suggèrent que le nouveau protocole ISET® pour isoler les cellules tumorales vivantes ne modifie pas le phénotype et le génotype cellulaire. En effet, la viabilité des cellules tumorales après leur isolement du sang est restée très élevée (> 85%).

Depuis le premier rapport de xénogreffes dérivées de CTC réussies en 2000 (Pretlow *et al.*, 2000), plusieurs publications de recherche se sont concentrées sur la propagation *ex vivo* des CTC à travers une *culture in vitro* à court terme (Bobek *et al.*, 2014; Gao *et al.*, 2014; Yu *et al.*, 2014), l'injection directe dans des souris immunodéprimées (Baccelli *et al.*, 2013; Hodgkinson *et al.*, 2014; Kolostova *et al.*, 2014) ou bien la culture 3D à long terme par l'établissement de lignées cellulaires de cancer de la prostate et du cancer colorectal dérivées de CTC (Cayrefourcq *et al.*, 2015). Cependant, la culture *in vitro* à long terme des CTC reste un défi technique, avec un pourcentage généralement très faible de croissance réussie. Des connaissances supplémentaires sur les conditions de culture sont nécessaires pour obtenir une croissance in vitro de populations de CTC hétérogènes et très rares. Cependant, la première exigence dans ce but est la possibilité d'extraire des cellules tumorales du sang sans biais de sélection, en gardant leur phénotype, leur viabilité, leur génotype et leurs capacités de croissance potentiellement intactes. Le nouveau protocole que nous avons développé pour l'isolement des cellules tumorales vivantes à partir du sang est très sensible, rapide, direct et ne modifie pas leurs caractéristiques biologiques, ce qui devrait aider à poursuivre les études axées sur l'expansion et l'analyse *ex vivo* des CTC.

Jusqu'à présent, la culture *ex vivo* des CTC a été réalisée en utilisant des échantillons de patients ayant plusieurs centaines de CTC par 7,5 ml de sang. Les taux de réussite de l'expansion des CTC en culture demeurent faibles à travers les différentes méthodes d'isolement et les conditions de culture. Une explication possible de ce faible taux de réussite a été suggérée par Grillet et ses collègues qui ont démontré la présence de CTC avec tous les attributs fonctionnels des cellules souches cancéreuses (CSC) dans le sang des patients atteints de cancer colorectal (Grillet *et al.*, 2016). Les CSC ont des propriétés cruciales (Abbaszadegan *et al.*, 2017) qui les rendent les mieux adaptées pour initier une croissance à long terme *in vitro* et Grillet *et al.* ont été en mesure d'établir plusieurs lignées cellulaires en sélectionnant la sous-population de CSC parmi les CTC des patients atteints de cancer colorectal. Cela a permis d'évaluer les caractéristiques moléculaires des CSC et des CTC parmi les lignées CTC pour déterminer que le métabolisme des médicaments est surexprimé dans ces cellules, en accord avec leur résistance observée aux composés cytotoxiques (Grillet *et al.*, 2016). Les CSC sont encore plus rares que les CTC dans le flux sanguin et l'amélioration de la sensibilité de la récupération des CSC peut s'avérer utile pour améliorer les taux de réussite de la culture *ex vivo* à long terme de CTC.

L'excellente sensibilité du protocole d'isolement de cellules vivantes ISET® et la preuve qu'il permet la croissance de cellules tumorales en culture devraient aider les tests de culture pour des études fondamentales des CTC et des tests de dépistage *ex vivo* (Yu *et al.*, 2014; Malara *et al.*, 2016; Wenjun *et al.*, 2017).

3.3. Perspectives et applications futures

Compte tenu de la transition actuellement en cours des traitements anticancéreux cytotoxiques systémiques vers une thérapie moléculaire personnalisée, il devient évident que la caractérisation moléculaire en masse de la tumeur primaire ne peut pas récapituler les caractéristiques moléculaires hautement hétérogènes de toutes les cellules cancéreuses individuelles qui constituent ensemble le fardeau du cancer d'un patient donné (Qian *et al.*, 2017). Par conséquent, parce que les marqueurs moléculaires sont actuellement évalués à partir de populations entières de cellules extraites de la tumeur primaire à des fins théranostiques, les stratégies thérapeutiques ne visent que les sous-clones tumoraux prédominants qui caractérisent une masse tumorale donnée à un moment donné de son développement (c.-à-d. au moment de la biopsie ou chaque fois que d'autres méthodes d'échantillonnage de tumeur sont effectuées). Cette stratégie "d'analyse collective" a montré des limites importantes en ce qui concerne la détection de sous-clones minoritaires résistants à la thérapie, ainsi que pour distinguer la résistance préexistante de la résistance acquise aux traitements anticancéreux (Tirosh *et al.*, 2016).

D'autre part, les méthodologies de séquençage à haut débit de cellules uniques ont grandement amélioré notre compréhension de la biologie du cancer, y compris notre conception du processus métastatique (Gao *et al.*, 2017b). En outre, ces développements technologiques récents ont favorisé un intérêt croissant de la communauté scientifique pour les applications du séquençage d'ARN sur cellules uniques (RNAseq) en oncologie prédictive (Zhu *et al.*, 2017). Bien que des études récentes aient souligné la nécessité de réaliser des améliorations techniques supplémentaires avant que les méthodologies RNAseq sur cellules uniques puissent être mises en œuvre de manière fiable dans des contextes cliniques (Yan *et al.*, 2017), d'autres ont déjà mis en évidence l'énorme potentiel de l'ARN pour inférer des stratégies thérapeutiques en médecine personnalisée (Kim *et al.*, 2016) ainsi que pour retracer le voyage évolutif d'une cellule donnée pour déterminer sa nature exacte (Trapnell, 2015). De telles analyses transcriptomiques posent la restriction nécessaire d'être appliquée aux cellules intactes et viables, une exigence qui s'applique à toutes les études fonctionnelles.

Avec l'avènement des technologies applicables à la cellule unique (Khoo *et al.*, 2016), y compris les domaines émergents de la protéomique sur cellules uniques (Lu *et al.*, 2017; Sinkala *et al.*, 2017) et la méthylomique sur cellules uniques (Yu *et al.*, 2017), de nouvelles stratégies méthodologiques sont de plus en plus disponibles pour l'application dans le domaine des cellules rares. Afin de permettre la combinaison de la filtration ISET® avec l'une de ces stratégies émergentes pour l'analyse des cellules uniques, des solutions de rechange au protocole standard ISET® ont été développées et une évaluation complète des paramètres techniques optimaux a été effectuée. Nos résultats valident la faisabilité du séquençage de nouvelle génération (SNG) pour interroger l'hétérogénéité génétique des CRC enrichi par ISET® au niveau de la cellule unique. En effet, l'analyse individuelle de CTC a récemment ouvert une nouvelle fenêtre sur la complexité de l'hétérogénéité des tumeurs, car on pense que les CTC représentent la population invasive de cellules tumorales dérivées de

tous les sites du cancer, y compris des sites métastésiques éloignés (Miyamoto *et al.*, 2016). Bien que l'analyse de l'ADN tumoral circulant (ADNtc) se présente comme une approche directe pour l'analyse génétique du fardeau tumoral, les CTC sont particulièrement adaptées pour interroger l'hétérogénéité fonctionnelle en combinant l'évaluation génétique et transcriptomique d'une seule CTC (Klein *et al.*, 2002) ou par une analyse parallèle du transcriptome et de l'épigénome d'une unique CTC (Zhao *et al.*, 2017). Par conséquent, nos développements méthodologiques s'orientent vers une recherche passionnante pour comprendre plus en détail le processus métastatique et interroger la biologie du cancer en général.

Le nouveau protocole ISET® pour enrichir les CTC vivantes du sang sans les coller au filtre fournit de nouvelles possibilités pour les études génétiques de cellules uniques, tout en évitant la microdissection. Les CTC peuvent être simplement capturées manuellement de manière individuelle après l'enrichissement par micropipetage ou en utilisant des approches commerciales actuelles (comme CellCelector™ (ALS) ou DEPArray™ (Silicon Biosystems) ou QiaScout (Qiagen)). Un protocole de travail optimisé pour la caractérisation moléculaire des CTC individuelles, isolées avec sensibilité sans biais lié aux anticorps, devrait être un outil intéressant. Nous avons signalé ici un protocole de travail optimisé comprenant : 1) l'isolement hautement sensible des CTC du sang sans biais, 2) la capture de CTC individuelles, 3) l'amplification du génome entier d'une seule cellule, 4) un séquençage efficace à haut débit en utilisant une analyse de panel multigène avec l'approche Ion Torrent™. Nos résultats montrent la faisabilité d'appliquer le SNG aux cellules individuelles vivantes et fixées enrichies du sang par ISET® et récupérées en suspension, en évaluant les mutations sur une variété d'oncogènes incluant KRAS et PIK3CA. Ceux-ci sont importants pour examiner les besoins théranostiques, car les mutations de ces gènes peuvent prédire la résistance à certains traitements. Les applications diagnostiques et théranositiques de l'analyse moléculaire de CTC individuelles pourraient aider à développer une médecine non-invasive et personnalisée de plus en plus précise pour les patients atteints de cancer (Polzer *et al.*, 2014; Grillet *et al.*, 2016).

Conclusion

Le travail présenté ici a porté sur le développement de méthodes pour l'étude des cellules rares circulantes (CRC) individuelles, avec des applications à la fois en oncologie prédictive et en diagnostic prénatal.

Le concept d'analyse moléculaire individuelle de trophoblastes isolés à partir du col de l'utérus entre 8 et 12 SA en utilisant ISET® a été validé pour un DPNI des maladies monogéniques récessives. La combinaison de cette stratégie avec la collecte de cellules trophoblastiques fœtales à partir d'échantillons de sang maternel serait probablement très avantageuse compte tenu de la rareté extrême de ces cellules. En permettant la récupération de trois fois plus de cellules fœtales par volume d'échantillon, le prelèvement endocervical suivi d'une filtration fournit du matériel biologique supplémentaire pour le DPNI.

Dans le domaine de l'oncologie, les cellules cancéreuses circulantes (CCC) et les microemboles sont des populations importantes à étudier puisqu'elles représentent le risque de développement de métastases et impliquent donc environ 90% des décès liés au cancer (Siegel *et al.*, 2015). La cytopathologie permet un diagnostic fiable, mais nos données expérimentales suggèrent que l'analyse moléculaire individuelle de CRC associée à la cytopathologie permet de trancher en cas de doute morphologique et est à considérer comme complémentaire. Pour aller plus loin, des développements méthodologiques ont été réalisés pour permettre l'interrogation simultanée de multiples cibles génétiques à partir d'une cellule circulante en utilisant le séquençage à haut débit. Ces approches trouveraient une utilité clinique à des fins non seulement diagnostiques, mais également théranostiques, en fournissant des indications pour choisir la thérapie ciblée adéquate, en suivi de la réponse et en dépistage précoce de la résistance au traitement (Alix-Panabières and Pantel, 2016). Le développement ultérieur et la validation des analyses du génome et du transcriptome complet des CRC individuelles après isolement par ISET® se révéleront certainement intéressants à des fins cognitives en vue de leur application clinique. Et enfin, le domaine émergent de l'épigénomique promet d'apporter des nouvelles informations sur l'hétérogénéité et la plasticité cellulaire des populations de CCC (Miyamoto *et al.*, 2016). Ainsi, l'étude des CRC individuelles, techniquement complexe, est susceptible de tirer bénéfice des grandes avancées techniques moléculaires pour enrichir la compréhension de ce domaine afin d'améliorer le diagnostic et le suivi des patients avec cancer ainsi que le diagnostic des maladies génétiques.

Références

Abbaszadegan, M. R., Bagheri, V., Razavi, M. S., Momtazi, A. A., Sahebkar, A., and Gholamin, M. (2017). Isolation, identification, and characterization of cancer stem cells: A review. J. Cell. Physiol. *232*, 2008–2018.

Abbosh, C. *et al.* (2017). Phylogenetic ctDNA analysis depicts early-stage lung cancer evolution. Nature *545*, 446–451.

Abdallah, E. A. *et al.* (2016). MRP1 expression in CTCs confers resistance to irinotecan-based chemotherapy in metastatic colorectal cancer. Int. J. Cancer *139*, 890–898.

Adinolfi, M., and Sherlock, J. (2001). Fetal cells in transcervical samples at an early stage of gestation. J. Hum. Genet. *46*, 99–104.

Alix-Panabières, C., and Pantel, K. (2016). Clinical Applications of Circulating Tumor Cells and Circulating Tumor DNA as Liquid Biopsy. Cancer Discov. *6*, 479–491.

Baccelli, I. *et al.* (2013). Identification of a population of blood circulating tumor cells from breast cancer patients that initiates metastasis in a xenograft assay. Nat. Biotechnol. *31*, 539–544.

Beaudet, A. L. (2016). Using fetal cells for prenatal diagnosis: History and recent progress. Am. J. Med. Genet. C Semin. Med. Genet. *172*, 123–127.

Béroud, C., Karliova, M., Bonnefont, J. P., Benachi, A., Munnich, A., Dumez, Y., Lacour, B., and Paterlini-Bréchot, P. (2003). Prenatal diagnosis of spinal muscular atrophy by genetic analysis of circulating fetal cells. Lancet Lond. Engl. *361*, 1013–1014.

Bianchi, D. W., Zickwolf, G. K., Weil, G. J., Sylvester, S., and DeMaria, M. A. (1996). Male fetal progenitor cells persist in maternal blood for as long as 27 years postpartum. Proc. Natl. Acad. Sci. U. S. A. *93*, 705–708.

Bidard, F.-C., Weigelt, B., and Reis-Filho, J. S. (2013). Going with the flow: from circulating tumor cells to DNA. Sci. Transl. Med. *5*, 207ps14.

Bobek, V., Kacprzak, G., Rzechonek, A., and Kolostova, K. (2014). Detection and cultivation of circulating tumor cells in malignant pleural mesothelioma. Anticancer Res. *34*, 2565–2569.

Bolnick, J. M., Kilburn, B. A., Bajpayee, S., Reddy, N., Jeelani, R., Crone, B., Simmerman, N., Singh, M., Diamond, M. P., and Armant, D. R. (2014). Trophoblast retrieval and isolation from the cervix (TRIC) for noninvasive prenatal screening at 5 to 20 weeks of gestation. Fertil. Steril. *102*, 135–142.e6.

Brabletz, T., Jung, A., Spaderna, S., Hlubek, F., and Kirchner, T. (2005). Opinion: migrating cancer stem cells - an integrated concept of malignant tumour progression. Nat. Rev. Cancer *5*, 744–749.

Breman, A. M. *et al.* (2016). Evidence for feasibility of fetal trophoblastic cell-based noninvasive prenatal testing. Prenat. Diagn. *36*, 1009–1019.

Buim, M. E. *et al.* (2015). Detection of KRAS mutations in circulating tumor cells from patients with metastatic colorectal cancer. Cancer Biol. Ther. *16*, 1289–1295.

Cabel, L., Proudhon, C., Gortais, H., Loirat, D., Coussy, F., Pierga, J.-Y., and Bidard, F.-C. (2017). Circulating tumor cells: clinical validity and utility. Int. J. Clin. Oncol. *22*, 421–430.

Calzado-Martín, A., Encinar, M., Tamayo, J., Calleja, M., and San Paulo, A. (2016). Effect of Actin Organization on the Stiffness of Living Breast Cancer Cells Revealed by Peak-Force Modulation Atomic Force Microscopy. ACS Nano *10*, 3365–3374.

Cancer Genome Atlas Research Network (2013). Comprehensive molecular characterization of clear cell renal cell carcinoma. Nature *499*, 43–49.

Cayrefourcq, L. *et al.* (2015). Establishment and characterization of a cell line from human circulating colon cancer cells. Cancer Res. *75*, 892–901.

Cheng, L., MacLennan, G. T., Zhang, S., Wang, M., Zhou, M., Tan, P.-H., Foster, S., Lopez-Beltran, A., and Montironi, R. (2008). Evidence for polyclonal origin of multifocal clear cell renal cell carcinoma. Clin. Cancer Res. Off. J. Am. Assoc. Cancer Res. *14*, 8087–8093.

Cohen, S. J. *et al.* (2008). Relationship of circulating tumor cells to tumor response, progression-free survival, and overall survival in patients with metastatic colorectal cancer. J. Clin. Oncol. Off. J. Am. Soc. Clin. Oncol. *26*, 3213–3221.

Cristofanilli, M. *et al.* (2004). Circulating tumor cells, disease progression, and survival in metastatic breast cancer. N. Engl. J. Med. *351*, 781–791.

Czarnecka, A. M., Kornakiewicz, A., Kukwa, W., and Szczylik, C. (2014). Frontiers in clinical and molecular diagnostics and staging of metastatic clear cell renal cell carcinoma. Future Oncol. Lond. Engl. *10*, 1095–1111.

Dagher, J., Kammerer-Jacquet, S.-F., Dugay, F., Beaumont, M., Lespagnol, A., Cornevin, L., Verhoest, G., Bensalah, K., Rioux-Leclercq, N., and Belaud-Rotureau, M.-A. (2017). Clear cell renal cell carcinoma: a comparative study of histological and chromosomal characteristics between primary tumors and their corresponding metastases. Virchows Arch. Int. J. Pathol.

Danila, D. C. *et al.* (2007). Circulating tumor cell number and prognosis in progressive castration-resistant prostate cancer. Clin. Cancer Res. Off. J. Am. Assoc. Cancer Res. *13*, 7053–7058.

Dumontet, C., and Jordan, M. A. (2010). Microtubule-binding agents: a dynamic field of cancer therapeutics. Nat. Rev. Drug Discov. *9*, 790–803.

Faas, B. H. W., de Ligt, J., Janssen, I., Eggink, A. J., Wijnberger, L. D. E., van Vugt, J. M. G., Vissers, L., and Geurts van Kessel, A. (2012). Non-invasive prenatal diagnosis of fetal aneuploidies using massively parallel sequencing-by-ligation and evidence that cell-free fetal DNA in the maternal plasma originates from

cytotrophoblastic cells. Expert Opin. Biol. Ther. *12 Suppl 1*, S19-26.

Fadini, G. P., Ciciliot, S., and Albiero, M. (2017). Concise Review: Perspectives and Clinical Implications of Bone Marrow and Circulating Stem Cell Defects in Diabetes. Stem Cells Dayt. Ohio *35*, 106–116.

Farace, F. *et al.* (2011). A direct comparison of CellSearch and ISET for circulating tumour-cell detection in patients with metastatic carcinomas. Br. J. Cancer *105*, 847–853.

Faugeroux, V., Pailler, E., Auger, N., Taylor, M., and Farace, F. (2014). Clinical Utility of Circulating Tumor Cells in ALK-Positive Non-Small-Cell Lung Cancer. Front. Oncol. *4*, 281.

Fidler, I. J. (1975). Biological behavior of malignant melanoma cells correlated to their survival in vivo. Cancer Res. *35*, 218–224.

Fidler, I. J. (2003). The pathogenesis of cancer metastasis: the "seed and soil" hypothesis revisited. Nat. Rev. Cancer *3*, 453–458.

Gao, D. *et al.* (2014). Organoid cultures derived from patients with advanced prostate cancer. Cell *159*, 176–187.

Gao, W., Li, W., Xiao, T., Liu, X. S., and Kaelin, W. G. (2017a). Inactivation of the PBRM1 tumor suppressor gene amplifies the HIF-response in VHL-/- clear cell renal carcinoma. Proc. Natl. Acad. Sci. U. S. A. *114*, 1027–1032.

Gao, Y. *et al.* (2017b). Single-cell sequencing deciphers a convergent evolution of copy number alterations from primary to circulating tumour cells. Genome Res.

Gerlinger, M. *et al.* (2012). Intratumor heterogeneity and branched evolution revealed by multiregion sequencing. N. Engl. J. Med. *366*, 883–892.

Gerlinger, M. *et al.* (2014). Genomic architecture and evolution of clear cell renal cell carcinomas defined by multiregion sequencing. Nat. Genet. *46*, 225–233.

Gerstung, M., Beisel, C., Rechsteiner, M., Wild, P., Schraml, P., Moch, H., and Beerenwinkel, N. (2012). Reliable detection of subclonal single-nucleotide variants in tumour cell populations. Nat. Commun. *3*, 811.

Greenberg, J. I. *et al.* (2008). A role for VEGF as a negative regulator of pericyte function and vessel maturation. Nature *456*, 809–813.

Grillet, F. *et al.* (2016). Circulating tumour cells from patients with colorectal cancer have cancer stem cell hallmarks in ex vivo culture. Gut.

Guck, J. *et al.* (2005). Optical deformability as an inherent cell marker for testing malignant transformation and metastatic competence. Biophys. J. *88*, 3689–3698.

Gulati, S. *et al.* (2014). Systematic evaluation of the prognostic impact and intratumour heterogeneity of clear cell renal cell carcinoma biomarkers. Eur. Urol. *66*, 936–948.

Harouaka, R. A., Nisic, M., and Zheng, S.-Y. (2013). Circulating tumor cell enrichment based on physical properties. J. Lab. Autom. *18*, 455–468.

Hayata, K., Hiramatsu, Y., Masuyama, H., Eto, E., Mitsui, T., and Tamada, S. (2017). Discrepancy between Non-invasive Prenatal Genetic Testing (NIPT) and Amniotic Chromosomal Test due to Placental Mosaicism: A Case Report and Literature Review. Acta Med. Okayama *71*, 181–185.

Heise, R. L., Link, P. A., and Farkas, L. (2016). From Here to There, Progenitor Cells and Stem Cells Are Everywhere in Lung Vascular Remodeling. Front. Pediatr. *4*, 80.

Hodgkinson, C. L. *et al.* (2014). Tumorigenicity and genetic profiling of circulating tumor cells in small-cell lung cancer. Nat. Med. *20*, 897–903.

Hofman, V. *et al.* (2011a). Preoperative circulating tumor cell detection using the isolation by size of epithelial tumor cell method for patients with lung cancer is a new prognostic biomarker. Clin. Cancer Res. Off. J. Am. Assoc. Cancer Res. *17*, 827–835.

Hofman, V. *et al.* (2012). Morphological analysis of circulating tumour cells in patients undergoing surgery for non-small cell lung carcinoma using the isolation by size of epithelial tumour cell (ISET) method. Cytopathol. Off. J. Br. Soc. Clin. Cytol. *23*, 30–38.

Hofman, V. *et al.* (2013). Usefulness of immunocytochemistry for the detection of the BRAF(V600E) mutation in circulating tumor cells from metastatic melanoma patients. J. Invest. Dermatol. *133*, 1378–1381.

Hofman, V. *et al.* (2014). Detection of circulating tumor cells from lung cancer patients in the era of targeted therapy: promises, drawbacks and pitfalls. Curr. Mol. Med. *14*, 440–456.

Hofman, V., Ilie, M. I., Long, E., Selva, E., Bonnetaud, C., Molina, T., Vénissac, N., Mouroux, J., Vielh, P., and Hofman, P. (2011b). Detection of circulating tumor cells as a prognostic factor in patients undergoing radical surgery for non-small-cell lung carcinoma: comparison of the efficacy of the CellSearch Assay™ and the isolation by size of epithelial tumor cell method. Int. J. Cancer *129*, 1651–1660.

Hofman, V. J. *et al.* (2011c). Cytopathologic detection of circulating tumor cells using the isolation by size of epithelial tumor cell method: promises and pitfalls. Am. J. Clin. Pathol. *135*, 146–156.

Hofman, V. J., Ilie, M., and Hofman, P. M. (2016). Detection and characterization of circulating tumor cells in lung cancer: Why and how? Cancer Cytopathol. *124*, 380–387.

Hunkapiller, N. M., and Fisher, S. J. (2008). Chapter 12. Placental remodeling of the uterine vasculature. Methods Enzymol. *445*, 281–302.

Hüsemann, Y. *et al.* (2008). Systemic spread is an early step in breast cancer. Cancer Cell *13*, 58–68.

Ilie, M. *et al.* (2012). ALK-gene rearrangement: a comparative analysis on circulating tumour cells and tumour tissue from patients with lung adenocarcinoma. Ann. Oncol. Off. J. Eur. Soc. Med. Oncol. *23*, 2907–2913.

Ilie, M., Hofman, V., Long-Mira, E., Selva, E., Vignaud, J.-M., Padovani, B., Mouroux, J., Marquette, C.-H., and Hofman, P. (2014). "Sentinel" circulating tumor cells allow early diagnosis of lung cancer in patients with chronic obstructive pulmonary disease. PloS One *9*, e111597.

Imudia, A. N., Suzuki, Y., Kilburn, B. A., Yelian, F. D., Diamond, M. P., Romero, R., and Armant, D. R. (2009). Retrieval of trophoblast cells from the cervical canal for prediction of abnormal pregnancy: a pilot study. Hum. Reprod. Oxf. Engl. *24*, 2086–2092.

Jain, C. V. *et al.* (2016). Fetal genome profiling at 5 weeks of gestation after noninvasive isolation of trophoblast cells from the endocervical canal. Sci. Transl. Med. *8*, 363re4.

Kats-Ugurlu, G. *et al.* (2009). Circulating tumour tissue fragments in patients with pulmonary metastasis of clear cell renal cell carcinoma. J. Pathol. *219*, 287–293.

Kervancioglu Demirci, E., Salamonsen, L. A., and Gauster, M. (2016). The role of CX3CL1 in fetal-maternal interaction during human gestation. Cell Adhes. Migr. *10*, 189–196.

Khoja, L. *et al.* (2012). A pilot study to explore circulating tumour cells in pancreatic cancer as a novel biomarker. Br. J. Cancer *106*, 508–516.

Khoja, L., Shenjere, P., Hodgson, C., Hodgetts, J., Clack, G., Hughes, A., Lorigan, P., and Dive, C. (2014). Prevalence and heterogeneity of circulating tumour cells in metastatic cutaneous melanoma. Melanoma Res. *24*, 40–46.

Khoo, B. L., Chaudhuri, P. K., Ramalingam, N., Tan, D. S. W., Lim, C. T., and Warkiani, M. E. (2016). Single-cell profiling approaches to probing tumor heterogeneity. Int. J. Cancer *139*, 243–255.

Kim, K.-T. *et al.* (2016). Application of single-cell RNA sequencing in optimizing a combinatorial therapeutic strategy in metastatic renal cell carcinoma. Genome Biol. *17*, 80.

Klein, C. A. *et al.* (2002). Combined transcriptome and genome analysis of single micrometastatic cells. Nat. Biotechnol. *20*, 387–392.

Klein, C. A. (2009). Parallel progression of primary tumours and metastases. Nat. Rev. Cancer *9*, 302–312.

Kolostova, K., Zhang, Y., Hoffman, R. M., and Bobek, V. (2014). In vitro culture and characterization of human lung cancer circulating tumor cells isolated by size exclusion from an orthotopic nude-mouse model expressing fluorescent protein. J. Fluoresc. *24*, 1531–1536.

Kølvraa, S. *et al.* (2016). Genome-wide copy number analysis on DNA from fetal cells isolated from the blood of pregnant women. Prenat. Diagn. *36*, 1127–1134.

Krebs, M. G. *et al.* (2012). Analysis of circulating tumor cells in patients with non-small cell lung cancer using epithelial marker-dependent and -independent approaches. J. Thorac. Oncol. Off. Publ. Int. Assoc. Study Lung Cancer *7*, 306–315.

Küsters, B., Kats, G., Roodink, I., Verrijp, K., Wesseling, P., Ruiter, D. J., de Waal, R. M. W., and Leenders, W. P. J. (2007). Micronodular transformation as a novel mechanism of VEGF-A-induced metastasis. Oncogene *26*, 5808–5815.

Latif, F., Tory, K., Gnarra, J., Yao, M., Duh, F. M., Orcutt, M. L., Stackhouse, T., Kuzmin, I., Modi, W., and Geil, L. (1993). Identification of the von Hippel-Lindau disease tumor suppressor gene. Science *260*, 1317–1320.

Li, J., Guo, L., and Ai, Z. (2017). An integrated analysis of cancer genes in clear cell renal cell carcinoma. Future Oncol. Lond. Engl. *13*, 715–725.

de Ligt, J., Veltman, J. A., and Vissers, L. E. L. M. (2013). Point mutations as a source of de novo genetic disease. Curr. Opin. Genet. Dev. *23*, 257–263.

Long, E. *et al.* (2016). High expression of TRF2, SOX10, and CD10 in circulating tumor microemboli detected in metastatic melanoma patients. A potential impact for the assessment of disease aggressiveness. Cancer Med. *5*, 1022–1030.

López, J. I. (2013). Renal tumors with clear cells. A review. Pathol. Res. Pract. *209*, 137–146.

Lu, Y., Yang, L., Wei, W., and Shi, Q. (2017). Microchip-based single-cell functional proteomics for biomedical applications. Lab. Chip *17*, 1250–1263.

Lubensky, I. A., Schmidt, L., Zhuang, Z., Weirich, G., Pack, S., Zambrano, N., Walther, M. M., Choyke, P., Linehan, W. M., and Zbar, B. (1999). Hereditary and sporadic papillary renal carcinomas with c-met mutations share a distinct morphological phenotype. Am. J. Pathol. *155*, 517–526.

Malara, N. *et al.* (2016). Ex-vivo characterization of circulating colon cancer cells distinguished in stem and differentiated subset provides useful biomarker for personalized metastatic risk assessment. J. Transl. Med. *14*, 133.

Maltepe, E., Bakardjiev, A. I., and Fisher, S. J. (2010). The placenta: transcriptional, epigenetic, and physiological integration during development. J. Clin. Invest. *120*, 1016–1025.

Mandriota, S. J. *et al.* (2002). HIF activation identifies early lesions in VHL kidneys: evidence for site-specific tumor suppressor function in the nephron. Cancer Cell *1*, 459–468.

Mantzaris, D., and Cram, D. S. (2015). Potential of syncytiotrophoblasts isolated from the cervical mucus for early non-invasive prenatal diagnosis: evidence of a vanishing twin. Clin. Chim. Acta Int. J. Clin. Chem. *438*, 309–315.

McCRACKEN, W. J. (1948). On the diagnosis of various malignancies by Papanicolaou smear. Can. J. Med. Technol. *10*, 114–117.

Medina, R. J. *et al.* (2017). Endothelial Progenitors: A Consensus Statement on Nomenclature. Stem Cells Transl. Med. *6*, 1316–1320.

Mego, M. *et al.* (2012). Expression of epithelial-mesenchymal transition-inducing transcription factors in primary breast cancer: The effect of neoadjuvant therapy. Int. J. Cancer *130*, 808–816.

Mejlvang, J., Kriajevska, M., Vandewalle, C., Chernova, T., Sayan, A. E., Berx, G., Mellon, J. K., and Tulchinsky, E. (2007). Direct repression of cyclin D1 by SIP1 attenuates cell cycle progression in cells undergoing an epithelial mesenchymal transition. Mol. Biol. Cell *18*, 4615–4624.

Miyamoto, D. T., Ting, D. T., Toner, M., Maheswaran, S., and Haber, D. A. (2016). Single-Cell Analysis of Circulating Tumor Cells as a Window into Tumor Heterogeneity. Cold Spring Harb. Symp. Quant. Biol. *81*, 269–274.

Montani, M., Heinimann, K., von Teichman, A., Rudolph, T., Perren, A., and Moch, H. (2010). VHL-gene deletion in single renal tubular epithelial cells and renal tubular cysts: further evidence for a cyst-dependent progression pathway of clear cell renal carcinoma in von Hippel-Lindau disease. Am. J. Surg. Pathol. *34*, 806–815.

Morris, K. L. *et al.* (2014). Circulating biomarkers in hepatocellular carcinoma. Cancer Chemother. Pharmacol. *74*, 323–332.

Morrow, C. J. *et al.* (2016). Tumourigenic non-small-cell lung cancer mesenchymal circulating tumour cells: a clinical case study. Ann. Oncol. Off. J. Eur. Soc. Med. Oncol. *27*, 1155–1160.

Mouawia, H., Saker, A., Jais, J.-P., Benachi, A., Bussières, L., Lacour, B., Bonnefont, J.-P., Frydman, R., Simpson, J. L., and Paterlini-Brechot, P. (2012). Circulating trophoblastic cells provide genetic diagnosis in 63 fetuses at risk for cystic fibrosis or spinal muscular atrophy. Reprod. Biomed. Online *25*, 508–520.

Nel, I., Gauler, T. C., Bublitz, K., Lazaridis, L., Goergens, A., Giebel, B., Schuler, M., and Hoffmann, A.-C. (2016). Circulating Tumor Cell Composition in Renal Cell Carcinoma. PloS One *11*, e0153018.

Nieto, M. A. (2011). The ins and outs of the epithelial to mesenchymal transition in health and disease. Annu. Rev. Cell Dev. Biol. *27*, 347–376.

Oudejans, C. B. M., Tjoa, M. L., Westerman, B. A., Mulders, M. A. M., Van Wijk, I. J., and Van Vugt, J. M. G. (2003). Circulating trophoblast in maternal blood. Prenat. Diagn. *23*, 111–116.

Pailler, E. *et al.* (2013). Detection of circulating tumor cells harboring a unique ALK rearrangement in ALK-positive non-small-cell lung cancer. J. Clin. Oncol. Off. J. Am. Soc. Clin. Oncol. *31*, 2273–2281.

Pailler, E. *et al.* (2015). High level of chromosomal instability in circulating tumor cells of ROS1-rearranged non-small-cell lung cancer. Ann. Oncol. Off. J. Eur. Soc. Med. Oncol. *26*, 1408–1415.

Pan, Q. *et al.* (2014). A prenatal case with discrepant findings between non-invasive prenatal testing and fetal genetic testings. Mol. Cytogenet. *7*, 48.

Pantel, K., Denève, E., Nocca, D., Coffy, A., Vendrell, J.-P., Maudelonde, T., Riethdorf, S., and Alix-Panabières, C. (2012). Circulating epithelial cells in patients with benign colon diseases. Clin. Chem. *58*,

936–940.

Park, S., Ang, R. R., Duffy, S. P., Bazov, J., Chi, K. N., Black, P. C., and Ma, H. (2014). Morphological differences between circulating tumor cells from prostate cancer patients and cultured prostate cancer cells. PloS One *9*, e85264.

Park, W.-H., and Eisen, T. (2007). Prognostic factors in renal cell cancer. BJU Int. *99*, 1277–1281.

Paterlini-Bréchot, P. (2014). Circulating Tumor Cells: Who is the Killer? Cancer Microenviron. Off. J. Int. Cancer Microenviron. Soc. *7*, 161–176.

Pfeifer, I. *et al.* (2016). Cervical trophoblasts for non-invasive single-cell genotyping and prenatal diagnosis. Placenta *37*, 56–60.

Pinzani, P., Salvadori, B., Simi, L., Bianchi, S., Distante, V., Cataliotti, L., Pazzagli, M., and Orlando, C. (2006). Isolation by size of epithelial tumor cells in peripheral blood of patients with breast cancer: correlation with real-time reverse transcriptase-polymerase chain reaction results and feasibility of molecular analysis by laser microdissection. Hum. Pathol. *37*, 711–718.

Podsypanina, K., Du, Y.-C. N., Jechlinger, M., Beverly, L. J., Hambardzumyan, D., and Varmus, H. (2008). Seeding and propagation of untransformed mouse mammary cells in the lung. Science *321*, 1841–1844.

Polzer, B. *et al.* (2014). Molecular profiling of single circulating tumor cells with diagnostic intention. EMBO Mol. Med. *6*, 1371–1386.

Poruk, K. E. *et al.* (2016). Circulating Tumor Cell Phenotype Predicts Recurrence and Survival in Pancreatic Adenocarcinoma. Ann. Surg. *264*, 1073–1081.

Pretlow, T. G. *et al.* (2000). Prostate cancer and other xenografts from cells in peripheral blood of patients. Cancer Res. *60*, 4033–4036.

Qian, M., Wang, D. C., Chen, H., and Cheng, Y. (2017). Detection of single cell heterogeneity in cancer. Semin. Cell Dev. Biol. *64*, 143–149.

Reed, J. D., and Chesley, R. F. (1948). The routine use of Papanicolaou vaginal smears in gynecologic practice. Bull. Margaret Hague Matern. Hosp. Jersey City NJ *1*, 104–106.

Runge, J., Reichert, T. E., Fritsch, A., Käs, J., Bertolini, J., and Remmerbach, T. W. (2014). Evaluation of single-cell biomechanics as potential marker for oral squamous cell carcinomas: a pilot study. Oral Dis. *20*, e120-127.

Saker, A., Benachi, A., Bonnefont, J. P., Munnich, A., Dumez, Y., Lacour, B., and Paterlini-Brechot, P. (2006). Genetic characterisation of circulating fetal cells allows non-invasive prenatal diagnosis of cystic fibrosis. Prenat. Diagn. *26*, 906–916.

Sato, Y. *et al.* (2013). Integrated molecular analysis of clear-cell renal cell carcinoma. Nat. Genet. *45*, 860–

867.

Schraml, P., Struckmann, K., Hatz, F., Sonnet, S., Kully, C., Gasser, T., Sauter, G., Mihatsch, M. J., and Moch, H. (2002). VHL mutations and their correlation with tumour cell proliferation, microvessel density, and patient prognosis in clear cell renal cell carcinoma. J. Pathol. *196*, 186–193.

Siegel, R. L., Miller, K. D., and Jemal, A. (2015). Cancer statistics, 2015. CA. Cancer J. Clin. *65*, 5–29.

Sifakis, S., Ghatpande, S., Seppo, A., Kilpatrick, M. W., Tafas, T., Tsipouras, P., Fejgin, M., and Amiel, A. (2010). Prenatal diagnosis of trisomy 21 through detection of trophoblasts in cervical smears. Early Hum. Dev. *86*, 311–313.

Sinkala, E. *et al.* (2017). Profiling protein expression in circulating tumour cells using microfluidic western blotting. Nat. Commun. *8*, 14622.

Song, Y., Tian, T., Shi, Y., Liu, W., Zou, Y., Khajvand, T., Wang, S., Zhu, Z., and Yang, C. (2017). Enrichment and single-cell analysis of circulating tumor cells. Chem. Sci. *8*, 1736–1751.

Sugino, T., Yamaguchi, T., Ogura, G., Saito, A., Hashimoto, T., Hoshi, N., Yoshida, S., Goodison, S., and Suzuki, T. (2004). Morphological evidence for an invasion-independent metastasis pathway exists in multiple human cancers. BMC Med. *2*, 9.

Swaminathan, V., Mythreye, K., O'Brien, E. T., Berchuck, A., Blobe, G. C., and Superfine, R. (2011). Mechanical stiffness grades metastatic potential in patient tumor cells and in cancer cell lines. Cancer Res. *71*, 5075–5080.

Tabor, A., and Alfirevic, Z. (2010). Update on procedure-related risks for prenatal diagnosis techniques. Fetal Diagn. Ther. *27*, 1–7.

Thiele, J.-A., Bethel, K., Králíčková, M., and Kuhn, P. (2017). Circulating Tumor Cells: Fluid Surrogates of Solid Tumors. Annu. Rev. Pathol. *12*, 419–447.

Tirosh, I. *et al.* (2016). Dissecting the multicellular ecosystem of metastatic melanoma by single-cell RNA-seq. Science *352*, 189–196.

Trapnell, C. (2015). Defining cell types and states with single-cell genomics. Genome Res. *25*, 1491–1498.

Vega, S., Morales, A. V., Ocaña, O. H., Valdés, F., Fabregat, I., and Nieto, M. A. (2004). Snail blocks the cell cycle and confers resistance to cell death. Genes Dev. *18*, 1131–1143.

Voss, M. H. *et al.* (2014). Tumor genetic analyses of patients with metastatic renal cell carcinoma and extended benefit from mTOR inhibitor therapy. Clin. Cancer Res. Off. J. Am. Assoc. Cancer Res. *20*, 1955–1964.

Wang, X., Tanaka, M., Krstin, S., Peixoto, H. S., Moura, C. C. de M., and Wink, M. (2016). Cytoskeletal interference - A new mode of action for the anticancer drugs camptothecin and topotecan. Eur. J.

Pharmacol. *789*, 265–274.

Wenjun, W., Zhihua, W., Zhuo, W., Yuliang, D., and Qihui, S. (2017). Fast isolation and ex vivo culture of circulating tumor cells from the peripheral blood of lung cancer patients. Yi Chuan Hered. *39*, 66–74.

Xu, W., Mezencev, R., Kim, B., Wang, L., McDonald, J., and Sulchek, T. (2012a). Cell stiffness is a biomarker of the metastatic potential of ovarian cancer cells. PloS One *7*, e46609.

Xu, X. *et al.* (2012b). Single-cell exome sequencing reveals single-nucleotide mutation characteristics of a kidney tumor. Cell *148*, 886–895.

Yan, B. *et al.* (2017). Single-cell genomic profiling of acute myeloid leukemia for clinical use: A pilot study. Oncol. Lett. *13*, 1625–1630.

Yu, B., Dong, X., Gravina, S., Kartal, Ö., Schimmel, T., Cohen, J., Tortoriello, D., Zody, R., Hawkins, R. D., and Vijg, J. (2017). Genome-wide, Single-Cell DNA Methylomics Reveals Increased Non-CpG Methylation during Human Oocyte Maturation. Stem Cell Rep.

Yu, M. *et al.* (2013). Circulating breast tumor cells exhibit dynamic changes in epithelial and mesenchymal composition. Science *339*, 580–584.

Yu, M. *et al.* (2014). Cancer therapy. Ex vivo culture of circulating breast tumor cells for individualized testing of drug susceptibility. Science *345*, 216–220.

Zhao, C., Hu, S. 'en, Huo, X., and Zhang, Y. (2017). Dr.seq2: A quality control and analysis pipeline for parallel single cell transcriptome and epigenome data. PloS One *12*, e0180583.

Zhao, C., Tynan, J., Ehrich, M., Hannum, G., McCullough, R., Saldivar, J.-S., Oeth, P., van den Boom, D., and Deciu, C. (2015). Detection of fetal subchromosomal abnormalities by sequencing circulating cell-free DNA from maternal plasma. Clin. Chem. *61*, 608–616.

Zhu, S., Qing, T., Zheng, Y., Jin, L., and Shi, L. (2017). Advances in single-cell RNA sequencing and its applications in cancer research. Oncotarget.

Lucile BRONCY

université PARIS-SACLAY | ÉCOLE DOCTORALE Structure et dynamique des systèmes vivants (SDSV) | UNIVERSITÉ PARIS SUD

Title : Isolation and molecular characterization of single circulating rare cells: development of innovative methods in predictive oncology and non-invasive prenatal diagnosis.

Keywords : Circulating rare cells (CRC), circulating tumor cells (CTC), clear cell renal cell carcinoma (ccRCC), circulating fetal trophoblastic cells (CFTC), non-invasive prenatal diagnosis (NIPD), ISET® (Isolation by SizE of Tumor/Trophoblastic cells) blood filtration.

Abstract : The aim of this doctoral research project is the development of reliable and reproducible methodological approaches enabling the genetic characterization of circulating rare cells (CRC) isolated by ISET® filtration (Rarecells®, France). The first application developed consists in detecting mutations of the VHL (Von Hippel Lindau) tumor suppressor gene in single CRC isolated from the blood of 30 patients with clear cell renal cell carcinoma (ccRCC), assessed according to the results obtained by cytopathological analysis. In parallel, genetic analysis of VHL mutations was conducted in the corresponding tumor tissues.
Results revealed a potential complementarity of the molecular genetic approach targeted to single cells with the reference method of cytopathological analysis and suggested that combining both strategies could improve the sensitivity of circulating cancer cells' detection in patients with ccRCC.
A second application consisted in the development of an innovative approach for non-invasive prenatal diagnosis of recessive genetic diseases by analysis of rare trophoblastic cells collected from the cervix.
Finally, further developments allowed to optimize high-throughput sequencing analyses and to apply them to single CRC isolated by ISET®. This approach, combined with the isolation of living CRC, enabled us to obtain broader genetic data from the whole exome and should foster innovative applications to both predictive oncology and non-invasive prenatal diagnosis.

Titre : Isolement et caractérisation moléculaire de cellules rares circulantes individuelles : développement de nouvelles approches méthodologiques en oncologie prédictive et diagnostic prénatal.

Mots clés : Cellules rares circulantes (CRC), cellules tumorales circulantes (CTC), carcinome rénal à cellules claires (CRCC), cellules fœtales trophoblastiques circulantes (CFTC), diagnostic prénatal non-invasif (DPNI), filtration sanguine ISET® (Isolation by SizE of Tumor/Trophoblastic cells).

Résumé : L'objectif principal de ce projet de recherche doctorale est la mise au point d'approches méthodologiques fiables et reproductibles permettant la caractérisation génétique de cellules rares circulantes isolées par la méthode de filtration ISET® (Rarecells®, France). La première application développée consiste en la détection des mutations du gène suppresseur de tumeur VHL (Von Hippel Lindau) dans les cellules rares circulantes (CRC) uniques isolées du sang de 30 patients atteints de carcinome rénal à cellules claires (CRCC), et réalisée comparativement à l'analyse cytopathologique. L'étude génétique a également été conduite en parallèle dans les 30 tissus tumoraux correspondants.
Les résultats ont mis en lumière une potentielle complémentarité de l'approche de génétique moléculaire sur cellules uniques avec l'analyse cytomorphologique de référence et suggèrent que combiner ces approches permettrait d'obtenir une plus grande sensibilité de détection des cellules cancéreuses circulantes chez les patients atteints de CRCC.
Une deuxième application a consisté en le développement d'une approche innovante pour le diagnostic prénatal non-invasif des maladies génétiques recessives par analyse de cellules trophoblastiques rares collectées au niveau du col de l'utérus.
Enfin, des développements supplémentaires ont permis d'optimiser les analyses de séquençage à haut débit et de les appliquer à des CRC individuelles isolées par ISET®. Cette nouvelle approche, associée à l'isolement de CRC non fixées, est en mesure de fournir des données génétiques élargies à l'exome entier pour des applications à la fois en oncologie prédictive et en diagnostic prénatal non invasif.

Université Paris-Saclay
Espace Technologique / Immeuble Discovery
Route de l'Orme aux Merisiers RD 128 / 91190 Saint-Aubin, France

Inserm | Rarecells